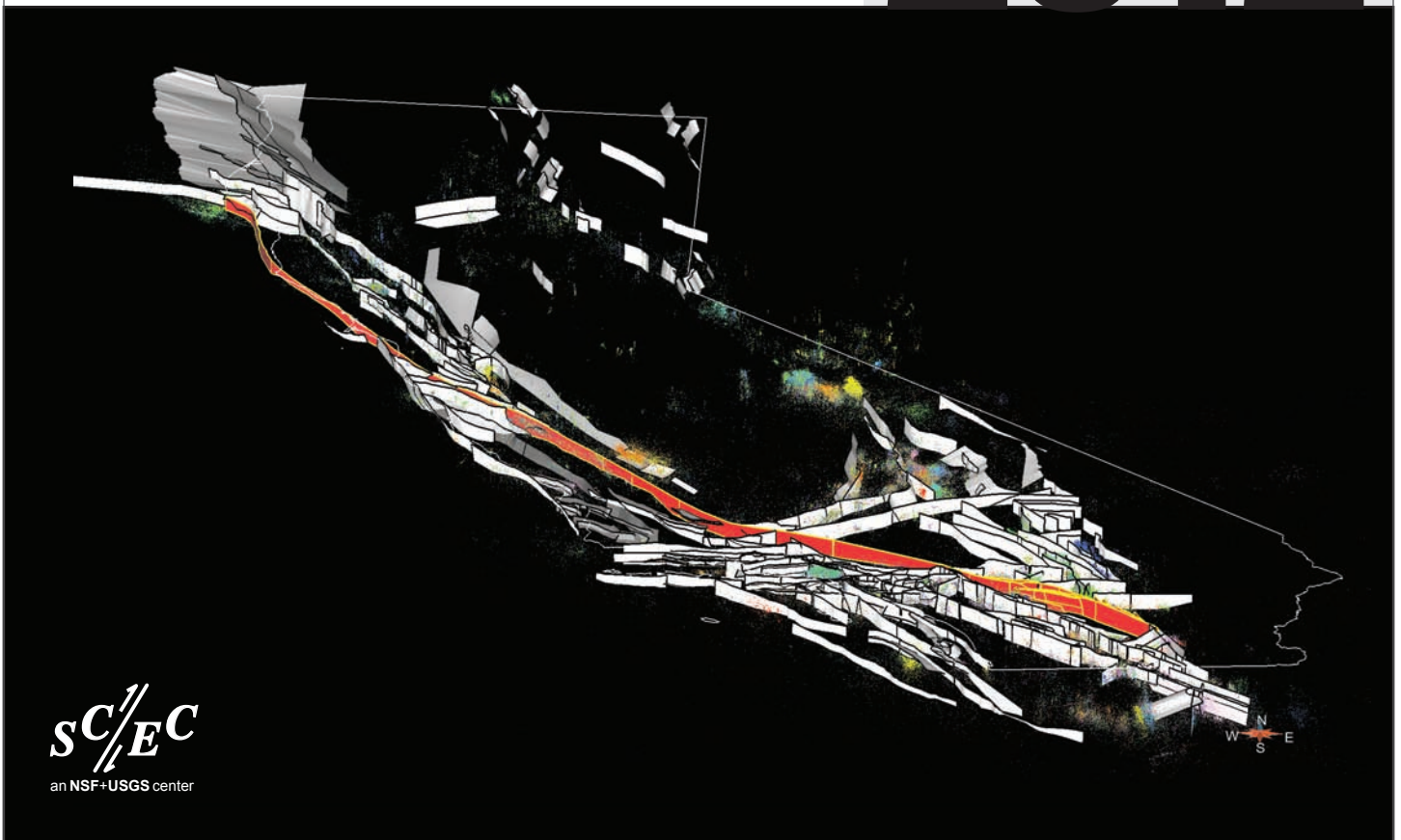


Southern California Earthquake Center
ANNUAL MEETING

2012



SC/EC
an NSF+USGS center

1985

1990

1995

2000

2005

2010

MEETING PROGRAM

September 8-12, 2012

SCEC LEADERSHIP

The Board of Directors (BoD) is the primary decision-making body of SCEC; it meets three times annually to approve the annual science plan, management plan, and budget, and deal with major business items. The Center Director acts as Chair of the Board. The liaison members from the U.S. Geological Survey are non-voting members.

The leaders of the Disciplinary Committees and Interdisciplinary Focus Groups serve on the Planning Committee (PC) for three-year terms. The PC develops the annual Science Collaboration Plan, coordinates activities relevant to SCEC science priorities, and is responsible for generating annual reports for the Center. Leaders of SCEC Special Projects (i.e., projects with funding outside the core science program) also serve on the Planning Committee. They ensure the activities of the Special Projects are built into the annual science plans.

The external Advisory Council (AC) provides guidance in all aspects of Center activities, including basic and applied earthquake research and related technical disciplines, formal and informal education, and public outreach. Members of the AC are elected by the Board for three-year terms and may be re-elected. The Council meets annually to review Center programs and plans, and prepares a report for the Center.

Core Institutions and Board of Directors (BoD)

| | | | | |
|-----------------------------------|--------------------------------|--|---------------------------------------|---|
| USC Tom Jordan* | Harvard Jim Rice | UC Los Angeles Peter Bird | UC Santa Cruz Emily Brodsky | USGS Pasadena Rob Graves |
| Caltech Nadia Lapusta** | MIT Tom Herring | UC Riverside David Oglesby | UNR Glenn Biasi | At-Large Member Roland Bürgmann |
| CGS Chris Wills | SDSU Steve Day | UC San Diego Yuri Fialko | USGS Golden Jill McCarthy | At-Large Member Judi Chester |
| Columbia Bruce Shaw | Stanford Paul Segall | UC Santa Barbara Ralph Archuleta | USGS Menlo Park Ruth Harris | * Chair ** Vice-Chair |

Science Working Groups & Planning Committee (PC)

| | Disciplinary Com. | Interdisciplinary Focus Groups | Special Projects |
|---------------------------------|--|---|---|
| PC Chair Greg Beroza* | Seismology Egill Hauksson* Elizabeth Cochran | USR John Shaw* Brad Aagaard | FARM Judi Chester* Pablo Ampuero |
| | Tectonic Geodesy Jessica Murray* Dave Sandwell | SoSAFE Kate Scharer* Ramon Arrowsmith | SDOT Kaj Johnson* Thorsten Becker |
| | EQ Geology Lisa Grant Ludwig* Mike Oskin | EFP Jeanne Hardebeck* Ilya Zaliapin | GMP Kim Olsen* Rob Graves |
| | Computational Sci Yifeng Cui* Eric Dunham | EElI Jack Baker* Jacobo Bielak | WGCEP Ned Field* |
| | | | * PC Members |

Advisory Council (AC)

| | | | |
|---|--|-----------------------------------|--|
| Jeff Freymueller , Chair U Alaska | Susan Cutter U South Carolina | Bob Lillie Oregon State | Farzad Naeim John A Martin |
| Gail Atkinson Western Ontario | Donna Eberhart-Phillips UC Davis | Anne Meltzer Lehigh | John Vidale U Washington |
| Roger Bilham U Colorado | Jim Goltz CalEMA (retired) | M. Meghan Miller UNAVCO | Andrew Whittaker MCEER/Buffalo |

Center Management

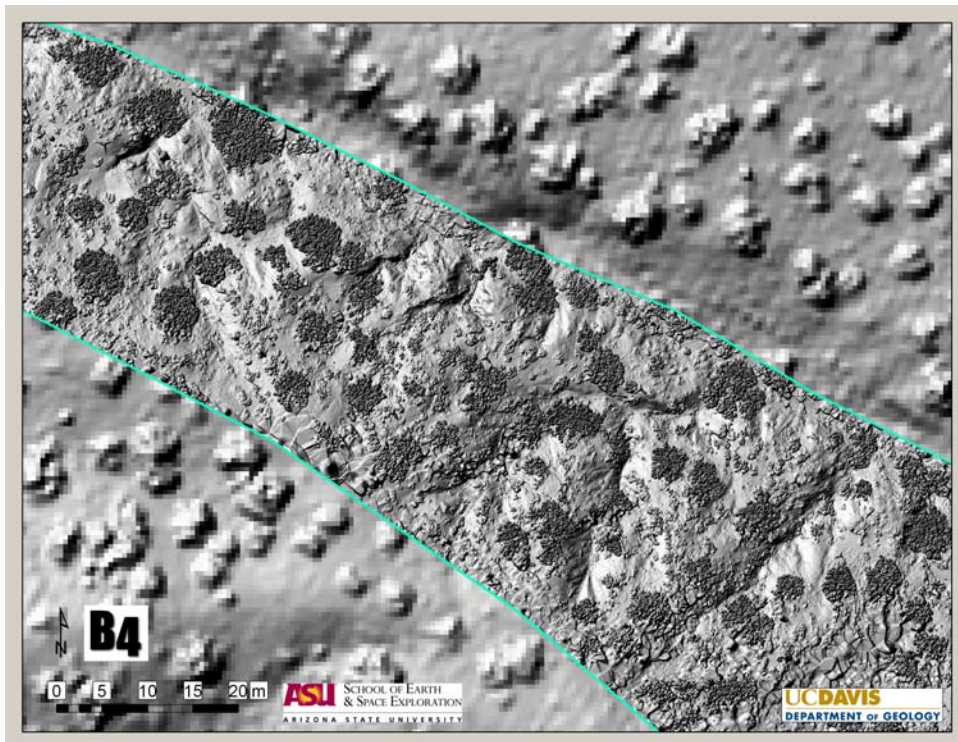
| | Center Administration | Communication, Education & Outreach | Information Technology |
|---------------------------------------|--|--|--|
| Center Director Tom Jordan | Associate Director John McRaney | Associate Director Mark Benthien | Associate Director Phil Maechling |
| Deputy Director Greg Beroza | Special Projects/Events Tran Huynh | Education Programs Bob de Groot | Research Programmer Scott Callaghan |
| | Contracts & Grants Karen Young | Digital Products John Marquis | Masha Liukis Kevin Milner Fabio Silva |
| | Admin Coordinator Deborah Gormley | | Systems Programmer John Yu |

Table of Contents

| | |
|--|------------|
| SCEC Leadership | 2 |
| Table of Contents | 3 |
| Saturday, September 8 | 4 |
| Sunday, September 9..... | 5 |
| Monday, September 10..... | 8 |
| Tuesday, September 11 | 9 |
| Wednesday, September 12 | 9 |
| State of SCEC, 2012 | 10 |
| 2011 Report of the Advisory Council | 17 |
| Communication, Education, and Outreach Highlights | 22 |
| SCEC3 Research Accomplishments | 30 |
| SCEC4 Science Milestones | 47 |
| Draft 2013 Science Plan | 51 |
| Plenary Talk Presentations | 72 |
| Poster Presentations | 77 |
| Ground Motion Prediction (GMP)..... | 77 |
| Earthquake Engineering Implementation Interface (EEII) | 78 |
| Community Modeling Environment (CME) | 78 |
| Earthquake Early Warning (EEW) | 78 |
| Collaboratory for the Study of Earthquake Predictability (CSEP) | 78 |
| Working Group on California Earthquake Probabilities (WGCEP) | 78 |
| Earthquake Forecasting and Predictability (EFP)..... | 79 |
| Fault Rupture and Mechanics (FARM) | 79 |
| Stress and Deformation Over Time (SDOT) | 80 |
| Unified Structural Representation (USR) | 80 |
| Southern San Andreas Fault Evaluation (SoSAFE)..... | 81 |
| Earthquake Geology | 81 |
| Seismology | 82 |
| Tectonic Geodesy | 83 |
| Summer Undergraduate Research Experience (SURE)..... | 84 |
| Communication, Education, and Outreach (CEO) | 84 |
| General | 85 |
| Undergraduate Studies in Earthquake Information Technology (UseIT) | 85 |
| Meeting Abstracts | 86 |
| Meeting Participants | 154 |
| SCEC Institutions | 159 |

Saturday, September 8

- 10:00 - 21:00 Southern San Andreas Fault Evaluation (SoSAFE) Fieldshop I**
Explore mapping techniques, base maps, and quality ranking that affect the measurement of small channel offsets, uncertainties and reproducibility.
Conveners: Kate Scharer (USGS), Ramon Arrowsmith (ASU)
Location: in the field
- 10:00 Depart Hilton Lobby
- 12:00 Meet at First Field Site (106 Street E in Pearblossom, CA)
Participants will be split into groups and given base maps and tapes to map and measure offsets near Pearblossom, CA. Each offset will be measured and mapped by multiple groups. In addition to examining reproducibility of measurements, the goal of the field activity is to generate questions and discussion on how offset uncertainties can be recorded, features that limit measurement precision, and recommendations on nomenclature for describing the features and their quality. Participants must turn in completed measurements at the end of the day to be compiled for discussion the following day. Lunch will be provided.
- 17:00 Depart
- 18:00 Group Dinner
- 20:00 Depart Restaurant
- 21:00 Arrive at Hilton Lobby



Hillshade from 5 cm DEM (terrestrial LiDAR scan courtesy of Peter Gold, Tracy Compton, and Eric Cowgill [UC Davis]) draped over hillshade from 50 cm B4 DEM

- 14:00 - 17:00 SCEC Annual Meeting Registration & Check-In at Hilton Lobby**

Sunday, September 9

- 07:00 - 18:30 **SCEC Annual Meeting Registration & Check-In** at Hilton Lobby
- 07:00 - 08:00 **Breakfast** at Hilton Poolside
- 08:00 - 20:00 **Poster Set-Up** in Plaza Ballroom

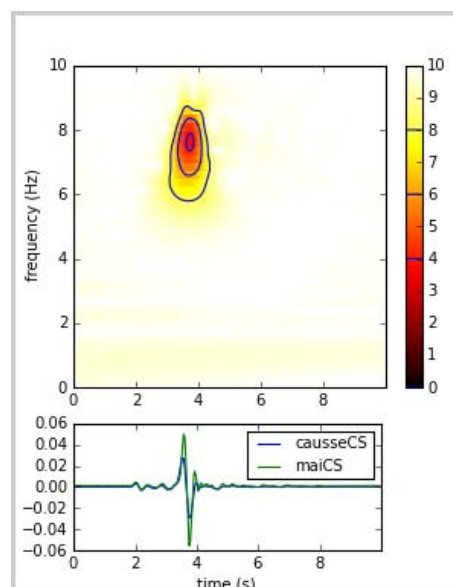
08:00 - 12:00 **Workshop: Source Inversion Validation (SIV)**

Develop strategies for automated source inversion algorithms that require no (or minimal) human interaction and provide testable rupture model output with rigorously quantifiable uncertainties.

Conveners: P. Martin Mai (KAUST), Danijel Schorlemmer (GFZ), and Morgan Page (USGS)

Location: Palm Canyon Room, Hilton Palm Springs

- 08:00 Introduction and overview of workshop goals (Martin Mai)
- 08:10 Current SIV benchmarks and results (Martin Mai)
- 08:30 Recent developments in source inversion using the W-phase (Zacharie Duputel)
- 09:00 Rapid extraction of seismic source properties - strengths and limitations of teleseismic body-wave data (Martin Vallée)
- 09:30 On rapid automated finite-fault inversions, Guangfu Shao (Chen Ji)
- 10:00 Break
- 10:15 Quantifying the quality of kinematic source optimizations through rigorous testing and automatization (Henriette Sudhaus & Danijel Schorlemmer)
- 10:45 Open Discussion
 - Current and future SIV benchmarks
 - Towards an SIV testing center
 - General SIV strategy and funding
- 12:00 Adjourn



Source Inversion Validation benchmark solution showing goodness of fit for the time frequency envelope between two signals in the database. A goodness of fit between 8 and 10 is considered excellent, between 6 and 8 good, between 4 and 6 fair, and below 4 poor.

08:00 - 12:00 **Workshop: Modeling Advances in SCEC Geodesy**

Present findings, progress, and next steps for three closely linked efforts within the SCEC community: development of the Community Geodetic Model (CGM), geodetic transient detection, and geodetic source inversion validation.

Conveners: Rowena Lohman (Cornell), Jessica Murray (USGS)

Location: Horizon Ballroom, Hilton Palm Springs

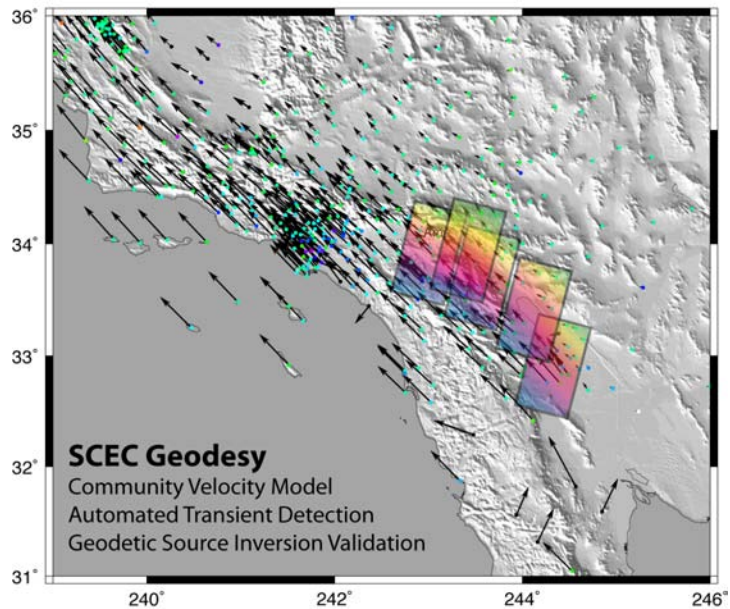
Community Geodetic Model (CGM)

- 08:00 Introduction/Overview of motivation and goals/target audiences (Jessica Murray)
- 08:10 CGM as input for the Uniform California Earthquake Rupture Forecast (UCERF) and Community Stress Model (CSM) (Kaj Johnson & Jessica Murray)
- 08:30 Geodetic Coverage: GPS and InSAR (Jessica Murray & Scott Baker)
- 08:50 Approaches available for integrating GPS and InSAR
Quantifying uncertainties - what precision is needed and possible? (Roland Bürgmann)
- 09:15 General Discussion
- 09:30 Break

continued on next page ...

Sunday, September 9

- 08:00 - 12:00** **Workshop: Modeling Advances in SCEC Geodesy** *(continued)*
 Geodetic Transient Detection
 10:00 Introduction/Summary of effort so far (Rowena Lohman)
 10:10 Presentations by groups on results from their approaches, (William Holt, Tom Herring/Kang Ji)
 10:30 Presentation on "operational" portion of effort (Masha Liukis)
 10:40 General Discussion
 10:50 Break
 Geodetic Source Inversion Validation
 11:10 Introduction and motivation (Rowena Lohman)
 11:20 New approaches (Brendan Meade)
 11:30 Unveiling of initial data sets and framework for comparisons (Rowena Lohman)
 11:40 General Discussion
 12:00 Adjourn



- 08:00 - 12:00** **Community Modeling Environment (CME) Group Meeting**
 Convener: Phil Maechling (USC)
 Location: Tapestry Room, Hilton Palm Springs

- 09:00 - 16:00** **NEES@UCSB Workshop and Site Visit: Using Earthquake Field Data in Research and Education**

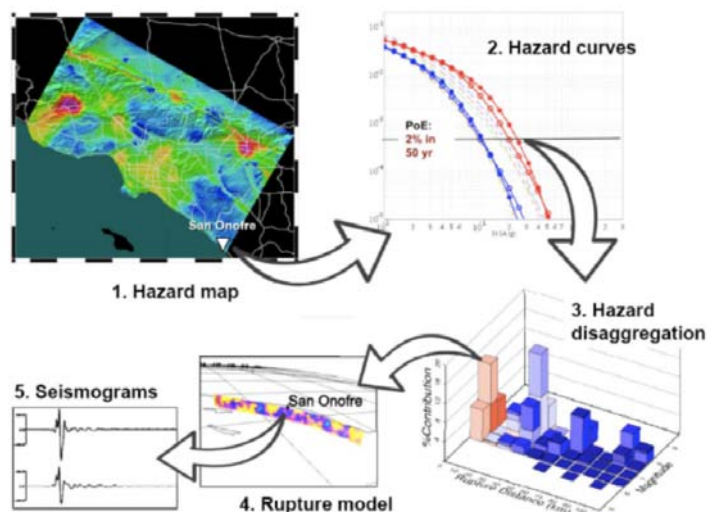
Garner Valley Downhole Array:
nees.ucsb.edu/facilities/gvda

- Conveners: Jamie Steidl (UCSB), Sandy Seale (UCSB)
- Location: Start at Cahuilla Room, Spa Resort Casino
- 09:00 Introduction to the Garner Valley Downhole Array (GVDA)
- 11:00 Travel to and Tour of GVDA Field Site
- 14:00 Depart GVDA
- 15:00 Follow-Up Session and Q&A at Spa Resort Hotel
- 16:00 Adjourn

- 12:00 - 13:00** **Lunch** at Hilton Palm Springs Restaurant and Poolside

Sunday, September 9

- 13:00 - 17:00 Workshop: Ground Motion Simulation Validation Progress**
 Develop near-term plans for validation of ground motion simulation models on (or soon to be on) the SCEC Broadband Platform, for use in developing the median part of ground motion prediction equations for elastic spectral acceleration.
Convener: Nico Luco (USGS)
Location: Horizon Ballroom, Hilton Palm Springs
- 13:00 Welcome and Background of GMSV Technical Activity Group and Broadband Platform Validation Project (Tom Jordan)
- 13:05 Overview of Agenda (Nico Luco)
SCEC Broadband Platform Validation Project
Moderator: Phil Maechling
- 13:10 Session Introduction (Phil Maechling)
- 13:15 Motivation and Needs (Norm Abrahamson)
- 13:30 Validation Plans (Christine Goulet)
- 13:45 Simulation Plans (Paul Somerville)
- 14:00 Discussion
- 14:30 Break
SCEC GMSV Technical Activity Group Projects
Moderator: Nico Luco
- 14:45 Session Introduction (Nico Luco)
- 14:50 Engineering Perspective on Simulation Validation and Use of the Broadband Platform (Jack Baker, Lynne Burks)
- 15:05 Validation of Broadband Platform Ground Motion Simulations for Historical Events (Farzin Zareian, Sanaz Rezaeian)
- 15:20 Comparison of CyberShake Hazard Models with NGA Models Using Averaging-Based Factorization (Feng Wang, Tom Jordan)
- 15:35 Discussion
- 15:50 Break
Priority GMSV Activities for 2013
SCEC Science Collaboration Plan
Moderator: Kim Olsen
- 16:05 Session Introduction (Kim Olsen)
- 16:10 Summary and Background of 2012 Priorities (Nico Luco)
- 16:20 Discussion
- 16:50 Summary of Discussions (Kim Olsen, Nico Luco)
- 17:00 Adjourn



The prototype CyberShake hazard model (CSHM-1, showing layer of hazard information. (1) Hazard map for the Los Angeles region. (2) Hazard curves computed for a site near San Onofre Nuclear Generating Station. (3) Disaggregation of hazard in terms of rupture magnitude and distance. (4) Rupture model of the earthquake with the highest hazard to the site. (5) Seismograms simulated for the earthquake with the highest hazard to site. Arrows show how users can query the model starting at highest levels (e.g. hazard map) to access information at progressively lower levels (e.g. seismograms).

Sunday, September 9

- 13:00 - 17:00 Southern San Andreas Fault Evaluation (SoSAFE) Fieldshop II**
 Explore mapping techniques, base maps, and quality ranking that affect the measurement of small channel offsets, uncertainties and reproducibility.
 Conveners: Kate Scharer (USGS), Ramon Arrowsmith (ASU)
Location: in the field
- 13:00 Introduction / Overview (Kate Scharer, Ramon Arrowsmith)
 Review obtained measurements and draft a ranking system and nomenclature for geomorphic offsets. A few short presentations of geomorphic offset studies will be given so that participants can discuss the results and interpretations in light of the field activity. Computer-based approaches for measuring offsets will be discussed and available for comparison.
- Offset channel measurement validation (Barrett Salisbury)
 - Terrestrial Laser Scanner data acquisition and processing: example from Little Rock along the San Andreas Fault (Tracy Compton)
 - Cumulative offset probability distributions (Ramon Arrowsmith)
 - Additional short presentations and discussions
- 17:00 Adjourn
- 17:00 - 18:00 Annual Meeting Ice-Breaker** in Hilton Lobby and Plaza Ballroom
- 18:00 - 19:00 Distinguished Speaker Presentation** in Horizon Ballroom
- 19:00 - 20:30 Welcome Dinner** at Hilton Poolside
- 19:00 - 20:30 SCEC Advisory Council Meeting** in Tapestry Room
- 20:30 - 22:00 Poster Session 1** in Plaza Ballroom

Distinguished Speaker Presentation (Sunday 18:00)
Rupture to Rafters on a Global Scale,
 David Wald (USGS) – see p.72

Monday, September 10

- 07:00 - 08:00 SCEC Annual Meeting Registration & Check-In** at Hilton Lobby
- 07:00 - 08:00 Breakfast** at Hilton Poolside
- 08:00 - 10:30 The State of SCEC**
Location: Horizon Ballroom, Hilton Palm Springs
- 08:00 Welcome and State of the Center (Tom Jordan)
 08:30 Report from the National Science Foundation (Greg Anderson)
 08:45 Report from the U.S. Geological Survey (Bill Leith)
 09:00 Communication, Education, & Outreach (Mark Benthien)
 09:30 SCEC Science Accomplishments (Greg Beroza)
- 10:30 - 11:00 Break
- 11:00 - 13:00 Risky Business - Risk Perception and Risk Communication**
Moderators: Lisa Grant-Ludwig (UCR), Mark Benthien (USC)
Location: Horizon Ballroom, Hilton Palm Springs
- 13:00 - 14:30 Lunch** at Hilton Restaurant, Tapestry Room, and Poolside
- 14:30 - 16:00 Poster Session 2** in Plaza Ballroom
- 16:00 - 18:00 The Importance of Faking It - Ground Motion Simulation for Earthquake Engineering**
Moderators: Rob Graves (USGS), Brad Aagaard (USGS)
Location: Horizon Ballroom, Hilton Palm Springs
- 19:00 - 21:00 SCEC Honors Banquet** at Hilton Poolside
- 21:00 - 22:30 Poster Session 3** in Plaza Ballroom

Science Session 1 (Monday 11:00)
Communicating Earthquake Risk: The Intersection of Earth and Social Sciences,
 Lucy Jones (USGS) and Tim Sellnow (Kentucky) – see p.72

Science Session 2 (Monday 16:00)
The Role SCEC Can Play in Improving Seismic Provisions in US Codes through Ground-Motion Simulations, C.B. Crouse (URS Corp) – see p.72

Tuesday, September 11

- 07:00 - 08:00** Breakfast at Hilton Poolside
- 08:00 - 10:00** **Out There - New Approaches to Modeling Extreme Events**
 Moderators: P. Martin Mai (KAUST), Jessica Murray (USGS)
 Location: Horizon Ballroom, Hilton Palm Springs
- 10:00 - 10:30** Break
- 10:30 - 12:30** **The Third Pillar - The Value of Computational Science as a Disciplinary Group in SCEC4**
 Moderators: Yifeng Cui (SDSC), Eric Dunham (Stanford)
 Location: Horizon Ballroom, Hilton Palm Springs
- 12:30 - 14:00** Lunch at Hilton Restaurant, Tapestry Room, and Poolside
- 12:30 - 14:00** **SCEC Advisory Council Executive Session** in Boardroom
- 14:00 - 15:30** **Poster Session 4** in Plaza Ballroom
- 15:30 - 17:30** **Super-Natural Laboratories - Special Fault Study Areas**
 Moderators: Kate Scharer (USGS), Mike Oskin (UC Davis)
 Location: Horizon Ballroom, Hilton Palm Springs
- 19:00 - 21:00** Dinner at Hilton Poolside
- 20:00 - 22:00** **SCEC Advisory Council Executive Session** in Boardroom
- 21:00 - 22:30** **Poster Session 5** in Plaza Ballroom

Wednesday, September 12

- 07:00 - 08:00** **Poster Removal** from Plaza Ballroom
- 07:00 - 08:00** **Breakfast** at Poolside
- 08:00 - 10:00** **The Endless Frontier - Issues Arising from the UCERF3 Project**
 Moderators: Morgan Page (USGS), Kaj Johnson (Indiana)
 Location: Horizon Ballroom, Hilton Palm Springs
- 10:30 - 12:00** **The Future of SCEC**
 Location: Horizon Ballroom, Hilton Palm Springs
- 10:30 2013 Science Collaboration and RFP (Greg Beroza)
- 11:00 Report from the SCEC Advisory Council (Jeff Freymueller)
- 11:30 Concluding Remarks (Tom Jordan)
- 12:00 Adjourn
- 12:00 - 14:00** **SCEC Planning Committee Lunch Meeting** in Palm Canyon Room
- 12:00 - 14:00** **SCEC Board of Directors Lunch Meeting** in Tapestry Room

Science Session 3 (Tuesday 08:00)
Imaging and modeling the unexpected rupture path of an extreme event: the 2012 Mw 8.6 off-Sumatra earthquake, Jean-Paul Ampuero (Caltech) – p.72
August 2012 Brawley Earthquake Swarm in Imperial Valley, Egill Hauksson (Caltech) – p.73

Science Session 4 (Tuesday 10:30)
Potential of High-Performance Computing for Solid-Earth Science, Jeroen Tromp (Princeton) – see p.73
Understanding earthquake source physics through computation, Jeremy Kozdon (Stanford) – see p.74

Science Session 5 (Tuesday 15:30)
The Ventura Region Special Fault Study Area: Towards an Understanding of the Potential for Large, Multi-Segment Thrust Ruptures in the Transverse Ranges, James Dolan (USC) – see p.74
SCEC Workshop on San Geronio Pass: Structure, Stress, Slip, and the Likelihood of Through-Going Rupture, Doug Yule (CSUN) – see p.75

Science Session 6 (Wednesday 08:00)
What can crustal deformation tell us about California's earthquake future? Lessons from UCERF3, Tom Parsons (USGS) – see p.75

State of SCEC, 2012

Thomas H. Jordan, SCEC Director

Welcome to the 2012 Annual Meeting!

The week's activities mark the first year of the five-year phase of the Center (SCEC4) that began on February 1 of this year. This meeting will focus on the collaboration plan for the science to be pursued under SCEC4, with a particular emphasis on those elements and initiatives that are new to the collaboration.

The Planning Committee has put together a compelling program that features keynote speakers on thought-provoking subjects, discussion sessions on major science themes, poster sessions on research results, technical demonstrations, education/outreach activities, and some lively social gatherings. There will be a number of workshops, group meetings, and two "fieldshops" during the weekend before the main meeting begins.

On Sunday afternoon, David Wald, of the USGS Golden, will kick-off the meeting with a plenary presentation "Rupture to Rafters on a Global Scale." Lucy Jones and Tim Sellnow will speak to the topic of effective risk communication on Monday morning, and C. B. Crouse will speak on the utility of ground motion simulations for earthquake building codes on Monday afternoon. Tuesday morning, Pablo Ampuero will give a talk on new approaches to seismic imaging and characterizing extreme events and Egill Hauksson will provide an update on the recent earthquake swarm near Brawley. That will be followed by a session on computational science in SCEC4 featuring a pair of talks by Jeroen Tromp and Jeremy Kozdon. Late that afternoon we will have a discussion on Special Fault Study Areas, and Wednesday morning there will be a forward-looking presentation by Tom Parsons on scientific questions motivated by UCERF3.

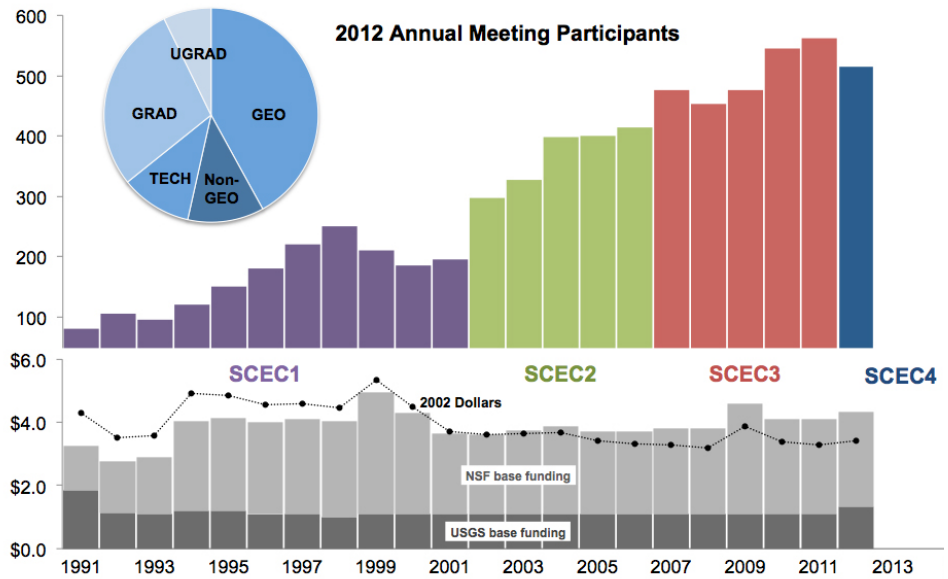


Figure 1. Registrants at SCEC Annual Meetings 1991-2012. Number for 2011 (516) is pre-registrants. Pie chart shows the demographic profile for 2012 pre-registrants. Note the large number of undergraduate (37) and graduate students (146)! The lower bar chart is the history of SCEC base funding in as-spent dollars; the connected dots are the base-funding totals in 2002 dollars.

The week's activities will bring together one of the largest collaborations in geoscience: 516 people have pre-registered (Figure 1), and almost 275 poster abstracts have been submitted. This year's pre-registrants include more than 140 first-time attendees, so we will welcome many new scientists and proto-scientists (37 undergraduate and 146 graduate students).

Veterans of past SCEC meetings know that much of the action happens in the poster sessions. In a change from recent years, posters will stay up for the entire meeting. To accomplish this, we had to reduce the size of posters by half. So we've put a premium on concision in the expectation that keeping the posters up will lead to more and better interactions. We are always looking for ways to improve the meeting, so if you have comments on how to improve this, or other aspects of it, please let the SCEC leadership know.

SCEC Accomplishments

Greg Beroza and the Planning Committee have assembled an impressive report on the SCEC3 research accomplishments, which is included in your online meeting volume, highlighting the science projects supported by SCEC during the past five years. This summary demonstrates our substantial progress in attaining the basic SCEC3 objectives. Greg will summarize the research results, with an emphasis on our more recent accomplishments, in his plenary address on Monday morning. The poster presentations at the Annual Meeting will provide a forum for more detailed discussions and interchange of ideas.

The Challenges of SCEC4

The SCEC4 scientific program is framed in terms of a very challenging, long-term research theme: *to understand how seismic hazards change across all time scales of interest, from millennia to seconds*. This problem is well suited to SCEC’s integrated approach to earthquake system science. The practical goals of SCEC4 research program are focused on time-dependent seismic hazard analysis—the geoscience required to “track earthquake cascades.” The basic research that will be needed to move towards these goals has been articulated in terms of six fundamental problems in earthquake physics (Table 1). These problems are interrelated and require an interdisciplinary, multi-institutional approach.

Table 1. Fundamental Problems of Earthquake Science for SCEC4

| | |
|----|--|
| 1. | Stress transfer from plate motion to crustal faults: long-term fault slip rates |
| 2. | Stress-mediated fault interactions and earthquake clustering: evaluation of mechanisms |
| 3. | Evolution of fault resistance during seismic slip: scale-appropriate laws for rupture modeling |
| 4. | Structure and evolution of fault zones and systems: relation to earthquake physics |
| 5. | Causes and effects of transient deformations: slow slip events and tectonic tremor |
| 6. | Seismic wave generation and scattering: prediction of strong ground motions |

Our organizational structure, reformulated in accordance with the overall SCEC4 research plan, comprises disciplinary working groups, interdisciplinary focus groups, special projects, and technical activity groups (Figure 2). A set of special projects funded separately by the NSF, USGS, and other agencies (the pink boxes in Figure 2) will continue to leverage core research support.

We are now well into the first year of SCEC4, and much of the meeting will be devoted to ambitious new activities, such as the development of the Community Geodetic Model, the Community Stress Model, and the Special Fault Study Areas. I urge you to step up with your ideas on how to push these and other initiatives forward.

At NSF’s request, we have drafted a set of milestones to guide the base research program, as well as a set of metrics and milestones to guide the SCEC/CEO program. The current draft of these research milestones, which were refined at the SCEC Leadership Retreat last June, are given in this meeting volume for your review. This is intended to be a “living document,” updated each year as the SCEC4 program progresses. Please share with us your comments on how they might be modified to improve their effectiveness as guidelines, while avoiding an unwarranted degree of specificity that would overly constrain the creative research essential to the SCEC mission.

New Projects

The SCEC leadership has been very active in securing new funding to support major research initiatives and infrastructure. Since the last Annual Meeting, we have been awarded major grants and contracts from the following agencies:

- NSF/OCI SI2-SSI Program for support of the SCEC Community Modeling Environment: “A Sustainable Community Software Framework for Petascale Earthquake Modeling.”
- NSF Geoinformatics Program for the support of seismic tomography: “Community Computational Platforms for Developing Three-Dimensional Models of Earth Structure.”
- Department of Homeland Security Office of Science and Technology to support CSEP: “Development of Infrastructure and Procedures for Evaluating Earthquake Forecasts and Predictions.”
- NSF Science Across Virtual Institutes (SAVI) Program to develop a major scientific collaboration with Japan: “Virtual Institute for the Study of Earthquake Systems (VISES) – A US-Japan Partnership in Earthquake Science.”

The last of these will come as a substantial supplement to the SCEC4 Cooperative Agreement (\$200K/yr) to enhance our growing scientific partnership with academic institutions in Japan. On the Japanese side, VISES will be led by the Earthquake Research Institute of Tokyo University and the Disaster Prevention Research Institute of Kyoto University. The structure of the Virtual Institute will be a major topic for discussion at this meeting, and we seek your input on how activities under VISES should be prioritized. We are especially interested in fostering scientific and educational exchanges that involve students early-career scientists.

STATE OF SCEC

We have signed MOUs with the Pacific Gas and Electric Company and with Southern California Edison Company for a long-term cooperative program on the study of earthquake hazards. New funding will also come from the USGS to support tsunami research (“Tsunami Modeling in Support of the USGS Science Application for Risk Reduction Project”) and SCEC participation in a collaborative earthquake early warning project with UC Berkeley and Caltech (“Prototype Development of the New CISEN Earthquake Alert System”).

Funding for CEO is increasing rapidly through support for ShakeOut activities. In Fall 2011, CEO received indirect funding from FEMA via a CalEMA subcontract to support Earthquake Country Alliance (ECA) activities and from the ATC for national ShakeOut development. In Fall 2012, SCEC will enter a direct cooperative agreement with FEMA to continue support for ECA and national ShakeOut activities. Additional support from other parts of FEMA is also possible in the next year, and private sector sponsorship will increase as ShakeOut becomes increasingly nationwide. This summer, we submitted a pre-proposal to the NSF Advancing Informal STEM Learning (AISL) program to further develop the EPIcenter Network. This week, we are submitting a proposal to NSF/REU to continue the UseIT program for 4 years.

Organization and Leadership

SCEC is an institution-based center, governed by a Board of Directors, who represent its members. The membership continues to evolve because SCEC is an open consortium, available to all qualified individuals and institutions seeking to collaborate on earthquake science in Southern California. The membership currently stands at 17 core institutions and—as of August of this year—36 institutions who have applied for and received participating status (page 159 of this meeting volume). **For those of you attending this meeting who don’t see your institution on this list, please note that it’s easy to apply; all we need is a letter from a cognizant official (e.g., your department chair or dean) that requests this status and appoints an institutional representative who will act as the point-of-contact with SCEC.**

As you can see from the list, SCEC institutions are not limited to universities, nor to U.S. organizations. The California Geological Survey has joined the SCEC4 core institutions, and URS Corporation will continue as a participation institution. We are very pleased that three of the major USGS offices—Menlo Park, Pasadena, and Golden—will remain core institutions represented by liaison (non-voting) members on the SCEC Board. There are currently 10 foreign institutions recognized as partners with SCEC through a growing list of international agreements.

SCEC currently involves more than 800 scientists and other experts in active SCEC projects. A key measure of the size of the SCEC community—registrants at our Annual Meetings—is shown for the entire history of the Center in Figure 1. For the last three years, more than 500 people have registered for each of the Annual Meetings.

Board of Directors. Under the SCEC4 by-laws, each core institution appoints one member to the Board of Directors, and two at-large members are elected by the Board from the participating institutions. The Board of Directors is the primary decision-making body of SCEC; it meets three times annually to approve the annual science plan, management plan, and budget, and deal with major business items. The liaison members from the U.S. Geological Survey are non-voting members. The Board is chaired by the Center Director, who also serves as the USC representative. I’m very pleased to announce that, at its first meeting in February, the SCEC4 Board elected Nadia Lapusta of Caltech as its Vice-Chair.

In an invitation sent to all SCEC3 domestic participating institutions, nominations were requested for the two at-large board positions. A number of outstanding nominations were received. As

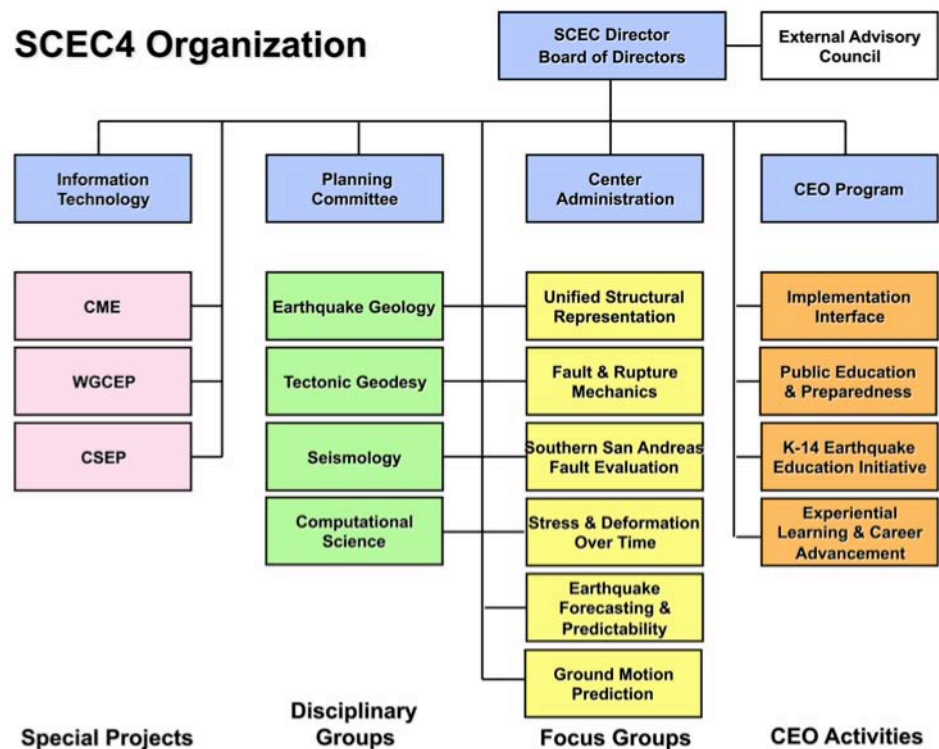


Figure 2. The SCEC3 organization chart, showing the disciplinary committees (green), focus groups (yellow), special projects (pink), CEO activities (orange), management offices (blue), and the external advisory council (white).

outlined in the by-laws, a secret ballot of the permanent core board members elected Judi Chester of Texas A&M and Roland Bürgmann of UC-Berkeley to the two at-large board positions. I congratulate Roland and Judi and welcome them to the Board! The complete Board of Directors is listed on page 2 of the meeting volume.

Advisory Council. The SCEC4 external Advisory Council is chaired by Dr. Jeffrey Freymueller of the University of Alaska. The AC is charged with developing an overview of SCEC operations and advising the Director and the Board. Since the inception of SCEC in 1991, the AC has played a major role in maintaining the vitality of the organization and helping its leadership chart new directions. A verbatim copy of the AC's 2011 report follows this report in the meeting volume.

We thank our distinguished colleague, John Filson (USGS, emeritus), who is rotating off the AC, for his excellent service. We also welcome Susan Cutter (University of South Carolina), who will be joining the AC this year. The current AC membership is listed on page 2 of the meeting volume.

Working Groups. The SCEC organization comprises a number of disciplinary committees, focus groups, special project teams, and technical activity groups. These working groups have been our engines of success. The discussions organized by the working-group leaders at the Annual Meeting provide critical input to the SCEC planning process. The current working group structure of SCEC4 is shown in Figure 2.

The Center supports disciplinary science through standing committees in Seismology, Tectonic Geodesy, and Earthquake Geology. A new disciplinary committee in Computational Science has been added for SCEC4. These groups (green boxes of Figure 2) are responsible for disciplinary activities relevant to the SCEC Science Plan, and they make recommendations to the Planning Committee regarding the support of disciplinary research and infrastructure.

SCEC coordinates earthquake system science through interdisciplinary focus groups (yellow boxes). Four of these groups existed in SCEC3: Unified Structural Representation (USR), Fault & Rupture Mechanics (FARM), Earthquake Forecasting & Predictability (EFP), and Ground Motion Prediction (GMP). The Southern San Andreas Fault Evaluation (SoSAFE) project, funded by the USGS Multi-Hazards Demonstration Project for the last four years, has been transformed into a standing interdisciplinary focus group to coordinate research on the San Andreas and the San Jacinto master faults. A new focus group called Stress and Deformation Through Time (SDOT) has merged the activities of two SCEC3 focus groups, Crustal Deformation Modeling and Lithospheric Architecture and Dynamics. Research in seismic hazard and risk analysis is being bolstered through a reconstituted Implementation Interface (an orange box in Figure 2) that includes educational as well as research partnerships with practicing engineers, geotechnical consultants, building officials, emergency managers, financial institutions, and insurers.

SCEC sponsors Technical Activity Groups (TAGs), which self-organize to develop and test critical methodologies for solving specific problems. TAGs have formed to verify the complex computer calculations needed for wave propagation and dynamic rupture problems, to assess the accuracy and resolving power of source inversions, and to develop geodetic transient detectors and earthquake simulators. TAGs share a modus operandi: the posing of well-defined “standard problems”, solution of these problems by different researchers using alternative algorithms or codes, a common cyberspace for comparing solutions, and meetings to discuss discrepancies and potential improvements. An important new TAG in SCEC4 is the Ground Motion Simulation Validation (GMSV) group, led by Nico Luco, which is developing procedures for the validation of numerical earthquake simulations that are consistent with earthquake engineering practice.

Planning Committee. The SCEC Planning Committee (PC) is chaired by the SCEC Deputy Director, Greg Beroza, and comprises the leaders of the SCEC science working groups—disciplinary committees, focus groups, and special project groups—who together with their co-leaders guide SCEC's research program (page 2). The PC has the responsibility for formulating the Center's science plan, conducting proposal reviews, and recommending projects to the Board for SCEC support. Its members will play key roles in formulating the SCEC4 proposal. Therefore, I urge you to use the opportunity of the Annual Meeting to communicate your thoughts about future research plans to them.

Center Budget and Project Funding

In 2012, SCEC received \$3.0M from NSF and \$1.34M from the USGS under the first year of the new current cooperative agreements with these two agencies. Supplementing the \$4.34M in base funding was \$406K from Pacific Gas & Electric, the Keck Foundation, and the geodesy royalty fund. In total, SCEC core funding for 2012 is \$4,746K, up slightly from \$4,591K in 2011.

The base budget approved by the Board of Directors for this year allocated \$3.404M for science activities managed by the SCEC Planning Committee; \$407K (including \$25K for intern programs) for communication, education, and outreach activities, managed by the CEO Associate Director, Mark Benthien; \$170K for information technology, managed by Associate Director for Information Technology, Phil Maechling; \$325K for administration and \$310K for meetings, managed by the Associate Director for Administration, John McRaney; and \$130K for the Director's reserve account.

STATE OF SCEC

Structuring of the SCEC program for 2012 began with the working-group discussions at our last Annual Meeting in September, 2011. An RFP was issued in October, 2011, and 193 proposals requesting a total of \$6.6M were submitted in November, 2011. Including collaborative proposals, there were 270 individual budget requests. All proposals were independently reviewed by the Director and Deputy Director. Each proposal was also independently reviewed by the leaders and/or co-leaders of three relevant focus groups or disciplinary committees. (Reviewers were required to recuse themselves when they had a conflict of interest.) The Planning Committee met on January 19-20, 2012, and spent two days discussing every proposal. The objective was to formulate a coherent, budget-balanced science program consistent with SCEC's basic mission, short-term objectives, long-term goals, and institutional composition. Proposals were evaluated according to the following criteria:

1. Scientific merit of the proposed research
2. Competence and performance of the investigators, especially in regard to past SCEC-sponsored research
3. Priority of the proposed project for short-term SCEC objectives as stated in the RFP
4. Promise of the proposed project for contributing to long-term SCEC goals as reflected in the SCEC3 science plan
5. Commitment of the P.I. and institution to the SCEC mission
6. Value of the proposed research relative to its cost
7. Ability to leverage the cost of the proposed research through other funding sources
8. Involvement of students and junior investigators
9. Involvement of women and underrepresented groups
10. Innovative or "risky" ideas that have a reasonable chance of leading to new insights or advances in earthquake physics and/or seismic hazard analysis.
11. The need to achieve a balanced budget while maintaining a reasonable level of scientific continuity given very limited overall center funding.

The recommendations of the PC were reviewed by the SCEC Board of Directors at a meeting on January 29-30, 2012. The Board voted unanimously to accept the PC's recommendations. After minor adjustments and a review of the proposed program by the NSF and USGS, I as Center Director approved the final program in March 2012. This year proved more difficult than usual to manage as final funding from NSF did not come through until July.

The total number of proposals received and the total requested funding were both records by large margins. The process to construct a budget for 2012 was the most difficult in the history of SCEC. Funds awarded compared to total requested funds are only 51.5% where historically the ratio has been closer to 65%. Some tough choices had to be made in finalizing the budget.

Communication, Education, and Outreach

Through its CEO Program, SCEC offers a wide range of student research experiences, web-based education tools, classroom curricula, museum displays, public information brochures, online newsletters, workshops, and technical publications. Highlights of CEO activities for the past year are reported in the meeting volume by the Associate Director for CEO, Mark Benthien, who will present an oral summary on Monday morning.

SCEC has led the development of the Earthquake Country Alliance (ECA), an umbrella organization, now statewide, that includes earthquake scientists and engineers, preparedness experts, response and recovery officials, news media representatives, community leaders, and education specialists. The ECA has become our primary framework for developing partnerships, products, and services for the general public. SCEC maintains the ECA web portal (www.earthquakecountry.org), which provides multimedia information about living in earthquake country, answers to frequently asked questions, and descriptions of other resources and services provided by ECA members. Mark is the ECA Executive Director.

A major focus of the CEO program since 2008 has been organizing the *Great California ShakeOut* drills and coordinating closely with ShakeOuts in other states and countries. The purpose of the Shakeout is to motivate all Californians to practice how to protect ourselves during earthquakes ("Drop, Cover, and Hold On"), and to get prepared at work, school, and home. 8.6 million people participated in the 2011 California ShakeOut, up from 7.8 million in 2009. Recruitment is well underway for the 2012 ShakeOut, with over 7.5 million participants registered as of September 8th. The goal is to exceed 9 million. I would like to encourage California members of the SCEC community to register for the ShakeOut (at www.shakeout.org) and to encourage their institutions to join USC and others that are already registered.

ShakeOut has spread across the country and around the world with more than 12.5 million participants in 2011. In February 2012, nine states of the Central U.S. commemorated the 1811-1812 New Madrid earthquake bicentennial with their second ShakeOut drill, involving 2.4 million participants. SCEC collaborated with colleagues in Japan to coordinate their first ShakeOut on the one-year anniversary of the great Tohoku earthquake and tsunami, and now local ShakeOut drills are now spreading throughout Japan and are expected to be consolidated nationally. And in April Utah held its first ShakeOut with

more than 940,000 participants. The first nationwide Shakeout is being held in September 2012 in New Zealand, with more than 1 million people already registered, already achieving their goal.

The “big event” will happen on October 18, 2012, when the entire west coast will participate with individual drills: Alaska (new), Arizona (new), British Columbia, California, Idaho, Nevada, Oregon, and Washington (new), with schools participation in Baja California (new). The Southeast US from Georgia to Maryland is holding its first regional drill on the same day, along with other US drills in Guam and Puerto Rico (new), and the US Navy has organized a ShakeOut drill for bases and local residents in Southern Italy (new).

All told, more than 15 million people worldwide are expected to participate in 2012. By 2014 all US drills will shift to the October timeframe, with additional states participating. ShakeOut sites now exist in Spanish (Puerto Rico), Italian, and soon French (for Canada), such that our ability to engage additional countries, especially in Latin America, will likely expand ShakeOut participation further.

SCEC CEO staff continues to work with museums and other informal education venues to develop content and programs for earthquake education and to distribute SCEC resources, such as the extensive set of publications that has grown out of *Putting Down Roots in Earthquake Country*. In 2008, SCEC organized a group of museums and other locations interested in earthquake education into a network of *Earthquake Education and Public Information Centers* (Earthquake EPIcenters), which has since been expanded to over 60 venues distributed throughout California and growing into other regions. The EPIcenters are essential partners in the ShakeOut, as many hold public events on drill day, help promote participation, and build capacity. SCEC is collaborating with San Bernardino County Museum (SBCM) to develop regional educational resources such as the Palmett Creek paleoseismic trench. In addition to rehabilitating the trench, a visitor’s guide and website are under development. The USGS, SBCM, Stanford, NEES, and SCEC are bringing the Quake Catcher Network to informal learning venues throughout the state by installing research sensors and developing educational products.

SCEC is very active in the earth science education community, participating in organizations such as the National Association of Geoscience Teachers, the Coalition for Earth System Education, and statewide and national science educator organizations (e.g. CSTA). SCEC Education Program Manager Bob de Groot leads these efforts and runs the SCEC Teacher Workshops and K-12 partnerships. Since 2009, SCEC has been collaborating with EarthScope and California State University, San Bernardino to conduct a campaign GPS research program involving both high school teachers and their students. In 2012, six teachers and eight students participated in the program and their poster is on display at this meeting.

Bob de Groot is also skillfully leading SCEC’s Office for Experiential Learning and Career Development. His office manages two SCEC intern programs: Summer Undergraduate Research Experience (SURE, 247 interns since 1994), Undergraduate Studies in Earthquake Information Technology (UseIT, 220 interns since 2002). The ELCA office promotes diversity in the

scientific workforce and the professional development of early-career scientists (Figure 3). As someone very involved in these intern programs, I really enjoy seeing the students grapple with the tough but engaging problems of cutting-edge earthquake science. For example, the “grand challenge” for this year’s UseIT program was to *develop visualization capabilities based on SCEC-VDO and GIS that can display earthquake rupture forecasts, and publish visualization products that can be used to educate the general public about the Uniform California Earthquake Rupture Forecasts, including the new forecasting model, UCERF3*. Many of the summer interns will be presenting their work at this meeting, and I hope you’ll have the opportunity to check out their posters and demos.



Figure 3. This “Brady Bunch” picture shows the students from around the country who participated in the 2012 UseIT summer program at USC. Several will be attending the Annual Meeting to present posters, demos, and animations.

A Word of Thanks

SCEC has been successful because of the collaborative efforts of many people over many years. As SCEC Director, I want to express my deep appreciation to all of you for your attendance at the Annual Meeting and your sustained commitment to the collaboration. Greg Beroza and the PC have developed another outstanding program, so the entire meeting should be a very pleasant experience.

| Center Administration | Communication, Education, and Outreach | Information Technology |
|--|--|---|
|  <p>Associate Director John McRaney</p> |  <p>Associate Director Mark Benthien</p> |  <p>Associate Director Phil Maechling</p> |
|  <p>Special Projects and Events Tran Huynh</p> |  <p>Education Programs Bob de Groot</p> |  <p>Research Programmer Scott Callaghan</p> |
|  <p>Contracts and Grants Karen Young</p> |  <p>Digital Products John Marquis</p> |  <p>Research Programmer Masha Liukis</p> |
|  <p>Admin Coordinator Deborah Gormley</p> | |  <p>Research Programmer Kevin Milner</p> |
| | |  <p>Research Programmer Fabio Silva</p> |
| | |  <p>Systems Programmer John Yu</p> |

Figure 4. The SCEC staff, a special group of individuals with exceptional skills and tremendous dedication to the Center and its participants.

Special recognition is in order for SCEC staff, which comprises individuals of remarkable skills and dedication (Figure 4). We all benefit immensely from the financial wizardry and personal empathy of John “The Chaplain” McRaney, the organizational skills of Mark “Mr. ShakeOut” Benthien, and the innovative expertise of Phil “Big-Iron” Maechling.

And we all owe a very special *thank you!* to Tran Huynh and Deborah Gormley, the SCEC Meetings Team, and their diligent associates, Karen Young, John Marquis, Matt Goldberg, Kelsey Richards, and David Gill, for their exceptional efforts in organizing this meeting and arranging its many moving parts. Please do not hesitate to contact me, Greg, Tran, or other members of the SCEC team if you have questions or comments about our meeting activities and future plans. Now please enjoy the sessions, the meals, and the pool in the spectacular, though perhaps a bit toasty, setting of Palm Springs!

2011 Report of the Advisory Council

Jeff Freymueller, *SCEC Advisory Council Chair*

Introduction

The SCEC Advisory Council (AC) met several times at the SCEC Annual Meeting in Palm Springs, September 11--14, 2011. The AC met with SCEC leadership, including representatives of the SCEC Board of Directors, with representatives of the funding agencies, and in informal settings with individual SCEC scientists and students. Prior to meeting, the SCEC leadership sent us copies of the SCEC 4 proposal, reviews, and panel summaries, along with a confidential letter from SCEC Director Tom Jordan that summarized SCEC's response to last year's Advisory Council recommendations and highlighted some new and continuing issues to solicit the Council's opinion this year. The AC set its agenda for discussion based on a combination of issues raised in the SCEC4 proposal reviews, those raised by the Director, and unresolved issues from previous AC reports.

The discussion in the AC meetings mostly fell into the following categories:

- Governance of the Center
- Transition to the yet-to-be-identified SCEC5 Director
- Prioritization of SCEC activities given flat funding
- Defining the advisory structure for SCEC CEO
- Setting the goals and metrics to keep SCEC CEO on a productive path
- The SCEC interface with the engineering community
- Opportunities and challenges in risk communication

As in past years, the AC is deeply impressed by the SCEC organization and community. SCEC is viewed positively by the broader earthquake science community and by its funding agencies, and this impression has been well earned. The SCEC collaboration remains vibrant, with enthusiastic participation across many disciplines.

We congratulate the SCEC leadership and community on success of SCEC4 proposal. The proposal was developed through a process that involved the SCEC community in an effective way. The proposal reflects the priorities and goals of the community. It proposed an ambitious, comprehensive and compelling scientific vision for the next 5 years of SCEC activities, and this was reflected in the laudatory reviews. We consider that the science planning process for SCEC4 is making appropriate progress based on the proposal and further community input. As in past years, input from the broader SCEC community is being integrated into the process in an effective manner.

Membership

Nine members of the Advisory Council attended the SCEC Annual Meeting and participated in all discussions of the AC at that venue. This report is a collaborative product of these AC members. The members who attended are:

Jeffrey T. Freymueller, Chair (University of Alaska Fairbanks)
 Gail Atkinson (University of Western Ontario)
 Roger Bilham (University of Colorado)
 Jim Goltz (CalEMA)
 Bob Lillie (Oregon State University, emeritus)
 Anne Meltzer (Lehigh University)
 Dennis Miletti (University of Colorado, emeritus)
 Farzad Naeim (John A. Martin & Associates)
 John Vidale (University of Washington)

Four additional members of the Advisory Council were not able to attend the meeting, although their input was sought in evaluating the draft report:

Donna Eberhart-Phillips (UC Davis)
 John Filson (US Geological Survey, emeritus)
 M. Meghan Miller (UNAVACO)
 Andrew Whittaker (University of Buffalo)

Governance and Transition from SCEC4 to SCEC5

The current governance structure is working well. Although the SCEC Director has considerable influence on the decisions, there was no discernible sentiment that this is a problem. Instead, there is enthusiasm for his energy, accessibility, fairness, and good judgment in steering SCEC to its current successes. The Director seeks and heeds effective input from the SCEC community into critical decisions at many levels.

As the current Director intends to step down before the start of SCEC5, should it be funded, plans have been discussed for an orderly succession to the next Director. The current succession planning, which we endorse, has the strong and early engagement of the SCEC Board of Directors with USC in the search, and a realistic timeline and process for searching and bringing the new Director on board.

We note that the existing infrastructure and current staff are very strong, and efforts should be made to ensure continuity through the transition to preserve them. We believe that it would benefit both the incoming director and SCEC staff to have documentation available to describe the roles of key individuals. We recommend that SCEC develop such documents over the next few years.

Elements of the SCEC structure may evolve during the transition to the next Director, but it was considered important that the changes should arise as a result of discussion with candidates and the chosen successor, rather than before a successor is appointed. The current arrangements between SCEC and USC have great stability and strength that would be difficult to match.

Prioritization with Flat Funding

The Advisory Council endorses the overarching science priorities outlined in the SCEC4 proposal. Seeing no serious weaknesses and plenty of judicious planning within SCEC, we offer only general advice here.

- Top priority should be for continued support for key staff members and infrastructure to make the Center run smoothly.
- Next in priority is the CEO effort that received both applause for its successes, and concern for its perceived absence of specific targets and quantitative measures of its effectiveness. At the very least the CEO program needs to be sustained and its momentum maintained despite tight budgets. The current CEO program brings tremendous visibility to SCEC despite its lean operations.
- A third priority is improving interactions with the earthquake engineering community. It is possible that these collaborative ventures with the engineering community may lead to additional CEO opportunities, in addition to scientific advances.
- Despite the flat funding, we encourage SCEC to keep its web presence up to date – the web remains a key interface both within the SCEC community and with external audiences.
- We recognize that as much as possible, it is important for SCEC to use its core funds to support activities and research that both are important to SCEC and are less likely to be supported by other sources.

Advice on Initiatives in Earthquake Simulation and Ground Motion Prediction and Building Collaboration with the Earthquake Engineering Community

The Advisory Council commends SCEC for its continued progress in broadband and large-scale ground motion simulations, and for its recent efforts to draw the engineering community more directly into the SCEC community to assist in effective utilization of these resources. Significant progress has been made in confirmation of these simulations through comparison with recorded data and through assessments of the consistency and accuracy of results from various investigators.

The scientific foundations and methods used in this work are solid and the potential applications, as a supplement to recorded data, are significant. The utilization of ground motion simulations within engineering practice remains a challenge. Despite the wide range of scenarios for which simulations can be computed, far exceeding the number of events with recorded data, the engineering community has remained muted in their acceptance of simulated time histories. Without general acceptance by the engineering profession, the ground motion simulation projects of SCEC will not realize their full potential. The reservations of the engineering profession regarding simulated ground motions apparently have several causes, including:

- The difficulty in validating the simulations with existing recordings of strong motions.
- The difficulty in capturing the sensitivity of simulations to the range of unpredictable parameters, i.e., quantifying the uncertainty in a useful way.
- Lack of knowledge of the scientific underpinnings of the simulation methods, and lack of awareness of recent advances in simulation studies.

- Lack of general availability of “user--friendly” access and well-documented sets of simulations that are readily useable. The research engineering community needs these data for comparing use of such simulations against use of real recordings.
- “Cultural” barriers to effective communication between the engineering and scientific communities

Despite these difficulties, it is the view of the Advisory Council that bridging the gap between the engineering and science communities with regards to the use of simulated earthquake records is of critical importance to the long--term relevance and survival of SCEC. The Advisory Council recognizes that SCEC is taking meaningful and significant steps to engage the engineering community to address these issues. We laud the initiative that SCEC has taken in recruiting high profile and highly talented members of the earthquake engineering to the SCEC Advisory Council and Board, and in engaging engineers in the SCEC technical activity group on ground--motion simulation. While these steps are excellent, we believe that SCEC needs to go still further to build effective collaborations with engineering organizations such as EERI, PEER, NEES, and CUREE. SCEC needs a stronger presence at engineering meetings. We note that there appears to be a natural basis for collaboration with NEES, as both SCEC and NEES have an embedded simulation---based approach to problem solving.

The Advisory Council believes that while SCEC needs to concentrate on its core science and CEO objectives, building a strong and vibrant relationship with the practicing earthquake engineering professionals is vital for the long---term success of SCEC. Earthquake engineering professionals on a local and national level must be engaged to realize the full potential benefits of SCEC efforts to enhance their state of practice. Equally important is for SCEC to realize the issues of practitioners so that the practical significance of various SCEC activates can be assessed and refined. The Advisory Council is of the opinion that SCEC scientists and professional practitioners have a lot to learn from each other to enhance the quality and relevance of their efforts. Furthermore, the wholehearted recognition of and support for SCEC by practicing engineers may prove vital to the long-term success of SCEC.

The Advisory Council recommends the following actions to the SCEC leadership:

- This year’s session on ground--motion simulation was rich in engineering content and featured excellent presentations on the engineering--seismology interface, including talks by prominent engineers. It was highly successful as an engagement vehicle, in our view. We recommend having one such session (with topics rotating as appropriate) at every annual SCEC meeting.
- We recommend that SCEC consider holding a collaborative engineering--- seismology interface workshop, centered on the generation and use of simulated earthquake records, perhaps just before the next annual SCEC meeting. Such a workshop could be jointly organized with a collaborating organization such as EERI, NEES or PEER.
- Investigate methods of delivering and promoting simulations to the engineering community by making them more comprehensive and accessible. Engineers typically use web tools to search and/or scale a database of “time histories” to match given target scenarios and conditions. Appropriate simulation--based databases could be compiled (and accessed through a similar tool); this would make it apparent how these simulations extended the possible scenarios for study over the limited set available just from recorded time histories, and also enable comparisons.
- Actively seek to involve young engineering students in SCEC’s student intern programs to build more integration into the next generation of engineers.

Communication, Education, and Outreach (CEO) Advisory Structure

The 2010 Advisory Council Report offered the following recommendation:

- Expand CEO Oversight Structure so that an increased number and more diverse set of outreach and education experts can offer advice and oversight to the SCEC CEO Program, and confer more often than once yearly, which now is the case. We think this is best done through a dedicated subcommittee reporting to the Advisory Council.

The Advisory Council therefore recommends that SCEC populate the Advisory Council with a workable number of members (we recommend 2-4 total members) with expertise and interest in CEO activities. The AC further recommends that these members be constituted as a subcommittee of the Advisory Committee to serve as a CEO--focused Advisory Group. The CEO Advisory Group should:

- Meet separately, as it sees fit, from the Advisory Council as a whole to carry out its work.
- Invite people from the SCEC and outside communities to meet and work with them, as they see fit, to broaden expertise and experience in areas such as social psychology, marketing, advertising, science and risk communication, public science education, emergency management, etc.
- Provide advice to the SCEC CEO Program through reporting directly to the SCEC Advisory Council.

The Advisory Council also recommends that SCEC work to increase engagement between the SCEC science community and SCEC CEO, toward greater participation by the community in CEO. Also SCEC would benefit from a greater dialogue between CEO and the rest of the community to choose the SCEC science for inclusion in CEO activities.

Set Goals for CEO

The Advisory Council recommends that the CEO program develop a comprehensive list of SCEC4 targets—those that are “social process orientated” as well as those with more readily quantified targets. The targets should first be generated and then metrics should be developed to measure progress toward them. SCEC CEO staff should articulate clear goals, milestones, and metrics and should distinguish between short--term and long---term goals. We note that in the long term, this is critical for full support from funding agencies. The CEO Advisory Group (i.e. the AC subcommittee) described above can review goals, milestones, and metrics, and provide feedback. The Advisory Council also recommends that SCEC CEO staff receive input from the SCEC community.

Finally, the Advisory Council notes that the ShakeOut has been a tremendous success, but other aspects of CEO need to be nurtured to maintain overall CEO Program progress. At the present time, the Advisory Council thinks that the revised CEO overview structure and target development will go a long way in addressing this issue and help the small CEO staff negotiate future conflicting demands on time and resources.

Training in Risk Communication

The Advisory Council continues to recommend that risk/crisis communication training for SCEC members likely to talk about earthquake science or earthquake hazard in southern California on the radio, in front of a television camera, or via other public media. We note that expertise in this area is available in other centers at USC. We also note that this training could be offered in conjunction with the SCEC Annual Meeting, and that different levels and types of training are likely appropriate for different types and levels of SCEC participants. We believe that many SCEC scientists are enthusiastic about the opportunity to learn more about effective risk communication.

Intern Program

The Advisory Council was impressed with the number, quality, diversity and commitment of SCEC interns. The SCEC mentors have done an outstanding job in leveraging SCEC funds to achieve a successful program. While we agree that as many interns as possible should attend the SCEC annual meeting, the costs of accommodating all interns presents a strain on SCEC’s budget. The Advisory Council discussed several possible ways to include interns in the annual meeting while reducing the overall cost to SCEC.

- Make attendance at the annual meeting an option. Interns may feel an obligation to attend and if this perception were removed, there might be a self---selection process that would result in fewer interns attending.
- Consider seeking support from sources other than SCEC to support the attendance of any SCEC intern who wishes to attend the annual meeting. Possible sources of support are the intern’s home institution, if that is not a SCEC institution, and foundations, grant programs, etc.
- Institute an application system that involves attendance as a competitive or semi--competitive process. Successful applicants could claim SCEC annual meeting attendance as an achievement that could be documented on a resume or CV.

CSEP and Public Information

The Collaboratory for the Study of Earthquake Predictability (CSEP) has strong potential to become an essential component in an operational earthquake forecasting system in conjunction with existing systems for the examination of prediction methods, models and actual predictions/forecasts. Existing systems include the National Earthquake Prediction Evaluation Council (NEPEC) and the California Earthquake Prediction Evaluation Council (CEPEC). SCEC should work with the US Geological Survey, the California Geological Survey and state agency emergency management agencies in the development of protocols for communicating both the function and objectives of CSEP.

Of equal importance, the Advisory Council recommends that communication of outputs of CSEP be informed by established and accepted risk communication science and the insights of the social science disaster research community. The Advisory Council acknowledged that development of short---term operational earthquake forecasting presents new challenges in terms of public information. Again, it is important that SCEC scientists become familiar with the state of the art in the social sciences regarding communicating natural hazards information and warnings. Given the current situation in Italy, it is also essential that SCEC scientists become aware of the legal implications of issuing public forecasts, particularly those representing private institutions. Close coordination with emergency management agencies is also highly recommended.

Presenting SCEC to the Outside World

The Advisory Council affirmed the importance of the SCEC web site as the “public face” of SCEC and urges both SCEC scientists and staff to keep the site current and vital. We acknowledge that doing so is a challenge given the number of participating institutions in SCEC, the press of scientific work being pursued, and time constraints on staff. As the website is

refreshed for SCEC4, we recommend that consideration be given for easy updating of scientific content, and that SCEC scientists be engaged in submitting graphics and text for the website (possibly through a wiki or other collaborative internal site), so that the work of updating can be distributed. Some of the SCEC research highlights shown at the Annual Meeting would be ideal to show on the website, for example.

Individual SCEC scientists can serve as effective ambassadors for SCEC and its scientific activities. We encourage SCEC staff to provide graphic files and similar support to SCEC scientists so that they can easily incorporate SCEC logos, community models and other products in their general scientific presentations as appropriate.

Communication, Education, and Outreach Highlights

Mark Benthien, SCEC Associate Director for CEO

SCEC’s Communication, Education, and Outreach (CEO) program is organized to facilitate learning, teaching, and application of earthquake research. SCEC CEO is integrated within the overall SCEC enterprise, and engages in a number of partnership-based programs with overarching goals of improving knowledge of earthquake science and encouraging actions to prevent, mitigate, respond to, and recover from earthquake losses. CEO programs seek to improve the knowledge and competencies of the general public, “gatekeepers” of knowledge (such as teachers and museums), and technical partners such as engineers and policy makers.

SCEC CEO has been very successful in leveraging its base funding with support from the California Earthquake Authority (CEA), FEMA, Cal-EMA, USGS, additional NSF grants, corporate sponsorships, and other sources. For example, for its *Putting Down Roots in Earthquake Country* publication SCEC CEO has leveraged an additional \$4.4 million for advertising and printing since 2004. The 2007 *Dare to Prepare* campaign and ShakeOut drills in 2008 and 2009 benefited from more than \$5 million in monetary and in-kind contributions by other organizations. SCEC’s intern programs have been supported with more than \$1 million in additional support from several NSF programs and a private donor.

2009 Program Evaluation

At the recommendation of the SCEC External Advisory Council, an external evaluation team was hired in 2009 to conduct a mixed-methods program evaluation to assess selected programmatic areas and the broader impacts of the SCEC CEO program. The effort was led by Mehrmaz Davoudi, Davoudi Consulting Services, in consultation with Dr. Deborah Glik, UCLA School of Public Health, who combined have over 25 years of program evaluation. The evaluation used existing and newly collected primary data from key-informant interviews, online surveys, and observations. A detailed evaluation report was prepared and presented to an external review panel that met September 16-17, 2009.

The panel included participants that span the scope of the SCEC CEO programs: Farzad Naeim (EERI President, Engineering), Thalia Anagnos (San Jose State, Engineering), Diane Baxter (San Diego Supercomputer Center, Education Director), Carlyn Buckler (Museum of the Earth, Cornell University), Johanna Fenton (FEMA Region IX Earthquake Program Manager), Dennis Mileti (University of Colorado, Emeritus, Social Science), and Mary Lou Zoback (RMS, Inc., and Chair, SCEC Advisory Council).

The external review panel submitted a comprehensive report based on the evaluation team’s findings and conclusions, and additional program review and data requested by the panel. Recommendations for each CEO area are included along with an analysis of the SCEC CEO program with regards to the NSF Broader Impacts criterion (see Table 1.2). The overall results are very positive and indicate that the SCEC CEO program plays an important role in earthquake education and preparedness in California and beyond (see **Box 2.2**). The review panel recommendations have greatly influenced the CEO program plan for SCEC4 (see §III.D).

Box 2.2. Summary of Review Panel Findings

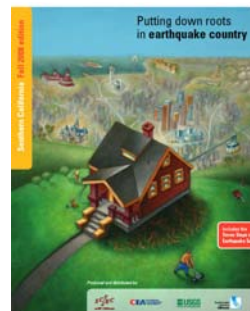
- Strong consensus that the SCEC CEO program has been an overwhelming success both in terms of breadth and impact
- CEO has succeeded in motivating the public to be better informed and prepared for the next big earthquake
- CEO has served as an honest broker and provided the leadership and trust to bring together a broad community of public, academic, and private groups
- At the same time they have created public outreach/museum programs, carried out effective K-12 teacher training, and have developed outstanding undergraduate internships which have become a magnet for attracting very bright and diverse students
- CEO should serve as a national model for other science centers
- CEO has effectively expanded and grown by leveraging dollars and strategic partnerships

Major Activities and Results

The primary SCEC3 CEO objective was to create reproducible “CEO frameworks” for using earthquake system science to inform and encourage preparedness and reduce earthquake risk. Research in the social sciences was applied during SCEC3, along with research and experience in K-12 education and undergraduate education and career advancement. The external review process documented several major accomplishments, which are summarized here.

Expansion of the Putting Down Roots in Earthquake Country portfolio

Putting Down Roots in Earthquake Country, a 32-page handbook, has provided earthquake science, mitigation, and preparedness information to the public since 1995. *Roots* was first updated in 2004, including the creation of the *Seven Steps to Earthquake Safety* to organize the



preparedness content. Since then the handbook has undergone five additional revisions and printings totaling 3.5 million copies. The first Spanish version of *Roots* was produced in 2006. The Fall, 2008 version added overviews of the ShakeOut Earthquake Scenario and the Uniform California Earthquake Rupture Forecast study [Field et al., 2009]. The 2011 version included new tsunami science and preparedness content.

The booklet has spawned the development of region specific versions for the San Francisco Bay Area, California's North Coast, Nevada, Utah, Idaho, and the Central U.S. (totaling an additional 4 million copies, see **Fig 2.24**). In Fall 2008, SCEC and its partners developed a new supplement to *Putting Down Roots* titled *The Seven Steps to an Earthquake Resilient Business*, a 16-page guide for businesses to develop comprehensive earthquake plans. It and other *Roots* handbooks can be downloaded and ordered from the main ECA website [<http://www.earthquakecountry.org>].

As part of the CEO evaluation, an online survey was conducted of people who recently ordered the southern California version of *Roots*, and compared to data collected when copies of the handbooks are requested. The survey indicates a clear increase in levels of household earthquake preparedness from the time they ordered the handbook to the time of the survey.

The *Putting Down Roots* framework (including the *Seven Steps to Earthquake Safety*) extends beyond the distribution of printed brochures and online versions. For example, the Birch Aquarium in San Diego and Fingerprints Youth Museum in Hemet both based earthquake exhibits on the booklet, and the Los Angeles County Emergency Survival Program based its 2006 and 2009 campaigns on the *Seven Steps*. Bogota, Colombia adapted the *Seven Steps* as the basis of the city's brilliant "Con Los Pies en la Tierra" (With Feet on the Ground) campaign [<http://www.conlospiesenlatierra.gov.co>]. This partnership resulted from SCEC CEO's involvement in the *Earthquakes and Megacities initiative*.



Figure 2.24. Related products of the *Putting Down Roots in Earthquake Country* series: (1) Original 1995 Southern California publication. (2) *Living with Earthquakes in Nevada* (1998). (3) *Echando Raíces en Tierra de Terremotos* (So Cal, 2006). (4) *Seis Jugadas Maestras* (Bogota, Colombia campaign, 2007). (5) *Putting Down Roots* (Utah, 2008). (6) *Putting Down Roots* (Bay Area, 2005). (7) *Protecting Your Family From Earthquakes* (Bay Area Multi-Language booklets, 2006). (8) *7 Steps to an Earthquake Resilient Business* (2008). (9) *Living on Shaky Ground* (North Coast CA, 2009). (10) Fifth update since 2004 of the Southern California version (2008). Versions for the Central U.S., Pacific Northwest, and elsewhere are in discussion.

Creation and development of the Earthquake Country Alliance and its activities

The ECA is a public-private partnership of people, organizations, and regional alliances, each of which are committed to improving preparedness, mitigation, and resiliency. People, organizations, and regional alliances of the ECA collaborate in many ways: sharing resources; committing funds; and volunteering significant time towards common activities. ECA's mission is to support and coordinate efforts that improve earthquake and tsunami resilience. The Earthquake Country Alliance is now the primary SCEC mechanism for maintaining partnerships and developing new products and services for the general public.

SCEC created the Earthquake Country Alliance (ECA) in 2003 and continues to play a pivotal role in developing and sustaining this statewide (as of 2009) coalition [<http://www.earthquakecountry.org>] with similar groups in the Bay Area and North Coast. Participants develop and disseminate common earthquake-related messages for the public, share or promote existing resources, and develop new activities and products. SCEC develops and maintains all ECA websites (www.earthquakecountry.org, www.shakeout.org, www.dropcoverholdon.org, and www.terremotos.org), has managed the printing of the "Putting Down Roots" publication series throughout the state, SCEC Associate Director for CEO Mark Benthien serves as Executive Director of the ECA.

Feedback from selected ECA members collected through key informant interviews, indicate that the foundation and development of the ECA very much rests upon SCEC leadership and its credibility and reputation as a trusted science and research consortium. SCEC is viewed as a 'neutral' and trusted leader, who employs a collaborative model to organizing stakeholders around a common cause and event. SCEC's "culture of collaboration" has provided for a bottom-up rather than a top down approach to building the ECA community.

Strategic planning in 2006 (just prior to SCEC3) identified the following six major projects for the ECA to implement. All have been completed or are continuing.

COMMUNICATION, EDUCATION, & OUTREACH HIGHLIGHTS

- **DARE to Prepare.** ECA's 2007 Earthquake Readiness Campaign encouraged everyone to "secure your space" (so objects won't fall and cause injury or damage). A new website [<http://www.daretoprepare.org>] was developed by SCEC, along with public events throughout the region and a comprehensive media campaign with commercials, on-air interviews, and more. In addition, a new Spanish-language website [<http://www.terremotos.org>] was created and is also hosted by SCEC.
- **Policy Summits.** Two major earthquake policy conferences were coordinated by ECA partners. The first was led by the Southern California Association of Governments in August 2007, and the second by the City of Los Angeles in 2008 (International Earthquake Conference during ShakeOut).
- **USGS Southern San Andreas Shakeout Scenario.** This major study led by Dr. Lucy Jones (USGS) involved over 300 scientists, engineers, and decision makers, was completed in May, 2008 [Jones et al., 2008]. It portrays the consequences of a magnitude 7.8 earthquake on the southernmost San Andreas Fault. A SCEC simulation of the scenario earthquake [Graves et al., 2008] was used as basis for scenario development.
- **Major regional earthquake response exercise.** The ShakeOut Scenario became the basis of the State of California's Golden Guardian Exercise in November 2008, coordinated with the ECA-led first-ever regional public drill at the same time, The Great Southern California ShakeOut. SCEC CEO has worked with many other states and several countries to extend the ShakeOut model, and as of April 2012 manages 11 ShakeOut websites (<http://www.shakeout.org>) (See next section).
- **Comprehensive survey of earthquake awareness and readiness.** SCEC initiated the process that led to this largest-ever survey of California household earthquake readiness, conducted by Dr. Linda Bourque (UCLA) with state funding. The results of this survey will help shape future ECA activities.
- **Development of the Earthquake Country Alliance.** Because of the success of the 2008 ShakeOut, the ECA is now a statewide coalition of four regional alliances. "ECA Associates" work together to educate and inform the public and recruit their participation in the ShakeOut.

In November 2010, the ECA held a Strategic Planning Workshop to discuss next steps for the organization's expanding programs and to increase engagement in the planning, management, and funding of initiatives. In this Workshop, the five researched solutions presented and discussed included the ECA becoming a 1) 501(c)(3) non-profit; 2) a 501(c)(4) non-profit; 3) a 501(c)(6) non-profit; 4) remaining as the same structure- a loosely organized confederation that cannot accept/administer grant funds directly; or, 5) becoming a program of SCEC under as part of SCEC's USC-based structure. Pros and cons were listed for all options looking at management, funding/budget, legal, governmental requirements, and other implications. The unanimous consensus of ECA leadership was to organize the ECA at USC to be administered by SCEC, under the direction of a statewide Steering Committee made up of regional ECA leaders, with these considerations:

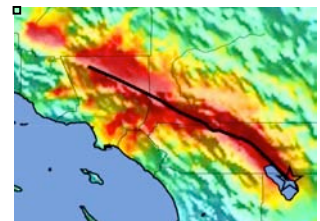
- Recognize the diverse and voluntary nature and size of ECA's component organizations and allow participation by the widest possible net of stakeholders, with an emphasis on regional groupings;
- Acknowledge that although most ECA Associates represent organizations, certain organizations need a role in the management structure;
- Minimize the size and role of the statewide effort in favor of supporting and connecting component organizations and regional alliances;
- Foster information sharing and provide effective and direct means of communication within and among ECA groups.

ECA Associates benefit from their participation by coordinating their programs with larger activities to multiply their impact; being recognized for their commitment to earthquake and tsunami risk reduction; having access to a variety of resources on earthquake and tsunami preparedness; networking with earthquake professionals, emergency managers, government officials, business and community leaders, public educators, and many others; and connecting with ECA sector-based committees to develop customized materials and activities. To participate, visit www.earthquakecountry.org/alliance/join.html.

The Earthquake Country Alliance (ECA) has coordinated outreach and recruitment for the California ShakeOut since 2008. Because of the creation and growth of the ShakeOut, and other activities and products, ECA has received national recognition. In 2011 ECA was recognized by FEMA with the "Awareness to Action" award, which resulted in SCEC's Associate Director for CEO Mark Benthien being named a "Champion of Change" by the White House. In April 2012 ECA also received the "Overall National Award in Excellence" at the quadrennial National Earthquake Conference held in Memphis.

Great ShakeOut Earthquake Drills. A major focus of the CEO program since 2008 has been organizing the *Great California ShakeOut* drills and coordinating closely with ShakeOuts in other states and countries. The purpose of the Shakeout is to motivate people to practice how to protect ourselves during earthquakes ("Drop, Cover, and Hold On"), and to get prepared at work, school, and home.

The ShakeOut began in southern California in 2008, to involve the general public in a large-scale emergency management exercise based on an earthquake on the San Andreas fault (the "ShakeOut Scenario"). ShakeOut communicates scientific and preparedness information



based on 30 years of research about why people choose to get prepared. SCEC developed advanced simulations of this earthquake used for loss estimation and to visualize shaking throughout the region. In addition, SCEC also hosted the ShakeOut website (www.ShakeOut.org) and created a registration system where participants could be counted in the overall total. In 2008 more than 5.4 million Californians participated.

Immediately following the 2008 ShakeOut (initially conceived as a “once-in-a-lifetime” event), participants began asking for the date of the 2009 ShakeOut. After significant discussion among ECA partners and state agencies, the decision was made to organize an annual, statewide Shakeout drill to occur on the third Thursday of October. This date is ideal for our school partners and follows National Preparedness Month in September, which provides significant exposure prior to the drill.

While K-12 and college students and staff comprise the largest number of participants, the ShakeOut has also been successful at recruiting participation of businesses, non-profit organizations, government offices, neighborhoods, and individuals. Each year participants are encouraged to incorporate additional elements of their emergency plans into their ShakeOut drill. Surveys conducted after each drill are being analyzed and results will be presented in 2012.

7.9 million people participated in the 2010 ShakeOut, up from 6.9 million in 2009. Many participants renew their participation each year, with nearly 5.5 million being staff and students from K-12 schools. The rest are people and organizations that typically do not have earthquake drills. In addition to registered participants, millions more see or hear about the ShakeOut via the news media. A list of over 300 print and online news stories is available on the ShakeOut web page, which in 2010 included a front-page photo in the New York Times. More than 500 TV and radio news stories across the state and country aired in the days surrounding the drill. A lengthy story on CBS Sunday Morning featured the ShakeOut in 2010.

The ShakeOut has been so successful that it has spread across the country, and even around the world. In October 2010 Nevada (110,000 participants) and Guam (38,000) joined with California, In January 2011, Oregon (38,000) and British Columbia (470,000) held drills to commemorate the anniversary of the 1700 Cascadia earthquake, and in April 2011 eleven states of the Central and Southern U.S. (Alabama, Arkansas, Georgia, Illinois, Indiana, Kentucky, Mississippi, Missouri, Oklahoma, South Carolina, and Tennessee) commemorated the 1811-1812 New Madrid earthquake bicentennial with a ShakeOut drill that grew to 3 million participations. Idaho held its first ShakeOut in October 2011 and Utah in April 2012. All of these areas are now holding ShakeOut drills annually (see www.shakeout.org/regions). SCEC provides consultation and manages the website for each drill. In 2011, 8.6 million Californian’s participated along with 4 million additional people participated in *Great ShakeOut* drills worldwide (see chart).

Growth of ShakeOut Drills

- 2008: 5.4 million**
Southern California
- 2009: 6.9 million**
California, New Zealand West Coast
- 2010: 7.9 million**
California, Nevada, Guam
- 2011: 12.5+ million**
CA, NV, GU, OR, ID, BC
130,000 in 5 Central Asia countries
Central US (AL, AR, GA, IN, IL, KY, MI, MO, OK, SC, TN)
- 2012: 15+ million (projected)**
All above plus:
UT, WA, NC, VA, Puerto Rico,
New Zealand (nationwide), Tokyo
- 2013 and beyond:**
AK, HI, American Samoa
Japan (nationwide)
Mexico, other Latin America
India, other Central Asian countries
US military bases/consulates



Other areas considering ShakeOut drills include Washington (2012), Alaska (2014), and also Hawaii, Puerto Rico, New Zealand (2012), and Turkey. SCEC is now collaborating with colleagues in Tokyo, to help them coordinate their first ShakeOut on the one-year anniversary of March 2011 devastating earthquake and tsunami. ShakeOut is changing the way people and organizations are approaching the problems of earthquake preparedness.

The ShakeOut’s impact has been more than just as a one-day event. Each registered participant receives periodic reminders leading up to the ShakeOut as well as drill instructions, preparedness information and access to a host of resources available on the ShakeOut website. Participants can download a soundtrack to play during their Drop, Cover, and Hold On Drill, ShakeOut posters and flyers, and web banners to place on their own websites encourage others to participate. ShakeOut flyers are available in

many versions including custom flyers for schools, individuals and families, businesses, state and local government, retirement communities, museums and libraries and many other participant categories. Information is also available in

COMMUNICATION, EDUCATION, & OUTREACH HIGHLIGHTS

Spanish, Korean, Vietnamese, and Chinese. The ECA has also created several drill manuals for schools, non-profits, businesses, and government agencies, respectively. Each version of the manual has information specific to the type of institution and has multiple drill levels, from a simple drill, to an advanced emergency simulation drill. These manuals include topics for discussion among the organizations leaders, evacuation procedures, and suggestions for making the simulation more engaging for employees or students. Access to these important earthquake resources is one of the most important benefits of being involved in the ShakeOut.

The ShakeOut has been the focus of significant media attention and has gone a long way to encourage dialogue about earthquake preparedness in California. Through the ShakeOut, the ECA does more than simply inform Californians about their earthquake risk. The ShakeOut teaches people a life-saving response behavior while fostering a sense of community that facilitates further dialogue and preparedness, and as such is an effective structure for advocacy of earthquake preparedness and mitigation.

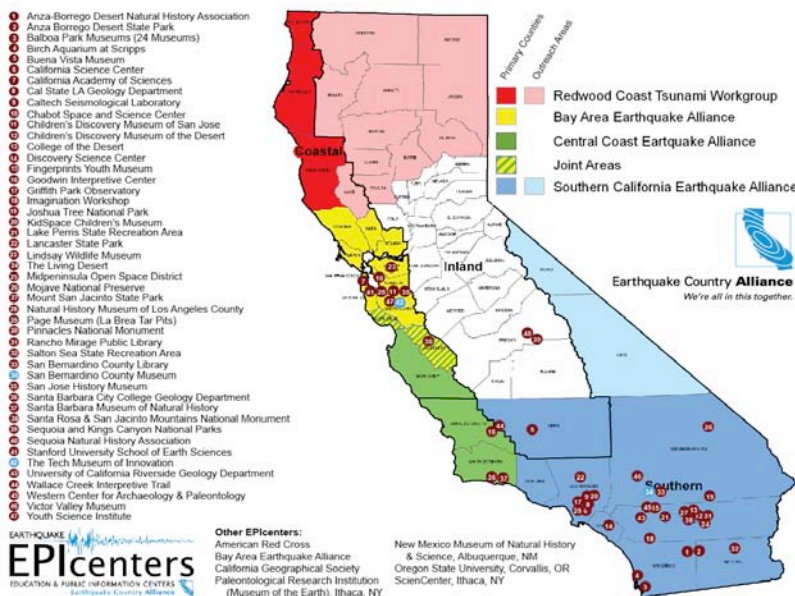
Development of the *EPIcenter* informal education network

SCEC CEO has developed exhibits and partnered with information education venues for many years, including an interpretive trail on the San Andreas fault at Wallace Creek, a permanent earthquake exhibit at a youth museum in Hemet, CA, and a temporary earthquake exhibit at the UCSD Birch Aquarium. The expansion of these partnerships, especially with the San Bernardino County Museum (SBCM) in 2007, led SCEC to create the Earthquake Education and Public Information Centers (EPIcenters) network in 2008. EPIcenters include museums, science centers, libraries, universities, parks, and other places visited by a variety of audiences including families, seniors, and school groups. Thus far, SCEC CEO has established relationships with over sixty institutional partners (Figure 1.3), who have implemented a variety of activities including displays and talks as part of earthquake exhibitions related to the ShakeOut, and other activities year round. The statewide Network is coordinated by SCEC Education Program Manager Robert de Groot with Kathleen Springer (San Bernardino County Museum) and Candace Brooks (The Tech Museum) coordinating Network activities in Southern and Northern California respectively.

These partners share a commitment to encouraging earthquake preparedness. They help coordinate Earthquake Country Alliance activities in their county or region (including the ShakeOut), lead presentations or organize events in their communities, develop earthquake displays, or in other ways provide leadership in earthquake education and risk reduction.

Through key informant interviews, EPIcenter members have indicated that the EPIcenter model produces institutional and professional benefits which support collaboration among partners, such as a) access to innovative, cutting-edge earthquake science findings, educational materials, visualizations and other means of presenting information, b) technical assistance with exhibit and/or gallery design, c) earthquake science education training for educators and interpreters, d) resource-sharing for enhanced patron experiences and efficient use of funds, e) increased capacity for partnership development, f) enhanced ability to apply disaster preparedness training, g) increased credibility as perceived by institutional leadership and patrons, and h) opportunities to showcase achievements at professional meetings and EPIcenter meetings.

In 2009, the EPIcenter network collaborated with EarthScope in hosting an interpretive workshop at SBCM. This activity broadened participation and brought a new and diverse community to the network. SCEC is now serving as a regional coordinator for EarthScope's program as well as building membership among EPIcenters. The statewide EPIcenter network is part of the Earthquake Country Alliance.



materials (durable signage, brochure content, and a website at www.scec.org/wallacecreek with additional information and directions to the trail). BLM has agreed to maintain the site and print the brochure into the foreseeable future.

The *ShakeZone Earthquake Exhibit* at Fingerprints Youth Museum in Hemet, CA was developed originally in 2001, was redesigned in 2006, and was retired from display in 2011. The redesigned version of the exhibit is based on SCEC's *Putting Down Roots in Earthquake Country* handbook. Major partners involved in the exhibit redesign included Scripps Institution of Oceanography and Birch Aquarium at Scripps. With funding from the United Way and other donors ShakeZone will be expanded in 2010 to include a section on Earthquake Engineering.

In 2006 SCEC has embarked on a long-term collaboration with the San Bernardino County Museum (SBCM) in Redlands, California. SCEC participated in the development and implementation of *Living on the Edge Exhibit*. This exhibit explains and highlights natural hazards in San Bernardino County (e.g. fire, floods, and earthquakes). SCEC provided resources in the development phase of the project and continues to supply the exhibit with copies of *Putting Down Roots in Earthquake Country*.

As a result of the successful collaboration on *Living on the Edge*, SCEC was asked to participate in the development of SBCM's *Hall of Geological Wonders*. To be completed in 2012, the Hall is a major expansion of this important cultural attraction in the Inland Empire. One of the main objectives of the Hall is to teach about the region from a geologic perspective. The museum is devoting a large space to the story of Southern California's landscape, its evolution and dynamic nature. SCEC has played an ongoing advisory role, provided resources for the development of the earthquake sections of the exhibit, and will have an ongoing role in the implementation of educational programming

The most recent debut of an EPIcenter earthquake display is the *Earthquake Information Center* at the Rancho Mirage Public Library in Rancho Mirage, CA. This exhibit, created in partnership with the City of Rancho Mirage, features a computer screen showing recent worldwide and local earthquakes. Located in the computer resource room this exhibit also displays the seven steps to earthquake safety and components of a basic earthquake disaster supply kit. Many hundreds of local residents from the desert communities pass by the exhibit every day on their way to accessing other resources in the library. Recently, the Development of other EPIcenter exhibits and resource areas are occurring at the The California Science Center, Los Angeles, and the Natural History Museum of Los Angeles County.

Expansion and improvement of SCEC's internship programs

SCEC offers a set of internship opportunities that are connected into an intellectual pipeline that encourages students to choose STEM (Science, Technology, Engineering, and Math) careers and is improving the diversity of the scientific workforce. Since 1994, SCEC has provided 457 internships to undergraduate and graduate students (some students participate in multiple years and are counted each time). SCEC currently offers two summer internship programs (SCEC/SURE and SCEC/UseIT) and in 2010 completed a year-round program for both undergraduate and graduate students (ACCESS). These programs are the principal framework for undergraduate student participation in SCEC, and have common goals of increasing diversity and retention. In addition to their research projects, participants come together several times during their internship for orientations, field trips, and to present posters at the SCEC Annual meeting. Students apply for both programs at www.scec.org/internships.

- The **Summer Undergraduate Research Experience (SURE)** internship places undergraduate students in research projects with SCEC scientists. Internships are supported from base SCEC funding and funding from internship mentors. 221 internships have been supported since 1994 (150 since 2002).
- SCEC/SURE has supported students working on numerous projects in earthquake science, including the history of earthquakes on faults, risk mitigation, seismic velocity modeling, science education, and earthquake engineering.
- The **Undergraduate Studies in Earthquake Information Technology (UseIT)** internship brings together undergraduates from many majors and from across the country in an NSF Research Experience for Undergraduates Site at USC. The eight-week program develops and enhances computer science skills while teaching the critical importance of collaboration for successful learning, scientific research and product development. UseIT interns tackle a scientific "Grand Challenge" that varies each year but always entails developing software and resources for use by earthquake scientists or outreach professionals, including SCEC-VDO (visualization software developed and refined each summer by UseIT interns). 167 students have participated since 2002.
- Our UseIT and CME experience identified a "weak link" in cyberinfrastructure (CI)-related career pathways: the transition from discipline-oriented undergraduate degree programs to problem-oriented graduate studies in earthquake system science. We worked to address this educational linkage problem through a CI-TEAM implementation project entitled the *Advancement of Cyberinfrastructure Careers through Earthquake System Science (ACCESS)* which ended in late 2010 with 29 internships having been awarded. The objective of the ACCESS project was to provide a diverse group of students with research experiences in earthquake system science that will advance their careers and encourage their creative participation in cyberinfrastructure development. Its overarching goal was to prepare a diverse, CI-savvy workforce for solving the fundamental problems of system science. Undergraduate (ACCESS-U) internships support CI-related research in the SCEC Collaboratory by undergraduate students working toward senior theses or other research enhancements of the

COMMUNICATION, EDUCATION, & OUTREACH HIGHLIGHTS

bachelor's degree. Graduate (ACCESS-G) internships supported up to one year of CI-related research in the SCEC Collaboratory by graduate students working toward a master's thesis.

Since 2002, over 1100 eligible applications for SCEC internship programs were submitted, with 384 awarded among the three programs. Leveraging of additional funding has allowed SCEC to double the number of internships offered each year (from 23 in 2002 to 54 in 2011). On average 30% of interns were underrepresented minority students, with some years near 50%. A 22% gender gap in 2002 has effectively been erased with near-parity since 2005. First generation college attendees have also increased from 24% in 2004 to more than 30% by the end of SCEC3.

Much of the success in increasing diversity has come from increased efforts to recruit students from other states and also from community colleges, making the internship programs an educational resource that is available to a broader range of students.

Past interns report that their internship made lasting impacts on their course of study and career plans, often influencing students to pursue or continue to pursue earthquake science degrees and careers. By observing and participating in the daily activities of earth science research, interns reported having an increased knowledge about what it's like to work in research and education. When interns developed good relationships with their mentors, they reported an increased ability to work independently, which coupled with networking at the SCEC annual meeting, gave them the inspiration and confidence to pursue earth science and career options within the field. Interns also report that their experience with the SCEC network (fellow interns, students and mentors) has been rewarding in terms of community building and networking, and a key component in creating and retaining student interest in earthquake science and related fields.

Development of K-12 educational activities and products

For the past eight years, SCEC has engaged in a number of activities – including educational workshops, materials development and distribution, field trips, school visits, and technical assistance – to provide K-12 educators with useful tools for teaching earthquake-related science, as well as to provide educators a direct connection to developers of these resources. SCEC uses a collaborative approach for two aspects of K-12 professional development: delivering workshops and developing materials. By building connections and coordinating with peer organizations, SCEC helps to ensure that educators are receiving the best resources available. SCEC has partnered with institutions such as USGS, IRIS, EarthScope, and USC to deliver workshops and develop curricula and materials.

Partnerships with Science Education Advocacy Groups and Organizations with Similar Missions. SCEC is an active participant in the broader earth science education community including participation in organizations such as the National Association of Geoscience Teachers, the Coalition for Earth System Education, and local and national science educator organizations (e.g. NSTA). Improvement in the teaching and learning about earthquakes hinges on improvement in earth science education in general. Hence, SCEC contributes to the community through participation on outreach committees wherever possible, co-hosting meetings or workshops, and building long-term partnerships. An example of a current project is a partnership with EarthScope to host a San Andreas Fault workshop for park and museum interpreters that was held in Spring 2009. In 2010 SCEC is collaborating with IRIS and EarthScope in developing the content for the San Andreas fault Active Earth Kiosk. The Active Earth Kiosk is an interactive website where visitors learn about earth hazards in a particular region. EarthScope is creating an Active Earth Kiosk for each of the regions covered by its Interpretive Workshops. Also in 2010 Arizona State University, the OpenTopography Facility, and SCEC developed three earth science education products to inform students and other audiences about LiDAR and its application to active tectonics research. First, a 10-minute introductory video titled *LiDAR: Illuminating Earthquakes* was produced and is freely available online. The second product is an update and enhancement of the Wallace Creek Interpretive Trail website. LiDAR topography data products have been added along with the development of a virtual tour of the offset channels at Wallace Creek using the B4 LiDAR data within the Google Earth environment. Finally, the virtual tour to Wallace Creek is designed as a lab activity for introductory undergraduate geology courses to increase understanding of earthquake hazards through exploration of the dramatic offset created by the San Andreas Fault (SAF) at Wallace Creek and Global Positioning System-derived displacements spanning the SAF at Wallace Creek. This activity is currently being tested in courses at Arizona State University. The goal of the assessment is to measure student understanding of plate tectonics and earthquakes after completing the activity. Including high-resolution topography LiDAR data into the earth science education curriculum promotes understanding of plate tectonics, faults, and other topics related to earthquake hazards.

Teacher Professional Development. SCEC offers teachers 2-3 professional development workshops each year with one always held at the SCEC Annual Meeting. The workshops provide connections between developers of earthquake education resources and those who use these resources in the classroom. The workshops include content and pedagogical instruction, ties to national and state science education standards, and materials teachers can take back to their classrooms. Workshops are offered concurrent with SCEC meetings, at National Science Teachers Association annual meetings, and at the University of Southern California. In 2003 SCEC began a partnership with the Scripps Institution of Oceanography Visualization Center to develop teacher workshops. Facilities at the Visualization Center include a wall-sized curved panorama screen (over 10m wide). The most recent teacher workshop held in partnership with Mt. San Antonio College was held in April 2010 at the GSA Cordilleran Section meeting.

COMMUNICATION, EDUCATION, & OUTREACH HIGHLIGHTS

Since 2009, SCEC has been collaborating with the Cal State San Bernardino/EarthScope RET program led by Sally McGill. During the course of the summer 7-10 high school teachers and their students conduct campaign GPS research along the San Andreas and San Jacinto faults. SCEC facilitates the education portion of the project through the implementation of the professional development model called Lesson Study. This allows for interaction with the teachers for an entire year following their research. For the second year all of the members of the RET cohort participate in the SCEC Annual Meeting by doing presentation of their research, participating in meeting activities such as talks and works culminating in presenting their research at one of the evening poster sessions.

Sally Ride Science Festivals. Attended by over 1000 middle school age girls (grades 5–8) at each venue, Sally Ride Science Festivals offer a festive day of activities, lectures, and social activities emphasizing careers in science and engineering. Since 2003, SCEC has presented workshops for adults and students and participated in the Festival’s “street fair,” a popular venue for hands-on materials and science activities. At the street fair SCEC demonstrates key concepts of earthquake science and provides copies of *Putting Down Roots in Earthquake Country*. The workshops, presented by female members of the SCEC community share the excitement and the many career opportunities in the Earth sciences.

National Science Teachers Association and California Science Teachers Association. Earthquake concepts are found in national and state standards documents. For example, earthquake related content comprises the bulk of the six grade earth science curriculum in California. SCEC participates in national and statewide science educator conferences to promote innovative earthquake education and communicate earthquake science and preparedness to teachers in all states. .

Plate Tectonics Kit. This new teaching tool was created to make plate tectonics activities more accessible for science educators and their students. SCEC developed a user-friendly version of the *This Dynamic Earth* map, which is used by many educators in a jigsaw-puzzle activity to learn about plate tectonics, hot spots, and other topics. At SCEC’s teacher workshops, educators often suggested that lines showing the location of plate boundary on the back of the maps would make it easier for them to correctly cut the map, so SCEC designed a new (two-sided) map and developed an educator kit.

ShakeOut Curricula. With the advent of the Great Southern California ShakeOut in 2008, SCEC CEO developed a suite of classroom materials focused primarily on preparedness to be used in conjunction with the drill. An important result of the ShakeOut is that it has enhanced and expanded SCEC’s reach into schools at all levels from county administrators to individual classroom educators.

SCEC3 Research Accomplishments

Greg Beroza, *SCEC Deputy Director*

The SCEC3 program was guided by the 19 research objectives (**Box 1**). They are organized under four priority objectives: (1) improve the unified structural representation and employ it to develop system level models for earthquake forecasting and ground motion prediction; (2) develop an extended earthquake rupture forecast; (13) predict broadband ground motions for a comprehensive set of large scenario earthquakes; and (19) prepare post-earthquake response strategies. We use this framework to describe SCEC3 accomplishments. Objectives (3)-(12) are subsidiary to (2), the main Earthquake Rupture Forecast (ERF) objective, and (14)-(18) are subsidiary to (13), the main Ground Motion Prediction (GMP) objective.

Box 1. SCEC3 Priority Research Objectives

- 1. **Improve the unified structural representation and employ it to develop system-level models for earthquake forecasting and ground motion prediction.**
 2. **Develop an extended earthquake rupture forecast to drive physics-based SHA.**
 3. Define slip rates and earthquake history of southern San Andreas fault system for last 2000 years.
 4. Investigate implications of geodetic/geologic rate discrepancies.
 5. Develop a system-level deformation and stress-evolution model.
 6. Map seismicity and source parameters in relation to known faults.
 7. Develop a geodetic network processing system that will detect anomalous strain transients.
 8. Test of scientific prediction hypotheses against reference models to understand the physical basis of earthquake predictability.
 9. Determine the origin and evolution of on- and off-fault damage as a function of depth.
 10. Test hypotheses for dynamic fault weakening.
 11. Assess predictability of rupture extent and direction on major faults.
 12. Describe heterogeneities in the stress, strain, geometry, and material properties of fault zones and understand their origin and interactions by modeling ruptures and rupture sequences.
 13. **Predict broadband ground motions for a comprehensive set of large scenario earthquakes.**
 14. Develop kinematic rupture representations consistent with dynamic rupture models.
 15. Investigate bounds on the upper limit of ground motion.
 16. Develop high-frequency simulation methods and investigate the upper frequency limit of deterministic ground motion predictions.
 17. Validate earthquake simulations and verify simulation methodologies.
 18. Collaborate with earthquake engineers to develop rupture-to-rafters simulation capability for physics-based risk analysis.
 19. **Prepare post-earthquake response strategies.**

Develop the Unified Structural Representation

The Unified Structural Representation (USR) refers to a combined set of structural models, which include the Community Velocity Models (CVMs) and the Community Fault Models (CFMs). The USR Focus Group supports the development, improvement, and extension of these models using 3D tomography, seismic exploration data and other geophysical surveys, geologic field mapping, precise earthquake relocations, and fault-system modeling. Signal accomplishments in research related to the USR in SCEC3 include development of waveform tomography and incorporation of results from it into CVM-H; incorporation of mantle tomography and Moho depths from receiver functions into CVM-H; addition of a shallow geotechnical layer to CVM-H; development of a new formal benchmarking and release protocol for CVM; the extension of the Community Fault Model to encompass the entire state of California, and improvements to the CFM through precise earthquake location, targeted paleoseismological studies, and shallow structural imaging.

Tomography to Improve CVM-H. SCEC has developed two crust and upper mantle velocity models: CVM-S [Kohler *et al.*, 2003] and CVM-H [Süss and Shaw, 2003]. These consist of basin descriptions, including structural representations of basin shapes and sediment velocity parameterizations, embedded in regional tomographic models. Development during SCEC3 focused on improvements to CVM-H, which include new v_p , v_s , and density parameterizations within the Santa Maria and Ventura basins, and the Salton Trough. They also include improved tomographic models [Hauksson, 2000] that extend to 35 km depth and a new upper mantle tomographic model that extends to 300 km depth.

SCEC took the lead in developing full-3D waveform tomography, in which the starting model is 3D and the full physics of 3D anelastic wave propagation is used to extract waveform information. Chen *et al.* [2007] used the scattering integral approach to develop the first full-3D waveform inversion-based model of the Los Angeles Basin using finite-difference simulations, and Tape *et al.* [2009] developed a tomographic model for all of Southern California using adjoint methods and spectral-element simulations. The new model used 6800 wavefield simulations and nearly 1 million CPU hours, and shows strong velocity

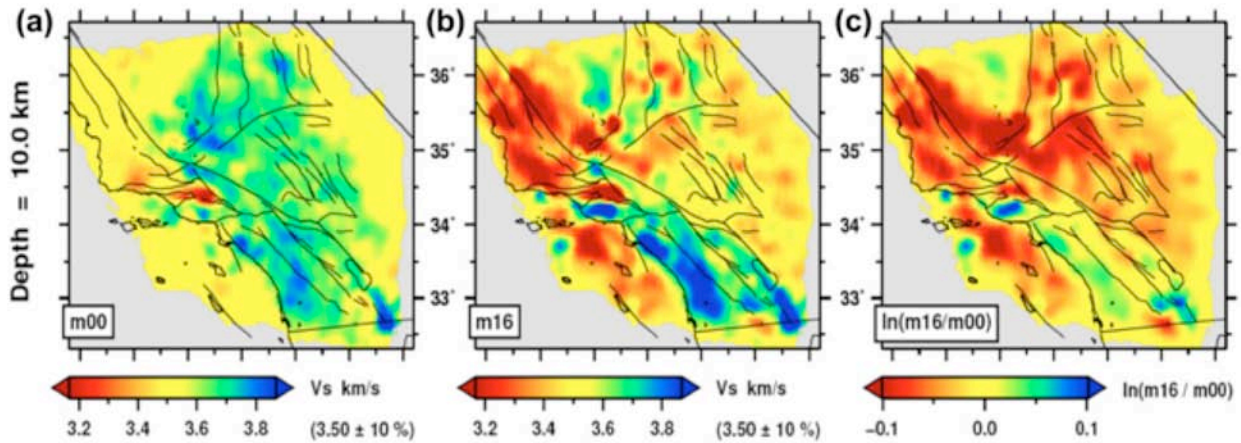


Figure 1. Horizontal sections of Vs adjoint tomographic model: (a) starting model CVM-H, (b) adjoint model after 16 iterations, (c) model differences. [Tape et al., 2009].

heterogeneity related to major tectonic features (**Fig. 1**). Changes in wave speeds are up to 30% of the background, and highlight basin structures not represented in the original model, such as the San Joaquin Basin. The scattering-integral method has also been extended to image the crustal structure of Southern California using waveform data from both local earthquakes and ambient-noise Green's functions. The first iteration used more than 3500 phase-delay measurements from local earthquakes and about 800 finite-difference wave-propagation simulations [Chen et al., 2009]. The model perturbation reveals a strong contrast in S-wave speed across the San Andreas Fault in the upper- to mid-crust and the updated model provides significantly better fit to observed waveforms. CVM-H 6.2 is the first release that fully integrates 3D waveform tomography into the community velocity model.

Additional Improvements to CVM-H. Additional improvements include a revised Moho (**Fig. 2**) [Yan and Clayton, 2007; Chulick et al., 2002]. An important improvement for strong ground motion prediction is the implementation of a new bedrock geotechnical layer [Plesch et al., 2007] based on the depth-velocity relations [Boore and Joyner, 1997]. Because of their affect on strong ground motion, sedimentary basins are a particularly important component of the Community Velocity Model. As data on the structure of sedimentary basins improves, it is systematically incorporated into updated releases of the CVM (**Fig. 3**). The cumulative effect of these changes is a dramatically improved CVM-H (**Fig. 4**).

Further improvements in the CVM should come rapidly now that waveform tomography is operational and a pathway into the velocity models is established. Ambient-seismic-field Green's functions [Prieto and Beroza, 2008; Ma et al., 2008] will provide new constraints on the elastic [Chen et al., 2009] and anelastic [Prieto et al., 2009] structure. A strength of the ambient-noise approach to CVM development is that it provides constraints in areas are important for seismic hazard analysis that currently lack recordings of earthquakes with which to validate models (most notably for paths from the San Andreas Fault). SCEC is

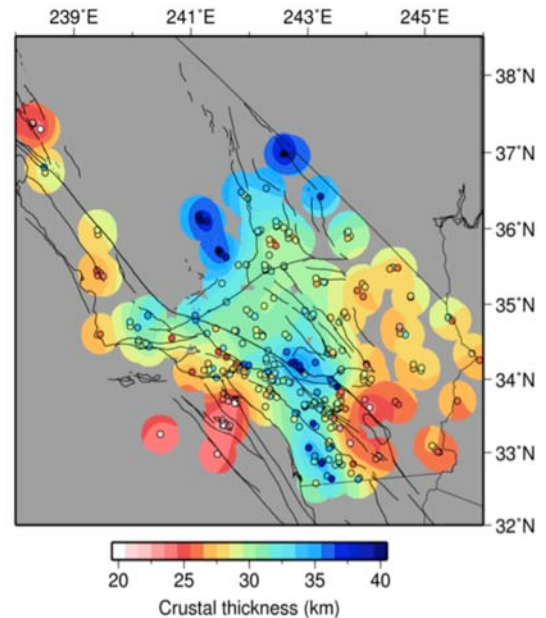


Figure 2. CVM-H was updated to include Moho depth from receiver functions. [Yan and Clayton, 2007].

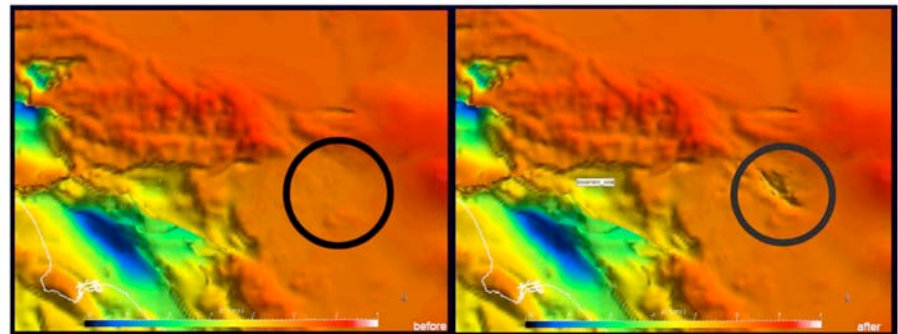


Figure 3. CVM-H basement surface before (left) and after (right) definition of the San Bernardino Basin (circled).

SCEC3 RESEARCH ACCOMPLISHMENTS

also developing eTree, and other representations, as well as parallel HPC codes to facilitate use of community models in large computational meshes and grids.

Assessing the Accuracy of Ground Motion Predictions. The primary use of the CVM is to predict ground motion for physics-based seismic hazard analysis. To assess these ground motion predictions SCEC scientists developed a flexible goodness-of-fit metric that compares simulated and observed ground motions [Olsen and Mayhew, 2010] according to criteria that can be tailored to specific applications. The method includes a set of user-weighted metrics such as peak ground motions, response spectrum, the Fourier spectrum, cross correlation coefficient, energy flux, and inelastic elastic displacement ratios. It has been used to validate CVM-H and CVM-S simulations of the 2008 M5.4 Chino Hills earthquake.

A Statewide Community Fault Model. The community fault model improved rapidly during SCEC3, and extends statewide as the result of a joint effort with the USGS and CGS. The statewide model (SCFM) consists of the CFM in southern California [Plesch et al., 2007] and new representations of faults in northern California (Fig. 5). This was a key requirement for developing a statewide rupture forecast model in UCERF2, and for use in simulating seismicity catalogs. The CFM in southern California continues to be improved using re-located earthquake catalogs [Hauksson and Shearer, 2005; Shearer et al., 2005; Lin et al., 2007; Waldhauser et al., 2008], which provide significantly improved resolution of many faults, particularly in areas of complex fault junctions [Nicholson et al., 2008]. The Uniform California Earthquake Rupture Forecast (UCERF3) project is critically dependent on the statewide CFM.

Develop an Extended Earthquake Rupture Forecast

Many elements of the SCEC3 research program contribute to the development of an “extended” earthquake rupture forecast; i.e., one with the requisite elements for physics-based simulations. Development of extended rupture forecasts draws on the full range of geoscience disciplines within SCEC and requires information from the entire range of temporal and spatial scales involved in the earthquake process. Signal accomplishments in developing an extended earthquake rupture forecast include: new understanding of the south-central San Andreas Fault that increases its seismic hazard; discovery and development of paleoseismic sites on the San Andreas system; improved understanding of earthquake potential from compressional structures at and near the Southern California Coast, progress in resolving geologic vs. geodetic slip-rate

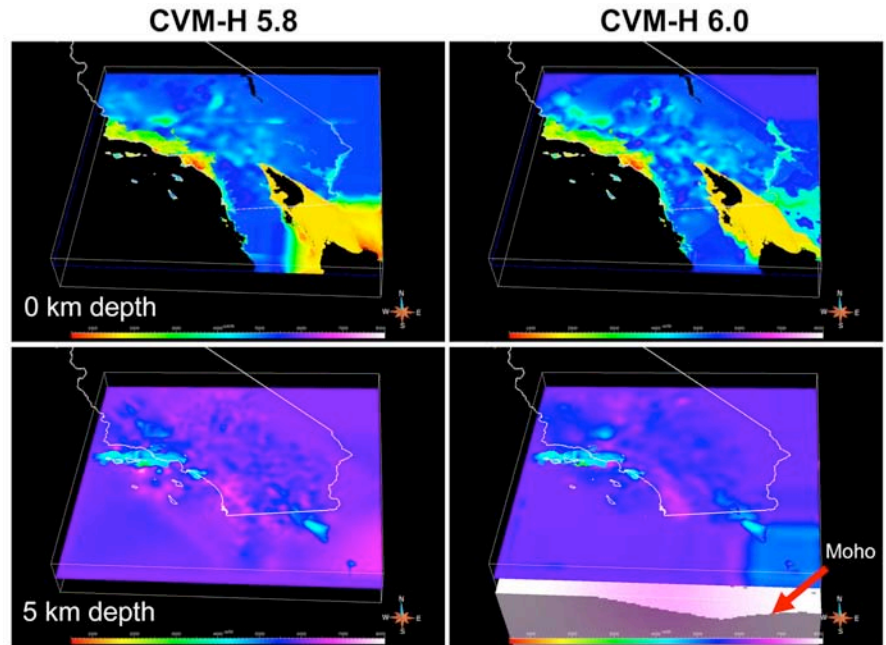


Figure 4. SCEC Community Velocity Model, CVM-H 6.0, and later revisions include basin structures embedded in the 3D waveform inversion model, and an explicit representation of the Moho.

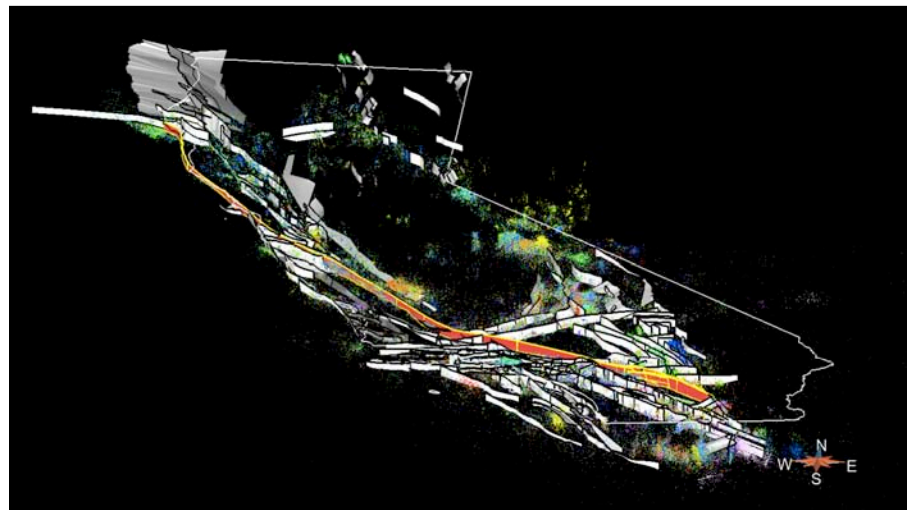


Figure 5. Perspective view of statewide Community Fault Model with precisely relocated seismicity. San Andreas Fault is highlighted in red.

discrepancies; progress in modeling fault systems to include realistic geometry and loading; precision seismicity and source parameter catalogs; development of detection algorithms for aseismic transients; new infrastructure for earthquake predictability experiments; new understanding of the importance of off-fault deformation; and tests of dynamic fault-weakening mechanisms.

More Frequent Large Earthquakes on the South-Central San Andreas Fault. A key to understanding the likely future behavior of the Southern California Fault System, is to refine our understanding of its past. A centerpiece of this effort is the Southern San Andreas Fault Evaluation (SoSAFE) special project, which received support from the USGS Multi-Hazards Demonstration Project. This research venture, coordinated through SCEC, has led to fundamental advances in understanding of the size, frequency, and predictability of major earthquakes on the principal plate boundary structures in southern California. Progress in this area during SCEC3 led to a dramatically different view of the earthquake potential of the San Andreas Fault.

Research on slip-rate and slip-per-event blossomed with the release of the B4 LiDAR data set that imaged the entire southern San Andreas Fault. We are just beginning to realize the potential of lidar observations, but an early highlight of this work is the result from Zielke *et al.* [2010] and Grant Ludwig *et al.* [2010] demonstrating numerous, subtle 5m offsets along the Carrizo Plain section of the San

Andreas Fault (Fig. 6). The youngest offsets cut by half the ~8 m slip attributed to the 1857 Fort Tejon earthquake by Sieh [1978]. This agrees well with new paleoseismic results from the Bidart fan paleoseismic site, which imply that major events on the south-central San Andreas Fault are about twice as frequent as previously believed. In other words, the entire southern San Andreas Fault is “locked and loaded” and could rupture in one, or a series, of large earthquakes at any time.

Earthquake Recurrence and Slip-Rate Variations. Several critical paleoseismic data gaps have been filled and important new developments unfolded from synthesis of paleoseismology, slip-rate, and slip-per-event data. New investigations at the Frazier Mountain site are filling a critical data gap in the northern Big Bend of the San Andreas, which should allow correlation of records from the Carrizo Plain to the Mojave Section [Biasi and Weldon, 2009]. Findings to date support the idea that most of the prehistoric earthquakes that ruptured the Carrizo Plain reached Frazier Mountain and about half can be connected to Pallett Creek (Fig. 7). Work at the Frazier Mountain site continues, now externally supported by the NSF Tectonics program. Another focus of the SoSAFE project has been the Coachella Valley – the only portion of the San Andreas that has not ruptured historically [Philibosian *et al.*, 2007]. The northern San Jacinto Fault was also identified as a target of interest because of the potential trade-off of activity with the nearby San Andreas [Bennett *et al.*, 2004; McGill *et al.*, 2008]. The emerging view is that slip is approximately equally partitioned between the

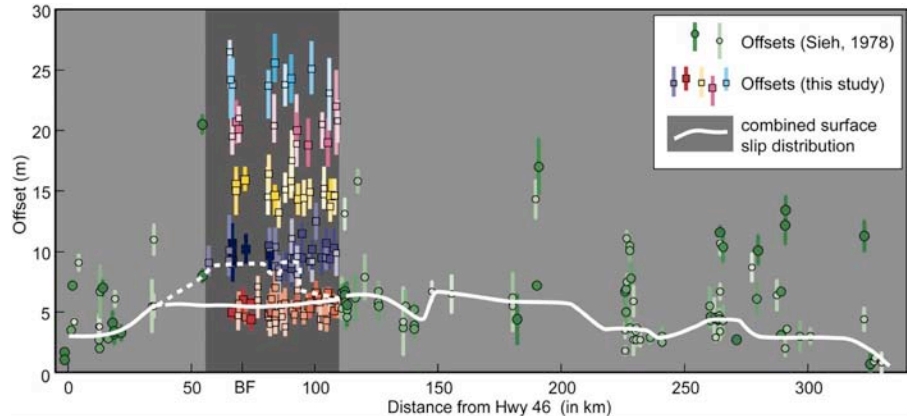


Figure 6. Combined surface slip distribution associated with the 1857 earthquake (solid white line). Measurements show quality rating increasing with increasing color intensity. Our measurements along the Carrizo Plain suggest an average slip of 5.3 ± 1.4 m during this event. The previously reported 9.0 ± 2.0 m offsets (dashed white line) represent the cumulative slip of at least two earthquakes. [Zielke *et al.*, 2010]

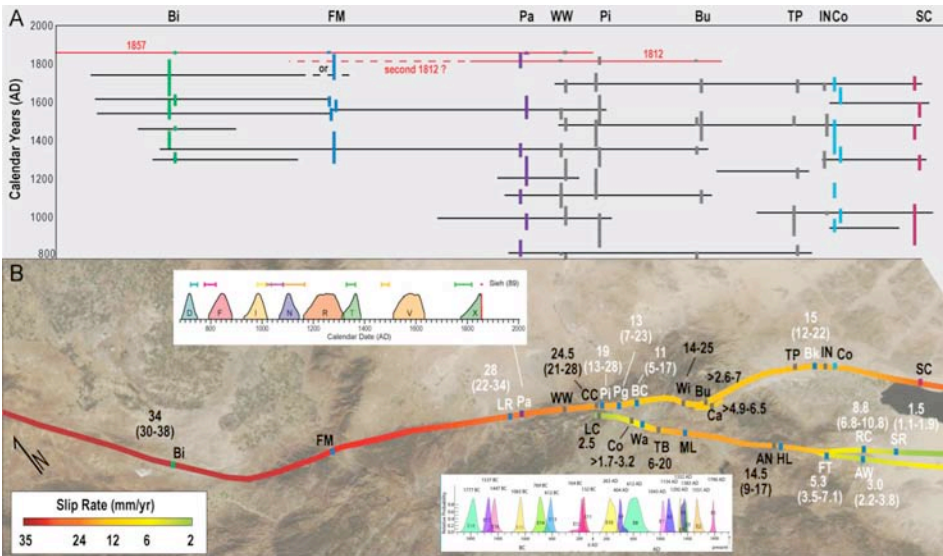


Figure 7. San Andreas Fault system data collected during SCEC3. (A) 2σ range for paleoearthquakes on the San Andreas identified/dated during SCEC3 (in color). Correlations based on age (black) suggest preference for N and S events. Color shows slip rate (mm/yr). Insets show PDFs for Hog Lake (lower) and Pallett Creek (upper).

SCEC3 RESEARCH ACCOMPLISHMENTS

San Andreas and northern San Jacinto Faults (**Fig. 7**). The discovery of a new paleoseismic site along the San Jacinto Fault at Mystic Lake [Onderdonk *et al.*, 2009; Sharpe, 1981] has great potential to yield a long record of earthquake recurrence. Ongoing work at sites on the San Andreas Fault will further refine event-dates and slip-per-event.

Quantifying the Threat from Other Faults. New paleoseismic records from the eastern California shear zone and from large blind thrust fault systems that underlie the coastal basins will further test the size of potential earthquakes. The ongoing research will help to quantify the threat from faults that lie closest to urban centers; in particular, the large blind thrust systems directly beneath Los Angeles. Leon *et al.* [2007] developed evidence for Holocene ($M > 7$) earthquakes on the Puente Hills thrust, under downtown Los Angeles, and Leon *et al.* [2009] made the case for similar events on the Compton thrust, further to the south, but still under metropolitan Los Angeles. Future work on the thrust systems of the western Transverse Ranges will examine the possibility that major faults could link into a very large event similar to the 2008 Wenchuan earthquake. Provocative results [Rockwell, personal communication] indicate 6-7 m of coseismic uplift of the Ventura Anticline in a very large event about 1000 yrs ago.

Resolving Geologic vs. Geodetic Slip-Rate Discrepancies. At the end of SCEC2, some geodetic/geologic slip rate discrepancies were substantial and difficult to understand (**Fig. 8**). Work at new sites on the San Jacinto Fault tested for temporal variation of slip rate [Bennett *et al.*, 2004; McGill *et al.*, 2008; Onderdonk *et al.*, 2009]. Geologically based slip-rate studies focused on a possible trade-off in activity between the southernmost San Andreas and San Jacinto Faults. These include an intensive study of slip rate from the Biskra Palms site on the San Andreas [Behr *et al.*, 2010; Fletcher *et al.*, 2010], documentation of slip rates showing a gradient in activity on the San Bernardino section north of San Geronio Pass [Bennett *et al.*, 2004; McGill *et al.*, 2008], and a multi-site investigation of slip rates on the San Jacinto [Onderdonk *et al.*, 2009; Blisniuk *et al.*, 2010; Janecke *et al.*, 2011]. Evidence for earthquake clustering [Rockwell *et al.*, 2006] and temporal variation in slip rate of the San Jacinto [Blisniuk *et al.*, 2010; Janecke *et al.*, 2011] suggest that its activity may oscillate with the southernmost San Andreas Fault.

SCEC played a central role in establishing continuously recording Global Positioning System (GPS) measurements in southern California with the Southern California Integrated GPS Network [Hudnut *et al.*, 2002] (which, in many ways, was the prototype for EarthScope's Plate Boundary Observatory). SCEC continues to support new GPS observations, with a focus on campaign GPS data in strategically important locations that complement continuous GPS coverage. SCEC researchers are collecting data along the San Bernardino section of the San Andreas, in Joshua Tree National Park, near Anza, and in the Salton Trough to address discrepancies between geologically and geodetically determined slip rates and to characterize the important details of deformation in these high strain-rate regions.

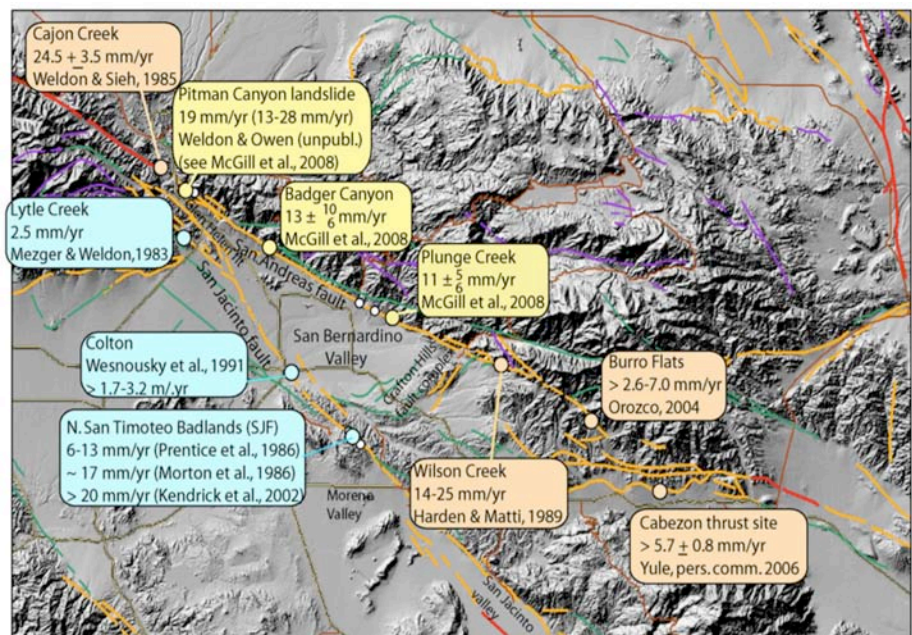


Figure 8. Summary of geologic slip rates across the San Andreas and San Jacinto Faults [McGill, Weldon *et al.*]. All slip rates exceed 5 mm/yr as estimated geodetically [Meade and Hager, 2005].

Geodetic observations can only be interpreted as slip rates through crustal deformation modeling. SCEC3 scientists have taken a number of different modeling approaches to infer fault slip rates from geodetic, geologic, and stress data. Of particular note are significant discrepancies between slip rates predicted by the elastic block model and geologic estimates of fault slip rates. Relative to geologic rates, the elastic model predicts low rates on the Mojave and San Bernardino segments of the San Andreas as well as the Garlock fault, and high rates in the Eastern California Shear Zone. These discrepancies with geologic measurements [Loveless and Meade, 2011] have been largely resolved by more recent block modeling; they now point to 9-11 mm/yr rates on the SBSAF, in agreement with the geologic rates. The slip rates from the block model (**Fig. 9**) increased largely due to changes in the representation of fault system geometry, pointing to the importance of an accurate CFM. This illustrates how interdisciplinary collaborations can resolve research questions.

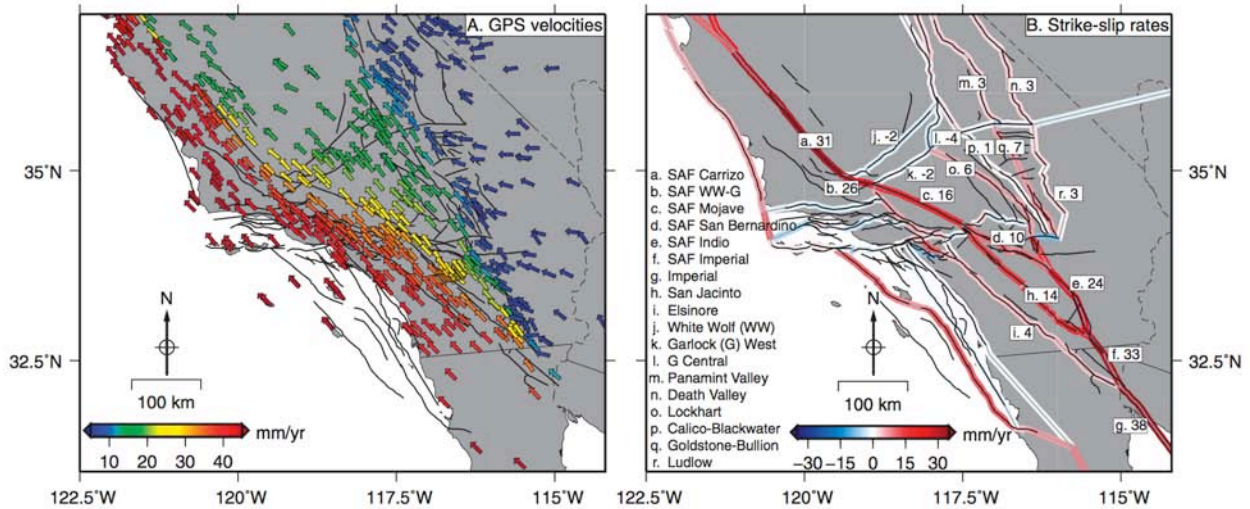


Figure 9. Left: Interseismic velocity field based on several GPS networks, relative to stable North America. Speed is denoted by color. Right: Estimated slip rates on block-bounding faults (right lateral is positive). Block geometry constructed from SCEC CFM. SAF—San Andreas Fault. [Loveless and Meade, 2011]

In addition to the block modeling, viscoelastic earthquake cycle models for Southern California predict slip rates on the San Andreas and in the Eastern California shear zone that are largely consistent with geologic rates [Chuang *et al.*, 2009]. Thus, viscous relaxation between large earthquakes may account for the apparent low rates across the San Andreas and Garlock Faults, and high rates across the Eastern California shear zone, and shows the effect of varying time since the last large earthquake (Fig. 10).

Progress in Modeling Fault Systems.

System-level deformation and stress-evolution modeling requires understanding heterogeneities in stress, strain, geometry, and material properties. A goal is to determine how plate motion is resolved onto the San Andreas Fault system. An important element of this is resolving absolute stress levels acting on faults. A novel approach to this uses seismic tomography of the upper mantle, which can be interpreted in terms of density anomalies that exert known loads on the Southern California crust and upper mantle [Fay *et al.*, 2008]. This load is substantial, is consistent with geodetic anomalies (Fig. 11), and provides an important constraint on absolute stress [Fay and Humphreys, 2008].

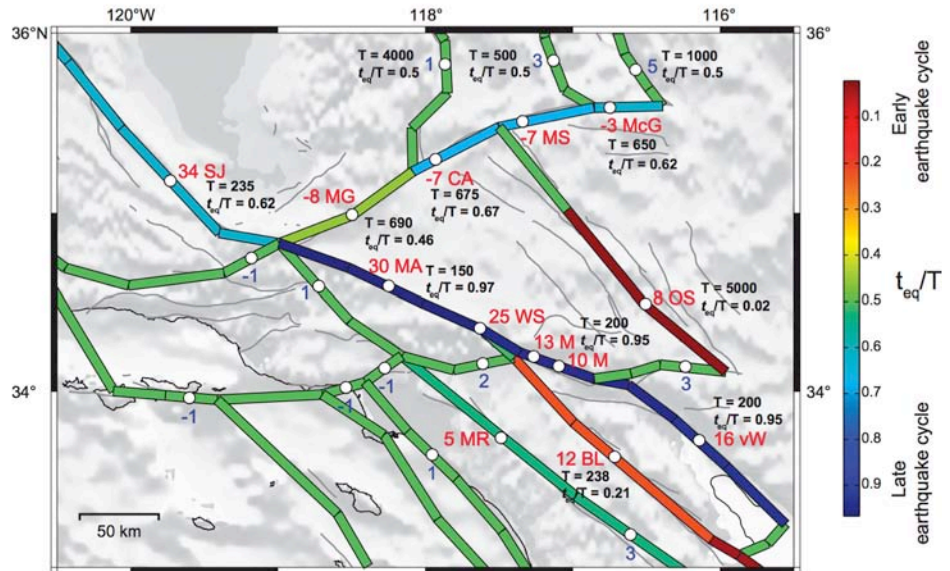


Figure 10. Summary of assumed geologic rates, recurrence interval (T), and time since last earthquake (t) in Southern California. Blue numbers are expert opinion slip rates from Working Group on California Earthquake Probabilities (2008) and red numbers are from other paleoseismology data. Color of rupture segment represents ratio of time since last earthquake and recurrence interval. Hot (red) colors show segments are in early earthquake cycle, and cold (blue) colors show late earthquake cycle. [Chuang and Johnson, 2011]

Development of earthquake simulators, aimed at generating synthetic earthquake catalogs over a range of spatial and temporal scales [Tullis *et al.*, 2009; Dieterich and Richards-Dinger, 2010], emerged as an important activity in SCEC3. Results on a sequence of standardized simulation problems were generated by the participating groups, comparisons have been made, and more complex problems formulated. An example of a simulated sequence of earthquakes on the San Andreas system is shown in Fig. 12. The simulator is based a quasi-static boundary-element calculation that employs a Dieterich nucleation model and can handle complex fault geometries [Dieterich and Richards-Dinger, 2010]. The vision for simulator-based seismicity catalogs is that they will provide important input into time-dependent earthquake rupture forecasts by combining short-term triggering with long-term stress renewal.

SCEC3 RESEARCH ACCOMPLISHMENTS

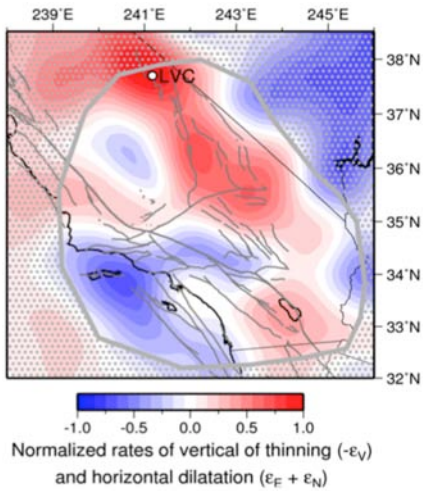


Figure 11. Predicted rates of vertical and horizontal strain inferred from seismic tomography of the upper mantle. [Fay et al., 2008]

Precision Catalogs. As earthquake rupture simulators show, fault geometry has a strong effect on earthquake size and occurrence. Much of what we know about fault structure at depth comes from earthquake locations. Recent development of precise location techniques, and their application to large Southern California catalogs [Hauksson and Shearer, 2005; Shearer et al., 2005; Lin et al., 2007; Waldhauser et al., 2008], have allowed researchers to discern structures that were previously obscured by location uncertainties (**Fig. 13**). Incorporating this new information into the Community Fault Model is a major activity in SCEC3. Work is also underway to develop the capability for precise locations in near real time. Improved stress measurements from earthquakes is an important objective. We are working to improve and interpret both catalogs of stress drops and earthquake focal mechanisms that account for SH/P amplitude ratios as well as first motions to reduce uncertainty. Algorithms for improved focal mechanism determination are currently being automated.

Aseismic Transient Detectors. A Transient Detection Technical Activity Group was organized in SCEC3 to develop geodetic transient detectors. This group is organized like the Earthquake Simulators and Rupture Dynamics Code Verification TAGS, and their objective is to develop new approaches to geodetic transient detection. Test data are distributed to participants who apply their detection methodologies and report on any transient signals they find through

an online forum and at small workshops (**Fig. 14**). So far, test data have been time series of synthetic GPS observations possibly containing an unknown transient fault slip signal and contaminated by a realistic combination of noise sources. As the exercise progresses, more complexity will be added to the synthetic data, test datasets consisting of real GPS time series will be incorporated, and other data types such as InSAR and strainmeter observations will be included. The eventual goal, to make geodetic transient detection an operational capability, was in the process of being realized with a sub-set of the detectors by the end of the SCEC3 project.

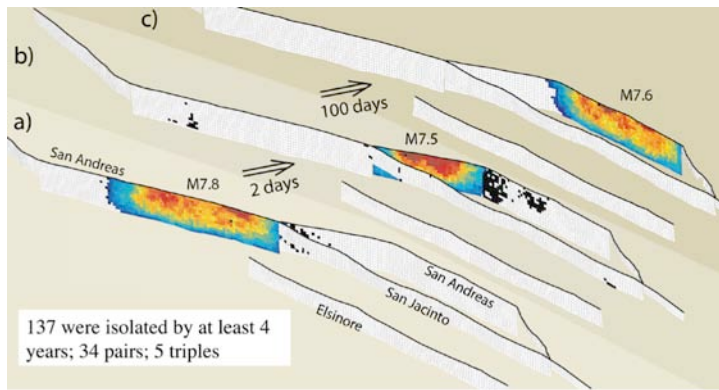


Figure 12. Example output from earthquake simulator showing sequence of earthquakes on the San Andreas Fault. There were 72 aftershocks in the 2-day interval between the M 7.8 and M 7.5 events, and 183 aftershocks in the 100-day interval between that and the M 7.6 event. Over the long term, the simulation led to 227 $M > 7$ earthquakes on these faults. [Dieterich and Richards-Dinger, 2010]

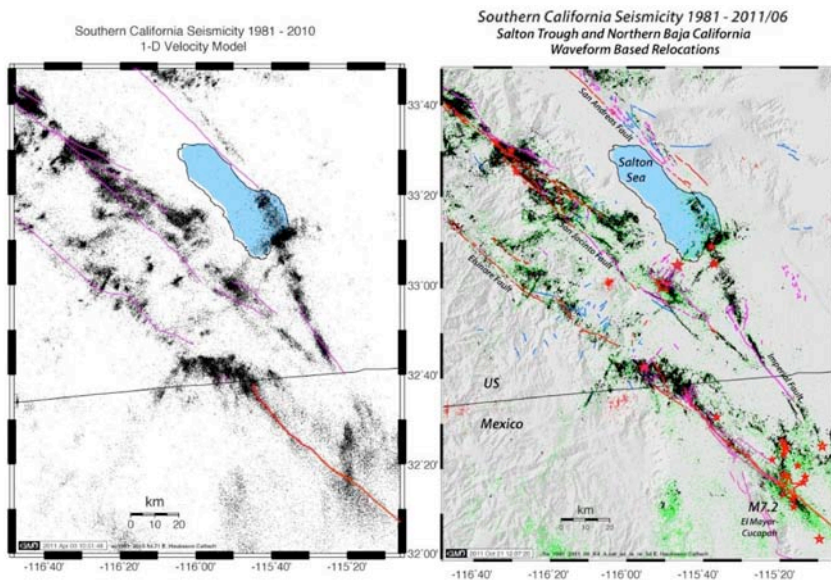


Figure 13. Seismicity located with 1-D mode (left) and precisely relocated (right) from 1981 through mid-2011. Similar-event clusters (black) relocated using cross-correlation. Events in SCSN catalog (and uncorrelated events from other catalogs) are shown in color. $M \geq 5.5$ shown with stars. Late Quaternary faults in red, and early Quaternary in blue. [Hauksson et al., submitted]

Earthquake Predictability Experiments. The Collaboratory for the Study of Earthquake Predictability (CSEP) is developing a virtual, distributed laboratory that supports a wide range of scientific prediction experiments in regional or global natural laboratories, and provides means for conducting and evaluating earthquake prediction experiments, with the goal of determining the extent to which the earthquake rupture process is predictable. CSEP has developed rigorous procedures for comparative testing of predictions as part of an infrastructure, including authorized data sets and monitoring products [Zechar et al., 2009]. A major focus of CSEP is to develop international collaborations between regional testing centers and to accommodate a wide-ranging set of prediction experiments involving geographically distributed fault systems in diverse tectonic environments. Nucleated as a special project within SCEC with funding from the W. M. Keck Foundation, CSEP has rapidly become a large international organization, with testing centers in Switzerland, New Zealand, , Japan, and, China; and with testing regions that include: California, Italy, Japan, Northwest Pacific, Southwest Pacific, New Zealand, and global.

Work on short-term earthquake forecast models for CSEP testing has focused on models, such as the Epidemic Type Aftershock Sequence (ETAS), which are updated and tested on a daily schedule. Models based on ETAS have been submitted to CSEP, some with a focus on California, while others are global, including both long-term and short-term global earthquake forecasts based on earthquake branching models and estimates of tectonic deformation (Fig. 15). There are currently more than 100 earthquake forecasts being testing by CSEP, and the global forecasts are being evaluated at the SCEC testing center. Considerable work has gone into the development of appropriate statistical tests for alarm-based earthquake forecasts [Zechar and Jordan, 2008]. This represents an important expansion of CSEP’s capabilities, as it allows CSEP to test classical earthquake predictions defined by a magnitude, time and location window.

Importance of Off-Fault Deformation. The need to account for off-fault deformation in ground motion modeling, dynamic rupture modeling, and in crustal deformation modeling more broadly, has emerged as a major theme of SCEC3. This includes damage in the very near field, and there is great progress in understanding the origin and effects of damaged and pulverized rocks along faults. Shallow drilling and coring of the pulverized zone adjacent to the San Andreas at Little Rock is the first borehole sampling effort to disentangle the mechanism of pulverization from near-surface weathering. Weschler et al. [2008; 2009] found clear evidence for pulverized rock that had undergone extensive tensile failure, and multiple fracture-healing cycles indicating they are earthquake-generated. Studies of pulverized rocks along major southern California faults [Rockwell et al., 2008; Dor et al., 2009] point to an origin caused by dynamic slip, but at relatively

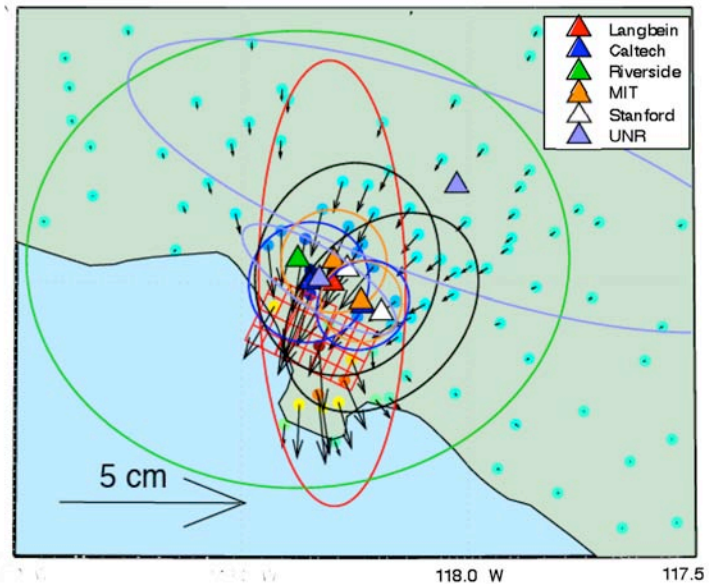


Figure 14. Summary of test results from a test dataset used in the Transient Detection Blind Test Exercise. Triangles with ellipses mark centroid location and extent of the transient cumulative displacement detected by each participating group. Cumulative noiseless synthetic displacements that were added to the test data are shown by vectors, and source fault geometry is shown by the red grid.

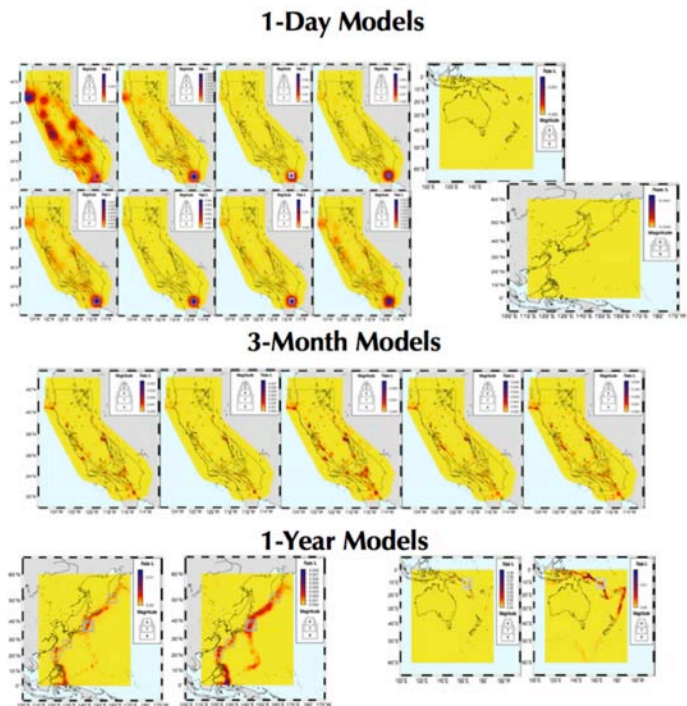


Figure 15. Example of earthquake forecast models under evaluation at the CSEP testing center.

SCEC3 RESEARCH ACCOMPLISHMENTS

shallow depth. The need to assess the contribution of fracture and comminution to the earthquake energy budget also motivated improved techniques to determine particle size distributions in fine-grained fault rocks [Rockwell et al., 2008; Dor et al., 2009]. The presence of damage has been shown to have a strong effect on dynamic rupture in the laboratory [Biegel et al., 2009; Bhat et al., 2010].

Central to earthquake rupture forecasts is the ability to predict extent and direction of rupture on major faults. Fault geometry is thought to play a major role in the former, and there are indications that material contrasts across a fault might play a controlling role in the latter. Slip on non-planar faults leads to geometric incompatibilities that grow in proportion to slip if the crust is assumed to behave elastically. In SCEC2 almost all numerical simulations assumed elastic yielding, whereas in SCEC3 inelastic effects have been examined and found to be important.

Much of the initial impetus for modeling off-fault plasticity (Fig. 16) came from the Extreme Ground Motion (ExGM) special project, which is designed to understand absolute limits on maximum possible ground motion at the proposed Yucca Mountain Nuclear Waste Repository [Andrews and Hanks, 2007]. The most recent efforts of the SCEC Rupture Dynamics Code Validation TAG [Harris et al., 2009] tested the effects of elastic vs. plastic yielding during super-shear and complete stress-drop earthquakes (extreme events) in both 2D and 3D. The maximum vertical ground motion (velocity) at a 300-m deep repository site was produced when 2D elastic assumptions were adopted, while ground motions were lowest for 3D simulations with plastic-yielding. The importance of off-fault yielding extends far beyond the Extreme Ground Motion project, however. The potential “smoothing” effect of near crack tip plasticity may, for example, counteract the need to resolve finer and finer spatial details in numerical simulations due to Lorentzian contraction during high-speed rupture propagation.

Tests of Dynamic Fault-Weakening. Identifying new mechanisms of dynamic fault weakening was an important achievement of SCEC2. The same research area remains as a research thrust in SCEC3, but the focus now is on understanding which dynamic weakening effects are most important and, which are most likely to be operative on real faults, and how might their signature be expressed in the field, and during fault rupture. Dunham and Rice [2008] and Noda et al. [2009] developed numerical methods for incorporating flash heating and pore fluid pressurization into a boundary integral code for dynamic rupture propagation. Recent models simulating spontaneous ruptures, constrained by lab and field data and incorporating rate-and-state friction laws, show that flash heating on faults with initially low ratios of shear to effective normal stress promote self-healing slip pulse behavior and predict stress drops consistent with seismic observations. Critical to understanding the role of fault geometry on dynamic rupture is determining how strength changes with normal stress changes. Plate-impact experiments demonstrate that sudden changes in normal stress cause friction to gradually approach a new steady-state level [Yuan and Prakash, 2008], reflecting the current state of the interface.

Theory [Rice, 2006; Beeler et al., 2008] indicates the velocity at the onset of weakening due to flash heating varies inversely with contact size. Tullis and Goldsby [2007] tested this prediction, but found that samples of large initial roughness do not demonstrate dramatic weakening. The discrepancy reflects the development and shearing of a gouge layer. This emphasizes the importance of slip localization and contact size in determining the degree to which flash heating is an important weakening mechanism in nature. Sagy et al. [2007] and Sagy and Brodsky [2009] find that slip surfaces bound a cohesive layer that has undergone granular flow, that the topography of the surfaces reflects variations in the thickness of this layer, and that it thins with displacement. Kitajima et al. [2010] developed a new understanding of the interactions between changing normal stress, temperature, and displacement in the formation and behavior of slip surfaces in high displacement fault zones using detailed microscopy and thermo-mechanical modeling. They found that dynamic weakening initiates above a critical temperature and is associated with slip localization and formation of a fluidized gouge layer (Fig. 17). These and related findings, have significant implications for improving models of slip on faults that incorporate realistic geological and geometrical complexities.

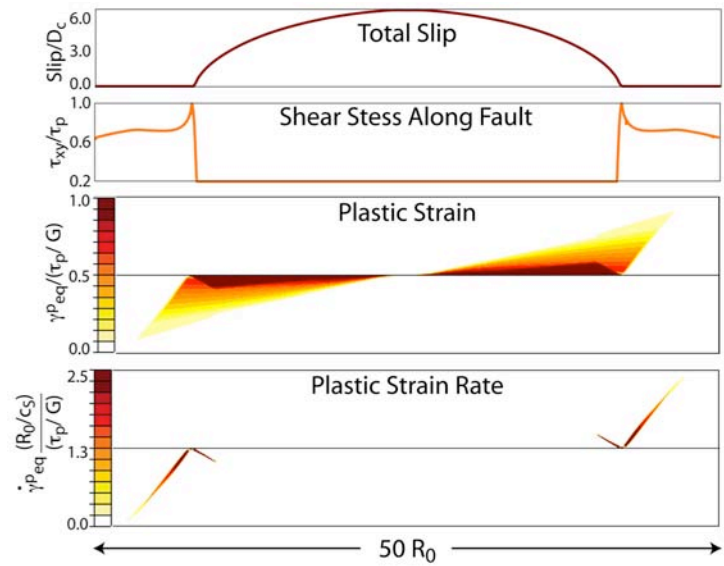


Figure 16. Accumulation and evolution of plastic strain during rupture propagation. Plastic strain accumulates in a narrow zone near the crack tip. [Templeton et al., 2009]

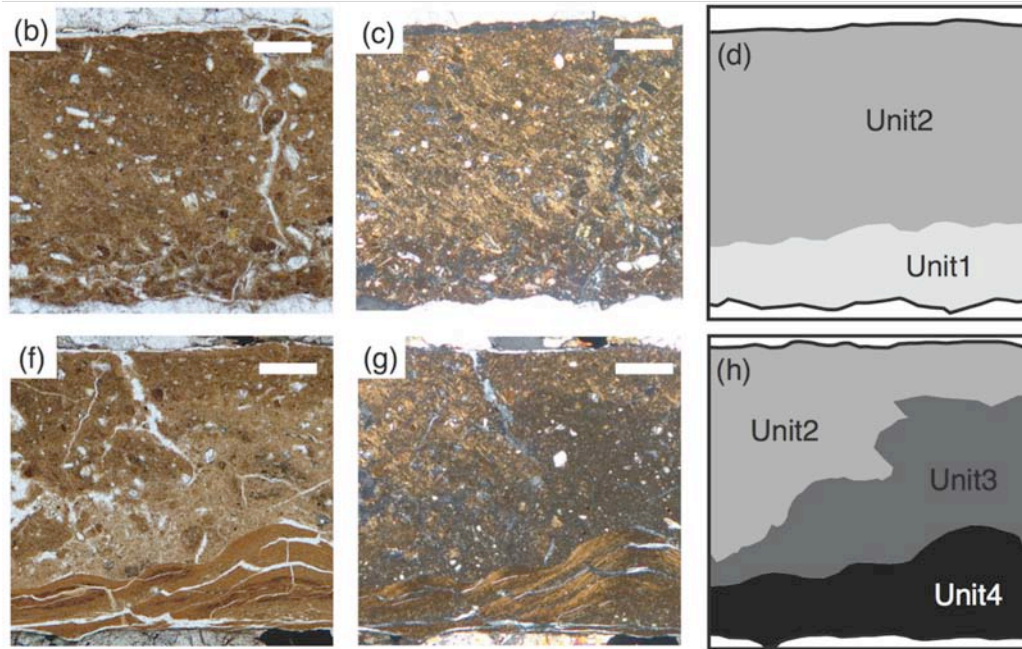


Figure 17. Characteristic structure of gouge units showing progressive evolution with slip. Unit 4 has been repeatedly imbricated and stacked. [Kitajima et al., 2010].

Predict Broadband Ground Motions

The critical tie between improved earthquake rupture forecasts, and earthquake risk reduction is accurate ground motion prediction. SCEC’s goal is the development of fully validated strong ground motion prediction based on a fundamental, physics-based understanding of earthquake rupture and seismic wave propagation. Simulating strong ground motion for large scenario earthquakes is one of the overarching research objectives of SCEC3, and there are a number of elements of the SCEC3 research program that contribute directly to this effort, including much of the research within the Community Modeling Environment (CME). Signal accomplishments in developing and extended earthquake rupture forecast include: verification of wave propagation and dynamic rupture algorithms; development of improved pseudo-dynamic representations; improved understanding of the possible effects of super-shear rupture; new ideas for modeling excitation of high-frequency ground motion; and new approaches to validations of strong ground motion simulations.

Another category of accomplishments in this area is the application of ground motion simulations for specific purposes. The Seismic Hazard and Risk Analysis focus group coordinates this research within SCEC. Here too, SCEC3 has an impressive list of accomplishments: ground motion simulations for extreme events, in support of NGA and the new National Seismic Hazard Maps, and for the PEER Tall Building Initiative; and for end-to-end simulations.

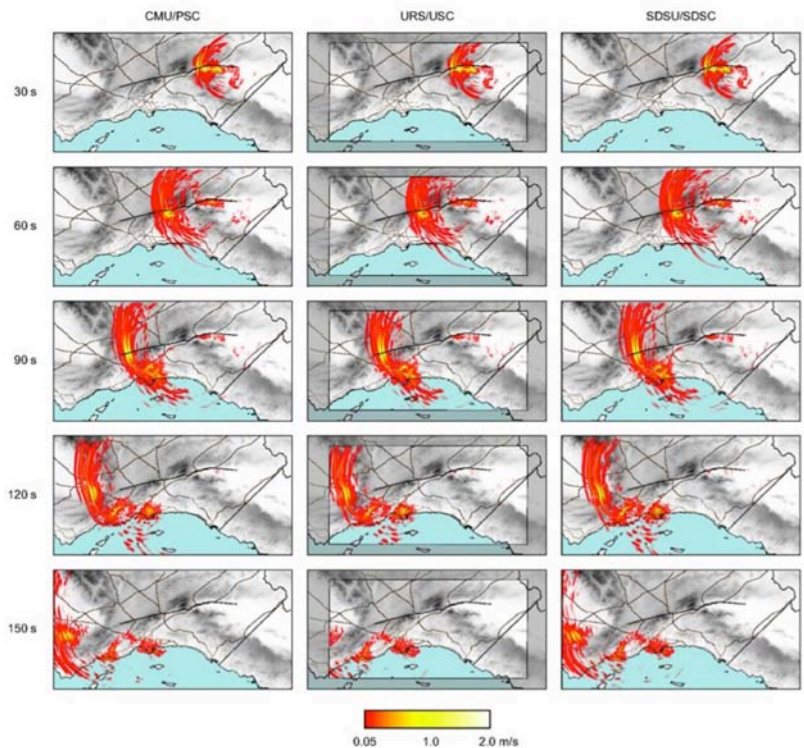


Figure 18. Snapshots at 5 different times, of horizontal velocity for 3 ShakeOut simulations. Groups/computer centers are from left to right CMU/PSC, URS/USC, and SDSU/SDSC.

SCEC3 RESEARCH ACCOMPLISHMENTS

Verification of Algorithms. Simulating ground motions from complex ruptures in a 3D Earth is a task that absolutely *requires* high-performance computing (HPC). For that reason, SCEC3 developed special projects that enable the requisite HPC, in particular the CME. These projects are a major success for SCEC in their own right (but not described here). As with any simulation, verification that algorithms are properly solving the wave propagation problem as posed is a challenge. SCEC has a long and successful history of code verification exercises, a history that is continuing not just with ground motion prediction, but with other tasks, such as dynamic rupture modeling [Harris et al., 2009] and ground motion modeling of large scenario earthquakes, such as the ShakeOut scenario [Bielak et al., 2010] (Fig. 18).

Improved Pseudo-Dynamic Rupture Models. Dynamic rupture models incorporate the physics of earthquake rupture that can improve simulations for ground motion prediction; however, developing dynamic rupture models of sufficient spatial and temporal detail to simulate the full frequency range of engineering interest is not yet possible. For that reason, SCEC3 has an objective of developing kinematic rupture representations that are consistent with dynamic rupture models. These “pseudo-dynamic” models are kinematically prescribed, but incorporate the salient features of dynamic models required for strong ground motion prediction [Guatteri et al., 2004; Song et al., 2009; Schmedes et al., 2010]. Multiple dynamic-rupture variations have been calculated for the ShakeOut scenario earthquake to estimate long-period spectral acceleration within the basins of greater Los Angeles. Predicted ground motions were a factor of 2–3 lower than the corresponding kinematic predictions, which stems from the less coherent wavefield excited by the complex rupture paths of the dynamic sources. An unanticipated result of those simulations was that dynamic predictions (at a given site) were very stable (Fig 19). This suggests that simulation ensemble variances may be substantially reduced through use of sources based on spontaneous rupture simulations.

Effect of Super-shear Rupture. It has become apparent that super-shear rupture can occur over substantial parts of the fault in large strike-slip earthquakes. This is in line with theoretical predictions from decades ago [Andrews, 1976], but we are still coming to grips with the implications for ground motion prediction because sub- and super-shear ruptures exhibit qualitatively different characteristics [Aagaard and Heaton, 2004; Dunham and Archuleta, 2004; Dunham and Bhat, 2008]. Super-shear rupture is observed in dynamic rupture simulations, such as the “wall-to-wall” earthquake rupture of the entire southern San Andreas Fault (Fig. 20). The long, straight section of the Carrizo segment of the San Andreas is consistent with the conditions thought to be conducive to super-shear rupture [Das, 2007] and the lack of on-

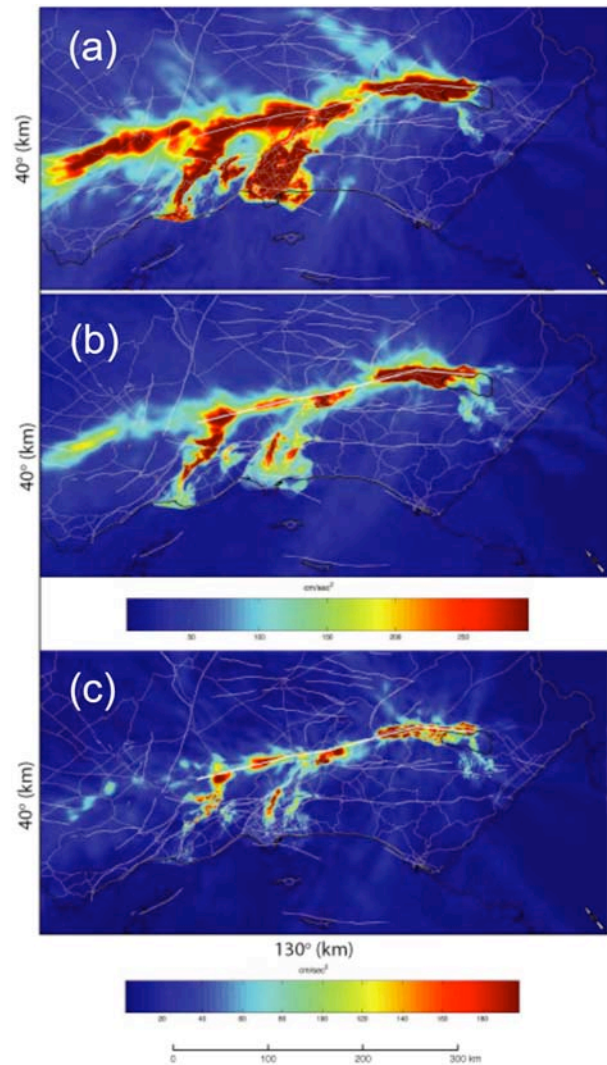


Figure 19. 3s Spectral acceleration for (a) kinematic, (b) mean dynamic, and (c) standard deviation of dynamic for ShakeOut scenario earthquake simulations.

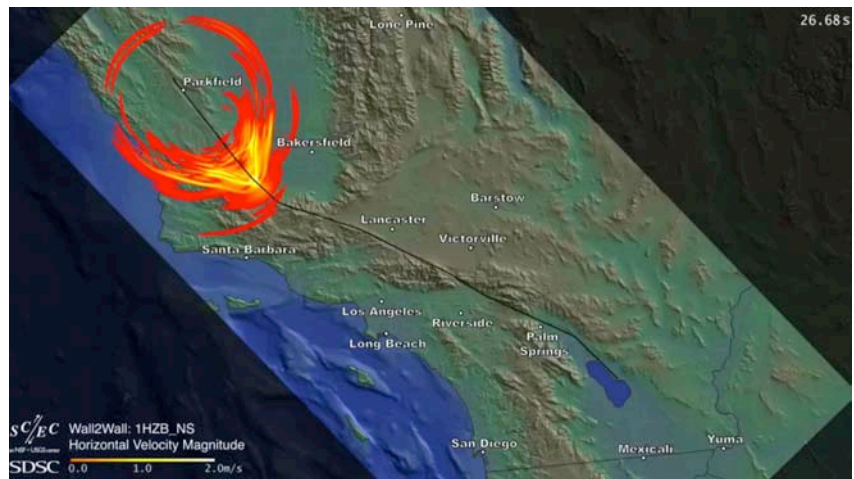


Figure 20. Supershear rupture on the Carrizo segment of the San Andreas Fault. In this dynamic simulation of NW-SE rupture, a classic Mach cone - the seismic equivalent of a sonic boom - is formed behind the rupture front.

fault seismicity on the San Andreas, here and elsewhere, is also suggestive [Bouchon and Karabulut, 2008]. Super-shear rupture adds a layer of complexity to ground motion simulation, because it may not occur in most earthquakes used to develop ground motion attenuation relations. It underscores the need for simulation-based ground motion predictions.

High-Frequency Excitation. We are working to address a pressing need in engineering seismology, viz., to develop improved high-frequency simulation methods and investigate the upper frequency limit of deterministic ground motion predictions. Current methods to simulate high frequency ground motions use rather ad hoc approaches. It has long been known that high-frequency ground motion is generated by short scale-length variations in slip rate or rupture velocity. Dunham et al. [2011] have pioneered a promising method that couples these phenomena in a physically realistic way. In their model, high-frequency ground motions are generated by normal stress variations that arise from dynamic rupture of a rough fault surface (Fig. 21). They include the effects of off-fault plasticity in their simulations. Plasticity enhances the effect due to its role as an energy sink.

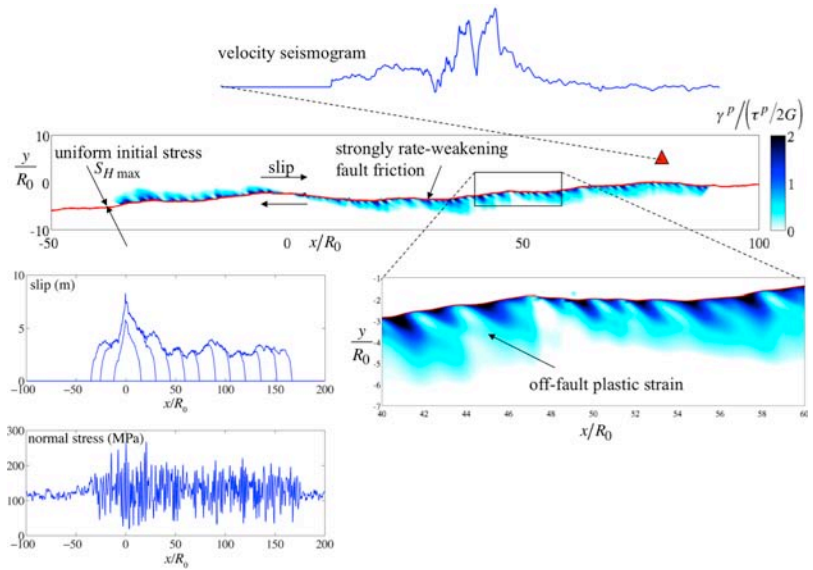


Figure 21. Simulation of rupture on fractally rough fault. Material is elastic-plastic. Stress perturbations (lower left) lead to fluctuations in rupture speed and slip (middle left), which are accentuated by plastic yielding (center). The result is production of high frequency ground motion (top).

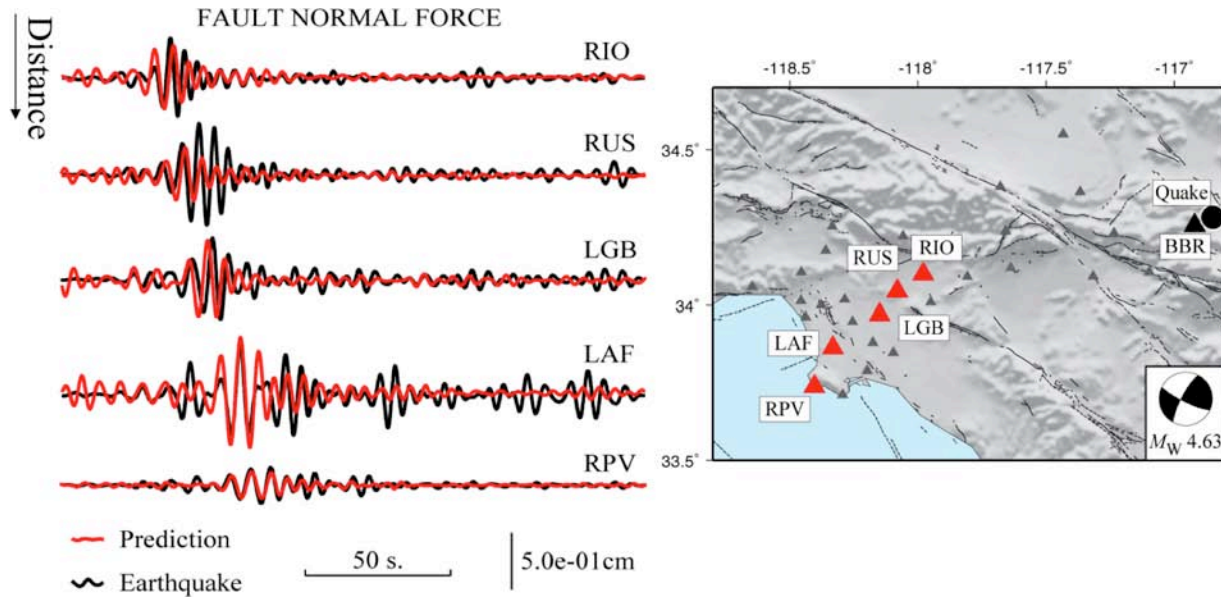


Figure 21. Simulation of rupture on fractally rough fault. Material is elastic-plastic. Stress perturbations (lower left) lead to fluctuations in rupture speed and slip (middle left), which are accentuated by plastic yielding (center). The result is production of high frequency ground motion (top).

New Approaches to Validation of Ground Motion Simulations. The need to validate simulated ground motions with data is listed explicitly as a SCEC3 priority. This is a challenge, however, because southern California has not suffered recent large earthquakes against which to compare simulations. SCEC has attacked this problem creatively and pioneered new approaches. The wave propagation part of validation can be accomplished through ground motion predictions for smaller earthquakes. The goodness-of-fit analysis for the 2008 M5.4 Chino Hills earthquake [Olsen and Mayhew, 2010] demonstrates this approach. This is not possible for many paths of interest, however, owing to the lack of appropriate earthquake sources. Prieto and Beroza [2008] showed it was possible to develop “virtual earthquakes,” which can be constructed

SCEC3 RESEARCH ACCOMPLISHMENTS

anywhere that a seismic station is available, using the ambient seismic field. As proof of concept, **Fig. 22** shows that a virtual earthquake developed from data recorded at broadband seismic station BBR reproduces the amplification and duration of waves within the L.A. Basin in just the same way as a real earthquake. Using stations in areas of particular interest, such as along the San Andreas Fault, allows SCEC scientists to validate ground motion predictions and, where necessary, improve the Community Velocity Model. Corrections for moment tensor and source-depth can be included using the SCEC CVM [Denolle et al., submitted].

Uncertainties in the source are at least as large as those associated with wave propagation and the source characterization too must be validated. An obvious approach to this is to compare ground motion predictions with data from other large earthquakes. Perhaps the most directly relevant earthquake for which we have intensity data is the 1906 San Francisco earthquake. SCEC scientists were leaders in efforts to simulate of the 1906 San Francisco earthquake for its centennial [Aagaard et al., 2008a; Aagaard et al., 2008b]. Another approach to validation is the approach of using precariously balanced rocks (PBRs) to test probabilistic seismic hazard analysis. PBRs have the advantage of having been in place for thousands of years, and thus sample many earthquake cycles. There are challenges, of course, because to use them as quantitative constraints on hazard requires measurement of the age of their precarious state as well as their sensitivity to strong shaking (**Fig. 23**). PBRs continue to be discovered in strategically important areas, and can provide constraints on PSHA that may otherwise be unobtainable.

Simulation of Extreme Events. Recordings of large earthquakes at close distances are few, and are insufficient for assessing the range of motions for performance based design or evaluation of important structures (such as tall buildings and bridges in Los Angeles and San Francisco). SCEC3 has generated scientifically based representative ground motions via simulations to fill this void. SCEC simulated records have been utilized by practicing engineers and researchers dealing with design and evaluation of important structures [e.g., Bozorgnia et al., 2007; Naeim and Graves, 2006; Somerville et al., 2007]. A number of buildings and bridges have been designed or evaluated using such records as well.

Contributions to NGA and National Hazard Maps. The Next Generation Attenuation relations used in the calculation of the 2008 USGS National Seismic Hazard Maps, which form the basis for impending national seismic design standards, such as ASCE 7-10 and International Building Code. Owing to the critical shortage of earthquake recordings, the NGA database has been supplemented with a number of SCEC simulated records for representation of motions produced by large nearby earthquakes. As a result, SCEC simulated records are having an impact on the building codes that will be used nationwide by practicing engineers.

Contributions to the PEER Tall Building Initiative. The Pacific Earthquake Engineering Research Center (PEER) is in the midst of a multi-year project sponsored by a variety of sources including NSF, USGS, California Seismic Safety Commission and Building Departments of Los Angeles and San Francisco, for establishing performance objectives and design guidelines for tall buildings. Numerous researchers and practicing engineers are actively involved in the PEER Tall Building Initiative. An important part of this research is a detailed parametric investigation of the performance of tall buildings designed by various methods, obtained by subjecting them to thousands of recorded and simulated earthquake ground motions. Another part of this research compares characteristics of recorded and simulated ground motions to validate the simulations. Tens of thousands of records generated by SCEC are being used in these exercises. The PEER Tall Building Initiative project will result in a set of guidelines and source materials that will be widely used and referenced by practicing engineers and building officials. This illustrates how SCEC has been vital to advancing state of the art and practice of earthquake resistant design.

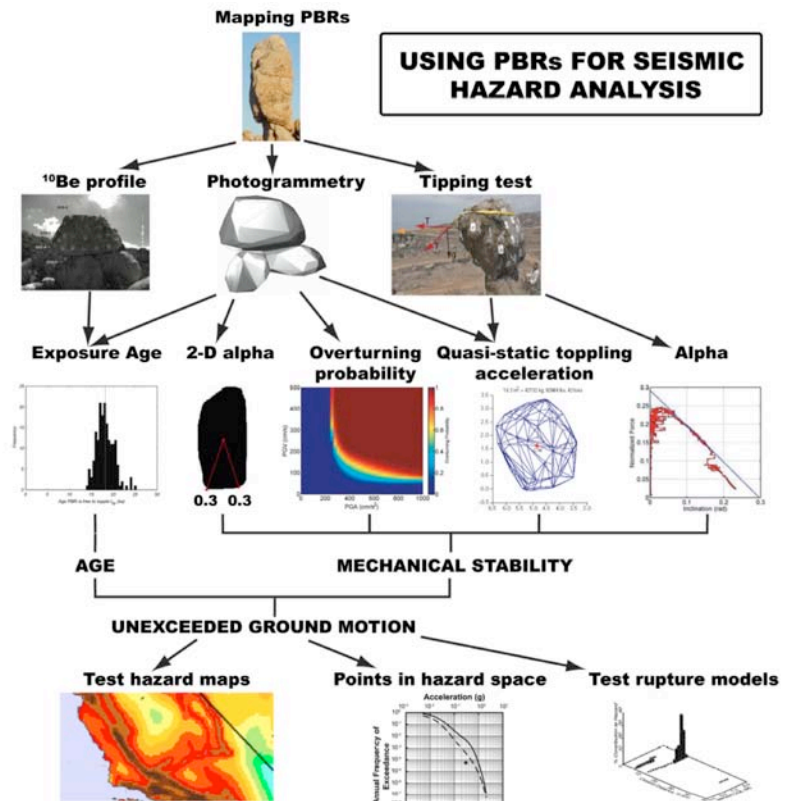


Figure 23. Methodology used to address seismic hazards with Precariously Balanced Rocks. Methodologies developed in SCEC3 use these methods to produce ground motion constraints for strategically selected PBRs. [Grant-Ludwig, 2012]

End-to-End Simulations. Ground motion predictions are only useful only if they inform engineering practice, disaster preparedness, or public policy. A priority for SCEC has been to work with earthquake engineers to develop rupture-to-rafters simulation capability for physics-based risk analysis. This type of end-to-end simulation is illustrated in **Fig. 24**. In such calculations, computer models of representative buildings (in the case of Fig. 24, a 2-story woodframe house) are spread throughout a geographical region and subjected to simulated ground motion scenarios, and the results are used to assess the performance of the representative buildings. The SCEC computational platforms such as TeraShake and CyberShake are especially suited for simulating ground motions appropriate for end-to-end calculations.

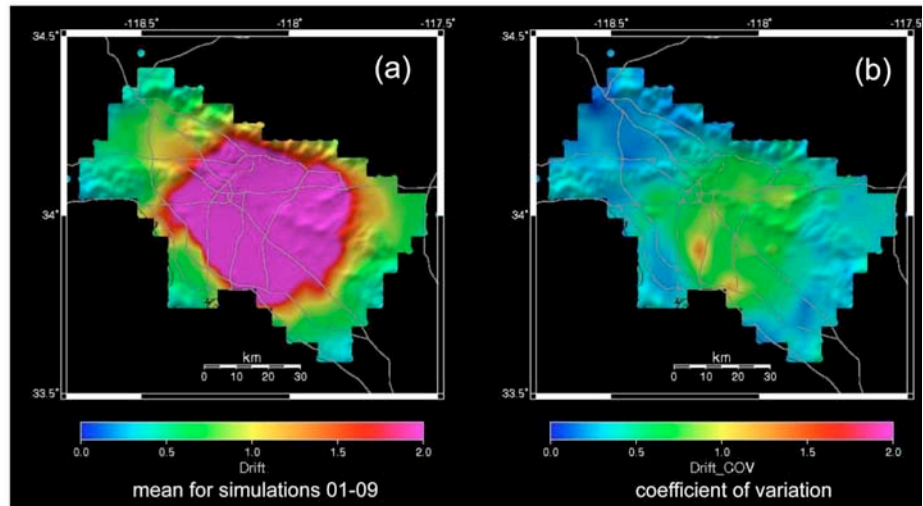


Figure 24. Peak inter-story drift (inches) and coefficient of variation throughout the Los Angeles region in a 2-story 1980s-2000s index woodframe house from a M 7.1 earthquake on the Puente Hills Blind Thrust. Values in excess of 2 inches (pink areas) would likely cause total loss and potential collapse.

Prepare Post-Earthquake Scientific Response Strategies

SCEC must be prepared to respond if a large earthquake strikes California. The last earthquake to have had a significant impact on Southern California was the 1994 Northridge earthquake (the M 5.4 Chino Hills earthquake of 2008 doesn't really count). Thus, it has been a long time since we have responded to an earthquake in Southern California. SCEC has therefore conducted exercises to coordinate the post-event scientific response of the academic science community with USGS, CGS, and other organizations and constructed new tools to facilitate this response.

ShakeOut Scientific Response Exercises. To prepare the SCEC scientific community, we held simulated earthquake response exercises during the 2008 and 2009 ShakeOut scenario exercises. These featured realistic injects in real time, with the responses being largely simulated. The simulated responses uncovered a number of issues that we needed to resolve, and they have helped to enable a more effective response to the real thing. The exercise is now an annual event.

Earthquake Response Content Management System. We also tested communications over satellite phones at key SCEC institutions and exchanged information using a new SCEC Response Content Management System, which is hosted at USC and mirrored at Caltech and Stanford for redundancy (in the event a large earthquake renders one of the hosting sites inoperable). In developing the Earthquake Response CMS, we have gathered information on instrumental resources, and contacts, from UNAVCO, IRIS, and universities.

References

- Aagaard, B. T., and T. H. Heaton (2004), Near-source ground motions from simulations of sustained intersonic and supersonic fault ruptures, *Bull. Seismol. Soc. Am.*, **94**, 2064–2078, doi:10.1785/0120030249.
- Aagaard, B. T., T. M. Brocher, D. Dolenc, D. Dreger, R. W. Graves, S. Harmsen, S. Hartzell, S. Larsen, M. L. Zoback (2008), Ground-Motion Modeling of the 1906 San Francisco Earthquake, Part I: Validation Using the 1989 Loma Prieta Earthquake, *Bull. Seismol. Soc. Am.*, **98**, 989-1011, doi: 10.1785/0120060409.
- Aagaard, B. T., T. M. Brocher, D. Dolenc, D. Dreger, R. W. Graves, S. Harmsen, S. Hartzell, S. Larsen, K. McCandless, S. Nilsson, N. A. Petersson, A. Rogers, B. Sjogreen, M. L. Zoback (2008), Ground-Motion Modeling of the 1906 San Francisco Earthquake, Part II: Ground-Motion Estimates for the 1906 Earthquake and Scenario Events, *Bull. Seismol. Soc. Am.*, **98**, 1012-1046, doi: 10.1785/0120060410.
- Akciz, S. O., L. Grant Ludwig, and J. R. Arrowsmith (2009), Revised dates of large earthquakes along the Carrizo section of the San Andreas fault, California, since A.D. 1310 \pm 30, *Journal of Geophysical Research*, **114**, B01313.
- Akciz, S. O., L. Grant Ludwig, J. R. Arrowsmith, and O. Zielke (2010), Century-long average time intervals between ruptures of the San Andreas fault in the Carrizo Plain, *Geology*, **38**, 787-790, doi: 10.1130/G30995.1.

SCEC3 RESEARCH ACCOMPLISHMENTS

- Andrews, D. J. (1976). Rupture velocity of plane strain shear cracks, *J. Geophys. Res.*, **81**, 5679–5687.
- Andrews, D.J. and T.C. Hanks (2007). Physical limits on ground motion at Yucca Mountain, *Bull. Seismol. Soc. Am.*, **97**, 1771-1792, doi:10.1785/0120070014.
- Beeler, N. M., T. E. Tullis, and D. L. Goldsby (2008), Constitutive relationships and physical basis of fault strength due to flash heating, *J. Geophys. Res.*, **113**, B01401, doi: 10.1029/2007JB004988
- Behr, W.M., Rood, D.H., Fletcher, K.E., Guzman, N., Finkel, R., Hanks, T.C., Hudnut, K.W., Kendrick, K.J., Platt, J.P., Sharp, W.D., Weldon, R.J., and Yule, J.D. (2010), Uncertainties in slip-rate estimates for the Mission Creek strand of the southern San Andreas fault at Biskra Palms Oasis, southern California. *GSA Bulletin*, **122**, 1360–1377; doi: 10.1130/B30020.1.
- Bennett, R. A., A.M. Friedrich, A. M., and K. P. Furlong (2004), Codependent histories of the San Andreas and San Jacinto fault zones from inversion of fault displacement rates, *Geology*, **32**, 961-964.
- Bhat, H. S., R. L. Biegel, A. J. Rosakis, and C. G. Sammis (2010) The Effect of Asymmetric Damage on Dynamic Shear Rupture Propagation II: With Mismatch in Bulk Elasticity, *Tectonophysics*, **493**, 263-271, doi:10.1016/j.tecto.2010.03.016.
- Biasi, G., and Weldon, R. (2009), San Andreas Fault rupture scenarios from multiple paleoseismic records; stringing pearls, *Bull. Seismol. Soc. Am.*, **99**, 471-498.
- Biegel, R. L., H.S. Bhat, C.G. Sammis, A.J. Rosakis, A.J. (2009) The Effect of Asymmetric Damage on Dynamic Shear Rupture Propagation I: No Mismatch in Bulk Elasticity, *J. Geophys. Res.*, (submitted).
- Bielak, J., R. Graves, K. Olsen, R. Taborda, L. Ramirez-Guzman, S. Day, G. Ely, D. Roten, T. Jordan, P. Maechling, J. Urbanic, Y. Cui, and G. Juve (2010) The ShakeOut earthquake scenario: verification of three simulation sets, *Geophys. J. Int.*, **180**, 375-404.
- Blisniuk, K., Rockwell, T., Owen, L., Oskin, M., Lippincott, C., Caffee, M., and Dorch, J. (2010), Late Quaternary slip-rate gradient defined using high-resolution topography and ¹⁰Be dating of offset landforms on the southern San Jacinto fault, California, *J. Geophys. Res.*, **115**, B08401, doi:10.1029/2009JB006346.
- Boore, D. M. and W. B. Joyner (1997). Site amplifications for generic rock sites, *Bull. Seismol. Soc. Am.*, **87**, 327-341.
- Bouchon, M. and H. Karabulut (2008). The Aftershock Signature of Supershear Earthquakes, *Science*, **320**, 1323-1325, doi:10.1126/science.1155030.
- Bozorgnia, Y., K. W. Campbell, N. Luco, J. P. Moehle, F. Naeim, P. Somerville, and T. Y. Yang (2007), Ground motion issues for seismic analysis of tall buildings: a status report, *The Structural Design of Tall Buildings*, **16**, 665-674.
- Chen, P., T. H. Jordan, S. Callaghan, P. Maechling (2009), Tera3d: Full-3D Waveform Tomography and Near-Real-Time Seismic Source Inversion in Southern California. SSA Annual Meeting Abstract.
- Chen, P., L. Zhao and T.H. Jordan (2007), Full 3D Tomography for Crustal Structure of the Los Angeles Region, *Bull. Seismol. Soc. Am.*, **97**, 1094-1120, doi: 10.1785/0120060222.
- Chuang, Y. R., and K. M. Johnson (2009), Are there geologic/geodetic fault slip rate discrepancies in southern California? 2009 SCEC Annual Meeting Proceedings.
- Chulick, G. S., and W. D. Mooney (2002), Seismic structure of the crust and uppermost mantle of North America and adjacent oceanic basins: A synthesis, *Bull. Seismol. Soc. Am.*, **92**, 2478–2492.
- Das, S. (2007), The need to study speed, *Science*, **317**, 906-907, doi:10.1126/science.1142143.
- Day, S. M., R. Graves, J. Bielak, D. Dreger, S. Larsen, K. B. Olsen, A. Pitarka & L. Ramirez-Guzman (2008), Model for Basin Effects on Long-Period Response Spectra in Southern California, *Earthquake Spectra*, **24**, 257-277.
- Denolle, M., E. M. Dunham, G. A. Prieto, and G. C. Beroza (submitted), Ground motion prediction of realistic earthquake sources using the ambient seismic field, *J. Geophys. Res.*
- Dieterich, J.H. and K.B. Richards-Dinger (2010), Earthquake recurrence in simulated fault systems, *Pure and Applied Geophysics*, **167**, 30.
- Dor, O., J.S. Chester, Y. Ben-Zion, J. Brune, T.K. Rockwell (2009), Characterization of Damage in Sandstones Along the Mojave Section of the San Andreas Fault: Implications for the Shallow Extent of Damage Generation, *Pure and Applied Geophysics*, **166**, 1747-1773, doi:10.1007/s00024-009-0516-z.
- Dunham, E. M. and R. J. Archuleta (2004). Evidence for a Supershear Transient during the 2002 Denali Fault Earthquake, *Bull. Seismol. Soc. Am.*, **94**, S256-S268.
- Dunham, E. M., D. Belanger, L. Cong, and J. E. Kozdon (2011), Earthquake ruptures with strongly rate-weakening friction and off-fault plasticity, 2: Nonplanar faults, *Bulletin of the Seismological Society of America*, **101**, 2308-2322, doi:10.1785/0120100076.
- Dunham, E. M. and H. S. Bhat (2008), Attenuation of radiated ground motion and stresses from three-dimensional supershear ruptures, *J. Geophys. Res.*, **113**, B08319, doi:10.1029/2007JB005182.
- Dunham, E. M. and J. R. Rice (2008), Earthquake slip between dissimilar poroelastic materials, *J. Geophys. Res.*, **113**, B09304, doi:10.1029/2007JB005405.
- Fay, N., R. Bennett, J. Spinler, and E. Humphreys (2008), Small-scale upper mantle convection and crustal dynamics in southern California, *Geochem. Geophys. Geosyst.*, **9**, Q08006.
- Field, E.H., T.E. Dawson, K.R. Felzer, A.D. Frankel, V. Gupta, T.H. Jordan, T. Parsons, M.D. Petersen, R.S. Stein, R.J. Weldon II & C.J. Wills (2009), Uniform California Earthquake Rupture Forecast, Version 2 (UCERF 2), *Bull. Seismol. Soc. Am.*, **99**, 2053-2107, doi:10.1785/0120080049. (Originally released as USGS Open File Report 2007-1437.)
- Fletcher, K.E., Sharp, W.D., Kendrick, K.J., Behr, W.M., Hanks, T.C. (2010), ²³⁰Th/^U dating of a late Pleistocene alluvial fan offset along the southern San Andreas fault, *GSA Bulletin*, **122**, 1360–1377, doi: 10.1130/B30020.1.

- Grant Ludwig, L., S. O. Akciz, G. R. Noriega, O. Zielke & J. R. Arrowsmith (2010). Climate- modulated channel incision and rupture history of the San Andreas fault in the Carrizo Plain, *Science*, doi:10.1126/science.1182837.
- Graves, R., S. Callaghan, E. Deelman, E. Field, N. Gupta, T. H. Jordan, G. Juve,, C. Kesselman, P. Maechling, G. Mehta, D. Meyers, D. Okaya & K. Vahi (2008). Physics-based probabilistic seismic hazard calculations for Southern California, *Proc. 14- World Conference on Earthquake Engineering*, Beijing, China, 8 pp., October, 2008.
- Graves, R., T. H. Jordan, S. Callaghan, E. Deelman, E. Field, , G. Juve, C. Kesselman, P. Maechling, G. Mehta, K. Milner, D. Okaya, and P. Small (2011), CyberShake: A physics-based probabilistic seismic hazard calculations for Southern California, *PAGEOPH*, **168**, 367-381, doi:10.1007/s00024-010-0161-6.
- Guatteri, M., P. M. Mai, and G. C. Beroza, (2004) A pseudo-dynamic approximation to dynamic rupture models for strong ground motion prediction, *Bull. Seism. Soc. Amer.*, **94**, 2051-2063.
- Harris, R.A., M. Barall, R. Archuleta, B. Aagaard, J.-P. Ampuero, H. Bhat, V. Cruz-Atienza, L. Dalguer, P. Dawson, S. Day, B. Duan, E. Dunham, G. Ely, Y. Kaneko, Y. Kase, N. Lapusta, Y. Liu, S. Ma, D. Oglesby, K. Olsen, A. Pitarka, S. Song, and E. Templeton (2009), The SCEC/USGS Dynamic Earthquake Rupture Code Verification Exercise, *Seismol. Res. Lett.*, **80**, 119-126, doi:10.1785/gssrl.80.1.119.
- Hauksson, E. (2000), Crustal Structure and Seismicity Distribution Adjacent to the Pacific and North America Plate Boundary in Southern California, *J. Geophys. Res.*, **105**, 13875-13903.
- Hauksson, E. and P. Shearer (2005), Southern California hypocenter relocation with waveform cross-correlation, Part 1: Results using the double-difference method, *Bull. Seismol. Soc. Am*, **95**, 896, DOI: 10.1785/0120040167.
- Hauksson, E. and W. Yang, and P. M. Shearer, *Waveform Relocated Earthquake Catalog for Southern California (1981 to June 2011) (submitted)*. *Bull. Seismol. Soc. Am*.
- Hudnut, K. W., Y. Bock, J. E. Galetzka, F. H. Webb, and W. H. Young (2002). *The Southern California Integrated GPS Network*, Seismotectonics in Convergent Plate Boundaries, ed. Y. Fujinawa and A. Yoshida, 167-189.
- Janecke, S., Dorsey, R., Froand, D., Steely, A., Kirby, S., Lutz, A., Housen, B., Belgarde, B., Langenheim, V., and Rittenhour, T., (2011). High geologic slip rates since early Pleistocene initiation of the San Jacinto and San Felipe fault zones in the San Andreas fault system, southern California, USA, *GSA Special Papers*, **475**, 1-49, doi:10.1130/2010.2475.
- Kitajima, H., J.S. Chester, F.M. Chester, F.M., T. Shimamoto (2010), High-speed Friction of the Punchbowl Fault Ultracataclasite in Rotary Shear: Characterization of Frictional Heating, Mechanical Behavior, and Microstructural Evolution, *J. Geophys. Res.* **115**, B08408, doi:10.1029/2009JB007038.
- Kohler, M., Magistrale, H., and Clayton, R. (2003). Mantle heterogeneities and the SCEC three-dimensional seismic velocity model version 3, *Bull. Seismol. Soc. Am.*, **93**, 757-774.
- Lin, G., P. M. Shearer, and E. Hauksson (2007), Applying a 3D velocity model, waveform cross-correlation, and cluster analysis to locate southern California seismicity from 1981 to 2005, *J. Geophys. Res.*, **112**, doi:10.1029/2007JB004986.
- Loveless, J. P., and B. J. Meade (2011), Loveless, J. P. and B. J. Meade (2011), Stress modulation on the San Andreas fault by interseismic fault system interactions, *Geology*, **39**, 1035-1038; doi:10.1130/G32215.1.
- Ma, S., G. Prieto, and G. C. Beroza (2008), Testing Community Velocity Models for Southern California Using the Ambient Seismic Field, *Bull. Seismol. Soc. Am.*, **98**, 2694-2714, DOI: 10.1785/0120080947.
- McGill, S., Weldon, R., and Owen, L. (2008), Preliminary slip rates along the San Bernardino strand of the San Andreas Fault, 2008 SCEC Annual Meeting Proceedings.
- Naeim F, and R. W. Graves (2006), The case for seismic superiority of well-engineered tall buildings. *Structural Design of Tall and Special Buildings*, **14**, 401-416.
- Nicholson, C., E. Hauksson, A. Plesch, G. Lin, and P. Shearer (2008), Resolving 3D fault geometry at depth along active strike-slip faults: simple or complex? 2008 SCEC Annual Meeting, Palm Springs, CA.
- Noda, H., E. M. Dunham, and J. R. Rice (2009), Earthquake ruptures with thermal weakening and the operation of major faults at low overall stress levels, *J. Geophys. Res.*, **114**, B07302, doi:10.1029/2008JB006143.
- Olsen, K.B., and J.E. Mayhew (2010). Goodness-of-fit Criteria for Broadband Synthetic Seismograms, With Application to the 2008 Mw5.4 Chino Hills, CA, Earthquake, *Seism. Res. Lett.* **81** , 715-723.
- Onderdonk, N., McGill, S., and Rockwell, T. (2009), New slip-rate, slip-history, and fault structure data from the northern San Jacinto fault zone, 2009 SCEC Annual Meeting Proceedings.
- Plesch A., J. H. Shaw, C. Benson, W. A. Bryant, S. Carena, M. Cooke, J. Dolan, G. Fuis, E. Gath, L. Grant, E. Hauksson, T. Jordan, M. Kamerling, M. Legg, S. Lindvall, H. Magistrale, C. Nicholson, N. Niemi, M. Oskin, S. Perry, G. Planansky, T. Rockwell, P. Shearer, C. Sorlien, M. P. SSM., J. Suppe, J. Treiman, R. Yeats (2007), Community Fault Model (CFM) for Southern California, *Bull. Seismol. Soc. Am.*, **97**, 1793-1802.
- Philibosian, B., T. Fumal, R. Weldon, K. Kendrick, K. Scharer, S. Bemis, R. Burgette, and B. Wisely (2007), Paleoseismology of the San Andreas fault at Coachella, California, 2007 SCEC Annual Meeting Proceedings.
- Power, M., B. Chiou, N. Abrahamson, Y. Bozorgnia, T. Shantz, and C. Roblee (2008). An Overview of the NGA Project, *Earthquake Spectra*, **24**, 3-21.
- Prieto, G. A. and G. C. Beroza (2008), Earthquake Ground Motion Prediction Using the Ambient Seismic Field, *Geophys. Res. Lett.*, **35**, L14304.
- Prieto, G. A., J. F. Lawrence, and G. C. Beroza (2009), Anelastic Earth Structure from the Coherency of the Ambient Seismic Field, *J. Geophys. Res.*, **114**, B07202, doi:10.1029/2008JB006067.
- Rice, J. R. (2006), Heating and weakening of faults during earthquake slip, *J. Geophys. Res.*, **111**, B05311, Doi 10.1029/2005jb004006.

SCEC3 RESEARCH ACCOMPLISHMENTS

- Rockwell, T., Seitz, G., Dawson, T., Young, J. (2006), The Long Record of San Jacinto fault paleoearthquakes at Hog Lake: Implications for Regional Patterns of Strain Release in the southern San Andreas fault system, *Seismol. Res. Lett.*, **77**, 270.
- Rockwell, T K, Sisk, M, Stillings, M, Girty, G, Dor, O, Wechsler, N, Ben-Zion, Y (2008), Chemical and Physical Characteristics of Pulverized Granitic Rock Adjacent to the San Andreas, Garlock and San Jacinto Faults: Implications for Earthquake Physics, *Eos Trans. AGU*, Fall Meet. Suppl., **89**, Abstract T53F-02.
- Sagy, A., and E. E. Brodsky (2009), Geometric and rheological asperities in an exposed fault zone, *J. Geophys. Res.* **114**, B02301, doi:10.1029/2008JB005701.
- Sagy, A., E.E. Brodsky, and G.J. Axen (2007), Evolution of fault-surface roughness with slip, *Geology*, **35**, doi: 10.1130/G23235A.1, 283-286.
- Schmedes, J., R. J. Archuleta, and D. Lavallee (2010). Correlation of earthquake source parameters inferred from dynamic rupture simulations, *J. Geophys. Res.*, **115**, doi:10.1029/2009JB006689.
- Shearer, P. M., G. A. Prieto, and E. Hauksson (2005), Comprehensive analysis of earthquake source spectra in southern California, *J. Geophys. Res.*, **111**, B06303, doi:10.1029/2005JB003979.
- Sharp, R. V. (1981), Variable rates of late Quaternary strike slip on the San Jacinto fault zone, southern California, *J. Geophys. Res.*, **86**, 1754-1762. doi:10.1029/JB086iB03p01754.
- Sieh, K. (1978), Slip along the San Andreas Fault associated with the great 1857 earthquake, *Bull. Seismol. Soc. Am.*, **68**, 1421-1448.
- Somerville, P.G., R.W. Graves, S.M. Day, and K.B. Olsen (2007), Ground Motion Environment of the Los Angeles Region', *The Structural Design of Tall and Special Buildings*, **15**, 483-494.
- Song, S., A. Pitarka, and P. Somerville (2009). Exploring spatial coherence between earthquake source parameters, *Bull. Seism. Soc. Am.* **99**, 564-2,571.
- Süss, M. P., and Shaw, J. H. (2003), P-wave seismic velocity structure derived from sonic logs and industry reflection data in the Los Angeles basin, California, *J. Geophys. Res.* **108**, 2170, doi: 10.1029/2001JB001628.
- Tape, C., Liu, Q., Maggi, A., and Tromp, J. (2009), Adjoint tomography of the Southern California crust, *Science*, **325**, 988-992.
- Templeton, E. L., A. Baudet, H. S. Bhat, R. Dmowska, J. R. Rice, A. J. Rosakis, and C.-E. Rousseau (2009) Finite element simulations of dynamic shear rupture experiments and dynamic path selection along kinked and branched faults, *J. Geophys. Res.*, **114**, B08304, doi:10.1029/2008JB006174.
- Tullis, T. and D. Goldsby (2007), Laboratory Experiments on Fault Shear Resistance Relevant to Coseismic Earthquake Slip, SCEC 2007 Final Report.
- Tullis, T. E., H. Noda, H., K. B. Richards-Dinger, N. Lapusta, J. H. Dieterich, Y. Kaneko, and N. M. Beeler (2009), Comparison of earthquake simulators employing rate and state-friction, 2009 SCEC Annual Meeting Proceedings.
- Waldhauser, F. and D.P. Schaff (2008), Large-scale relocation of two decades of Northern California seismicity using cross-correlation and double-difference methods, *J. Geophys. Res.*, **113**, B08311, doi:10.1029/2007JB005479.
- Ward, S. N. (2009), ALLCALL earthquake simulator - recent progress, 2009 SCEC Annual Meeting Proceedings.
- Wechsler, N, Allen, E E, Rockwell, T K, Chester, J S, Girty, G H, Ben-Zion, Y (2008), Physical and chemical characterization of pulverized granite from a shallow drill along the San Andreas Fault, Little Rock, CA, *Eos Trans. AGU*, Fall Meet. Suppl., Abstract T51A-1861.
- Wechsler, N., Allen, E.E., Rockwell, T.K., Chester, J., and Ben-Zion, Y. (2009), Characterization of Pulverized Granite from a Traverse and a Shallow Drill along the San Andreas Fault, Little Rock, CA, Seismological Society of America Annual meeting, *Seismol. Res. Lett.*, **80**, 2, 319.
- Yan, Z., and R. W. Clayton (2007), Regional mapping of the crustal structure in southern California from receiver functions, *J. Geophys. Res.*, **112**, B05311, doi:10.1029/2006JB004622.
- Yuan, F., and Prakash, V. (2008) Slip weakening in rocks and analog materials at co-seismic slip rates. *J. Mech. Phys. Sol.*, **56**, 542-560; Yuan, F. and V. Prakash (2008), Use of a Modified Torsional Kolsky Bar to Study Frictional Slip Resistance in Rock-Analog Materials at Coseismic Slip Rates, *International Journal of Solids and Structures*, Elsevier.
- Zechar, J., and T. H. Jordan (2008) Testing alarm-based earthquake predictions, *Geophys. J. Int.*, **172**, 715-724, doi 10.1111/j.1365-246x.2007.03676.x.
- Zechar, J.D., D. Schorlemmer, M. Liukis, J. Yu, F. Euchner, P.J. Maechling, & T.H. Jordan, 2009. The Collaboratory for the Study of Earthquake Predictability perspective on computational earthquake science, *Concurrency and Computation: Practice and Experience*, doi:10.1002/cpe.1519.
- Zielke, O., J. R. Arrowsmith, L. Grant Ludwig, and S. O. Akciz (2010), Slip in the 1857 and earlier large earthquakes along the Carrizo Plain, San Andreas fault, *Science*, doi:10.1126/science.1182781.

SCEC4 Science Milestones

Southern California Earthquake Center, September 2012

TABLE 1. SCEC4 FUNDAMENTAL PROBLEMS OF EARTHQUAKE PHYSICS

- I. Stress transfer from plate motion to crustal faults: long-term slip rates.
- II. Stress-mediated fault interactions and earthquake clustering: evaluation of mechanisms.
- III. Evolution of fault resistance during seismic slip: scale-appropriate laws for rupture modeling.
- IV. Structure and evolution of fault zones and systems: relation to earthquake physics.
- V. Causes and effects of transient deformations: slow slip events and tectonic tremor.
- VI. Seismic wave generation and scattering: prediction of strong ground motions.

Milestones

NSF has requested that we submit an annualized list of milestones as part of a revised SCEC4 plan for 2012-2017. According to NSF instructions, these milestones are based on the six fundamental problems in earthquake physics described in the SCEC4 proposal (see Table 1 of this supplement). Our response to the NSF request adopts the premise that milestones are to be used by SCEC and its sponsoring agencies as indicators of research progress along unknown conceptual pathways rather than, say, lists of working-group tasks, timelines for IT developments, or absolute measures of research volume from individual research groups.

We have therefore concentrated on targets for SCEC's interdisciplinary activities in earthquake system science, such as those related to the SCEC Community Models, which will include a new Community Geodetic Model (CGM) and a Community Stress Model (CSM); those related to a proposed new set of Special Fault Study Areas (SFSAs); and those coordinated through the Technical Activity Groups (TAGs), such as the newly established Ground Motion Simulation Validation TAG, which brings earthquake engineers together with ground motion modelers. Because SCEC interdisciplinary activities in some cases depend on ancillary support from special projects (e.g., IT developments, HPC resources), reaching some of the milestones will be contingent on receiving this ancillary support.

The milestones are organized by a numbered research topic or collaboration. The problems addressed by each numbered item are listed parenthetically at the end of each paragraph; e.g., [I-VI] indicates that the milestones for that topic or collaboration are relevant to all six problems. Owing to the unpredictable nature of basic research, the milestones for the first two years are more explicit than those for the out-years of the SCEC4 program.

Year 1 (2012-2013)

12. **Improved Observations.** Archive and make available at the SCEC waveforms, refined catalogs of earthquake locations and focal mechanisms for the period 1981-2011. Begin cataloging validation earthquakes and associated source descriptions and strong ground motion observations for California for use in ground motion simulation validation. Implement automated access to EarthScope GPS data for transient detections. Initiate planning with IRIS and UNAVCO to improve the scientific response capabilities to California earthquakes. [I-VI]
13. **Transient Geodetic Signals.** Develop data-processing algorithms that can automatically detect geodetic transients localized within Southern California using continuously recorded GPS data. Provide access to authoritative GPS data streams through CSEP. Implement at least two detection algorithms as continuously operating procedures within CSEP. [V]
14. **Community Modeling Environment.** Implement, refine, and release software tools for accessing the SCEC CVMs. Define reference calculations and evaluation criteria for 3D velocity models. Conduct comparative evaluations among different CFMs and CVMs. Deliver statewide versions of CFMs for use by WGCEP in UCERF3. Develop dynamic rupture verification exercises that incorporate effects of large-scale branching fault geometry on dynamic rupture and ground motions. [II, III, IV, VI]
15. **Community Geodetic Model.** Obtain input from the SCEC community via a workshop in order to define the conceptual and geographic scope of the CGM, including the time-independent and time-dependent model components, the data to be assimilated into the model, and the type and spatial distribution of model output. [I, V]

SCEC4 SCIENCE MILESTONES

16. **Community Stress Model.** Develop a strategy for archiving and curating observational and model-based constraints on the tectonic stress field in Southern California. Based on this strategy, begin developing components of the database that will underlie the CSM. Organize a SCEC collaboration to contribute existing observational and model-based constraints to this database. [I, II]
17. **Special Fault Study Areas.** Identify requirements for SFSA Science Plans. Solicit SFSA Science Plan(s) from SCEC community to be ratified by PC and then included into 2013 RFP. Coordinate interdisciplinary activities, including workshops, to prototype at least one SFSA. [I-VI]
18. **Ground Motion Simulation Validation.** Develop a set of validation procedures suitable for the application of ground motion simulations in seismic hazard analysis and earthquake engineering. Identify a set of ground motions recorded in large California earthquakes to use for validation. Use codes available in the CME to simulate the ground motions. Compare these simulations with the observed recordings and other empirical models where they are well-constrained. [VI]
19. **Source Modeling.** Assess field evidence for the importance of specific resistance mechanisms during fault rupture, and plan fieldwork to collect new diagnostic data. Develop laboratory experiments that explore novel weakening mechanisms. Standardize observations from key earthquakes for the testing of different methods of finite-fault source inversion, and set up standardized inverse problems as cross-validation exercises. [III, VI]
20. **Time-Dependent Earthquake Forecasting.** Support WGCEP in the development and release of UCERF3. Reduce the updating interval of the short-term forecasting models being tested in CSEP. Improve methods for detecting, classifying, and analyzing various types of seismic clustering. [II, V]

Year 2 (2013-2014)

1. **Improved Observations.** Begin cataloging SCEC-supported geochronology analyses available for Southern California. Complete cataloging validation earthquakes and associated source descriptions and strong ground motion observations for California for use in ground motion simulation validation. Start comparing InSAR and GPS data to flag any suspect data as a first step to integrated use of GPS and InSAR in the CGM. Start developing plans for enhanced seismic instrument deployments in the SFSAs and elsewhere in Southern California. Update coordination of earthquake response capabilities of the SCEC community with partner organizations, including USGS, IRIS, and UNAVCO. [I-VI]
2. **Transient Geodetic Signals.** Increase the number of geodetic transient detection algorithms automated within CSEP that continuously operate on authoritative GPS data streams. Assess and refine detection thresholds through the use of synthetic data for a range of earthquake sizes for all operating detectors. [V]
3. **Community Modeling Environment.** Improve CVMs by applying full-3D waveform tomography to data from hundreds of earthquakes. Perform reference calculations and apply goodness-of-fit measures to evaluate CVMs against earthquake waveform data. Improve stochastic kinematic rupture models that incorporate source complexity observed in dynamic rupture simulations, including supershear rupture. Provide access to the UCERF3 statewide hazard model via the OpenSHA software platform. Develop methodology for calculating an extended ERFs based on UCERF3. [II, III, IV, VI]
4. **Community Geodetic Model.** Start generating a unified GPS time series dataset for secular and transient deformation and compiling LOS velocity maps from available SAR catalogs. Establish strategy for estimating secular rate as well as temporally variable signals (e.g., seasonal, postseismic). Assess the feasibility and the potential benefits of incorporating additional datasets (e.g., strainmeter, LiDAR) into CGM. Specify the CGM output needed for input to the CSM and transient detection and begin providing preliminary datasets as available. [I, V]
5. **Community Stress Model.** Populate the CSM data system with existing observational and model-based constraints. Begin coordination efforts with developers of the CGM and earthquake models. Investigate the variations in directions and magnitudes of stresses and stressing rates predicted by different existing models. [I, II, IV]
6. **Special Fault Study Areas.** Solicit SFSA Science Plan(s) from SCEC Community to be ratified by PC and then included into 2014 RFP. Re-examine requirements for SFSA Science Plans. Evaluate whether SCEC should increase the number of SFSA-oriented studies in the SCEC base program. [I-VI]
7. **Ground Motion Simulation Validation.** Develop a list of metrics identified by earthquake scientists and engineers as needed to validate ground motion predictions for application to seismic hazard analysis and earthquake engineering. Use the observed ground motions of well-recorded California earthquakes to evaluate existing ground motion simulation methods and recommend improvements. Establish the Broadband Simulation Platform as a high-performance cyberfacility for ground motion simulation by outside research communities, including earthquake engineers. [III, VI]
8. **Source Modeling.** Develop numerical methods that simultaneously resolve fault zone processes and large-scale rupture, including fault interaction, complex geometries, heterogeneities and multiple fault physics. Assess data available to distinguish source from path/site effects at high frequencies. Develop a methodology for uncertainty quantification in finite-fault source inversion and back-projection source imaging, tested on standardized data sets. [III, VI]

9. **Time-Dependent Earthquake Forecasting.** Assess the capabilities of UCERF3 for time-dependent forecasting through comparisons with earthquake catalogs or synthetic catalogs from earthquake models. Through CSEP and in collaboration with the USGS and CGS, test the suitability of deploying UCERF3 as an operational earthquake forecast. Couple UCERF3 to the Cybershake simulation suite for the Los Angeles region to prototype a time-dependent urban seismic hazard model. [II, VI]
10. **Progress Report on SCEC4 Problems.** Report to the SCEC4 community and Advisory Council on the progress made so far in formulating and testing hypotheses that address the six fundamental problem areas of earthquake physics.

Year 3 (2014-2015)

1. **Improved Observations.** Archive and make available at the SCEDC waveforms, refined catalogs of earthquake locations and focal mechanisms for the period 1981-2013. Continue cataloging SCEC-supported geochronology analyses available for Southern California. Submit a proposal to NSF/Earthscope that focuses on high-resolution imaging of SFSA and elsewhere in Southern California. Begin developing catalogs of prehistoric surface rupturing events along major faults in the system. [I-VI]
2. **Transient Geodetic Signals.** Using the first two years of results from Southern California, assess the capability and consistency of the geodetic transient detection procedures. Develop ensemble-based detection procedures that combine the output of multiple detection algorithms. [II, V]
3. **Community Modeling Environment.** Incorporate results from the Salton Seismic Imaging Project into the CVMs. Incorporate stochastic descriptions of small-scale heterogeneities into the upper layers of the CVMs, and evaluate the importance of these heterogeneities in ground motion models. Integrate and evaluate a statewide unified CVM suitable for 3D ground motion modeling. Incorporate new information on fault complexity from SFSA projects into the CFM. [II, III, IV, VI]
4. **Community Geodetic Model.** Integrate InSAR and GPS in order to formulate a uniform resolution model for secular surface velocities and associated uncertainties and covariances. Revise or refine the technical specifications of the CGM based on results obtained in years 1 and 2 and input from the CSM and the Geodetic Transient Detection TAG. Define the framework and infrastructure for maintaining CGM. Identify and test algorithms for time-dependent InSAR analysis. [I, V]
5. **Community Stress Model.** Quantitatively assess discrepancies between various stress models. Begin the process of identifying classes of alternative stress models or branches for the CSM. [I, II, IV]
6. **Special Fault Study Areas.** Continue to execute coordinated plans for disciplinary fieldwork and interdisciplinary synthesis in SFSA. Finalize the set of SFSA to be investigated in SCEC4. [I-VI]
7. **Ground Motion Simulation Validation.** Develop scientific and engineering criteria for appropriate use of deterministic and stochastic frequencies in ground motion simulations. Based on the Year-2 evaluation, assess how future SCEC simulation efforts can best assist seismic hazard analysis, risk analysis, and earthquake engineering. Use SCEC4 research on dynamic weakening and the effect of geometrical heterogeneity on faulting to improve estimates of high-frequency wave excitation by seismic sources. [III, VI]
8. **Source Modeling.** Verify numerical methods and assess physical formulations of fault geometries. Develop and calibrate parameterization of resistance mechanisms that are suitable for large scale models of dynamic ruptures, including interaction with fault roughness and damage-zone properties. Develop improved source inversion approaches with enhanced information extraction from high frequencies, including by intergration with back-projection imaging. [III, VI]
9. **Time-Dependent Earthquake Forecasting.** Develop approaches for using physics-based earthquake models in forecasting. Employ these models for studying the predictability of large events and constraining seismic cycle parameters (maximum magnitude, inter-event time, etc.). Conduct prospective forecasting experiments in CSEP that test the key hypotheses that underlie time-dependent forecasting methods. [II]
10. **Progress Report on SCEC4 Problems.** Report to the SCEC4 Community and Advisory Council on the progress made so far in formulating and testing hypotheses that address the six fundamental problem areas of earthquake physics and report to SCEC4 community.

Year 4 (2015-2016)

1. **Improved Observations.** Refine catalogs of prehistoric surface rupturing events along major faults in the system and, if needed, document more events, including paleo-magnitudes, with more robust uncertainty measurements. Initiate the use of GPS data to better constrain 3D motion observed by InSAR, especially in the North/South direction. [I-VI]
2. **Transient Geodetic Signals.** Incorporate the CGM into the transient detection procedures as the reference model for time-dependent geodetic signals. Using the data collected in Southern California and elsewhere on geodetic transients, assess the observational constraints on the spectrum of deformation transients that might be associated with earthquake processes in San Andreas Fault system. [II, IV, V]

SCEC4 SCIENCE MILESTONES

3. **Community Modeling Environment.** Develop a prototype CyberShake hazard model for the Los Angeles region based on extensions of UCERF3 and large suites of ground motion simulations up to 1 Hz calculated from improved CVMs. Provide interactive access to this layered seismic hazard model. [II, III, IV, VI]
4. **Community Geodetic Model.** Use SAR data catalogs from previous and current SAR missions to generate LOS displacement time series over Southern California, and conduct comparisons between InSAR and GPS time series results. [I, V]
5. **Community Stress Model.** Integrate the various stress model developed in years 1-3 into a full-scale version of the CSM that includes both time-independent and time-dependent components. Begin applying results to the problem of discriminating between competing models of fault system loading. [I, II]
6. **Special Fault Study Areas.** Through workshops and other collaborative mechanisms, begin to examine how SFSA's results can be integrated into SCEC products and activities and address SCEC science questions. [I-VI]
7. **Ground Motion Simulation Validation.** Extend validation studies to high-frequency ground motion simulations that incorporate improved representations of source physics, source complexity, attenuation, and high-frequency scattering by near-surface heterogeneities. [VI]
8. **Source Modeling.** Incorporate more realistic models of fault-resistance evolution into CFM- and CSM-based simulations of the earthquake cycle. Compare fault interaction patterns from dynamic rupture models to earthquake simulators. Generate a uniform database of kinematic source models of past earthquakes and extract constraints on mechanical fault properties. Develop fundamental insight into source inversion uncertainties and implications for seismic network design. [III, VI]
9. **Time-Dependent Earthquake Forecasting.** Prototype numerical forecasting earthquake models, and evaluate their utility in developing new versions of a Uniform California Earthquake Rupture Forecast. [II]
10. **Progress Report on SCEC4 Problems.** Report on the progress made so far by SCEC4 investigations of the six fundamental problem areas of earthquake physics. Synthesize the current state of interdisciplinary knowledge in each of these problem areas, and evaluate which among the alternate hypotheses described in the SCEC4 proposal are now favored by the observational data and model-based constraints. This report will be used as input to the SCEC5 proposal. [I-VI]

Year 5 (2016-2017)

1. **Improved Observations.** Archive and make available at the SCEC waveforms, refined catalogs of earthquake locations and focal mechanisms for the period 1981-2015. Document results from significant earthquakes that occurred during SCEC4. Continue refinement of the catalog of prehistoric surface rupturing events along major faults in the system including realistic uncertainty estimates. Initiate new project for archiving and making available InSAR datasets from Sentinel and ALOS2 acquisitions, which pertain to geological problems being studied by SCEC investigators. Complete comparing InSAR and GPS data to flag any suspect anomalies in GPS data as a first step to resolving discrepancies between GPS and InSAR strain rates. [I-VI]
2. **Transient Geodetic Signals.** Using the data collected in Southern California and elsewhere on geodetic transients during SCEC4, assess the validated and potential utility of geodetic data in time-dependent earthquake forecasting. [II, IV, V]
3. **Community Modeling Environment.** Perform reference calculations and apply goodness-of-fit measures to evaluate a SCEC California statewide CVM using earthquake waveform data. Calculate statewide CyberShake hazard model based on extensions of UCERF3, the California statewide CVM, and large suites of ground motion simulations up to 1 Hz. Provide interactive and programmable access to this layered seismic hazard model. [II, III, IV, VI]
4. **Community Geodetic Model.** Develop a full-scale version of the CGM that integrates data types and includes both time-independent and time-dependent components. Provide outputs from the CGM that can be used as input to the CSM, transient detectors, and time-dependent earthquake forecasting. [I, V]
5. **Community Stress Model.** Release the final SCEC4 version of the CSM and assess its implications for earthquake physics. Recommend guidelines for future data collection and modeling studies to improve resolution of the CSM. [I, II]
6. **Special Fault Study Areas.** Publish synthesis studies of the SCEC4 SFSA's. Assess the utility of these syntheses in improving seismic hazard models for California. [I-VI]
7. **Ground Motion Simulation Validation.** Complete an evaluation of the simulated ground motions produced by the current versions of the Broadband Platform and the statewide CyberShake model. [VI]
8. **Source Modeling.** Develop realistic broadband kinematic source models of well-recorded earthquake in California that are consistent with source inversion and dynamic rupture modeling. Work with USGS/Golden to migrate improvements in source inversion into operational methods. [III, VI]
9. **Time-Dependent Earthquake Forecasting.** Use earthquake models, the CFM and CSM, and other modeling tools to quantify how fault-system complexities govern the probabilities of large earthquakes and rupture sequences. [II]
10. **Progress Report on SCEC4 Problems.** Conduct a final assessment of SCEC4 investigations of the six fundamental problem areas of earthquake physics, and evaluate the utility of new knowledge in time-independent and time-dependent seismic hazard analysis. [I-VI]

Draft 2013 Science Plan

SCEC Planning Committee, September 2012

I. Preamble

The Southern California Earthquake Center (SCEC) coordinates basic research in earthquake science using Southern California as its natural laboratory. SCEC emphasizes the connections between information gathering by sensor networks, fieldwork, and laboratory experiments; knowledge formulation through physics-based, system-level modeling; improved understanding of seismic hazard; and actions to reduce earthquake risk and promote resilience. The Center is a consortium of institutions that coordinates earthquake system science within Southern California. SCEC's long-term goal is to understand how seismic hazards change across all time scales of scientific and societal interest, from millennia to seconds. The fourth phase of SCEC (SCEC4) will move earthquake science forward through highly integrated collaborations that are coordinated across scientific disciplines and research institutions and enabled by high-performance computing and advanced information technology. It will focus on six fundamental problems of earthquake physics:

1. Stress transfer from plate motion to crustal faults: long-term fault slip rates.
2. Stress-mediated fault interactions and earthquake clustering: evaluation of mechanisms.
3. Evolution of fault resistance during seismic slip: scale-appropriate laws for rupture modeling.
4. Structure and evolution of fault zones and systems: relation to earthquake physics.
5. Causes and effects of transient deformations: slow slip events and tectonic tremor.
6. Seismic wave generation and scattering: prediction of strong ground motions.

The six fundamental problems constitute the basic-research focus of SCEC. They are interrelated and require an interdisciplinary, multi-institutional approach. Interdisciplinary research initiatives will focus on special fault study areas, the development of a community geodetic model for Southern California, and a community stress model. The latter will be a new platform where the various constraints on earthquake-producing stresses can begin to be integrated. Improvements will be made to SCEC's unified structural representation and its statewide extensions.

Collaboration Plan. On February 1, 2012, the Southern California Earthquake Center (SCEC) transitioned from SCEC3 to SCEC4 under joint funding from NSF/EAR and the U.S. Geological Survey. SCEC4 is funded for the period February 2012 through January 2017. This document, referred to as the Collaboration Plan, solicits proposals from individuals and groups to participate in the second year of the SCEC4 research program.

II. Guidelines for Proposal Submission

- A. **Due Date.** Monday, November 5, 2012, 5:00 pm PST. Late proposals will not be accepted. Note the different deadline for submitting annual progress reports below.
- B. **Delivery Instructions.** Proposals must be submitted through the SCEC Proposal Submission System, accessible at <http://www.scec.org/proposals>. See "Formatting Instructions" below for requirements and procedure for submitting proposals.
- C. **Formatting Instructions.**

Cover Page. The cover page should be headed with the words "2013 SCEC Proposal" and include the Project Title, Principal Investigator(s), Institutional Affiliation(s), Amount of Request per Investigator, Total Amount of Request, and Proposal Category (see Section IV). Collaborative proposals involving multiple investigators and/or institutions should list all Principal Investigators. Proposals do not need to be formally signed by institutional representatives, and should be for one year, with a start date of February 1, 2012. Also on the cover page, list - in order of priority - three SCEC science objectives (Section VII) that your proposal addresses (e.g. 1a, 3c and 4b). If your proposal includes undergraduate student funding, please be sure to note this on the cover page.

Technical Description. In five pages maximum (including figures), describe the technical details of the proposed project and how it relates to the short-term objectives outlined in the SCEC Research Priorities and Requirements (Section VII). If the proposed project is a continuation of a previously funded SCEC project, the technical description must also include a one-page summary of previous research results. This research summary is part of the five-page limit. References are not included in the five-page limit. See note below on submission of collaborative proposals.

Budget Page. Budgets and budget explanations should be constructed using NSF categories (http://www.nsf.gov/pubs/policydocs/pappguide/nsf11001/gpg_2.jsp). Under guidelines of the SCEC

Cooperative Agreements and A-21 regulations, secretarial support and office supplies are not allowable as direct expenses.

Current Support. Statements of current support should be included for each Principal Investigator, following NSF guidelines (http://www.nsf.gov/pubs/policydocs/pappguide/nsf11001/gpg_2.jsp). Any proposal without a current and pending support statement will not be reviewed.

Labeling the Submitted PDF Proposal. Proposals must be submitted as PDF documents and follow the SCEC proposal naming convention. Investigators must label their proposals with their last name followed by 2013 (e.g. Beroza2013.pdf). If there is more than one proposal, then the file should be labeled as follows: Beroza2013_1.pdf (for the 1st proposal) and Beroza2013_2.pdf (for the 2nd proposal).

2011 Annual Progress Report. Scientists funded by SCEC in 2012 must submit a progress report by March 15, 2013 (5:00 pm PST). Submission of this report is critical to preparing the annual progress report to the funding agencies. **To receive 2013 SCEC funding, all prior SCEC-funded project reports must be submitted and up to date.** Reports should be a maximum of five pages (text and figures). Reports should include references to any SCEC publication during the past year (including papers submitted and in review), including their SCEC contribution number. Publications are assigned numbers when they are submitted to the SCEC publication database (via <http://www.scec.org/signin>).

Special Note on Workshop Reports. Reports on results and recommendations of workshops funded by SCEC in 2013 are to be submitted no later than 30 days following the completion of the workshop. The reports will be posted on the SCEC website as soon as possible after review by SCEC directors.

- D. **Principal Investigator Responsibilities.** Principal investigators are expected to interact with other SCEC scientists on a regular basis (e.g., by attending the annual meeting, workshops and working group meetings) and to contribute data, analysis results, and/or models to the appropriate SCEC data center (e.g., Southern California Earthquake Data Center—SCEDC), database, or community model (e.g., Community Velocity Model—CVM). Publications resulting entirely or partially from SCEC funding must include a publication number (<http://www.scec.org/core/cis/pubsearch.php>). By submitting a proposal, investigators are agreeing to these conditions.
- E. **Eligibility.** Proposals can be submitted by eligible Principal Investigators from:
- U.S. academic institutions
 - U.S. private corporations
 - International institutions (funding will mainly be for travel to SCEC-sponsored meetings in the U.S.). Due to limited funding, requests for travel to the SCEC annual meeting must be cost shared by the international participants. Cost sharing should be described in the proposal.
- F. **Collaborative Proposals.** Collaborative proposals with investigators from the USGS are encouraged. USGS employees should submit their requests for support through USGS channels.
- Collaborative proposals involving multiple investigators and/or institutions are strongly encouraged. A collaborative proposal should be submitted only by the lead investigator. Information on all investigators (including budgets and current support statements) must be included in the proposal submission. Collaborative proposals may include one extra page per investigator to report results of previous research.
- G. **Budget Guidance.** Typical SCEC grants funded under this Science Plan fall in the range of \$10,000 to \$35,000. This is not intended to limit SCEC to a fixed award amount, nor to a specified number of awards, rather it is intended to calibrate expectations for proposals written by first-time SCEC investigators. **Field research investigations outside southern California will not be supported.**
- H. **Award Procedures.** The Southern California Earthquake Center is funded by the National Science Foundation and the U.S. Geological Survey through a cooperative agreement with the University of Southern California. All awards will be funded by subcontract from the University of Southern California.

III. SCEC Organization

A. **Mission and Science Goal.** SCEC is an interdisciplinary, regionally focused organization with a mission to:

- Gather data on earthquakes in Southern California and other places where such data has direct relevance to southern California
- Integrate information into a comprehensive, physics-based understanding of earthquake phenomena
- Communicate understanding to the world at large as useful knowledge for reducing earthquake risk

SCEC's primary science goal is to develop a comprehensive, physics-based understanding of earthquake phenomena in Southern California through integrative, multidisciplinary studies of plate-boundary tectonics, active fault systems, fault-zone processes, dynamics of fault ruptures, ground motions, and seismic hazard analysis.

B. **Disciplinary Activities.** The Center sustains disciplinary science through standing committees in Seismology, Geodesy, Geology, and Computational Science. These committees will be responsible for planning and coordinating disciplinary activities relevant to the SCEC Science Collaboration Plan, and they will make recommendations to the SCEC Planning Committee regarding support of disciplinary research and infrastructure. High-priority disciplinary activities are summarized in Section VIII.

C. **Interdisciplinary Focus Areas.** Interdisciplinary research is organized into science focus areas: Unified Structural Representation (USR), Fault and Rupture Mechanics (FARM), Stress and Deformation Over Time (SDOT), Earthquake Forecasting and Predictability (EFP), Ground Motion Prediction (GMP), Southern San Andreas Fault Evaluation (SOSAFE), and Earthquake Engineering Implementation Interface (EII). High-priority activities are listed for each of these interdisciplinary focus areas in Section IX.

D. **Technical Activity Groups.** Various groups of experts have formed Technical Activity Groups (TAGs) to verify the complex computer calculations needed for wave propagation and dynamic rupture problems, to assess the accuracy and resolving power of source inversions, and to develop geodetic transient detectors and earthquake simulators. TAGs can be thought of as "mini-collaboratories" that pose well-defined "standard problems", encourage solution of these problems by different researchers using different algorithms or codes, develop a common cyberspace for comparing solutions, and facilitate meetings to discuss discrepancies and potential improvements.

E. **Communication, Education, and Outreach.** The theme of the CEO program during SCEC4 is *Creating an Earthquake and Tsunami Resilient California*. CEO will continue to manage and expand a suite of successful activities along with new initiatives, within four CEO interconnected thrust areas:

- a. The *Implementation Interface* connects SCEC scientists with partners in earthquake engineering research, and communicates with and trains practicing engineers and other professionals.
- b. The *Public Education and Preparedness* thrust area educates people of all ages about earthquakes, and motivates them to become prepared.
- c. The *K-14 Earthquake Education Initiative* seeks to improve earth science education and school earthquake safety.
- d. Finally, the *Experiential Learning and Career Advancement* program provides research opportunities, networking, and more to encourage and sustain careers in science and engineering.

Opportunities for participating in the CEO program are described in Section XI.

IV. Proposal Categories

A. **Data Gathering and Products.** SCEC coordinates an interdisciplinary and multi-institutional study of earthquakes in Southern California, which requires data and derived products pertinent to the region. Proposals in this category should address the collection, archiving and distribution of data, including the production of SCEC community models that are online, maintained, and documented resources for making data and data products available to the scientific community.

B. **Integration and Theory.** SCEC supports and coordinates interpretive and theoretical investigations on earthquake problems related to the Center's mission. Proposals in this category should be for the integration of data or data products from Category A, or for general or theoretical studies. Proposals in Categories A and B should address one or more of the goals in Section VII, and may include a brief description (<200 words) as to how the proposed research and/or its results might be used in a special initiative (see Section X) or in education and/or outreach (see Section XI).

- C. **Special Fault Study Areas.** Special Fault Study Areas (SFSA) are integrated, multidisciplinary projects focused on areas of complex fault behavior within southern California. There are two primary goals of SFSA, as articulated in the SCEC4 proposal: (1) To understand how fault complexities affect the propagation of earthquake ruptures and the heterogeneity of stress in the crust, and (2) To investigate how tremor and microseismicity (including induced seismicity) affect the nucleation of large earthquakes. Tackling these problems will require the assembly of teams of researchers with diverse expertise. For example, research areas of fault complexity may seek to merge geological, seismological, and potential-field data to elucidate fault structure and paleoseismic history, integrate this information with geodetic data to derive fault loading and stressing rates, and apply dynamic rupture simulations to explore how earth structure and rupture history affect the potential sizes of future earthquakes. One of the anticipated advantages of SFSA is to leverage the impact of new and/or densified instrumentation. It is expected that collaborations built around SFSA will be open to the community, and generate open community data sets.

- *SFSA Science Plans:* Starting this year, an additional requirement for these and any new SFSA will be a SFSA Science Plan that describes the general structure and scientific questions to be addressed by the group. Groups that are interested in formalizing SFSA for 2013 are encouraged to self-organize and develop Science Plans now or propose a workshop (through the standard SCEC workshop proposal process) to explore a new SFSA. SFSA Science Plans should be developed and written by a group of SCEC investigators and be on the order of 2 pages long. They are due with the SCEC 2013 proposals in early November. The plans should detail:
- Identification of key questions and research targets that address fundamental problems in earthquake science with an interdisciplinary plan for achieving these goals within SCEC4
- Discussion of integrative activities and broader impacts
- Assessment of resources needed to achieve these goals and identification of outside resources that may be required
- Timeline identifying short and long term goals and completion date

SCEC 2013 Proposals associated with a SFSA: Each PI will submit a separate, standard 5 page SCEC proposal for 2013 that clearly ties the investigator's work to the Science Plan, provides additional background and details on the data collection and/or analyses to be completed by that investigator, and a budget for that investigator. Each investigator's proposal will be evaluated separately through the standard SCEC proposal process (see SCEC Science Collaboration Plan 2013). Workshop proposals for activities around the SFSA should be developed according to the standard workshop proposal process as outlined in the 2013 Collaboration Plan. The SFSA website (<http://www.scec.org/research/sfsa.html>) contains details about the SFSA process and structure, updates from proposed SFSA, and contact information.

- D. **Workshops.** SCEC participants who wish to host a workshop between February 1, 2012 and January 31, 2013 should submit a proposal for the workshop in response to this Collaboration Plan.

Please notify Tran Huynh (scecmeet@usc.edu) before submitting the proposal if you want to organize a workshop around the time of the SCEC Leadership Retreat (June) or SCEC Annual Meeting (September). Note that workshops scheduled in conjunction with the SCEC Annual Meeting are restricted to half-day session only.

Workshops in the following topics are particularly relevant:

- Organizing collaborative research efforts for the five-year SCEC program (2012-2017). In particular, interactive workshops that engage more than one focus and/or disciplinary group are strongly encouraged.
- Engaging earthquake engineers and other partner and user groups in SCEC-sponsored research.
- Participating in national initiatives such as EarthScope, the Advanced National Seismic System (ANSS), and the George E. Brown, Jr. Network for Earthquake Engineering Simulation (NEES).

- E. **Communication, Education, and Outreach.** SCEC has developed a long-range CEO plan and opportunities for participation are listed in Section XI. Investigators who are interested in participating in this program should contact Mark Benthien (213-740-0323; benthien@usc.edu) before submitting a proposal.

- F. **SCEC/SURE Intern Project.** Each year SCEC coordinates the Summer Undergraduate Research Experience (SCEC/SURE) Program, which supports undergraduate students working one-on-one with SCEC scientists on diverse research projects. Recruitment for SURE intern mentors begins in the fall. Potential research projects are published on the SCEC Internships website (<http://www.scec.org/internships>), where undergraduate students may apply and identify their preferred projects. Interested SCEC scientists are encouraged to include support for an undergraduate SURE intern in their SCEC proposals. SURE mentors are required to provide at

least \$2500 of the \$5000 intern stipend. Mentor contributions can come from any source, including SCEC-funded research projects.

Questions about the SCEC/SURE Program should be referred to Robert de Groot (degroot@usc.edu).

If your proposal includes undergraduate student funding, please be sure to note this on the cover page.

- G. **SCEC Annual Meeting participation.** This category includes proposals by investigators requesting travel funding only for participation at the SCEC Annual Meeting. Investigators who are (a) already funded to study projects that would be of interest to the SCEC community, and/or (b) new to SCEC who would benefit from exposure to the SCEC Annual Meeting in order to fine-tune future proposals are encouraged to apply.

V. Evaluation Process and Criteria

- A. Proposals should be responsive to the Collaboration Plan. A primary consideration in evaluating proposals will be how directly the proposal addresses the main objectives of SCEC. Important criteria include (not necessarily in order of priority):
1. Scientific merit of the proposed research,
 2. Competence and performance of the investigators, especially in regard to past SCEC-sponsored research,
 3. Priority of the proposed project for short-term SCEC objectives as stated in the Collaboration Plan,
 4. Promise of the proposed project for contributing to long-term SCEC goals,
 5. Commitment of the principal investigator and institution to the SCEC mission,
 6. Value of the proposed research relative to its cost,
 7. Ability to leverage the cost of the proposed research through other funding sources,
 8. Involvement of students and junior investigators,
 9. Involvement of women and underrepresented groups, and
 10. Innovative or "risky" ideas that have a reasonable chance of leading to new insights or advances in earthquake physics and/or seismic hazard analysis.
- B. Proposals may be strengthened by describing:
1. Collaboration
 - Within a disciplinary or focus group
 - Between disciplinary and/or focus groups
 - In modeling and/or data gathering activities
 - With engineers, government agencies, and others.
 2. Leveraging additional resources
 - From other agencies
 - From your institution
 - By expanding collaborations
 3. Development and delivery of products
 - Community research tools, models, and databases
 - Collaborative research reports
 - Papers in research journals
 - End-user tools and products
 - Workshop proceedings and CDs
 - Fact sheets, maps, posters, public awareness brochures, etc.
 - Educational curricula, resources, tools, etc.
 4. Educational opportunities

DRAFT 2013 SCIENCE PLAN

- Graduate student research assistantships
 - Undergraduate summer and year-round internships (funded by the project)
 - K-12 educator and student activities
 - Presentations to schools near research locations
 - Participation in data collection
- C. All research proposals will be evaluated by the appropriate disciplinary committees and focus groups, the Science Planning Committee, and the Center Director. CEO proposals will be evaluated by the CEO Associate Director and the Center Director.
- D. The Science Planning Committee is chaired by the Deputy Director and comprises the chairs of the disciplinary committees, focus groups, and special projects. It is responsible for recommending a balanced science budget to the Center Director.
- E. Recommendations of the planning committees will be combined into an annual spending plan and forwarded to the SCEC Board of Directors for approval.
- F. Final selection of research projects will be made by the Center Director, in consultation with the Board of Directors.
- G. The review process should be completed and applicants notified by the end of February 2012.

VI. Coordination of Research between SCEC and USGS-EHRP

Earthquake research in Southern California is supported both by SCEC and by the USGS Earthquake Hazards Program (EHP). EHP's mission is to provide the scientific information and knowledge necessary to reduce deaths, injuries, and economic losses from earthquakes. Products of this program include timely notifications of earthquake locations, size, and potential damage, regional and national assessments of earthquake hazards, and increased understanding of the cause of earthquakes and their effects. EHP funds research via its External Research Program, as well as work by USGS staff in its Pasadena, Menlo Park, and Golden offices. The EHP also directly supports SCEC.

SCEC and EHP coordinate research activities through formal means, including USGS membership on the SCEC Board of Directors and a Joint Planning Committee, and through a variety of less formal means. Interested researchers are invited to contact Dr. Rob Graves, EHP coordinator for Southern California, or other SCEC and EHP staff to discuss opportunities for coordinated research.

The USGS EHP supports a competitive, peer-reviewed, external program of research grants that enlists the talents and expertise of the academic community, state and local governments, and the private sector. The investigations and activities supported through the external program are coordinated with and complement the internal USGS program efforts. This program is divided into six geographical/topical 'regions', including one specifically aimed at Southern California earthquake research and others aimed at earthquake physics and effects and at probabilistic seismic hazard assessment (PSHA). The Program invites proposals that assist in achieving EHP goals.

The EHP web page, <http://earthquake.usgs.gov/research/external/>, describes program priorities, projects currently funded, results from past work, and instructions for submitting proposals. The EHP external funding cycle is several months offset from SCEC's, with the RFP due out in February and proposals due in May. Interested PIs are encouraged to contact the USGS regional or topical coordinators for Southern California, Earthquake Physics and Effects, and/or National (PSHA) research, as listed under the "Contact Us" tab.

The USGS internal earthquake research program is summarized by topic at <http://earthquake.usgs.gov/research/topics.php>.

VII. SCEC4 Fundamental Problems of Earthquake Physics: Research Priorities and Requirements

The six fundamental problems constitute the basic-research focus of SCEC4 and are listed in the preamble. They are interrelated and require an interdisciplinary, multi-institutional approach. Interdisciplinary research initiatives will focus on special fault study areas, the development of a community geodetic model for Southern California, and a community stress model. The latter will be a new platform where the various constraints on earthquake-producing stresses can begin to be integrated. Improvements will be made to SCEC's unified structural representation and its statewide extensions.

1. *Stress transfer from plate motion to crustal faults: long-term fault slip rates.*

Priorities and Requirements

1a. Mapping and studying faults in Southern California for which brittle/ductile transitions have been exposed by detachment faulting or erosion.

1b. Focused laboratory, numerical, and geophysical studies of the character of the lower crust, its rheology, stress state, and expression in surface deformation. We will use surface-wave dispersion to improve depth resolution relative to teleseismic studies.

1c. Regional searches for seismic tremor at depth in Southern California to observe if (some) deformation occurs by slip on discrete structures.

1d. Development of a Community Geodetic Model (CGM) for California, in collaboration with the UNAVCO community, to constrain long-term deformation and fault-slip models.

1e. Combined modeling/inversion studies to interpret GPS and InSAR geodetic results on postseismic transient deformation without traditional simplifying assumptions.

2. *Stress-mediated fault interactions and earthquake clustering: evaluation of mechanisms*

Priorities and Requirements

2a. Improvement of earthquake catalogs, including non-point-source source descriptions, over a range of scales. Traditional aftershock catalogs can be improved through better detection of early aftershocks. Long-term (2000-yr) earthquake chronologies, including slip-per-event data, for the San Andreas Fault system are necessary to constrain long-term clustering behavior.

2b. Improved descriptions of triggered earthquakes. While temporal earthquake clustering behavior (Omori's Law) is well known, the spatial and coupled temporal-spatial behavior of triggered earthquakes, potentially key diagnostics, are not well constrained.

2c. Lowered thresholds for detecting aseismic and infraseismic transients, and improved methods for separating triggering by aseismic transients from triggering by other earthquakes.

2d. Development of a Community Stress Model (CSM) for Southern California, based on merging information from borehole measurements, focal mechanisms, paleo-slip indicators, observations of damage, topographic loading, geodynamic and earthquake-cycle modeling, and induced seismicity. We will use seismicity to constrain CSM and investigate how stress may control earthquake clustering and triggering. We plan to collaborate with other organizations in fault-drilling projects for in situ hypothesis testing of stress levels.

2e. Development of physics-based earthquake simulators that can unify short-term clustering statistics with long-term renewal statistics, including the quasi-static simulators that incorporate laboratory-based nucleation models.

2f. Better understanding of induced seismicity, specifically induced by geothermal power production in the Salton Sea area, which warrant study as potential hazards.

3. *Evolution of fault resistance during seismic slip: scale-appropriate laws for rupture modeling*

Priorities and Requirements

3a. Laboratory experiments on fault materials under appropriate confining stresses, temperatures, and fluid presence through targeted experiments in collaboration with rock mechanics laboratories.

3b. Search for geological, geochemical, paleo-temperature, and hydrological indicators of specific resistance mechanisms that can be measured in the field. In particular, we will look for evidence of thermal decomposition in exhumed fault zones.

3c. Theoretical and numerical modeling of specific fault resistance mechanisms for seismic radiation and rupture propagation, including interaction with fault roughness and damage-zone properties. At the scale of meters to hundreds of meters, the behavior of the near-fault layer with evolving damage may have to be included in the fault constitutive relations.

3d. Development of parameterized fault rheologies suitable for coarse-grained numerical modeling of rupture dynamics and for simulations of earthquake cycles on interacting fault systems. Currently, the constitutive laws for co-seismic slip are often represented as complex coupled systems of partial differential equations, contain slip scales of the order of microns to millimeters, and hence allow detailed simulations of only small fault stretches.

3e. Dynamic rupture modeling to constrain stress levels along major faults, explain the heat-flow paradox, and understand extreme slip localization, the dynamics of self-healing ruptures, and the potential for repeated slip on the fault during the earthquake. We will collaborate with other organizations in fault-drilling projects to measure temperature on faults before and after earthquakes and thus constrain co-seismic resistance.

3f. Development of earthquake simulators that can incorporate realistic models of fault-resistance evolution during the earthquake cycle.

4. *Structure and evolution of fault zones and systems: relation to earthquake physics*

Priorities and Requirements

4a. Establishment of special fault study areas for detailed geologic, seismic, geodetic, and hydrologic investigations of fault complexities

4b. Investigations of along-strike variations in fault roughness and complexity as well as the degree of localization and damage perpendicular to the fault.

4c. Improvements to the CFM using better mapping, including LIDAR, and precise earthquake relocations. We will also extend the CFM to include spatial uncertainties and stochastic descriptions of fault heterogeneity.

4d. Use of special fault study areas to model stress heterogeneities both deterministically and stochastically. We will integrate the results of these special studies into the CSM.

4e. Use of earthquake simulators and other modeling tools, together with the CFM and CSM, to quantify how large-scale fault system complexities govern the probabilities of large earthquakes and rupture sequences.

5. *Causes and effects of transient deformations: slow slip events and tectonic tremor*

Priorities and Requirements

5a. Improvement of detection and mapping of the distribution of tremor across southern California by applying better instrumentation and signal-processing techniques to data collected in the special study areas, such as those outlined in the proposal.

5b. Application of geodetic detectors to the search for aseismic transients across southern California. We will use the CGM as the time-dependent geodetic reference frame for detecting geodetic anomalies.

5c. Collaboration with rock mechanics laboratories on laboratory experiments to understand the mechanisms of slow slip and tremor.

5d. Development of physics-based models of slow slip and tectonic tremor. We will constrain these models using features of tremor occurrence and its relationship to seismicity, geodetic deformation, and tectonic environment, as well as laboratory data.

5e. Use of physics-based models to understand how slow slip events and tremor activity affect earthquake probabilities in Southern California.

6. *Seismic wave generation and scattering: prediction of strong ground motions*

Priorities and Requirements

6a. Development of a statewide anelastic Community Velocity Model (CVM) that can be iteratively refined through 3D waveform tomography. We will extend current methods of full-3D tomography to include ambient-noise data and to estimate seismic attenuation, and we will develop methods for estimating and representing CVM uncertainties.

6b. Modeling of ruptures that includes realistic dynamic weakening mechanisms, off-fault plastic deformation, and is constrained by source inversions. The priority is to produce physically consistent rupture models for broadband ground motion simulation. An important issue is how to treat multiscale processes; specifically, does off-fault plasticity regularize the Lorentzian scale collapse associated with strong dynamic weakening? If not, how can adaptive meshing strategies be most effectively used to make full-physics simulations feasible?

6c. Develop stochastic representations of small-scale velocity and attenuation structure in the CVM for use in modeling high-frequency (> 1 Hz) ground motions. We will test the stochastic models with seismic and borehole logging data and evaluate their transportability to regions of comparable geology.

6d. Measure earthquakes with unprecedented station density using emerging sensor technologies (e.g., MEMS). The SCEC Portable Broadband Instrument Center will work with IRIS to make large portable arrays available for aftershock and flexible array studies.

6e. Collaborate with the engineering community in validation of ground motion simulations. We will establish confidence in the simulation-based predictions by continuing to work with engineers in validating the simulations against empirical attenuation models and exploring coherency and other standard engineering measures of ground motion properties.

VIII. Disciplinary Activities

The Center will sustain disciplinary science through standing committees in Seismology, Geodesy, Geology, and Computational Science. These committees will be responsible for planning and coordinating disciplinary activities relevant to the SCEC Science Collaboration Plan, and they will make recommendations to the SCEC Planning Committee regarding the support of disciplinary infrastructure. High-priority disciplinary objectives include the following tasks:

A. Seismology

Objectives

The objectives of the Seismology group are to gather data on the range of seismic phenomena observed in southern California and to integrate these data into physics-based models of fault slip. Of particular interest are proposals that foster innovations in network deployments, data collection, real-time research tools, and data processing. Proposals that provide community products that support one or more of the SCEC4 goals or those that include collaboration with network operators in Southern California are especially encouraged. Proposers should consider the SCEC resources available including the Southern California Earthquake Data Center (SCEDC) that provides extensive data on Southern California earthquakes as well as crustal and fault structure, the network of SCEC funded borehole instruments that record high quality reference ground motions, and the pool of portable instruments that is operated in support of targeted deployments or aftershock response.

Example Research Strategies

- Enhancement and continued operation of the SCEDC and other existing SCEC facilities particularly the near-real-time availability of earthquake data from SCEDC and automated access.
- Real-time processing of network data such as improving the estimation of source parameters in relation to faults, especially evaluation of the short-term evolution of earthquake sequences and real-time stress perturbations on major fault segments.
- Enhance or add new capabilities to existing earthquake early warning (EEW) systems or develop new EEW algorithms. Develop real-time finite source models constrained by seismic and GPS data to estimate evolution of rupture and potentially damaging ground shaking; develop strategies for robust uncertainty quantification in finite-fault rupture models.
- Advance innovative and practical strategies for densification of seismic instrumentation, including borehole instrumentation, in Southern California and develop innovative algorithms to utilize data from these networks. Develop metadata, archival and distribution models for these semi-mobile networks.
- Develop innovative methods to search for unusual signals using combined seismic, GPS, and borehole strainmeter data; collaborations with EarthScope or other network operators are encouraged.
- Investigate near-fault crustal properties, evaluate fault structural complexity, and develop constraints on crustal structure and state of stress.
- Collaborations, for instance with the ANSS and NEES projects, that would augment existing and planned network stations with downhole and surface instrumentation to assess site response, nonlinear effects, and the ground coupling of built structures.
- Preliminary design and data collection to seed future passive and active experiments such as dense array measurements of basin structure and large earthquake properties, OBS deployments, and deep basement borehole studies.

Priorities for Seismology in 2012

1. **Tremor.** Tremor has been observed on several faults in California, yet it does not appear to be ubiquitous. We seek proposals that explore the distribution and source characteristics of tremor in California and those that explore the conditions necessary for the generation of seismically observable tremor.
2. **Low-cost seismic network data utilization and archiving.** Several groups are developing seismic networks that use low-cost MEMS accelerometers. We seek proposals that would address development of seismological algorithms to utilize data from these networks in innovative ways. We also seek proposals that would develop metadata and archiving models for these new semi-mobile networks, as well as archive and serve these data to the SCEC user community.
3. **Short-Term Earthquake Predictability.** We seek proposals that develop new methods in earthquake statistics or analyze seismicity catalogs to develop methods for determining short-term (hours to days) earthquake probability gain.

B. Tectonic Geodesy

Tectonic Geodesy activities in SCEC4 will focus on data collection and analysis that contribute to improved earthquake response and to a better understanding of fault loading and stress transfer, the causes and effects of transient deformation, and the structure and evolution of fault zones and systems. The following are research strategies aimed at meeting these broad objectives:

1. **Contribute to the development of a Community Geodetic Model (CGM).** The goal of this effort is to develop a time-dependent geodetic data product for southern California that leverages the complementary nature of GPS and InSAR time series data. The resulting product will consist of well-constrained, temporally and spatially dense horizontal and vertical displacement time series that can be used in meeting a variety of SCEC4 objectives. This will require development of optimal methods for combining GPS and InSAR data, characterizing seasonal/hydrologic/anthropogenic signals, incorporating new data, and accounting for earthquake effects as needed.

Data collection and analysis designed to address specific questions regarding geodetic/geologic slip rate discrepancies, to assess the role of lower crust/upper mantle processes in driving fault loading, to constrain more physically realistic deformation models, and to provide input to the development of Community Stress Models are also encouraged, as are studies that pursue integrated use of geodetic, geologic, seismic, and other observations targeting special fault study areas. Proposals for the development of new data products or collection of new data should explicitly motivate the need for such efforts and state how the resulting data or products will be used. Resulting data should be provided for inclusion in the CGM. In compliance with SCEC's data policy, data collected with SCEC funding must be made publically available upon collection by archiving at an appropriate data center (e.g., UNAVCO or SCEC). Annual reports should include a description of archive activities.

2. **Improve our understanding of the processes underlying detected transient deformation signals and/or their seismic hazard implications through data collection and development of new analysis tools.** Work that advances methods for near-real-time transient detection and applies these algorithms within the SCEC transient detection testing framework to search for transient deformation in southern California is encouraged. Approaches that can be automated or semi-automated are the highest priority, as is their inclusion in the testing framework now in place at SCEC. Extension of methods to include InSAR and strainmeter data and, when available, the CGM is also a priority.

Targeted collection and analysis of all types of geodetic data to constrain physics-based models of slow slip and tremor, as well as work that develops means for incorporating the output of transient detection algorithms into time-dependent earthquake forecasting, are also encouraged.

Develop and apply algorithms that use real-time high-rate GPS data in concert with seismic data for improved earthquake response.

C. Earthquake Geology

Objectives

The Earthquake Geology Disciplinary Committee promotes studies of the geologic record of the Southern California natural laboratory that advance SCEC science. Its primary focus is on the Late Quaternary record of faulting and ground motion, including data gathering in response to major earthquakes. Geologic observations provide important contributions, either directly or indirectly, to all six of the fundamental problems in earthquake physics identified in the SCEC4 proposal. Earthquake Geology also fosters research activities motivated by outstanding seismic hazard issues, understanding of the structural framework and earthquake history of special fault study areas (see Section VII, Problem 4), or will contribute significant information to the statewide Unified Structural Representation. Collaborative proposals that cut across disciplinary boundaries are encouraged.

Example Research Strategies

- Gathering well-constrained slip-rates on the southern California fault system, with emphasis on major structures (Problem 1).
- Mapping and analysis of fault-zone properties where the seismogenic zone or brittle-ductile transition has been exhumed (Problems 1a, 3b).
- Paleoseismic documentation of earthquake ages and displacements, with emphasis on long paleoseismic histories, slip-per-event, and slip-rate histories, including a coordinated effort to develop slip rates and slip-per-event history of southern San Andreas fault system (Problem 2a, in collaboration with the SoSAFE focus group).

- Studies to improve understanding of special fault study areas (Problem 4a) or to improve the statewide community fault model, especially that take advantage of high-resolution topographic data sets to better define fault traces, spatial uncertainty, and stochastic heterogeneity of fault geometry (Problem 4c).
- Quantifying along-strike variations in fault roughness, complexity, strain localization, and damage in relation to the rupture propagation processes, including evaluation of the investigating the processes and likelihood of multi-fault ruptures (Problem 4b).
- Validation of ground motion prediction through analysis and dating of precariously balanced rocks and other fragile geomorphic features (Problem 6).

Geochronology Infrastructure

The shared geochronology infrastructure supports C-14, optically stimulated luminescence (OSL), and cosmogenic dating for SCEC-sponsored research. The purpose of shared geochronology infrastructure is to allow flexibility in the number and type of dates applied to each SCEC-funded project as investigations proceed. Investigators requesting geochronology support should clearly state in their proposal an estimate of the number and type of dates required. For C-14 specify if sample preparation will take place at a location other than the designated laboratory. For cosmogenic dating, investigators are required to arrange for sample preparation. Sample preparation costs must be included in the proposal budget unless preparation has been pre-arranged with one of the laboratories listed. Investigators are strongly encouraged to contact the investigators at the collaborating laboratories prior to proposal submission. Currently, SCEC geochronology has established relationships with the following laboratories:

- C-14: University of California at Irvine (John Southon, jsouthon@uci.edu) and Lawrence Livermore National Laboratory (Tom Guilderson, tguilderson@llnl.gov),
- OSL: University of Cincinnati (Lewis Owen, lewis.owen@uc.edu) and Utah State University (Tammy Rittenour, tammy.rittenour@usu.edu), and
- Cosmogenic: Lawrence Livermore National Laboratory (Susan Zimmerman, zimmerman17@llnl.gov).

Investigators may alternatively request support for geochronology outside of the infrastructure proposal for methods not listed here or if justified on a cost-basis. These outside requests must be included in the individual proposal budget. Please direct questions regarding geochronology infrastructure to the Earthquake Geology group co-leader, Mike Oskin (meoskin@ucdavis.edu).

Data Reporting Requirements

Studies under Earthquake Geology gather diverse data that are at times challenging to consistently archive per NSF data reporting requirements. Under SCEC4, PIs will be required to provide full reporting of their geochronology samples, including raw data, interpreted age, and geographic/stratigraphic/geomorphic context (what was dated?). This reporting requirement will be coordinated with the geochronology infrastructure program. A priority at the outset of SCEC4 is to do define additional, achievable goals for geology data reporting to be followed by Earthquake Geology community.

Priorities for Earthquake Geology

- Establish research strategies for special fault study areas and begin data collection.
- Prioritize and coordinate research objectives with respect to SoSAFE focus group goals, targets for slip-rate studies, and mechanisms to achieve progress on exhumed fault-zone problems.
- Define consistent and achievable data reporting requirements for Earthquake Geology in SCEC4. Archive data from SCEC3.
- Improve understanding of the seismogenic faults along the coast and offshore. Search for possible tsunami deposits from offshore sources, including both faults and landslides.

D. Computational Science

Objectives

The Computational Science group promotes the use of advanced numerical modeling techniques and high performance computing (HPC) to address the emerging needs of SCEC users and application community on HPC platforms. The group works with SCEC scientists across a wide range of topics to take advantage of rapidly changing computer architectures and algorithms. It also engages and coordinates with HPC labs/centers as well as the vendor community in crosscutting efforts enabling SCEC petascale computing milestones. The group encourages research using national supercomputing resources, and supports students from both geoscience and computer science backgrounds to develop their skills in the area. Projects

DRAFT 2013 SCIENCE PLAN

listing Computational Science as their primary area should involve HPC in some way; research utilizing standard desktop computing should list the most relevant non-Computational Science disciplinary or focus group as the primary area.

Example Research Strategies

1. Porting and optimization of high performance codes on new architectures, and utilize advanced high performance computing programming techniques such as hybrid MPI/OpenMP, MPI/CUDA, PGAS, and auto-tuning.
2. Novel algorithms for earthquake simulation, particularly those that either improve efficiency and accuracy or expand the class of problems that can be solved (e.g., adaptive mesh refinement).
3. Optimization of earthquake simulators that can resolve the faulting processes across the range of scales required to investigate stress-mediated fault interaction, including those caused by dynamic wave propagation, generate synthetic seismicity catalogs, and assess the viability of earthquake rupture forecasts.
4. Tools and algorithms for uncertainty quantification in large-scale inversion and forward-modeling studies, for managing I/O, data repositories, workflow and data analysis.
5. Data-intensive computing tools, including but not limited to 3D tomography, cross-correlation algorithms used in ambient noise seismology, and other signal processing techniques used, for example, to search for tectonic tremor.

Key Problems in Computational Science

1. Seismic wave propagation
 - Validate SCEC community velocity models.
 - Develop high-frequency simulation methods and investigate the upper frequency limit of deterministic ground motions.
 - Extend existing simulation methodologies to a set of stochastic wavefield simulation codes that can extend the deterministic calculations to frequencies as high as 20 Hz, providing the capability to synthesize “broadband” seismograms.
2. Tomography
 - Assimilate regional waveform data into the SCEC community velocity models.
3. Rupture dynamics
 - Evaluate proposed fault weakening mechanisms in large-scale earthquake simulations, determine if small-scale physics is essential or irrelevant, and determine if friction law parameters can be artificially enhanced without compromising ground motion predictions.
 - Evaluate different representations of source complexity, including stress heterogeneity, variability in frictional properties, fault geometrical complexity, and dynamic rupture propagation in heterogeneous media.
4. Scenario earthquake modeling
 - Model a suite of scenario ruptures, incorporating material properties and fault geometries from the unified structural representation projects.
 - Isolate causes of enhanced ground motion using adjoint-based sensitivity methods.
5. Data-intensive computing
 - Develop computational tools for advanced signal processing algorithms, such as those used in ambient noise seismology and tomography
6. Data-intensive computing
 - Develop computational tools for advanced signal processing algorithms, such as those used in ambient noise seismology and tomography

IX. Interdisciplinary Focus Areas

Interdisciplinary research will be organized into seven science focus areas: Unified Structural Representation (USR), Fault and Rupture Mechanics (FARM), Stress and Deformation Over Time (SDOT), Earthquake Forecasting and Predictability (EFP),

Ground Motion Prediction (GMP) Southern San Andreas Fault Evaluation (SOSAFE) and Earthquake Engineering Implementation Interface (EII). Collaboration within and across focus areas is strongly encouraged.

A. Unified Structural Representation (USR)

The Unified Structural Representation group develops three-dimensional models of active faults and earth structure (velocity, density, attenuation, etc.) for use in fault-system analysis, ground-motion prediction, and hazard assessment. This year's efforts will focus on (1) making improvements to existing community models (CVM, CFM) that will facilitate their uses in SCEC science, education, and post-earthquake response planning and (2) developing methods to represent smaller scale features, such as the detailed representations needed for the special fault study areas and stochastic variations of seismic velocities and attenuation structure.

- **Community Velocity Model (CVM).** Improve the current SCEC CVMs, with emphasis on more accurate representations of V_p , V_s , density, attenuation, and basin structure. Generate improved mantle V_p and V_s models, as well as more accurate descriptions of near-surface properties that can be incorporated into the models' geotechnical layers. Perform 3D waveform tomographic inversions and ambient noise analysis for evaluating and improving the CVMs. Develop and apply procedures (i.e., goodness-of-fit measures) for evaluating the existing and future models with data (e.g., waveforms, gravity) to distinguish alternative representations and quantify model uncertainties; apply these methods for well-recorded earthquakes in southern California to delineate areas where CVM updates are needed. Develop databases, models, and model building tools that will help facilitate expansion of the CVMs to statewide and plate-boundary scale velocity representations. These efforts should be coordinated with the SCEC CME special project.
- **Community Fault Model (CFM).** Improve and evaluate the CFM and statewide CFM (SCFM), placing emphasis on defining the geometry of major faults that are incompletely, or inaccurately, represented in the current model. Refine representations of the linkages among major fault systems. Extend the CFM to include spatial uncertainties and stochastic descriptions of fault heterogeneity. Evaluate the CFM with data (e.g., seismicity, seismic reflection profiles, geologic slip rates, and geodetic displacement fields) to distinguish alternative fault models. Update the CFM-R (rectilinear fault model) to reflect improvements in the CFM.
- **Unified Structural Representation (USR).** Develop better IT mechanisms for delivering the USR, particularly the CVM parameters and information about the model's structural components, to the user community for use in generating and/or parameterizing numerical models. Generate maps of geologic surfaces compatible with the CFM that may serve as strain markers in crustal deformation modeling and/or property boundaries in future iterations of the USR.

B. Fault and Rupture Mechanics (FARM)

The primary mission of the Fault and Rupture Mechanics focus group in SCEC4 is to develop physics-based models of the nucleation, propagation, and arrest of dynamic earthquake rupture. We specifically solicit proposals that will contribute to the six fundamental problems in earthquake physics defined in the SCEC 4 proposal and enhance understanding of fault system behavior through interdisciplinary investigation of the special fault study areas. We encourage researchers to address this mission through field, laboratory, and modeling efforts directed at characterizing and understanding the influence of material properties, geometric irregularities and heterogeneities in stress and strength over multiple length and time scales, and that will contribute to our understanding of earthquakes in the Southern California fault system.

Priorities for FARM in 2013

- Investigate the relative importance of different dynamic weakening and fault healing mechanisms, and the slip and time scales over which these mechanisms operate (3a, 3b, 3c, 3e).
- Determine the properties of fault cores and damage zones (1a, 1b, 3a, 3b, 4a, 4b) and characterize their variability with depth and along strike (1a, 1b, 4a, 4b) to constrain theoretical and laboratory studies, including width and particle composition of actively shearing zones, signatures of temperature variations, extent, origin and significance of on- and off-fault damage, healing, and poromechanical behavior.
- Determine the relative contribution of on- and off-fault damage to the total earthquake energy budget (3c, 4a, 4b), and the absolute levels of local and average stress (3e).
- Develop, test, and apply innovative source-inversion strategies to image the space-time rupture evolution of earthquakes reliably, propose source-inversion methods with minimal assumptions, and provide robust uncertainty quantification of inferred source parameters; collaboration with the Technical Activity Group (TAG) on Source Inversion Validation (SIV) is encouraged.
- Develop realistic descriptions of heterogeneity in fault geometry, rock properties, stresses and strains, and tractable ways to incorporate heterogeneity in numerical models of single dynamic rupture events and multiple earthquake cycles (3e, 3f, 4b, 4d, 6b). Test dynamic rupture modeling that incorporates these heterogeneities

first by verifying the computational algorithms with benchmark exercises of the Dynamic Rupture Code Verification Technical Activity Group (TAG), then by comparing the results with geological and geophysical observations.

- Understand the significance of fault zone characteristics and processes on fault dynamics (3a, 3b, 3c) and formulate constitutive laws for use in dynamic rupture models (3d).
- Evaluate the relative importance of fault structure, material properties, interseismic healing, and prior seismic and aseismic slip to earthquake dynamics, in particular, to rupture initiation, propagation, and arrest, and the resulting ground motions (3c, 3d, 3f).
- Characterize earthquake rupture, fault loading, degree of localization, and constitutive behavior at the base of and below the seismogenic zone (1a, 1b, 1e, 4a).
- Develop observations of slow slip events and non-volcanic tremors in southern California and understand their implications for constitutive properties of faults and overall seismic behavior (3a, 5a-5e).
- Assess the predictability of rupture direction and directivity of seismic radiation by collecting and analyzing field and laboratory data (4a, 4b), and conducting theoretical investigations to understand implications for strong ground motion.
- Develop physics-based models that can describe spatio-temporal patterns of seismicity (2e, 4e).
- Explore similarities between earthquakes and offshore landslide sources with the goal of better understanding their mechanics and the tsunami hazard from sources in southern California.

C. Stress and Deformation Over Time (SDOT)

The focus of the interdisciplinary focus group Stress and Deformation Over Time (SDOT) is to improve our understanding of how faults are loaded in the context of the wider lithospheric system evolution. SDOT studies these processes on timescales from 10s of Myr to 10s of yrs, using the structure, geological history, and physical state of the southern California lithosphere as a natural laboratory. The objective is to tie the present-day state of stress and deformation on crustal-scale faults and the lithosphere as a whole to the long-term, evolving lithospheric architecture, through 4D geodynamic modeling, constrained by the widest possible range of observables from disciplines including geodesy, geology, and geophysics.

One long-term goal is to contribute to the development of a physics-based, probabilistic seismic hazard analysis for southern California by developing and applying system-wide deformation models of lithospheric processes at time-scales down to the earthquake cycle. These deformation models require a better understanding of a range of fundamental questions such as the forces loading the lithosphere, the relevant rock rheology, fault constitutive laws, and the spatial distribution of absolute deviatoric stress. Tied in with this is a quest for better structural constraints, such as on density, Moho depths, thickness of the seismogenic layer, the geometry of lithosphere-asthenosphere boundary, as well as basin depths, rock type, temperature, water content, and seismic velocity and anisotropy.

Projects Solicited for SDOT

- Contributions to our understanding of geologic inheritance and evolution, and its relation to the three-dimensional structure and physical properties of present-day crust and lithosphere. Contributions to efforts of building a 4D model of lithospheric evolution over 10s of Myr for southern California.
- Seismological imaging of crust, lithosphere and upper mantle using interface and transmission methods with the goal of characterizing the 3D distribution of isotropic and anisotropic wave speed variations.
- Contributions to the development of a Community Stress Model (CSM), a set of spatio-temporal (4D) representations of the stress tensor in the southern California lithosphere.
- Geodynamic models of southern California dynamics to allow hypothesis testing on issues pertaining to post-seismic deformation, fault friction, rheology of the lithosphere, seismic efficiency, the heat flow paradox, stress and strain transients, fault system evolution, as tied in with stress and deformation measurements across scales.
- Development of models of interseismic and earthquake cycle deformation, including efforts to estimate slip rates on southern CA faults, fault geometries at depth, and spatial distribution of slip or moment deficits on faults. Assessments of potential discrepancies of models based on geodetic, geologic, and seismic data. Development of deformation models (fault slip rates and locking depths, off-fault deformation rates) for UCERF (Unified California Earthquake Rupture Forecast).
- Research into averaging, simplification, and coarse-graining approaches across spatio-temporal scales, addressing questions such as the appropriate scale for capturing fault interactions, the adequate representation of frictional behavior and dynamic processes in long-term interaction models, fault roughness, structure,

complexity and uncertainty. Modeling approaches may include analytical or semi-analytical methods, spectral approaches, boundary, finite, or distinct element methods, and a mix of these, and there are strong links with all other SCEC working groups, including FARM, Earthquake Simulators, and USR.

D. Earthquake Forecasting and Predictability (EFP)

The Earthquake Forecasting and Predictability (EFP) focus group coordinates five broad types of research projects: (1) the development of earthquake forecast methods, (2) the development of testing methodologies for evaluating the performance of earthquake forecasts, (3) expanding fundamental physical or statistical knowledge of earthquake behavior that may be relevant for forecasting earthquakes, (4) the development and use of earthquake simulators to understand predictability in complex fault networks, and (5) fundamental understanding of the limits of earthquake predictability.

We seek proposals that will increase our understanding of how earthquakes might be forecast, to what extent and precision earthquakes are predictable, and what is a physical basis for earthquake predictability. Proposals of any type that can assist in this goal will be considered. In order to increase the amount of analyzed data, and so decrease the time required to learn about predictability, proposals are welcome that deal with global data sets and/or include international collaborations.

For research strategies that plan to utilize the Collaboratory for the Study of Predictability (CSEP), see Section X to learn of its capabilities. Successful investigators proposing to utilize CSEP would be funded via core SCEC funds to adapt their prediction methodologies to the CSEP framework, to transfer codes to the externally accessible CSEP computers, and to be sure they function there as intended. Subsequently, the codes would be moved to the identical externally inaccessible CSEP computers by CSEP staff who will conduct tests against a variety of data as outlined in the CSEP description.

Priorities for EFP in 2013

- Support the development of statistical or physics-based real-time earthquake forecasts.
- Utilize and/or evaluate the significance of earthquake simulator results.
- Study how to properly characterize and estimate various earthquake-related statistical relationships (including the magnitude distribution, Omori law, aftershock productivity, etc.).
- Focus on understanding patterns of seismicity in time and space, as long as they are aimed toward understanding the physical basis of earthquake predictability.
- Develop useful measurement/testing methodology that could be incorporated in the CSEP evaluations, including those that address how to deal with observational errors in data sets.

E. Ground-Motion Prediction (GMP)

The primary goal of the Ground-Motion Prediction focus group is to develop and implement physics-based simulation methodologies that can predict earthquake strong-motion waveforms over the frequency range 0-10 Hz. Source characterization plays a vital role in ground-motion prediction. At frequencies less than 1 Hz, the methodologies should deterministically predict the amplitude, phase and waveform of earthquake ground motions using fully three-dimensional representations of Earth structure, as well as dynamic or dynamically compatible kinematic representations of fault rupture. At higher frequencies (1-10 Hz), the methodologies should predict the main character of the amplitude, phase and waveform of the motions using a combination of deterministic and stochastic representations of fault rupture and wave propagation.

Research Topics in GMP

- Developing and/or refining physics-based simulation methodologies, with particular emphasis on high frequency (1-10 Hz) approaches. This work could include implementation of simulation methodologies onto the Broadband Simulation Platform, or implementation of more efficient approaches in wave and rupture propagation schemes (in collaboration with CME), allowing accurate simulation of higher frequency ground motion.
- Waveform modeling of past earthquakes to validate and/or refine the structure of the Community Velocity Model (CVM) (in collaboration with USR). This includes exploration of the effects of statistical models of structural and velocity heterogeneities on the ground motion, the significance of the lowest (S-wave) velocities as frequencies increase, and development and validation of improved (possibly frequency-dependent) attenuation (intrinsic or scattering) models in physics-based simulations (in collaboration with USR).
- Incorporation of non-linear models of soil response, off-fault plasticity into physics-based simulation methodologies used to simulation ground motions at higher frequencies (>1Hz).
- Development of more realistic implementations of dynamic or kinematic representations of fault rupture, including simulation of higher frequencies (up to 10+ Hz). Possible topics include simulation of dynamic rupture on nonplanar faults and studying the effects of fault roughness on the resulting synthetic ground motion, and

DRAFT 2013 SCIENCE PLAN

development of kinematic representations based on statistical models constrained by observed and/or dynamic ruptures. This research could also include the examination of current source-inversion strategies and development of robust methods that allow imaging of kinematic and/or dynamic rupture parameters reliably and stably, along with a rigorous uncertainty assessment. Close collaboration with the Technical Activity Group (TAG) on Source Inversion Validation (SIV) is encouraged.

- Verification (comparison against theoretical predictions) and validation (comparison against observations) of the simulation methodologies with the objective to develop robust and transparent simulation capabilities that incorporate consistent and accurate representations of the earthquake source and three-dimensional velocity structure. Comparison of synthetic ground motions from deterministic and stochastic approaches to data for overlapping bandwidths. Close collaboration with the Technical Activity Group (TAG) on Ground Motion Simulation Validation (GMSV).

It is expected that the products of the Ground-Motion Prediction group will have direct application to seismic hazard analysis, both in terms of characterizing expected ground-motion levels in future earthquakes, and in terms of directly interfacing with earthquake engineers in the analysis of built structures. Activities within the Ground-Motion Prediction group will be closely tied to several focus areas, including the GMSV TAG, with particular emphasis on addressing ground motion issues related to seismic hazard and risk (see EEII below).

F. Southern San Andreas Fault Evaluation (SoSAFE)

The SCEC Southern San Andreas Fault Evaluation (SoSAFE) Project continues to increase our knowledge of slip rates, paleo-event chronology, and slip distributions of past earthquakes, for the past two thousand years on the southern San Andreas fault system. From Parkfield to Bombay Beach, and including the San Jacinto fault, the objective is to obtain new data to clarify and refine relative hazard assessments for each potential source of a future 'Big One'.

Priorities for SoSAFE in 2013

- Lengthen existing paleoearthquake chronologies or start new sites in key locations along the fault system that will improve understanding of the last 2000 years of this fault system.
- Determine slip rates at many time scales, so that possible system-level interaction can be documented.
- Obtain the best possible measurements of geomorphic slip distributions from past earthquakes using field and LiDAR approaches and to validate the different measures.
- Explore chronometric, geomorphic, or statistical approaches to linking geomorphic offsets to dated paleoearthquakes.
- Use novel methods for estimating slip rates from geodetic data.
- Investigate methodologies for integrating paleoseismic (including geomorphic measures of slip) and geologic data into rupture histories. For example, studies may improve or inform interactions between SoSAFE results and scenario rupture modeling or rupture forecasts.

Requests for geochronology support (e.g., to date 12 radiocarbon samples) are encouraged and shall be coordinated with Earthquake Geology; a portion of SoSAFE funds will be contributed towards joint support for dating. We also welcome proposals that seek to add other data (such as climate variations) to earthquake chronologies, which may be used to improve age control, understanding of the formation of offset features, or site-to-site correlation of events.

Research by single or multi-investigator teams will be supported to advance SCEC research towards meeting priority scientific objectives related to the mission of the SoSAFE Interdisciplinary Focus Group. SoSAFE objectives also foster common longer-term research interests and facilitate future collaborations in the broader context of a decade-long series of interdisciplinary, integrated and complementary studies on the southern San Andreas Fault system such as those targeted by teams investigating Special Fault Study Areas.

G. Earthquake Engineering Implementation Interface (EEII)

The purpose of the Earthquake Engineering Implementation Interface is to create and maintain collaborations with research and practicing engineers, much as the Seismic Hazard and Risk Analysis focus group did during SCEC3. These activities may include ground motion simulation validation, rupture-to-rafter simulations of building response as well as the end-to-end analysis of large-scale, distributed risk (e.g., ShakeOut-type scenarios). Our goal of impacting engineering practice and large-scale risk assessments require even broader partnerships with the engineering and risk-modeling communities, which motivates the activities described next.

Technical Activity Group (TAG) on Ground Motion Simulation Validation (GMSV)

A TAG focusing on validation of ground motion simulations has been established to develop and implement testing/rating methodologies via collaboration between ground motion modelers and engineering users. A 2011 workshop on this topic (<http://www.scec.org/workshops/2011/gmsv/index.html>) and the GSMV Plenary Session at the Annual Meeting identified the following initial efforts as potential priority activities in this area. Proposals on these topics will be reviewed with all other SCEC proposals in January of 2012. Interested researchers are invited to contact Dr. Nicolas Luco (nluco@usgs.gov) to discuss opportunities for coordinated research. Note that any PIs funded to work on GSMV-related projects will become members of the TAG and will be required to coordinate with each other, in part via participation in approximately two coordination workshops.

- Generate simulated ground motions for the following past earthquakes, preferably (but not necessarily) via the Broadband Simulation Platform: 1971 San Fernando, 1979 Imperial Valley, 1983 Coalinga, 1984 Morgan Hill, 1986 North Palm Springs, 1987 Whittier Narrows, 1989 Loma Prieta, 1992 Landers, 1992 Big Bear, 1994 Northridge, 1999 Hector Mine, 2004 Parkfield, and 2010 El Mayor-Cucapah.
- Develop validation methodologies that use elastic and inelastic response spectra, and demonstrate them with existing simulated ground motions (preferably, but not necessarily, from the Broadband Simulation Platform) and their recorded counterparts.
- Develop and demonstrate validation methodologies that use common models of structures of interest (e.g. multi-degree-of-freedom nonlinear models of building or geotechnical systems).
- Comprehensive analysis and documentation of the sensitivity of simulated ground motions to model input parameters and their interactions and uncertainties.
- Research on important ground motion or structural (e.g. building or geotechnical system) response parameters and statistics that should be used in validation of simulations.
- Demonstrate validation methodologies with ground motions simulated with deterministic and stochastic methods above 1 Hz.

Improved Hazard Representation

- Develop improved hazard models that consider simulation-based earthquake source and wave propagation effects that are not already well reflected in observed data. These could include improved methods for incorporating rupture directivity effects, basin effects, and site effects in the USGS ground motion maps, for example. The improved models should be incorporated into OpenSHA.
- Use broadband strong motion simulations, possibly in conjunction with recorded ground motions, to develop ground motion prediction models (or attenuation relations). Broadband simulation methods must be verified (by comparison with simple test case results) and validated (against recorded strong ground motions) before use in model development. The verification, validation, and application of simulation methods must be done on the SCEC Broadband Simulation Platform. Such developments will contribute to the future NGA-H Project.
- Develop ground motion parameters (or intensity measures), whether scalars or vectors, that enhance the prediction of structural response and risk.
- Investigate bounds on the median and variability of ground motions for a given earthquake scenario, in coordination with the Extreme Ground Motion Project.

Ground Motion Time History Simulation

- Develop acceptance criteria for simulated ground motion time histories to be used in structural response analyses for building code applications or risk analysis. This relates closely to the GMSV section above.
- Assess the advantages and disadvantages of using simulated time histories in place of recorded time histories as they relate to the selection, scaling and/or modification of ground motions for building code applications or risk analysis.
- Develop and validate modules for simulation of short period ground motions (< 1 sec) for incorporation in the Broadband Platform.
- Develop and validate modules for the broadband simulation of ground motion time histories close to large earthquakes, and for earthquakes in the central and eastern United States, for incorporation in the Broadband Platform.
- Develop and validate modules for nonlinear site response, including models for under what circumstances nonlinear modeling is required.

Collaboration in Structural Response Analysis

DRAFT 2013 SCIENCE PLAN

- Tall Buildings and Other Long-Period Structures. Enhance the reliability of simulations of long period ground motions in the Los Angeles region using refinements in source characterization and seismic velocity models, and evaluate the impacts of these ground motions on tall buildings and other long-period structures (e.g., bridges, waterfront structures). Such projects could potentially build on work done in the PEER TBI Project.
- End-to-End Simulation. Interactively identify the sensitivity of structural response to ground motion parameters and structural parameters through end-to-end simulation. Buildings of particular interest include non-ductile concrete frame buildings.
- Reference Buildings and Bridges. Participate with PEER investigators in the analysis of reference buildings and bridges using simulated broadband ground motion time histories. The ground motions of large, rare earthquakes, which are poorly represented in the NGA strong motion database, are of special interest. Coordination with PEER can be done through Yousef Bozorgnia (yousef@berkeley.edu).
- Earthquake Scenarios. Perform detailed assessments of the results of scenarios such as the ShakeOut exercise, and the scenarios for which ground motions were generated for the Tall Buildings Initiative (including events on the Puente Hills, Southern San Andreas, Northern San Andreas and Hayward faults) as they relate to the relationship between ground motion characteristics and structural response and damage.

Ground Deformation

- Investigate the relationship between input ground motion characteristics and local soil nonlinear response, liquefaction, lateral spreading, local soil failure, and landslides -- i.e., geotechnical hazards. Investigate hazards due to surface faulting and to surface deformation caused by subsurface faulting and folding.

Risk Analysis

- Develop improved site/facility-specific and portfolio/regional risk analysis (or loss estimation) techniques and tools, and incorporate them into the OpenRisk software.
- Use risk analysis software to identify earthquake source and ground motion characteristics that control damage estimates.

Other Topics

- Proposals for other innovative projects that would further implement SCEC information and techniques in seismic hazard, earthquake engineering, risk analysis, and ultimately loss mitigation, are encouraged.

X. Special Projects and Initiatives

The following are special projects for which SCEC has obtained funding beyond the core program. This Collaboration Plan is not for those funds, which are committed; rather it is for SCEC core funding for research projects that are consonant with these special projects. This is consistent with SCEC policy that requires that special projects be aligned with core SCEC goals.

A. Working Group on California Earthquake Probabilities (WGCEP)

Following the 2008 release of the Uniform California Earthquake Rupture Forecast version 2 (UCERF2), the WGCEP is now working on finishing UCERF3 (the time-independent model being due by Jan 2013), and planning for future models. Our primary goals are to relax segmentation, add multi-fault ruptures, and include spatial-temporal clustering (earthquake triggering). As the latter will require robust interoperability with real-time seismicity information, UCERF3 will bring us into the realm of operational earthquake forecasting (OEF). These models are being developed jointly by SCEC, the USGS, and CGS, in close coordination with the USGS National Seismic Hazard Mapping Program, and with support from the California Earthquake Authority (CEA).

The following are examples of SCEC activities that could make direct contributions to WGCEP goals:

- Reevaluate fault models in terms of the overall fault connectivity (important for understanding the likelihood of multi-fault ruptures) and the extent to which faults represent a well-defined surface versus a proxy for a braided deformation zone.
- Develop improved or a wider range of viable deformation models (defined as giving rakes and slip rates for each fault in a fault model, plus an "off fault" strain-rate map). Of particular interest is the extent to which slip rates taper toward the ends of faults that terminate (do not connect with other faults).
- Help determine the average along-strike slip distribution of large earthquakes, especially where multiple faults are involved (e.g., is there reduced slip at fault connections?).

- Help determine the average down-dip slip distribution of large earthquakes (the ultimate source of existing discrepancies in magnitude-area relationships).
- Develop a better understanding of the distribution of creeping processes and their influence on both rupture dimension and seismogenic slip rate.
- Contribute to the compilation and interpretation of mean recurrence-interval constraints from paleoseismic data and/or develop models for the probability of events going undetected at a paleoseismic site.
- Develop earthquake rate models that relax segmentation and include multi-fault ruptures (e.g., using physics-based simulators).
- Develop ways to constrain the spatial distribution of maximum magnitude for background seismicity (for earthquakes occurring off of the explicitly modeled faults).
- Address the question of whether every small volume of space exhibits a Gutenberg Richter distribution of nucleations (even those on faults)?
- Develop improved estimates (including uncertainties) of the long-term rates of observed earthquakes for different sized volumes of space.
- Develop methods for quantifying elastic-rebound based probabilities in un-segmented fault models.
- Help quantify the amount of slip in the last event, and/or average slip over multiple events, on any major faults in California (including variations along strike).
- Develop models for fault-to-fault rupture probabilities, especially given uncertainties in fault endpoints.
- Determine the proper explanation for the apparent post-1906 seismicity-rate reduction (the so-called Empirical Model of previous WGCEPs). How temporally variable are seismicity rates (e.g., more so than implied by aftershock statistics)?
- Develop applicable methods for adding spatiotemporal clustering to forecast models (e.g., based on empirical models such as ETAS, or derived from physics-based simulators). Are sequence-specific parameters warranted?
- Is there a physical difference between a multi-fault rupture and a separate event that was triggered quickly?
- Contribute the robust acquisition of real-time earthquake information needed for operational earthquake forecasting (e.g., a real-time model giving the probability of undetected events as a function of time, space, and magnitude).
- Develop more objective ways of setting logic-tree branch weights, especially where there are either known or unknown correlations between branches.
- Develop easily computable hazard or loss metrics that can be used to evaluate and perhaps trim logic-tree branches.
- Develop techniques for down-sampling event sets to enable more efficient hazard and loss calculations.
- Develop novel ways of testing UCERF3, especially ones that can be integrated with CSEP.

Further suggestions and details can be found at <http://www.WGCEP.org>, or by contacting the project leader (Ned Field: field@usgs.gov; (626) 644-6435).

B. Collaboratory for the Study of Earthquake Predictability (CSEP)

CSEP is developing a virtual, distributed laboratory—a collaboratory—that supports a wide range of scientific prediction experiments in multiple regional or global natural laboratories. This earthquake system science approach seeks to provide answers to the questions: (1) How should scientific prediction experiments be conducted and evaluated? and (2) What is the intrinsic predictability of the earthquake rupture process? Contributions may include:

- Establishing rigorous procedures in controlled environments (testing centers) for registering prediction procedures, which include the delivery and maintenance of versioned, documented code for making and evaluating predictions including intercomparisons to evaluate prediction skills;
- Constructing community-endorsed standards for testing and evaluating probability-based, alarm-based, and event-based predictions;
- Developing hardware facilities and software support to allow individual researchers and groups to participate in prediction experiments;

DRAFT 2013 SCIENCE PLAN

- Providing prediction experiments with access to data sets and monitoring products, authorized by the agencies that produce them, for use in calibrating and testing algorithms;
- Reducing testing latency by reducing the updating interval of the short-term forecasting models (e.g., STEP and ETAS) in order to explore the potential information gain in aftershock sequences. Most desirable is testing on an event by event basis to adapt the testing frequency to the seismic activity;
- Establishing seismicity-based reference models as norms against which the skill of candidate models can be evaluated;
- Developing testing procedures that explicitly recognize that real-time catalogs are incomplete and have larger errors in source parameters;
- Working to develop testable fault-based forecast models;
- Intensifying the collaboration with Japan and New Zealand with a special emphasis on the effect of the Darfield and Tohoku-oki earthquakes, and using data collected from these sequences to retrospectively calibrate and prospectively test improved forecasting models;
- Initiating joint efforts with China;
- Initiating new experiments in existing or new testing regions;
- Re-assessing the geophysical, neotectonic, and paleoseismic data on the long-term recurrence of high-magnitude events and re-examining time-dependent hazard models;
- Developing experiments to test basic physical principles of earthquake generation (e.g., models for estimating the largest possible earthquake on a given fault are important to earthquake scenarios like ShakeOut and to earthquake hazard models. We seek proposals to develop quantitative tests of such models);
- Evaluating hypotheses critical to forecasting large earthquakes, including the characteristic earthquake hypothesis, the seismic gap hypothesis, and the maximum-magnitude hypothesis;
- Expanding the range of physics-based models to test hypotheses that some aspects of earthquake triggering are dominated by dynamic rather than quasi-static stress changes and that slow slip event activity can be used to forecast large earthquakes; and
- Conducting workshops to facilitate international collaborations.

A major focus of CSEP is to develop international collaborations between the regional testing centers and to accommodate a wide-ranging set of prediction experiments involving geographically distributed fault systems in different tectonic environments.

SPECIAL NOTE: Global travel grants for CSEP from 2006 to 2010 were funded with a grant from the W. M. Keck Foundation, which ended in early 2011. Future funding for CSEP global travel has not been obtained at the time of the release of this document.

C. Community Modeling Environment (CME)

The Community Modeling Environment is a SCEC special project that develops improved ground motion forecasts by integrating physics-based earthquake simulation software, observational data, and earth structural models using advanced computational techniques including high performance computing. CME projects often use results, and integrate work, from SCEC groups including Interdisciplinary Focus Groups Technical Activity Groups.

The SCEC research community can contribute research activities to CME by providing scientific or computational capability that can improve ground motion forecasts. The following paragraphs briefly describe several current CME computational goals so researchers can propose to develop a needed element that can be integrated into a larger CME calculation.

Examples of CME research requirements include earth structural models, curated data sets to support forecast validation, and scientific software that simulates physical processes in the earth including dynamic ruptures (such as those that are verified in the Dynamic Rupture Code Verification Technical Activity Group (TAG)), and wave propagation simulations. Proposals are encouraged that work towards improving the accuracy of the statewide community velocity model (SCVM).

CME computationally based research projects include three types of forecast evaluation and testing systems; transient detection and forecast evaluation, earthquake early warning earthquake parameter and ground motion forecast evaluation, and short-term earthquake forecast evaluation.

CME is developing ground motion simulations that produce broadband seismograms. These simulation tools include rupture generators, low frequency wave propagation models, high frequency stochastic models, non-linear site response modules, and validation capabilities including assembled observational strong motion data sets and waveform-matching goodness of

fit algorithms and information displays. Proposals that enhance our ability to extend ground motion simulations to higher frequencies through high frequency source generation models, and stochastic models of source, propagation, and site effects are encouraged.

Ground motion simulation validation computational and organizational tools are needed to establish repeatable validation of ground motion simulations to engineering standards. Research in this area would contribute to the efforts under the ground motion simulation validation TAG.

Proposals that seek to use existing CyberShake simulations as a research database are encouraged.

CME is working to improve probabilistic seismic hazard calculations. CME PSHA research requires a high resolution 3D velocity model for California, a pseudo-dynamic rupture generator capable of generating an extended earthquake rupture forecast from UCERF3.0, highly efficient reciprocity-based seismogram calculations, and probabilistic hazard model information system providing access to calculation results. Proposals that develop improved pseudo-dynamic models, including parameterizations that include the possibility of super-shear rupture, are encouraged.

D. National Partnerships through EarthScope

The NSF EarthScope project (<http://www.earthscope.org>) provides unique opportunities to learn about the structure and dynamics of North America. SCEC and the NSF EarthScope program encourage proposals that integrate the goals of the SCEC Science Plan with the many overlapping goals of the EarthScope Science Plan (<http://www.earthscope.org/ESSP>). Topics of interest include applying EarthScope observational resources to SCEC science and hazard problems; characterizing the crust and lithosphere of the natural laboratory of Southern California; exploring stress and deformation over time using EarthScope resources (including high resolution topography); testing hypothesis and enhancing models of earthquakes, faulting, and the rheology of the lithosphere; developing innovative contributions to identifying earthquake hazard and community response; and promoting Earth Science literacy in education and outreach in SCEC and EarthScope topic areas. These partnerships should seek to strengthen the connections across the organizations and leverage SCEC and EarthScope resources.

XI. Communication, Education, and Outreach

The theme of the CEO program during SCEC4 is *Creating an Earthquake and Tsunami Resilient California*. CEO will continue to manage and expand a suite of successful activities along with new initiatives, within four CEO interconnected thrust areas:

1. The *Implementation Interface* connects SCEC scientists with partners in earthquake engineering research, and communicates with and trains practicing engineers and other professionals.
2. The *Public Education and Preparedness* thrust area educates people of all ages about earthquakes, and motivates them to become prepared.
3. The *K-14 Earthquake Education Initiative* seeks to improve earth science education and school earthquake safety.
4. Finally, the *Experiential Learning and Career Advancement* program provides research opportunities, networking, and more to encourage and sustain careers in science and engineering.

These thrust areas present opportunities for members of the SCEC community to partner with CEO staff. Limited funding (typically no more than \$2000-\$5000) may be available as direct payments from SCEC (not subcontracts) for materials or activities and typically does not require a formal proposal. For larger activities, joint proposals with SCEC CEO to potential sources are the best approach. Those interested in partnering with SCEC CEO on activities, submitting a joint proposal, or in submitting a CEO proposal responding to this Collaboration Plan should first contact the Associate SCEC Director for CEO (Mark Benthien: benthien@usc.edu, 213-740-0323).

Plenary Talk Presentations

Rupture to Rafters on a Global Scale, *David J. Wald (USGS)*

Sunday, September 9, 2012 (18:00)

The U.S. Geological Survey's Prompt Assessment of Global Earthquakes for Response (PAGER) system provides rapid and automated alerting of estimated economic and human impacts following earthquakes around the globe. Although PAGER's primary purpose is to quantify any earthquake's severity for situational awareness and response decision-making, the underlying tools developed are utilized for many other scientific and mitigation efforts. PAGER is an end-to-end system of scientific and engineering results combined for the purpose of loss estimation, analogous to SCEC's notion of "rupture to rafters" computations. There are four components of the PAGER system. First, earthquakes trigger rapid source characterization; second, these source parameters inform our estimates of shaking-distribution (e.g., ShakeMap). Third, losses are then modeled by computed populations exposed per shaking intensity level, and country-specific and shaking-dependent loss functions are used to provide estimates of economic impact and potential casualties. Finally, these uncertain loss estimates are communicated in an appropriate form for actionable decision-making among a variety of users. Rapidly and automatically assessing the wide range of seismological, demographic, building inventory, and vulnerability information necessary to make such loss estimates entails a requisite balance of empirical & physics-based modeling strategies. Several aspects of our problem cannot yet be adequately solved with purely empirical, nor solely mechanistic, approaches. The "physics-based" model components of the PAGER system are essential for informing empirical models where they are data-limited, and for providing a framework for better understanding the causative pathways that dominate earthquake losses around the globe. In the course of explaining the end-to-end strategies and science/engineering employed by the PAGER system, we also describe what pragmatic choices were made in balancing the uncertainties in and benefits provided by our empirical, semi-empirical, expert-opinion, and physical models. We then relate these trade-offs to similar challenges faced by SCEC scientists. Recognizing and reconciling the complimentary benefits of data-driven versus theoretical problem-solving is at the core of the PAGER system, as it is for a wide variety of other challenges within the earth sciences.



Communicating Earthquake Risk: The Intersection of Earth and Social Sciences, *Lucy M. Jones (USGS) & Timothy L. Sellnow (U Kentucky)*

Monday, September 10, 2012 (11:00)

Earth scientists and engineers face significant challenges in communicating earthquake risk to decision makers, members of the media, and the public. Some earth scientists have empirically developed an understanding of the opportunities and challenges in expressing the risk posed by earthquakes to non-specialists. Independently, researchers in psychology and communications have completed extensive research on the variability of the public's response to a range of risk communication strategies. This session will compare the empirical experience of scientists in communicating the risk with the results of research in psychology in risk communication. We will focus on three major topics: 1) the challenges of communicating probabilities, 2) the fallacy of the teachable moment – what the public can perceive at times of fear, and 3) lessons from ShakeOut – what the success of ShakeOut tells us about motivating people to take action to protect themselves. For each topic, we will examine the experience of seismologists, compare with social science research that bears on these issues, and seek participation from the audience. The goal is to arrive at practical approaches for earth scientists and engineers to facilitate productive interaction with decision makers, media, and the public.

The Role SCEC Can Play in Improving Seismic Provisions in US Codes through Ground-Motion Simulations, *C.B. Crouse (URS Corp)*

Monday, September 10, 2012 (16:00)

Through its Uniform California Earthquake Rupture Forecast (UCERF) project, SCEC has collaborated with the USGS to establish seismic source models for California. These models will be used to prepare ground-motion maps for possible inclusion in the next edition of the ASCE 7 standard, which will be incorporated by reference in the International Building Code. Probabilistic and deterministic seismic hazard analysis (PSHA and DSHA) methods will use these models and empirical ground-motion prediction equations (GMPEs), derived from accelerogram data recorded worldwide, to develop the maps. However, these GMPEs are limited in their ability to model long period ground motions in 3-D basin structures, such as those in the greater Los Angeles region. As an alternative to using empirical GMPEs, SCEC's CyberShake project used numerical simulations to generate the ground motions used in a PSHA for Los Angeles; one result was a contour map of 5%

damped response spectral acceleration at 3-sec natural period and 2475-year return period. Expanding this effort to include a range of natural periods in the 1 to 10-sec band and forming a subcommittee, consisting of SCEC/USGS seismologists performing the simulations and engineers involved in seismic code development, is recommended to determine whether and how to incorporate the results into regional ground-motion maps for inclusion in the ASCE 7 standard. If the method is judged feasible during this pilot study, then it would be formally introduced in the code-development process and applied to other urban areas where the 3-D velocity structures are well known. If the resulting maps are approved by the code seismic committees, SCEC should store the simulated accelerograms in a data bank that could be easily accessed by structural engineers for dynamic response analysis of long period structures. Depending on the structure, a stochastic component may need to be added to the accelerograms to extend their useful period band to shorter periods < 1 sec, in order to cover higher mode responses.

Imaging and modeling the unexpected rupture path of an extreme event: the 2012 Mw 8.6 off-Sumatra earthquake, Jean-Paul Ampuero (Caltech)

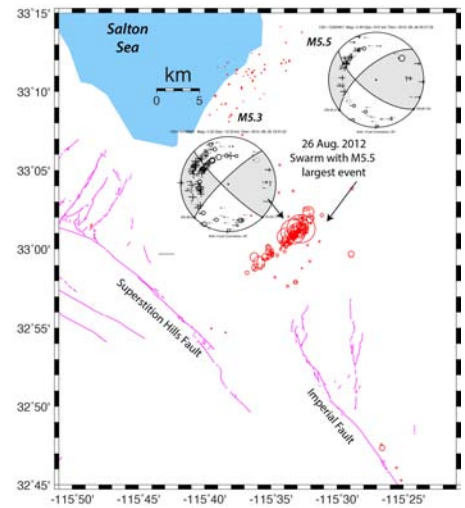
Tuesday, September 11, 2012 (08:00a)

On April 11th 2012 a Mw 8.6 earthquake, the largest strike-slip event known to date, occurred in a diffuse deformation zone in the Indian Ocean, off-shore Sumatra. I will summarize what has been learned so far about this rare event and which puzzles remain unsolved, while highlighting those aspects that are relevant to research in SCEC4, especially on Fault and Rupture Mechanics. Due to its remote location, this earthquake is a good example of the unique information about earthquake rupture processes that can be obtained by high-resolution back-projection source imaging based on teleseismic array data. This technique reveals a complicated rupture path, involving multiple segments of a network of conjugate, almost-orthogonal faults and unexpected features like branching despite compressional dynamic stresses. I will discuss implications of these observations for a range of topics, including earthquake source imaging, dynamic rupture branching, rupture linkage across stepovers, rheology of the deep lithosphere and the maximal depth extent of earthquake rupture, the possibility of rupture through nominally stable fault regions, the timely characterization of rupture growth.

August 2012 Brawley Earthquake Swarm in Imperial Valley, Egill Hauksson (Caltech)

Tuesday, September 11, 2012 (08:00b)

The 2012 Imperial Valley Brawley swarm started near the City of Brawley on 22nd of August with six events of $M < 2.0$. The seismic activity picked up early on 23rd of August with increasing rate early in the day. The three largest earthquakes (M5.5, M5.3, and M4.9) in the sequence occurred over a time period of 90 minutes, starting at 12:33 pm on August 23rd. The high rate of seismic activity lasted about 24 hours. This sequence that so far consists of more than 600 events forms a 12 km long linear northeast trending distribution, mostly in the depth range of 8 to 12 km. The focal mechanisms predominantly exhibit strike-slip motion on northeast or northwest striking planes. This swarm occurred in the immediate vicinity of the largest (M5.8) aftershock of the 1979 Mw6.4 Imperial Valley earthquake. Similar seismic swarms have occurred in the Brawley seismic zone in the past, especially in the 1970s and 1980s but in the 1990s the region was seismically quiet. The Brawley seismic zone is the northern most spreading center of the Gulf of California rift zone, which transfers slip from the Imperial fault in the south to the San Andreas fault in the north.



Map of CISM/SCSN relocations with 3D and HypoDD: Brawley Swarm, August 2012, from the SCSN website (www.scsn.org/2012Brawley.html).

Potential of High-Performance Computing for Solid-Earth Science, Jeroen Tromp (Princeton)

Tuesday, September 10, 2012 (10:30a)

In recent years, modeling, simulation and computation have come to play a central role in modern solid-Earth science in general, and seismology in particular. With dramatic increases in the quality and quantity of geophysical data and the availability of sophisticated open-source numerical modeling tools, there is a need for a more organized, community-driven approach to computational solid-Earth science. As an example, the California Seismic Network, the EarthScope USArray Transportable Array, the permanent Backbone Array, and the Flexible Array are providing seismologists with a wealth of new data. Data analysis is keeping up with data acquisition only for the computationally simplest analysis methods, as even computationally modest analysis is often still labor intensive. Modeling of and imaging with this data requires powerful numerical modeling tools, automation of routine analysis tasks, and dedicated high-performance computing facilities.

Most simulations are currently performed on modest in-house facilities, or through grants at various national supercomputing centers. A dedicated simulation facility would accommodate the substantial computational demands of modern solid-Earth science, including, for example, kinematic

and dynamic rupture simulations to assess seismic hazard, data assimilation simulations in geodynamics, seismology, and geomagnetism, and full waveform inversions in global and regional seismology. Such a facility would not obviate the need for local resources, instead the local facilities would be used for development, scenario testing, and education, acting as the on-ramp to the earth science HPC facility. The facility would benefit investigators at universities that have limited HPC resources by providing hardware, software engineering, training and a community specific environment to draw on. The goal of such a computational solid-Earth science center should be to provide our community a system structured specifically for our simulation/imaging needs, which include large fast storage capacity, large memory, and a large number of cores, configured in a system designed for long run-times, which also allows for user interaction between iterations in compute intensive inversions.

Understanding earthquake source physics through computation, *Jeremy E. Kozdon (Stanford)*

Tuesday, September 11, 2012 (10:30b)

What are the physical mechanisms for incoherent, high-frequency ground motion? How does complex geometry affect the rupture process? At what scales must we model events to have reliable and physically realistic simulations? What processes give rise to self-similarity in earthquakes? How does the stress evolve over multiple earthquake cycles? In this talk, I will present highlights of how our group is using dynamic rupture models and high-performance computing to explore these questions. Though our focus will be on dynamic rupture models, the lessons we have learned can aid the SCEC community at large in thinking about computations.

We initially explored incoherence of high-frequency ground motion through fault roughness. As a rupture encounters local stress heterogeneities it accelerates and decelerates which, along with fluctuations in slip, excites incoherent ground motion. Recently, we have begun considering the importance of path effects in a heterogeneous medium. Scattering both generates incoherent ground motion and feeds back into the rupture process leading to further incoherence. Untangling the relative importance of these mechanisms requires dynamic rupture simulations.

Computation can help answer other geometry and material structure related questions. Using dynamic rupture models of the Tohoku earthquake, we are exploring how ruptures can reach the seafloor through a shallow velocity strengthening fault segment and what hydroacoustic signals might tell us about shallow slip. Though subduction zone events may not be directly related to the primary SCEC objectives, rupture dynamics in other geometrically complex fault systems featuring spatially variable frictional properties are. For instance, which branch will a rupture take in a fault network? Can an earthquake in this system jump to another fault? How do local fault geometry and frictional properties affect segmentation?

Rupture processes are multiscale and using laboratory measured parameters requires millimeter resolution. Even with exascale resources, this is impossible for regional simulations with fixed grids. One way forward is adaptive mesh refinement (AMR). In AMR, resolution is added as and where required, significantly reducing the computational overhead. Currently, we are using AMR to explore self-similarity and possible physical mechanisms (in particular, off-fault plasticity and/or thermal pressurization) underlying observed earthquake energy balance and scaling laws.

The Ventura Region Special Fault Study Area: Towards an Understanding of the Potential for Large, Multi-Segment Thrust Ruptures in the Transverse Ranges, *James F. Dolan (USC), John H. Shaw (Harvard), & Thomas K. Rockwell (SDSU)*

Tuesday, September 11, 2012 (15:30a)

The recent occurrence of several highly destructive thrust fault earthquakes (e.g., 1994 Mw 6.7 Northridge; 1999 Mw 7.6 Chi-Chi; 2005 Mw 7.5 Kashmir; 2008 Mw 7.9 Wenchuan; 2011 Mw 7.2 Van) and the growing recognition of the hazards posed by such structures to urban centers around the world highlight the need to better understand the behavior of these faults and their associated folds. The 2008 Wenchuan earthquake, in particular, emphasized that ruptures may link together various thrust faults to generate extremely large-magnitude earthquakes. The growing realization of the possibility of multi-fault ruptures, coupled with the presence of numerous large reverse faults within the Transverse Ranges, emphasizes the necessity of assessing the hazards posed by such multi-segment thrust earthquakes in southern California. The major reverse faults of the Transverse Ranges form an interconnected, >200-km-long network that could potentially rupture together during very large-magnitude events similar to the Wenchuan earthquake. Of particular importance is the complex network of faults in the Ventura area. These faults could potentially serve as linking structures connecting large thrust ramps to the west (e.g., Pitas Point fault) with the large thrust and reverse faults to the east (e.g., San Cayetano, Santa Susana, and Sierra Madre-Cucamonga faults, the latter extending all the way across the northern edge of the Los Angeles metropolitan region.

The critical need to understand the faults of the Ventura region has led SCEC to designate this as a Special Fault Study Area (SFGSA). The goal of this SFGSA is to focus multi-disciplinary efforts of many SCEC researchers on the common problem of understanding the structure, state of activity, slip rates, and seismic hazards of the Ventura region faults, and more generally on assessing the degree to which these faults provide potential structural linkages for through-going, large-magnitude multi-segment ruptures. Much of this research is already under way with SCEC funding, including 3D structural modeling using industry well and seismic reflection data and newly collected high-resolution reflection data, both onshore and offshore paleoseismologic work aimed at determining the slip rates of these faults and the ages and displacements of ancient earthquakes that they have generated, studies of tsunami records preserved in estuarine sediments, mechanical modeling of regional fault interactions, and dynamic rupture simulations. In addition to describing preliminary results from these studies at the SCEC Annual Meeting, we will also discuss the format of a planned SCEC workshop on this SFGSA to be held in 2013.

SCEC Workshop on San Geronio Pass: Structure, Stress, Slip, and the Likelihood of Through-Going Rupture, Doug Yule (CSUN), Michele L. Cooke (UMass), & David Oglesby (UCR)

Tuesday, September 11, 2012 (15:30b)

This workshop explored the San Geronio Pass "knot" region as a candidate for a SCEC Special Fault Study Area and outlined a plan to fill existing knowledge gaps. Specific topics included the geometry of active subsurface faulting, the potential for earthquakes on the complex fault system in this region, and the likelihood of a 'super-earthquake' that would propagate along the San Andreas system through the pass, leading to a very large-magnitude and damaging event. The workshop brought together geoscientists from a wide spectrum of interests including tectonic geomorphology, structural geology, mechanical modeling, rupture modeling, gravity and magnetic modeling, seismology, geochronology, geodesy, and fault and rock mechanics. The first day was a blend of short science talks on case studies with discussions of specific topics. On the second day, we took a field trip to view key sites in San Geronio Pass. Our discussions focused on three major questions for the San Geronio Pass.

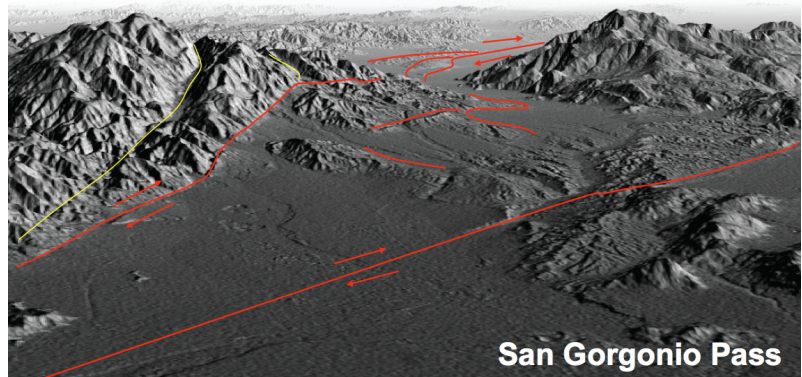


Image courtesy of Mike Oskin (UC Davis)

1. How do we reconcile near-surface observations with subsurface evidence for active fault configuration? The pattern of active faulting revealed by seismicity seems to be quite different below about 10-12 km from that expressed in the upper crust or at the surface. Potential field data suggest fault configurations representative of older fault strands with larger cumulative displacements than those interpreted as currently active from other data sets.

2. What is the earthquake potential of faults in the San Geronio Pass? Slip rates, slip per event and uplift rates provide critical data for assessment of earthquake potential. While the UCERF3 seeks to provide critical seismic hazard information, it fails to capture active deformation within the SGP because of erroneous fault geometry. Forward mechanical models show that small changes in fault geometry can produce large differences in slip rates and uplift patterns.

3. Can large earthquakes rupture through the San Geronio Pass? The patterns of precarious rocks and temporal correlation of slip events between trenches provide some constraints on the rupture extent of paleo-earthquakes through the Pass. In addition to these constraints, dynamic earthquake rupture models can determine the likelihood of the SGP allowing a 'super-event' to propagate through this region of extreme fault complexity. Recent advances in numerical methodology indicate that we are ready to incorporate enough realism into such models.

What can crustal deformation tell us about California's earthquake future? Lessons from UCERF3, Tom Parsons (USGS)

Wednesday, September 12, 2012 (08:00)

We want to characterize seismogenic deformation in California to make earthquake probability calculations. UCERF assumes that earthquake rates are proportional to deformation rates; in particular, the rates that faults slip. Extensive use of GPS observations is a new feature brought into UCERF3. Geodetic measurements tend to be more areally comprehensive than geologic offset observations. However, all measures are subject to considerable uncertainty that include dating errors and modeling assumptions. The ~150-yr earthquake catalog is shown to identify sites of future activity in California, but it is temporally limited and may be incomplete for infrequent high magnitude events.

PLENARY TALK PRESENTATIONS

How best to balance these deformation measures into a form that can be translated into future earthquakes? I describe our efforts to test, compare, contrast, and apply five candidate deformation models that use geodetic and/or geologic measurements to calculate fault slip rate and residual “off-fault” seismogenic deformation: (1) a group of block models, (2) an FEM, (3) a buried dislocation model, (4) a geologic model, and (5) the UCERF2 deformation model. We find that all fit the vast majority of observed data well, and at first glance are viable representations of California deformation within data constraints.

However, every model had problems that required iterations and revisions. This is caused in part by the UCERF3 earthquake rate approach that breaks faults into ~5-10 km long subsections, meaning more section rates must be found than before. Even if a given model fits 95% of subsections to data - an acceptable standard for a scientific publication - it only takes a few anomalous results to cause important changes to hazard.

Traditional PSHA methods of working from identified earthquake sources may underreport hazard when applied to an area as large as California, where it is unlikely that every fault has been discovered. By contrast, geodetic techniques may overreport hazard because they record virtually all surface strain whether it is seismogenic or not. Indeed geodetic deformation models imply increased moment release (14%-25%) compared with the UCERF2 model and the earthquake catalog.

The UCERF3 process offers hope that complimentary data are applicable to hazard assessment. However, there remains an information gap that necessitates consensus judgments on how best to balance some conflicting results from different temporal and spatial deformation measures.

Poster Presentations

View full abstracts at www.scec.org/meetings/2012am

Sunday, September 9, 2012

20:00 – 22:00 Poster Session 1

Monday, September 10, 2012

14:30 – 16:00 Poster Session 2

21:00 – 23:00 Poster Session 3

Tuesday, September 11, 2012

14:00 – 15:30 Poster Session 4

21:00 – 23:00 Poster Session 5



Ground Motion Prediction (GMP)

Posters 001-027

- 001 **Maximum peak ground velocity in Los Angeles Basin**, *Norman H. Sleep*
- 002 **Importance of 1-point statistics in earthquake source modeling for ground motion simulation**, *Seok Goo Song and Luis A. Dalguer*
- 003 **Ground Motion Prediction Equations for data recorded within and around the San Jacinto Fault Zone**, *Ittai Kurzon, Frank L. Vernon, Yehuda Ben-Zion, and Gail Atkinson*
- 004 **Using the SCEC Broadband Platform for Supplementing Empirical Data on Fling Effects**, *Ronnie Kamai, Kathryn Wooddell, and Norman Abrahamson*
- 005 **Fragile Geologic Features and Points in Hazardspace in New Zealand**, *Mark W. Stirling and Dylan H. Rood*
- 006 **Strong ground motions of the Mw 6.3 2009 L'Aquila earthquake: modeling and validation**, *Frantisek Gallovic, Gabriele Ameri, and Francesca Pacor*
- 007 **Analysis of Terrain Proxy Using Measured Vs30 Data**, *Alan Yong*
- 008 **Kinematic earthquake rupture scenarios for the Salt Lake segment, Wasatch fault**, *Morgan P. Moschetti, Stephen Angster, Leonardo Ramirez-Guzman, Stephen Hartzell, Stephen Personius, and William Stephenson*
- 009 **Using Averaging-Based Factorization to Compare Seismic Hazard Models Derived from 3D Earthquake Simulations with NGA Ground Motion Prediction Equations**, *Feng Wang and Thomas H. Jordan*
- 010 **Nonlinear amplification factors at SC strong motion stations**, *Dominic Assimaki, Jian Shi, and Alan Yong*
- 011 **Testing seismic hazard models with Be-10 exposure ages for precariously balanced rocks**, *Dylan H. Rood, Rasool Anooshehpour, Greg Balco, Glenn Biasi, James Brune, Richard Brune, Lisa Grant-Ludwig, Katherine Kendrick, Matthew Purvance, and Inyo Saleeby*
- 012 **Estimation of path effects on the ground motion standard deviation based on the empirical data and the simulated waveforms from the CyberShake platform**, *Manuela Villani and Norman Abrahamson*
- 013 **Development of excess pore water pressure in liquefiable soils inferred from vertical array records**, *Daniel Roten, Donat Fäh, and Fabian Bonilla*
- 014 **On the Prediction of Earthquake Ground Motion**, *Daniel Lavallee, Jan Schmedes, and Ralph J. Archuleta*
- 015 **Simulation of the 1994 Northridge Earthquake Including Nonlinear Soil Behavior**, *Doriam Restrepo, Ricardo Taborda, and Jacobo Bielak*
- 016 **Improved Green's Functions Using Physical Constraints**, *Marine AM. Denolle and Gregory C. Beroza*
- 017 **3-D Rocking Response of Precariously Balanced Rocks**, *Swetha Veeraghavan and Swaminathan Krishnan*
- 018 **A Recursive Division Stochastic Strike-Slip Seismic Source Algorithm Using Insights from Laboratory Earthquakes and Implications of a Big One in the Los Angeles Basin**, *Hemanth Siriki and Swaminathan Krishnan*
- 019 **Deterministic High-Frequency Ground Motions from Simulations of Dynamic Rupture along Rough Faults**, *Kyle B. Withers, Kim B. Olsen, Zheqiang Shi, Rumi Takedatsu, and Steve Day*
- 020 **New Earthquake Classification Scheme for Mainshocks and Aftershocks in the NGA – West2 Ground Motion Prediction Equations (GMPEs)**, *Kathryn E. Wooddell and Norman A. Abrahamson*
- 021 **Understanding the NGA-West ground-motion prediction equations for PGA and PGV SSA Abstract 2012**, *Annemarie S. Baltay, Gregory C. Beroza, and Thomas C. Hanks*
- 022 **Broadband Ground Motion Simulations Using Hybrid of Low Frequency deterministic and High Frequency Source- and Site-Specific Empirical Greens Function Approach**, *Ramses Mourhatch and Swaminathan Krishnan*
- 023 **Ground Motions from Large-Scale Dynamic Rupture Simulations**, *Zheqiang Shi and Steven M. Day*
- 024 **Using the SCEC Broadband Platform for Strong Ground Motion Simulation and Validation**, *Fabio Silva, Phillip J. Maechling, Kim Olsen, Ralph Archuleta, Robert Graves, Christine Goulet, Paul Somerville, Thomas H. Jordan, and Broadband Platform Working Group*
- 025 **Geomorphic Erosional Models for Estimating Ages of Precariously Balanced Rocks from Cosmogenic Isotope Data**, *Richard J. Brune, Lisa Grant-Ludwig, Katherine Kendrick, and James N. Brune*
- 026 **Testing CyberShake Using Precariously Balanced Rocks**, *Jessica R. Donovan, Thomas H. Jordan, and James N. Brune*
- 027 **Source and Basin Structure Studies using the 8 August 2012 Yorba Linda Earthquake Sequence**, *Shengji Wei, Robert W. Graves, Dunzhu Li, and Don Helmbarger*

Earthquake Engineering Implementation Interface (EII)

- 028 **Response of a tall building far from the epicenter of the March 11, 2011 M=9.0 Tohoku, Japan earthquake and aftershocks**, Mehmet Celebi, Izuru Okawa, Toshidate Kashima, Shin Koyama, and Masanori Iiba
- 029 **Engineering validation of hybrid broadband ground motion simulations**, Lynne S. Burks and Jack W. Baker
- 030 **Engineering Validation of Ground Motion Simulation: Part 1. Tall Buildings**, Carmine Galasso, Peng Zhong, and Farzin Zareian
- 031 **Engineering Validation of Ground Motion Simulation: Part 2. Skewed Bridges**, Farzin Zareian, Carmine Galasso, and Peyman Kaviani

Posters 028-032

- 032 **Spatial Correlations in Building Response Using Simulated and Recorded Earthquake Scenarios**, David J. DeBock, Jack W. Garrison, and Abbie B. Liel

Community Modeling Environment (CME)

- 033 **The influence of complex fault geometry on uplift patterns in the Coachella Valley and Mecca Hills of Southern California**, Laura Fattaruso and Michele Cooke
- 034 **Assessment of site conditions and empirical site response at stations recording near-field extreme ground motions during the 2008 Mogul, Nevada earthquake swarm**, Aasha Pancha, Satish Pullammanappallil, Glenn Biasi, John N. Louie, and Craig dePolo
- 035 **A 77-Fold Speedup and 100 Tflops Acceleration of Seismic Wave Propagation AWP-ODC on Heterogeneous Supercomputers**, Efecan Poyraz, Jun Zhou, Dong Ju Choi, Amit Chourasia, and Yifeng Cui
- 036 **Full-3D Waveform Tomography for Southern California**, En-Jui Lee, Po Chen, Thomas Jordan, Philip Maechling, Marine Denolle, and Gregory Beroza
- 037 **Optimizing the CyberShake Platform for Probabilistic Seismic Hazard Analysis**, Scott Callaghan, Philip Maechling, Gideon Juve, Gaurang Mehta, Karan Vahi, Mats Rynge, Robert Graves, Kim Olsen, and Thomas H. Jordan

Posters 033-039

- 038 **Spatial Variability of Shallow Velocity Measurements in the Los Angeles Area**, William H. Savran, Kim B. Olsen, and Bo H. Jacobsen
- 039 **Investigating absolute stress in southern California: How well do stress models of compensated topography and fault loading match earthquake focal mechanisms?**, Karen M. Luttrell, Bridget R. Smith-Konter, and David T. Sandwell

Earthquake Early Warning (EEW)

- 040 **Improved Ground-Motion Predictions for Earthquake Early Warning During Large Earthquakes**, Maren Boese, Tom Heaton, Egill Hauksson, Robert Graves, Scott Callaghan, and Philip Maechling
- 041 **The ARIA project: Advanced Rapid Imaging and Analysis for Natural Hazard Monitoring and Response.**, Susan E. Owen, Frank Webb, Mark Simons, Paul Rosen, Jennifer Cruz, Sang-Ho Yun, Eric Fielding, Angelyn Moore, Hook Hua, Piyush Agram, and Paul Lundgren

Posters 040-042

- 042 **Rapid Source Characterization of the 2011 Tohoku-oki Earthquake with Real-Time GPS and Strong Motion Data**, Brendan W. Crowell, Diego Melgar, and Yehuda Bock

Collaboratory for the Study of Earthquake Predictability (CSEP)

- 043 **Betting against the house and peer-to-peer gambling: a Monte Carlo view of earthquake forecasting**, Jeremy D. Zechar and Jiancang Zhuang
- 044 **Study on the Earthquake Potential Risk in Western United States by LURR Method Based on Seismic Catalogue, Fault Geometry and Focal Mechanisms**, Yongxian Zhang, M. Burak Yikilmaz, and John B. Rundle
- 045 **Comparison of earthquake forecasting tests in Kanto district and all over Japan**, Sayoko Yokoi, Hiroshi Tsuruoka, Kazuyoshi Nanjo, and Naoshi Hirata
- 046 **Very Short-Term (Sub-24h) and Event-Based Earthquake Forecasting Experiments in California**, Maximilian J. Werner, Agnes Helmstetter, David D. Jackson, and Yan Y. Kagan
- 047 **Collaboratory for the Study of Earthquake Predictability: Recent Developments and Extensions**, Maria Liukis, Danijel Schorlemmer, John Yu, Philip J. Maechling, Jeremy D. Zechar, Maximilian J. Werner, Thomas H. Jordan, and the CSEP Working Group

Posters 043-047

Working Group on California Earthquake Probabilities (WGCEP)

- 048 **Initial Results from the UCERF3 Long-term Earthquake Rupture Forecast**, Morgan T. Page, Edward H. Field, and Kevin Milner
- 050 **Using Risk Targeted Ground Motions to Evaluate Seismic Hazard Models**, Peter M. Powers

Posters 048-051

- 051 **A Fault-based Crustal Deformation Model for UCERF3 and Its Implication to Seismic Hazard Analysis**, Yuehua Zeng and Zhengkang Shen

Earthquake Forecasting and Predictability (EFP)

- 052 **Characteristic Earthquake Model, 1884 – 2011, R.I.P.**, Yan Y. Kagan, David D. Jackson, and Robert J. Geller
- 053 **Different types of seismicity clusters in southern California: A case study of non-universal behavior**, Ilya Zaliapin and Yehuda Ben-Zion
- 054 **Information gains of a hybrid earthquake forecasting model**, David A. Rhoades
- 055 **An Analysis of Tradeoffs in Element Size and Approximation Schemes for Earthquake Simulation**, Eric M. Heien, Michael K. Sachs, Galen Danziger, John B. Rundle, and Louise H. Kellogg
- 056 **Modeling seismicity rate changes in Oklahoma and Arkansas**, Andrea L. Llenos and Andrew J. Michael
- 057 **1/f and the Earthquake Problem: Scaling constraints to facilitate operational earthquake forecasting**, Mark R. Yoder, John B. Rundle, and Donald L. Turcotte
- 058 **Using Static Coulomb Models with Rate- and State-Friction Models to Estimate Seismicity Rates for the Canterbury, New Zealand, Earthquake Sequence**, Charles A. Williams, Sandy Steacy, Matthew Gerstenberger, and David Rhoades
- 059 **Using Socioeconomic Data to Calibrate Loss Estimates**, James R. Holliday and John B. Rundle

Posters 052-063

- 060 **Quantifying the seismic risk with Gutenberg-Richter relation**, Yi-Hsuan Wu, Chien-Chih Chen, Donald L. Turcotte, and John B. Rundle
- 061 **Revising Canterbury, New Zealand seismic design levels to account for time-varying hazard from the continuing Canterbury earthquake sequence.**, Matthew C. Gerstenberger and The NZ NSHM Team
- 062 **Aftershock Probabilities on Southern California Faults from a Million-Year RSQSim Catalog**, Kevin R. Milner, Thomas H. Jordan, Keith B. Richards-Dinger, and James H. Dieterich
- 063 **The Role of Deep Creep in the Timing of Large Earthquakes**, Charles G. Sammis and Stewart W. Smith

Fault Rupture and Mechanics (FARM)

- 064 **Are b-values a good indicator of stress?: A view based on laboratory stick-slip experiments**, Thorsten W. Becker, Thomas Goebel, Danijel Schorlemmer, and Georg Dresen
- 065 **Subsurface Rock Damage Structure of the M7.1 Darfield and M6.3 Christchurch Earthquake Sequence Viewed with Fault-Zone Trapped Waves**, Yong-Gang Li, Gregory De Pascale, and Darren Gravely
- 066 **Reversed-polarity secondary deformation structures near fault stepovers**, Yehuda Ben-Zion, Thomas Rockwell, Zheqiang Shi, and Shiqing Xu
- 067 **Non-equilibrium thermodynamics in sheared hard-sphere materials**, Charles K. Lieou, Ahmed E. Elbanna, James S. Langer, and Jean M. Carlson
- 068 **Coseismic slip gradient and rupture jump on parallel fault systems**, Zaifeng Liu and Benchun Duan
- 069 **Laboratory Earthquakes: Measuring surface displacements with high-speed digital image correlation**, Vito Rubino, Ares J. Rosakis, and Nadia Lapusta
- 070 **Shear Localization and the Evolution of Fault Strength**, Jiangzhi Chen and Alan W. Rempel
- 071 **Systematic reduction of pore pressure response near the San Jacinto fault**, Andrew J. Barbour
- 072 **Key results from JFAST: location and structure of the plate boundary in the area of maximum slip during the 2011 Tohoku-Oki earthquake**, James D. Kirkpatrick and Expedition 343 Scientists
- 073 **Observation of far-field Mach waves generated by the 2001 Kokoxili supershear earthquake**, Martin Vallée and Eric M. Dunham
- 074 **Numerical and theoretical analyses of in-plane dynamic rupture on a frictional interface and off-fault yielding patterns at different scales**, Shiqing Xu and Yehuda Ben-Zion
- 075 **Temperature dependence of frictional stability of gabbro and granite**, Erica K. Mitchell, Kevin M. Brown, and Yuri Fialko
- 076 **An earthquake in a maze: compressional rupture branching during the 11 April 2012 M8.6 off-Sumatra earthquake**, Lingsen Meng
- 077 **Ground Shaking and Seismic Source Spectra for Large Earthquakes Around the Megathrust Fault Offshore of Northeastern Honshu, Japan**, Lingling Ye, Thorne Lay, and Hiroo Kanamori
- 078 **Analysis of the Shallow Slip Deficit Using Sub-Pixel Image Correlation: Implications for Fault Slip Rates, and Seismic Hazards**, James Hollingsworth, James Dolan, Chris Milliner, Sebastien Leprince, Francois Ayoub, and Jean-Philippe Avouac
- 079 **Using a multi-cycle earthquake simulator to specify heterogeneous initial conditions for modeling rupture dynamics.**, Jacquelyn J. Gilchrist, James H. Dieterich, Keith B. Richards-Dinger, and David D. Oglesby
- 080 **Factors controlling shallow co-seismic deformation: Quantifying distributed co-seismic deformation of the 1992 Landers earthquake.**, Chris W. Milliner, James Hollingsworth, James Dolan, Sebastien Leprince, and Francois Ayoub
- 081 **Modeling slow slip events, non-volcanic tremor and large earthquakes in the**

Posters 064-106

- Guerrero subduction zone (Mexico) with space-variable frictional weakening and creep**, Dimitri Zigone, Yehuda Ben-Zion, and Michel Campillo
- 082 **Inferring the Initial Stress State of Large Earthquakes: Fault Branching and Incomplete Slip Partitioning in the 2008 M8 Wenchuan Earthquake Suggest Rotations of the Stress Field**, Benchun Duan
- 083 **Regional extent of the large coseismic slip zone of the 2011 Mw 9.0 Tohoku-Oki Earthquake delineated by on-fault aftershocks**, Aitaro Kato, Toshihiro Igarashi, and Jun'ichi Fukuda
- 084 **Dynamics of anti-plane shear ruptures with off-fault plasticity**, Ahmed E. Elbanna and Ralph Archuleta
- 085 **An old question revisited: the mechanics of shallow creep events on strike slip faults**, Meng Wei, Yajing Liu, and Jeff McGuire
- 086 **Earthquake rupture dynamics in complex geometries using coupled summation-by-parts high-order finite difference methods and node-centered finite volume methods**, Ossian J. O'Reilly, Eric M. Dunham, Jeremy E. Kozdon, and Jan Nordström
- 087 **Rupture Dynamics and Ground Motion from Earthquakes in Heterogeneous Media**, Samuel A. Bydlon, Jeremy E. Kozdon, and Eric M. Dunham
- 088 **"Melt Welt" Mechanism of Extreme Weakening of Gabbro at Seismic Slip Rates**, Kevin M. Brown and Yuri Fialko

POSTER PRESENTATIONS

- 089 **Dynamic rupture at low mean shear stress initiated with rate/state friction and sustained by thermal pressurization**, *Stuart V. Schmitt, Andrew M. Bradley, Eric M. Dunham, and Paul Segall*
- 090 **Self-healing slip pulses driven by thermal decomposition: Towards identifying dynamic weakening mechanisms in seismic observations**, *John D. Platt, Robert C. Viesca, and Dmitry Garagash*
- 091 **Modeling Crack-like/Pulse-like Ruptures on Dip-Slip Faults using Rate-State Friction with a Normal-Stress-Dependent State**, *Kenny J. Ryan and David D. Oglesby*
- 092 **The Role of Fluid Pressure on Frictional Behavior at the Base of the Seismogenic Zone**, *Greg Hirth and Nick Beeler*
- 093 **Reconstructing Initial Stress Condition for the 1987 Superstition Hills Earthquake**, *Qiming Liu and Ralph J. Archuleta*
- 094 **Dynamics of migrating earthquake swarms at Yellowstone and Mount Rainier: Evidence for fluid triggering?**, *David R. Shelly, Seth C. Moran, David P. Hill, Frédéric Massin, Jamie Farrell, and Robert B. Smith*
- 095 **Using Multiscale Dynamic Rupture Simulations with Adaptive Mesh Refinement to Explore the Role of Off-Fault Plasticity in the Energy Balance and Self-Similarity of Earthquakes**, *Jeremy E. Kozdon and Eric M. Dunham*
- 096 **Variability of seismic source spectra derived from cohesive-zone models of a circular rupture propagating at a constant speed**, *Yoshihiro Kaneko and Peter M. Shearer*
- 097 **Steady slip pulses on faults with rate- and state-dependent friction and strong velocity-weakening friction due to flash heating**, *Robert C. Viesca and Dmitry I. Garagash*
- 098 **Do Large Earthquakes Penetrate below the Seismogenic Zone? Potential Clues from Microseismicity**, *Junle Jiang and Nadia Lapusta*
- 099 **What Can Surface Slip Distributions Tell Us About Fault Connectivity at Depth?**, *David D. Oglesby*
- 100 **Assessment of uncertainties in coseismic and long-term slip variability along the Borrego section of the El Mayor-Cucapah surface rupture using terrestrial lidar**, *Peter O. Gold, Michael E. Oskin, Austin J. Elliott, Alejandro Hinojosa-Corona, Michael H. Taylor, Oliver Kreylos, Eric Cowgill*
- 101 **Dynamic models of potential earthquakes within the San Geronio Pass, CA**, *Jennifer M. Tarnowski and David D. Oglesby*
- 102 **Preliminary dynamic rupture and ground motion models on the Claremont-Casa Loma stepover of the San Jacinto Fault, incorporating realistic fault geometry**, *Julian C. Lozos, David D. Oglesby, Kim B. Olsen, and James N. Brune*
- 103 **Stress Drop Variability Reduction with Root-Mean-Square Acceleration**, *Jorge G. Crempien and Ralph J. Archuleta*
- 104 **The SCEC-USGS Dynamic Earthquake Rupture Code Verification Exercise - Recent Progress**, *Ruth A. Harris*
- 105 **Surface Slip During Large Owens Valley Fault Earthquakes**, *Elizabeth K. Haddon, Colin B. Amos, and Roland Bürgmann*
- 106 **Strong weakening and energy partition in a model of sheared dry gouge with thermally varying material properties**, *Jean M. Carlson and Ahmed E. Elbanna*

Stress and Deformation Over Time (SDOT)

- 107 **Contribution to the SCEC Community Stress Model Project: Two Stress Models from Focal Mechanism Inversion**, *Jeanne L. Hardebeck*
- 108 **Seismic Potential and Slip Behavior of Corrugated Reverse Fault Surfaces**, *Scott T. Marshall and Anna C. Morris*
- 109 **Stratigraphic Record of Vertical Crustal Motions in the Past 2-3 Ma Along the Coachella Valley Segment of the San Andreas Fault, Mecca Hills, California**, *James C. McNabb and Rebecca J. Dorsey*
- 110 **Space-Time Model and Analysis of Repeating Earthquakes in Parkfield Segment**, *Shunichi Nomura, Yosihiko Ogata, and Robert M. Nadeau*
- 111 **Integrating short-term and long-term deformation in numerical models: some benchmark examples using SULEC, Abaqus and Pylith**, *Susan Ellis, S Buitter, and C Williams*
- 112 **Postseismic Deformation Following the 1999 Chi-Chi Earthquake, Taiwan: Implication for Lower-Crust Rheology**, *Sylvain D. Barbot, Baptiste Rousset, Jean-Philippe Avouac, and Ya-Ju Hsu*
- 113 **Dynamics of western North America**, *Attreyee Ghosh, Thorsten W. Becker, and Gene Humphreys*
- 114 **Can self-organization of shear zones control the scale and structure of plate boundaries?**, *John P. Platt, Louis Moresi, and Thorsten W. Becker*
- 115 **Moment Accumulation Rate in Southern California**, *Kaj M. Johnson*
- 116 **Finite-fault earthquake cycle models incorporating viscous shear zones**, *Elizabeth H. Hearn*

Posters 107-116

Unified Structural Representation (USR)

- 117 **Width and dip of the southern San Andreas fault from modeling of magnetic and gravity data**, *Victoria E. Langenheim, Noah D. Athens, Daniel S. Scheirer, and Gary S. Fuis*
- 118 **High-Resolution Mapping and Analysis of Borderland Faults Using Multibeam Bathymetry Data**, *Mark R. Legg, Monica D. Kohler, Dayanthie Weeraratne, and Natsumi Shintaku*
- 119 **The Role of Fault Geometry on Geologic and Interseismic Deformation Along the Southern SAF and ECSZ**, *Justin W. Herbert, Michele L. Cooke, and Scott T. Marshall*
- 120 **Investigating Earthquake Hazards in the Northern Salton Trough, Southern California, Using Data from the Salton Seismic Imaging Project (SSIP)**, *Gary S. Fuis, John A. Hole, Joann M. Stock, Neal W. Driscoll, Graham M. Kent, Alistair J. Harding, Annie Kell, Mark R. Goldman, Elizabeth J. Rose, Rufus D. Catchings, Michael J. Rymer, Victoria E. Langenheim, Daniel S. Scheirer, Noah D. Athens, and Jennifer M. Tarnowski*
- 121 **Quaternary Deformation of the Newport-Inglewood-Carlsbad-Coronado Bank-Descanso Fault System: Long Beach to San Diego, California**, *Jonathan Bennett, Christopher Sorlien, Marie-Helene Cormier, Robert Bauer, and Brian Campbell*
- 122 **Upgrades and Improvements to the SCEC Community Fault Model: Increasing 3D fault complexity and compliance with surface and subsurface data**, *Craig Nicholson, Andreas Plesch, John Shaw, and Egill Hauksson*

Posters 117-123, 281

- 123 **Post-1 Ma deformation history of the anticline forelimb above the Pitas Point-North Channel fault in Santa Barbara Channel, California**, *Christopher C. Sorlien, Courtney J. Marshall, Craig Nicholson, Richard J. Behl, James P. Kennett, Sarah H. Decesari, Marc J. Kamerling*
- 281 **Stochastic Descriptions of Basin Velocity Structure from Analyses of Sonic Logs and the SCEC Community Velocity Model (CVM-H)**, *Thomas H. Jordan, Andreas Plesch, and John H. Shaw*

Southern San Andreas Fault Evaluation (SoSAFE)

- 124 **Extending the paleoseismic record back in time at the Mystic Lake site on the Claremont fault, northern San Jacinto fault zone**, *Nate W. Onderdonk, Sally McGill, Tom Rockwell, Neta Wechsler, Erik Gordon, and Erik Haaker*
- 125 **Geologically determined uplift rates through the central San Gorgonio Pass**, *Richard V. Heermann, Doug Yule, Paul McBurnett, and Shahid Ramzan*
- 126 **Earthquakes through the Big Bend: Comparison of earthquake ages from Frazier Mountain, Bidart Fan, and Pallett Creek, CA**, *Katherine M. Scharer, Ray Weldon, and Ashley Streig*
- 127 **Mapping offset features using high-resolution LiDAR data and field observations along the San Andreas fault in the San Bernardino/ Cajon Pass area, southern California**, *Ziad Sedki, Nate Onderdonk, and Sally McGill*
- 128 **Fault Nomenclature for the San Gorgonio Pass Region**, *Jerome A. Treiman, Jonathan C. Matti, William A. Bryant, and Katherine J. Kendrick*
- 129 **A New slip rate estimate for the San Andreas fault zone in the Coachella Valley at Pushawalla Canyon, California**, *Kimberly D. Blisniuk, Kate Scharer, Roland Burgmann, Warren Sharp, Mike Rymer, Thomas Rockwell, Patrick Williams*
- 130 **Generating a preliminary Holocene slip history along the Mojave section of the San Andreas fault**, *Tracy Compton, Eric Cowgill, Katherine M. Scharer, Ryan Gold, Rolf Westerteiger, and Tony Bernardin*

Earthquake Geology

- 134 **Rupture arrest at a strike-slip restraining double-bend observed in nature and numerical simulations**, *Austin J. Elliott, Zaifeng Liu, Michael E. Oskin, Benchun Duan, and Jing Liu-Zeng*
- 135 **Preservation of the seismic cycle in a continental low-angle, oblique-normal fault: West Salton detachment fault, USA**, *Mitchell R. Prante, Susanne U. Janecke, and James P. Evans*
- 136 **Western Transverse Ranges Tsunami Project: Do Great Earthquakes Occur on a Linked Western Transverse Ranges Thrust System?**, *Thomas K. Rockwell, Robert Peters, Eileen Hemphill-Haley, Mary McGann, Bruce Richmond, Bruce Jaffe, Rick Wilson, and Stephanie Ross*
- 137 **Using offset geomorphic features to estimate paleo-earthquake slip distribution on the Claremont fault, northern San Jacinto fault zone.**, *Scott Kenyon and Nate Onderdonk*
- 138 **Luminescence dating inter-comparison for sediments associated with the Puente Hills Blind-Thrust System recovered from cores**, *Wendy A. Barrera, Edward J. Rhodes, Madhav K. Murari, Lewis A. Owen, Michael J. Lawson, Kristian J. Bergen, James F. Dolan, and John H. Shaw*
- 139 **The Length to which an Earthquake will go to Rupture: Information Gathering**, *Alexander E. Morelan, Steven G. Wesnousky, and Glenn P. Biasi*
- 140 **Preliminary Results from the 2012 Dry Lake Valley Paleoseismic Site on the central Creeping Section of the San Andreas Fault**, *Nathan A. Toke, Tsurue Sato, Larry Kellum, Nicole Abueg, James Anderson, Jeff Selck, James B. Salisbury, and J.R. Arrowsmith*
- 141 **Vegetation Lineaments Near Pearblossom as Possible Indicators of San Andreas Foreberg-Style Faulting**, *David K. Lynch, Kenneth W. Hudnut, and Frank Jordan*
- 142 **Assessing different strategies to improve the reliability and applicability of luminescence dating of high energy sediment deposition and neotectonic contexts**, *Michael J. Lawson, Edward J. Rhodes, Wendy A. Barrera, Guadalupe T. Ochoa, and Belinda J. Roder*
- 143 **Various Visualization Techniques for Exploring the El Mayor-Cucaph Rupture using LiDAR**, *Divya Banesh, Michael E. Oskin, Xin Wang, Oliver Kreylos, and Bernd Hamann*
- 144 **Contributions of Precarious Rock Evidence to Ground Motion Prediction and**

Posters 124-133

- 131 **Comparing the Size and Frequency of Ruptures of the San Andreas fault system at the Burro Flats, Millard Canyon, and Cabazon Paleoseismic Sites**, *Doug Yule, Paul McBurnett, Shahid Ramzan, and Kerry Sieh*
- 132 **Quaternary geology, geochronology and geomorphology of the San Gorgonio Pass Region, southern California**, *Katherine J. Kendrick and Jonathan C. Matti*
- 133 **Paleoseismology of the San Jacinto Fault Zone, Claremont segment, at Mystic Lake, California**, *Rainer Luptowitz, Sally McGill, Nate W. Onderdonk, Thomas K. Rockwell, Neta Wechsler, Joseph Berg, Breeanna Copeland, and Michelle Smith*

Posters 134-149, 280

- Simulations**, *Glenn P. Biasi, James N. Brune, and Lisa Grant-Ludwig*
- 145 **New observations from the Elizabeth Lake paleoseismic site: Current results and future directions**, *Sean P. Bemis, Kate Scharer, Laurel Walker, and Patrick Taylor*
- 146 **Reevaluation of faulting in the vicinity of Cedar Springs Dam, San Bernardino County, California**, *Sean L. Dunbar, Ray J. Weldon II, Don F. Hoirup, Jr., Robert G. Barry, and Justin T. Pearce*
- 147 **Progress towards developing an improved chronology for slip-rate and paleoseismic record of the central Garlock fault using luminescence dating**, *Steven G. Okubo, Evan M. Wolf, Belinda J. Roder, Edward J. Rhodes, Sally F. McGill, James F. Dolan, Lee J. McAuliffe, Mike J. Lawson, and Wendy A. Barrera*
- 148 **Subjectivity of LiDAR-Based Offset Measurements: Results from a Public Online Survey**, *J. Barrett Salisbury, J. Ramon Arrowsmith, Thomas K. Rockwell, David E. Haddad, Olaf Zielke, and Christopher M. Madugo*
- 149 **Off-Fault Deformation in the Eastern California Shear Zone Can Account for Slip Rate Discrepancies**, *Ohilda Difo, Michele L. Cooke, and Justin W. Herbert*

POSTER PRESENTATIONS

- 280 **A user-friendly online tool for inferring surface ages from ^{10}Be depth profiles**, A. Joshua West and John Yu

Seismology

- 150 **Repeating earthquakes in the lab (not the ones you're thinking of)**, Thomas H. Goebel, Jeremy D. Zechar, Thorsten W. Becker, and Georg Dresen
- 151 **Taming the Dragons: Insights into Biases in Historical Intensity Distributions From Analysis of Spatial Variability of DYFI Intensities** Susan E. Hough
- 152 **Effects of Implementing Coulomb Stress Changes into Southern California Earthquake Forecasts**, Anne E. Strader and David D. Jackson
- 153 **Seismotectonic Crustal Stress Field and Style of Faulting Along the Pacific North America Plate Boundary in Southern California**, Wenzheng Yang and Egill Hauksson
- 154 **Complex Fault Interaction in the Yuha Desert**, Kayla A. Kroll, Elizabeth S. Cochran, Keith B. Richards-Dinger, and Danielle F. Sumy
- 155 **Salton Seismic Imaging Project Line 7: Data and Analysis to Date**, Mark R. Goldman, Gary S. Fuis, Rufus D. Catchings, Mike J. Rymer, Neal W. Driscoll, Graham M. Kent, Alistair J. Harding, Annie Kell, John A. Hole, and Joann M. Stock
- 156 **Investigating the spatial and temporal distribution of earthquakes and tremor along the Cholame segment of the San Andreas fault**, Danielle F. Sumy, Elizabeth S. Cochran, Rebecca M. Harrington, and Justin R. Brown
- 157 **Rapid Triggering of Micro-Earthquake Repeating Sequences in West Taiwan: Observations and modeling**, Yen-Yu Lin, Nadia Lapusta, and Kuo-Fong Ma
- 158 **Effects of Uncertain Primary Assumptions on Earthquake Source Imaging**, Hoby Razafindrakoto and Martin Mai
- 159 **Envelope inversion for the spatial distribution of high-frequency energy radiators of the M9.0 Tohoku-Oki earthquake**, Asaf Inbal, Jean-Paul Ampuero, and Don Helmberger
- 160 **Seismic Imaging of a bimaterial interface along the Hayward Fault, CA, with Fault Zone Head Waves and Direct P Arrivals**, Amir A. Allam, Yehuda Ben-Zion, and Zhigang Peng
- 161 **Multiple sources inversion techniques on GPU/CPU hybrid platform**, Yongfei Wang and Sidao Ni
- 162 **Biases in the Coseismic Slip Models of Shallow Subduction Zone Earthquakes Induced by Using Elastic Green's Functions**, Qian Yao and Shuo Ma
- 163 **Volumetric changes in source regions of earthquakes in the San Jacinto fault zone and the eastern California shear zone**, Zachary E. Ross, Yehuda Ben-Zion, and Lupei Zhu
- 164 **California foreshock sequences suggest underlying aseismic process** Xiaowei Chen, Peter M. Shearer, and Egill Hauksson
- 165 **Detecting Ambient Tectonic Tremors in Southern California**, Justin R. Brown, Susan E. Hough, and Jean-Paul Ampuero
- 166 **Broadband Near-Field Ground Motion Simulations in 3D Scattering Media**, Walter Imperatori
- 167 **Array analysis of Love-wave data in the Southern California Seismic Network (SCSN) to Detect Azimuthal Anisotropy**, Stephanie D. Tsang and Toshiro Tanimoto
- 168 **The 2001 – Present Triggered Seismicity Sequence in the Raton Basin of Southern Colorado/Northern New Mexico**, Justin L. Rubinstein, William L. Ellsworth, and Arthur McGarr
- 169 **The relationship between slow slip, tectonic tremor, and triggered seismicity in Cascadia and Hikurangi**, Noel M. Bartlow, John Beavan, Laura Wallace, Stephen Bannister, Aaron Wech, and Paul Segall
- 170 **Foreshock sequence of the April 11, 2012, Mw 8.6 Indian Ocean earthquake**, Xiangyu Li, Guangfu Shao, and Chen Ji
- 171 **Theoretical and Numerical Results on Effects of Attenuation and Dispersion in Correlation Functions of Ambient Seismic Noise**, Xin Liu, Yehuda Ben-Zion, and Thomas H. Jordan
- 172 **Earthquake source inversion with dense networks**, Surendra Nadh Somala, Jean-Paul Ampuero, and Nadia Lapusta
- 173 **Extensive Poroplastic Deformation as a Unifying Interpretation to Anomalous Earthquake Characteristics and Tsunami Generation in the Shallow Subduction Zone**, Evan T. Hiramawa and Shuo Ma
- 174 **Dynamic Strains at Regional and Teleseismic Distances**, Duncan C. Agnew and Frank K. Wyatt
- 175 **Aftershock Decay with Distance from a Fault**, Deborah A. Weiser, Lucile M. Jones, and Egill Hauksson
- 176 **Mapping the Crust-Mantle Transition Beneath Parkfield and Tectonic Tremor**, Han Yue, Susan Y. Schwartz, and Geoffrey Abers
- 177 **Tomographic imaging of the tectonic tremor zone beneath the San Andreas fault in the Parkfield region**, Dana E. Peterson, Clifford H. Thurber, David R. Shelly, Ninfa L. Bennington, Haijiang Zhang, and Justin R. Brown
- 178 **Seismic response to injection and production at the Salton Sea geothermal field, southern California** Lia J. Lajoie and Emily E. Brodsky
- 179 **Earthquake Nests as Natural Laboratories for the Study of Intermediate-Depth Earthquake Mechanics**, German A. Prieto
- 180 **Systematic search for missing earthquakes in Southern California around the 2010 Mw7.2 El Mayor-Cucapah earthquake**, Xiaofeng Meng, Zhigang Peng, Xiao Yu, and Bo Hong
- 181 **Understanding Seismicity in the Context of Complex Fault Systems and Crustal Geophysics**, Egill Hauksson
- 182 **Do aftershock focal mechanisms agree with the stress tensors at aftershock hypocenters?**, Elizabeth H. Madden, Gregory Beroza, and David D. Pollard
- 183 **Correlations of small and large earthquakes with tidal and seasonal stresses**, Karin A. Dahmen, Braden Brinkman, Michael Leblanc, Yehuda Ben-Zion, and Jonathan Uhl
- 184 **Moo, Whoosh, Vroom, Beep, Twinkle: Identifying Non-Seismic Signals Recorded by EarthScope's USArray Transportable Array (TA) Stations**, Debi L. Kilb, Aaron A. Velasco, and Kristine L. Pankow
- 185 **Investigation of Seasonal Variations in the Response of the Soil-Foundation-Structure-Interaction Test Structure**, Sandra H. Seale, Emily Stinson, Jamison H. Steidl, and Paul Hegarty
- 186 **Anisotropy of the Mexico Subduction Zone Based on Shear-Wave Splitting**, Igor Stubailo and Paul M. Davis
- 187 **Geometry of fault slip zones at depth from quantitative analysis of seismic catalogs**, Yaman Ozakin and Yehuda Ben-Zion

Posters 150-203, 279

- 188 **High resolution imaging of slow earthquakes using dense seismic arrays**, *Abhijit Ghosh, John E. Vidale, and Kenneth C. Creager*
- 189 **The Effects of Off-Fault Plasticity in Earthquake Cycle Simulations**, *Brittany A. Erickson and Eric M. Dunham*
- 190 **The Magnitude Distribution of Triggered Earthquakes**, *Stephen Hernandez, Emily E. Brodsky, and Nicholas J. van der Elst*
- 191 **Measuring Material Properties with a Permanently Deployed Cross-Hole Experiment**, *Jamison H. Steidl, Timothy A. Lamere, Sandra H. Seale, Robin Gee, and Paul Hegarty*
- 192 **Spatiotemporal evolution of the 2012 Mw 8.6 Sumatra earthquake constrained by teleseismic body and surface waves**, *Guangfu Shao, Xiangyu Li, and Chen Ji*
- 193 **Products and Services Available from the Southern California Earthquake Data Center (SCEDC) and the Southern California Seismic Network (SCSN)**, *Ellen Yu, Aparna Bhaskaran, Shang-Lin Chen, Faria Chowdhury, Doug Given, Kate Hutton, Egill Hauksson, and Rob Clayton*
- 194 **Dynamic Triggering of Deep Non-Volcanic Tremor in Cuba and Southern Chile**, *Gregory Armstrong, Zhigang Peng, Kevin Chao, Chastity Aiken, Hector Gonzalez-Huizar, and Bladimir Moreno*
- 195 **Triggering of Tremor along the San Jacinto Fault near Anza, California**, *Tien-Huei Wang, Elizabeth S. Cochran, Duncan Agnew, and David D. Oglesby*
- 196 **Upper crustal structure beneath the Salton Sea as imaged by active source marine seismic refraction in conjunction with the Salton Seismic Imaging Project**, *Annie M. Kell, Valerie Sahakian, Alistair Harding, Graham Kent, and Neal Driscoll*
- 197 **When Are Noise Correlation Amplitudes Useful?**, *Victor C. Tsai and Zhongwen Zhan*
- 198 **Utilizing methods of subspace detection on an earthquake sequence in the Big Bear region**, *Sarah A. Barrett and Greg Beroza*
- 199 **Dispersion observations from the 2011 Tohoku tsunami waveforms recorded on the spatially dense ALBACORE OBS array**, *Monica D. Kohler, Fan-Chi Lin, and Dayanthie S. Weeraratne*
- 200 **Evaluation of the Scattering Models in the Crust for Mexico and Long Beach**, *Luis A. Dominguez, Paul Davis, and Dan Hollis*
- 201 **Spatiotemporal Behaviors in Earthquake Multiplets at the Geysers Geothermal Field, CA**, *Taka'aki Taira*
- 202 **Salton Seismic Imaging Project Line 5—the San Andreas Fault and Northern Coachella Valley Structure, Riverside County, California**, *Michael J. Rymer, Gary S. Fuis, Rufus D. Catchings, Mark R. Goldman, Jennifer M. Tarnowski, John A. Hole, Joann M. Stock, and Jonathan C. Matti*
- 203 **Salton Seismic Imaging Project Line 6: San Andreas Fault and Northern Coachella Valley Structure, Riverside and San Bernardino Counties, California**, *Rufus D. Catchings, Gary S. Fuis, Michael J. Rymer, Mark R. Goldman, Jennifer M. Tarnowski, John A. Hole, Joann M. Stock, and Jonathan C. Matti*
- 279 **SKS Splitting offshore California from ALBACORE**, *Joseph Ramsay, Paul M. Davis, and Monica D. Kohler*

Tectonic Geodesy

- 204 **InSAR Time Series Error Characteristics and Mitigation**, *William D. Barnhart and Rowena B. Lohman*
- 205 **A systematic estimation of fault creep rates along major faults in California from L-band radar interferometry**, *Xiaopeng Tong, David Sandwell, and Bridget Smith-Konter*
- 206 **Quantifying 3D ground deformation using multi-angle high resolution optical imagery**, *Sebastien Leprince, Francois Ayoub, James Hollingsworth, Jean-Philippe Avouac, and James Dolan*
- 207 **Automated Determination of Fault Slip Model from GPS Network Signals After an Earthquake**, *Jay W. Parker, Margaret Glasscoe, and Andrea Donnellan*
- 208 **Mechanisms of Postseismic Deformation Following the 2010 El Mayor-Cucapah Earthquake**, *John C. Rollins, Sylvain Barbot, and Jean-Philippe Avouac*
- 209 **Visible Earthquakes – a web-based tool for visualizing and modeling InSAR earthquake data**, *Gareth J. Funning and Rowan B. Cockett*
- 210 **Network estimation of time-dependent noise in GPS data**, *Ksenia Dmitrieva and Paul Segall*
- 211 **Decadal-Scale Crustal Deformation Transients in Japan Prior to the March 11, 2011 Tohoku Earthquake**, *Andreas P. Mavrommatis, Paul Segall, Shin'ichi Miyazaki, Susan E. Owen, and Angelyn W. Moore*
- 212 **Total variation denoising of interseismic deformation in southern California**, *Eileen L. Evans and Brendan J. Meade*
- 213 **Status of GPS Network Operations at USGS Pasadena**, *Daniel N. Determan, Aris G. Aspiotes, Ken W. Hudnut, Nancy E. King, and Keith F. Stark*
- 214 **3-D earthquake surface displacements from differencing pre- and post-event LiDAR point clouds**, *Edwin Nissen, Ramon Arrowsmith, Aravindhan Krishnan, and Srikanth Saripalli*
- 215 **Southern California Educators and Their Students Contribute to Crustal Deformation Studies Within San Bernardino and Riverside Counties**, *Thomas Castiglione, Helen Corral-Bonner, Robert de Groot, Joshua Drake, Jacob Drake, Anna Foutz, Steven Husa, Sally McGill, Eric Sahl, Joshua Spinler, Bernadette Vargas, and Rick Bennett*
- 216 **Towards an improved GPS velocity solution in the presence of earthquakes, and accurate assessment of inter-, co- and post-seismic motions**, *Michael A. Floyd and Thomas A. Herring*
- 217 **Analyzing UAVSAR Data using the QuakeSim Computational Environment**, *Andrea Donnellan*
- 218 **Present-day loading rate of faults in southern California and northern Baja California, Mexico, and post-seismic deformation following the M7.2 April 4, 2010, El Mayor-Cucapah earthquake from GPS Geodesy**, *Joshua C. Spinler and Richard A. Bennett*
- 219 **Teachers Using Continuous GPS Data to Learn About Earthquakes: Sharing Research Results in the Classroom Through Lesson Study – 2012 Campaign**, *Robert M. de Groot, Sally McGill, Thomas Castiglione, Helen Corral-Bonner, Anna M. Foutz, Steve G. Husa, Eric Sahl, Bernadette E. Vargas, and Seth Wallace*
- 220 **Fault slip rate estimates for southwestern US from GPS data and non-block viscoelastic sheet models**, *Ray Y. Chuang and Kaj M. Johnson*
- 221 **Unified Western US Crustal Motion Map**, *Zheng-Kang Shen and Min Wang*
- 222 **Studying Fault Movement Throughout the San Bernardino Mountains**, *Tiffany N. Anderson*
- 223 **An inverse modeling code for obtaining earthquake source parameters from InSAR data**, *Erika Noll*
- 224 **UNAVCO-PBO Southwest Region Network Operations**, *Christian Walls, Doerte Mann, Andre Basset, Jacob Sklar, Chelsea Jarvis, Travis Pitcher, Shawn Lawrence, and Karl Feaux*

Posters 204-240

POSTER PRESENTATIONS

- 225 **Evaluation of transient deformation from two decades of continuous GPS time series analysis in Southern California and Cascadia**, *Yehuda Bock, Brendan W. Crowell, Peng Fang, Sharon Kedar, Zhen Liu, and Angelyn W. Moore*
- 226 **Interseismic Strain Accumulation Across Metropolitan Los Angeles: Puente Hills Thrust**, *Donald F. Argus, Zhen Liu, Michael B. Heflin, Angelyn W. Moore, Susan Owen, Paul Lundgren, Vicki G. Drake, and Ivan I. Rodriguez-Pinto*
- 227 **Constraining Moment Accumulation Rate on the Creeping Segment of the San Andreas Fault**, *Jeremy L. Maurer, Kaj M. Johnson, and Paul Segall*
- 228 **Using GPS Derived Shear Strain Rates in Southern California to Constrain Fault Slip Rate, Locking Depth, and Residual Off-Fault Strain Rates**, *William E. Holt, Atreyee Ghosh, and Yu Chen*
- 229 **Application of a sequential optimization algorithm for GPS network augmentation at Parkfield and Sumatra**, *Piyush S. Agram and Sylvain Barbot*
- 230 **Southern California crustal deformation map and long-term transient from InSAR time series analysis**, *Zhen Liu, Paul Lundgren, and Sylvain Barbot*
- 231 **Integration and Analysis of Seismic, Pore Pressure, and Strain signals at the PBO Borehole Stations**, *Francesco Civilini and Jamison H. Steidl*
- 232 **Using GPS to measure San Andreas and San Jacinto fault movement in the San Bernardino area**, *Joseph Berg, Sally McGill, William Buckley, Ashley Covarrubias, Rainer Luptowitz, Joshua Spinler, and Richard A. Bennett*
- 233 **Two New Optical Fiber Strainmeters for Earth Strain Measurement**, *Scott DeWolf, Frank K. Wyatt, Mark A. Zumberge, Duncan C. Agnew, Don Elliott, and Billy Hatfield*
- 234 **Application of Cluster Analysis to Interpreting Regional GPS Velocity Fields in California**, *Wayne Thatcher, James Savage, and Robert Simpson*
- 235 **Using GPS to measure slip rates on the Honey Lake/Warm Springs and Mohawk Valley fault systems, Northern Walker Lane.**, *Jayne M. Bormann, William C. Hammond, Corné Kreemer, and Geoffrey Blewitt*
- 236 **Detection of Strain Transient Anomalies in Southern California Using Retrospective and Near Real Time Analyses**, *Gina Shcherbenko and William E. Holt*
- 237 **Properties of Shallow creep on the Southern San Andreas Fault from InSAR and GPS**, *Eric O. Lindsey, Yuri Fialko, and Yehuda Bock*
- 238 **Evolution of the October 1999 Hector Mine Earthquake surface rupture: a decadal view**, *Frank J. Sousa, Joann M. Stock, and Sinan O. Akciz*
- 239 **Investigations into effects of different modeling codes and rheology on predicted coseismic and postseismic surface deformation**, *David T. Sandwell, Sylvain D. Barbot, Charles A. Williams, Andrew Freed, Susan Ellis, Mong-Han Huang, and Bridget R. Smith-Konter*
- 240 **El Mayor-Cucapah (Mw 7.2) earthquake: Early Postseismic Deformation from InSAR and GPS observations**, *Alejandro Gonzalez-Ortega, David T. Sandwell, Yuri Fialko, John M. Fletcher, Alex Nava, Jose J. González-García, Brad P. Lipovsky, Michael A. Floyd, and Gareth J. Funning*

Summer Undergraduate Research Experience (SURE)

- 250 **Role of Geotechnical Velocity Models in Shake Zone Scenarios of South Lake Tahoe**, *Kelley A. Hall and John Louie*
- 251 **Earthquake Preparedness Education Program**, *Michelle J. Vanegas, Monica Barajas, Nick Scruggs, Aaron Hoogstraten, and Robert M. de Groot*
- 252 **Discovery and paleoseismic investigation of the Bidart Fault, a subparallel oblique-slip strand of the San Andreas fault in the Carrizo Plain**, *Terry M. Cheiffetz, Tsurue Sato, Sinan Akciz, and Lisa Grant-Ludwig*
- 253 **Tracking the Moho and the lithosphere-asthenosphere boundary along the margin of the Salton Trough with variations in basaltic magmas**, *Elinor S. Utevsy, Andrew P. Barth, and Drew S. Coleman*
- 254 **Analyzing ShakeOut Participant Feedback to Improve Future Drills**, *Erica Garland and Michele Wood*

Posters 250-256

- 255 **Integration of Significant Data from SCEC Borehole Sites with the NEES@UCSB Database**, *Matthew Cook, Jamison Steidl, Sandra Seale, and Paul Hegarty*
- 256 **The Effects of Boundary Conditions on Auto-Acoustic Compaction**, *Kevin Bernardo, Emily E. Brodsky, and Nicholas J. van der Elst*

Communication, Education, and Outreach (CEO)

- 257 **The Impact of the Earthquake Country Alliance (ECA) Earthquake Education and Public Information Center (EPIcenter) Network**, *Irene N. Gow, Robert M. de Groot, and Thomas H. Jordan*
- 258 **Low risk does not equal no risk: understanding barriers to earthquake risk-reduction in low seismic hazard zones**, *David Johnston, Caroline Orchiston, Craig Weaver, Julia Becker, Sarah McBride, Douglas Paton, John McClure, and Tom Wilson*
- 259 **Using Videogames in Geoscience Education**, *Daniel Rohrlack, Alan Yang, and Debi Kilb*
- 260 **GeoTrek: An Educational Framework for K-12 Free-Choice Learning at the San Bernardino County Museum's Hall of Geological Wonders**, *Karina Chung, Robert de Groot, and Kathleen Springer*
- 261 **New Videos Developed for Outreach and Education in Earthquake Engineering**, *Val V. Gorbunov, Nicholas Perez, Justin*

Posters 257-262

- Morris, Sandra H. Seale, and Jamison H. Steidl*
- 262 **Citizen Science with the Quake-Catcher Network: Promoting seismology research and broader impacts activities in museums, libraries, and other free-choice learning venues**, *William M. Luedtke, Kevin Chan, Danielle Sumy, Robert de Groot, Elizabeth Cochran, Nick Rousseau, Thomas Jordan*

General

- 263 **Present-day rheology of the lithospheric mantle beneath the Mojave region from naturally deformed peridotite xenoliths,** *Whitney M. Behr and Greg H. Hirth*
- 265 **Observation of Forward-Directivity Effects in the Near-Fault Ground Motions of the 2010-11 Canterbury, New Zealand Earthquakes,** *Varun A. Joshi and Brendon A. Bradley*
- 266 **Seismic Response of the Instrumented UC Physics Building in the Canterbury Earthquakes,** *Sam A. McHattie and Brendon A. Bradley*
- 267 **Is deep non-volcanic tremor just a swarm of low frequency earthquakes?,** *Naum I. Gershenzon and Gust Bambakidis*
- 268 **Understanding Slip on Triggered Faults in the Presence of a Large Regional Deformation,** *Moises M. Ponce-Zepeda, Andrea Donnellan, and Jay Parker*

- 269 **Exploration of slip-rate discrepancies and distributed deformation via linkages between the Calico, Harper Lake and Blackwater Faults,** *Jacob Selander and Michael Oskin*
- 270 **Continuous Record of Permeability inside the Wenchuan Earthquake Fault Zone,** *Lian Xue, Emily E. Brodsky, Haibing Li, Huan Wang, and Junling Pei*
- 271 **What PGD and PGV values collapse mid-rise steel, special moment frames or make them unreparable?** *Anna H. Olsen and Thomas H. Heaton*
- 272 **Evidence for Active Northeast Tilting Across the Southern Coachella Valley and Santa Rosa Mountains,** *Rebecca J. Dorsey, Victoria E. Langenheim, and James C. McNabb*
- 273 **Bio-inspired Techniques for Novel Earthquake Research,** *Liwen Shih*

- 274 **Investigation of structure and seismicity in the Los Angeles basin with a dense array,** *Dunzhu Li, Fan-Chi Lin, Brandon Schmandt, and Rob Clayton*
- 275 **Data Democracy in Simultaneous Monte Carlo Optimizations of Geodetic and Seismic Data,** *Henriette Sudhaus and Sebastian Heimann*
- 276 **Formation and suppression of strike-slip fault systems,** *Ivy S. Curren*
- 277 **Imaging the upper crustal velocity structure in the northern Salton Sea: Results from the Salton Sea Imaging Project's (SSIP) marine refraction experiment,** *Valerie J. Sahakian, Annie Kell, Alistair Harding, Neal Driscoll, and Graham Kent*
- 278 **A Quasi-DYNAMIC Earthquake Simulator (QDYN) for earthquake cycle, slow slip and tremor modeling,** *Yingdi Luo and Jean-Paul Ampuero*

Posters 263-278

Undergraduate Studies in Earthquake Information Technology (UseIT)

- 295 **Creation of additional GIS capabilities for SCEC-VDO: Added support for new earthquake catalogs for the SCEC-VDO software and improved functionality of existing SCEC-VDO plugins for the 2012 UseIT Grand Challenge,** *Kevin Centeno, Aaron Hoogstraten, Kameron Johnson, Dave Smith, Bridget Hellige, Nick Rousseau, Thomas H. Jordan, and Robert M. de Groot*
- 296 **Enhancing the Functionality for SCEC-VDO: Surface Map Coloring and Earthquake Statistics,** *Nolan Mattox, Christian Vanderwall, Chris Kohlenberger, Michael Hodges, Marshall Rogers-*

- Martinez, Thomas H. Jordan, Robert de Groot, Nick Rousseau, and Kevin Milner*
- 297 **SCEC-VDO and GIS Integration for the USEIT 2012 Grand Challenge,** *Rebecca N. Greenwood, Marianne Jara, Laura Gerbi, Eduardo Andino, Thomas Jordan, Robert de Groot, Yao-Yi Chiang, and Nick Rousseau*
- 298 **SCEC-VDO Scripting Team Visualizations for the 2012 USEIT Grand Challenge,** *Laura M. Gerbi, Eduardo Andino, Shanna Williamson, Jose Cruz, Thomas Jordan, Robert de Groot, Nick Rousseau, Sam Reed, and Bridget Hellige*

- 299 **The Grand Challenge: Documenting the Scientific Collaboration and other Experiential Learning Activities of the UseIT Class of 2012,** *Nick Rousseau, Alysia Gonzales, Carlos Landa, Will Ilgen, Madeline Berger, Thomas Jordan, and Robert de Groot*

Posters 295-299

Meeting Abstracts

Dynamic Strains at Regional and Teleseismic Distances, Duncan C. Agnew and Frank K. Wyatt (Poster 174)

There are increasing amounts of data for, and interest in, the ability of large earthquakes to trigger different kinds of seismicity, both conventional earthquakes and non-volcanic tremor, at distances such that largest stress changes are caused by radiated seismic waves. The amplitudes of these are almost always inferred from recorded (or inferred) ground motions, since few measurements of deformation are available. The longbase laser strainmeters at Pinyon Flat Observatory (PFO) provide a unique, well-calibrated measure of the complete strain tensor. We have examined strain data from 81 earthquakes between 1977 and the present, with magnitudes from 6.5 through 9.0, and at distances from 500 to 16,000 km. It is possible to fit these data, to within a factor of 3, with a simple regression of log strain against log distance and magnitude. For example, peak strain in the direction to the earthquake is given by $\log(E) = 0.95M - 1.65 \log(\text{dist}) - 2.8$, with distance in degrees and strain in nanostrain. Similar relationships give other peak strains, and also the maximum power and total energy dissipated in a unit volume. Theory predicts zero extensional

strain perpendicular to the back-azimuth, but this is not what is observed; the rms transverse strain is at least 20% of the radial, and can be larger than radial strain for some events. This remains true even if the back-azimuth is allowed to vary to allow for wave refraction. The strains seem to be least isotropic for paths through relatively uniform structure (from the SW Pacific) and most for paths along the plate boundary, suggesting a possible effect from multipathing. Both areal and fault-parallel shear are systematically larger at the strainmeter sites in the Salton Trough (SCS and DHL) than at PFO.

Application of a sequential optimization algorithm for GPS network augmentation at Parkfield and Sumatra, Piyush S. Agram and Sylvain Barbot (Poster 229)

We present a simple sequential selection algorithm for optimizing geodetic networks to monitor specific geophysical phenomena. Our approach is a generalized version of sequential subset algorithms used in the medical imaging community [Reeves and Zhe, 1999; Broughton et al., 2010]. We demonstrate the strength of our algorithm by applying it to two real world examples - 1) monitoring the seismogenic zone between the hypocenters of the 1966 and the 2004 Parkfield earthquakes and 2) monitoring of the locked Mentawai segment of the Sunda megathrust from the trench to below the brittle-ductile transition. In each case, we observe that our ability to resolve slip in the presumed seismogenic zone on the fault using geodetic observations from existing continuous GPS networks is poor. We apply our algorithm to identify possible station locations that will allow enable us to maximally resolve slip in the seismogenic zone. Specifically, our algorithm maximizes the improvement in the minimum model resolution in the seismogenic zone with addition of every new station.

We show that the pre-2004 continuous GPS network at Parkfield is more sensitive to 1 cm of slip at depths shallower than 6 km than to 50 cm of slip in the deeper seismogenic zone, to which only two far-field stations are most sensitive. The augmentation of the GPS network following the 2004 event allows us to constrain deeper slip, but more coverage is needed at strategic points to detect anomalous, and perhaps precursory, fault slip in the seismogenic zone during the current inter-seismic period before the next anticipated Mw 6 Parkfield rupture. We present the optimal spatial distribution of the 20 new GPS stations that are required to resolve the seismogenic zone geodetically.

The locked Mentawai segment of the Sunda Megathrust has accumulated about 10m of fault slip deficit since the great 1797 Mw8.9 earthquake. We present the most favourable combination of island and mainland stations to augment the Sumatra GPS Array (SuGAR), that will theoretically enable us to perfectly resolve fault slip from the trench to

depths greater than 100km with a 30 x 30km spatial resolution. The presence of the Batu, Siberut, Sipora and Pagai islands hundred kilometers off the mainland is a favourable circumstance that allows us, in principle, to monitor fault activity with unprecedented accuracy.

Seismic Imaging of a bimaterial interface along the Hayward Fault, CA, with Fault Zone Head Waves and Direct P Arrivals, Amir A. Allam, Yehuda Ben-Zion, and Zhigang Peng (Poster 160)

We show the existence and image properties of a seismic velocity contrast along the Hayward fault using moveout analysis and joint inversion of fault zone head waves (FZHW) and direct P arrivals. The analysis is based on FZHW and P arrival times for 5834 earthquakes recorded at up to 27 stations of the Berkeley Digital Seismic Network (BDSN) and the Northern California Seismic Network (NCSN). Robust identification of FZHW requires the combination of multiple techniques due to the diverse instrumentation of the BDSN and NCSN. For single-component short-period instruments, FZHW are identified by examining sets of waveforms from both sides of the fault, and finding on one (the slow) side emergent reversed-polarity arrivals before the direct P waves. For three-component broadband and strong-motion instruments, the FZHW are identified with polarization analysis that detects early arrivals from the fault direction before the regular body waves with polarizations in the source-receiver directions. The initial results indicate a velocity contrast of 5-12% along the central portion of the Hayward fault, with the southwest side having faster P wave velocity in agreement with tomography results. A systematic moveout between the FZHW and direct P waves for a roughly 70 km long fault section suggest a single continuous fault interface over that distance. We also find some complexities near the junction with the Calaveras fault in the southernmost portion and near the city of Oakland. Regions giving rise to variable FZHW arrival times can be correlated to first order with the presence of lithological complexity, including slivers of high-velocity metamorphic rocks and serpentinized rocks. The seismic velocity contrast and geological complexity have important implications for earthquake and rupture dynamics of the Hayward fault.

Imaging and modeling the unexpected rupture path of an extreme event: the 2012 Mw 8.6 off-Sumatra earthquake, Jean-Paul Ampuero (Talk Tue 08:00)

On April 11th 2012 a Mw 8.6 earthquake, the largest strike-slip event known to date, occurred in a diffuse deformation zone in the Indian Ocean, off-shore Sumatra. I will summarize what has been learned so far about this rare event and which puzzles remain unsolved, while highlighting those aspects that are relevant to research in SCEC4, especially on Fault and Rupture Mechanics. Due to its remote location, this earthquake is a good example of the unique information about earthquake rupture processes that can be obtained by high-resolution back-projection source imaging based on teleseismic array data. This technique reveals a complicated rupture path, involving multiple segments of a network of conjugate, almost-orthogonal faults and unexpected features like branching despite compressional dynamic stresses. I will discuss implications of these observations for a range of topics, including earthquake source imaging, dynamic rupture branching, rupture linkage across stepovers, rheology of the deep lithosphere and the maximal depth extent of earthquake rupture, the possibility of rupture through nominally stable fault regions, the timely characterization of rupture growth.

Studying Fault Movement Throughout the San Bernardino Mountains, Tiffany N. Anderson (Poster 222)

California State University, San Bernardino students in the PRISM (Proactive Recruitment in Introductory Science and Mathematics) program have used GPS equipment to survey and study movement along southern California's San Andreas Fault system. This area's movement has been researched by California State University, San

Bernardino since 2002. This geographic area had previously not been sufficiently investigated due to some of the difficulties of time and physical efforts needed to set up equipment at these sites. The GPS data collected in 2012 will be processed at the University of Arizona. The data show that the San Andreas and San Jacinto faults are the fastest moving faults in the plate boundary fault system. The best-fitting model has a slip rate of 12 mm/yr for the San Andreas Fault and 9 mm/yr for the San Jacinto fault. Other models, however, can also fit the data reasonably well with slip rates for either fault ranging from 0 to 24 mm/yr.

Interseismic Strain Accumulation Across Metropolitan Los Angeles:

Puente Hills Thrust, *Donald F. Argus, Zhen Liu, Michael B. Hefflin, Angelyn W. Moore, Susan Owen, Paul Lundgren, Vicki G. Drake, and Ivan I. Rodriguez-Pinto* (Poster 226)

Twelve years of observation of the Southern California Integrated GPS Network (SCIGN) are tightly constraining the distribution of shortening across metropolitan Los Angeles, providing information on strain accumulation across blind thrust faults. Synthetic Aperture Radar Interferometry (InSAR) and water well records are allowing the effects of water and oil management to be distinguished. The Mojave segment of the San Andreas fault is at a 25° angle to Pacific-North America plate motion. GPS shows that NNE-SSW shortening due to this big restraining bend is fastest not immediately south of the San Andreas fault across the San Gabriel mountains, but rather 50 km south of the fault in northern metropolitan Los Angeles. The GPS results we quote next are for a NNE profile through downtown Los Angeles. Just 2 mm/yr of shortening is being taken up across the San Gabriel mountains, 40 km wide (0.05 micro strain/yr); 4 mm/yr of shortening is being taken up between the Sierra Madre fault, at the southern front of the San Gabriel mountains, and South Central Los Angeles, also 40 km wide (0.10 micro strain/yr). We find shortening to be more evenly distributed across metropolitan Los Angeles than we found before [Argus et al. 2005]. Elastic models of interseismic strain accumulation is fit to the GPS observations using the Back Slip model of Savage [1983]. Rheology differences between crystalline basement and sedimentary basin rocks are incorporated using the EDGRN/EDCMP algorithm of Wang et al. [2003]. We find, along the NNE profile through downtown, that: (1) The deep Sierra Madre Thrust cannot be slipping faster than 2 mm/yr, and (2) The Puente Hills Thrust and nearby thrust faults (such as the upper Elysian Park Thrust) are slipping at 9 ± 2 mm/yr beneath a locking depth of 12 ± 5 km (95% confidence limits). Incorporating sedimentary basin rock either reduces the slip rate by 10 per cent or increases the locking rate by 20 per cent. The 9 mm/yr rate for the Puente Hills Thrust and nearby faults exceeds the cumulative 3–5 mm/yr rate estimated using paleoseismology along the Puente Hills Thrust (1.2–1.6 mm/yr, Dolan et al. 2003), upper Elysian Park Thrust (0.6–2.2 mm/yr, Oskin et al. 2000), and western Compton Thrust (1.2 mm/yr, Leon et al. 2009), though all the paleoseismic estimates are minimums. We infer that M 7 earthquakes in northern metropolitan Los Angeles may occur more frequently than previously thought.

Dynamic Triggering of Deep Non-Volcanic Tremor in Cuba and Southern Chile

Gregory Armstrong, Zhigang Peng, Kevin Chao, Chastity Aiken, Hector Gonzalez-Huizar, and Bladimir Moreno (Poster 194)

Triggered tremors are well documented and known to occur in subduction zones and along strike-slip faults where ambient tremors also occur. Despite many observations, the physical mechanisms responsible for this phenomena are still uncertain. Here, we study the strike-slip fault system of Cuba from 2007 to mid-2012 and along the subduction zone of southern Chile from late-2004 to 2006. In Cuba, we select regional and teleseismic events with a magnitude-based estimated dynamic stress [e.g. van der Elst, 2010] greater than 1 kPa. In Chile, the mainshocks so far include only teleseismic events (e.g., distance larger than 1000 km) with a magnitude greater than Mw7.5 and a calculated dynamic stress greater than 0.5 kPa. We classify triggered tremor bursts as having low-frequency (~1 to 10 Hz), long-duration, and coincidence with large-amplitude surface waves from the mainshock. In southern Chile, we have found 3 triggered tremors from teleseismic events - the 2004/12/26 Mw9.1 Sumatra, the 2005/03/28 Mw8.6 Sumatra, and the 2006/05/03 Mw8.0 Tonga earthquakes. On the other hand, in Cuba we have identified 6 regional/teleseismic events triggering deep tremor, including

the 2010/02/27 Mw8.8 Chile and the 2011/03/11 Mw9.0 Japan earthquakes that have been analyzed previously (Gonzalez-Huizar et al., 2012; Peng et al., 2012). Our initial locations suggest that tremors occur near active plate boundary faults in both regions. However, the tremor depth is not well constrained, so we set the depth to be as 25 km in Cuba and 35 km in Southern Chile. In both regions, we use the peak ground velocities to estimate the dynamic stresses, and found an apparent triggering threshold of 10 kPa and ~6 kPa in Cuba and Chile, respectively. It is worth noting that ambient tremor in Cuba has not been identified yet. In southern Chile, Ide (2012) have found clear ambient tremor very close to our study region. Our next step is to examine the relationship between ambient and triggered tremor in southern Chile, and perform a detailed search for ambient tremor in Cuba.

Nonlinear amplification factors at SC strong motion stations, *Dominic Assimaki, Jian Shi, and Alan Yong* (Poster 010)

In this study, we compile H/V ambient vibration inversion data at strong motion station sites in Southern California with generic nonlinear soil properties for typical sedimentary deposits, and develop nonlinear site-specific amplification factors for implementation in ground motion simulations. Until recently, limited information existed on the soil properties and amplification effects at many of the strong motion stations in Western US. Acknowledging the critical role of nonlinear site response for inversion and prediction of broadband ground motions, geotechnical characterization of a large number of station sites has taken place as part of an ongoing effort led by the USGS. To date, site classification of a large number of station sites has been completed based on the average soil velocity in the top 30m (Vs30). While Vs30 provides a quantitative measure of the soil stiffness, however, it does not reflect the profile susceptibility to nonlinear effects during strong seismic shaking. Furthermore, empirical amplification factors that have been computed for a large number of stations are primarily based on weak seismic motions, thus reflecting the linear response of the sediments. We here compile available geotechnical information at selected station sites, conduct site-specific response analyses by means of validated nonlinear models available on the SCEC Broadband Simulation Platform, study the parametric uncertainty introduced by the geotechnical input parameters, and develop intensity-dependent, site-specific amplification factors that account for nonlinear effects. Comparison of our results with empirical amplification factors, currently employed in large-scale ground motion predictions to simulate site effects, will indicate the sites where nonlinear effects are anticipated to play an important role, and provide improved measures of site response for ground motion validation. Future work includes the development of frequency- and intensity-dependent site amplification factors that can be integrated in the Southern California Broadband simulation platform to improve the accuracy and efficiency of ground motion predictions accounting for nonlinear effects in the near-surface.

Understanding the NGA-West ground-motion prediction equations for PGA and PGV *SSA Abstract 2012, Annemarie S. Baltay, Gregory C. Beroza, and Thomas C. Hanks* (Poster 021)

Next Generation of Attenuation (NGA) ground-motion prediction equations (GMPE) use as many as 19 parameters to empirically describe peak ground acceleration (PGA) and peak ground velocity (PGV) as a function of magnitude and distance; these parameters are complexly related and may trade off in ways that are not easily understood. We use the simple point-source models of Hanks and McGuire [1979], McGarr [1984], and Boore [1983] to fit PGA and PGV dependent on magnitude and source-site distance to the NGA-West 2012 data set, finding a single stress drop for all of the data. The fit results in a stress drop of ~5 MPa for all events, consistent with stress drop studies in similar active regions; Class 1 events, analogous to mainshocks, in the NGA data set, however, have stress drops greater than that of the Class 2 events, on-plane aftershocks.

Between M 4.5 – M 7, the theoretical relation for PGA matches the four most commonly used NGA-West GMPEs very well. Only knowledge of stress drop, as well as the material parameters ρ , β , and f_{max} , are necessary to model the theoretical relationship. At large magnitudes, however, these physics-based point source models over predict both the PGA and PGV data. Assuming contributions to PGA from points on the

MEETING ABSTRACTS

fault farther than 30 km are negligible at recording distances less than 20 km due to the high-frequency nature of PGA, earthquakes above magnitude ~ 6.7 are theoretically saturated for PGA. PGV saturates at a slightly higher magnitude of 7, consistent with the notion that contributions to PGV can come from farther distances, as PGV is less attenuated than PGA. Statistical tests also confirm that the data becomes saturated at these magnitudes. Above the saturation magnitudes, we indeed find a constant PGA of $\sim 0.3g$ and constant PGV of ~ 40 cm/s, albeit in the midst of considerable scatter. At small magnitudes, $M < 4.5$, the point-source models again over predict the NGA West data. We modify the point-source models to account for near-site shallow crustal attenuation, κ , where f_{max} relates to κ as $f_{max} = 1/\pi\kappa$. By incorporating the effect of κ , the point-source relationships are able to model the decrease in PGA and PGV in the small magnitude data. That these very simple constant stress-drop, point-source models, together with the finite-fault approximation at large magnitudes, match the NGA PGA and PGV data well suggest that considerable simplicity underlies the parametrically complex NGA-West GMPEs.

Various Visualization Techniques for Exploring the El Mayor-Cucapah Rupture using LiDAR, Divya Banesh, Michael E. Oskin, Xin Wang, Oliver Kreylos, and Bernd Hamann (Poster 143)

One of the best ways to analyze deformations in the landscape due to earthquake surface ruptures is to use point-based visualizations, such as LidarViewer. LidarViewer is a visualization system devised by a team of UC Davis researchers, which we have used as a basis for the visualization approaches presented here. Grid-based techniques often fail to adequately represent 3-D features, such as scarps and vegetation, and introduce aliasing artifacts that are undesirable when the deformation signal sought is less than the point spacing. In the case of the El Mayor-Cucapah earthquake, pre-earthquake airborne LiDAR data, which was collected as part of a regional survey, is very sparse (0.013 pts/m²) compared to the post-earthquake survey (9 pts/m²). A simple, χ^2 minimization approach to matching these data sets takes advantage of this dramatic resolution difference to extract 3-D ground motion. The resulting dense field of 3-D displacement vectors show the deformation along various parts of the landscape that occurred as a result of the earthquake, but are difficult to visualize together with the terrain, limiting interpretation of these results. To resolve this problem, we visualize the resulting displacement field in a 3-D environment using streamline-based approaches having their origin in flow field visualization, colored by elevation change, and superimposed on the post-earthquake topography. This fused data product makes possible exploration and assessment of the deformation signal and its relationship to landscape features, such as fault scarps, vegetation, and topographic relief. Of the two streamline-based approaches we have employed, the first method creates a set of typical streamlines, where each streamline is a path traced by a massless particle as it moves through a vector field. This approach is a more comprehensive visualization than a vector field, and allows for changes in landscape deformation to be easily noticed. The second method, line-integral convolution (LIC), is a very "dense version" of streamline visualization and while streamlines are placed some distance apart, a LIC visualization affects every pixel in the image. The resulting image resembles the result of a paint brush outlining the flow of the particles in the vector field. Both methods enhance the analysis of these data sets.

Postseismic Deformation Following the 1999 Chi-Chi Earthquake, Taiwan: Implication for Lower-Crust Rheology, Sylvain D. Barbot, Baptiste Rousset, Jean-Philippe Avouac, and Ya-Ju Hsu (Poster 112)

On 1999 September 21, the Mw 7.6 Chi-Chi earthquake ruptured a segment of the Chelungpu Fault, a frontal thrust fault of the Western Foothills of Taiwan. The stress perturbation induced by the rupture triggered a transient deformation across the island, which was well recorded by a wide network of continuously operated GPS stations. The analysis of more than ten years of these data reveals a heterogeneous pattern of postseismic displacements, with relaxation times varying by a factor of more than ten, and large cumulative displacements at great distances, in particular along the Longitudinal Valley of eastern Taiwan, where relaxation times are also longer. We show that while afterslip is the

dominant relaxation process in the epicentral area, viscoelastic relaxation is needed to explain the pattern and time evolution of displacements at the larger scale. We model the spatio-temporal behavior of the transient deformation as the result of afterslip on the décollement that extends down-dip of the Chelungpu thrust, and viscoelastic flow in the lower crust and in the mid-crust below the Central Range. We construct a model of deformation driven by coseismic stress change where afterslip and viscoelastic flow are fully coupled. The model is compatible with the shorter relaxation times observed in the near field, which are due to continued fault slip, and the longer characteristic relaxation times and the reversed polarity of vertical displacements observed east of the Central Range. Our preferred model shows a viscosity of 0.5-1 E19 Pa s at lower-crustal depths and 5x1E17 Pa s in the mid-crust below the Central Range, between 10 and 30 km depth. The low-viscosity zone at mid-crustal depth below the Central Range coincides with a region of low seismicity where rapid advection of heat due to surface erosion coupled with underplating maintain high temperatures, estimated to be between 300°C and 600°C from the modeling of thermo-chronology and surface heat flow data.

Systematic reduction of pore pressure response near the San Jacinto fault, Andrew J. Barbour (Poster 071)

In the shallow crust, the relationship between pore pressure and strain changes is complicated by the presence of permeable fractures or joints, and large through-going faults. Information on poroelastic parameters traditionally comes from a joint analysis of the response of water-well levels to tides or seismic waves, and deformations (tilt or strain) associated with those natural sources. We have analyzed records of strain and pore pressure from Plate Boundary Observatory borehole sites around the San Jacinto Fault zone (SJF) in southern California to examine the response to surface waves from large earthquakes. Our catalog consists of a total of 55 events from late 2006 (the start of the data) to the present, and provides a wide range of dynamic strains with source magnitudes ranging from 4.5 to 9.0. We use timeseries of strain from calibrated 20Hz borehole strainmeter data and 1Hz pore pressure data which we filter to remove energy outside seismic frequencies (< 10 –3 Hz) and transformed into envelope functions using the Hilbert transform. For each station we fit a linear model to the entire set of responses of pore pressure to dynamic strains by robust regression using iteratively re-weighted least squares.

We observe a systematic reduction in response at sites within a 5 km zone near the SJF system, relative to others farther away. At stations far from the fault in mostly intact granodiorite, there is very high correlation between pressure and strain timeseries, indicating a linear relationship with essentially zero time lag; however, at stations close to the fault, pore-pressure variations are much smaller and lag strain significantly. These findings provide strong evidence (supported by borehole logs and regional patterns of stress orientation) of differences in fracture orientation and density around the fault. In light of recent findings of significant mechanical and chemical alteration of SJF fault-core and damage zone material, our findings provide support to the hypothesis that vigorous fluid flow near the fault acts as an advective heat-dissipation mechanism for ruptures on the fault.

InSAR Time Series Error Characteristics and Mitigation, William D. Barnhart and Rowena B. Lohman (Poster 204)

Observations of ground motion from (InSAR) are impeded by error sources that are well documented by the user community. One significant source is correlated noise due to signal propagation delays through the stratified atmosphere. In many cases, atmospheric-induced noise may be as large as large as 3cm and is often correlated to short- and long-wavelength topographic features. The correlation of atmospheric noise to topography is especially problematic for tectonic studies when investigating tectonic signals that are expected to mimic the topography, such as anticlinal uplift or interseismic motion across basin-bounding faults. InSAR time series techniques (e.g. stacks, SBaS, PS) are expected to minimize the influence of correlated atmospheric noise. Theoretically, while atmospheric noise may correlate in a single interferogram, the sign of the noise should be random and should cancel out when many independent SAR acquisitions are used to build a time series. In most locations, InSAR observations histories are not ideal, meaning

acquisitions are unevenly spaced temporally, demonstrate seasonal biases, or are insufficient in number (< 50 acquisitions) to fully characterize the noise characteristics. In this work, we use independent observations of precipitable water vapor in the atmosphere to illustrate characteristics of atmospheric noise that can propagate into InSAR time series. We use MODIS observations acquired daily that correlate near-infrared measurements to total precipitable water vapor. We show that while time series techniques do reduce the impact of correlated atmospheric noise, apparent signals over both long- (>100 km) and short-wavelengths (>100 km) are propagated to the final time series. We show that in some cases, abrupt changes in InSAR-derived time series can be correlated to individual storm events. We present an algorithm to estimate errors in time series caused by correlated atmospheric noise that uses the MODIS observations. Using a Monte Carlo approach, we generate multiple MODIS time series with acquisition date histories similar to that of the InSAR time series. We then use the population of MODIS time series to assess the variability in apparent signal at each SAR acquisition date. The variability is then used to assign error bounds to the time series. This method is beneficial in that it captures variability in signals induced by both seasonal weather fluctuations and individual, multi-day storm events.

Luminescence dating inter-comparison for sediments associated with the Puente Hills Blind-Thrust System recovered from cores, *Wendy A. Barrera, Edward J. Rhodes, Madhav K. Murari, Lewis A. Owen, Michael J. Lawson, Kristian J. Bergen, James F. Dolan, and John H. Shaw* (Poster 138)

Initial results of an on-going laboratory inter-comparison project based on samples recovered by coring of sediments associated with the Puente Hills Blind-Thrust System, Los Angeles, CA are presented. Conventional quartz OSL (optically stimulated luminescence) age estimates were determined at the Cincinnati Luminescence Laboratory for nine samples spanning the full depth range; while at the UCLA Luminescence Laboratory, IRSL (infra-red stimulated luminescence) measurements of K-feldspar were made for just five samples. C-14 age controls exist for the upper samples, where quartz OSL ages provide good agreement, while K-feldspar IRSL for one sample may be too old. Quartz OSL ages appear to reach a maximum value of around 35 ka at greater depths, but K-feldspar results provide older age estimates, more in line with prior expectation. Assessment of the characteristics of quartz grains separated at UCLA suggest that for these samples the OSL signal is dominated by contributions from quartz, with little sign of contamination from mineral inclusions of different composition (feldspar, zircon etc). Further experiments will be undertaken to help determine the source of age estimate discrepancies, in order to develop a reliable chronology for this sequence.

Utilizing methods of subspace detection on an earthquake sequence in the Big Bear region, *Sarah A. Barrett and Greg Beroza* (Poster 198)

Implications about time-dependent processes are critically reliant on a complete catalog, especially when the source is repeating or near-repeating. However, often a catalog of events is incomplete. In the past, various methods such as incoherent energy detectors or waveform templates have been used to identify missing events. We investigate the results of using a subspace detector as an alternative method. Subspace detectors are formed using a design set of earthquakes, as identified by cluster analysis. A singular value decomposition of a matrix of the design set waveforms is performed, yielding a set of basis vectors that describe the events in the subspace. This subspace presumably spans a range of signals that encompass slight variations in the source, making this method advantageous for detecting earthquakes using template matching, since a given earthquake might not be well described by the template event. We test this technique using a sequence of earthquakes in the Big Bear region occurring in 2003. Initial results of the largest singular vector show remarkable similarities to the stack of design events. We investigate the dimensions of the subspace and apply the technique to identify events in the sequence not included in the catalog.

The relationship between slow slip, tectonic tremor, and triggered seismicity in Cascadia and Hikurangi, *Noel M. Bartlow, John Beavan,*

Laura Wallace, Stephen Bannister, Aaron Wech, and Paul Segal (Poster 169)

Recently, tectonic tremor has been observed on the Parkfield segment of the San Andreas fault (Shelly, Nature, 2010), and slow slip is assumed to accompany this tremor although it has not been directly observed by geodetic instruments. Subduction environments where slow slip is geodetically observed have presumably higher slip magnitudes and a more favorable geometry for geodetic detection. Slow slip events may increase stress on seismically locked regions, with implications for hazard assessment. It is therefore important to study the relationship between tremor and slip in multiple subduction environments to learn what conclusions can be applied to the San Andreas tremor by extrapolation. For example, tremor and slip appear to be collocated in Cascadia (Bartlow et al, GRL, 2011); however, this does not appear to hold everywhere. Specifically, we show that in Hikurangi a small catalog of tremor locations is significantly offset from the actively slipping region. By extension, if there is slow slip accompanying the observed tremor on the San Andreas, it may be either co-located or offset. We also find that although slow slip in Hikurangi can trigger swarms of low magnitude earthquakes (e.g., Delahaye et al., 2008, EPSL), it does not always do so, even when the slip is adjacent to areas with a high background seismicity rate.

Are b-values a good indicator of stress?: A view based on laboratory stick-slip experiments, *Thorsten W. Becker, Thomas Goebel, Danijel Schorlemmer, and Georg Dresen* (Poster 064)

The failure of rock samples in the laboratory is commonly preceded by seismically active micro-cracking which can provide insight in preparatory processes at various scales. We investigated the relationship between cyclical stress changes and temporal variations in seismic event statistics during stick-slips on rough fracture surfaces using four cylindrical (radius = 4 cm, height = 10.7 cm) Westerly granite samples. Each specimen contained notches at a thirty degree angle to the loading axis to localize deformation at its center. We first fractured the intact part between the notches, then locked the resulting fault through increasing the confining pressure and reactivated the fault. The last stage led to the creation of series of stick-slip events with large stress drop which were partially preceded by events with smaller stress drops as an expression of fault heterogeneity. While large slip events were connected to whole fault displacements some of the smaller stress drop events may be connected to localized fracture or slip. During the inter-slip periods between large slips, we observed repeating acoustic emission (AE) patterns, i.e., increasing AE-rates and seismic moments whereas b-values decreased throughout most of the cycle. We observed periods of low b-values, ranging from seconds before failure to about 34% of the inter-slip period. After the slip events, b-values increased abruptly and seismic moments were comparatively low. b-values and differential stresses showed an inverse linear relationship for a specific range of stresses (50-90% of the maximum stress) but also showed deviations from linearity especially at high stresses. High stress regimes showed a spectrum of b-value behavior from a simple continuation of the linear relationship to a succession of b-value jumps, which could partially be linked to small stress drop events before large slips. The amount of increase in b-values after individual stress drops may be indicative of the effectiveness of an event to decrease the stress level on the fracture surface, so that slip events with large stress drops would result in a larger increase in b-values. Our results support a connection between b-value variations and stress but also highlight the importance of spatial and temporal scales when attempting to link b-value variations to physical mechanisms like stress variations and structural complexities.

Present-day rheology of the lithospheric mantle beneath the Mojave region from naturally deformed peridotite xenoliths, *Whitney M. Behr and Greg H. Hirth* (Poster 263)

We characterize the rheological properties of a lithospheric mantle section using a suite of naturally deformed peridotite xenoliths erupted from the dominantly Pleistocene Cima volcanic field in the tectonically active Mojave desert of California. The Cima field consists of over 70 cinder cones and associated basalt flows that cover an area of ~150 km² within the central Mojave. Approximately 10% of the cones and several

MEETING ABSTRACTS

of the flows contain abundant lower crustal and mantle derived gabbro, pyroxenite, and spinel- and plagioclase-facies peridotite xenoliths, several of which are metamorphosed and penetratively deformed. The part of the Mojave from which the Cima xenoliths are derived is a region in which several models of both the transient and steady-state rheology structure of the lithosphere have been made from surface velocity measurements following the Landers (1992) and Hector Mine (1999) earthquakes. It is also a region where geophysical observations (including seismic velocity and attenuation, and receiver function studies) highlight a drop in shear velocity that is rapid in depth, interpreted to be the seismological lithosphere-asthenosphere boundary; the magnitude of the shear velocity drop is too abrupt to be explained by temperature contrasts alone. The compositional and rheological properties of the mantle lithosphere here are therefore critical to understanding what influences both the large-wavelength post-seismic signal, and the abrupt transition from lithospheric lid to low viscosity, low velocity asthenospheric mantle.

We document how stress, temperature, water content, deformation mechanism, lattice preferred orientation and style of localization vary with increasing depth (down to at least 45 km) in the lithospheric mantle from which the Cima xenoliths are derived. These natural measurements of rheological parameters are used to a) test the applicability of experimentally derived flow laws and predictions of LPO development to mantle rocks, b) develop a naturally constrained stress profile of the upper mantle in the Mojave region and c) examine how the rheological parameters measured influence a range of larger-scale geophysical models for the region.

New observations from the Elizabeth Lake paleoseismic site: Current results and future directions, Sean P. Bemis, Kate Scharer, Laurel Walker, and Patrick Taylor (Poster 145)

Elizabeth Lake is located in the middle of a critical stretch of the southern San Andreas Fault between well-established paleoseismic sites at Pallett Creek and Frazier Mountain. This 100 km long gap in the known paleoearthquake chronology for the southern San Andreas Fault produces uncertainty in the correlation of earthquakes between sites and the resultant implications regarding potential earthquake rupture lengths and timing. We undertook paleoseismic studies at Elizabeth Lake to evaluate this site's utility for paleoearthquake studies and begin to constrain the paleoearthquake history. The active trace of the San Andreas Fault through the Elizabeth Lake area is characterized by an uphill-facing scarp against which alluvial fans have accumulated with several local closed depressions. We targeted the largest depression, between Blue Hills Road and Ranch Club Road, for our paleoseismic investigations because it appears wet during most historic imagery and it appears to correspond with a small extensional stepover in the trace of the San Andreas Fault. Our first trench, EL1, crosses the well-defined surface trace of the fault to the west of the stepover, whereas the second trench, EL2, is east of the stepover and crosses the southern margin of the pond. EL1 exposed evidence of multiple deformation events, with the most recent event (presumably the 1857 Fort Tejon earthquake) creating a small graben structure. Sediment involved in the most recent deformation appears to also onlap onto an anticlinal structure near the base of our exposure, indicating potential evidence for a previous event, but we have yet to establish a clear connection of this deformation to an exposed fault displacement due to a high water table. EL2 did not expose evidence of large tectonic deformation, but did have pervasive sand-filled sub-vertical cracks for several meters at the graben margin, possibly evidence of distributed shear in the coarse sand and gravel debris flow units present at that location. Radiocarbon dating to constrain the age of events and the exposed stratigraphic section is underway. Our results demonstrate the suitability of this site for further paleoseismic investigations and highlight the value of examining the older portions of the stratigraphy.

Reversed-polarity secondary deformation structures near fault stepovers, Yehuda Ben-Zion, Thomas Rockwell, Zheqiang Shi, and Shiqing Xu (Poster 066)

We study volumetric deformation structures in stepover regions using numerical simulations and field observations, with a focus on small-scale features near the ends of rupture segments that have opposite-polarity

from the larger-scale structures that characterize the overall stepover region. The reversed-polarity small-scale structures are interpreted to be generated by arrest phases that start at the barriers and propagate some distance back into the rupture segment. Dynamic rupture propagating as a symmetric bilateral crack produces similar (anti-symmetric) structures at both rupture ends. In contrast, rupture in the form of a predominantly unidirectional pulse produces pronounced reversed-polarity structures only at the fault end in the dominant propagation direction. Several observational examples at different scales from strike-slip faults of the San Andreas system in southern California illustrate the existence of reversed-polarity secondary deformation structures. In the examples shown, relatively-small pressure-ridges are seen only on one side of relatively-large extensional stepovers. This suggests frequent predominantly unidirectional ruptures in at least some of those cases, although multi-signal observations are needed to distinguish between different possible mechanisms. The results contribute to the ability of inferring from field observations on persistent behavior of earthquake ruptures associated with individual fault sections.

Quaternary Deformation of the Newport-Inglewood-Carlsbad-Coronado Bank- Descanso Fault System: Long Beach to San Diego, California, Jonathan Bennett, Christopher Sorlien, Marie-Helene Cormier, Robert Bauer, and Brian Campbell (Poster 121)

Previously, offshore faults between Long Beach and San Diego have been interpreted as discontinuous and certain faults have been interpreted as thrusts. However, our geometric fault interpretation based on ~2,500 km of seismic reflection data is significantly different from these models. In particular, we interpret new faults not presented in the SCEC Community Fault Model (CFM), and propose that the central Oceanside "thrust" currently found in the CFM exhibits no evidence for Quaternary activity.

Our work based on deep-penetration industry multi-channel seismic reflection (MCS) data as well as high resolution U.S. Geological Survey reflection profiles indicate that many of the offshore faults are more geometrically continuous than previously reported, including the San Mateo-Carlsbad, Coronado Bank, and Descanso faults. We interpret a ~18 km wide right step-over from the Newport-Inglewood-San Mateo-Carlsbad positive flower structure in the north to the Coronado Bank-Descanso negative flower structure in the south, adjacent to San Diego. These digital fault and stratigraphic horizon surfaces were gridded and depth converted using the SCEC Community Velocity Model-H, and results were used for modeling displacement of the San Mateo-Carlsbad fault.

Four late Quaternary unconformities (Q1, Q2, Q3, and Q4) are interpreted through much of the study area. We correlate the Q horizons to core holes in Los Angeles harbor and constrain their ages as follows: Q1 is 160-300 ka; Q2 is ~300 ka; Q3 300-450 ka; and Q4 ~600 ka. These ages are several times older than recently published stratigraphic age models and an order of magnitude older for the Top Lower Pico horizon (1.8Ma). Fault slip rates modeled using our new ages are correspondingly slower than would be the case using the previous age models.

We estimate an average right-lateral slip rate of ~0.44mm/yr since 1.8 Ma on the central and southern San Mateo-Carlsbad, which had been previously identified as a thrust. The structural relief pattern exhibited by Q3 and Q4 is similar to that of top Lower Pico which suggests that the style of late Quaternary deformation has remained similar to the average post-1.8 Ma deformation. Our modeling also indicates that the San Mateo-Carlsbad fault is kinematically continuous for at least 60 km through a major bend that is a northern part of the 18 km-wide right step-over. This bend and step-over mark a boundary between transpression in the north and transtension in the south.

Using GPS to measure San Andreas and San Jacinto fault movement in the San Bernardino area, Joseph Berg, Sally McGill, William Buckley, Ashley Covarrubias, Rainer Luptowitz, Joshua Spinler, and Richard A. Bennett (Poster 232)

We collected new GPS data from 18 sites in and around the San Bernardino Mountains in order to constrain fault slip rates. We tested over 400,000 possible slip rate combinations of the 14 faults in a transect across the plate boundary through the San Bernardino Mountains. We

created an envelope to help better define the range of “acceptable” fitting models. To do this we took a running average of twice the outer ends of the error bars on the GPS velocities. Of the models that came closest to falling within this envelope, the slip rate across the San Andreas fault in the San Bernardino transect has been found to be 8-14 mm/yr, and the rate across the San Jacinto fault was 6-10 mm/yr. The slip rates we found are similar to those observed in previous studies.

The Effects of Boundary Conditions on Auto-Acoustic Compaction, *Kevin Bernardo, Emily E. Brodsky, and Nicholas J. van der Elst* (Poster 256)

The rheology of granular flows may be studied to describe the interactions of gouge filled faults. Angular grain flows have been studied extensively in previous experiments and the kinematics of grains sliding and rolling past each other is well documented. In this presentation we focus on the effect of acoustics in those processes and provide evidence establishing an acoustic regime of granular flow.

Two distinct regimes of granular flow have been widely recognized; the quasi-static regime at low shear rates and the inertial regime at high shear rates. Traditionally, shearing of granular media is expected to produce increased dilation as shear velocity increases. However, at the shear rates between the quasi-static and inertial regimes, angular media produces a pronounced compaction in the shear zone. The recent study of acoustics in rheology has introduced a new regime occupying those transitional shear rates. This transitional or “acoustic regime” is useful in describing the unexpected observation of shear zone thinning at intermediate shear rates. Previous investigations into the acoustic regime were conducted by observing the occurrence while applying a constant normal force during shearing and measuring the change in shear zone volume at various shear rates. Our trials further the research by performing similar trials but at a constant volume and measuring the resultant change in normal force as the shear zone grains aim to dilate or compact.

Here we show the connection between shear zone compaction and acoustic pulses created by the grain interactions. Observations include: 1) a link between increased acoustic amplitude and decreases in normal stress at intermediate shear rates, 2) an increase in acoustic amplitude driven by increased shear rates and, 3) an increase in grain comminution under constant volume. This presentation will provide evidence to further support: 1) the existence of an acoustic regime at intermediate shear velocities and 2) the phenomenon of auto-acoustic compaction of shear zones.

The rheology of granular media in the acoustic regime can help describe the forces affecting the rupture and cessation of seismic activity of gouge filled faults. Auto-acoustic compaction and normal force weakening of angular media responding to acoustic pressure can be a mechanism of fault zone weakening.

Contributions of Precarious Rock Evidence to Ground Motion Prediction and Simulations, *Glenn P. Biasi, James N. Brune, and Lisa Grant-Ludwig* (Poster 144)

Estimates of strong ground motion parameters at 1,000 to 10,000 year return times are only generally constrained by the observed strong-motion data set. As a result, the USGS National Seismic Hazard Maps 1% and 2% in 50 year hazard maps, for example, require multiple assumptions about the variability of ground motion, e.g., the ergodic assumption, attenuation relationships, random background earthquake size, frequency and location, directions of rupture propagation, relative hanging wall-foot wall ground motions, and ground motions at step-overs. SCEC initiatives for Ground Motion Simulation Validation and CyberShake also provide ground motion hazard curves at long return times. In southern California precariously balanced rocks (PBRs) comprise a resource to constrain these ground motion predictions. SCEC-sponsored efforts to develop this resource have led to improvements in quantifying rock fragilities (e.g., Purvance et al., *Eqk. Eng'g Struct. Dynam.*, 2008a; Purvance et al., *BSSA*, 2008b) and age constraints (Balco et al., *Quat. Geochr.*, 2011; Rood et al., *SCEC Ann. Mtg.*, 2011; R. Brune et al., *SCEC Ann. Mtg.*, 2012). PBRs are located near eighteen CyberShake grid points close enough to contribute ground motion constraints. We used logistic regressions by Purvance et al. (2008a,b) developed from shake-table overturning experiments and 2-D

estimates of rock parameters to provide vector probability of overturning estimates for these rocks. In preliminary comparisons, several rocks near grid points in the Mojave area are inconsistent with current CyberShake predictions (Donovan et al., *SCEC Ann. Mtg.*, 2012). To extend the usefulness of PBR constraints we are continuing to develop the archive of PBR resources. Location metadata associated with several hundred rocks in southern California have been recovered and are being integrated, along with rock dimensions not initially available for 2-D analysis. Screening of over 3,000 additional photos of southern California rocks has been completed in preparation for inclusion in a relational database.

A New slip rate estimate for the San Andreas fault zone in the Coachella Valley at Pushawalla Canyon, California, *Kimberly D. Blisniuk, Kate Scharer, Roland Burgmann, Warren Sharp, Mike Rymer, Thomas Rockwell, Patrick Williams* (Poster 129)

Although previous studies have produced detailed maps of the San Andreas fault zone comprising the Mission Creek and Banning fault strands in the Coachella Valley, understanding how slip is distributed across the zone and into the San Geronio Pass or into the Eastern California Shear Zone remains an important question for seismic hazard assessment in southern California. To better understand the kinematic role and the associated seismic hazard of the San Andreas fault zone at this latitude, we combine LiDAR topographic data, geologic field mapping of offset landforms, and 10Be and U-series Quaternary geochronology to obtain precise estimates of fault slip rates over 104 to 105 year timescales. Four study sites located on the southern San Andreas fault zone have been identified to constrain geologic slip rates. At these sites, we have conducted detailed geomorphic mapping and initial sample collection from: (1) 2 of 3 channels completely beheaded from Pushawalla Canyon due to offset by the Mission Creek fault strand, (2) offset late Pleistocene and Holocene alluvial fans on the Mission Creek fault strand at Dell Wash, just south of Pushawalla Canyon, (3) a late Pleistocene fan deposit offset by the Banning fault strand located between Thousand Palms Canyon and Pushawalla Canyon, and (4) an offset Holocene alluvial fan deposit offset along 2 strands of the Mission Creek fault strand at Thermal Wash. Our initial mapping and dating of an alluvial deposit confined within a beheaded channel at Pushawalla Canyon offset by the Mission Creek fault strand define slip rates of 17-24 mm/yr since ~50-70 ka, similar to contemporary rates derived from GPS data and previously published estimates at Biskra Palms (12-22 mm/yr; 14-17 mm/yr preferred). By inference, we suggest that slip on the Mission Creek strand of the San Andreas fault zone in the Coachella Valley may have remained constant over the past >50 ka. When combined with published paleoseismic studies that show the last earthquake to rupture the Coachella section of the San Andreas fault occurred over 300 years ago (ca. 1690), the new data further support the interpretation that this section of the San Andreas fault zone accumulated a slip deficit of 5.0 to 7.5 m over the past 300 years which could be relieved in a large-magnitude earthquake.

Evaluation of transient deformation from two decades of continuous GPS time series analysis in Southern California and Cascadia, *Yehuda Bock, Brendan W. Crowell, Peng Fang, Sharon Kedar, Zhen Liu, and Angelyn W. Moore* (Poster 225)

As part of a NASA MEaSUREs project and its contribution to EarthScope, we are producing a combined 24-hour position time series for more than 1000 stations in Western North America based on independent analyses of continuous GPS data at JPL (using GIPSY software) and at SIO (using GAMIT software), using the SOPAC archive as a common source of metadata. Included are all EarthScope/PBO stations as well as stations from other networks still active (SCIGN, BARD and PANGA), and pre-PBO era data some already two decades old. The time series are appended weekly and the entire data set is filtered once a week using a modified principle component analysis (PCA) algorithm. Both the unfiltered and filtered data undergo a time series analysis with QOCA software. All relevant time series are available through the NASA GPS Explorer data portal and its interactive Java-based time series utility. Also available are associated modeled parameters (e.g., station velocities, postseismic deformation) and relevant metadata (e.g., non-tectonic offsets). In addition, we provide estimates and animations of strain

MEETING ABSTRACTS

accumulation for Western North America based on the combined filtered time series, providing synoptic view of temporal evolution of the shear and dilatational strain across the plate boundary.

After a comprehensive process of re-analysis and quality control, we have evaluated the time series for transient deformation, that is, time series that deviate from linear behavior due to coseismic and postseismic deformation, slow slip events, volcanic events, and strain anomalies. In addition, we have observed non-tectonic effects from hydrologic, magmatic and anthropogenic sources which are manifested primarily in the vertical but sometimes bleed over into the horizontal, making tectonic interpretation and transient detection difficult. We will present an overview of our analysis workflow as well as examples of transient tectonic deformation from Cascadia, such as the episodic slip events, and Southern California, such as continued postseismic deformation after the 2010 El Mayor-Cucapah earthquake.

Improved Ground-Motion Predictions for Earthquake Early Warning

During Large Earthquakes, *Maren Boese, Tom Heaton, Egill Hauksson, Robert Graves, Scott Callaghan, and Philip Maechling* (Poster 040)

Scientists and engineers at the California Institute of Technology (Caltech), UC Berkeley, the Swiss Federal Institute of Technology (ETH), and the University of Southern California (USC) started in 2007 to develop and implement an earthquake early warning (EEW) demonstration system for California, called CISEN ShakeAlert. One of the major challenges in CISEN ShakeAlert and EEW in general is the site-specific real-time prediction of ground-motion intensity measures for large earthquakes ($M > 6.5$). Commonly, site-specific ground-motion parameters are predicted from magnitude and distance from rupture to site using empirical ground-motion attenuation relations. This approach though bears two major problems: (1) the extent of fault ruptures is usually unknown in real-time and the earthquake has to be approximated by a simple point-source; (2) directivity and basin effects are generally neglected. This can lead to a serious under estimation of ground-motions and result in warnings not being issued.

We will present two approaches to overcome these shortcomings. First, to provide rapid estimates of fault rupture extent during large earthquakes we have developed an algorithm called FinDer (Finite Fault Rupture Detector). FinDer uses image recognition techniques to detect automatically surface-projected fault ruptures in real-time (assuming a line source) by estimating their current centroid position, length L , and strike θ . Our approach is based on a rapid high-frequency near/far-source classification of ground motion amplitudes in a dense seismic network, and comparison with a set of pre-calculated templates using Matching by Correlation; to increase computational efficiency, we perform the correlation in the wavenumber domain.

The second approach that we will present to improve the ground-motion predictions for large earthquakes is based on statistical models (Support Vector Machines) that combine the effects of fault geometries, wave propagation, and rupture directivity to provide site-specific ground-motion estimates. Our models were trained using source and ground-motion parameters from the SCEC CyberShake dataset that consists of around 400,000 full 3D wave-propagation simulations ($6.5 \leq M \leq 8.5$) at around 200 locations in and around the Los Angeles (LA) basin.

We will show how our two approaches will improve ground-motion predictions for EEW during large earthquakes in California and elsewhere.

Using GPS to measure slip rates on the Honey Lake/Warm Springs and Mohawk Valley fault systems, Northern Walker Lane.,

Jayne M. Bormann, William C. Hammond, Corné Kreemer, and Geoffrey Blewitt (Poster 235)

The Honey Lake/Warm Springs and Mohawk Valley faults are parallel, northwest striking, dextral fault systems separated by ~50 km in the westernmost part of the Northern Walker Lane (NWL). These faults work as a cooperative pair to accommodate 3-5 mm/yr of the total 8 mm/yr of right-lateral strain geodetically observed across the NWL, however it is unclear which fault is dominant. Geologic studies report right-lateral slip rates of 1-2.5 mm/yr on the Honey Lake fault and a minimum of 0.3 mm/yr on the Mohawk Valley fault. In contrast, previous geodetic studies

estimate slip rates of ~1 mm/yr on the Honey Lake fault and ~3 mm/yr on the Mohawk Valley fault. To explore this discrepancy, we use new GPS data to constrain an elastic block model focusing on the Honey Lake/Warm Springs and Mohawk Valley faults. We present a dense velocity solution (~10 km average station spacing) that includes semi-continuous and continuous GPS data collected during the summer of 2012. The density of our velocity field and recent advances in data processing give us unprecedented precision in the measurement of contemporary deformation in the NWL. We use the velocity solution to solve for slip rates on the companion fault systems and explore the effects of block model geometry assumptions and tradeoffs.

Our preferred model predicts slip rates of 1.1 ± 0.2 mm/yr for the Honey Lake fault and 2.3 ± 0.3 mm/yr for the Mohawk Valley fault. Uncertainties in fault geometry and block boundary position affect block model predictions, but are difficult to quantify. For example, including the Grizzly Valley fault (a minor parallel fault located between the Honey Lake and Mohawk Valley faults) reduces slip rates on the Honey Lake and Mohawk Valley faults to 0.5 mm/yr and 1.8 mm/yr, respectively, and predicts ~1.5 mm/yr of dextral slip on the Grizzly Valley fault. Adding this fault results in a small but insignificant improvement to the model RMS residual velocities. We conclude that geodetic data allows for, but does not require dextral slip along the Grizzly Valley fault. Due to the weak geomorphic expression of the Grizzly Valley fault, the fault is not included in our preferred model. Despite changes to block model geometry, the Mohawk Valley fault consistently accommodates ~1 mm/yr more slip than the Honey Lake fault. Our results support the conclusion of previous geodetic studies that the Mohawk Valley fault is currently the dominant fault accommodating right-lateral deformation in the NWL.

Detecting Ambient Tectonic Tremors in Southern California,

Justin R. Brown, Susan E. Hough, and Jean-Paul Ampuero (Poster 165)

In every tectonic setting where it is observed, tremor proves difficult to detect due to its long durations and low amplitudes close to the noise band. This is particularly true in southern California where cultural noise sources are both spatially and temporally pervasive. Ambient tectonic tremor in circum-Pacific subduction zones was shown to consist of repeating low-frequency earthquakes and locate at the deep extent of the primary seismogenic zone in a region down dip of historical $M 8+$ earthquakes. In the strike-slip setting, families of deep ambient tremors near the Parkfield-Cholame segment of the San Andreas fault were shown to be possible probes of deep fault slip there. Whether ambient tremor occurs in a similar fashion in southern California remains unclear.

Running autocorrelation and matched-filter techniques were successfully used elsewhere to detect and locate tremor/low-frequency earthquakes. We scan continuous seismic recordings of the Southern California Seismic network near the San Jacinto fault from 2008-2012 to detect tremor signals and subsequently locate it. We target this area on account of the abundance of seismic stations including borehole stations. Also, since tremor was triggered by the passing surface waves of the 2002 $M 7.8$ Denali earthquake in vicinity of the San Jacinto fault we expect an ambient signal to occur in the same area. The application of a spectral discriminator is particularly needed in this region, where previous analysis identified recurrent transients with a spectrum peaked between 3 and 4 Hz associated with heavy train traffic along the Coachella Valley.

"Melt Welt" Mechanism of Extreme Weakening of Gabbro at Seismic Slip Rates,

Kevin M. Brown and Yuri Fialko (Poster 088)

We conducted high-speed friction experiments on gabbro to investigate the nature of strong velocity weakening at seismic slip rates. The critical weakening velocity is normal stress (i.e. pre-weakening shear stress) and slip distance dependent implying a thermally-activated mechanism. The mechanism initiates when the average rate of frictional heating exceeds a critical power density of 0.1-0.35 MW/m². Weakening is associated with formation of heterogeneously distributed thermally expanded shot spots and macroscopic streaks of melt ("melt welts"). A net shear zone dilation of as little as ~ 5-10 μm partially unloads portions of the interface initiating weakening. Upon weakening, elevated temperatures localized near melt welts while the surrounding areas of the slip interface cooled. Anti-correlated variations in temperature across the ring sample in the post-

weakening regime indicate that hot spots can migrate across the slip interface. A time delay Δt_c to the onset of weakening seen at near critical velocities at various stress levels occurs because there are two components to the temperature field: (1) A generally rising average back ground component, and (2) a superimposed relatively short lived transient peak component associated with heterogeneities. The small thermally elevated stress heterogeneities hit solidus coincident with weakening while average shear zone temperatures are still well below solidus (250-450 °C) and we propose that both the elastic thermal and phase transition related expansion components are involved. Presumably the concentrators could be any heterogeneity on naturally rough fractal fault surface. The subsequent onset of strengthening in our experiments is associated with formation of a continuous through-going layer of melt that covers the entire contact, in agreement with previously published results. Our proposed mechanism does not preclude the occurrence of all other potential additional mechanisms of strong dynamic weakening (particularly aquathermal pressurization). In fact, such an additional mechanism may be required to reconcile the inferred low dynamic strength of earthquake ruptures with scarcity of pseudotachylites on exhumed natural faults.

Geomorphic Erosional Models for Estimating Ages of Precariously Balanced Rocks from Cosmogenic Isotope Data, *Richard J. Brune, Lisa Grant-Ludwig, Katherine Kendrick, and James N. Brune* (Poster 025)

Grant Ludwig et al. (SCEC 3 Final Report) pointed out that estimates of the ages of precariously balanced rocks (PBRs) from cosmogenic data will depend on the geomorphic erosion model assumed. This point was also made by Balco et al. (2011). One extreme model, i.e. rapid erosion rate from a large distance above the top of the rock to the top of the pedestal., was assumed in the first estimates of the ages of PBRs by Bell et al. (1998).

In this work we present another assumption, constant erosion rate from above the top of the rock to near the top of the PBR pedestal, and then assuming the same rate to the current ground level and dividing the height of the pedestal by that rate. Calculation is carried out with a simple spread sheet. We then compare the inferred erosion rates and PBR ages with similar values for three other models. The models assumed are:

- (1) The new constant erosion rate model presented here.
- (2) The assumption of very rapid erosion from above the rock to the top of the pedestal (Bell et al., 1998 model).
- (3) Published results from the Balco et al. (2011) three erosion rate model (two prior and one during exhumation).
- (4) Dividing the pedestal height by an independently derived regional erosion rate.

We conclude that precise results for erosion rates and pedestal ages depend on the models assumed, as suggested in the Grant Ludwig (2012) final report for SCEC 3, but that all methods give age dates of thousands to tens of thousands of years for most rocks, and that for most rocks an approximate age date can be obtained by simply dividing the pedestal height by a reasonable erosion rate.

Engineering validation of hybrid broadband ground motion simulations, *Lynne S. Burks and Jack W. Baker* (Poster 029)

Hybrid broadband ground motion simulation methods are a quickly developing tool. If these simulations can be substituted for recordings, then the engineering community could potentially use simulations in situations where recordings are limited, like large magnitude and short distance events. However, engineers remain hesitant to use simulations because of a lack of sufficient validation for engineering application. This poster focuses on the comparison of basic engineering parameters between recordings and simulations similar to the 1994 Northridge earthquake. There are seven sets of Northridge simulations, each computed using the SCEC Broadband Platform software system. The first set was computed using the validation module, which starts from an inverted rupture time history. The other six sets use the rupture generator modules, which start from a basic description of the fault and generate a detailed rupture time history. Three sets were simulated using the URS rupture generator code and three sets using the UCSB code. Engineering

parameters like elastic response spectra, epsilon, near-fault pulse characteristics, and example building collapse capacities were calculated and compared between the recordings and seven sets of simulations. Results indicate that the UCSB rupture generator produces a relatively smoother rupture time history and weaker elastic response spectra at some long periods. All simulations tend to predict near-fault pulses more frequently and with a longer period than expected, which leads to epsilon with variability that is too small at short periods and too high at long periods. But if the recordings and simulations are pruned to have similar pulse periods and spectral shape, then structural collapse capacities are consistent between recordings and simulations.

Rupture Dynamics and Ground Motion from Earthquakes in Heterogeneous Media, *Samuel A. Bydlon, Jeremy E. Kozdon, and Eric M. Dunham* (Poster 087)

Heterogeneities in the material properties of Earth's crust scatter propagating seismic waves. The effects of scattered waves are reflected in the seismic coda and depend on the relative strength of the heterogeneities, spatial arrangement, and distance from source to receiver. In the vicinity of the fault, scattered waves influence the rupture process by introducing fluctuations in the stresses driving propagating ruptures. Further variability in the rupture process is introduced by naturally occurring geometric complexity of fault surfaces, and the stress changes that accompany slip on rough surfaces. We have begun a modeling effort to better understand the origin of complexity in the earthquake source process, and to quantify the relative importance of source complexity and scattering along the propagation path in causing incoherence of high frequency ground motion. To do this we extended our two-dimensional high order finite difference rupture dynamics code to accommodate material heterogeneities. We generate synthetic heterogeneous media using Von Karman correlation functions and their associated power spectral density functions. We then nucleate ruptures on either flat or rough faults, which obey strongly rate-weakening friction laws. Preliminary results for flat faults with uniform frictional properties and initial stresses indicate that off-fault material heterogeneity alone can lead to a complex rupture process. Our simulations reveal the excitation of high frequency bursts of waves, which radiate energy away from the propagating rupture. The average rupture velocity is thus reduced relative to its value in simulations employing homogeneous material properties. In the coming months, we aim to more fully explore parameter space by varying the correlation length, Hurst exponent, and amplitude of medium heterogeneities, as well as the statistical properties characterizing fault roughness.

Optimizing the CyberShake Platform for Probabilistic Seismic Hazard Analysis, *Scott Callaghan, Philip Maechling, Gideon Juve, Gaurang Mehta, Karan Vahi, Mats Rynge, Robert Graves, Kim Olsen, and Thomas H. Jordan* (Poster 037)

SCEC researchers have developed and used the CyberShake computational platform to perform probabilistic seismic hazard analysis (PSHA) in the Los Angeles region (Graves et al., 2010) using deterministic wave propagation simulations at frequencies up to 0.5 Hz, combined with stochastic methods, to produce broadband seismograms up to 10 Hz. CyberShake uses seismic reciprocity to calculate synthetic seismograms for a suite of more than 600,000 rupture realizations. From this set of seismograms we compute intensity measures, which are then combined into a PSHA hazard curve for the site of interest at various periods. We use scientific workflows running on high performance computing clusters for job execution and data management.

To increase the scale at which hazard curves can be calculated, we have targeted large shared clusters, such as NICS Kraken, for execution. Due to the highly optimized nature of such clusters, code and workflow modifications are often required to get good performance. We will discuss the changes and improvements we have made to the CyberShake scientific workflows, including combining execution steps, reducing memory footprint, and simplifying the workflow. We will also describe our validation procedure for checking the correctness of CyberShake results, and explore the scale at which we can execute future CyberShake runs.

Strong weakening and energy partition in a model of sheared dry

MEETING ABSTRACTS

gouge with thermally varying material properties, *Jean M. Carlson and Ahmed E. Elbanna* (Poster 106)

We quantify the effect of thermal softening on the stress-slip response and energy partition in uniformly sheared thin gouge layers (). We use the shear transformation zone (STZ) theory to model the plastic strain accumulation due to the local granular rearrangements. We incorporate thermal softening by including the temperature dependence of the minimum flow stress (aka yield stress) in the STZ theory formulation. We show that at small strain rates, the steady state sliding shear stress depends weakly on strain rate. As the strain rate approaches a critical value, the steady state sliding shear stress shows strong strain rate dependence and drops to values very close to the system minimum flow stress. By accounting for the decrease in the minimum flow stress with increasing temperature, we obtain slip weakening behavior comparable to what is inferred from seismic observations for statically-strong-dynamically-weak systems. We discuss the implications of our results for understanding gouge friction and dynamics of earthquake ruptures.

Southern California Educators and Their Students Contribute to Crustal Deformation Studies Within San Bernardino and Riverside Counties,

Thomas Castiglione, Helen Corral-Bonner, Robert de Groot, Joshua Drake, Jacob Drake, Anna Foutz, Steven Husa, Sally McGill, Eric Sahl, Joshua Spinler, Bernadette Vargas, and Rick Bennett (Poster 215)

In conjunction with California State University, San Bernardino, Inland Empire high school teachers and students have used GPS to monitor movement along the San Andreas and San Jacinto faults within the Inland Empire, San Bernardino Mountains and high desert regions of Southern California since 2002. Stations observed in 2012 were selected from those that previously had relatively poorly constrained time series, so as to contribute useful new velocity constraints for use by the SCEC community and others. Procedures for the study included setting up a tripod (or spike mount), antennae and receiver over existing survey monuments for an 8 hour period each day for 5 days. GPS data were processed at the University of Arizona and benchmark positions were compared to those in previous years. Time series graphs were used to estimate the north, east and vertical velocities of each site. Velocities for our sites were combined with velocities from SCEC's Crustal Motion Model version 4. One-dimensional elastic modeling of the combined data set was used to infer fault slip rates within a transect across the plate boundary through the San Bernardino Mountains. Results indicate that the combined slip rate of the 11 faults within our transect is 44-46 mm/yr. The San Andreas (SAF) and San Jacinto (SJF) faults have the highest rate of movement within the transform plate boundary system, with a range of 4-14 mm/yr along the SAF and 3-11 mm/yr along the SJF, among the well fitting models explored in an ad hoc manner by participants in the program. The combined slip rate of SAF, SJF and Elsinore faults within our transect is 19-25 mm/yr. This is substantially less than the published 35 mm/yr slip rate of the SAF alone in central California. Nonetheless our inferred slip rates for the SAF and SJF are consistent with previously published slip rates for these faults in southern California over late Quaternary time scales.

Salton Seismic Imaging Project Line 6: San Andreas Fault and Northern Coachella Valley Structure, Riverside and San Bernardino Counties,

Rufus D. Catchings, Gary S. Fuis, Michael J. Rymer, Mark R. Goldman, Jennifer M. Tarnowski, John A. Hole, Joann M. Stock, and Jonathan C. Matti (Poster 203)

The Salton Seismic Imaging Project (SSIP) is a large-scale, active- and passive-source seismic project designed to image the San Andreas fault (SAF) and adjacent basins (Imperial and Coachella Valleys) in southernmost California. Data and preliminary results from many of the seismic profiles are reported elsewhere (including Fuis et al., Rymer et al., Goldman et al., Langenheim et al., this meeting). Here, we focus on SSIP Line 6, one of four 2-D seismic profiles that were acquired across the Coachella Valley. The 44-km-long, SSIP-Line-6 seismic profile extended from the east flank of Mt. San Jacinto northwest of Palm Springs to the Little San Bernardino Mountains and crossed the SAF (Mission Creek (MCF), Banning (BF), and Garnet Hill (GHF) strands) roughly normal to strike. Data were generated by 10 downhole explosive sources (most spaced about 3 to 5 km apart) and were recorded by approximately 347

Texan seismographs (average spacing 126 m). We used first-arrival refractions to develop a P-wave refraction tomography velocity image of the upper crust along the seismic profile. The seismic data were also stacked and migrated to develop low-fold reflection images of the crust. From the surface to about 7 km depth, P-wave velocities range from about 2.5 km/s to about 7.2 km/s, with the lowest velocities within an ~2-km-deep, ~20-km-wide basin, and the highest velocities below the transition zone from the Coachella Valley to Mt. San Jacinto and within the Little San Bernardino Mountains. The BF and GHF strands bound a shallow sub-basin on the southwestern side of the Coachella Valley, but the underlying shallow-depth (~4 km) basement rocks are P-wave high in velocity (~7.2 km/s). The lack of a low-velocity zone beneath BF and GHF suggests that both faults dip northeastward. In a similar manner, high-velocity basement rocks beneath the Little San Bernardino Mountains suggest that the MCF dips vertically or southwestward. However, there is a pronounced low-velocity zone in basement rocks between about 2 and 7 km depth beneath and southwest of the MCF, suggesting a vertical or slightly southwest-dipping MCF. The apparent northeast dip of the BF and the apparent vertical or southwest dip of the MCF suggests that the two main strands of the SAF (MCF and BF) merge at about 10 km depth. A plot of double-difference earthquake hypocenters (Hauksson, 2000) along the seismic profile shows events that occurred between 1980-2000 (excluding those in 1992, prior to and after the Joshua Tree and Landers earthquakes) are largely confined to the vicinity of the basement low-velocity zone between the MCF and BF. However, a separate alignment of hypocenters occurs southwest of the BF and projects toward the surface beneath Mt. San Jacinto. Collectively, the velocity images and the seismicity data suggest the BF strand of the SAF dips to the northeast at about 50 degrees in the upper 10 km, and the MCF strand is either vertical or dips southwestward about 80 degrees, with both strands merging at about 10 km depth and forming a near-vertical zone of faults to at least 15 km depth. The SSIP Line 6 data are consistent with structures interpreted by Catchings et al. (2009).

Response of a tall building far from the epicenter of the March 11, 2011

M=9.0 Tohoku, Japan earthquake and aftershocks, *Mehmet Celebi, Izuru Okawa, Toshidate Kashima, Shin Koyama, and Masanori Iiba* (Poster 028)

The March 11, 2011 M=9.0 Tohoku (also known as Great East Japan) earthquake generated significant, long-duration shaking that propagated hundreds of kilometers from the epicenter and affected urban areas throughout much of Honshu. Recorded responses of a tall building 770 km from the epicenter of the mainshock and other related or unrelated aftershocks show how structures sensitive to long-period motions can be affected by distant sources. Even when the largest peak input motion to the building is about 3% g, the strong shaking duration was about 140 s. The 300-1000 s prolonged recorded responses of the building are primarily due to a combination of surface waves, site resonance (e.g. structural fundamental frequency ~0.15 Hz and site frequency ~0.13-0.17 Hz) and low damping (~1-2 %) of the structure. Response modification technologies can improve the response of the building during future earthquakes. The need to consider risks to the built environment from distant sources is vital.

a) Earthquake Science Center, USGS, Menlo Park, Ca. 94025

b) Building Research Institute, Tsukuba, Japan

Creation of additional GIS capabilities for SCEC-VDO: Added support for new earthquake catalogs for the SCEC-VDO software and improved functionality of existing SCEC-VDO plugins for the 2012 UseT Grand Challenge, *Kevin Centeno, Aaron Hoogstraten, Kameron Johnson, Dave Smith, Bridget Hellige, Nick Rousseau, Thomas H. Jordan, and*

Robert M. de Groot (Poster 295)

The 2012 Undergraduate Studies in Earthquake Information Technology (UseIT), Development Team 1 was given the task of creating additional Geographic Information Systems (GIS) capabilities, as well as adding support for new earthquake catalogs for the SCEC-Virtual Display of Objects (SCEC-VDO) software. New GIS features include updated 2010 U.S. census data for California population density, updated California infrastructure data, and an improved orthoimagery downloader. Combined with SCEC-VDO's new ShakeMap and Seismic Hazard Map

plugins, the newly implemented data will provide users with important information on the risk impact of earthquakes on various California populations. Development Team 1's other improvements include the ability to import UCERF3 catalogs and a general catalog parser to facilitate the importing of future catalogs without the need to know a catalog's particular formatting. With the addition of improved functionalities users now have the ability to render earthquakes in discrete colors that correspond to magnitude and can create custom color legends through the Legends submenu. These improvements are the result of Development Team 1's goal to provide a more intuitive interface and increase user accessibility in SCEC-VDO.

Discovery and paleoseismic investigation of the Bidart Fault, a subparallel oblique-slip strand of the San Andreas fault in the Carrizo Plain, Terry M. Cheiffetz, Tsurue Sato, Sinan Akciz, and Lisa Grant-Ludwig (Poster 252)

The San Andreas Fault (SAF) is the most significant source of seismic hazard in densely populated Southern California. Recent field reconnaissance, ground penetrating radar (GPR) investigations, and LiDAR image analysis revealed a linear structural anomaly sub-parallel to the main trace of the SAF between Wallace Creek and the Bidart Fan paleoseismic sites. This previously unrecognized fault strand is located ~400m to the northeast of the main SAF trace. We excavated two paleoseismic trenches across the anomaly to confirm prior surface rupture and investigate recency and style of deformation. Trenches revealed distinct stratigraphy which included fissures, upward termination of faults, vertical apparent offset, lateral unit thickness changes, and colluvial wedges, and exposed evidence for as many as five Holocene earthquake events. We propose this linear structural anomaly could have accommodated some of the lateral slip variation between the main strand of the SAF at the Wallace Creek site and the Bidart Fan during the 1857 earthquake. Dates of surface ruptures are constrained using detrital charcoal that was emplaced during debris flows events and embedded in micro-paleosols. Of the 37 charcoal samples collected throughout the stratigraphy in both trenches, we estimate that 20 will produce useable C14 dates to resolve the ages of the individual earthquakes and determine if they can be correlated to the previously reported ruptures along the main strand of the SAF.

Shear Localization and the Evolution of Fault Strength, Jiangzhi Chen and Alan W. Rempel (Poster 070)

Within the relatively thick gouge layers that characterize mature fault surfaces, field investigations have identified much finer structures, down to 10–20 μm thickness. This is consistent with observations from laboratory experiments of high-speed friction, which also find that most strain occurs in narrow shear zones of several tens to hundreds of microns in width. However, thermomechanical considerations suggest that the frictional heat generated during moderate-sized earthquakes (e.g. $M_w \geq 6$) may not be confined to such narrow zones because this would cause macroscopic melting to occur, which is inconsistent with the reportedly rare distribution of pseudotachylytes along mature faults. We describe a kinematic model that predicts the evolution of temperature and shear-zone thickness during earthquakes. We show how decreases in the lifetimes of asperity contacts cause flash heating to produce rate-strengthening friction at elevated temperatures and typical co-seismic slip rates. This introduces a delocalizing effect that competes with the localizing influence of thermal pressurization to determine how the shear-zone thickness changes as the temperature increases and the effective stress drops. Using this framework, numerical simulations are performed that track the increasing shear thickness as melting conditions are approached, allowing heat to be dissipated over an increasingly broad region. As a result, the maximum temperature within the shear zone is reduced, and this may help to explain the apparent lack of pseudotachylytes along mature faults.

California foreshock sequences suggest underlying aseismic process, Xiaowei Chen, Peter M. Shearer, and Egill Hauksson (Poster 164)

Foreshocks are the clearest precursors to mainshocks, and understanding their characteristics is of great interest. In this study, we analyze immediate foreshock sequences (within 2 days and 5 km) for mainshocks in California using precisely relocated catalogs and find that 27 out of 61 mainshocks of $M \geq 5$ have at least one immediate foreshock. Among the 27 foreshock sequences, 9 consist of just one event, 3 are aftershocks of a previous event, and 13 are swarm-like sequences (more than 4 events, not starting with the largest foreshock). For 5 swarm-like foreshock sequences (Landers, Hector Mine, El Mayor-Cucapah, Chalfant, Mt-Lewis earthquakes), there are enough events to determine that they exhibit significant spatial migration, with migration velocities comparable to swarms in southern California (e.g., Chen et al., 2011). To study if there are systematic changes between foreshocks and aftershocks, we apply an iterative deconvolution approach [Shearer et al., 2006] to obtain earthquake source spectra. We then estimate earthquake stress drops using a multi-event empirical Green's function (EGF) method. These 5 foreshock sequences have much lower median stress drops than aftershocks from the same region. To confirm this difference, we shift the source spectra along an f^{-3} curve to facilitate a direct comparison of the frequency content of the source spectra for different sized events. The foreshocks have a stronger fall off at high frequencies compared to the aftershocks. We are currently studying, using a source-specific EGF approach, whether attenuation changes could explain some of these frequency differences. These observations of spatially migrating foreshock sequences and their apparently low stress drops indicate that there is likely an underlying aseismic process, such as fluid flow or slow slip, that triggers both the foreshocks and the mainshocks. Such aseismic processes are thought to drive many swarms and some observations have suggested that aseismic slip may occur prior to large earthquakes [e.g., Roeloffs, 2006].

Fault slip rate estimates for southwestern US from GPS data and non-block viscoelastic sheet models, Ray Y. Chuang and Kaj M. Johnson (Poster 220)

Fault slip rate estimates from geodetic data are becoming increasingly important for earthquake hazard studies. In order to estimate fault slip rates, GPS-constrained kinematic models such as elastic block models are widely used. However, kinematic block models are inherently non-unique and provide limited insight into the mechanics of deformation. Furthermore, assumed discrete tectonic blocks may not exist everywhere as not every region of the western US displays mature, through-going geologic structures that naturally divide the crust into tectonic blocks. For example, the eastern California shear zone and regions of the Basin and Range Province are best described as broad zones of interacting, discontinuous fault strands.

We are building towards mechanical models of present-day surface motions in which deformation is a response to plate boundary forces, gravitational loading, and rheological properties of the lithosphere. To model fault slip rates in the southwestern US, we populate an elastico-visco thin sheet (plane stress) with thin viscous shear zones (faults) and impose far-field plate motions and gravitational loading to compute the long-term fault slip rates and crustal motions. Interseismic deformation due to locking of faults is modeled with backslip on dislocations in an elastic half-space or in an elastic plate over a viscoelastic half-space. The total present-day deformation field (long-term plus interseismic) is compared with the GPS-derived velocity field and the model stress tensor is compared with the stress state inferred from stress-inversions of focal mechanism data.

GeoTrek: An Educational Framework for K-12 Free-Choice Learning at the San Bernardino County Museum's Hall of Geological Wonders, Karina Chung, Robert de Groot, and Kathleen Springer (Poster 260)

The San Bernardino County Museum (SBCM) in Redlands, California, is building exhibits for the new Hall of Geological Wonders. The SBCM partners with SCEC's Communication, Education and Outreach Program, and under the Earthquake Country Alliance umbrella, is the southern California nexus of the Earthquake Education and Public Information Centers (EPICenter) network, which includes 60+ free-choice learning institutions committed to disseminating earthquake science information. Concomitant with the opening of the new Hall of Geological Wonders, the SBCM seeks to create educational scaffolding where none currently exist. The cornerstone of this new informal learning framework is the creation of the Hall of Geological Wonders Learning Treks Program

The San Bernardino County Museum (SBCM) in Redlands, California, is building exhibits for the new Hall of Geological Wonders. The SBCM partners with SCEC's Communication, Education and Outreach Program, and under the Earthquake Country Alliance umbrella, is the southern California nexus of the Earthquake Education and Public Information Centers (EPICenter) network, which includes 60+ free-choice learning institutions committed to disseminating earthquake science information. Concomitant with the opening of the new Hall of Geological Wonders, the SBCM seeks to create educational scaffolding where none currently exist. The cornerstone of this new informal learning framework is the creation of the Hall of Geological Wonders Learning Treks Program

GeoTrek: An Educational Framework for K-12 Free-Choice Learning at the San Bernardino County Museum's Hall of Geological Wonders, Karina Chung, Robert de Groot, and Kathleen Springer (Poster 260)

The San Bernardino County Museum (SBCM) in Redlands, California, is building exhibits for the new Hall of Geological Wonders. The SBCM partners with SCEC's Communication, Education and Outreach Program, and under the Earthquake Country Alliance umbrella, is the southern California nexus of the Earthquake Education and Public Information Centers (EPICenter) network, which includes 60+ free-choice learning institutions committed to disseminating earthquake science information. Concomitant with the opening of the new Hall of Geological Wonders, the SBCM seeks to create educational scaffolding where none currently exist. The cornerstone of this new informal learning framework is the creation of the Hall of Geological Wonders Learning Treks Program

MEETING ABSTRACTS

(GeoTreks). The model outlines a K-12 field trip to the SBCM. As exhibits come on-line, the timing of this program presents a unique opportunity to participate in the interaction between the GeoTrek programs and exhibits during their simultaneous creation. A long-term goal of the program is to establish individual GeoTreks for different ages of school groups and Hall of Geological Wonders exhibits.

The GeoTrek activity is based on Lesson Study, an educational approach using observations of student learning to inform small, incremental improvements to the lesson. Lesson Study focuses on a specific, observable learning goal, determined prior to the activity chosen to address the particular aspect of learning. Although Lesson Study had its advent in Japan, it is gaining popularity in formal education environments in the United States. This project is a free-choice learning adaptation of Lesson Study. In addition to a Lesson Study based activity, each GeoTrek will include student and facilitator guides, an observation rubric, pre-and post-surveys, as well as additional materials that pertain to the lesson. The pilot GeoTrek was developed for 6th grade curriculum in California in conjunction with the museum's Paleoseismology exhibit. Exhibit content includes a re-creation of a paleoseismic trench on the San Andreas fault, and explains the science of paleoseismology by the exhibition of two peels from Pallett Creek and Wrightwood. Taken together, the visitor's immersion into the field of paleoseismology will highlight the collaborative nature of science in the 21st century, as well as showcase paleoseismology as one of the lines of evidence necessary for creating an earthquake rupture forecast.

Integration and Analysis of Seismic, Pore Pressure, and Strain signals at the PBO Borehole Stations, *Francesco Civilini and Jamison H. Steidl* (Poster 231)

The borehole stations of the Earthscope Plate Boundary Observatory (PBO) are providing unprecedented observations of co-located pore pressure and strain measurements over time scales of seconds to years, and over wide geographic and tectonic environments. Water level fluctuations in response to tides are well documented and understood, however the response to earthquakes, especially at the dynamic co-seismic, and short-term post-seismic time scales is less well understood. Observations of strain and water level steps due to earthquakes are presented and we hypothesize the mechanism responsible for these changes based on the co-located strain observations. For each earthquake, the water table change is consistent with the co-seismic areal strain change. There appears to be no correlation between the intensity of ground shaking and the magnitude of the pore pressure response. Two methodologies, one using Fourier transforms and the other cross correlation, were developed for calculating phase and amplitude differences of tidal forces before and after the earthquakes. Temporary phase and amplitude differences in the tidal signal were observed for the gradual post-seismic pore pressure increase at PBO 84 Piñon Flats during the El Mayor-Cuicapah earthquake, implying a change in hydrological parameters. A smaller amplitude difference is also detected for the gradual decrease observed at PBO 88 Sky Oaks during the Collins Valley earthquake. Using information from geotechnical logs, the fracture orientation was determined for each borehole and compared to the directions of maximum compression and dilatation of the earthquake. Out of the three chosen earthquakes, two of these had optimal fracture orientations for the observed pore pressure response. Lastly, the accuracy of these methods was tested for a pore pressure record for which there was no co-located strain.

Generating a preliminary Holocene slip history along the Mojave section of the San Andreas fault, *Tracy Compton, Eric Cowgill, Katherine M. Scharer, Ryan Gold, Rolf Westerteiger, and Tony Bernardin* (Poster 130)

Measuring histories of fault slip spanning multiple (10-100) ruptures has the potential to advance understanding of fault and fault-system behavior, including temporal variations in the rate of strain release. The Mojave section of the San Andreas fault (MSAF) shows an apparent discrepancy between slip rates where

Integration of Significant Data from SCEC Borehole Sites with the NEES@UCSB Database, *Matthew Cook, Jamison Steidl, Sandra Seale, and Paul Hegarty* (Poster 255)

The NEES@UCSB facility maintains and operates multiple permanently-instrumented geotechnical field sites that monitor strong motions and pore pressure response to earthquakes and are also used for active testing. Data from these sites are collected and placed in a database, processed, and then published to the Data Portal hosted on the NEES@UCSB website. The establishment of this cyberinfrastructure allows the public access to these stores of geotechnical data, which are of great interest to scientists, researchers, and engineers across various disciplines and locations. The range and efficacy of data dissemination from the NEES@UCSB facility are being improved by updating the database and Data Portal to include additional stations that are part of the SCEC Borehole Instrumentation Program.

The expanded database will include data and station information for 17 stations that are a collaboration between SCEC and UCSB. For these stations, the process of database integration involves data collection and organization and using Antelope code for data processing. Additionally, station information and instrument histories are documented and archived to accompany the Data Portal expansion. The NEES@UCSB Data Portal and website will continue to add stations to improve the distribution of data to the public.

Stress Drop Variability Reduction with Root-Mean-Square Acceleration, *Jorge G. Crempien and Ralph J. Archuleta* (Poster 103)

Stress drop is a fundamental property of the earthquake source. For a given tectonic region, stress drop is assumed to be constant, allowing for the scaling of earthquake spectra. However, the variability of stress drop, either worldwide or regional catalogs is quite large. The variability around the median is well above the order of 2 in log10 units according to Allman & Shearer (2009). A possible explanation for this large variability might be attributed to the epistemic uncertainty in the regional properties of Q and the number of earthquakes needed to constrain a robust statistically significant value of stress drop. Oth (personal communication) computed a mean value stress drop of 0.034 (1.1MPa in log10 units) for the Tottori aftershock sequence with 38 earthquakes, and a standard deviation of ~0.3 (factor of 2 in log10 units) reducing by half the findings of Allmann and Shearer (2009). The log10 based stress drop values are in good agreement with a Gaussian distribution. A possible explanation for the reduction of stress drop variability found by Oth is that he used a detailed regional analysis of Q using the work of Oth et al. (2011) for Japan.

One question that continues to pervade the analysis of stress drop is whether this variability is an inherent characteristic of the Earth or is an artifact of the determination of stress drop via the use of the spectral analysis. It is simple to see that the stress drop determined by seismic moment times corner frequency cubed that errors in the corner frequency will strongly influence the variability in the stress drop. To avoid this strong dependence on corner frequency cubed, we have examined the determination of stress drop based on the approach proposed by Hanks (1979), namely using the root-mean-square acceleration. The stress drop determined using rms acceleration might be advantageous because the stress drop is only affected by the square root of the corner frequency. To test this approach we have determined stress drops for the 2000 Tottori earthquake and its aftershocks. For this, we only consider recorded data within 40 km of hypocentral distance. We use both the classic method of fitting to a spectrum as well as rms acceleration based method. For a preliminary analysis of eight aftershocks and the mainshock we find that the variability in stress drop is reduced by about a factor of two. This approach needs more careful analysis with more events, which will be shown at the meeting.

The Role SCEC Can Play in Improving Seismic Provisions in US Codes through Ground-Motion Simulations, *C.B. Crouse* (Talk Mon 16:00)

Through its Uniform California Earthquake Rupture Forecast (UCERF) project, SCEC has collaborated with the USGS to establish seismic source models for California. These models will be used to prepare ground-motion maps for possible inclusion in the next edition of the ASCE 7 standard, which will be incorporated by reference in the International Building Code. Probabilistic and deterministic seismic hazard analysis (PSHA and DSHA) methods will use these models and empirical ground-motion prediction equations (GMPEs), derived from accelerogram data recorded worldwide, to develop the maps. However,

these GMPEs are limited in their ability to model long period ground motions in 3-D basin structures, such as those in the greater Los Angeles region. As an alternative to using empirical GMPEs, SCEC's CyberShake project used numerical simulations to generate the ground motions used in a PSHA for Los Angeles; one result was a contour map of 5% damped response spectral acceleration at 3-sec natural period and 2475-year return period. Expanding this effort to include a range of natural periods in the 1 to 10-sec band and forming a subcommittee, consisting of SCEC/USGS seismologists performing the simulations and engineers involved in seismic code development, is recommended to determine whether and how to incorporate the results into regional ground-motion maps for inclusion in the ASCE 7 standard. If the method is judged feasible during this pilot study, then it would be formally introduced in the code-development process and applied to other urban areas where the 3-D velocity structures are well known. If the resulting maps are approved by the code seismic committees, SCEC should store the simulated accelerograms in a data bank that could be easily accessed by structural engineers for dynamic response analysis of long period structures. Depending on the structure, a stochastic component may need to be added to the accelerograms to extend their useful period band to shorter periods < 1 sec, in order to cover higher mode responses.

Rapid Source Characterization of the 2011 Tohoku-oki Earthquake with Real-Time GPS and Strong Motion Data, *Brendan W. Crowell, Diego Melgar, and Yehuda Bock* (Poster 042)

Saturation of seismometers in the near field and problems with the double integration of accelerometer data into displacements degrades rapid magnitude estimation and source characterization for large earthquakes. Although Japan possesses the most advanced earthquake and tsunami early warning system in the world, it took about 20 minutes using

telesismic waves from distant seismic networks to determine that the 11 March 2011 Tohoku-oki earthquake was an Mw 9.0 event – earlier estimates based on local seismic networks ranged from M7.2 to M8.0. We present a seismogeodetic network model that can estimate on-the-fly the full dynamic range and spectrum of seismic motions for large earthquakes using observations starting in the near field. Replaying local Japanese data in a simulated real-time mode from 785 GPS stations and 190 accelerometers during the Tohoku-oki earthquake, we demonstrate that an accurate centroid moment tensor solution to ascertain the type of earthquake, immediately followed by a finite fault slip model could have been obtained in about 3 minutes, providing more accurate and timely warnings of the severity of the impending tsunami and assisting first responders with evacuation and recovery efforts. The seismogeodetic network model is sufficiently accurate to detect P wave arrivals in the near field for large events, leading to improved earthquake early warning (EEW) methodologies that predict the arrival and intensity of S waves. Using a maximum P wave amplitude scaling relationship from displacements estimated for 175 stations during three historical large earthquakes including Tohoku-oki, we demonstrate that an accurate first estimate of magnitude may be able to be obtained within a few seconds of P wave arrival at a handful of stations closest to the epicentre. Furthermore, we use the rapid slip inversion to model the ensuing tsunami.

Formation and suppression of strike-slip fault systems, *Ivy S. Curren* (Poster 276)

In orogens elongated parallel to a great circle about the Euler pole for the two bounding plates, theory requires simple-shear deformation in the form of distributed deformation or velocity discontinuities across strike-slip faults. This type of deformation, however, does not develop at all plate boundaries requiring toroidal motion. Using the global model of plate boundaries, PB2002 [Bird, 2003], as the basis for identifying areas where expected simple-shear deformation is absent or underdeveloped, it was also possible to identify two potential causes for this behavior: (1) the presence of extensive fracturing at right angles to the shear plane and (2) regional cover of flood basalts or andesites containing columnar joints. To test this hypothesis, a new plane-stress finite-strain model was developed to study the effects of such pre-existing structures on the development of simple shear in a clay cake. A homogenous kaolinite-

water mixture was poured into a deforming parallelogram box and partially dried to allow for brittle and plastic deformation at and below the surface of the clay, respectively. This was floated on a dense fluid foundation, effectively removing basal friction, and driven by a motor in a sinistral direction from the sides of the box. Control experiments produced classic Riedel model fault assemblages and discrete, through-going primary deformation zones (PDZs); experiments with pre-existing structures developed the same, though subdued and distributed, fault assemblages but did not develop through-going PDZs. Although formation of strike-slip faults was underdeveloped at the surface in clay with pre-existing structures, offset within the clay cake (measured, with respect to a fixed point, by markers on the clay surface) as a fraction of total offset of the box was consistently larger than that of the control experiments. This suggests that while the extent of surface faulting was lessened in clay with pre-existing structures, slip was still occurring at depth. Selected areas on Earth with anomalously undeveloped strike-slip faulting where plate models would predict otherwise were compared with results from the analog model experiments in this study. Physical similarities between the model results and Brothers Fault Zone (BFZ), Walker Lane (WL) and the South Iceland Seismic Zone (SISZ) imply that strike-slip faulting may be suppressed at the surface in these regions due to the presence of pre-existing structures.

Correlations of small and large earthquakes with tidal and seasonal stresses, *Karin A. Dahmen, Braden Brinkman, Michael Leblanc, Yehuda Ben-Zion, and Jonathan Uhl* (Poster 183)

We study whether correlations of triggered small events with tidal, seasonal and other oscillatory stresses indicate fault failure, and, if so, which oscillatory stresses best predict impending large earthquakes. We develop a simple probabilistic model of earthquake triggering to simulate earthquake sequences on a fault subject to an external periodic stress of amplitude F_0 and frequency ω . Our model predicts that the oscillation amplitude needed to observe significant correlations with large events varies with the oscillation frequency: For oscillation periods larger than typical large earthquake inter-event times (ω small), the amplitude needed to observe correlations scales with frequency as $F_0 \sim 1/\omega$. For oscillation periods much less than the typical large earthquake inter-event times (ω large), F_0 is a constant independent of frequency. The behavior of F_0 at intermediate frequencies depends on the spread in the average large earthquake inter-event times. For sharply peaked inter-event time distributions, the required amplitude $1/\omega$ behavior breaks down into decaying oscillations with minima when $\omega/2\pi$ times the average inter-event time is an integer. When the inter-event time distributed is not sharp, the $1/\omega$ regime smoothly decays into the constant regime with no visible oscillations.

Our model also predicts that $F_0(\omega)$ depends on the number of events detected as $1/n^{1/2}$. This result has important consequences for large earthquake analyses: using typical values of tidal stress amplitudes, we find that observation of thousands or more of large earthquakes are needed to observe significant correlations between large earthquakes and tidal stresses. This is consistent with findings that few large earthquakes exhibit tidal stress correlations. Seasonal thermoelastic stress, with amplitudes that may be >5 KPa at seismogenic depth and much longer period than the tidal period, should trigger more events than tides. We note that for materials testing in the lab, the model predicts that only tens to hundreds of events are required to observe significant correlations.

We also calculate small-event correlations in our simulations using the same analysis as Tanaka (2010) to compute the degree of correlation between the oscillatory stresses and small earthquakes. In our model, the number of small earthquakes increases as the fault approaches failure, and so does the degree of correlation. We use the degree of correlation to compute the probability of having a large earthquake. We examine two frequencies, characteristic of either tidal or seasonal stresses, for several amplitudes less than the failure stress of our model fault. This allows us to compare which periodic stress is a better indicator of an impending large earthquake.

Teachers Using Continuous GPS Data to Learn About Earthquakes: Sharing Research Results in the Classroom Through Lesson Study – 2012

MEETING ABSTRACTS

Campaign, Robert M. de Groot, Sally McGill, Thomas Castiglione, Helen Corral-Bonner, Anna M. Foutz, Steve G. Husa, Eric Sahl, Bernadette E. Vargas, and Seth Wallace (Poster 219)

This SCEC and EarthScope funded project is a collaboration between high school science teachers and their students, undergraduate and graduate students, and faculty from California State University San Bernardino, University of Arizona, and SCEC. As high school teachers and their students work alongside one another, they are exposed to and contribute to an authentic research process that will lead to publishable results. The scientific goal of this project is to measure plate tectonic movement within the San Bernardino mountain area and the Inland Empire region of Southern California utilizing GPS. Teachers and high school students collected survey-mode GPS data from 6 sites (among a total of 16 sampled by the larger group of participants) during a 5-day campaign from July 27 to August 1, 2012. The information obtained will be useful for understanding and characterizing seismic hazards in that region of Southern California. To enhance this experience, all of the teachers and their students have been invited to present their results at the SCEC Annual Meeting in September 2012. As part of the classroom implementation phase of the program the teachers are introduced to the Lesson Study approach. Lesson Study is a professional development process where teachers systematically examine their practice with the goal of becoming more effective. This process centers on teachers working collaboratively on a small number of Research Lessons. First, they identify the areas where their students are encountering challenges in learning standards-based content. The challenging areas are identified through results from standardized exams (e.g. California Standards Tests) or other assessment tools. To address areas of difficulty the teachers develop, test, and improve an instructional experience that promotes student learning of that standards-based material. Lesson Study is different from "lesson planning" because it focuses on what teachers want students to learn rather than on what teachers plan to teach. The 2012 teachers divided into two groups and each group is developing a Research Lesson. One of each of the group members teaches the lesson while the others observe the student learning. After the Research Lesson is taught the entire group comes together to debrief the lesson, make revisions, and another member of the group re-teaches the lesson (at a later date and at a different school) to incorporate what has been learned.

Spatial Correlations in Building Response Using Simulated and Recorded Earthquake Scenarios, David J. DeBock, Jack W. Garrison, and Abbie B. Liel (Poster 032)

Regional seismic risk assessment, e.g. for portfolios of buildings or geographically distributed infrastructure systems, requires appropriate treatment of spatial correlations in ground shaking intensity and in building response. Spatial correlations in ground motion intensity have previously been shown to be significant; underestimating these correlations leads to errors in assessing seismic risk for geographically distributed systems (Park et al. 2007). This study focuses on quantifying correlations in building response. Correlations are computed from nonlinear response history simulation of multi-degree-of-freedom models subjected to ground motions from two recorded and two simulated earthquake scenarios. The simulated earthquake scenarios are the Graves et al. (2008) ShakeOut scenario on the southern San Andreas Fault ($M_w=7.8$) and the Graves et al. (2005) scenario along the Puente Hills fault in the Los Angeles Basin ($M_w=7.2$). Correlations in building response are quantified and illustrated using two approaches: by linear correlation coefficients dependent on site separation distance and through semivariograms. Using these methods, spatial correlation metrics are analyzed to determine over what range correlations are significant, and what factors contribute to stronger or weaker correlations. Results show that correlations are significant for closely-spaced, similar buildings.

Building response correlations are also compared to spatial correlations of spectral acceleration intensity at the buildings' fundamental periods. Spectral acceleration is a common intensity measure, and its value, and the spatial correlations therein, can be predicted by modern ground motion prediction equations and correlation models. Results show that, for the regions and earthquake magnitudes considered, spatial

correlations in the spectral accelerations at building fundamental periods and in their nonlinear dynamic responses are often indistinguishable from one another. This finding indicates that recent models for computing spatial correlations in ground motion intensity can also be used for estimating spatial correlations of building responses such as peak drifts and floor accelerations. These results may be useful for incorporation into models for regional seismic risk assessment of building portfolios in the future.

This abstract reflects work funded by SCEC in 2011 and 2012

Improved Green's Functions Using Physical Constraints, Marine AM. Denolle and Gregory C. Beroza (Poster 016)

Estimating accurate ambient noise Green's functions from temporarily deployed seismic arrays is challenging because non-homogenous noise source distribution, or large contribution of local noise, can introduce biases and slow convergence to the true Green's function. We use the physical constraints of Green's function symmetry and causality as constraints to determine optimal weights for the correlations that are stacked to estimate the Green's function. We treat Green's function estimation as an inverse problem and simultaneously minimize the energy in the acausal window and maximize the symmetry using a set of non-negative weights on the components that are stacked. We carry this out using Non-Negative Linear Least Squares stabilized by Tikhonov Regularization, but replace the roughness norm to be minimized by the Green's function symmetry conditions. We use generalized cross-validation to find the optimal damping parameter. We show the clear improvement of the Green's functions for specific stations in the Los Angeles sedimentary basin. To constrain the Los Angeles sedimentary basin response, we installed broadband sensors in the Coachella Valley along the San Andreas Fault (SAVELA experiment), in a 3-month deployment during which the April 4th, 2010, $M7.2$, El Mayor-Cucapah earthquake occurred. Although the earthquake and its aftershocks interfere with our ability to use the ambient noise, they do provide signals in the form of scattered waves of the coda. We take advantage of the aftershock data to improve our estimate of the Green's functions further. The resulting Green's functions provide clearer information on the sedimentary basin structure.

Status of GPS Network Operations at USGS Pasadena, Daniel N. Determan, Aris G. Aspiotes, Ken W. Hudnut, Nancy E. King, and Keith F. Stark (Poster 213)

The US Geological Survey (USGS) Pasadena field office operates over 100 permanent, continuously-operating Global Positioning System (GPS) stations in southern California. These stations are primarily located throughout the urban Los Angeles area and along the southern San Andreas fault. Construction of the stations began in 1994 and continues today. The majority of the sites were constructed during the Southern California Integrated GPS Network project in the late 1990s through 2001. Three new GPS stations were added in 2012. Two of these have both seismic and GPS instrumentation. One site we recently installed co-located seismic and GPS instrumentation, is a critical infrastructure site that monitors the integrity of the fresh water tunnel that crosses the San Andreas Fault. This site was established in partnership with the Los Angeles Department of Water and Power. Two more GPS stations will be added in 2013, with several more being proposed. The proposed sites will be located at another critical fresh water infrastructure location that crosses the Casa Loma section of the San Jacinto fault. These sites will be established in partnership with the Metropolitan Water District.

The USGS GPS network in southern California consists of three types of geodetic grade GPS receivers: the Ashtech Z-XII, the Trimble NetRS, and the TOPCON Net-G3A. The Ashtech Z-XII is being phased out this year, as the TOPCON Net-G3As and future JAVAD Sigmas have the additional capability of tracking other Global Navigation Satellite Systems. All of the receivers in the network record 1 sample every 15 seconds locally onto the receiver. Almost all of them also transmit that data using phone lines, spread spectrum radios, cell modems, and the Internet, to a database where the data is processed and archived. In addition, the USGS currently has over 80 of their 104 GPS stations streaming real-time high rate (1 sample per second) data, which scientists and others can utilize immediately from anywhere in the world.

Improvements for the network include upgrading all stations to the newly acquired TOPCON Net-G3A receivers (JAVAD Sigmas will be installed at future sites), and having all stations streaming high-rate real-time data with minimal data gaps. One important goal of the GPS network is to add a geodetic component to an effective earthquake early warning system.

Two New Optical Fiber Strainmeters for Earth Strain Measurement, *Scott DeWolf, Frank K. Wyatt, Mark A. Zumberge, Duncan C. Agnew, Don Elliott, and Billy Hatfield* (Poster 233)

Optical fiber interferometers offer an attractive means to measure Earth strain because they are capable of sensing very small displacements over long baselines and can average the noise from localized effects. However, the design of such sensors presents a range of challenges. In the past year we have deployed two new systems at the Piñon Flat Observatory, adjacent to the existing long-base laser strainmeters that locally provide ground-truth. Both of the systems use standard single-mode telecom fiber and passive optical components.

The first is a 250-m vertical borehole strainmeter in operation since December 2011. Stretched between a clamping point 4 meters below the surface and an anchor at depth, this sensor is comprised of three unequal-arm interferometers in two separate optical fiber cables. These provide redundant measurements of vertical strain relatively immune from surface temperature fluctuations. An additional unequal arm interferometer provides the means to track the wavelength drift of the light source, an unstabilized infrared laser. As a completely optical system there are no down-hole electronics.

The second is a 180-m horizontal strainmeter in operation since July 2012. This sensor is tensioned between two poured-concrete blocks at the ends of a 1-m deep trench. Operated as an equal-arm interferometer, the sensing element is a single extended fiber with an equal length of fiber wrapped onto a quartz reference mandrel, all buried at the same depth. The mandrel provides the dual benefit of eliminating the need for a frequency-stabilized laser as well as temperature compensation for the otherwise highly temperature sensitive sensing portion of the strainmeter.

In addition to the details of each sensor's design and deployment, we present an examination of their noise and responses to Earth tides and earthquakes. For the vertical borehole strainmeter, this analysis includes a current strain rate of +1.5 microstrain per year, a differential strain rate of -150 nanostrain per year between the redundant fibers, a -130 dB intertidal noise level, and an RMS noise of 20-30 picostrain in the 1-10 Hz band.

Given the near-surface setting of the horizontal strainmeter, the aim of this system is to provide good estimates of the earth tides and to capture the seismic band. Records show the (separable) diurnal-strain signals and solid earth tides to be comparable in amplitude, establishing the viability of optical fibers for horizontal strain sensing

Off-Fault Deformation in the Eastern California Shear Zone Can Account for Slip Rate Discrepancies, *Ohilda Difo, Michele L. Cooke, and Justin W. Herbert* (Poster 149)

The Eastern California Shear Zone (ECSZ) shows a discrepancy between geologic strike-slip rates and slip rates from geodetic inversions. The sum of estimated geologic slip rates across six faults in the ECSZ are at most 6.2 mm/yr, half of the geodetic rates of 12 mm/yr (Oskin et al. 2008). We use three-dimensional mechanical models to investigate if this discrepancy may be due to unaccounted off-fault deformation surrounding the faults. We start with the fault configuration of the Southern California Earthquake Center (SCEC) Community Fault Model (CFM). The CFM is a compilation of active fault surfaces in southern California that approximates the mapped fault traces. Within the ECSZ, several faults are over-connected with the CFM. We modified the CFM to improve the accuracy of the fault geometry and investigate the resulting deformation. The revisions to the model provide better matches to the geologic strike-slip rate data. Our modeling yields off-fault deformation field consistent with long-term patterns of uplift and subsidence in the area. (e.g., Meigs et al., 2008, Cooke and Dair 2011). Within the model, off-fault deformation accounts for 30% of the total strain and accommodates ~3 mm/yr of deformation. This suggests that half of the discrepancy between the geologic slip rates and rates from

geodetic inversion in the ECSZ could owe to unaccounted off-fault deformation in the inversions.

Network estimation of time-dependent noise in GPS data, *Ksenia Dmitrieva and Paul Segall* (Poster 210)

GPS position time series are widely used for measuring crustal deformation. However, the uncertainty in station velocity is in particular strongly influenced by long-period noise, typically modeled as power-law noise, including random walk and flicker noise. Hence a good understanding of GPS noise is essential for knowing the velocity uncertainly.

We develop a network noise estimator that is able to determine the time-dependent noise properties of GPS time series in regions of low deformation rates. Specifically, we investigate spatial correlations of different components of the data. In our filtering approach we decompose the signal within a stable plate interior into a spatially coherent plate rotation (possibly plus post-glacial rebound) and noise. Currently the noise is a sum of flicker, random walk, and white noise. Assuming that there are no other signals in stable parts of the plate, we process all stations simultaneously use a Kalman filter to estimate the different components of the data. We use maximum likelihood estimation (MLE) to solve for the best fitting variance parameters in the noise model.

Preliminary work using synthetic data shows that our method can recover even low levels of time-dependent noises in the data. We compare our network method with commonly used "baseline fit" MLE techniques by running both methods on sets of synthetic data with constant white and flicker noise, but varying random walk variance. Each method can determine flicker noise and white noise values well; however, the baseline fit fails to detect random walk if its magnitude is significantly lower than flicker noise. For example, for flicker noise of 2 mm/yr0.25 and random walk of 0.38 mm/yr0.5, the baseline fit finds no random walk, and yet our network approach estimates a value of 0.3 mm/yr0.5. Even low values of random walk significantly affect the uncertainty in the site velocity.

The Ventura Region Special Fault Study Area: Towards an Understanding of the Potential for Large, Multi-Segment Thrust Ruptures in the Transverse Ranges, *James F. Dolan, John H. Shaw, and Thomas K. Rockwell* (Talk Tue 15:30a)

The recent occurrence of several highly destructive thrust fault earthquakes (e.g., 1994 Mw 6.7 Northridge; 1999 Mw 7.6 Chi-Chi; 2005 Mw 7.5 Kashmir; 2008 Mw 7.9 Wenchuan; 2011 Mw 7.2 Van) and the growing recognition of the hazards posed by such structures to urban centers around the world highlight the need to better understand the behavior of these faults and their associated folds. The 2008 Wenchuan earthquake, in particular, emphasized that ruptures may link together various thrust faults to generate extremely large-magnitude earthquakes. The growing realization of the possibility of multi-fault ruptures, coupled with the presence of numerous large reverse faults within the Transverse Ranges, emphasizes the necessity of assessing the hazards posed by such multi-segment thrust earthquakes in southern California. The major reverse faults of the Transverse Ranges form an interconnected, >200-km-long network that could potentially rupture together during very large-magnitude events similar to the Wenchuan earthquake. Of particular importance is the complex network of faults in the Ventura area. These faults could potentially serve as linking structures connecting large thrust ramps to the west (e.g., Pitas Point fault) with the large thrust and reverse faults to the east (e.g., San Cayetano, Santa Susana, and Sierra Madre-Cucamonga faults, the latter extending all the way across the northern edge of the Los Angeles metropolitan region.

The critical need to understand the faults of the Ventura region has led SCEC to designate this as a Special fault Study Area (SFSA). The goal of this SFSA is to focus multi-disciplinary efforts of many SCEC researchers on the common problem of understanding the structure, state of activity, slip rates, and seismic hazards of the Ventura region faults, and more generally on assessing the degree to which these faults provide potential structural linkages for through-going, large-magnitude multi-segment ruptures. Much of this research is already under way with SCEC funding, including 3D structural modeling using industry well and seismic reflection data and newly collected high-resolution reflection data, both

MEETING ABSTRACTS

onshore and offshore paleoseismologic work aimed at determining the slip rates of these faults and the ages and displacements of ancient earthquakes that they have generated, studies of tsunami records preserved in estuarine sediments, mechanical modeling of regional fault interactions, and dynamic rupture simulations. In addition to describing preliminary results from these studies at the SCEC Annual Meeting, we will also discuss the format of a planned SCEC workshop on this SFSA to be held in 2013.

Evaluation of the Scattering Models in the Crust for Mexico and Long Beach, Luis A. Dominguez, Paul Davis, and Dan Hollis (Poster 200)

Modeling of scattered waves in the crust has been highly controversial in the past 40 years. From the initial models of back-scattering proposed by Keiiti Aki in 1969; to the recent models of scattering based on kinetic theory of gases. Different groups have relied on a priori assumptions about the medium, the mode of propagation and the physics of the rocks. These constraints have led to a large variety of models with notorious differences in the phenomenological basis with an apparent success fitting the data. Perhaps one of the major hurdles to achieve a unifying theory lies in the sparse nature of the current seismic networks. A novel experiment deployed by Nodal Seismic provides an unprecedented set of data to analyze scattered wavefields at high frequencies and short wavelengths. A set of ~5400 seismic instruments, spaced every 100m, was installed for a period 6 months in the Long Beach area to mainly image the geological structure of the area for oil exploration purposes. Nonetheless, our interest focuses on the examination of coda waves and their statistical and physical properties. In the first instance, we compute the frequency-wavenumber diagrams as a function of time to detect the sources of coda and their evolution in time. In addition, we analyze the entropy of the network as seismic waves propagate through the array. Entropy marks the transition between the coherent direct body waves and the onset of coda waves. This result suggests that the seismic record is mostly dominated by forward scattered body waves for a time comparable to the arrival of the s-wave before the transition to omnidirectional coda waves occurs. Additionally, we evaluate independent measurements of intrinsic and scattering attenuation for a dense array in Mexico (station spacing ~5km). In this case, we analyzed the different components of the MLTW method (Hoshiya 1991) to reconcile the results obtained by the application of this method and laboratory experiments. We examine the effects of assuming spherical geometrical spreading of the wavefield, the depth of the sources, the preferential mode of propagation and the absorption of energy into the mantle. Unlike Long Beach, Mexico is situated in a tectonically different environment that can be used to test different scenarios. Ongoing efforts may shed light on the validity of these models and their applicability both in the frequency and space domain.

Analyzing UAVSAR Data using the QuakeSim Computational Environment, Andrea Donnellan (Poster 217)

QuakeSim is a computational environment for analyzing GPS and InSAR geodetic imaging data products, and integrating multiple data sources into models of the earthquake cycle. NASA has been collecting UAVSAR Repeat Pass Interferometry in California on its airborne interferometric synthetic aperture radar imaging platform since 2009. The 2010 El Mayor – Cucapah Earthquake was imaged, as well as slip on several faults north of the main rupture, including the Superstition Hills, Imperial, and Yuha faults. Using QuakeSim's InSAR profile tool we have identified slip on the southern part of the Superstition Hills fault of 15 ± 0.3 mm and in excess of 60 cm of ground range change from the main rupture. UAVSAR data products suffer from error due to troposphere and unmodeled residual aircraft motion. Using QuakeSim's InSAR profile tool we have found the differencing data across profile removes some of this correlated error. We have also found areas in which lineations parallel to faults observed in the RPI images are not due to tectonic motion, but rather some other error source. Inversions of the UAVSAR data products show that surface slip extended 10–20 km deep in the crust.

Testing CyberShake Using Precariously Balanced Rocks, Jessica R. Donovan, Thomas H. Jordan, and James N. Brune (Poster 026)

Precariously balanced rocks (PBRs) are fragile geologic features that are expected to be overturned by ground accelerations less than about 0.5 g

and represent the only currently available dataset for constraining maximum ground motions over multiple large earthquake cycles (Brune and Whitney, 1992). Previous research (e.g., Brune, 1996; Anooshehpour et al., 2004; Purvance et al., 2008) shows how estimates of the overturning response of these rocks is used to estimate maximum ground motion over time scales of up to ~20 ky (Bell et al., 1998). These ground motion constraints have been compared in the literature to probabilistic seismic hazard models that are based on empirical ground motion prediction equations (GMPEs, sometimes called attenuation relations) (e.g., Brune, 1996; Brune, 1999; Purvance et al., 2008; Brune et al., 2006).

In this study we apply PBR constraints to test the Southern California Earthquake Center's physics-based ground motion simulator, CyberShake (Graves et al., 2011), which currently extends the Uniform California Earthquake Rupture Forecast, version 2 (UCERF2). We use a catalog of 17 PBR locations within the southern California CyberShake region and compute overturning probabilities for the ground motions predicted by the CyberShake hazard model. We find a discrepancy between high overturning probabilities for some PBRs and the observation that these rocks are not overturned, particularly in the Mojave section of the San Andreas Fault. We discuss the possible sources of discrepancy in terms of uncertainties in the overturning response of the PBRs, unrealistic ruptures or incorrect assumptions in the extended earthquake rupture forecast, and incorrect ground motion calculations. We then address the implications of these discrepancies for future versions of UCERF as well as future CyberShake runs.

Evidence for Active Northeast Tilting Across the Southern Coachella Valley and Santa Rosa Mountains, Rebecca J. Dorsey, Victoria E. Langenheim, and James C. McNabb (Poster 272)

The southern San Andreas fault (SAF) system provides an excellent natural laboratory for the study of rapid vertical crustal motions in a continental strike-slip fault zone. Here we describe a hypothesis for active NE tilting of a crustal-scale (~30 x 40 km) tilt block in the southern Coachella Valley and Santa Rosa Mts, between the San Jacinto fault zone on the SW (dated in other studies at ~1.2 Ma) and the SAF on the NE. The Santa Rosa fault (SRF), a strand of the San Jacinto fault zone, marks the steep SW flank of the Santa Rosa Mts and merges with the Clark fault beneath Clark Valley. The SRF is an active normal fault with well developed triangular facets, steeply SW-dipping fault zone with brittle gouge and microfaults, and narrow footwall canyons that feed steep alluvial fans in the hanging wall (east side of Clark Valley). The Clark basin is ~4 km deep, and the pre-SRF West Salton detachment fault projects ~1.5 km above the valley floor in the Santa Rosa Mts. A steep linear gravity gradient reveals combined vertical separation of ~5.5 km across the SRF and Clark fault, for an implied slip rate of ~4.5 mm/yr across the two faults. The NE side of the Santa Rosa Mts has a gentler surface gradient and no large-offset active faults. The ratio of alluvial fan area to catchment area is 0.5-0.6 for fan-catchment pairs along the SRF, compared to an average of 1.1-1.2 on the NE slope of the Santa Rosa Mts, suggesting rapid subsidence in the hanging wall and relatively slow subsidence in the NE-tilting footwall of the SRF. The depth of the southern Coachella Valley increases from the SW side, where sediments onlap crystalline rock of the Santa Rosa Mts, to 4-5 km near the SAF on the NE side of the valley. NE of the SAF in the Mecca Hills, crystalline basement has been exhumed from ~1.3 km depth to the surface since 740 ka at ~1.8 mm/yr. If just 3 km of the Coachella Valley basin fill is post-1.2 Ma, the net rate of vertical offset across the SAF is ca. 4-5 mm/yr. The data suggest rapid NE tilting of a large tilt block about a NW-trending horizontal axis since initiation of the San Jacinto FZ ~1.2 Ma. To the south in the Salton Sea, a large positive gravity anomaly reveals the presence of thin mafic crust beneath basin-filling sediment. NE tilting, if correct, may result from translation of crust through large releasing and restraining bends in the SAF system, and/or vertical loading in the lower crust or upper mantle related to recent lithospheric rupture.

Inferring the Initial Stress State of Large Earthquakes: Fault Branching and Incomplete Slip Partitioning in the 2008 M8 Wenchuan Earthquake Suggest Rotations of the Stress Field, Benchun Duan (Poster 082)

The 2008 M8 Wenchuan earthquake exhibits complex rupture propagation on a geometrically complex fault system and incomplete slip partitioning, i.e., the Beichuan fault experienced both strike-slip and thrust motions, while slip on the shallow-dipping Pengguan fault was primarily thrust. These two faults are parallel on the surface and merge at depth. These features of dynamic branching and slip partitioning in the event await a physical explanation. In this study, we perform 3D dynamic rupture modeling to investigate physical conditions that can produce these features. In our finite element models, we use natural cubic spline functions to characterize the smoothly curved Beichuan and Pengguan faults that are suggested by geologic and geodetic studies. Given the branched fault geometry, we are particularly interested in exploring effects of different initial stress fields along the fault system just before the dynamic event on rupture propagation and slip partitioning. We resolve depth-dependent effective principal stresses, one of which is vertical, onto the branched fault system in setting up the initial stress field, which may be characterized by the angle α between the horizontal maximum principal stress and the fault strike. We find that a uniform regional stress field on the fault system, e.g., α being 90 or 60 degree along the entire fault system, cannot produce dynamic branching and slip partitioning features observed in the 2008 event. However, when we set different values of α along the two faults, e.g., α being 90 and 50 degrees for the Pengguan and Beichuan faults, respectively, dynamic branching and incomplete slip partitioning can be reproduced. In particular, further introducing variations of α (i.e., stress rotations) along the Beichuan fault can reproduce a feature in rupture propagation reported by some kinematic inversions based on near-field strong-motion recordings, i.e., the rupture started on the Pengguan fault and triggered failure of the Beichuan fault ~40 km northeast of the hypocenter after ~17 seconds of the rupture initiation. We observe that fault branching in these scenarios is generated by dynamic triggering at shallow depth, not rupture propagating through the branching point from below. These numerical experiments illustrate that we may infer the initial stress field of recent large earthquakes by integrating various observations and dynamic rupture models.

Reevaluation of faulting in the vicinity of Cedar Springs Dam, San Bernardino County, California, Sean L. Dunbar, Ray J. Weldon II, Don F. Hoirup, Jr., Robert G. Barry, and Justin T. Pearce (Poster 146)

A review of active faulting in the vicinity of Cedar Springs Dam, which impounds Silverwood Lake in the Western San Bernardino Mountains, revealed a lower level of seismic activity than previously inferred. The Cleghorn fault is the predominant fault in the vicinity of the dam, with fault scarps, offset and beheaded stream channels, and other types of geomorphic evidence supporting Quaternary activity, and possibly Holocene activity. No other faults in the vicinity of the dam show similarly young tectonic geomorphology, and thus all other faults appear to have much lower slip rates. While the Cleghorn fault is clearly active, its published slip rate (3 mm/yr) was overestimated due to miscorrelation of late Quaternary fluvial terrace levels (Qt1 and Qt2) with the dated Quaternary sequence in Cajon Pass. Subsequent mapping to better link the terraces between the two systems (especially along drainage divides within the San Bernardino Mountains and the Summit Pass/Inface Bluffs region), the development of published soils chronosequences, and the growing number of cosmogenic surface exposure dates on surfaces within the San Bernardino Mountains suggest that the respective ages of Qt1 and Qt2 are ~60,000 and ~500,000 years old rather than ~12,000 and ~60,000 years old, as previously inferred. Thus, the slip rate on the Cleghorn fault is now estimated to be 5-10 times less than previously inferred (0.3 to 0.6 mm/yr). In addition, this suggests that mapped faults in the foundation of Cedar Springs Dam should be considered "conditionally active" rather than "active" according to DSOD criteria.

The faults under Cedar Springs Dam are not likely connected to the North Frontal fault zone of the San Bernardino Mountains, since the North Frontal fault zone terminates against a series of west-to-northwest striking faults in the Grass Valley fault zone. The faults under the dam may be related to the Grass Valley fault zone, which appears to have a very low level of active strike slip faulting, but are most likely late Miocene faults that have been reactivated under the current stress regime. In either case, the geomorphic expression suggests that faults

under the dam are less active than the Cleghorn fault, and are thus inferred to have slip rates less than 0.3 to 0.6 mm/yr.

Dynamics of anti-plane shear ruptures with off-fault plasticity, Ahmed E. Elbanna and Ralph Archuleta (Poster 084)

We investigate the effect of off-fault plasticity on the dynamics of anti-plane shear ruptures propagating on frictional interfaces characterized by linear slip weakening friction and instantaneous healing at zero slip rate. We discretize the equations of elasto-plasticity using a second order finite difference approximation and integrate them in time using the second-order Newmark scheme. The yield surface is modeled by a Mohr-Coloumb criterion and isotropic hardening with a constant hardening parameter. We explore the dynamics for different values of confining pressure as well as the strength parameter (S). We find that the rupture speed quickly accelerates to values near its limiting speed even in the presence of off-fault dissipation. Off-fault plasticity, however, limits the peak slip rate compared to the linear elastic case. The increase in slip with propagation distance in the former case is achieved by changing the shape of the slip pulse making its peak broader. For constant pressure, the width of the plastic zone increases with propagation distance. To simulate depth dependence, we model a few cases with linearly varying pressure. The dynamics of the slip pulse in these cases is more complicated with and that the width of the plastic zone was found not to necessarily increase as the value of confining pressure decreases. We discuss the implications of our findings on the energy partition of real earthquakes.

To examine the impact of plastic deformation on seismicity and the evolution of the prestress due to repeated ruptures, we developed a modified version of the spring block slider model with non-linear inter-block springs. We find that plasticity leads to an increase in the number of small events and to the evolution of heterogeneous prestress characterized by a white-noise spectrum. We discuss the implications of our results on the continuum case.

Rupture arrest at a strike-slip restraining double-bend observed in nature and numerical simulations, Austin J. Elliott, Zaifeng Liu, Michael E. Oskin, Benchun Duan, and Jing Liu-Zeng (Poster 134)

Static frictional stresses at bends or stepovers along a fault impede earthquake ruptures, but heterogeneous residual stresses from prior earthquakes may overcome this effect, enabling rupture to propagate through such barriers. Understanding the circumstances that lead to rupture propagation through known stress barriers is central to the debate over whether a southern San Andreas rupture would pass through the San Gorgonio Pass restraining double-bend. To evaluate the relative impacts of fault geometry and rupture history on earthquake size at such a bend, we pair field observations of paleoearthquakes with numerical rupture models of the similar, but superficially less complex Aksay restraining bend and stepover of the rapidly slipping (~1cm/yr) sinistral Altyn Tagh fault in western China. We find that the most recent major rupture of this fault system terminated in both directions at restraining double-bends. The westward terminus was identified by Washburn et al. (2004). We mapped its eastward extent along a 65 km reach of fault marked by distinct moletracks and numerous small (~4m) offsets. Beyond the rupture tip, an additional ~150 km reach of the fault shows no expression of earthquake rupture in late Holocene deposits and only highly relaxed scarps cutting features >6ka. The eastern rupture terminus coincides with the 098°-striking reach of the fault most highly inclined to the regional fault strike of 072°. In this zone of marked transpression, slip steps over to an adjacent fault; slip on each fault wanes where they overlap. Our numerical models of stress evolution over multiple dynamic seismic cycles on this fault system show that individual ruptures propagating along the fault are commonly arrested in the misaligned reach. After many model cycles, representing a long history of large (>250km length) ruptures, residual stresses within the bend enable small amounts of slip beyond the boundaries of major ruptures, sometimes as individual moderate earthquakes, sometimes as the tail ends of large ruptures. However, individual ruptures do not propagate far beyond the bend on either fault strand. On the basis of our field and model results, we suggest that restraining bends of the size and angle exemplified by the Aksay bend form sufficiently resistant static stress barriers to consistently block earthquake ruptures.

MEETING ABSTRACTS

Integrating short-term and long-term deformation in numerical models: some benchmark examples using SULEC, Abaqus and Pylith, *Susan Ellis, S Buiter, and C Williams* (Poster 111)

Lagrangian finite element codes based on an elastic formulation are a powerful tool to investigate short-term responses to earth phenomena such as earthquakes. Integrating deformation in such codes over millennia requires careful consideration of the effects of finite strain – both numerically (meshes and geometry) and physically (fault development and strain weakening). An alternative approach is to start from a viscous formulation, in which only the shear effects of elasticity are modelled, according to the method outlined in Moresi et al. (2003, 2007). This approach can handle many hundreds of per cent finite strain, by integrating all variables through time and space using tracer particles. It can also be used in a limited fashion to investigate coseismic and postseismic deformation, and thus has the potential to jump from short to much longer timescales. However, because it uses a continuum approach, discrete faults must be represented by softened shear zones. We contrast the two modelling approaches by presenting several benchmark problems comparing SULEC (a 3D arbitrary Eulerian-Lagrangian finite element code based on Stokes creeping flow) with Lagrangian codes Abaqus and Pylith. The benchmarks include: long-term development of a through-going strike-slip fault; quasi-static propagation (with elastic unloading) of a crack; and modelling surface response to postseismic creep. These benchmark exercises are a necessary first step in our long-term goal of integrating the two approaches. We would eventually like to achieve near-steady-state behavior over long time scales using the SULEC-type approach, while addressing behavior over individual earthquake cycles using a Lagrangian code such as Pylith.

The Effects of Off-Fault Plasticity in Earthquake Cycle Simulations, *Brittany A. Erickson and Eric M. Dunham* (Poster 189)

Field observations of damage zones around faults reveal regions of fractured or pulverized rocks on the order of several hundred meters surrounding a highly damaged fault core. It has been postulated that these damage zones are the result of the fracturing and healing within the fault zone due to many years of seismogenic cycling. We are developing an efficient numerical method to simulate full earthquake cycles of multiple events with rate-and-state friction laws and off-fault plasticity. Our method evolves the system through the interseismic period, generating self-consistent initial conditions prior to rupture. Large time steps can be taken during the interseismic period while much smaller time steps are required to fully resolve quasi-dynamic rupture. So far our simulations have been done assuming a linear elastic medium. We have concurrently begun developing methods for allowing plastic deformation in our cycle simulations where the stress is constrained by a Drucker-Prager yield criterion. The idea is to simulate multiple events which allow for inelastic response, in order to understand how plasticity alters the rupture process during each event. We will use this model to see what fraction of coseismic strain is accommodated by inelastic deformation throughout the entire earthquake cycle. Modeling earthquake cycles with plasticity will also allow us to study how an initial plastic strain distribution affects subsequent rupture. We consider a vertical strike slip fault where constant creep is imposed at the downdip extension of the fault. For the volume discretization required for plasticity we use high order summation-by-parts finite difference operators. We assume antiplane deformation in 2D and our numerical methods achieve high order convergence for the static elastic problem in the time-stepping method. We are currently integrating plasticity into this routine to allow for inelastic response throughout the entire cycle. Incorporating the constitutive relations for plasticity furnishes a nonlinear equilibrium equation for displacement. The equilibrium equation is solved by an iterative solution procedure which makes use of an elastoplastic tangent stiffness tensor and the return mapping theorem to solve for stresses consistent with the constitutive theory. During each iteration the equilibrium equation requires finite difference operators for variable material properties where we show second order convergence.

Total variation denoising of interseismic deformation in southern California, *Eileen L. Evans and Brendan J. Meade* (Poster 212)

Geodetic observations of interseismic deformation provide constraints on microplate rotations, earthquake cycle processes, and slip partitioning across the Pacific-North America plate boundary. These measurements may be interpreted using block models, in which the upper crust is divided into microplates bounded by mapped faults. The number and geometry of microplates are typically defined with boundaries representing a limited sub-set of the large number of potentially seismogenic faults. An alternative approach is to include all possible faults in a dense array of microplates, and then deterministically estimate the boundaries at which strain is localized. This is possible with a regularization technique called total variation denoising (TVDN), which simultaneously minimizes of the L_1 -norm of the data residuals and L_1 -norm of the variation in the estimated state vector. Applied to three-dimensional spherical block models, TVDN reduces the total variation between estimated rotation vectors, creating groups of microplates that rotate together as larger blocks, and therefore localizing fault slip on the boundaries of these larger blocks. Here we develop a block model comprised of hundreds of microplates based on detailed fault maps, and deterministically identify the kinematically most important faults in southern California using TVDN regularization.

The influence of complex fault geometry on uplift patterns in the Coachella Valley and Mecca Hills of Southern California, *Laura Fattaruso and Michele Cooke* (Poster 033)

Detailed 3D surfaces for active faults in southern California have been compiled within the Southern California Earthquake Center Community Fault Model (CFM) based on data from geologic maps, seismic reflection data, and microseismicity. 3D mechanical models that use the CFM version 3.5 and apply plate motions on the boundaries produce fault slip rates and uplift patterns that match geologic observations, validating that the CFM well represents active fault geometry in many portions of southern California. One region of lingering mismatch is the Coachella Valley segment of the San Andreas fault (SAF). Model uplift patterns produced by a vertical Coachella segment do not match the pattern of sedimentation in the Coachella valley and rapid ongoing uplift in the Mecca Hills northeast of the SAF.

The Coachella Valley segment of the SAF consists of a single main fault that branches into the Mission Creek and Banning strands in the northwest. While the fault has previously been modeled as vertical, seismic and structural studies suggest a steep (60-70°) northeast dip on the main segment that shallows to the northwest, where the fault merges at depth with the north-dipping San Geronio Pass fault zone. A northeast dip to the Coachella Valley segment of the SAF is also consistent with the inferred position of locking depth of this fault from InSAR data.

The most recent version of the CFM (v. 4.0) has seen the addition of several secondary faults in Indio Hills and Mecca Hills as well as the addition of a dipping fault at depth striking sub-parallel to the Coachella Valley segment. We compare uplift patterns and slip rates produced by mechanical models with a variety of alternative fault configurations— a northeast dipping Coachella segment, and a vertical Coachella segment with a sub-parallel northeast dipping fault (CFM 4.0). Both of these Coachella Valley alternatives were run with and without the five secondary faults on the northeast side of the Coachella segment of the SAF. A northeast dipping Coachella Valley segment tilts the Coachella Valley to the east, better matching sedimentation patterns. The addition of the secondary faults east of the Coachella segment into the model produces localized uplift in the Mecca Hills region. These variations in fault configuration demonstrate the impact of complex regional fault geometry on uplift/subsidence patterns and slip rates in the Coachella Valley and Mecca Hills.

Towards an improved GPS velocity solution in the presence of earthquakes, and accurate assessment of inter-, co- and post-seismic motions, *Michael A. Floyd and Thomas A. Herring* (Poster 216)

The Plate Boundary Observatory's GPS velocity solution contains some anomalous sites, especially in the Mojave Desert around the locations of the 1992 Landers and 1999 Hector Mine earthquakes. These anomalous velocities are most likely due to incorrectly modeled post-seismic motions, which propagate into and contaminate the steady inter-seismic

tectonic motions in which we are generally interested for the problem of fault slip rates. We wish to investigate methods for simultaneously separating and solving for the contribution of post-seismic and other non-secular motions to improve velocity solutions contaminated by such motions. Here we present preliminary tests into a simple inversion method for typical post-seismic parameters such as elastic and viscoelastic layer thicknesses and rheological properties. We perform numerous forward models to predict the motion with time at given observation sites and set of parameters using analytical models for post-seismic viscoelastic relaxation (e.g. Savage and Prescott, 1978). From this, a linearized system of equations is formed using the partial derivatives of displacement (with time) with respect to the parameters we wish to solve for. Ultimately, we hope to perform the forward model operations using more sophisticated numerical software such as PyLith to represent more accurately Earth's response to particular earthquakes. Furthermore, we anticipate that such methods may be able to account for episodic transient motions in a similar manner.

Investigating Earthquake Hazards in the Northern Salton Trough, Southern California, Using Data from the Salton Seismic Imaging Project (SSIP)

Gary S. Fuis, John A. Hole, Joann M. Stock, Neal W. Driscoll, Graham M. Kent, Alistair J. Harding, Annie Kell, Mark R. Goldman, Elizabeth J. Rose, Rufus D. Catchings, Michael J. Rymer, Victoria E. Langerheim, Daniel S. Scheirer, Noah D. Athens, and Jennifer M. Tarnowski (Poster 120)

The southernmost San Andreas fault (SAF) system, in the northern Salton Trough (Salton Sea and Coachella Valley), is considered likely to produce a large-magnitude, damaging earthquake in the near future. The geometry of the SAF and the velocity and geometry of adjacent sedimentary basins will strongly influence energy radiation and strong ground shaking during a future rupture. The Salton Seismic Imaging Project (SSIP) was undertaken, in part, to provide more accurate information on the SAF and basins in this region.

We report preliminary results from modeling four seismic profiles (Lines 4-7) that cross the Salton Trough in this region. Lines 4 to 6 terminate on the SW in the Peninsular Ranges, underlain by Mesozoic batholithic rocks, and terminate on the NE in or near the Little San Bernardino or Orocochia Mountains, underlain by Precambrian and Mesozoic igneous and metamorphic rocks. These lines cross the Coachella Valley, which is underlain by Miocene to Holocene sedimentary deposits. Line 7 crosses the Salton Sea and sedimentary basin deposits to the northeast similar to those of the Coachella Valley. On three lines (7, 4, 6) there is evidence from our seismic imaging, potential-field studies, and (or) earthquakes that active strands of the SAF dip moderately NE.

From south to north, on Lines 7, 4, 5, and 6, maximum sedimentary basin depths are approximately 5.5, 5.5, 3.5, and 3.5 km, respectively, as measured from the surface to the 5.3 km/s velocity contour. (In prior studies of the Imperial Valley, unmetamorphosed sediment is interpreted to lie above this approximate velocity contour.) Basement rocks that can be traced from the Peninsular Ranges to depth beneath the Coachella Valley are characterized by relatively high velocities, averaging 4.9 km/s at the surface and 6.4 km/s at a depth of 4 km. They are also characterized by high velocity gradients, averaging $> 0.4/s$. In contrast, rocks of the Little San Bernardino and Orocochia Mountains are characterized by relatively low velocities, averaging 3.9 km/s at the surface and 6.1 km/s at a depth of 4 km; and they are characterized by low velocity gradients, averaging $< 0.4/s$. The rocks of the Peninsular Ranges can be seen on Lines 4 and 6 extending at depth northeastward beyond the active surface trace(s) of the SAF.

Strong ground shaking from the ShakeOut Scenario Earthquake will be recalculated using our new non-vertical geometry for the SAF and new basin information.

Visible Earthquakes – a web-based tool for visualizing and modeling

InSAR earthquake data, Gareth J. Funning and Rowan B. Cockett (Poster 209)

Despite the utility of the technique and its widespread adoption by the research community, InSAR does not feature in the teaching curricula of most university geoscience departments. This is, we believe, due to a lack of accessibility to software and data. Existing tools for the

visualization and modeling of interferograms are often research-oriented, command line-based and/or prohibitively expensive. Here we present a new web-based interactive tool for comparing real InSAR data with simple elastic models. The overall design of this tool was focused on ease of access and use.

The tool, provisionally named 'Visible Earthquakes', uses web-based technologies to instantly render the displacement field that would be observable using InSAR for a given fault location, geometry, orientation, and slip. The user can adjust these 'source parameters' using a simple, clickable interface, and see how these affect the resulting model interferogram. By visually matching the model interferogram to a real earthquake interferogram (processed separately and included in the web tool) a user can produce their own estimates of the earthquake's source parameters. Once satisfied with the fit of their models, users can submit their results and see how they compare with the distribution of all other contributed earthquake models, as well as the mean and median models.

We envisage that the ensemble of contributed models will be useful both as a research resource and in the classroom. Locations of earthquakes derived from InSAR data have already been demonstrated to differ significantly from those obtained from global seismic networks (Weston et al., 2011), and the locations obtained by our users will enable us to identify systematic mislocations that are likely due to errors in Earth velocity models used to locate earthquakes. If the tool is incorporated into geophysics, tectonics and/or structural geology classes, in addition to familiarizing students with InSAR and elastic deformation modeling, the spread of different results for each individual earthquake will allow the teaching of concepts such as model uncertainty and non-uniqueness when modeling real scientific data. Additionally, the process students go through to optimize their models can be tied into teaching concepts of forward and inverse modeling, which are universal in geophysics.

Engineering Validation of Ground Motion Simulation: Part 1. Tall

Buildings, Carmine Galasso, Peng Zhong, and Farzin Zareian (Poster 030)

Challenges in defining seismic input for design and assessment of tall buildings in high seismic regions are numerous. For instance, it is generally required that these buildings are designed for collapse prevention under rare earthquakes, although ground motion databases rarely include appropriate records for such an assessment. Simulated (or synthetic) ground motion accelerograms are a valuable tool to overcome the scarcity of real (i.e. recorded) signals in empirical databases. However, the validation of simulation methodologies in terms of seismic structural demand is an essential step in establishing synthetic records as a potentially reliable engineering tool. The study presented in this poster (which is the first of a set of two) addresses the issue of engineering validation of hybrid broadband ground motion simulations in terms of seismic response of tall buildings. In particular, this study utilizes nonlinear dynamic analysis to statistically compare the seismic demands due to simulated and recorded ground motions on three variations of a 40-storey buckling-restrained braced frame designed for high seismic hazard in the Los Angeles region. The three designs are referred to as a 'code-based design', based on the 2006 International Building Code (IBC), a 'performance-based design', based on criteria published by the Los Angeles Tall Building Design Council (LATBDC) and a "performance-based design plus", based on newly developed criteria from the Pacific Earthquake Engineering Research (PEER) Center. Seismic demands in terms of interstory drift ratio (IDR) and peak floor acceleration (PFA) are derived for the 1994 Mw 6.7 Northridge earthquake using simulations and actual recordings at 43 stations. The median IDR and PFA profiles over the height, the dispersion (i.e., intra-event variability) of IDR and PFA profiles and their correlation over the height are employed as statistical measures for the comparison. Sensitivity of the results to the closest distance to the fault and site class is finally investigated.

Strong ground motions of the Mw 6.3 2009 L'Aquila earthquake: modeling and validation, Frantisek Gallovic, Gabriele Ameri, and Francesca Pacor (Poster 006)

On April 6, 2009 a Mw 6.3 earthquake struck the L'Aquila city, one of the largest urban centers in the Abruzzo region (Central Italy), causing a large number of casualties and damage in the town and surrounding villages.

MEETING ABSTRACTS

The collected records represent a unique dataset in Italy in terms of number and quality of records, azimuthal coverage and presence of near-fault recordings. Despite the moderate magnitude of the L'Aquila earthquake, the strong-motion and macroseismic data in the vicinity of the fault depict a large variability of the observed shaking and damage.

In this study we present broadband (0.1 – 10 Hz) ground motion simulations of the 2009 L'Aquila earthquake to be used for engineering purposes in the region. We utilize Hybrid Integral-Composite (HIC, Galovic and Brokesova, 2007) approach based on a k-square kinematic rupture model, combining low-frequency coherent and high-frequency incoherent source radiation and providing omega-squared source spectral decay. We first model the recorded seismograms in order to calibrate source parameters and to assess the capabilities of the broadband simulation model. To this end, position and slip amount of the two main asperities, the largest asperity time delay and the rupture velocity distribution on the fault is constrained, based on the low-frequency slip inversion result. Synthetic Green's functions are calculated in a 1D-layered crustal model including 1D soil profiles to account for site-specific response (where available). Several goodness-of-fit criteria confirm a remarkable agreement between observed and simulated data at most of the stations. The results show that not only the local site effects improve the modeling results, but also that the spatial broadband ground-motion variability is to large extent controlled by the rupture kinematics revealed by the low-frequency inversion.

We simulate the ground motion at a grid of sites and compare the observed macroseismic intensity distribution with that converted from synthetic data. We find that the spectral ordinates at periods larger than 2s are well correlated with the macroseismic intensity pattern observed in the epicentral area. Finally, we compare the synthetic ground-motion parameters with estimates from several empirical ground motion prediction equations (GMPEs). The comparison highlights potential drawbacks in using GMPEs to validate simulated motions and/or when used for engineering purposes.

Analyzing ShakeOut Participant Feedback to Improve Future Drills, Erica Garland and Michele Wood (Poster 254)

The Earthquake Country Alliances' Great ShakeOut has engaged participants throughout California since it was initiated in 2008. Participant feedback is important to help better understand the involvement of groups such as businesses and organizations and to motivate preparedness behaviors, which can help speed recovery of the entire community following a disaster. ShakeOut registrants were invited via email to participate in an Internet-based survey following the 2011 ShakeOut. This presentation focuses on survey responses from California businesses and organizations (N = 1,042). Of particular note was the lack of involvement of disabled persons in the actual drill activities; a full 40% of those responding as organizations indicated the number of disabled individuals participating in the drill as "some, few, or none." A total of 15% of those responding as organizations did not plan to evaluate the drill despite the importance of evaluation. Attitudes about the drill were positive. Nearly all (94%) felt that participating in the ShakeOut led to improvements. The overwhelming majority (99%) indicated that they plan to participate in the 2012 ShakeOut. Almost all (91%) of those responding as organizations indicated having a disaster preparedness plan, and 72% indicated having "all, most, or some" plans for continuity of service. Organizational preparedness is critical because many organizations are employers, and their policies can affect workers' safety on the job as well as their preparedness behavior at home. Organizations also play vital infrastructure roles in a community in the event of a disaster, like media groups contributing to communications, health sector organizations offering health services, and neighborhood or faith-based assemblages contributing to the social and psychological needs of disaster survivors. Findings from these responding organizations can be used to help assess the success of the ShakeOut and to improve it in the future.

SCEC-VDO Scripting Team Visualizations for the 2012 USEIT Grand Challenge, Laura M. Gerbi, Eduardo Andino, Shanna Williamson, Jose Cruz, Thomas Jordan, Robert de Groot, Nick Rousseau, Sam Reed, and Bridget Hellige (Poster 298)

Visual representations of quantitative and qualitative Uniform California Earthquake Rupture Forecast, Version 3 (UCERF3) data are created by the 2012 Undergraduate Studies in Earthquake Information Technology (USEIT) Scripting Team utilizing the visualization capabilities of SCEC Virtual Display of Objects (SCEC-VDO). These visualizations illustrate fault slip rates with both large-scale and regional comparisons in California for the four deformation models: Averaged Block Model (ABM), Geologic Block Model (GEOL), NeoKinema (NeoK), and Zeng Buried Dislocation Model (Zeng). Multiple Fault Rupture Rate movies display fault participation rates during a chosen event for faults with the highest rupture probabilities and earthquake risks, while Solution Participation Rates show the frequency of different earthquake magnitudes on California faults. ShakeMap visualizations combine shaking intensity and CyberShake data to illustrate the relationship between wave propagation and velocity during ruptures, shaking, and seismic risk. Additionally, Felzer Earthquake Catalogue movies display earthquakes from 1769 to 2011. Animations of the catalogue reveal the complexity of seismicity over time. Using SCEC-VDO, vital differences between the deformation models have been discovered that can only be seen through virtual representation. These visualizations of UCERF3 data provide revolutionary 4D animations that can be used for education, analyses, and earthquake preparedness and are an essential tool for further development.

Is deep non-volcanic tremor just a swarm of low frequency earthquakes?, Naum I. Gershenzon and Gust Bambakidis (Poster 267)

Deep non-volcanic tremor arises inside of, or in close proximity to, well-developed subduction and transform faults at a certain depth ranges. It has been observed that (1) bursts of tremor accompany slip pulses in so-called Episodic Tremor and Slip phenomena; (2) seismic waves from either the local medium or from distant large earthquakes can trigger tremor; (3) the intensity of tremor varies with tidal stress. While the duration and amplitude of a tremor burst varies depending on the source, the spectral composition remains essentially the same. The question arises as to how various external stress disturbances, spanning a wide range of amplitudes and frequencies, can all trigger tremor in the 1 to 30 Hz range in the fault area.

We show that the model of plate dynamics developed earlier by us is an appropriate tool for describing tremor triggering. The specific features predicted by the model are (1) the central frequency of tremor is defined by the effective normal stress at the source location 2) the size of the emitted area is on the order of from a few to dozens km; (3) a comparatively small effective normal stress (hence high fluid pressure) is required to make model to be consistent with observed tremor parameters

It is commonly assumed that tremor is a superposition of many low frequency earthquakes (LFE) [Shelly, D.R., Beroza, G.C. & Ide, S., 2007, *Nature*, 446, 305–307]. In the model we proposed, tremor is a result of specific radiation generated inside a fault. This radiation may be initiated by LFEs as well as by the other types of local failure such as regular earthquake, very low frequency (VLF) earthquakes and aseismic slip.

Revising Canterbury, New Zealand seismic design levels to account for time-varying hazard from the continuing Canterbury earthquake sequence., Matthew C. Gerstenberger and The NZ NSHM Team (Poster 061)

We present updates of the time-dependent hazard modelling for the Canterbury plains region following the recent Canterbury earthquakes, and the subsequent updates of the NZS1170.5 (2004) earthquake design standards for Christchurch. Seismicity in the region continues to be very high relative to activity prior to the September 2010 earthquake, requiring development of earthquake hazard estimates that model time-varying seismicity rates (e.g., from aftershocks and longer-term clustering). Updates to the NSHM and the resulting changes to the design standard have occurred in a two-step procedure: firstly, in April 2011 a preliminary update was conducted which was followed by the convening of international expert panels in November 2011 and March 2012 to update, re-evaluate, and finalize the results.

The expert panels, made up of international and NZ-based scientists, were presented with questions for which they were expected to provide

weights. The questions were divided into five categories: 1) Time-dependent seismicity models, 1- and 50-year forecast (e.g., STEP, ETAS, EEPAS); 2) Long-term seismicity models, 50-year forecasts (e.g., PPE, NSHM, Helmstetter); 3) Minimum and maximum magnitude of forecast models; 4) Depth distribution of forecast models; and 5) GMPEs and variability in predicted ground motions. The experts were presented existing work done in response to the Canterbury sequence; the goal of the workshop was not to develop new ideas for immediate consideration in the NSHM. Understanding the uncertainty in the hazard was a primary goal of the workshop. To this end, the expert panel followed the methodology of Cooke where the responses of each expert were weighted based on answers to questions which targeted how well experts estimate the uncertainties in their own knowledge.

A particular challenge in understanding the influence of the aftershocks on hazard and risk comes from the earthquake magnitudes that are driving the hazard in the region. With the introduction of aftershock modelling, the dominant sources in the region are $M < 6$ earthquakes at close distances.

High resolution imaging of slow earthquakes using dense seismic arrays, *Abhijit Ghosh, John E. Vidale, and Kenneth C. Creager (Poster 188)*

Slow earthquakes, characterized by seismic tremor and geodetic slip, occur down-dip of the locked zones of major plate boundary faults that break in large destructive earthquakes. Spatiotemporal evolution of slow earthquakes and their controlling factors are, however, not clear mainly due to difficulties in detecting and locating tremor. We developed a novel multi-beam-backprojection (MBBP) technique to image slow earthquakes by detecting and locating tremor with high resolution using seismic arrays. It detects more duration of tremor activity, gives high-resolution tremor location, and allows a more complete imaging of slow earthquakes in space and time compared to existing methods. MBBP method is applied to continuous seismic data recorded in Cascadia using eight seismic arrays to image two large episodic tremor and slip (ETS) events and numerous smaller slow earthquakes that occurred during an inter-ETS time period.

We show that the majority of the tremor is occurring near the plate interface [Ghosh et al., JGR, 2012] in the Cascadia Subduction Zone. Tremor zone appears to be characterized by several patches with dimension of tens of kilometers. The patches behave like asperities, and possibly represent more seismic part of the fault embedded within a relatively aseismic background. Tremor asperities are spatially stable and marked by prolific tremor activity. These tremor asperities seem to control evolution of slow earthquakes and likely represent rheological and/or frictional heterogeneity on the fault plane.

MBBP method also allows us to track tremor activity minute by minute. During slow earthquakes, we observe strikingly different behavior of tremor over different time scales. The most prominent is near-continuous slip-parallel streaking of tremor at a velocity of ~ 100 km/hr [Ghosh et al., G-cubed, 2010]. In addition, along-strike rupture progression during large slow quake shows sharp change in propagation velocity that appears to be associated with asperity locations. Dynamically evolving state-of-stress during slow earthquakes and its interaction with the fault structures possibly govern the complex pattern of spatiotemporal distribution of tremor. Overall, high-resolution imaging of slow quakes are giving insights into the physics of fault slip, dynamics of slow earthquakes, and may provide important clues on interaction of fault segments characterized by different frictional regimes.

Dynamics of western North America, *Attreyee Ghosh, Thorsten W. Becker, and Gene Humphreys (Poster 113)*

The forces that cause deformation of western North America have been debated for decades. Recent studies, primarily based on analysis of crustal stresses in the western United States (US), have suggested that the deformation of the region is mainly controlled by gravitational potential energy (GPE) variations and boundary loads, with basal tractions due to mantle flow playing a relatively minor role. We address these issues by modeling the deviatoric stress field over western North America from a three-dimensional finite element mantle circulation model (CitcomS) with lateral viscosity variations. Our approach takes into account the contribution from both topography and shallow lithosphere

structure (GPE) as well as that from deeper mantle flow in one single model, as opposed to separate lithosphere and circulation models, as has been done so far. We ensure that the forces that arise in our models are dynamically consistent by additionally fitting the constraints of geoid, dynamic topography and plate motion both globally and over North America. We examine the sensitivity of the dynamic models to different lateral viscosity variations and find that both weak plate boundaries and strong cratonic keels along with a slightly stronger San Andreas fault fit the observational constraints best. Although GPE variations control a large part of the deformation of the western US, deeper mantle tractions also play a significant role. This model provides information on how long-distance forcing affects regional tectonics, such as in southern California. This in turn can provide a better understanding of how faults in this region are loaded and how strain is localized along the plate boundary.

Using a multi-cycle earthquake simulator to specify heterogeneous initial conditions for modeling rupture dynamics., *Jacquelyn J. Gilchrist, James H. Dieterich, Keith B. Richards-Dinger, and David D. Oglesby (Poster 079)*

Initial conditions used for dynamic models, particularly the heterogeneity of initial stresses, play a primary role in determining rupture characteristics and resulting ground motion. In natural fault systems, initial stress conditions are a product of prior slip history and fault-system interactions. In contrast to previous studies that used composed initial stress conditions, we use evolved stresses from the multi-cycle earthquake simulator RSQSim to define initial conditions for rupture simulations. RSQSim is a 3D boundary-element code that incorporates rate-state fault friction to simulate long sequences of earthquakes, typically $> 100,000$ events, in complicated, fully interacting fault systems. We use these evolved stresses to examine near-field ground motions with FaultMod, a finite-element code that models earthquake rupture dynamics with rate-state fault friction. In simulations with heterogeneous (non-evolving) properties, fault system interactions appear to be quite efficient in finding the optimal nucleation location and minimal stress state that enables ruptures to propagate. As a consequence, RSQSim events that result from these evolved stresses are qualitatively and quantitatively different from events produced by simulations that use homogeneous or statistical models of initial stress. Rupture propagation is sometimes intermittent, with local pauses up to several seconds. There is no lasting evidence of initial heterogeneities. Rupture speeds are often slower and the stress drops are lower. These effects result in reduced ground motions.

Repeating earthquakes in the lab (not the ones you're thinking of), *Thomas H. Goebel, Jeremy D. Zecher, Thorsten W. Becker, and Georg Dresen (Poster 150)*

Repeating earthquakes, which may result from the repeated failure of strong fault patches, could help advance the understanding of structural differences of faults; they also provide a framework to test basic assumptions in earthquake physics and to quantify earthquake predictability. In this study, we consider the smallest repeating earthquakes: those generated in a laboratory setting. We present results from stick-slip experiments conducted on saw-cut surfaces that had varying roughness. We identified repeating acoustic emissions (AEs), i.e., co-located AEs with highly correlated waveforms and related them to fault surface roughness. We conducted these experiments with 3 Westerly granite cores that were pre-cut at a 30 degree angle to the loading axis. Each saw-cut was ground to be parallel and to have a specified roughness. We loaded the surfaces axially at a confining pressure of 120-150 MPa until several (up to 7) stick-slips occurred; throughout the loading cycle we recorded mechanical data and AEs, including full waveforms. AE locations were estimated using automatically-picked first-arrival times of a 14-channel miniature seismic array. (The resulting location uncertainty was between 1-4 mm.) In identifying repeating AEs, we conducted a systematic sensitivity analysis. Initially, we only imposed constraints on waveform similarity and examined the influence of distance constraints on the identification process. For a more restrictive choice of cross-correlation coefficient and correlation windows, the total spatial extent of each repeating sequence did not grow beyond twice the AE location uncertainties. Thus, repeating AEs identified with our algorithm are representative of tectonic repeating earthquakes. The magnitude and duration of individual AEs could vary

MEETING ABSTRACTS

strongly within a given repeating sequence, but by definition all events in a sequence had highly similar waveforms. After establishing robust identification criteria, we compared sequences in samples with different roughness. Frequency and size distributions, as well as the average distance between repeating sequences, changed between smooth and rough faults. In particular, samples with rough faults witnessed a larger proportion of small sequences with smaller average inter-AE distances. Our results highlight that repeater characteristics and fault structure can be related in the laboratory.

Assessment of uncertainties in coseismic and long-term slip variability along the Borrego section of the El Mayor-Cucapah surface rupture using terrestrial lidar, Peter O. Gold, Michael E. Oskin, Austin J. Elliott, Alejandro Hinojosa-Corona, Michael H. Taylor, Oliver Kreylos, Eric Cowgill (Poster 100)

We analyze high-resolution (>104 points/m²) terrestrial lidar surveys of the 4 April 2010 El Mayor-Cucapah earthquake rupture (Baja California, Mexico), collected 12 to 18 days after the event at three sites. Using point cloud-based tools in an immersive, virtual-reality environment, we quantify coseismic fault slip for hundreds of meters along strike and construct densely constrained along-strike slip distributions from measurements of offset landforms. Uncertainty intervals ranging from ± 12 -17% (2 σ) for each offset or fault-perpendicular profile are determined empirically by repeatedly measuring each sequence of offsets. This analysis suggests that short wavelength (101-102 m) variations in displacement do not reflect recognizable earthquake mechanisms but rather are the result of epistemic (interpretive) uncertainties that are difficult to quantify in the field. At all three sites, a linear slip gradient either satisfies all measurement distributions or accounts for unmeasured sagging of the hangingwall detected with differential airborne lidar. Conversely, fitting an envelope curve above the local slip maxima overestimates true fault slip by ~30% and along-fault strain by over an order of magnitude by favoring measurements with large, positive, epistemic errors. In aggregate, these datasets show that the true slip distribution at each site is likely to be smoother than that implied by a single set of field- or virtual reality-based measurements. In addition, we measured two populations of striations on exposed fault faces plunging ~25° and ~56° to the southeast. The shallower set of striations overlaps within error the ~30° plunge of the 2010 slip vector determined from offset measurements, implying that the steeper striations preserve the slip direction from the penultimate earthquake. Fault-perpendicular profiles across a paleoscarp that we interpret to have resulted from a single pre-historic earthquake reveal ~3.2 m of vertical displacement. Thus we find that the Borrego fault produced ~2.5 m of strike-slip dominated displacement in 2010, and ~4 m of dip-slip dominated displacement in the penultimate earthquake. Both interpretations suggest that the Borrego fault violates the common assumption that faults produce kinematically similar slip events.

Salton Seismic Imaging Project Line 7: Data and Analysis to Date, Mark R. Goldman, Gary S. Fuis, Rufus D. Catchings, Mike J. Rymer, Neal W. Driscoll, Graham M. Kent, Alistair J. Harding, Annie Kell, John A. Hole, and Joann M. Stock (Poster 155)

The Salton Seismic Imaging Project (SSIP) was a large-scale, active- and passive-source seismic imaging program that imaged the San Andreas Fault (SAF) and adjacent basins (Imperial Valley and Coachella Valley) in southernmost California. Data and preliminary results from many of the seismic profiles are reported elsewhere (see Fuis et al., 2012; Stock et al., 2011; Davenport et al., 2011; and others). Here, we focus on SSIP Line 7, one of four 2-D NE-SW-oriented seismic profiles that were acquired across the SAF, parts of the Coachella Valley, and the Salton Sea. Seismic sources for Line 7 included both land-based downhole explosive sources and airgun sources within the Salton Sea. Data were recorded by 189 Texan seismographs on land (50 m spacing), 102 channels (10 m spacing) of a multi-channel cabled recording system near the San Andreas fault on land, and nine ocean bottom seismographs (OBS) (1.3 km spacing) within the Salton Sea. The Texans and OBS's recorded both airgun and explosive sources, and the cable array recorded explosions only. Data from the Texan and the multi-channel seismographs were organized as shotgathers, and the OBS data were arranged as receiver gathers. All data were merged into a single profile for analysis. The

seismic profile is approximately 23 km long and crosses the SAF at about 90 degrees, but an approximately 2-km-long segment of the profile at the SAF near the northeastern edge of the Salton Sea does not have either seismograph or seismic source coverage due to limited OBS data. Because the gap in the seismic profile was within about 500 m from the surface trace of the SAF, imaging of the SAF was limited. First arrivals from all data sets were combined to develop a refraction tomography velocity image of the upper crust. From the surface to about 6 km depth, P-wave velocities range from about 2 km/s to about 6 km/s, with basement (~6 km/s) shallower northeast of the SAF. The SAF also marks the southwestern boundary of a relatively high-velocity body in the near surface. Southwestward of the SAF, low-velocity (< 4 km/s) sediments occur that thicken to ~4 km beneath the Salton Sea. Northeast of the SAF, near-surface velocities (upper 2 km) infer complex structures that likely arise from multiple faults. Data were also stacked to develop low-fold reflection images, and we used pre-stack depth migration of automated line drawings to develop migrated images of the upper crust. Stacked and migrated line drawings also suggest an apparent northeast dip of sediments on the southwest side of the SAF. Although the dip of the SAF is not fully resolved with the data analysis to date, the termination of the northeast dipping sedimentary wedge southwest of the SAF and an apparent lack of offset of reflectors northeast of the SAF suggest the possibility of a vertical or slightly southwest dip of the SAF at depth.

References

Davenport, K., J.A. Hole, J.M. Stock, G.S. Fuis, E. Carrick, and B. Tikoff (2011). The Salton Seismic Imaging Project: Tomographic characterization of a sediment-filled rift valley and adjacent ranges, southern California, Am. Geophys. Union Fall Meeting 2011, Abstract #T31F-07, San Francisco

Fuis, G.S., J.A. Hole, J.M. Stock, N.W. Driscoll, G.M. Kent, A.J. Harding, A. Kell, M.R. Goldman, E.J. Rose, R.D. Catchings, M.J. Rymer, V.E. Langenheim, D.S. Scheirer, N.D. Athens, and J.M. Tarnowski (2012). Investigating earthquake hazards in the northern Salton Trough, southern California, using data from the Salton Seismic Imaging Project (SSIP), Abstracts, 2012 SCEC Annual Meeting, Palm Springs, California, Sept. 9-12, 2012.

Stock, J.M., J.A. Hole, G.S. Fuis, A. Gonzalez-Fernandez, O. Lazaro-Mancilla, N.W. Driscoll, G. Kent, S. Klemperer, S. Skinner, and J. Persico, (2011). The Salton Seismic Imaging Project (SSIP): Rift processes in the Salton Trough, Geol. Soc. Am. Abstr. With Programs, 43, 362., 9-12 October 2011, Minneapolis

El Mayor-Cucapah (Mw 7.2) earthquake: Early Postseismic Deformation from InSAR and GPS observations, Alejandro Gonzalez-Ortega, David T.

Sandwell, Yuri Fialko, John M. Fletcher, Alex Nava, Jose J. Gonzalez-Garcia, Brad P. Lipovsky, Michael A. Floyd, and Gareth J. Funning (Poster 240)

El Mayor-Cucapah earthquake occurred on April 4, 2010, in Northeastern Baja California just south of the USA/Mexico border. The earthquake rupture several previously mapped as well as unidentified faults, including the Pescadores, Borrego, Paso Inferior and Paso Superior in the Cucapah Mountains at the Sierra domain, and Indiviso fault in the Mexicali Valley at the Delta domain. We conducted several Global Position System (GPS) campaign surveys of pre-existing and newly established benchmarks within 30 km of the earthquake rupture. Most of the benchmarks were occupied within days after the earthquake, allowing us to capture the very early and entire postseismic transient. GPS timeseries indicate a gradual decay in postseismic velocities having the same motion sense as the coseismic displacements, with exponential characteristic decay time scale of 70 days in the near-fault deformation at the Sierra Cucapah domain. We also analyzed available Synthetic Aperture Radar (SAR) data from ENVISAT and ALOS satellites. The main deformation features seen in the line of sight (LOS) displacement maps indicate subsidence southern and northern part of the Indiviso fault in the Delta domain region, Laguna Salada basin and Paso Superior fault, respectively. We investigate to which extent GPS and Interferometric SAR (InSAR) observations can be explained by commonly assumed mechanism of postseismic deformation. In particular, we explore the

after slip model in a joint inversion context for the time period of 5 months after the earthquake.

New Videos Developed for Outreach and Education in Earthquake

Engineering, Val V. Gorbunov, Nicholas Perez, Justin Morris, Sandra H. Seale, and Jamison H. Steidl (Poster 261)

Over the past two years, the NEES@UCSB team has developed several videos for use in outreach and education. Here we present four videos that are targeted to specific audiences: (1) We present animation of the response of two test structures created with data recorded at the Garner Valley Downhole Array field site (GVDA) from two earthquakes and a shaker test. The two events were both located directly below GVDA and had magnitudes M3.1 and M3.6. The shaker test is a nightly sine sweep from 15 – 5Hz. Animation of the structures was created with Blender (<http://www.blender.org/>), an open source 3D content creation suite. The animation shows distinct resonances of the structures and seismic wave arrivals are clearly visible. (2) Visualization Services group at the San Diego Supercomputer Center created animation of the ground excitation at GVDA from a M4.1 earthquake. Using data recorded in the boreholes at GVDA, the animation clearly shows the amplification of the signal in the near surface materials. These visualizations created from actual earthquake data provide new insight into ground and structural response to strong motion. The animations will be used as teaching tools for college-level engineering courses. (3) Data that are recorded at the NEES@UCSB field sites are processed and made available to the public through the data portal on the website nees.ucsb.edu. We have developed a video tutorial for the use of the website data portal. (4) This summer, two student interns at UCSB produced “A Case Study of Earthquake Damage and Repair: The Santa Barbara Earthquake of 1925.” This is a film of Professor Arthur Sylvester giving a tour of the earthquake history of downtown Santa Barbara. Earth science is part of the 6th-grade framework for curriculum in California. This video will be distributed to 6th-grade teachers in California, along with a student workbook. It will also be made available through the NEES@UCSB and the NEEShub websites.

The Impact of the Earthquake Country Alliance (ECA) Earthquake Education and Public Information Center (EPICenter) Network, Irene N. Gow, Robert M. de Groot, and Thomas H. Jordan (Poster 257)

Ranging from designed spaces to everyday activities, informal learning environments account for the majority of the public’s science knowledge and education. Despite an increase in research of informal science learning over the past 50 years, there remains a need for comprehensive outcome measures. Established evaluation methods would improve overall science learning and the management and accountability of informal learning institutions. This study was conducted to address the current lack of methodology through the development of impact measures for the Earthquake Country Alliance (ECA) Earthquake Education Public Information Center (EPICenter) Network. Formed in 2008, the ECA EPICenter Network currently consists of over 60 informal learning institutions throughout California. Members of the Network are committed to encouraging earthquake and tsunami preparedness through demonstrated leadership in risk-reduction and education. Grounded Theory, a qualitative methodology, was used to develop evaluation methods for the Network through simultaneous data collection and analysis. Open-ended interviews were conducted with six Members of the Network’s Southern California Region, a convenience sample representing five types of informal learning institutions (e.g., museums, children’s museums, libraries, science centers, and outdoor areas). Data from the interviews were incorporated into logic models, graphical representations of program outcomes. The logic models for the six informal learning institutions and overall Network revealed similar theoretical long-term outcomes including strengthened community partnerships, development of the Network, increased awareness of earthquakes, and increased community earthquake education, earthquake preparedness, and knowledge of earthquake science. Continued refinement of the use of logic models to measure the impact of the Network and informal learning institutions is needed through the collection of quantitative data. The development of comprehensive impact measures will not only affect the sustainability of the ECA EPICenter Network and other informal learning institutions, but also affect

statewide, national, and international approaches to earthquake education and emergency preparedness.

SCEC-VDO and GIS Integration for the USEIT 2012 Grand Challenge,

Rebecca N. Greenwood, Marianne Jara, Laura Gerbi, Eduardo Andino, Thomas Jordan, Robert de Groot, Yao-Yi Chiang, and

Nick Rousseau (Poster 297)

The Grand Challenge of the 2012 Undergraduate Studies in Earthquake Information Technology (USEIT) summer internship program involved the development of visualization capabilities based on SCEC Virtual Display of Objects (SCEC-VDO) and Geographical Information Systems (GIS) in order to improve current methods and update past data sets. Using these tools, plug-ins were developed to display earthquake rupture forecasts and publish visualization products used to educate a variety of audiences including the scientific community about the Uniform California Earthquake Rupture Forecast, Version 3 (UCERF3). The GIS & Data team utilized ArcGIS to examine hazard areas from ShakeMaps and produce geographic maps that contain point, line, and polygon data that can be loaded into SCEC-VDO. Collections of various geographic data such as population density, landmarks, and road systems, focused on California areas of interest allow for the creation of complimentary maps with critical resources that will be vital in the event of an earthquake. Along with human geography datasets, physical datasets such as topography and hydrography have been produced for SCEC-VDO. Additionally, the team has developed a capability that allows for the importing of updated geographic datasets into SCEC-VDO. For files created by the 2012 USEIT GIS & Data team can be found at: <http://scec.usc.edu/internships/useit/challenge/2012>. Further examination of other GIS capabilities within SCEC-VDO will allow a more user friendly environment to the interface.

Surface Slip During Large Owens Valley Fault Earthquakes, Elizabeth K. Haddon, Colin B. Amos, and Roland Bürgmann (Poster 105)

Advances in our ability to image and analyze active faults using high-resolution lidar provide a unique opportunity to characterize the spatial distribution of slip during large earthquake surface ruptures. For strike-slip faults, along-strike compilation of laterally displaced geomorphic features measured using lidar enables the assessment of surface slip during historical and paleoearthquakes. Here, we seek to test whether surface slip during the 1872 Mw 7.4 – 7.9 Owens Valley earthquake, one of California’s three largest historic ruptures, mimics the displacement during earlier events. We utilize recently developed analysis and processing tools to investigate EarthScope lidar data spanning the ~140-km-long Owens Valley surface rupture. We present over 70 new measurements of laterally displaced channels, terrace risers, meander scars, lake shorelines, and fan edges, with offsets up to 25 m. Where possible, we test the precision of lidar-based measurements by comparing our results to published field estimates of surface slip during this event. Displacements attributed to the most recent event (MRE) range between ~2 and 9 m, with an average horizontal offset of $\sim 5 \pm 2$ m. Our along-strike compilation suggests that displacement gradients for the MRE are smooth at the >10 km length scale, in contrast with the distinctly peaked distribution estimated from previous field studies. Progressively larger offsets are attributed to earlier surface ruptures and may imply a similar amount of surface slip to the MRE (~5-7 m). Lateral slip during these events contributes to preliminary peaks in the cumulative offset frequency density at ~12 and ~18 m. The precision of these peaks likely reflects some bias toward well-preserved offsets, since the majority of offset features reflect displacement during the 1872 event. Taken together, our results indicate some variability in the amount of surface slip during Owens Valley surface ruptures, although large earthquakes appear to repeatedly rupture a similar fault extent. As we expand our database of offset measurements and further develop a long-term paleoseismic history, we will test whether or not similar patterns of surface slip are repeated as characteristic earthquakes during surface ruptures on the Owens Valley fault.

Role of Geotechnical Velocity Models in Shake Zone Scenarios of South Lake Tahoe, Kelley A. Hall and John Louie (Poster 250)

MEETING ABSTRACTS

The three major factors that control ground motion in an earthquake include: the source, the geometry of the basin, and the properties of the materials that the waves travel through. Using the Nevada Shake Zoning (NSZ) methodology developed by Dr. John Louie, we studied the role of the geotechnical data set on the ground motion. For these models, we analyzed the South Lake Tahoe Basin; specifically examining the impact of a rupture on the south end of the West Tahoe Fault. The South Lake Tahoe basin was of particular interest, given its location on the western edge of the Basin and Range province and the large tourist draw of the area. The West Tahoe Fault has the largest vertical offset in the area and last ruptured approximately 4000 years ago (Brothers et al. 2009). We sought to compare our limited geotechnical data set with more comprehensive but theoretical data sets. Our resulting scenarios generated PGV values of nearly 200 cm/sec. We also established that minor changes in Vs30 created amplifications of a factor of two and deamplifications of a factor of one-half. Our results imply that dense Vs30 measurements are necessary to fully understand potential hazards resulting from earthquakes in and around basins.

Contribution to the SCEC Community Stress Model Project: Two Stress Models from Focal Mechanism Inversion, *Jeanne L. Hardebeck* (Poster 107)

One major short-term goal of the SCEC Community Stress Model (CSM) project is to collect southern California stress models, and the relevant data, from the SCEC community. The contributed stress models will be compared with each other to identify areas of agreement, areas of disagreement that may become CSM branches, and targets for future research. One class of data-derived stress models are found by inverting earthquake focal mechanisms for stress orientations. I present two new stress orientation models, based on inversion of recent focal mechanism catalogs for southern (Yang et al., BSSA 2012) and central (Hardebeck, BSSA 2010; Thurber et al., BSSA 2006) California. The events are divided into spatial bins, and the bins are inverted simultaneously with damping between adjacent bins to produce the smoothest model that adequately fits the data (following Hardebeck and Michael, JGR 2006). Two different binning schemes are used: one that bins earthquakes according to their distance from the major faults of the San Andreas system, and one that divides the region into cubes of variable size depending on the earthquake density. I will show comparisons of the two stress models, and tests of both models against available data. These tests may serve as prototypes for the stress model comparisons to be carried out as part of the SCEC CSM project.

The SCEC-USGS Dynamic Earthquake Rupture Code Verification Exercise - Recent Progress, *Ruth A. Harris* (Poster 104)

We summarize recent progress by the SCEC-USGS Dynamic Rupture Code Verification Group, that examines if SCEC and USGS researchers' spontaneous-rupture computer codes agree when computing benchmark scenarios of dynamically propagating earthquake rupture. Our latest 3D benchmarks have involved dynamic rupture propagating on planar vertical strike-slip faults with heterogeneous initial stress conditions and cases of dynamic rupture on branching vertical strike-slip faults. The heterogeneous initial stress cases produced good agreement among the codes and we are confident that this was a successful endeavor. The branching fault cases will be a focus of continued study because those results were not as successful as hoped. We are examining the reasons for this mismatch of the branching fault benchmark results, and have a number of ideas to explore. Our next benchmark exercises will continue with dynamic rupture on branching vertical strike-slip faults, until we obtain good matches among the code results. We will also investigate another fault geometry, the case of a stepover in a vertical strike-slip fault.

Please also see our website, scecddata.usc.edu/cvws

August 2012 Brawley Earthquake Swarm in Imperial Valley, *Egill Hauksson* (Talk Tue 08:00)

The 2012 Imperial Valley Brawley swarm started near the City of Brawley on 22nd of August with six events of $M < 2.0$. The seismic activity picked up early on 23rd of August with increasing rate early in the day. The three largest earthquakes ($M_{5.5}$, $M_{5.3}$, and $M_{4.9}$) in the sequence

occurred over a time period of 90 minutes, starting at 12:33 pm on August 23rd. The high rate of seismic activity lasted about 24 hours. This sequence that so far consists of more than 600 events forms a 12 km long linear northeast trending distribution, mostly in the depth range of 8 to 12 km. The focal mechanisms predominantly exhibit strike-slip motion on northeast or northwest striking planes. This swarm occurred in the immediate vicinity of the largest ($M_{5.8}$) aftershock of the 1979 $M_{6.4}$ Imperial Valley earthquake. Similar seismic swarms have occurred in the Brawley seismic zone in the past, especially in the 1970s and 1980s but in the 1990s the region was seismically quiet. The Brawley seismic zone is the northern most spreading center of the Gulf of California rift zone, which transfers slip from the Imperial fault in the south to the San Andreas fault in the north.

Understanding Seismicity in the Context of Complex Fault Systems and Crustal Geophysics, *Egill Hauksson* (Poster 181)

We analyze the waveform relocated (1981 to 2011) catalog of more than 500,000 earthquakes recorded along the Pacific North-America plate boundary in southern California. This seismicity, with five mainshocks of $M > 6.5$, reflects regional plate-boundary tectonics and other crustal deformation processes in the crust as well as the physical properties of the crust. The plate boundary is expressed as a system of late Quaternary faults or principal slip zones (PSZs) that accommodate major earthquakes. There are numerous smaller slip surfaces adjacent to the PSZs, which accommodate background seismicity as well as in some cases aftershocks. The plate tectonic strain loading dominates the dynamic process and causes the largest earthquakes along the PSZs, moderate-sized events in their immediate vicinity, and small earthquakes across the whole region. To analyze earthquake scaling in the context of this fault system, we measure the Euclidian distance from every hypocenter to the nearest PSZs. In addition, we assign crustal geophysical parameters such as heat flow value and shear or dilatation strain rates to each epicenter. Stress drop values are available for a subset of ~60,000 events. We extend our catalog by adding these parameters to the standard earthquake parameters of each event such as date, location, depth, magnitude, seismic moment, and error estimates. We use this extended catalog to investigate seismogenic thickness and fault zone width as well as earthquake scaling. We find that the seismicity rate is a function of location, with the rate dying off exponentially with distance from the PSZ. The decay per kilometer is similar as the decay per kilometer of depth in the rate of earthquakes below 5 km. About 80% of the small earthquakes are located within 5 km of a PSZ. For small earthquakes, stress drops increase in size with distance away from the PSZs. The magnitude distribution near the PSZs suggests that large earthquakes are more common close to the PSZs, and they are more likely to occur at greater depth than small earthquakes. In contrast, small quakes can occur at any geographical location but tend to cluster at the top and bottom of the seismogenic zone.

Finite-fault earthquake cycle models incorporating viscous shear zones, *Elizabeth H. Hearn* (Poster 116)

One longstanding problem in earthquake science has been how to explain both localized interseismic deformation and broad-scale, rapidly decaying postseismic deformation around major faults with a single, realistic lithosphere model. To address this problem, I have developed a suite of finite-element earthquake-cycle models incorporating narrow viscous shear zones and finite (200-km-long) ruptures, and have compared the resulting surface deformation to that produced by models incorporating layered viscoelastic structure. I find that viscous shear zones localize deformation around faults, producing a more rapidly decaying postseismic transient and more stationary interseismic deformation than halfspace viscoelastic models producing similar early postseismic deformation in the near field. Models with finite ruptures produce smaller magnitude, more localized transients than 2D models with infinitely long ruptures (as has been noted previously by K. Johnson and F. Pollitz for the layered viscoelastic case). As expected, summing the modeled velocity perturbations for simultaneous, end-to-end finite ruptures gives the 2D solution. Finite rupture models incorporating a viscous shear zone in the lower lithosphere still require a transient or

power-law viscoelastic rheology to generate postseismic and late interseismic deformation consistent with observations from major faults.

Geologically determined uplift rates through the central San Gorgonio Pass, Richard V. Heermance, Doug Yule, Paul McBurnett, and Shahid Ramzan (Poster 125)

The San Gorgonio Pass (SGP), which has relatively infrequent thrust-fault rupture events (~600 yr recurrence), represents a structural knot that may inhibit through-going rupture between the Coachella and San Bernardino strands of the San Andreas fault (SAF). Recent interest in the SGP as a "Special Fault Study Area" has highlighted the need to determine long-term uplift and slip rates in an effort to test models of rupture propagation and reconcile slip deficits through the region. We present the surface uplift history of the Millard Canyon Fan in the central SGP area, based on measured vertical displacement across fault scarps and the inferred ages of fan surfaces. At least five surfaces, four Holocene (Qf1–Qf4) and one mid-late Pleistocene (Qh), have been documented through this area and contain excellent fault scarps of the Banning and San Gorgonio Pass Faults. Radiocarbon charcoal ages collected in fault trenches from Qf 1-3 imply surface ages of 627 ± 163 , 1270 ± 85 , and 2551 ± 196 yrs BP, respectively. These ages, however, are likely maxima as they are from sediment beneath the fan surface and may be older than the age of fan abandonment. Qf4 and Qh have not been directly dated, although new ^{10}Be exposure ages are currently pending for Qf3 and Qf4, and Qh is likely mid-late Pleistocene (500,000–200,000 yrs) based on its well-developed soil profile. The northern Holocene fault strand through Millard Canyon, the Banning Fault, cuts Qf2, Qf3, and Qh with scarps of ~2.5 m and ~5.2 m, and ~120 m respectively. The more southerly San Gorgonio Pass fault strand cuts surfaces Qf1, Qf3, Qf4, and Qh with heights of ~1.5, ~5, and ~12.5 and ~170 m respectively. The Qh surface uplift is a minimum estimate because the correlative surface is likely buried to some unknown depth (potentially 10s–100s of meters) in the footwall and the surface has been eroded since abandonment. Scarp heights, divided by the inferred surface ages, imply remarkably consistent uplift rates of ~2 mm/year across Qf 1-3 for a total of 4 mm/yr cumulative uplift within Millard Canyon. Uplift rates for scarps that cut the Qh surface range from 0.2–0.9 mm/yr, although these minimum long-term rates are very speculative due to our uncertain displacement and age data. These new data will be combined with ongoing USGS studies in the western (San Gorgonio River) and eastern (Whitewater Wash, Mission Creek Fan) to illustrate the uplift variability across the entire SGP region.

An Analysis of Tradeoffs in Element Size and Approximation Schemes for Earthquake Simulation, Eric M. Heien, Michael K. Sachs, Galen Danziger, John B. Rundle, and Louise H. Kellogg (Poster 055)

To better understand the spatial and temporal complexity of large scale fault zones, researchers are beginning to use earthquake simulators. These simulators use a model of the fault system under study to calculate long range stress interactions between faults over long time periods and short term rupture propagation during earthquake events. Because of the finite speed and storage available on computers, simulators must make approximations in the algorithms for stress and rupture calculation as well as the resolution of elements that is used to approximate fault surfaces. However, for some approximations little is known regarding the effect on the simulation behavior and statistics of the simulated seismic activity.

In this work we examine the effect of two key approximations made by earthquake simulators - the size of the elements representing the fault surface and the method of calculating interactions between fault elements. In order to calculate interactions between all elements, most simulators approximate fault surfaces as sets of segments ranging in size from 3000m to 1000m on a side. However, by using larger elements the effects of small scale stress release may be ignored and the interactions between nearby elements may be poorly approximated. Another approximation scheme is to use a Barnes-Hut style scheme for determining interactions between elements such that nearby interactions are calculated exactly and distant ones are simplified and approximated. In this work we quantify the effects of the fault size and Barnes-Hut

approximations by evaluating their impact on the results of the Virtual California earthquake simulation program.

The Role of Fault Geometry on Geologic and Interseismic Deformation Along the Southern SAF and ECSZ, Justin W. Herbert, Michele L. Cooke, and Scott T. Marshall (Poster 119)

We investigate discrepancies between geologic slip rates and results from models that invert GPS velocities for slip rates along the San Bernardino strand of the San Andreas Fault (SAF) and across the Eastern California Shear Zone (ECSZ). GPS derived slip rates are slower than geologic rates on the San Bernardino strand of the SAF and greater than geologic rates across the ECSZ. Differences between GPS-derived fault slip rates and longer-term geologic slip rates have been attributed to temporal variations in fault slip rate but may also owe to inadequate fault complexity within the models that use GPS data. Our three-dimensional Boundary Element Method models that use more complex fault geometries show significant spatial variation in both fault slip rates and interseismic surface velocities along each fault segment. Using a two-step, strain-driven forward model approach, we are able to simulate both fault slip rates that match the geologic rates and horizontal velocities that closely match permanent GPS station velocities without evoking temporal variations in fault slip rates. We also test the sensitivity of surface velocities to the orientation and magnitude of regional tectonic loading. Discrepancies between geologic and GPS-derived slip rates along the San Bernardino strand of the SAF may owe to over-simplified and over-connected fault network within the GPS block models. We test the role of fault geometry by comparing a simplified fault network with a CFM-based network, and show that slip along the San Bernardino Strand of the SAF decreases when other faults are over connected. We do the same for the ECSZ and find that a simpler fault network does not significantly increase the cumulative slip rate across the zone. The discrepancy between GPS-derived and geologic results could owe to remaining over-connectedness or to temporal variation in strain accumulation such as post-seismic deformation following the 1999 Hector Mine earthquake.

The Magnitude Distribution of Triggered Earthquakes, Stephen Hernandez, Emily E. Brodsky, and Nicholas J. van der Elst (Poster 190)

Large dynamic strains carried by seismic waves are known to trigger seismicity far from their source region. It is unknown, however, whether surface waves trigger only small earthquakes, or whether they can also trigger societally significant earthquakes. To address this question, we use a mixing model approach in which total seismicity is decomposed into 2 broad subclasses: "triggered" events directly initiated or advanced by far-field dynamic stresses, and "untriggered/ambient" events consisting of everything else. The b -value of a composite data set is decomposed into a weighted sum of b -values of its constituent components, b_T and b_U . For populations of Californian earthquakes subjected to the largest dynamic strains, the fraction of earthquakes that are likely triggered, f_T , is estimated via inter-event time ratios and used to invert for b_T . The distribution of b_T is found by nonparametric bootstrap resampling of the data, giving a 90% confidence interval for b_T of [0.74, 2.79]. This wide interval indicates the data are consistent with a single-parameter Gutenberg-Richter distribution governing the magnitudes of both triggered and untriggered earthquakes. Triggered earthquakes therefore seem just as likely to be societally significant as any other population of earthquakes.

Extensive Poroplastic Deformation as a Unifying Interpretation to Anomalous Earthquake Characteristics and Tsunami Generation in the Shallow Subduction Zone, Evan T. Hiraikawa and Shuo Ma (Poster 173)

The deficiency of high-frequency seismic radiation from shallow subduction zone earthquakes was first recognized in tsunami earthquakes (Kanamori, 1972), which produce larger tsunamis than expected from short-period (20 s) surface wave excitation. Shallow subduction zone earthquakes were also observed to have unusually low energy-to-moment ratios compared to regular subduction zone earthquakes (e.g., Newman and Okal, 1998; Venkataraman and Kanamori, 2004; Lay et al., 2012). What causes this anomalous radiation and how it relates to large tsunami generation has remained unclear.

MEETING ABSTRACTS

Here we show that these anomalous observations can be due to extensive poroplastic deformation in the overriding wedge, which provides a unifying interpretation.

Ma (2012) showed that the pore pressure increase in the wedge due to up-dip rupture propagation significantly weakens the wedge, leading to widespread Coulomb failure in the wedge. Widespread failure gives rise to slow rupture velocity and large seafloor uplift (landward from the trench) in the case of a shallow fault dip. Here we extend this work and demonstrate that the large seafloor uplift due to the poroplastic deformation significantly dilates the fault behind the rupture front, which reduces the normal stress on the fault and increases the stress drop, slip, and rupture duration. The spectral amplitudes of the moment-rate time function is significantly less at high frequencies than those from elastic simulations. Large tsunami generation and deficiency of high-frequency radiation are thus two consistent manifestations of the same mechanism (poroplastic deformation). Although extensive poroplastic deformation in the wedge represents a significant portion of total seismic moment release, the plastic deformation is shown to act as a large energy sink, leaving less energy to be radiated and leading to low energy-to-moment ratios as observed for shallow subduction zone earthquakes.

The Role of Fluid Pressure on Frictional Behavior at the Base of the Seismogenic Zone, Greg Hirth and Nick Beeler (Poster 092)

We describe a new approach for characterizing the evolution of the effective pressure law at conditions near the base of the seismogenic zone. The role of fluids on the processes responsible for the brittle-plastic transition (BPT) in quartz-rich rocks has not been explored at experimental conditions where the kinetic competition between microcracking and viscous flow is similar to that expected in the Earth. However, our initial analysis of this competition between brittle and ductile processes suggests that the effective pressure law should not work as efficiently near the brittle-plastic transition, if it works at all.

Our motivation comes from two observations. First, extrapolation of viscous creep laws for quartzite indicates the BPT occurs at a temperature of ~300°C at geologic strain rates for conditions where fault strength is controlled by a coefficient of friction (μ) of 0.6 with a hydrostatic pore-fluid pressure gradient (where the ratio pore-fluid pressure/lithostatic pressure (λ) is ~0.4). This observation remains consistent with microstructural observations of quartzite mylonites that preserve microstructures from conditions near the BPT (e.g., Behr and Platt, 2011). Second, by considering the influence of pore-fluids on brittle deformation, we suggest that the preservation of relatively high stress viscous microstructures indicates that the effective pressure law must evolve rapidly near the BPT - for example - from highly efficient to zero efficiency with increasing depth. This hypothesis is consistent with high temperature lab tests on quartzite in which the presence of fluid does not promote localized brittle failure (e.g., Chernak et al., 2009), even though these experiments are conducted under undrained conditions.

This suite of observations can be reconciled if changes in the real area of contact near the BPT are accounted for in the effective pressure law (Beeler et al., manuscript in preparation). The effect of pore-fluid pressure on mechanical behavior in the frictional regime is described using the relationship: $\sigma_{eff} = (\sigma_n - \alpha P_f)$, where for most applications the constant α is assumed to be unity. However, at high P-T conditions, where creep and crack healing processes are efficient, α may decrease significantly. Owing to the exponential temperature-dependence of thermally activated processes, changes in α may occur with relatively small spatial/temporal variations.

Using Socioeconomic Data to Calibrate Loss Estimates, James R. Holliday and John B. Rundle (Poster 059)

One of the loftier goals in seismic hazard analysis is the creation of an end-to-end earthquake prediction system: a "rupture to rafters" work flow that takes a prediction of fault rupture, propagates it with a ground shaking model, and outputs a damage or loss profile at a given location.

So far, the initial prediction of an earthquake rupture (either as a point source or a fault system) has proven to be the most difficult and least

solved step in this chain. However, this may soon change. The Collaboratory for the Study of Earthquake Predictability (CSEP) has amassed a suite of earthquake source models for assorted testing regions worldwide. These models are capable of providing rate-based forecasts for earthquake (point) sources over a range of time horizons. Furthermore, these rate forecasts can be easily refined into probabilistic source forecasts. While it's still difficult to fully assess the "goodness" of each of these models, progress is being made: new evaluation procedures are being devised and earthquake statistics continue to accumulate. The scientific community appears to be heading towards a better understanding of rupture predictability.

Ground shaking mechanics are better understood, and many different sophisticated models exist. While these models tend to be computationally expensive and often regionally specific, they do a good job at matching empirical data. It is perhaps time to start addressing the third step in the seismic hazard prediction system.

We present a model for rapid economic loss estimation using ground motion (PGA or PGV) and socioeconomic measures as its input. We show that the model can be calibrated on a global scale and applied worldwide. We also suggest how the model can be improved and generalized to non-seismic natural disasters such as hurricane and severe wind storms.

Analysis of the Shallow Slip Deficit Using Sub-Pixel Image Correlation: Implications for Fault Slip Rates, and Seismic Hazards,

James Hollingsworth, James Dolan, Chris Milliner, Sebastien Leprince, Francois Ayoub, and Jean-Philippe Avouac (Poster 078)

The pattern of surface displacement produced by an earthquake can be retrieved by sub-pixel correlation of optical satellite images, using the program COSI-Corr. This technique can provide robust measurements of displacement very close to fault ruptures, and is therefore a complementary tool to InSAR, which provides precise measurements of deformation in the far-field, but often de-correlates close to the fault. Inversions of InSAR data are commonly used to determine how slip varies on the fault plane during an earthquake. Previous inversion results for a number of large continental earthquakes suggest a deficit of slip occurs in the upper few kilometers of the crust. This 'missing' slip may occur later in the earthquake cycle, either in the post-seismic period as afterslip, or during the inter-seismic period as creep. Alternatively, this 'missing' slip could also be accommodated by distributed off-fault deformation not captured by InSAR. This latter point is significant, since any distributed off-fault deformation must be taken into account when calculating Quaternary fault slip-rates, that typically incorporate discrete offsets of geomorphic features measured over a narrow aperture. The goal of this study is to use optical image correlation to better determine fault displacements close to faults so we can address the nature of distributed versus discrete coseismic deformation. Firstly, we show the surface deformation field for a number of large continental strike-slip earthquake. Secondly, we develop a tool that allows along-strike fault displacement profiles to be extracted from displacement maps. We quantify the difference between COSI-Corr-derived and field-derived fault displacement measurements; any difference is assumed to result primarily from distributed deformation, which can be difficult to measure in the field. By comparing the component of distributed, off-fault deformation with geological parameters, such as the fault structural maturity, we attempt to better constrain the parameters controlling fault slip in the upper crust. This approach allows us to potentially correct Quaternary fault slip rates determined for any fault based on its structural maturity, thus accounting for any distributed component of deformation that may occur throughout the seismic cycle. Consequently, our results have significant implications for probabilistic seismic hazard assessment, which rely heavily on geologically determined fault slip rates.

Using GPS Derived Shear Strain Rates in Southern California to Constrain Fault Slip Rate, Locking Depth, and Residual Off-Fault Strain Rates,

William E. Holt, Attreyee Ghosh, and Yu Chen (Poster 228)

Strain rate fields within strike-slip regimes often possess complexity associated with along-strike slip rate variations. These along-strike slip rate variations produce dilatational components of strain rate within and near the fault zones and within the adjacent block areas. These dilatation

rates do not directly reflect the slip rate magnitude on the strike slip fault, but rather the relative change in along-strike slip rate. Displacement rates measured using GPS observations reflect the full deformation gradient field, which may involve significant dilatational components together with other off-fault deformation. Thus, using displacement rates to infer slip rate and locking depth of major strike-slip faults may introduce errors when along-strike slip rate variations are present. On the contrary, the shape and magnitude of the shear strain rates (pure strike-slip component) reflect the true strike-slip parameters of interest (locking depth and slip rate). In this study we use of shear strain rates alone (obtained from the full displacement rate field of the SCEC 4.0 velocity field in southern California) to infer fault slip rate and locking depth parameters along the San Andreas (up to 37° N) as well as the San Jacinto fault zones. Such an analysis is critical for accurate estimation of off-fault strain rates outside of the major shear zones. Results to date from this methodology applied to southern California using the SCEC 4.0 GPS velocity field show remarkably well-resolved and prominent shear strain rate bands that follow both the San Andreas and San Jacinto fault systems. The shear strain rates show evidence of dramatic along-strike slip rate variations. We obtain locking depths that are shallower than many previous estimates along several sections of the San Andreas system (e.g. Big Bend region). We hypothesize that contamination from off-fault strain rates can result in errors in fault locking depth and slip rate estimates. Our treatment of modeling only the shear strain rates acts as a 'filter' to remove signals in the displacement rate field that are unrelated to pure strike-slip deformation, thereby providing more accurate model estimates of slip rate and locking depth along these major strike-slip shear zones.

Taming the Dragons: Insights into Biases in Historical Intensity Distributions From Analysis of Spatial Variability of DYFI Intensities,
Susan E. Hough (Poster 151)

Careful assessments of macroseismic effects provide critical information to investigate important earthquakes in the pre-instrumental era, and to quantify seismic hazard. In this study I compare subjectively reassessed intensity distributions for both 19th century historical earthquakes and 20th century instrumentally recorded earthquakes with spatially rich "Did You Feel It?" (DYFI) intensity distributions for recent moderate earthquakes. There is a qualitative difference in the character of MMI(r) decay observed for subjectively assigned intensities versus intensities determined by the DYFI system. I discuss several alternative hypotheses to explain the discrepancy, including the possibility that intensity values determined subjectively from archival/media reports in either historical or relatively modern times are pervasively inflated due to reporting and sampling biases. A quantitative analysis of the DYFI intensity distribution for the Mineral, Virginia, earthquake, for which over 140,000 responses were received by the DFYI system, illustrates how reporting and sampling biases arise, and commonly inflate historical earthquake intensity assignments by a full intensity unit or more. This analysis also explains the difference in intensity distance decays for modern versus historical events. Thus, intensity maps for historical earthquakes tend to imply more pervasive and widespread damage patterns than are revealed by intensity distributions of modern earthquakes of comparable magnitude. This bias is significant even when intensities are reassigned following modern, conservative practices. One caveat to this conclusion is that intensity accounts of historical earthquakes often suggest that relatively larger structures such as courthouses were damaged more than smaller buildings. This in turn suggests long-period shaking effects that will not be fully captured fully by historical damage distributions due to a paucity of large structures in historical times. I further reconsider the intensity distributions and magnitudes of moderate earthquakes in the greater San Francisco Bay Area prior to 1906 to explore the extent to which catalog magnitude estimates for historical events are inflated. For late 19th century events I estimate significantly lower magnitudes than the preferred estimate in the WGCEP catalog, with differences commonly on the order of 0.5 magnitude units.

Broadband Near-Field Ground Motion Simulations in 3D Scattering Media, Walter Imperatori (Poster 166)

The heterogeneous nature of Earth's crust is manifested in the scattering of propagating seismic waves. In recent years, different techniques have

been developed to include such phenomenon in broadband ground-motion calculations, either considering scattering as a semi-stochastic or pure stochastic process. In this study, we simulate broadband (0-10 Hz) ground motions using a 3D finite-difference wave propagation solver using several 3D media characterized by Von Karman correlation functions with different correlation lengths and standard deviation values. Our goal is to investigate scattering characteristics and its influence on the seismic wave-field at short and intermediate distances from the source in terms of ground motion parameters. We also examine other relevant scattering-related phenomena, such as the loss of radiation pattern and the directivity breakdown. We first simulate broadband ground motions for a point-source characterized by a classic omega-squared spectrum model. Fault finiteness is then introduced by means of a Haskell-type source model presenting both sub-shear and super-shear rupture speed. Results indicate that scattering plays an important role in ground motion even at short distances from the source, where source effects are thought to be dominating. In particular, peak ground motion parameters can be affected even at relatively low frequencies, implying that earthquake ground-motion simulations should include scattering also for PGV calculations. At the same time, we find a gradual loss of the source signature in the 2-5 Hz frequency range, together with a distortion of the Mach cones in case of super-shear rupture. For more complex source models and truly heterogeneous Earth, these effects may occur even at lower frequencies. Our simulations suggests that Von Karman correlation functions with correlation length between several hundred meters and few kilometers, Hurst exponent around 0.3 and standard deviation in the 5-10% range reproduce the available observations, although an unambiguous random-media characterization of the Earth crust in the distance range currently cannot be achieved

Envelope inversion for the spatial distribution of high-frequency energy radiators of the M9.0 Tohoku-Oki earthquake, Asaf Inbal, Jean-Paul Ampuero, and Don Helmberger (Poster 159)

The March 11, 2011 M9.0 Tohoku-Oki earthquake was recorded by dense seismological and geodetical networks deployed in Japan, as well as by a vast number of seismic stations worldwide. These observations allow us to study the properties of the subduction interface with unprecedented accuracy and resolution. In particular, depth-dependent variations of fault behavior, a feature which has long been masked by strong heterogeneities along the fault strike, can now be probed successfully. Back-projection analysis of teleseismic data suggests that coherent high frequency energy (> 1 Hz) was mainly emitted from deep portions of the megathrust, at the bottom extent of the rupture zone. Here we study the details of high-frequency energy radiation during the M9.0 mainshock using local recordings.

In order to better constrain the timing, location and amplitude of high-frequency radiators, we invert waveform envelopes recorded by the dense Kiban Kyoshin borehole accelerometers network located in northeastern Japan. Conventional inversions of acceleration data suffer from the lack of resolution of local Earth models, and are thus capable of modeling only signals with periods of a few seconds or longer. Waveform envelopes, on the other hand, are less sensitive to structural complexities, and may be used efficiently to model signals at high frequencies. We compute theoretical envelopes for waves traveling in a heterogeneous scattering medium using the method of Nakahara et al. (1998). We assume constant rupture velocity, and perform a search for rupture velocity and rise time that will minimize the misfit between the observed and calculated envelopes in several frequency bands. A major difficulty in the inversion procedure is the separation of the source and the site effects. Strong trade-offs between these parameters render the inversion non-linear and thus extremely sensitive to the response of individual stations. We therefore adopt an empirical approach and iteratively separate the the source and site terms from the stacked spectra of numerous events recorded by the network. The output response functions are used to stabilize the inversion. Preliminary results are consistent with far-field observations and suggest that the origin of high-frequency energy emitted during the M9.0 event is at the down-dip limit of the rupture zone.

Do Large Earthquakes Penetrate below the Seismogenic Zone? Potential Clues from Microseismicity, Junle Jiang and Nadia Lapusta (Poster 098)

MEETING ABSTRACTS

It is typically assumed that slip in large earthquakes is confined within the seismogenic zone - often defined by the extent of the background seismicity - with regions below creeping. In rate-and-state friction, the locked seismogenic zone and the creeping fault extensions are velocity-weakening (VW) and velocity-strengthening (VS), respectively. Recently, it has been hypothesized that earthquake rupture could penetrate into the deeper creeping areas (Shaw and Wesnousky, 2008), and yet it is difficult to detect the deep slip due to limited resolution of source inversions with depth.

We hypothesize that absence of concentrated microseismicity at the bottom of the seismogenic zone may point to the existence of deep-penetrating earthquake ruptures. If the creeping-locked boundary (CLB) is at the bottom of the VW area, which supports earthquake nucleation, microseismicity should persistently occur there, as been observed on the Parkfield segment of the San Andreas Fault (SAF). However, such microseismicity would be inhibited if dynamic earthquake rupture penetrates well below the VW/VS transition, which would drop stress in the ruptured VS areas, making them effectively locked. Indeed, microseismicity concentration is not observed for several faults that hosted major earthquakes, such as the Carizzo segment of the SAF (the site of 1857 Mw 7.9 Fort Tejon earthquake).

We confirm this hypothesis by simulating earthquake sequences and aseismic slip in 3D fault models (Lapusta and Liu, 2009; Noda and Lapusta, 2010). VS areas surround a VW area on the fault, at the bottom of which, patches of smaller nucleation sizes simulate potential sources of microseismicity. On part of the fault, thermally-induced pore fluid pressurization (TP) is effective, leading to enhanced coseismic weakening. In the case where efficient TP is restricted to the VW zone, model-spanning earthquakes arrest quickly in the VS areas, and the CLB reaches the bottom of the VW area early in the earthquake cycle, producing microseismicity. In contrast, if efficient TP extends deeper (5 km), ruptures activate coseismic weakening in the VS areas, penetrating much deeper. The CLB, while moving up-dip with time, is below the VW area throughout the cycle, producing no microseismicity. The support of hypothesis is strongest under the assumption of localized shear zones below the brittle-ductile transition, supported by frictional postseismic slip and seismic tremor at the deeper fault extensions.

Moment Accumulation Rate in Southern California, Kaj M. Johnson (Poster 115)

Rate of moment release is an important parameter in probabilistic seismic hazard assessments such as UCERF. Geodetic data can be used to infer the moment accumulation rate on faults and/or within volumes of the crust. In this study we use deforming block models and GPS and InSAR data to constrain the moment accumulation rate on and off major faults in southern California. The deforming block model maps the majority of deformation onto slip on major block-bounding faults but also allows for some deformation to be distributed in the crust between faults. As in typical block models, we invert for both the long-term slip rates on block boundary faults and the interseismic creep rate (using the backslip approach). The rate of moment accumulation on faults is derived from the backslip rate. We solve a sequence of moment-bounded inversions in which we solve for the best-fitting backslip distribution on faults for a given moment rate. We find that the data are fit nearly equally well by models with moment accumulation rates on faults ranging from about 1.2-2.8 Nm/yr. Off-fault moment rate, computed from off-fault strain rates using a Kostrov-summation method, is about 1 Nm/yr. The sum of the on-fault moment accumulation rate and the off-fault moment rate is higher than the observed 150-year seismic moment release rate of 2.2 Nm/yr for the entire state of California. It remains unclear how much of the accumulated moment will be released in future earthquakes and how much is released aseismically.

Low risk does not equal no risk: understanding barriers to earthquake risk-reduction in low seismic hazard zones, David Johnston, Caroline Orchiston, Craig Weaver, Julia Becker, Sarah McBride, Douglas Paton, John McClure, and Tom Wilson (Poster 258)

Over the past few decades considerable effort has been devoted to improving our knowledge of seismic risk. Much of this work has resulted in improved seismic risk models and hazard maps, delineating variations

in relative risk. However, disparities are still common between these expert assessments and the manner in which the public and authorities interpret and act on seismic risk information. Public understanding of and response to earthquake risk is determined by a range of factors, including scientific information, and direct past experience of earthquakes, as well as the interaction of social, cultural, institutional and political processes. Many people in lower seismic hazard regions falsely interpret their relatively low seismic risk as a reason not to prepare. This phenomenon is common in many parts of the world. Recent research will be presented within the context of Canterbury, New Zealand and eastern Washington, USA, that explores barriers to earthquake risk reduction in low seismic hazard zones.

Communicating Earthquake Risk: The Intersection of Earth and Social Sciences, Lucile M. Jones and Timothy L. Sellnow (Talk Mon 11:00)

Earth scientists and engineers face significant challenges in communicating earthquake risk to decision makers, members of the media, and the public. Some earth scientists have empirically developed an understanding of the opportunities and challenges in expressing the risk posed by earthquakes to non-specialists. Independently, researchers in psychology and communications have completed extensive research on the variability of the public's response to a range of risk communication strategies. This session will compare the empirical experience of scientists in communicating the risk with the results of research in psychology in risk communication. We will focus on three major topics: 1) the challenges of communicating probabilities, 2) the fallacy of the teachable moment - what the public can perceive at times of fear, and 3) lessons from ShakeOut - what the success of ShakeOut tells us about motivating people to take action to protect themselves. For each topic, we will examine the experience of seismologists, compare with social science research that bears on these issues, and seek participation from the audience. The goal is to arrive at practical approaches for earth scientists and engineers to facilitate productive interaction with decision makers, media, and the public.

Stochastic Descriptions of Basin Velocity Structure from Analyses of Sonic Logs and the SCEC Community Velocity Model (CVM-H), Thomas H. Jordan, Andreas Plesch, and John H. Shaw (Poster 281)

Sustained increases in computational resources and the trend of numerical wave propagation studies to shorter periods create a demand for higher resolution velocity models. One way to parameterize such models is to characterize the small length scale (<100m) structure and implement this as a stochastic representation of the near-surface layers in regional velocity model. Here we analyze sonic logs in the Los Angeles basin in conjunction with the current velocity structure in the CVM-H in order to develop a stochastic representation of the near-surface to depths of 3 km. Sonic logs measure compressional and shear wave slowness at samples of tens of centimeters to a few meters, and we applied a de-spiking procedure to eliminate small (<10 ft) slowness anomalies that were likely caused by instrument error. Our first effort compared these observations directly with the velocity values represented at the well bore locations in the CVM-H. Given that smoothed (25 m sample) versions of these data were used to develop the velocity model, this analysis simply defined the scale of variability present in the data but not represented in the models. Our analysis shows a standard variation of 157 ms/m around a mean of 1.3 ms/m for the delta between compressional wave slowness in logs and model.

After removing longer scale trends by subtracting the velocity model, we then analyzed the well data to quantify the vertical and horizontal variability of the velocity structure that they sample. Vertical analyses were conducted in individual wells, whereas groups of closely-spaced wells were used to analyze horizontal variability. In the vertical analysis variances were computed for all lags (spacing between pairs of data) between 5 m and 500 m and plotted in a variogram. The smallest lag where variance starts to level out to a background level can be considered the largest correlation distance. Our results show a vertical correlation distance of about 80m at which variance levels reach about 430 ms²/m².

In the horizontal analysis, variograms were constructed with lags varying from 100 m to 8 km. The data set is divided into thin (10m to 100m)

horizontal layers, in which wells are paired and analysed. The resulting variances for each lag in each layer are combined in a variogram. While a trend to higher variances with increasing distance cannot be established, this analysis showed a maximum correlation distance of about 900m where variance reaches a high level of about 750 ms²/m². Thus, the model analysis suggests a ratio of horizontal to vertical correlation lengths of about 11:1.

To further analyze this fine scale basin structure, we propose to establish a series of natural laboratories in the Los Angeles basin where additional water well and geotechnical borehole data can be used to investigate velocity structure in the uppermost strata (<300 m), which are sparsely sampled by the industry wells. These areas should also include broadband seismic station to facilitate numerical studies that compare observed and synthetic waveforms developed using different velocity parameterizations. Ultimately, our goal is to generate future releases of the CVM-H that provide, as an option, stochastic representations of the finer scale velocity structure that can be used to simulate ground motions at higher frequencies

Observation of Forward-Directivity Effects in the Near-Fault Ground

Motions of the 2010-11 Canterbury, New Zealand Earthquakes, *Varun A. Joshi and Brendon A. Bradley* (Poster 265)

Near-fault ground motions recorded during the Mw7.1 Darfield (4 September, 2010) and Mw 6.2 Christchurch (22 February, 2011) earthquakes show clear evidence of forward-directivity effects. Due to the alignment of the rupture front and slip direction along the causative strike-slip fault during the Darfield event, forward-directivity effects are clearly observed in the form of a large pulse arriving at the beginning of the fault-normal velocity time-series. Although the time-series characteristics of the velocity pulse observed at 4 CBD strong ground motion stations are very similar, the effects of this pulse on the resulting pseudo-acceleration response spectra are significantly different considering that the source-to-site geometry for each station is essentially the same. In contrast, due to the complexity of the thrust fault rupture during the Christchurch event, forward-directivity effects are not clearly discernible in the fault-normal velocity time-series at many locations, and in most cases, the principal directivity pulse was observed in orientations similar to the fault-parallel direction.

The limitations of the automated pulse-classification algorithm developed by Baker (2007) are illustrated using an example from the Darfield event. In particular, the algorithm is unable to capture the initial forward-directivity pulse, and generally selects the large amplitude and long period ground motion generated by basin effects. As a result, manual intervention was required to appropriately characterise this pulse in terms of its amplitude and period. Comparisons of the pulse periods obtained from both the automated Baker (2007) algorithm and manual approaches yield larger pulse periods than empirical equations, possibly as a result of soft sedimentary soils underlying a majority of Christchurch city.

Characteristic Earthquake Model, 1884 -- 2011, R.I.P., *Yan Y. Kagan, David D. Jackson, and Robert J. Geller* (Poster 052)

Unfortunately, working scientists sometimes reflexively continue to use "buzz phrases" grounded in once prevalent paradigms that have been subsequently refuted. This can impede both earthquake research and hazard mitigation. Well-worn seismological buzz phrases include "earthquake cycle," "seismic cycle," "seismic gap," and "characteristic earthquake." They all assume that there are sequences of earthquakes that are nearly identical except for the times of their occurrence. If so, the complex process of earthquake occurrence could be reduced to a description of one "characteristic" earthquake plus the times of the others in the sequence. A common additional assumption is that characteristic earthquakes dominate the displacement on fault or plate boundary "segments." The "seismic gap" (or the effectively equivalent "seismic cycle") model depends entirely on the "characteristic" assumption, with the added assumption that characteristic earthquakes are quasi-periodic. However, since the 1990s numerous statistical tests have failed to support characteristic earthquake and seismic gap models, and the 2004 Sumatra earthquake and 2011 Tohoku earthquake both ripped through several supposed segment boundaries. Earthquake

scientists should scrap ideas that have been rejected by objective testing or are too vague to be testable.

Using the SCEC Broadband Platform for Supplementing Empirical Data on Fling Effects, *Ronnie Kamai, Kathryn Wooddell, and Norman Abrahamson* (Poster 004)

A large set of finite-fault simulations has been submitted to the SCEC broadband platform to be used for constraining the magnitude and distance dependence of the effects of permanent tectonic deformations on ground motion predictions. The simulations include 38 different earthquake scenarios, consisting of both strike-slip and reverse faults, with dips ranging from 45 to 90 degrees and magnitudes from 6.0-8.2. Each scenario includes 30 random realizations of the hypocentral location and the slip distribution and is recorded by about 100-200 stations per realization, at distances of 1.0-100 km from the fault.

The simulations were submitted to the platform by users who are not experts in the details of the model development and implementation. With support from SCEC IT staff, simulations were set up on the cluster. Thirty six out of the total 38 simulations were completed within a month, using 16 cores each. The two larger events were submitted later and were completed within an additional two weeks, using 32 cores each. This collaboration has demonstrated the accessibility and usability of the broadband platform to external users.

The results of the physics-based simulations are expected to supplement the available empirical data for the effects of permanent tectonic displacements and provide insight into the relative size of the transient and the permanent components of ground motions. The Fling study will use the simulation results to address the three following questions: (1) Do the existing empirical Ground Motion models capture the full extent of fling effects? Are there enough representative recordings in the dataset (mainly at short distances), and for the available recordings – how much of the fling effect has been taken out by standard signal processing? (2) How well are empirically-based predictions of PGV at short distances constrained? (3) What is the Magnitude and Distance dependence of the fling parameters (such as fling step amplitude, pulse period, and time of onset)?

Variability of seismic source spectra derived from cohesive-zone models of a circular rupture propagating at a constant speed, *Yoshihiro Kaneko and Peter M. Shearer* (Poster 096)

Static stress drop of earthquakes is often estimated from far-field body-wave spectra using measurements of corner frequencies, together with seismic moment, which can be computed from the low-frequency part of the spectrum. Corner frequencies are used to infer the source dimension based on a specific theoretical model. The most widely used model is from Madariaga (1976), who considered a bilateral rupture expanding at a constant speed on a circular fault. This model assumes that the rupture front is characterized by an abrupt change of fault strength from a uniform initial prestress to a kinetic frictional stress, and hence the stress is singular at the rupture front. In this study, we investigate variability of source spectra derived from dynamic models of expanding bilateral ruptures on a circular fault with a cohesive zone that prevents a stress singularity at the rupture front. We study the dependence of far-field body-wave spectra on the rate of frictional weakening (which controls the cohesive zone size), rupture speed, and dynamic stress drop. For each source model, we compute far-field body-wave displacement synthetics for a homogeneous elastic space using the representation theorem (Aki and Richards, 2002). Our results show that P- and S-wave corner frequencies of displacement spectra are systematically larger than those predicted by Madariaga (1976) and generally depend on the rate of frictional weakening in the source model, which affects the fracture-energy-density distribution on the fault. For a given rupture speed, the average of corner frequencies over the focal sphere is larger for source models with larger fracture energy. For ruptures propagating at 90% of the S-wave speed, the azimuthal average of P-wave corner frequencies in the case with the smallest fracture energy is about 20 percent larger than that of Madariaga (1976), which corresponds to about a factor-of-two difference in the inferred stress drop. Thus for these ruptures, application of the Madariaga model overestimates stress drops by factors of two or more, depending upon the fracture energy.

MEETING ABSTRACTS

Regional extent of the large coseismic slip zone of the 2011 Mw 9.0 Tohoku-Oki Earthquake delineated by on-fault aftershocks, Aitaro Kato, Toshihiro Igarashi, and Jun'ichi Fukuda (Poster 083)

In order to image the rupture process of the 2011 Tohoku-Oki earthquake, many fault source models have recently been developed following this giant earthquake by inverting for slip on the fault plane, based on a variety of collected geophysical data. Most of these studies suggest that the area of largest coseismic slip (30–80 m) was located near the mainshock hypocenter, extending eastward to a location near the Japan Trench axis. However, the estimated outer edges of the large-slip zone are substantially different between these models, due to the currently limited spatial resolution of slip along the fault. Consequently, there are insufficient constraints as to how far the large-slip zone extended along the plate interface during the mainshock rupture.

Here we delineate the outer edge of this large-slip zone in detail, by applying a spatial correlation between on-fault aftershocks and slip to the Tohoku aftershock sequence. We focus on the sharp density contrast observed for interplate, repeating, and down-dip compressional earthquakes induced by the Tohoku-Oki mainshock. The seismicity rate of interplate earthquakes changed significantly after the mainshock, probably as a result of stress perturbations by the large-slip, and here we use this information as qualitative constraints in constructing our model. The model that we present for the large-slip zone incorporates the main features of previously proposed fault source models, and also the observed fine-scale heterogeneities of fault slip associated with this event. It is important to highlight that the outer edge of this large-slip zone shows a remarkably complex shape. In particular, it is narrow and elongate southward along the ~35 km iso-depth contour of the plate boundary offshore of Fukushima and Ibaraki. This southward elongate slip zone corresponds to down-dip regions that appear to have produced higher relative levels of short-period seismic radiation. Although some intensive foreshocks, situated close to the initial rupture point of the Tohoku-Oki mainshock, were recorded [Kato et al., 2012, *Science*], any aftershock in this foreshock area was abruptly terminated.

We explore whether the coseismic geodetic data could be fit with a fault source model in which slip is confined to the large-slip zone delineated in this study. We assume a nonplanar fault plane along the plate boundary. In addition to the largest coseismic slip area off Miyagi, an isolated high slip region is imaged off Ibaraki.

Upper crustal structure beneath the Salton Sea as imaged by active source marine seismic refraction in conjunction with the Salton Seismic Imaging Project, Annie M. Kell, Valerie Sahakian, Alistair Harding, Graham Kent, and Neal Driscoll (Poster 196)

In the spring of 2011 we expanded a campaign of marine seismic reflection efforts in the Salton Sea in conjunction with the Salton Seismic Imaging Project (SSIP) to collect active-source marine refraction data using Ocean Bottom Seismometers (OBSs) and a marine airgun. The Salton Trough presents an opportunity to study rifting processes similar to those seen in the Gulf of California, as well as the seismic hazards associated with the southern terminus of the San Andreas Fault (SAF). An areal array, comprised of 78 OBS deployments, was focused in the southern part of the sea but also included a line parallel to the San Andreas Fault (SAF), line 1, extending then length of the sea, and a line perpendicular to the SAF, crossing the northern basin, line 7. These lines are collinear with high-resolution reflection profiles and existing chirp profiles. The OBS array was concentrated in the southern Salton Sea to investigate the pull-apart deformation reported by Brothers et al. (2009). Using the methods of Van Avendonk et al. (2004) we seek to constrain upper crustal velocities in this region by travel-time tomography. Beginning with P-wave arrival times we trace the ray paths through the model space and invert for seismic velocities. By iterating from the forward picking to the inversion, we reduce the chi-squared error to produce a 2D depth profile of the seismic velocities while maintaining a stable model. Line 1 uses 38 OBSs and 470 shots from a 210 cu. in. airgun to model the upper 4 km beneath the Salton Sea. Velocities vary from 1.5 km/s in the upper 1 km to an apparent 4 km deep basement velocity of 5.5 km/s. Velocity variations with depth agree with major boundaries in the co-linear seismic reflection profiles and the divergence toward the south/fault structure is also captured in these early models.

With this model, we seek to further understanding of the Salton Sea pull-apart system, as well as the active rifting processes seen in the region.

Quaternary geology, geochronology and geomorphology of the San Gorgonio Pass Region, southern California, Katherine J. Kendrick and Jonathan C. Matti (Poster 132)

The San Gorgonio Pass (SGP) region of southern California is a locus of long-continued Quaternary deformation and landscape evolution within a structural knot in the San Andreas Fault (SAF) zone. The geomorphology of the SGP region reflects the complex history of geologic events in the formation and resolution of this structural knot. We recognize five morphologically distinct terrains in and around SGP; our focus in this study is on two, the Pisgah Peak (PPB) and Kitching Peak blocks (KPB). Morphometric analyses, including drainage density, hypsometry, topographic profiles, and stream-power measurements and discontinuities, consistently demonstrate distinctions between the blocks, though the lithology is the same. KPB is bounded on the north by the Mission Creek strand of the SAF and on the east by the Whitewater Fault; PPB is bounded on the north by the San Bernardino strand of the SAF, which continues southeastward into the core of SGP and there separates PPB from KPB. KPB has significantly greater topographic relief than PPB. Canyons in KPB lack thick Quaternary alluvial fills, and hillslopes have shed numerous bedrock landslides. Canyons in PPB contain large volumes of Middle-Pleistocene through Holocene alluvium, associated with areally extensive relict geomorphic surfaces. We use the geomorphic differences, along with geologic factors, to reconstruct tectonically driven landscape evolution over the last 100–200 Ka years.

The KPB and PPB both are bounded southward by contractional structures of the San Gorgonio Pass Fault zone (SGPFZ), but geologic complexity within this zone differs markedly south of each block. South of KPB, the SGPFZ consists of multiple thrust-fault strands, some older than 500 ka, has a wide spatial footprint, and Holocene alluvium is disrupted by numerous fault scarps. South of PPB the SGPFZ consists of fewer thrust-fault strands, has a relatively narrow footprint, and faults breaking Holocene deposits are uncommon. The San Bernardino strand of the SAF intersects the SGPFZ at about the boundary between these two domains. Morphometric data indicate that the KPB has undergone significantly greater uplift than the PPB since inception of the San Bernardino strand, proposed by Matti and Morton (1993) to have occurred at ~125ka.

Using offset geomorphic features to estimate paleo-earthquake slip distribution on the Claremont fault, northern San Jacinto fault zone., Scott Kenyon and Nate Onderdonk (Poster 137)

Recent paleoseismic work at the Mystic Lake and Quincy sites along the northern San Jacinto fault zone has documented the timing of the last seven ground-rupturing earthquakes on the Claremont fault. Dating of offset features at the Quincy site suggest these earthquakes averaged about 3 m of lateral slip per event. However, we do not know the lateral extent or slip distribution of these ruptures.

To determine the extent and slip distribution of these ruptures we are conducting detailed geomorphic mapping along the Claremont fault to identify and catalog offset features. The offset features we are most interested in are the small features that have formed in the last one or two ruptures. We will then compile the data to map out the lateral extent of the identified ruptures as well as to estimate the magnitude of these events. This data will also be compared to a recent study by Salisbury et al. (2010) that identified and mapped the lateral extent of the last three surface ruptures along the central San Jacinto fault zone (Clark fault). By comparing the data we will be able to examine the patterns of recent coseismic slip distribution along much of the San Jacinto fault zone. We hope that this will also allow us to determine if any recent events have jumped the San Jacinto valley releasing step-over between the Clark and Claremont faults.

Presently, we have mapped most of the of the Claremont strand using B4 LiDAR data and field observations and are starting to measure and catalog offset features. We expect that this new mapping will also allow provide more details regarding the fault zone structure and can be used to look for more paleoseismic sites or slip rate sites to further the work being done at the Mystic Lake and Quincy sites.

Moo, Whoosh, Vroom, Beep, Twinkle: Identifying Non-Seismic Signals Recorded by EarthScope's USArray Transportable Array (TA) Stations,
Debi L. Kilb, Aaron A. Velasco, and Kristine L. Pankow (Poster 184)

The rapid increase in the rate of seismic data collection and data distribution is forcing seismologists to re-evaluate how they search data for important signals. Previously, it was common practice to examine seismograms individually in a non-automated manner to assess qualitatively the usefulness of a given data trace. Given today's technology advances in combination with the onslaught of data availability, this old-school method is now being replaced with automated processes that systematically identify potentially important signals within seismic data streams. The continuous data collected by EarthScope's USArray Transportable Array (TA) is prime for this type of automated processing techniques, as these data include 24-7 recordings of 3-component data at >400 seismic stations that are distributed in a regular grid throughout the contiguous US. We use an automated approach to examine TA data to test hypotheses related to the physics of dynamic triggering of remote aftershocks. To begin, we use the Antelope software's short-term average (STA) to long-term-average (LTA) ratio algorithm to create a catalog of "detections" at each station as a function of time. We define a detection as simply a signal above the noise level, which may, or may not, be an earthquake. We assume a strong change in the rate of detections during, and/or following, the passage of surface waves from a large teleseismic event could be indicative of remote triggering. As anticipated, some data is not useful for our purposes because the small signals we want to study are obscured. To identify non-optimal stations we create time-of-day histograms of the detections for each station. A skewed distribution in a detection histogram, for example detections mostly during daytime hours, is an indication that our detection algorithm might be primarily detecting non-seismic events. Examining the raw waveforms from these stations we can begin to estimate the cause of these disturbances, such as stations near airports (e.g., stations C03A, CIA, E44A, E44A, NEE2, P06A, R17A, R35A, and Y14A), live stalk or dairy farms (e.g., station J38A), car traffic patterns (e.g., station SOL) and mechanical movement from telescopes in an observatory (e.g., station UPAO). Our aim is not to eliminate these stations completely from our study, but instead to help us identify the cleanest data first (i.e., station R11A) to test our algorithms on and then subsequently move on and process the more challenging data.

Key results from JFAST: location and structure of the plate boundary in the area of maximum slip during the 2011 Tohoku-Oki earthquake,
James D. Kirkpatrick and Expedition 343 Scientists (Poster 072)

Integrated Ocean Drilling Project Expedition 343, Japan Trench Fast Drilling Project (JFAST), sailed on April 1st 2012 to investigate the shallow part of the Japan Trench subduction zone that ruptured in the M9 Tohoku-Oki earthquake in March 2011. The goals of the expedition were to establish the state of stress and the physical properties of the fault zone. Two holes were drilled through the plate boundary that provided logging while drilling (LWD) and measuring while drilling (MWD) data from the first hole and a total of 21 cores from the second. Analysis of the rocks and data show that the accretionary wedge is composed of ~820 m of disrupted, folded and faulted clayey to silty mudstones. Fault and bedding orientations in the wedge interpreted from LWD resistivity images strike ~NE, consistent with contraction parallel to the plate convergence direction. Lithologic and bedding orientation changes observed in both holes and stress magnitude changes indicated by borehole breakouts observed in LWD data show the down-going Pacific plate was penetrated at a depth of around 820 meters below sea floor. The décollement is defined in core by 1 m of intensely sheared clay containing a pervasive scaly fabric indicative of distributed shear over the 1 m zone. Extremely narrow discontinuities separate domains in the clay in which the foliation orientation and intensity change, which suggests localized brittle failure. Although core recovery through the fault zone was incomplete, the maximum possible thickness of the sheared clay is <5 m implying long-term deformation is localized onto a relatively narrow fault zone.

Dispersion observations from the 2011 Tohoku tsunami waveforms recorded on the spatially dense ALBACORE OBS array, Monica D. Kohler, Fan-Chi Lin, and Dayanthie S. Weeraratne (Poster 199)

The ALBACORE (Asthenosphere and Lithosphere Broadband Architecture from the California Offshore Region Experiment) ocean bottom seismometer (OBS) array recorded the March 2011 Mw=9.0 Tohoku tsunami with very high spatial resolution. In that array, 22 stations had differential pressure gauges (DPGs) that recorded water pressure waveform data continuously at 50 samples per second. Average station spacing was 75 km. This deployment of OBSs spanned a 150 km north-south by 400 km east-west off the coast of southern California, extending into deep open ocean west of the Patton escarpment. Several hours of the DPG tsunami waveforms were Gaussian filtered in narrow bands around 32 frequencies between 0.00067 and 0.0033 Hz (300 to 1500 sec), and both phase and group travel times were measured for the first arrival. Phase and group velocities were then calculated from arrival time differences across the ALBACORE stations based on eikonal tomography. At longer periods, velocities are higher and approximately constant as expected as they are only a function of water depth and not frequency, although the match is not exact even though bathymetry is well mapped at small spatial scale. The velocity measurements, however, are likely slightly biased by finite frequency effects such as wave interference due to multipathing. The frequency band of these calculations spans the transition from long-period, non-dispersive, shallow-water, gravity-driven ocean wave behavior to short-period, dispersive behavior, and this transition is apparent in the maps. At shorter periods in the phase velocity maps, there is a clearer correlation with bathymetry. In particular, velocity gradients are pronounced at the Patton Escarpment and near island plateaus. This is expected as the wavelengths of the tsunami waves are smaller and closer to the wavelengths of the local structures the waves are encountering. In the deep open ocean area, where waveforms are simpler and easier to interpret, the measured phase velocities are overall consistent with the theoretical dispersion predictions and have ~2% estimated uncertainty.

Understanding earthquake source physics through computation, Jeremy E. Kozdon (Talk Tue 10:30b)

What are the physical mechanisms for incoherent, high-frequency ground motion? How does complex geometry affect the rupture process? At what scales must we model events to have reliable and physically realistic simulations? What processes give rise to self-similarity in earthquakes? How does the stress evolve over multiple earthquake cycles? In this talk, I will present highlights of how our group is using dynamic rupture models and high-performance computing to explore these questions. Though our focus will be on dynamic rupture models, the lessons we have learned can aid the SCEC community at large in thinking about computations.

We initially explored incoherence of high-frequency ground motion through fault roughness. As a rupture encounters local stress heterogeneities it accelerates and decelerates which, along with fluctuations in slip, excites incoherent ground motion. Recently, we have begun considering the importance of path effects in a heterogeneous medium. Scattering both generates incoherent ground motion and feeds back into the rupture process leading to further incoherence. Untangling the relative importance of these mechanisms requires dynamic rupture simulations.

Computation can help answer other geometry and material structure related questions. Using dynamic rupture models of the Tohoku earthquake, we are exploring how ruptures can reach the seafloor through a shallow velocity strengthening fault segment and what hydroacoustic signals might tell us about shallow slip. Though subduction zone events may not be directly related to the primary SCEC objectives, rupture dynamics in other geometrically complex fault systems featuring spatially variable frictional properties are. For instance, which branch will a rupture take in a fault network? Can an earthquake in this system jump to another fault? How do local fault geometry and frictional properties affect segmentation?

Rupture processes are multiscale and using laboratory measured parameters requires millimeter resolution. Even with exascale resources, this is impossible for regional simulations with fixed grids. One way

MEETING ABSTRACTS

forward is adaptive mesh refinement (AMR). In AMR, resolution is added as and where required, significantly reducing the computational overhead. Currently, we are using AMR to explore self-similarity and possible physical mechanisms (in particular, off-fault plasticity and/or thermal pressurization) underlying observed earthquake energy balance and scaling laws.

Using Multiscale Dynamic Rupture Simulations with Adaptive Mesh Refinement to Explore the Role of Off-Fault Plasticity in the Energy Balance and Self-Similarity of Earthquakes, *Jeremy E. Kozdon and Eric M. Dunham* (Poster 095)

There is strong observational evidence that earthquakes are self-similar. That is, stress drop and rupture velocity are independent of source dimension, whereas slip and the energy release rate scale linearly with source dimension. The earthquake energy balance then requires that fracture energy must also scale linearly with source dimension. Though well supported observationally, it is not known what physical mechanism gives rise to this self-similarity. Assuming an ideally elastic off-fault material response, both slip-weakening and the standard rate-and-state friction laws fail to predict this scaling. The fundamental problem is that for both models the fracture energy is constant if the slip-weakening or state-evolution distance is independent of event size or propagation distance. Within the literature, there are two leading suggestions to overcome this: thermal pressurization (Rice, JGR, 2006) and off-fault plasticity (Andrews, JGR, 2005).

To test and compare these proposed mechanism with dynamic rupture simulations requires resolving the propagating rupture over many temporal and length scales. With fixed grid methods this is computationally infeasible. Adaptive mesh refinement (AMR), in which grid resolution is dynamically allocated in response to the local solution structure, can make these simulations possible. To this end we have developed Tetemoko, an extension of the Chombo AMR package. The equations of elastodynamics are integrated using a multidimensional finite volume scheme that allows for adaptivity in space and time, thus allowing grid cells to be advanced using locally optimal time steps. Plastic deformation is implemented using operator splitting, with a plastic correction occurring after every local elastic step. On the fault, the code handles both rate-and-state and slip-weakening friction, and the implementation of thermal pressurization is in progress.

Here we consider whether off-fault plastic deformation leads to a self-similar rupture process. Preliminary simulations of a 100 m rupture with laboratory scale friction parameters (26 μm state-evolution distance and 30 mm characteristic extent of state-evolution region) suggest that plasticity can lead to both a linearly increasing slip profile as well as a wedge-shaped region of plastic deformation. Both of these are required for a self-similar rupture process, suggesting that off-fault inelastic deformation might provide the necessary energy sink necessary for self-similarity.

Complex Fault Interaction in the Yuha Desert, *Kayla A. Kroll, Elizabeth S. Cochran, Keith B. Richards-Dinger, and Danielle F. Sumy* (Poster 154)

We determine precise hypocentral locations for 3,600 aftershocks that occurred in the Yuha Desert (YD) region following the 4 April 2010 Mw 7.2 El Mayor-Cuicapah (EMC) earthquake until 14 June 2010 originally located by the Southern California Seismic Network. To calculate precise hypocenters we used manually identified phase arrivals and cross-correlation delay times in a series of absolute and relative relocation procedures with algorithms including hypoinverse, velest and hypoDD. Location errors were reduced with this process to ~20 m horizontally and ~80 m vertically. The locations reveal a complex pattern of faulting with an echelon fault segments trending toward NW and an echelon conjugate features trending NE. The relocated seismicity correlates with the mapped faults that show triggered surface slip in response to the EMC mainshock. Aftershocks are located between depths of 2 and 11 km, consistent with previous studies of seismogenic thickness in the region. 3D analysis reveals individual and intersecting fault planes between 5 and 10 km in the along-strike and along-dip directions. These fault planes remain distinct structures at depth, indicative of conjugate faulting, and do not appear to coalesce onto a throughgoing fault segment. We

observe a complex spatiotemporal migration of aftershocks with individual fault strands active for relatively short time periods. In addition, events relocated by Hauksson et al. (2012) that occur in the 2 year period following the 15 June 2010 M5.7 Ocotillo earthquake show a majority of the seismicity occurs along the Laguna Salada-West branch. At the same time, seismicity along the Laguna Salada-East and other faults in the Yuha Desert abruptly shuts off suggesting fault activity is highly sensitive to local stress conditions. Furthermore, we locate >31,000 previously unreported aftershocks in with 8 seismometers installed in the YD during the same time period. For this analysis we automatically detect arrivals using an STA/LTA filter on continuously recorded data. Absolute locations were first determined with hypoinverse using the automated phase picks, and the velocity model used in the above relocation procedure. We refined the relative locations again with hypoDD. We use these newly detected earthquakes to further the investigation of fault geometry at the surface and how it relates to fault structure at depth, rheology of the crust, and the spatiotemporal migration patterns within the aftershock distribution

Ground Motion Prediction Equations for data recorded within and around the San Jacinto Fault Zone, *Ittai Kurzon, Frank L. Vernon, Yehuda Ben-Zion, and Gail Atkinson* (Poster 003)

We present a new set of Ground Motion Prediction Equations (GMPEs) for horizontal Peak Ground Acceleration (PGA), Peak Ground Velocity (PGV) and 5% damped pseudo-acceleration spectra (PSA), developed for the San Jacinto Fault Zone (SJFZ) area. The local set of GMPE developed for a specific fault zone can provide new insights into the parameters and physics controlling ground motion. The analyzed dataset includes ~22000 observations from ~650 events related to the MW 5.2 Anza-Clark (AC) earthquake in June 2005, the MW 5.4 Coyote Creek (CC) earthquake in July 2010, and the seismic activity during the recent time-period of January 2010 to April 2012. The events span the magnitude range $1.5 < M < 6.0$ and are recorded by up to 110 stations at distances ranging from meters to 150km. We first examined the data against several generic Ground Motion Prediction Equations (GMPEs), such as a few of the Next Generation Attenuation models (e.g. Boore & Atkinson, 2008 and Cua & Heaton 2008). The generic models tend to underestimate the PGA and PGV values observed in the SJFZ at the higher end of the magnitude range ($M > 4.0$), and to underestimate the PSA over the complete magnitude range ($1.5 \leq M \leq 6.0$). These initial observations provide justification for the development of a local GMPE to better describe the average motions and their scaling with magnitude and distance. We then developed a local GMPE for the SJFZ by applying classical regression techniques. Predictive variables that we examined include distance, and magnitude, site characteristics reflected by V_s30 , rupture directivity, Fault Zone amplification, and topographical amplification. Our results show that rupture directivity is a significant factor controlling the amplitudes, even for small events. Thanks to our dense network, directivity effects can be extracted quite well from the ground-motion dataset during the regression analysis process. The directivity tool implemented in our GMPE for the SJFZ reflects the main fault mechanism orientations as known from other studies. Fault Zone amplification is measured by a simple rotation of coordinates to the average azimuth of the fault and is seen clearly in the data. However, this is of secondary importance to the directivity effect and seems to only slightly reduce the variance of the GMPE.

Seismic response to injection and production at the Salton Sea geothermal field, southern California, *Lia J. Lajoie and Emily E. Brodsky* (Poster 178)

California hosts both the largest geothermal resource capacity and highest seismicity rate in the nation. With plans to increase geothermal output, and proven earthquake triggering in the vicinity of geothermal power plants worldwide, it is important to determine the local and regional effects of geothermal power production. This study examines the link between fluid injection and seismicity at the Salton Sea geothermal field in southern California by attempting to answer three motivating questions: 1) Does fluid injection at the geothermal field change local seismicity in a measurable way? 2) Are aftershocks triggered at the same rate inside and outside of the field? 3) How do the triggered aftershocks interact with regional fault networks, specifically,

could these aftershocks trigger a societally significant event on the southern San Andreas fault?

We use monthly fluid injection and production data from 1980 to 2012 for 88 wells at the Salton Sea geothermal field and seismic data for the same time span from the relocated Hauksson, Yang, and Shearer earthquake catalog for southern California to evaluate these issues. We find that seismicity is correlated in both time and space in the Salton Sea geothermal field to injection. The observations strongly suggest triggering in the field. We also find that earthquakes within the field trigger aftershocks at a higher rate than most earthquakes elsewhere in California. The combination of observations suggest that aftershocks from induced seismicity could extend beyond the edges of the field into the neighboring tectonic system.

Width and dip of the southern San Andreas fault from modeling of magnetic and gravity data, *Victoria E. Langenheim, Noah D. Athens, Daniel S. Scheirer, and Gary S. Fuis* (Poster 117)

We investigate the geometry and width of the southern San Andreas fault using potential-field data, including new marine magnetic data from the Salton Sea. Previous models of the geometry of the San Andreas fault using ground magnetic data along line 7 of the Salton Sea Imaging Project (near Salt Creek) were hampered by lack of data west of the San Andreas fault, which lies < 1 km east of the Salton Sea shoreline. The San Andreas fault in this area coincides with a complex magnetic signature, with <100-nT magnetic anomalies with a wavelength of < 1 km superposed on a broader magnetic anomaly that is at least 5 km wide. Marine magnetic data show that high-frequency magnetic anomalies extend more than 1 km west of the mapped trace of the San Andreas fault.

Two-dimensional forward modeling of these data indicates two magnetic sources, with the broader anomaly sourced by magnetic rocks with seismic P-wave velocities greater than 4 km/s (also supported by gravity data) and the higher-frequency anomalies sourced by the overlying sedimentary section. Magnetic susceptibility measurements indicate that sandstones in this section are weakly to moderately magnetic (0.5-5.5 $\times 10^{-3}$ SI) and thus capable of producing the high-frequency anomalies. The model supports a moderate to steep (> 50 degrees) northeast dip of the San Andreas fault, but also suggests that the sedimentary sequence is folded west of the fault because of the presence of high-frequency anomalies.

The lack of detailed gravity data in the Salton Sea precludes using these data to model with any precision the dip of the San Andreas fault. Gravity data, however, are sufficient to map structure on the east side of the fault. To first order, gravity anomalies are consistent with the modeled seismic velocity structure but suggest a deeper basin, bounded by the Hidden Springs and Hot Springs faults, than imaged by the seismic experiment. This basin extends southeast of Line 7 for nearly 20 km, with linear margins parallel to the San Andreas fault. These data suggest that the San Andreas fault is wider than suggested by its surface trace.

On the Prediction of Earthquake Ground Motion, *Daniel Lavallee, Jan Schmedes, and Ralph J. Archuleta* (Poster 014)

Using a slip-weakening dynamic model of rupture, we generated earthquake scenarios that provided the spatio-temporal evolution of the slip on the fault and the radiated field at the free surface. We observed scenarios where the rupture propagates at a supershear speed on some parts of the fault while remaining subshear for other parts of the fault. For some scenarios with nearly identical initial conditions, the rupture speed was always subshear. For both types of scenarios (mixture of supershear and subshear speeds and only subshear), we compute the peak ground accelerations (PGA) regularly distributed over the Earth's surface. We then calculate the probability density functions (PDF) of the PGA. For both types of scenarios, the PDF curves are asymmetrically shaped and asymptotically attenuated according to power law. This behavior of the PDF is similar to that observed for the PDF curves of PGA recorded during earthquakes. Based on these results, we investigate issues fundamental for the prediction of ground motion.

It is important to recognize that recorded ground motions during an earthquake sample a small fraction of the radiation field. It is not obvious

that such sampling will capture the largest ground motion generated during an earthquake, nor that the number of stations is large enough to properly infer the statistical properties associated with the radiation field. To quantify the effect of under (or low) sampling of the radiation field, we design two experiments. For a scenario where the rupture speed is only subshear, we construct multiple sets of observations. Each set is comprised of 100 randomly selected PGA values from all of the PGA's calculated at the Earth's surface. In the first experiment, we fit the PDF of the PGA of every set with probability laws discussed in the literature (e.g. lognormal). For each set, the probability laws are then used to compute the probability to observe a PGA value that will cause "moderate to heavy" potential damage according to Instrumental Intensity scale developed by USGS. For each probability law, we compare predictions based on the set with the prediction estimated from all the PGA. This experiment quantifies the reliability and uncertainty in predicting an outcome due to under sampling the radiation field. The second experiment consists in using the sets discussed above and repeats the comparison but this time with a scenario where the rupture has a supershear speed over part of the fault.

Assessing different strategies to improve the reliability and applicability of luminescence dating of high energy sediment deposition and neotectonic contexts, *Michael J. Lawson, Edward J. Rhodes, Wendy A. Barrera, Guadalupe T. Ochoa, and Belinda J. Roder* (Poster 142)

In order to overcome technical difficulties in applying conventional quartz OSL (optically stimulated luminescence) dating to certain types of sedimentary environments and in areas where the characteristics of available mineral grains are sub-optimal, we explore a range of alternative approaches. As contributions from very small volumes of mineral inclusions within quartz grains can significantly affect OSL behaviour, and potentially lead to erroneous age estimation, we have developed tests designed to quantify the degree of signal contamination. Other dating approaches explored include the use of K-feldspar and fine-grained polymineral IRSL (infra-red stimulated luminescence) and ITL (isothermal thermoluminescence). Sand-sized grains of K-feldspar were dated using several different protocols, including a post-infrared IRSL SAR (single aliquot regenerative-dose) protocol applied to both conventional multiple grain single aliquots and to single grains, and two novel approaches. The novel methods include a "selective SAR" protocol, comprising the measurement of the natural SAR cycle for 48 aliquots, followed by the remaining steps of a regular SAR protocol applied only to the 12 aliquots with the lowest sensitivity-corrected natural IRSL signals. This approach is focused at improved measurement efficiency and rapidly isolating the most fully bleached aliquots. A second approach, termed a SACoR (single aliquot combined regenerative-dose) protocol, is designed specifically to allow the effects of anomalous fading of feldspar luminescence signals to be reduced.

Full-3D Waveform Tomography for Southern California, *En-Jui Lee, Po Chen, Thomas Jordan, Philip Maechling, Marine Denolle, and Gregory Beroza* (Poster 036)

Our full-3D tomography (F3DT) uses 3D SCEC Community Velocity Model Version 4.0 (CVM4) in Southern California as initial model, a staggered-grid finite-difference code to simulate seismic wave propagation and the sensitivity (Fréchet) kernels are calculated based on the scattering integral and adjoint methods to iteratively improve the model. We use both earthquake recordings and ambient noise Green's function data, stacking of station-to-station correlations of ambient seismic noise, in our F3DT inversions. To reduce errors of earthquake sources, the epicenters and source parameters of earthquakes used in our F3DT are inverted based on full-wave method. An automatic waveform analysis algorithm that based on continuous wavelet transforms and a topological watershed method is used to pick waveforms full-wave inversions and make frequency dependent phase and amplitude measurements. Our current model shows many features that relate to the geological structures at shallow depth and contrasting velocity values across faults. The perturbations with respect to the initial model in some regions could up to 40% and relate to some structures do not exist in the initial model, such as southern Great Valley. The waveform fittings of earthquake waveforms and ambient noise Green's function data are both improved after iterations. The earthquake

MEETING ABSTRACTS

waveform misfit and summation of square of ambient noise Green's function group velocity delay time between observed waveforms and updated synthetic waveforms both reduced more than 50%.

High-Resolution Mapping and Analysis of Borderland Faults Using Multibeam Bathymetry Data, Mark R. Legg, Monica D. Kohler, Dayanthie Weeraratne, and Natsumi Shintaku (Poster 118)

We completed processing new high-resolution swath bathymetry data to map active Borderland fault structures and provide more accurate estimation of offshore earthquake and tsunami potential. New data obtained during deployment of the ALBACORE OBS array last year are combined with existing data offshore southern California to produce more complete maps of the seafloor morphology. Four areas of high-resolution bathymetry were mapped at 100-m grid spacing. The first area covers most of the northern Borderland from Point Arguello to the southern San Diego Trough offshore Baja California. The second area covers the northern part of the Inner Borderland and eastern Outer Borderland from San Nicolas Island to Oceanside centered around Catalina Basin and Santa Catalina Island. The third area covers the northern Outer Borderland, south of the Channel Islands and south of the San Nicolas Island escarpment. The fourth area covers the central Outer Borderland from San Nicolas Island to Velerio Basin west of northern Baja California. New multibeam bathymetry tracklines were chosen to follow major seafloor escarpments where active faulting is expressed by scarps and other lineaments in the seafloor morphology. Area 2 (Catalina) provides coverage of the major San Clemente fault system including triple junctions (fault wedge tips of Crowell, 1974) where major active faults intersect at each end of the Catalina Ridge. Area 3 (North Ferrello) provides coverage of the major Ferrello fault zone that extends to the southeast from Santa Rosa Island for more than 300-km into Mexican waters. The northern section of the East Santa Cruz Basin fault zone (ESCB) lies within the third area. Area 4 (South Ferrello) provides coverage of the southern two-thirds of the Ferrello fault zone that lies within U.S. waters; existing data provide some coverage of this fault zone in Mexican waters to the south. The southern sections of the ESCB fall within the South Ferrello map area. The transverse San Nicolas Island escarpment is covered by both Ferrello map areas, with the southern map providing coverage of the intersection with the ESCB to the east and the northern map covering the intersection with the Ferrello fault zone to the west. In our final analysis, we have identified numerous seafloor channels inferred to result from turbidite flows and deposition that may provide important piercing points where active faults are crossed, such as the San Diego Trough and San Pedro Basin fault zones.

Quantifying 3D ground deformation using multi-angle high resolution optical imagery, Sebastien Leprince, Francois Ayoub, James Hollingsworth, Jean-Philippe Avouac, and James Dolan (Poster 206)

We demonstrate how 3D ground deformations can be recovered using multi-angle high resolution satellite imagery such as provided by the Quickbird or Worldview satellites. In particular, we apply this technique to reconstruct the 3D displacement field induced by the Mw 7.2 2010 El-Mayor Cucapah earthquake. Full-field ground deformation is recovered using sub-pixel image matching and triangulation on a set of images acquired before the earthquake, and on a set of images acquired after the earthquake. This technique is implicitly equivalent to reconstructing two elevation models, before and after the earthquake, using stereoscopy, and matching them. We show that the results compete with the analysis of the pre and post-earthquake LiDAR acquisitions.

Investigation of structure and seismicity in the Los Angeles basin with a dense array, Dunzhu Li, Fan-Chi Lin, Brandon Schmandt, and Rob Clayton (Poster 274)

A recent 3D industrial survey in a subset of the Los Angeles basin near Long Beach, CA provides an remarkable opportunity to investigate the basin structure and local seismicity. The seismic dataset consist a 6 month nearly continuous recording of about 5400 vertical component geophone distributed across a 10 km by 7 km area with an average spacing of about 110 meters. Ambient noise correlations using 1 week of continuous data recover both surface-waves and P and S body-waves in the frequency range of 0.2-10 Hz. Eikonal tomography was applied to the

short period Rayleigh waves isolated by interferometry in order to invert for a shear velocity model of the upper 1 km. The model resolves clear structural contrasts associated with the Newport-Inglewood fault zone and it can aid in the active source reflection survey by constraining near-surface lateral velocity variations that are conventionally addressed through introduction of static correction. Efforts to robustly identify reflected and refracted body-wave phases and incorporate them into inversions for structure are ongoing. Teleseismic P waves for several events are clearly recorded in the frequency range of 0.3-1.5 Hz, and their utility for constraining upper crustal discontinuities via vertical component P receiver functions also is being explored. During the 6-month deployment of the array, approximately 20,000 small possible events were located, compared with 10 by the permanent stations of the Southern California Seismic Network. The daily counts of events show a very large variability. Updated results regarding structural imaging and characterization of local seismicity will be presented.

Foreshock sequence of the April 11, 2012, Mw 8.6 Indian Ocean earthquake, Xiangyu Li, Guangfu Shao, and Chen Ji (Poster 170)

The 2012 off northern Sumatra Indian Ocean earthquake sequence started with a Mw 7.2 earthquake in Jan 10th. According to USGS PDE locations, this foreshock's epicenter is 21 km northeast of the epicenter of the April 11 Mw 8.6 mainshock. Four of its aftershocks subsequently were located within 10 km of the mainshock epicenter (Ji et al., 2012). However, it is of interest to notice that right before the April 11 mainshock, no earthquake within 50 km of mainshock epicenter can be found in the same catalog during a half-month period from March 26 to April 10. Unfortunately, it is not clear yet whether this represents a pre-seismic "quiescence" period in seismic activity near the mainshock epicenter, which had been reported during the studies of several previous large earthquakes (Kanamori, 1981), or is simply caused by the incompleteness of the PDE catalog in this remote area. To answer this question we use hundreds of broadband records of the Jan 10th foreshock at global seismic stations as empirical Green's functions to locate the nearby earthquakes. For each station, the correlation between this record and the waveform from Jan10th to April 11th is calculated after bandpass filtering them between 0.01 and 0.033 Hz. A nearby earthquake with similar focal mechanism to the foreshock shall be associated with a peak in the resulted correlogram, though it might be invisible due to the ambient noise. After stacking hundreds of correlograms, our preliminary analysis captures over 500 events, one order of magnitude more than the number of nearby events in the PDE catalog during the same period. Seismic statistic analyses will be applied to this new catalog after --further improving the estimations of event locations and magnitudes. The seismic "quiescence" hypothesis will be testified. The proposed method shall be useful to study the foreshock and aftershock sequences of other oceanic large earthquakes in the remote area as well.

Subsurface Rock Damage Structure of the M7.1 Darfield and M6.3 Christchurch Earthquake Sequence Viewed with Fault-Zone Trapped Waves, Yong-Gang Li, Gregory De Pascale, and Darren Gravely (Poster 065)

The M6.3 Christchurch earthquake struck the Canterbury region in NZ's South Island on 22 February 2011, following ~6 months after the 2010 M7.1 Darfield earthquake in the same region. In order to document the subsurface structure of the damage zones caused by multiple slips in this earthquake sequence, we deployed two short linear seismic arrays in the Canterbury region to record aftershocks in 2011. Array 1 was across the Greendale fault (GF) on which the 4.5-m right-lateral slip was observed at surface rupture of the Darfield mainshock. Array 2 was located at the surface projection of aftershocks along the blind Port Hills fault (PHF) which ruptured in the Christchurch mainshock. We have examined waveform data for 853 aftershocks and identified prominent fault-zone trapped waves (FZTWs) with large amplitude and long wavetrains at stations of Array 1 within the ~200-m-wide rupture zone for aftershocks occurring along the GF and the PHF. The post-S durations of these FZTWs increase as event depth and epicentral distance increases, showing an effective low-velocity waveguide formed by severely damaged rocks extending along the GF and PHF at seismogenic depth,

but with variations in its geometry and velocity reduction along multiple rupture segments. The FZTWs infer that while the Darfield main rupture exposes at the surface over ~30 km along the E-W striking GF, it bifurcates two blind segments and extends eastward an additional ~5-8 km. The Christchurch main rupture is ~15-km in length on the blind PHF dipping to SSE, but it extends westward along the aftershock lineament approaching the eastern extension of the Darfield rupture. Two main rupture segments might connect through a weak portion of the low-velocity waveguide formed by rocks with milder damage beneath the dilatational fault step-over where accumulated seismic energy release was minimal in this earthquake sequence. The rupture segment of their largest M6 aftershock runs along an eastern blind branch of the PHF. Extensive observations and preliminary simulations of these FZTWs show that the main rupture zone on the GF is ~250-m wide with the maximum velocity reduction of 50% in the ~75-m-wide damage core zone, likely extending down to the depth of at least 8-10 km. Our study illuminates a potential approach to investigate the blind rupture zone in urban areas where the deployment of a seismic array is difficult, using FZTWs recorded at the array deployed at its surface section in suburban area.

Non-equilibrium thermodynamics in sheared hard-sphere materials,

Charles K. Lieou, Ahmed E. Elbanna, James S. Langer, and Jean M. Carlson (Poster 067)

We combine the shear-transformation-zone (STZ) theory of amorphous plasticity with Edwards' statistical theory of granular materials to describe shear flow in a disordered system of thermalized hard spheres, a prototypical model of granular fault gouge. The equations of motion for this system are developed within a statistical thermodynamic framework analogous to that which has been used in the analysis of molecular glasses. For hard spheres, the system volume replaces the internal energy as a function of entropy in conventional statistical mechanics. In place of the effective temperature, the compactivity characterizes the internal state of disorder. We derive the STZ equations of motion for a granular material accordingly, and predict the strain rate as a function of the ratio of the shear stress to the pressure for different values of a dimensionless, temperature-like variable near a jamming transition. We use a simplified version of our theory to interpret numerical simulations by Haxton, Schmiedeberg and Liu, and in this way are able to obtain useful insights about internal rate factors and relations between jamming and glass transitions in a granular system.

Rapid Triggering of Micro-Earthquake Repeating Sequences in West Taiwan: Observations and modeling,

Yen-Yu Lin, Nadia Lapusta, and Kuo-Fong Ma (Poster 157)

Repeating earthquake sequences (REs) – which consist of events with similar waveforms and locations – are used to study a wide range of earthquake science problems, from stress drops to rates of creep in surrounding areas. Using the TCDP borehole seismometers array, we discovered 290 REs during 35 months from November 2006 to September 2009 in west Taiwan, with magnitudes ranging from Mw -0.01 to 2.36. There are 2 to 13 events in each sequence. The locations of the REs, determined from stacked waveforms, show that the REs are distributed in a flat deformed zone within the depth of 9 to 13 km, similar to the overall micro-earthquakes distribution in the area (Lin et al., 2012). The majority of the REs, 207 out of 290, involve events with short recurrence times (< 7 days), called burst-type REs. The minimum recurrence time interval is 2 seconds. Such a short interval potentially indicates dynamic triggering between events. This result is in contrast to studies of the San Andreas fault, where burst-type REs are not common (Templeton et al., 2008).

To explore the potential mechanisms for rapid event recurrence, we are developing a model of repeating earthquakes based on rate-and-state friction laws. Such a model has been successfully used to explain the properties of REs on the San Andreas fault (Chen and Lapusta, 2009). In the model, several small patches governed by steady-state velocity-weakening friction are located in a close proximity to each other and surrounded by a larger velocity-strengthening region with a background loading slip rate. Our long-term simulations of slip in this model generate sequences of earthquakes of different magnitudes which trigger each other. Collectively, these events would appear as repeating, with similar waveforms and locations. We will report on our progress in determining

the source parameters compatible with the TCDP observations. Our focus is on exploring whether the rapid recurrence times of the order of seconds can be consistently achieved in this model, due to combination of dynamic triggering by seismic waves and rapid effects of postseismic slip, or whether additional factors such as fluid effects are required.

Properties of Shallow creep on the Southern San Andreas Fault from InSAR and GPS,

Eric O. Lindsey, Yuri Fialko, and Yehuda Bock (Poster 237)

We present a detailed characterization of surface creep and off-fault deformation along the Coachella Valley segment of the San Andreas Fault from 33.3-33.7 deg. North using a combination of campaign GPS and multiple InSAR viewing geometries. An array of 30 survey monuments spanning 3km across the fault at Painted Canyon was occupied with campaign-mode GPS between 2007 and 2012, providing a direct measurement of creep at that location; the rate of 3+/-1mm/yr is in good agreement with long-term geologic estimates of 2-4 mm/yr (Sieh and Williams, 1990). A combination of over 400 radar interferograms from ascending and descending Envisat (Tracks 356 and 77), ALOS (Tracks 213-214) (Tong et. al, 2012), and ERS (Track 356) were used to separate the creep signal from non-tectonic sources of deformation such as local subsidence, providing a high-resolution image of the near-fault horizontal deformation pattern. The results indicate a creep rate consistent with the GPS at Painted Canyon, and reveal along-strike variations in both the creep rate and effective shear zone width. This width varies from less than a few meters at Painted Canyon to as wide as 4km along the North Shore section of the fault. In this area, previous geologic and geodetic observations have not identified localized surface creep, while the satellite data indicates 3-4 mm/yr of fault-parallel surface deformation is distributed over a wide shear zone. Our data indicate non-steady behavior of shallow creep along strike as well as down-dip, implying that long periods of observations are needed to constrain average creep rates.

Reconstructing Initial Stress Condition for the 1987 Superstition Hills Earthquake,

Qiming Liu and Ralph J. Archuleta (Poster 093)

Dynamic rupture simulations have been widely used to study earthquake source physics and simulate ground motion from big earthquakes. Among the many ingredients (such as medium property, friction laws, state of stress, fault geometry, anelasticity, etc.) that go into dynamic rupture modeling, the most critical feature might be constructing the initial stress condition on the fault plane or even in the bulk (e.g. Andrews & Harris 2005). However, except in rare cases (e.g., SAFOD), the stress field near existing fault planes is not directly measurable. Instead, we have to resort to indirect methods to estimate the stress condition, such as borehole measurements, seismic focal mechanisms, topography and gravity fields, etc. One goal of SCEC4 is to integrate and reconcile various data sets to model the stress field (SCEC4 Community Stress Model).

Here we try to describe the stress condition on the Superstition Hills (SH) Fault just before the 1987 Mw 6.6 Superstition Hills earthquake. There are many factors that could make the stress condition heterogeneous, such as local elevation variation (e.g., Superstition Mountain), non-uniform subsurface medium properties, creeping behavior on part of the fault, conjugate fault systems in the region, etc. There is the additional factor: a Mw 6.2 earthquake and its aftershocks occurred on the conjugate Elmore Ranch (ER) Fault during the 12 hours before the SH earthquake. The projection of the Elmore Ranch Fault would intersect the Superstition Hills Fault almost exactly at the Mw 6.6 epicenter. It almost certainly must have perturbed the local stress field that then led to the nucleation of the Superstition Hills earthquake (Frankel & Wennerberg, 1989; Wald et al., 1990).

We will evaluate the effect of the Elmore Ranch sequence on the initial stress of the Superstition Hills Fault (e.g. Hardebeck & Michael, 2006). We will be cautious of the corresponding uncertainty due to the 3D velocity model, complex fault geometry in the preparation of initial stress condition for the next step dynamic rupture modeling.

MEETING ABSTRACTS

Theoretical and Numerical Results on Effects of Attenuation and Dispersion in Correlation Functions of Ambient Seismic Noise, *Xin Liu, Yehuda Ben-Zion, and Thomas H. Jordan* (Poster 171)

We use a simple theoretical approach to account for attenuation and dispersion in ambient noise cross-correlation functions with isotropic source distribution. The derivation of attenuation effects includes a quality factor $Q(\omega)$ and a complex phase velocity. Initial results show that attenuation generates asymmetry in the cross-correlation functions, and that attenuation and dispersion together shift the phases in the cross-correlation function. The theoretical derivations are compared with numerical simulations based on generation of synthetic noise waveforms by summing up contributions of numerous noise sources. We consider synthetic tests for situations involving isotropic/non-isotropic source distributions, far/near-field sources, and with/without attenuation. We also perform a 1D inversion for group/phase velocity in the synthetic tests. These tests indicate, in agreement with the theoretical results, that group velocity dispersion measurements might provide a more reliable metric than phase velocity measurements.

Coseismic slip gradient and rupture jump on parallel fault systems, *Zaifeng Liu and Benchun Duan* (Poster 068)

Field observations on historic slip distribution from large continental strike-slip earthquakes reveal a possible correlation between the abruptness of slip decreases as an earthquake rupture approaching a structural step in the fault system and the ability of the rupture to propagate through step. We set up numerical models with two parallel left-strike slip faults imbedded in an elastic medium to simulate the coseismic process of earthquake rupture, aiming to provide insights into the field observations. We find that the slip gradients calculated over the final 1 km of the ruptured fault have a linear relationship with both the corresponding average stress drop on the fault and the largest possible width of the step could be jumped by the propagating rupture. Our dynamic Coulomb stress analyses show that when the fault system has a smaller average stress drop during the coseismic process, the corresponding positive Coulomb stress region at the end of first fault is smaller, which reduces the largest width of steps that could be jumped. When the first fault has a larger average stress drop, the strong stopping phase at the end of the first fault produces a larger positive Coulomb stress region, which finally increases the ability of rupture to jump onto the nearby parallel fault.

Southern California crustal deformation map and long-term transient from InSAR time series analysis, *Zhen Liu, Paul Lundgren, and Sylvain Barbot* (Poster 230)

Differential interferometric synthetic aperture radar (InSAR) has a proven capability to image surface deformation of plate boundary zones at fine spatial resolution. The ~18 years of extensive SAR data collection over southern California makes it now possible to generate a long time interval InSAR-based line-of-sight (LOS) velocity map to examine the resolution of both steady-state and transient deformation processes. We present InSAR time series analysis results of crustal deformation in southern California using an extensive catalog of ERS-1/2 and Envisat data since 1992. We apply a variant of the Small Baseline Subset (SBAS) time series analysis approach to derive InSAR LOS velocity map and time series. A GPS derived crustal model is used to constrain long wavelength deformation signals while estimating and removing orbital ramp error. The spatiotemporal details of deformation signals provided by InSAR measurements, when combined with in-situ continuous GPS, enable the separation of tectonic and non-tectonic sources. We observe a clear transient variation over ~18 yrs across the Blackwater-Little lake fault system in the Eastern California Shear Zone. Integration with modeling results from viscoelastic models suggests that such long-term strain transient can be reasonably explained by a broad-scale viscoelastic relaxation process following the 1992 Landers and 1999 Hector Mine earthquakes. Our studies suggest that the long lasting postseismic transients from past large earthquakes can still perturb current strain observation near the faults in southern California and need to be accounted for in the estimates of fault slip rates and earthquake hazard.

Collaboratory for the Study of Earthquake Predictability: Recent Developments and Extensions, *Maria Liukis, Danijel Schorlemmer, John Yu, Philip J. Maechling, Jeremy D. Zechar, Maximilian J. Werner, Thomas H. Jordan, and*

the CSEP Working Group (Poster 047)

The Southern California Earthquake Center (SCEC) has been working with international partners to develop a Collaboratory for the Study of Earthquake Predictability (CSEP). The collaboratory is designed to support a global program for conducting prospective forecasting experiments under rigorous, controlled conditions and evaluating the results using transparent, community-accepted criteria specified in advance. There are now four testing centers in California, New Zealand, Japan, and Europe, with a total of 229 models under evaluation, and a fifth is being developed in China. In this presentation, we describe how the testing centers have evolved to meet the CSEP design goals and share our experiences in operating the centers since their inception. In particular, we detail the cyberinfrastructure improvements to the W. M. Keck Foundation Testing Center at SCEC. This prototype center has been operational since September 1, 2007, and currently hosts intermediate-term and short-term forecasts, both alarm-based and rate-based, for California and the Western Pacific, as well as for the global testing region. Current efforts are focused on the reduction of testing latencies and procedures for the evaluation of externally hosted forecasting experiments, with the goal of supporting the new USGS program in operational earthquake forecasting. We describe the open-source CSEP software available for personal use by scientists to perform independent study and evaluation of their models prior submitting them to the Testing Center (<http://northridge.usc.edu/trac/csep/wiki/MiniCSEP>). We also discuss how the CSEP infrastructure is being applied to geodetic transient detection and the evaluation of ShakeAlert system for earthquake early warning, and how CSEP procedures will be adapted to ground motion prediction experiments.

Modeling seismicity rate changes in Oklahoma and Arkansas, *Andrea L. Lenos and Andrew J. Michael* (Poster 056)

The rate of $M \geq 3$ earthquakes in the central and eastern US increased beginning in 2009, particularly in regions such as Oklahoma and central Arkansas where fluid injection has occurred (Ellsworth et al., SSA abs, 2012; Horton, SRL, 2012). We compare rate changes observed in Oklahoma, which had a low background seismicity rate before 2009, to rate changes observed in central Arkansas, which had swarms prior to the start of wastewater injection (Chiu et al., BSSA, 1984; Horton, SRL, 2012). In both cases, stochastic Epidemic-Type Aftershock Sequence (ETAS) models (Ogata, JASA, 1988) and statistical tests demonstrate that the background rate of independent events and the aftershock productivity must increase in 2009 in order to explain the observed increase in seismicity. Productivity is lower during the earlier tectonic swarms in Arkansas. The change in aftershock productivity may provide a way to distinguish manmade from natural earthquake rate changes and could provide insights into the physical mechanisms of induced seismicity.

We fit the ETAS model, which is based on empirical aftershock scaling laws such as Omori's Law and the Gutenberg-Richter magnitude distribution, to a 1973-2011 USGS PDE catalog of $M \geq 3$ Oklahoma earthquakes and a 1982-2012 ANSS catalog of $M \geq 2.2$ Arkansas earthquakes. To determine whether a rate increase is due to a change in background seismicity rate, aftershock productivity, or some combination of the two, we do the following: 1) fit the model parameters to the data, 2) convert origin times to transformed times (Ogata, JGR, 1992), and 3) use Runs and autocorrelation function tests to test the null hypothesis that the transformed times are drawn from a Poisson distribution with constant rate (as expected when no external processes trigger earthquakes besides a constant tectonic loading rate). In both cases a single set of parameters cannot fit the entire time period, suggesting that significant changes in the underlying process occurred. The null hypothesis is rejected in both Oklahoma ($p < 0.001$) and Arkansas ($p = 0.015$). Then, given a change point in 2009 (Ellsworth et al., SSA abs, 2012; Horton, SRL, 2012), we estimate ETAS parameters for both time periods to determine which parameters must vary. Space-time models

are unstable due to the low number of events and large location error in the earlier catalogs, but likelihood tests of the temporal models indicate the data are better fit when both background rate and productivity increase.

Preliminary dynamic rupture and ground motion models on the Claremont-Casa Loma stepover of the San Jacinto Fault, incorporating realistic fault geometry, *Julian C. Lozos, David D. Oglesby, Kim B. Olsen, and James N. Brune* (Poster 102)

The Claremont and Casa Loma strands of the San Jacinto Fault in southern California are separated by a 25 km long extensional stepover, which bounds a sedimentary basin. Both individual strands are themselves geometrically complex. A smaller fault strand is located within the stepover, approximately halfway between the two main strands. The width of the larger stepover approaches 4 km, which has been shown by prior observational and modeling work to be close to the upper limit for stepover width through which rupture may jump. The region within and surrounding the Claremont-Casa Loma stepover is densely populated, which further emphasizes the importance of understanding the rupture and shaking hazard associated with this fault system. We use the 3D finite element method to model dynamic ruptures on the Claremont-Casa Loma stepover, incorporating geometrical complexities based on the USGS Quaternary Fault Database and the SCEC Community Fault Model, in order to investigate the ability of the rupture to propagate through the geometrical complexities in this region, as well as the resulting ground motions. As compared to a stepover model with planar segments, the overall intensity and distribution of strong motion for the complex model is reduced, but there remains a region of decreased peak motions between the end of the nucleating fault and the second fault strand. In addition, rupture directivity is diminished near each bend in the fault. Due to this break in directivity, peak ground motions near the fault are weakest immediately after the rupture turns a bend, and are strongest and more widespread immediately before the next bend. Unlike the case of a stepover with planar segments, the shape and intensity of the ground motion distribution is not symmetrical across the fault; an alternating pattern of fault bends produces an alternating pattern for which side of the fault trace experiences higher ground motion. We are currently integrating a 3D velocity structure based on the SCEC Community Velocity Model into our dynamic models, which should significantly improve the accuracy of our ground motion estimates.

Citizen Science with the Quake-Catcher Network: Promoting seismology research and broader impacts activities in museums, libraries, and other free-choice learning venues, *William M. Luedtke, Kevin Chan, Danielle Sumy, Robert de Groot, Elizabeth Cochran, Nick Rousseau, Thomas Jordan* (Poster 262)

The Quake-Catcher Network (QCN) uses low-cost seismic sensors to record data in real-time on volunteer computers and engages participants in authentic science. The primary goal of this project was to develop pilot program to facilitate the installation and marketing of the QCN sensors for research and broader impacts activities in venues that provide free-choice learning opportunities. Achievements for this project include the installation of QCN research sensors at the San Bernardino County Museum, the University of Southern California-Department of Earth Sciences, and California State University, Los Angeles; Department of Geosciences. An installation protocol and QCN kit were developed to better facilitate future installations and promote program participation. The QCN website was updated to provide resources, content, and visibility for participating institutions. With sufficient density of sensors, the QCN may one day be used as an earthquake early-warning and forecasting tool, which complements the goals of the Uniform Earthquake Rupture Forecast (UCERF) version 3. UCERF provides an unparalleled opportunity to teach about the nature of scientific processes. Developed from multiple data sources and the collaborative efforts of many investigators UCERF is an example of how science is being done in the twenty-first century. Participation in QCN provides a concrete opportunity to engage with the science behind UCERF as well as a means to contribute to the data set for future versions of the Forecast. This project is a joint effort between the QCN and the

Earthquake Education and Public Information Center (EPIcenter) Network to further encourage earthquake and tsunami preparedness in California.

A Quasi-DYNAMIC Earthquake Simulator (QDYN) for earthquake cycle, slow slip and tremor modeling, *Yingdi Luo and Jean-Paul Ampuero* (Poster 278)

We have developed a Quasi-DYNAMIC earthquake simulator (QDYN), a boundary element software package to simulate earthquake cycles (tectonic fault slip) under the quasi-dynamic approximation (quasi-static elasticity with radiation damping). It is open-sourced and hosted online at <http://code.google.com/p/qdyn>. The code implements adaptive time stepping, shared-memory parallelization, and is capable to deal with multi-scale earthquake cycle simulations with fine details in both time and space. QDYN includes various forms of rate-and-state friction and state evolution laws, and handles complex fault geometry in 3D and 2D media, as well as spring-block simulations. It is equipped with a user-friendly interface and well-formatted graphical output.

In this presentation, we will show the details and applications of QDYN, including multi-scale simulations of Slow-Slip Event (SSE) and complex tremor migration patterns, conceptual cycle simulations of the 2011 Tohoku earthquake. In the simulations of SSE and tremor, we first generated the background SSE conveniently adapting cutting-off velocity for rate-and-state friction, then small brittle asperities (frictional unstable, velocity weakening patches) were applied and we successfully reproduced all the major tremor migration patterns observed in Northern Cascadia. In the conceptual Tohoku earthquake cycle simulation, we model the scenario with subduction zone with deep brittle asperities which producing both the high-frequency contents during the megathrust event and M7 earthquakes recurring every several years between each megathrust events. The results of QDYN simulations can also be used as initial conditions for fully dynamic simulations.

Paleoseismology of the San Jacinto Fault Zone, Claremont segment, at Mystic Lake, California, *Rainer Luptowitz, Sally McGill, Nate W.*

Onderdonk, Thomas K. Rockwell, Neta Wechsler, Joseph Berg, Breeanna Copeland, and Michelle Smith (Poster 133)

A new trench was excavated near Mystic Lake along a strand of the Claremont fault over a previous trench location. The new trench was excavated to a length of about 44 m and a depth of about 5 m. Prior work recognized 7 surface-rupturing earthquake events. This new, deeper trench exposed 4 older events. Some of the best evidence for these events is found in the north east half of the trench (see poster by Onderdonk). This poster will focus on the evidence in the southwest half of the trench which support the four older events. Event 8 is the latest of these events and is evident in one location in the southwestern half of the trench by a down warp of unit 700, overlain by a growth layer that pinches out against the folded unit 700, on top of which is the relatively horizontal unit 690. Event 9 is also only weakly suggested at two locations in the southwestern half of the trench, one where unit 800 (or 790?) caps a possible fissure, and elsewhere a clay seam terminates upward at the top of unit 800. Evidence for event 10 is seen where unit 900 is gently folded in several places with a growth layer pinching out against the fold and buried by unit 890. The earliest event noticed was event 11 with strong deformation of units 1000-1060 capped by units 940-960, which are only weakly deformed. These four new events extend the knowledge of the Claremont Fault paleoseismology. Aside from the four older events, additional evidence for previously documented event 7 was found in one location, where unit 600 and underlying units are offset 6-7 cm and then buried by unit 590 which was offset 1 cm or less in a younger event. Radiocarbon dates are pending.

Investigating absolute stress in southern California: How well do stress models of compensated topography and fault loading match earthquake focal mechanisms?, *Karen M. Luttrell, Bridget R. Smith-Konter, and David T. Sandwell* (Poster 039)

The 3-D orientation of the in situ stress field in Southern California is reflected in the focal mechanisms of moderate to large magnitude earthquakes. An extensive new catalog [Yang et al., 2012] contains 2310 high quality mechanisms from events with $M > 3$ in this region indicating a heterogeneous stress field, with strike-slip, reverse, and normal faulting

MEETING ABSTRACTS

in close proximity to one another. We attempt to reconstruct these observations by accounting for the stress fields from three sources: 1) the 3-D crustal stress imposed by topography of the surface and Moho, as constrained by gravity observations; 2) the 3-D earthquake cycle stress accumulated on locked fault segments; and 3) a 2-D regional stress field representing plate boundary scale tectonic driving stress. Based on the 3-D stress from topography, we are able to identify absolute lower bounds on the regional stress magnitude of 30 MPa NNE principal compression and 10 MPa ESE principal tension. We also solve for the best-fitting regional stress orientation for each focal mechanism. No single regional stress field is able to simultaneously predict orientations of both thrust and strike-slip earthquakes across southern California as a whole, although individual fault segments do suggest some smaller-scale homogeneity. By further analyzing spatial variations in the orientation of the best-fitting regional stress field, we can assess the significance of additional sources of stress such as secondary fault structures.

Vegetation Lineaments Near Pearblossom as Possible Indicators of San Andreas Foreberg-Style Faulting, David K. Lynch, Kenneth W. Hudnut, and Frank Jordan (Poster 141)

An isolated cluster of 24 natural vegetation lineaments (VLs) on and around Holcomb Ridge near Pearblossom, CA, were identified using Google Earth imagery. They ranged in length from 0.21 to 2.29 km (mean 0.8 km) and were ~15-20 m wide. The cluster and the VLs are ~3km north of the San Andreas fault and trend subparallel to it. The VLs mean headings strike $304^\circ \pm 11^\circ$ (1 sigma), or N56W, consistent with the local strike of the SAF. None of the VLs coincide with faults in USGS OF 2003-293 or in the CGS-USGS Quaternary Faults database, although one (VL15) clearly corresponds to a suspected fault identified by Dibblee (2002). The lineaments were visible on many earlier studies of the area (e.g. Barrows et. al 1975-1985) but were not marked or identified as being significant. Several lineaments cross the California aqueduct and were identified as faults in California Department of Water Resources reports.

Field reconnaissance revealed low, subtle scarps (0.5 - 2 m high) and offset channels (5-15 m) on several of the VLs. A few VLs coincide with metamorphic lineations mapped by Dibblee (2002) as Precambrian pendants of marble, dolomite, and mica schist. These VLs presumably indicate seasonally persistent moisture sources. If these VLs mark the surface traces of faults, they may indicate the presence of fractures associated with foreberg-like structures of the SAF. Florensov and Solonenko (1963) documented significant slip on similarly sized and oriented structures when mapping the 1957 Gobi-Altay earthquake surface ruptures.

Some lineaments (most notably V2, V3, and V4) are associated with recent topography. We infer that these are faults that have begun to move perhaps within the past few tens of thousands of years. Other VLs, (V9 & V10) appear to offset alluvial fan surfaces by several meters vertically. Further mapping is planned to determine the magnitude of any movement and its recency, whether or not the lineaments indicate foreberg-style structures, and if similar foreberg systems exist elsewhere along the SAF system. Such systems could accommodate nearly fault-normal compression by forming elongate doubly-plunging anticlinal folds that trend sub-parallel to the main through-going strike-slip system. These lineaments may indicate the presence of previously unrecognized hazards associated with secondary faults that subparallel the main strand of the SAF.

Do aftershock focal mechanisms agree with the stress tensors at aftershock hypocenters?, Elizabeth H. Madden, Gregory Beroza, and David D. Pollard (Poster 182)

Spatial correspondence between mainshock-induced Coulomb stress changes and aftershock distributions have been highlighted for many large earthquakes, suggesting that aftershocks occur because of mainshock stress increases. Therefore, the orientations of and slip along aftershock nodal planes are expected to be in general agreement with the stress change tensor at an aftershock hypocenter. However, the magnitudes of the remote stress field exceed those of the perturbed stress field, particularly away from the faults that slipped in the

mainshock, so an alternative hypothesis is that aftershocks respond predominantly to the remote stress field. This is assumed in typical inversions of aftershock focal mechanisms conducted to determine remote principal stress orientations and relative magnitudes. A third and persuasive alternative is that aftershocks respond to the total stress field present following the mainshock, due to the combined remote and perturbed stress fields. We evaluate this third hypothesis by modeling the total stress associated with slip during the 1992 M 7.3 Landers, California earthquake at the hypocenters of relocated aftershocks using the boundary element modeling program Poly3D. We compare the orientations of the aftershock slip vectors with the model shear stress resolved on aftershock nodal planes following the method of Beroza and Zoback (1994). This provides a rough assessment of the agreement between the model stress and aftershock orientations. We find that only 30 % of aftershocks agree with the model total stress and that this percentage decreases to 23 % over six years, when aftershocks are analyzed in cumulative bins. These results are consistent when models incorporate fault structures ranging from planar to non-planar and vertical to non-planar and dipping. Preliminary tests do not suggest that aftershock magnitude or focal mechanism quality influence results. We are currently running models to determine if aftershock depth and distance from the mainshock fault planes influence results. In the future, we will assess aftershock agreement with the remote stress field and the perturbed stress field alone. In addition, calculating the angle between the intermediate principal stress inferred from the aftershock focal mechanism and the model intermediate principal stress will quantitatively assess the mechanical agreement between aftershock orientations and model stress tensors.

Seismic Potential and Slip Behavior of Corrugated Reverse Fault Surfaces, Scott T. Marshall and Anna C. Morris (Poster 108)

To better understand the mechanics and seismic potential of non-planar fault surfaces, we present numerical modeling results of faults with sinusoidal corrugations in the down-dip direction. We introduce variations in corrugation wavelength, amplitude, and loading angle to determine the effects on slip behavior and seismic moment release. In general, model results suggest that corrugated faults slip less than planar faults. Changes in slip behavior are dominantly controlled by the amplitude/wavelength of corrugations and are thus nearly scale independent. Model results suggest that obliquely loaded wavy faults accumulate less strike-slip than a planar fault with the same tip line dimensions and average orientation. This result implies that slip direction is not a reliable indicator of regional stress direction and may at least partially explain repeated, nearly pure dip slip coseismic events at oblique plate boundaries. These results imply that using coseismic slip direction to infer regional stress direction may be unreliable, at least for single events. To assess the seismic potential of corrugated fault surfaces, we calculate the scalar moment release for all modeled faults. Although the scalar seismic moment release is always less for corrugated fault surfaces due to a greater reduction in slip compared to increased surface area, for geologically typical corrugation geometries, changes in total scalar moment release are not significant compared to planar faults. Techniques that utilize highly simplified fault geometries may therefore accurately reproduce scalar moment release, but will incorrectly predict coseismic slip magnitudes and distributions, as well as regional stress orientations.

Enhancing the Functionality for SCEC-VDO: Surface Map Coloring and Earthquake Statistics, Nolan Mattox, Christian Vanderwall, Chris

Kohlenberger, Michael Hodges, Marshall Rogers-Martinez, Thomas H. Jordan, Robert de Groot, Nick Rousseau, and Kevin Milner (Poster 296)

The 2012 Undergraduate Studies in Earthquake Information Technology (USEIT) Grand Challenge, Development Team 2 worked primarily on implementing generalized surface coloring functions to better visualize seismic datasets. In particular, the team implemented a more flexible coloring utility, allowing the user to color maps with a customizable color gradient, choose a discrete color scheme, or choose to color on a logarithmic or decimal scale. Additionally, the team created a more general seismic data interpolation function, allowing datasets of any size or shape to be properly colored based on a data point with associated intensity measurement values. This latter part coincided closely with a

new add-on in the SCEC-Virtual Display of Objects (SCEC-VDO) ShakeMap plugin called the "ShakeMap Generator", where VDO users can generate their own ShakeMap based on customizable parameters. The development team also developed an add-on to the earthquake catalog allowing the user to view and graph earthquake catalog data statistics, such as the magnitude frequency distribution. All of these new capabilities will allow users to visualize a variety of different surface maps (i.e. ShakeMaps and Seismic Hazard Maps) in customizable ways, as well as calculate and view statistics on various earthquake catalogs.

Constraining Moment Accumulation Rate on the Creeping Segment of the San Andreas Fault, *Jeremy L. Maurer, Kaj M. Johnson, and Paul Segall* (Poster 227)

The San Andreas Fault has historically been known for producing large earthquakes, especially in the Los Angeles and San Francisco areas. However, it is currently unclear whether the "creeping section" between these two areas, a 150-km long section of the fault extending from Parkfield to San Juan Bautista, could also produce large earthquakes. This section of the fault is known to be creeping at the surface and the along-strike variation of present-day creep between Parkfield and San Juan Bautista is well known from geodesy (e.g., Titus et al. [2006]). While some areas may creep at the long-term rate without accumulating strain in the surrounding rock, GPS data clearly show some level of strain accumulation in the creeping section; Ryder and Burgmann (2008) determined that the moment accumulation rate on the fault is equivalent to a M7.4 earthquake every 150 years. However, the fault slip inversion problem is well known to be underdetermined and therefore non-unique. Furthermore, it is ambiguous whether the slip deficit inferred from geodetic data will be recovered in future earthquakes or accelerated transient creep events. Our approach to the first problem is to estimate rigorous bounds on the moment deficit rate, independently of any regularizing functional (slip is not smoothed). Our approach to the second problem is to introduce physical constraints on the inversion that separate parts of the fault that are locked versus those that may be creeping at constant stress. We use GPS and InSAR data and an elastic block model and solve the constrained least squares problem for the backslip rate on the creeping section that minimizes the data misfit at a fixed moment accumulation rate. Systematically varying this fixed moment accumulation rate, we find that the data are fit by models with moment accumulation rates varying by as much as a factor of 3 with equivalent 150-year moment magnitudes of M6.8-7.6. However, physically-constrained inversions (creep constrained to constant stress) show that the area of the creeping section that is actually locked and accumulating stress is likely small and probably not capable of generating earthquakes as large as M6.8-7.6.

Decadal-Scale Crustal Deformation Transients in Japan Prior to the March 11, 2011 Tohoku Earthquake, *Andreas P. Mavrommatis, Paul Segall, Shin'ichi Miyazaki, Susan E. Owen, and Angelyn W. Moore* (Poster 211)

Excluding postseismic transients and slow-slip events, interseismic deformation is generally believed to accumulate linearly in time. We test this assumption using data from Japan's GPS Earth Observation Network System (GEONET), which provides high-precision time series spanning over 10 years. Here we report regional signals of decadal transients that in some cases appear to be unrelated to any known source of deformation. If this observation is commonplace, then it has strong implications for extrapolating contemporary deformation fields over the entire interseismic period.

We analyze GPS position time series processed independently, using the BERNESE and GIPSY-PPP software, provided by the GSI and a collaborative effort of JPL and Dr. Mark Simons (Caltech), respectively. We use time series from 891 GEONET stations, spanning an average of ~14 years prior to the M9 March 11, 2011 Tohoku earthquake. We assume a time series model that includes a constant velocity, as well as a constant acceleration. Postseismic transients are modeled by $A \log(1 + t/T)$. We also model seasonal terms and antenna offsets, and solve for the best-fitting parameters using standard nonlinear least squares. Uncertainties in model parameters are determined by linear propagation of errors. Noise parameters are inferred from time series that lack

obvious transients using maximum-likelihood estimation and assuming a combination of power-law and white noise.

Excluding stations with high misfit to the time series model, our results reveal several spatially coherent patterns of statistically significant apparent crustal acceleration in various regions of Japan. We interpret most of the accelerations to represent transient deformation due to known sources, including slow-slip events or postseismic transients due to large earthquakes prior to 1996. In addition to these signals, we find spatially coherent accelerations in the Tohoku and Kyushu regions. The Tohoku signal consists of east-southeastward acceleration covering ~200 km along the southeast coast of Tohoku and is spatially correlated with the extent of the March 11, 2011 M9 rupture area. We note that the inferred acceleration is present prior to the sequence of M7+ earthquakes beginning in 2003, and that short-term transients following these events have been accounted for in the analysis. A possible, although non-unique, cause of the acceleration is increased slip rate on the Japan Trench.

Seismic Response of the Instrumented UC Physics Building in the Canterbury Earthquakes, *Sam A. McHattie and Brendon A. Bradley* (Poster 266)

The Physics Building at the University of Canterbury is an eight storey reinforced concrete building comprised of structural frames and walls. The building was instrumented in 2006 with ten multidirectional accelerometers located on four different floors. These accelerometers recorded the ground motions from earthquakes on 4 September 2010 (M_w 7.1), 22 February 2011 (M_w 6.2) and many subsequent aftershocks. The recorded acceleration data was used to determine the gross structural characteristics of the building using response spectrum and frequency-domain techniques. Accelerometers on the first, fourth and eighth floors were used to examine the pseudo-spectral response amplification over the building height. The fundamental periods along both axes of the building were also computed based on several ground motion records. A simple numerical model of the structure with one node per floor was used to scrutinize typical assumptions in simplified structural modelling. The numerical model was able to match the observed peak floor displacements on the floors with accelerometers, poorer accuracy was achieved for modelling the time series of relative displacements on the 8th floor.

Stratigraphic Record of Vertical Crustal Motions in the Past 2-3 Ma Along the Coachella Valley Segment of the San Andreas Fault, Mecca Hills, California, *James C. McNabb and Rebecca J. Dorsey* (Poster 109)

Sedimentary rocks exposed on the NE margin of Coachella Valley in the Mecca Hills record vertical crustal motions along the San Andreas and associated strike-slip faults. We interpret a complex history of subsidence, transport, deposition, and uplift based on mapping and measuring of sedimentary rocks, analysis of sedimentary lithofacies, and determination of transport directions from clast imbrications and cross-bedding. The 330 m-thick Mecca Fm rests non-conformably on Precambrian and Cretaceous crystalline rocks SW of the Painted Canyon Fault (PCF), and is not present NE of the PCF. The Mecca Fm is likely late Pliocene or early Pleistocene in age (Boley et al., 1994), and consists of boulder conglomerate with SSE to WSW paleoflow. It fines up into sandstone and is gradationally overlain by the lower member of the Palm Spring Formation (PSF). The PSF is likely younger than 2.0-2.6 Ma (Boley et al., 1994) and older than the 0.74-Ma Thermal Canyon Ash high in the section (Rymer, 1989). The lower PSF is 340 m thick with SE paleoflow, and the main facies are fluvial sandstone, distal alluvial fan conglomerate, and a thin lacustrine limestone that correlates across the PCF. The contact between the lower and upper PSF changes from a local conformable contact in the central Mecca Hills to a widespread angular unconformity elsewhere. The upper PSF is ~650 m thick and displays transport to the SSE, with local exceptions. It is highly variable and includes alluvial-fan conglomerate, fluvial to eolian sandstone, lacustrine mudstone, and lake-margin facies. The capping Ocotillo Fm is an ~25 m thick conglomerate with SSW to WSW paleoflow that thickens into a wedge on the NE side of the PCF.

We infer that the PCF experienced SW-side-down slip during deposition of the Mecca Fm, and has recently been inverted as a steep, SW-side-up

MEETING ABSTRACTS

oblique-reverse fault. Stratigraphic thicknesses indicate that ~1.3 km of uplift has occurred at a rate of ~1.8 mm/yr since 740 ka. This study reveals a complex pattern of rapid, punctuated vertical motions that likely are driven by geometric complexities in the San Andreas Fault zone. A nearly continuous, 60 x 6 km strip on the NE side of Coachella Valley is undergoing uplift at a scale exceeding that of local fault-zone complexities, suggesting an additional regional control. Future work will refine the depositional ages, provenance, basin dynamics, and controls on 4D patterns of vertical strain along the San Andreas Fault in this area.

An earthquake in a maze: compressional rupture branching during the 11 April 2012 M8.6 off-Sumatra earthquake, Lingsen Meng (Poster 076)

Geophysical observations of the 2012 Mw 8.6 Sumatra earthquake reveal unprecedented complexity of dynamic rupture. The surprisingly large magnitude results from the combination of deep extent, high stress drop and rupture of multiple faults. Back-projection source imaging indicates that the rupture occurs on distinct planes in an orthogonal conjugate fault system, with relatively slow rupture speed. The ESE-WNW ruptures add a new dimension to the seismotectonics of the Wharton Basin which was previously thought to be controlled by N-S strike-slip faulting. The rupture followed an exceptionally tortuous rupture path. It featured two episodes of branching into fault segments that were experiencing increased compressive dynamic stresses, hence increased frictional strength. By conducting 2D dynamic rupture simulations, we find that the compressional branching can only occur under slow rupture speed and low apparent friction coefficient. Poroelastic effects can also contribute by buffering the dynamic clamping. We suggest that serpentinized minerals may provide low friction, fluids and dynamic weakening down to 25 km depth, and ductile shear heating instability may provide a weakening mechanism from 40 to 60 km depth. The absence of known weakening mechanism in the intermediate depth range suggests that rupture may penetrate over velocity-strengthening regions.

Systematic search for missing earthquakes in Southern California around the 2010 Mw7.2 El Mayor-Cucapah earthquake, Xiaofeng Meng, Zhigang Peng, Xiao Yu, and Bo Hong (Poster 180)

Whether static or dynamic stress changes is the dominant mechanism for triggering earthquakes in near field is currently under debate. Previous studies on earthquake triggering mostly examined seismicity rate changes around the occurrence time of large earthquakes based on existing earthquake catalogs. However, such catalogs could be incomplete immediately after the mainshock, which may cause apparent seismicity rate changes that are unrelated to stress changes. The 2010 Mw7.2 El Mayor-Cucapah earthquake induced significant static and dynamic stress changes in Southern California, where has dense seismic network coverage. Hence, the El Mayor-Cucapah earthquake is a perfect case for testing triggering mechanisms. According to the Southern California Seismic Network catalog, the seismicity rate near Salton Sea, where static Coulomb stress changes decreased, clearly increased immediately after the mainshock and dropped below the pre-mainshock level within a few tens of days. However, the seismicity rate near San Jacinto fault, where static Coulomb stress changes increased, remained high up to several months after the mainshock. Such pattern suggests that dynamic triggering may be dominant in short period, while static triggering took over in longer period. To check whether such patterns could be caused by catalog incompleteness, we apply a waveform-based matched filter technique to systematic detect possible missing events within Southern California one year before and after the El Mayor-Cucapah mainshock. We use ~40,000 template events covering a wide region in Southern California and run the detection codes on multiple GPU cards, which can significantly reduced the computation time. Our preliminary results show that 2167 template events are detected one day before and after the mainshock, which is ~2 times more than listed in existing catalog. We plan to extend the same analysis to longer times before and after the mainshock. With more complete catalog, we can identify the genuine seismicity rate changes for better comparison with the static and dynamic stress changes pattern, which could help to contribute to the aforementioned debate on static vs. dynamic triggering of aftershocks.

Factors controlling shallow co-seismic deformation: Quantifying distributed co-seismic deformation of the 1992 Landers earthquake.,

Chris W. Milliner, James Hollingsworth, James Dolan, Sebastien Leprince, and Francois Ayoub (Poster 080)

Near-field co-seismic deformation can be measured using sub-pixel optical image correlation. We use the program COSI-Corr to co-register, orthorectify and correlate pairs of high-resolution NAPP aerial photos taken before and after the 1992 Landers (Mw 7.3) earthquake. Using this technique, we are able to measure the detailed horizontal displacement field produced by this earthquake. Detailed investigation of both the surface displacement field and geology of the fault zone allow us to better quantify the extent to which geological properties, such as fault zone maturity and lithology, control variability in the location, width and magnitude of distributed deformation at the surface. Horizontal surface displacement of the Landers earthquake is determined by co-registering and correlating 14 image pairs, acquired 2 years before and 3 years after the earthquake. Although the spatial resolution of the aerial photos are ~1 meter, COSI-Corr can detect horizontal surface movements as low as 10 cm (corresponding to 1/10 of the input photo resolutions). We extract along-strike displacement profiles from the COSI-Corr-derived displacement maps, which are then compared to published coseismic displacement data measured by field geologists. COSI-Corr offers the advantage of measuring displacement over a far wider aperture than that available to field geologists who are often restricted to a small number of discrete offset markers. Thus, where field measurements underestimate those determined by optical image correlation, we assume this difference to result from distributed deformation missed by field surveys. Furthermore, using displacements measured by COSI-Corr we can quantify the width of the deformation zone across the fault by measuring the distance between the minimum and maximum displacements either side of the fault. Knowledge of the location, width and magnitude of distributed deformation for the Landers rupture has implications for understanding the mechanics of fault zones, as well as the geological factors which control near-surface co-seismic behavior, such as fault zone maturity and lithology.

Aftershock Probabilities on Southern California Faults from a Million-Year RSQSim Catalog, Kevin R. Milner, Thomas H. Jordan, Keith B. Richards-Dinger, and James H. Dieterich (Poster 062)

It is well known that the short-term rate of large aftershocks following a large earthquake on the Southern San Andreas Fault (SSAF) is high relative to the long-term rate (Reasenberg and Jones 1989), but the spatial distribution of the hazard increase is more challenging to quantify. We use a one-million-year synthetic earthquake catalog generated by the RSQSim physics-based simulator (Dieterich and Richards-Dinger 2010) to explore the spatiotemporal distribution of large aftershocks in the Southern California fault system. An interesting example is the Mojave section of the SSAF, where, in the first week following large (M7+) events, the average rate of equally large earthquakes increases by two orders of magnitude, and almost 3 orders of magnitude for M7.5+ events. The rate gains conform to magnitude-frequency distributions that are characteristic rather than Gutenberg-Richter: the rates of M7.5+ aftershocks are significantly higher than M7.0+ aftershocks. We quantify the spatial distribution of the hazard increase in the first year following initial events by analyzing participation rate gains on neighboring faults. For initial events on the Mojave section, the rate gains are highest on neighboring sections (suggesting an "unzipping" of the SSAF). In particular, the participation rate of the Coachella section in magnitude 7+ events increases tenfold, from $\sim 10^{-2.3}$ to $\sim 10^{-1.3}$. Similarly, the M7+ participation rate of the Carrizo section increases from $\sim 10^{-2.3}$ to $\sim 10^{-1.5}$, a rate gain of 6, and the Western Garlock's from $\sim 10^{-2.9}$ to $\sim 10^{-2.0}$, a rate gain of 8. The rate gain on the San Jacinto fault is much smaller, about 1.5. Elastic rebound explains the decrease by a factor of 5-10 in the M7+ participation rate on the rupture surface. This methodology is highly dependent on the fault geometries involved, and a variety of patterns are observed for initial events on different fault sections. We illustrate how post-event rate gains can be carried through to hazard calculations, producing short-term hazard and risk estimates.

Temperature dependence of frictional stability of gabbro and granite, Erica K. Mitchell, Kevin M. Brown, and Yuri Fialko (Poster 075)

We conducted a series of experiments using a direct shear apparatus to determine the rate-state friction parameter (a-b) as a function of temperature. We performed tests on fine-grained gabbro and Westerly granite. The setup used in our study has a relatively low stiffness compared to commonly used triaxial setups, and unstable slip occurs more readily under variable loading conditions. We employed three methods of determining (a-b). First, we performed velocity-stepping tests and in case of stable sliding we measured (a-b) directly. Second, we performed normal stress-stepping tests. We calculated (a-b) based on the critical normal stress required to initiate oscillations in coefficient of friction. Third, we fitted the time-series of stick-slip events using a model of a spring-slider that incorporates the rate-state constitutive equations (Ruina, 1983). We used a Monte Carlo algorithm to invert the observed time-series of stress and displacements for the parameters a and b. Results from the three methods are in general agreement. We find that (a-b) of gabbro is weakly negative at room temperature (-0.001), and increasingly negative up to 400 C (-0.003). Results from He et al., 2006 suggest that (a-b) of gabbro is weakly positive up to 500 C (0.002), and becomes strongly negative at 600 C (-0.01). He et al. noted that low total slip produces positive values of (a-b), while samples that have accumulated larger total slip have negative (a-b) values, possibly due to fabric development within the gouge. This may explain the difference between the results of our study and those reported by He et al., since our experiments were performed after multiple centimeters of "run-in" displacement. Our experiments on granite also revealed unstable behavior over almost the entire range of temperatures, with even stronger velocity-weakening. This is consistent with our previous results for frictional healing of granite at high temperature (Mitchell et al., in review), but is inconsistent with results from previous studies that suggest that granite should slip stably at temperatures greater than 300 C (Stesky et al., 1974; Blanpied et al., 1995). These results indicate that more experimental data are required to understand the nature of the brittle-ductile transition in the Earth's crust, and highlight the importance of rock composition, gouge fabric development, and the presence of fluids in a fault's ability to nucleate and propagate earthquake ruptures.

The Length to which an Earthquake will go to Rupture: Information Gathering, *Alexander E. Morelan, Steven G. Wesnousky, and Glenn P. Biasi* (Poster 139)

We expand on an existing empirical dataset to examine structural controls on earthquake rupture propagation and fault-to-fault jumps. The observational dataset is composed of mapped historical earthquake surface rupture traces in continental crust. The goal is to understand the connection between geometrical discontinuities and the ultimate extent to which a rupture will propagate. Empirical measures developed from actual earthquake ruptures provide independent data against which to compare predictions, including the Uniform California Earthquake Rupture Forecast 3. We define geometrical discontinuities as step-overs, gaps, splays, and parallel faults along the length of the rupture trace. The expanded dataset contains 62 earthquakes (35 strike-slip, 14 reverse, 13 normal). Results show that longer ruptures do not necessarily have more steps. Within the dataset, the number of earthquakes is a decreasing function of the number of steps observed along strike. The relationship also holds if the data are divided into strike-slip, normal, and reverse type subsets. These observations are consistent with dynamic modeling that associates steps with energy sinks that hinder and can stop rupture propagation. Within the dataset it is also observed that normal and reverse mechanism events have propagated across larger step sizes than have strike-slip ruptures. The difference seems to be associated with the mechanism of the earthquake. The rupture process of a dip-slip earthquake does not involve volumetric changes within steps as it does in steps along strike-slip ruptures. As such, geometric roughness and step sizes that would kinematically hinder strike-slip ruptures have less effect on dip-slip earthquakes.

Kinematic earthquake rupture scenarios for the Salt Lake segment, Wasatch fault, *Morgan P. Moschetti, Stephen Angster, Leonardo Ramirez-Guzman, Stephen Hartzell, Stephen Personius, and William Stephenson* (Poster 008)

We develop a fault model and kinematic earthquake rupture scenarios for the Salt Lake segment of the Wasatch fault to investigate the variability of

earthquake ground motions in the Salt Lake City, Utah region. The fault model incorporates geological observations and a geophysically derived basin model. Fault dip values within the basin are defined from field measurements and slip vector analysis of Bruhn et al. (1987). Beneath the sedimentary basin, as defined by the Wasatch Front community velocity model (Magistrale et al., 2006), we impose a constant fault dip of 50 degrees to seismogenic depths. An important feature of the fault model is that it is consistent with the mapped, left step-over between the Warm Springs and East Bench strands, which merge near 3 km depth. The step-over geometry presents an alternative to existing fault models that allow continuous surface rupture between the fault strands (e.g., Roten et al., 2011). Kinematic rupture scenarios are constructed for a M7 earthquake using correlated random distributions with the method of Liu et al. (2006) to derive spatial distributions of slip amplitude, rise times and rupture velocities. More than fifty rupture scenarios are generated, representing the use of three hypocenters, three correlation lengths for the calculation of slip distributions, three corner frequencies and two sub-shear average rupture velocities. We use a single fault model for all ruptures but vary the slip distributions, corner frequencies and average rupture velocities used to generate the rupture scenarios. To vary rupture directivity, we use three hypocenters for each kinematic scenario, producing northward and southward unilateral ruptures and a bilateral rupture. The ranges of the kinematic rupture parameters are constrained by empirical relations and seismological observations; values selected for the scenarios are appropriate to the target M7 normal-faulting earthquake and generally represent the mean and two-sigma values. Future work will use the rupture models in 3-D earthquake simulations to estimate the variability in ground motions that may be expected from a M7 earthquake on the Salt Lake segment of the Wasatch fault.

Broadband Ground Motion Simulations Using Hybrid of Low Frequency deterministic and High Frequency Source-and Site-Specific Empirical Greens Function Approach, *Ramses Mourhatch and Swaminathan Krishnan* (Poster 022)

The purpose of this work is to produce site-specific broadband ground motions in southern California from a suite of large earthquakes on the San Andreas fault. A key limitation of seismic wave propagation simulations is that the seismic wave-speed structure of the earth is not well resolved for propagating high-frequency waves. The current deterministic methods are capable of propagating waves with frequencies up to 0.5 Hz, well below that required for many engineering applications. We are using a hybrid approach for generating ground motions from large earthquakes. The low frequency content (< 0.5 Hz) of the ground motion is generated deterministically using a spectral element based program called SPECFEM3D, which incorporates the regional wave-speed structure in three dimensions. The low frequency content from such a deterministic simulation is then superposed with high frequency shaking generated using source- and site-specific approach. We adopt the classical empirical Green's function (EGF) approach of summing recorded seismograms from past small earthquakes with suitable time-shifts to generate seismograms for large events. Whereas, in the past, the magnitude of events used as EGFs were limited to within 1 or 2 units of the target event's magnitude, this source- and site-specific approach allows us to use a vast number of seismograms from very small earthquakes (magnitudes 2.5 - 3.5) as EGFs to produce the high-frequency content of large earthquakes (magnitudes 6.0 - 8.0). The key advances in this work are: (i) expanding the limits of applicability of the EGF method by utilizing the large quantity of the seismic data available in the low magnitude range and (ii) eliminating the need for filtering or convolution to match Brune's spectrum within the frequency band of interest using a subtle variation in the summing procedure. In this variation the small events are unevenly time shifted within the rise time of each subfault to best match its assigned source time function. We validate our approach by simulating the 2004 Parkfield (Mw 6.0) and 1999 Hector Mine (Mw 7.1) earthquakes at various stations across southern California.

Upgrades and Improvements to the SCEC Community Fault Model: Increasing 3D fault complexity and compliance with surface and subsurface data, *Craig Nicholson, Andreas Plesch, John Shaw, and Egill Hauksson* (Poster 122)

MEETING ABSTRACTS

We present major upgrades to the SCEC Community Fault Model (CFM) and anticipate formal release of these improvements as CFM v.4.0 this fall. The release incorporates improvements in 3D fault representations, a detailed fault surface trace layer, and a new fault naming and numbering scheme that allows for closer links to the USGS/CGS Quaternary Fault database (Qfaults). Fault representations in CFM are now available referenced to the modern WGS84 datum and the new surface layer in CFM allows upgraded 3D fault models to be registered to the more detailed Qfaults and other digital fault maps. However, registration of older CFM faults to the Qfault surface traces is still ongoing. We use alignments of hypocenters and nodal planes from relocated earthquake catalogs [e.g., Hauksson et al., 2012] to better define the subsurface geometry of active faults. These new revised CFM fault models and interpretations allow for more non-planar, multi-stranded 3D fault geometry, and help characterize a more complex pattern of fault interactions at depth between various fault sets and linked fault systems. This increasing 3D fault complexity for CFM representations is particularly evident along the multi-stranded San Andreas fault and adjacent secondary structures in the Coachella Valley and through San Geronio Pass, as well as for the complex surface and subsurface ruptures associated with the Laguna Salada and related faults involved in the El Mayor-Cucapah sequence. The CFM fault database hierarchical naming and numbering scheme was substantially revised and sent out for review, in addition to a requested ranking of revised CFM 3D fault representation quality. These rankings are being used to target areas of CFM for further improvements and upgrades, as well as to identify a preferred set of compatible fault models among the various alternative representations in CFM. The revised hierarchical naming scheme allows for flexible database searches and easier identification of fault components, alternative representations, and possible system-level associations of individual 3D fault elements that comprise CFM. This hierarchical scheme also allows for grouping related individual faults under a higher level fault system (e.g., Southern Frontal Fault System for the Raymond, Hollywood, Santa Monica, and Malibu Coast faults) to help facilitate identification of potentially larger earthquake ruptures between such kinematically linked fault segments.

3-D earthquake surface displacements from differencing pre- and post-event LiDAR point clouds, Edwin Nissen, Ramon Arrowsmith, Aravindhan Krishnan, and Srikanth Saripalli (Poster 214)

The explosion in sub-meter resolution aerial LiDAR topography along active faults across California provides a baseline against which to compare repeat LiDAR datasets collected after future earthquakes. We present a new method for determining 3-D coseismic surface displacements and rotations by differencing pre- and post-earthquake LiDAR point clouds using an adaptation of the Iterative Closest Point (ICP) algorithm, a point set registration technique widely used in medical imaging, computer vision and graphics. There is no need for any gridding or smoothing of the LiDAR data and the method works well even with large mismatches in the density of the two point clouds. To explore the method's performance, we simulate pre- and post-event point clouds using real (B4) LiDAR data on the southern San Andreas Fault perturbed with displacements of known magnitude. For input point clouds with 2 points per square meter, we are able to reproduce displacements with a 50 m grid spacing and with horizontal and vertical accuracies of approximately 20 cm and 4 cm, respectively. In the future, finer grids and improved precisions should be possible with higher shot densities and better survey geo-referencing. By capturing near-fault deformation in 3-D, LiDAR differencing with ICP will complement satellite-based techniques such as InSAR which map only certain components of the surface deformation and which often break down close to surface faulting or in areas of dense vegetation. It will be especially useful for mapping shallow fault slip and rupture zone deformation, helping inform paleoseismic studies and better constrain fault zone rheology. Because ICP can image rotations directly, the technique will also help resolve the detailed kinematics of distributed zones of faulting where block rotations may be common.

An inverse modeling code for obtaining earthquake source parameters from InSAR data, Erika Noll (Poster 223)

Current catalogs of earthquake source parameters from InSAR data are currently based upon the published literature (e.g. Weston et al., 2011). Published studies rely on a number of different inverse modeling programs that incorporate different assumptions and methodologies. They therefore give varying results, which can be difficult to compare with each other since it is difficult to separate the variability that arises from the data from variability that arises from using different methods or assumptions. In order to eliminate the model-based uncertainty, it may be necessary to use a single, uniform methodology and apply it to all future earthquakes. We are developing MATLAB codes to find the best-fitting earthquake source parameters from InSAR deformation data, and then evaluate the most efficient, accurate, and meaningful level of detail in the generated model that is permitted by the data.

We have tested our prototype codes against data from the 1995 Dinar, Turkey earthquake. The unwrapped ERS interferogram for the event was downsampled using quadtree decomposition to provide a manageable data set for inversion. The current code solves for nine parameters of a simple rectangular fault with uniform slip, and outputs the coordinates of the fault's endpoints and its dip, rake, slip, and minimum and maximum depths. The code currently solves for these parameters using one of MATLAB's basic nonlinear optimization solvers. Future improvements will include optimizing using the Metropolis algorithm in order to provide estimates of parameter uncertainties, solving for values linearly where possible, and implementing multiple, nested slip patches to provide a quantifiable level of complexity in models, which can then be used in statistical tests of model parameter significance.

Space-Time Model and Analysis of Repeating Earthquakes in Parkfield Segment, Shunichi Nomura, Yosihiko Ogata, and Robert M. Nadeau (Poster 110)

We propose a new space-time model for a set of earthquake sequences repeating at same hypocenters scattered on a tectonic plate boundary. Nadeau et al. (1995) discovered many series of earthquakes with almost the same hypocenters and seismic waves in Parkfield segment of San Andreas Fault, California. They recurred very regularly and therefore renewal process can be applied better than Poisson process as a stochastic model of the repeating earthquakes. But when we apply a renewal process to these sequences, we will confront with the problem that the inter-event times have non-stationary trends. These trends of the recurrence intervals are related to the changes of the slip rate near their hypocenters, and Nadeau and McEvilly (1999) estimated the space-time changes of the slip rate in Parkfield segment from their dataset.

In our study, we assume the stress loading process by Matthews et al. (2002), which models cyclic mechanism of repeating earthquakes with steady loading rate and Brownian perturbation. We incorporate the non-stationary trend by time-transformation as in Lindqvist (1993) and represent space-time structure by smooth cubic B-spline functions allocated to partitioned grids. On estimating the coefficients of spline bases, we use a penalty function for unsmooth change into the model to avoid over-fitting for the dataset. Thus, we analyzed the dataset of repeating earthquakes in Parkfield segment clustered and provided by Robert M. Nadeau. They are recorded by the HRSN and their moment magnitudes range from only M-0.7 to M1.8. This dataset contains the occurrence data from 1987 to 2011, including aftershocks of the 2004 Parkfield earthquake at M6.0. Since the seismicity pattern drastically and discontinuously changed by this main shock, we divided the dataset in into two periods, before and after it, and analyzed these two datasets independently. The same feature as Nadeau and McEvilly (1999) pointed out are seen in our results, and also the triggering effects of other large earthquakes exceeding M4 are seen in some sequences. After the 2004 earthquake, its aftershocks appeared at some sequences and decayed basically along the same Omori-Utsu law. However, their behaviours except for aftershock decay differ among repeating sequences. In our result, prominent change in loading rate occurred around the 2004 Sumatra-Andaman earthquake at M9.1 as pointed out by Taira et al. (2009), but showed contrastive behaviour among some sequences.

Earthquake rupture dynamics in complex geometries using coupled summation-by-parts high-order finite difference methods and node-

centered finite volume methods, *Ossian J. O'Reilly, Eric M. Dunham, Jeremy E. Kozdon, and Jan Nordström* (Poster 086)

We present a 2-D multi-block method for earthquake rupture dynamics in complex geometries using summation-by-parts (SBP) high-order finite differences on structured grids coupled to finite volume methods on unstructured meshes. The node-centered finite volume method is used on unstructured triangular meshes to resolve earthquake ruptures propagating along nonplanar faults with complex geometrical features. The unstructured meshes discretize the fault geometry only in the vicinity of the faults and have collocated nodes on the fault boundaries. Away from faults, where no complex geometry is present, the seismic waves emanating from the earthquake rupture are resolved using the high-order finite difference method on coarsened structured grids, improving the computational efficiency while maintaining the accuracy of the method.

In order for the SBP high-order finite difference method to communicate with the node-centered finite volume method in a stable manner, interface conditions are imposed using the simultaneous approximation term (SAT) penalty method. In the SAT method the interface conditions and boundary conditions are imposed in a weak manner. Fault interface conditions (rate-and-state friction) are also imposed in a provably stable manner using the SAT method. Another advantage of the SAT method is the ability to impose multiple boundary conditions at a single boundary node, e.g., at the triple junction of a branching fault.

The accuracy and stability of the numerical implementation are verified using the method of manufactured solutions and against other numerical implementations. To demonstrate the potential of the method, we simulate an earthquake rupture propagating in a nonplanar fault geometry resolved with unstructured meshes in the fault zone and structured grids in the far-field.

What Can Surface Slip Distributions Tell Us About Fault Connectivity at Depth?, *David D. Oglesby* (Poster 099)

Fault traces on the Earth's surface are often discontinuous. In many earthquakes, however, rupture propagates across numerous fault segments, leading to the question of whether these segments are connected by a single through-going fault at depth. To help answer this question, it would be useful if the connectivity of fault segments at depth were manifested as an observable feature of the surface slip distribution, which could be mapped in the field. In the present research, I use 3D dynamic models to investigate the impact of fault connectivity at depth on the surface slip distribution in an earthquake. In particular, I compare results for faults with several coplanar segments that are disconnected by locked patches on the surface but are connected to a through-going fault at varying depths, as well as faults that are entirely disconnected or entirely connected. I find that the deeper the depth of connection between the segments, the lower the slip on the individual segments. Segments that are entirely disconnected produce roughly elliptical surface slip profiles that are almost indistinguishable from those of segments that are connected at depths below around 8 km. For segments that are connected up to shallower depths, the surface slip distributions become flatter in the middle, with higher slip gradients near the segment edges. This effect is increased as the along-strike width of the segment increases. For small (< 20 km along strike) segments, though, these effects might not be easily distinguished from slip heterogeneity induced by other factors, such as heterogeneous stress, material properties, and fault geometry. These results appear to be robust with respect to whether the fault stress is depth-dependent or not. Thus, it may be difficult under most circumstances to discern fault connectivity at depth from surface slip mapping unless the connection is rather shallow (1-3 km) and/or fault segments are longer than 20 km; in such cases, high slip gradients near the segment edges might be indicative of connection below the surface. The results may have implications for the predictability of earthquake size, ground motion, and seismic hazard.

Progress towards developing an improved chronology for slip-rate and paleoseismic record of the central Garlock fault using luminescence dating, *Steven G. Okubo, Evan M. Wolf, Belinda J. Roder, Edward J. Rhodes, Sally F. McGill, James F. Dolan, Lee J. McAuliffe, Mike J. Lawson, and Wendy A. Barrera* (Poster 147)

We present updated luminescence dating results for samples from two sites along the central Garlock fault, California. At the site of El Paso Peaks, a well defined sequence of playa sediments trapped between a small alluvial fan and the shutter ridge of the central Garlock fault provides the opportunity to assess technical innovations in luminescence dating by comparison to a robust radiocarbon chronology. At this site, luminescence dating has the potential to provide improved resolution for the paleoseismic record, by dating sediment horizons from which no material suitable for radiocarbon dating was recovered. At the site of Christmas Canyon West, a few miles further east, numerous small offsets of depositional and erosional alluvial fan features provide the opportunity to determine slip rates for a variety of timescales spanning the past couple of thousand years. We review both the challenges involved in developing a reliable luminescence chronology for sediment deposition, and also in relating this chronology to erosional events and fault slip.

What PGD and PGV values collapse mid-rise steel, special moment frames or make them unrepairable?, *Anna H. Olsen and Thomas H. Heaton* (Poster 271)

For the SCEC Ruptures to Rafters initiative, we simulate the responses of eight steel, special moment frames in 64,765 synthetic ground motions from physics-based simulations of crustal, California earthquakes with magnitudes ranging from 6.3 to 7.8. We use fully nonlinear finite element models of six- or twenty-story moment frames with either a stiffer, higher strength design or a more flexible, lower strength design. The frame models have sound or fracture-prone welds. As an example of the results, both the six- or twenty-story, more flexible frames with sound welds (a design consistent with existing buildings in California) have a ten-percent probability of collapse in ground motions with a peak ground displacement (PGD) of roughly 1.2 m and peak ground velocity (PGV) of roughly 1.7 m/s. If the twenty-story frame has fracture-prone welds, however, it has a ten-percent collapse probability when PGD is roughly 0.7 m and PGV is roughly 0.7 m/s. Why find the PGD and PGV values corresponding to a ten-percent collapse probability? In the current approach to building design, engineers deem acceptable a ten-percent probability of collapse in the "maximum considered earthquake" ground motion. If these buildings were built today, the stated intensity-measure values would be consistent with "maximum considered earthquake" ground motions for the greater Los Angeles and San Francisco areas. Thus, we turn the engineering question "what building design has a ten-percent collapse probability in the 'maximum considered earthquake' ground motion" into a seismological question "what PGD and PGV values should engineers assume in Los Angeles or San Francisco to have an exceedance probability of roughly two-percent in fifty years (or a 2500-year return period)?"

Extending the paleoseismic record back in time at the Mystic Lake site on the Claremont fault, northern San Jacinto fault zone, *Nate W.*

Onderdonk, Sally McGill, Tom Rockwell, Neta Wechsler, Erik Gordon, and Erik Haaker (Poster 124)

The Mystic Lake paleoseismic site is located within a small (.4 km wide) step over within the Claremont fault zone in the northern San Jacinto Valley. Trenches excavated at the site in 2009 and 2010 provided exposures of seven ground-rupturing earthquakes in the upper 1.5 m of strata, which corresponds to the past 1700 years. The timing of these events is constrained by 50 radiocarbon dates. The most recent event occurred sometime between 1744 and 1853 AD and the oldest event occurred sometime between 579 and 846 AD. The average recurrence interval for these seven events was 160 to 210 years.

In June and July of 2012 we excavated a deeper (4 m deep) trench across the main fault to look for older events. The trench exposed evidence for an additional four earthquakes recorded in the deeper strata, which were expressed as upward terminations, fissure fills, folding, and thickening of units across faults. Approximately 200 detrital charcoal samples were collected and will be used to constrain the timing of these additional events. We anticipate that this longer record will allow better comparisons of the earthquake history at Mystic Lake with paleoseismic records from other nearby sites to help evaluate patterns of strain distribution along the San Jacinto fault in the late Holocene.

MEETING ABSTRACTS

The ARIA project: Advanced Rapid Imaging and Analysis for Natural

Hazard Monitoring and Response., Susan E. Owen, Frank Webb, Mark Simons, Paul Rosen, Jennifer Cruz, Sang-Ho Yun, Eric Fielding, Angelyn Moore, Hook Hua, Piyush Agram, and Paul Lundgren (Poster 041)

ARIA is a joint JPL/Caltech coordinated effort to automate geodetic imaging capabilities for hazard response and societal benefit. Over the past decade, space-based geodetic measurements such as InSAR and GPS have provided new assessment capabilities and situational awareness on the size and location of earthquakes following seismic disasters and on volcanic eruptions following magmatic events. Geodetic imaging's unique ability to capture surface deformation in high spatial and temporal resolution allow us to resolve the fault geometry and distribution of slip associated with any given earthquake in correspondingly high spatial & temporal detail. In addition, remote sensing with radar provides change detection and damage assessment capabilities for earthquakes, floods and other disasters that can image even at night or through clouds. These data sets are still essentially hand-crafted, and thus are not generated rapidly and reliably enough for informing decision-making agencies and the public following an earthquake.

We are building an end-to-end prototype geodetic imaging data system that would form the foundation for an envisioned operational hazard response center integrating InSAR, GPS, seismology, and modeling to deliver monitoring, actionable science, and situational awareness products. This prototype exploits state-of-the-art analysis algorithms from technologists and scientists. These algorithms enable the delivery of actionable products from larger data sets with enhanced modeling and interpretation, and the development of next generation techniques. We are collaborating with USGS scientists in both the earthquake and volcano science program for our initial data product infusion.

We present our progress to date on development of prototype data system and demonstration data products, and example responses we have run such as generating products for the 2011 M9.0 Tohoku-oki, M6.3 Christchurch earthquakes, the 2011 M7.1 Van earthquake, and several simulated earthquake response exercises.

Geometry of fault slip zones at depth from quantitative analysis of seismic catalogs, Yaman Ozakin and Yehuda Ben-Zion (Poster 187)

Seismic catalogs provide the highest resolution data for imaging the subsurface geometry of fault zones. In this study we use observed earthquake catalogs and basic scaling relations to calculate the cumulative density of seismic potency associated with the catalog data. The cumulative potency density provides direct information on the geometry of seismic slip zones at depth. We assign a potency density distribution for each event depending on its focal mechanism, location uncertainty and magnitude. Summing individual potency density distributions provides a potency density field that represents the geometry of the seismically active zones in the region covered by the catalog. The method is tested with synthetic catalogs, lab experiments and relocated catalogues. We apply the method for various sections of the San Jacinto fault zone. Results for the Hemet step-over region suggest the existence of a continuous fault zone structure within the complex volumetric structure in the region.

Initial Results from the UCERF3 Long-term Earthquake Rupture Forecast, Morgan T. Page, Edward H. Field, and Kevin Milner (Poster 048)

We present results from an inversion-based methodology developed for the 3rd Uniform California Earthquake Rupture Forecast (UCERF3) that simultaneously satisfies available slip-rate, paleoseismic event-rate, and magnitude-distribution constraints. Using a parallel simulated-annealing algorithm, we solve for the rates of all ruptures that extend through the seismogenic thickness on major mapped faults in California. This inverse approach eliminates the need for expert-opinion voting on rupture rates, allowing for more transparent, objective, and reproducible results than previous earthquake rupture forecasts. The inversion methodology also allows for the incorporation of multi-fault ruptures, which eliminates the magnitude-distribution misfits that were present in earlier models. We show that the UCERF3 inversion solutions match slip-rate and

paleoseismic event-rate data better than the previous model, UCERF2. Furthermore, many possible sets of rupture rates fit the available data. We present results from an array of logic-tree branches that span the range of plausible models.

Assessment of site conditions and empirical site response at stations recording near-field extreme ground motions during the 2008 Mogul, Nevada earthquake swarm, Aasha Pancha, Satish Pullammanappallil, Glenn Biasi, John N. Louie, and Craig dePolo (Poster 034)

The 26 April 2008 Mw 5.0 Mogul, Nevada earthquake, located at a shallow depth of 3.1 km, was the largest event during a shallow earthquake swarm that began in February 2008 and persisted for several months. Strong ground motions at the four closest stations installed at the time of the mainshock event all exceeded accelerations of 300 cm/s² and velocities of 14 cm/s. The largest peak acceleration vector during the mainshock event was recorded at station MOGL (1.19g; 1164 cm/s²), which at the time was among the 25 largest recorded earthquake accelerations worldwide. Aftershocks were measured at eight additional Mogul-area sites. As part of NEHRP-IMW grant, both shear-wave and P-wave geophysical techniques were used to characterize and map lateral velocity heterogeneity beneath these twelve near-field seismic sites. Shear-wave velocities were obtained as a function of depth to 100 m depth using refraction-microtremor (ReMi) arrays. A series of one-dimensional soundings along each of the arrays were interpolated to obtain a 2D shear-velocity section. 2D P-wave sections were obtained from hammer refraction surveys using a non-linear optimization approach. The 2D shear-velocity sections together with 2D P-wave sections show complex site conditions beneath these stations. Some of these sites may be crossed by local faults, and the velocity sections reflect this possibility. These resultant site condition assessments at these near-field sites will contribute towards quantification of local site response and calibration of the high peak ground motions recorded during both the mainshock event and the foreshock/aftershock swarm events. We also empirically evaluate spectral amplification, relative to a rock site, at each of the ANSS strong motion stations within the urban areas of Reno and Sparks, Nevada using ground motions from foreshocks and aftershocks of the 2008 Mogul earthquake. Response spectra from Mogul events show a strong similarity to those calculated using regional events. These empirically derived site effects are compared with average shallow-shear wave velocities to 30 m and 100 m depth (Vs30 and Vs100) beneath the ANSS sites. Statistical analyses show amplification tends to be smaller as Vs30 and Vs100 increase, showing a dependence of ground motion on site conditions.

Automated Determination of Fault Slip Model from GPS Network Signals After an Earthquake, Jay W. Parker, Margaret Glasscoe, and Andrea Donnellan (Poster 207)

The SCEC Workshops on Transient Anomalous Strain Detection are leading to a number of approaches for automatic characterization of local deformation events occurring in a region of dense GPS stations, such as PBO. We present a simple method, and show that it characterizes earthquake fault orientation and mechanism for four diverse coseismic cases: the Hector Mine earthquake, the San Simeon earthquake, the Parkfield (2004) earthquake, and a simulated event centered near Whittier, California (SCEC transient case IV-C). The steps of the characterization method are: a) choose a circular disk from initial reports of time, location and magnitude, or from examination of principal components of the regional GPS time series; b) Determine a coseismic displacement at each station by differencing the mean for a week before and a week after the event. c) spawn a suite of optimal inversion runs to determine a single fault-patch rectangle and slip (strike-slip, dip-slip, and tensile motion). The optimization application "simplex" has been found to converge more reliably when several strike and dip angle cases are used as seeds; since simplex uses the chi-square criterion as a measure of quality, only the best fitting inversion need be retained. d) report and plot observed vs. calculated displacements, calculated moment magnitude, and model-interpolated displacement fields on a dense grid of geographical points (including strain and tilt). Future improvements include treatment of seasonal signals, more complicated faulting, and long-term transient signals. But the method presented here by its

simplicity proves useful for quick inclusion into rapid earthquake characterization systems, for scientists and decision makers.

What can crustal deformation tell us about California's earthquake future? Lessons from UCERF3, Tom Parsons (Talk Wed 08:00)

We want to characterize seismogenic deformation in California to make earthquake probability calculations. UCERF assumes that earthquake rates are proportional to deformation rates; in particular, the rates that faults slip. Extensive use of GPS observations is a new feature brought into UCERF3. Geodetic measurements tend to be more areally comprehensive than geologic offset observations. However, all measures are subject to considerable uncertainty that include dating errors and modeling assumptions. The ~150-yr earthquake catalog is shown to identify sites of future activity in California, but it is temporally limited and may be incomplete for infrequent high magnitude events.

How best to balance these deformation measures into a form that can be translated into future earthquakes? I describe our efforts to test, compare, contrast, and apply five candidate deformation models that use geodetic and/or geologic measurements to calculate fault slip rate and residual "off-fault" seismogenic deformation: (1) a group of block models, (2) an FEM, (3) a buried dislocation model, (4) a geologic model, and (5) the UCERF2 deformation model. We find that all fit the vast majority of observed data well, and at first glance are viable representations of California deformation within data constraints.

However, every model had problems that required iterations and revisions. This is caused in part by the UCERF3 earthquake rate approach that breaks faults into ~5-10 km long subsections, meaning more section rates must be found than before. Even if a given model fits 95% of subsections to data - an acceptable standard for a scientific publication - it only takes a few anomalous results to cause important changes to hazard.

Traditional PSHA methods of working from identified earthquake sources may underreport hazard when applied to an area as large as California, where it is unlikely that every fault has been discovered. By contrast, geodetic techniques may overreport hazard because they record virtually all surface strain whether it is seismogenic or not. Indeed geodetic deformation models imply increased moment release (14%-25%) compared with the UCERF2 model and the earthquake catalog.

The UCERF3 process offers hope that complimentary data are applicable to hazard assessment. However, there remains an information gap that necessitates consensus judgments on how best to balance some conflicting results from different temporal and spatial deformation measures.

Tomographic imaging of the tectonic tremor zone beneath the San

Andreas fault in the Parkfield region, Dana E. Peterson, Clifford H. Thurber, David R. Shelly, Ninfa L. Bennington, Haijiang Zhang, and Justin R. Brown (Poster 177)

The fine-scale seismic velocity structure around zones of tectonic (nonvolcanic) tremor and low-frequency earthquakes (LFE's) has been imaged successfully in subduction zones. This success is due in part to the occurrence of earthquakes in the subducting slab beneath the zone of tremor and LFE's. Such studies have found the tremor and LFE's to lie within zones of reduced seismic velocity and high Vp/Vs, which have been interpreted to reflect high pore fluid pressure (e.g., Shelly et al., 2006). For the San Andreas fault, the observed tremor and LFE's in the Parkfield region occur at depths greater than 15 km, which is below the deepest conventional earthquakes in the region. This makes tomographic imaging of the tremor zone more challenging. We use a combination of P and S arrival times and corresponding differential times from stacked seismograms of LFE's (Shelly and Hardebeck, 2010) along with absolute and differential times from shallower microearthquakes to image the three-dimensional P- and S-wave velocity structure to ~20 km depth. Our initial results indicate the LFE's near SAFOD lie within or adjacent to zones with slightly reduced P-wave velocity and more sharply reduced S-wave velocity. The estimated Vp/Vs values are approximately 1.85 to 1.95 in these zones. The elevated Vp/Vs values are interpreted to reflect high pore fluid pressure and low effective stress. This is consistent with

results from subduction zones and with observations of triggering and tidal modulation of LFE's and tremor on this deep extension of the SAF.

Self-healing slip pulses driven by thermal decomposition: Towards identifying dynamic weakening mechanisms in seismic observations,

John D. Platt, Robert C. Viesca, and Dmitry Garagash (Poster 090)

Seismological observations indicate that earthquake ruptures commonly propagate as slip pulses, with slip duration at any location on the fault being much shorter than the total event duration [Heaton 1990]. Theoretical work has linked these slip pulses to low values of the background driving stress on the fault [Zheng and Rice 1998].

Recent experiments [Han et al. 2007; Brantut et al. 2008] have shown that fault materials may thermally decompose during shear. These endothermic reactions release pore fluid, leading to an increase in pore pressure and a decrease in temperature [Sulem and Famin 2009]. An Arrhenius kinetic controls the reaction rate, and dynamic weakening only occurs when the temperature reaches a critical temperature triggering the reaction. This is in contrast with thermal pressurization where the pore pressure increases smoothly with slip.

Previous theoretical studies of thermal decomposition have focused on simple mechanical systems with imposed slip rates [Sulem and Famin 2009], or coupling to a spring-slider model [Brantut et al. 2011]. We present the first solutions to couple thermal decomposition with dynamic rupture, extending the model in Garagash [2012] to solve for self-healing slip pulses. For a range of driving stresses there are two possible slip pulses, compared with a single solution for thermal pressurization alone. One solution corresponds to small slip and a low temperature rise that precludes the reaction; the other is a larger slip solution with weakening due to thermal pressurization at the rupture tip, and weakening due to thermal decomposition in the middle of the pulse. A dramatic drop in fault strength accompanies the onset of the reaction, leading to peak slip rates coinciding with the onset of the reaction.

For thermal pressurization alone the maximum strain rate always occurs at the rupture tip, and depends sensitively on the driving stress. Thermal decomposition is identified by slower rupture speeds, longer slip duration and more dramatic strength drops. The peak slip rates occur away from the rupture tip, and are insensitive to changes in the driving stress. For deeper events the ambient temperature is higher, causing the reaction to initiate earlier, and the peak slip rate to move towards the rupture tip. Often the total slip in a pulse is linked to a critical slip required to activate the reaction, suggesting a decrease in slip with depth.

Can self-organization of shear zones control the scale and structure of plate boundaries?, John P. Platt, Louis Moresi, and Thorsten W. Becker (Poster 114)

Several inter-related concepts suggest that ductile shear zones cutting the main body of the lithosphere can self-organize in such a way that they control their spacing and cumulative width at any given depth. Microstructural weakening involves damage processes such as grain-size reduction by dynamic recrystallization, the mixing and dispersal of phases in polymineralic rocks, and the development of lattice preferred orientations. These processes require that at any given depth and temperature (a) the yield strength of the undeformed material be exceeded, and (b) sufficient permanent strain occurs that these processes can cause weakening. The development of shear zones therefore requires that the ambient stress remain at the yield stress, and hence the shear zones are likely to develop a cumulative width such that they can accommodate the imposed plate boundary velocity at that level of stress. We examine the way shear zones evolve under these boundary conditions, and the controls on shear zone spacing and continuity under different temperature conditions and in different materials.

Dissipative heating complicates this picture because it has a strongly scale-dependent effect on the evolution of shear zones. If shear zones lose heat by conduction, they will reach an average temperature differential from the ambient value that depends on the square of their thickness and on the depth below the surface. Dissipative heating and temperature-dependent weakening will therefore favor small numbers of

MEETING ABSTRACTS

thick shear zones. We examine the inter-relationships between these two groups of effects.

Understanding Slip on Triggered Faults in the Presence of a Large Regional Deformation, *Moises M. Ponce-Zepeda, Andrea Donnellan, and Jay Parker* (Poster 268)

The Mw 7.2 El Mayor-Cucapah (EMC) earthquake occurred on April 4th 2010 with an epicenter 48 km SSE of Calexico, CA. Slip associated with the EMC event is on the order of 3 meters, whereas slip on the faults north of the rupture is measurable in centimeters. Unmanned Air Vehicle Synthetic Aperture Radar (UAVSAR) data has been collected in the Salton Trough, north of the US border since 2009, and has been flown six times since the EMC event in order to monitor change in the area. The resulting interferograms encompass the northern most extent of the main rupture, as well as the surrounding area north of the border. The interferograms show slip after the EMC event where there had previously been no evidence of faulting. The displayed slip corresponds to the Yuha fault, a recently discovered NE trending sinistral fault with 4.5 cm of displacement and a subtly expressed fault scarp. The large signal from the EMC event, superimposed over the much smaller signals from faults to the north-east, make it difficult to infer details of behavior on the responding faults. Using QuakeSim tools it is possible to test the level to which we can invert for slip on the corresponding faults north of the rupture. We used QuakeSim's forward dislocation modeling program called Disloc to create a UAVSAR equivalent interferogram of the published four fault mainshock slip parameters and slip from the Yuha Fault. We then used the Simplex component of QuakeSim to model elastic inversions of crustal deformation from the simulated interferograms. The series of models tested how well one can invert the synthetic data for small slips when there is a large regional deformation gradient from the main fault. One variation consisted of modeling fixed parameters for the main fault while varying different parameters for the Yuha fault such as strike, location, and strike slip and dip slip motions. The next step is to invert the observed UAVSAR interferogram for characteristics of slip along the Yuha fault. The QuakeSim tools make data accessible for scientists at every level to garner a better understanding of active tectonics earthquake processes.

Using Risk Targeted Ground Motions to Evaluate Seismic Hazard Models, *Peter M. Powers* (Poster 050)

The use of risk targeted ground motions (RTGM; Luco et al., 2007) simplifies the process of evaluating and comparing seismic hazard models. RTGM, which were adopted by the Building Seismic Safety Council (BSSC) in conjunction with the 2009 update to the NEHRP Provisions, have the advantage that they are scalar valued and consider an entire hazard curve at a particular site. Prior to 2009, "uniform-hazard" (e.g., the ground motion value with a 2% probability of being exceeded in 50 years) was used as the basis for the US Seismic Design Maps. Assuming that the capacity against collapse of structures designed for "uniform-hazard" ground motions is equal to the corresponding mapped value at the location of the structure, the probability of its collapse in 50 years is also uniform. In reality, there is significant uncertainty in the structural capacity of buildings, such that site-to-site variability in the shape of ground motion hazard curves results in a lack of uniformity. Designing for uniform-hazard ground motions does not necessarily result in buildings with uniform probability of collapse in 50 years, or "uniform-risk". To calculate RTGM, the hazard curve at a site is iteratively combined, via a "risk integral", with fragility functions for different target ground motions. The target ground motion is varied until the iterations converge on a result that would yield a 1% probability of collapse in 50 years. As a proxy for small and large buildings, RTGM values are calculated at 0.2 sec and 1.0 sec spectral accelerations, respectively. It should also be noted that, in engineering practice, RTGM is taken as the lesser of the probabilistic and deterministic ground motion at a site. For the purposes of this presentation, only the probabilistic component is considered. Such a straightforward metric that considers an entire hazard curve alleviates the need to examine multiple points on a curve for consistency (e.g., 2%, 5%, 10% in 50 years) and is particularly useful when dealing with a large number of hazard models. As an example, I use RTGM to compare the numerous branches of the 2nd and 3rd versions of the Uniform California Earthquake Rupture Forecasts

(UCERF2 and UCERF3) to the USGS 2008 National Seismic Hazard Map (NSHM) data as well as alternate implementations of the 2008 NSHM. This case study demonstrates how RTGM may be used to verify hazard software, as well as to identify deficiencies and evaluate assumptions that go into hazard model.

A 77-Fold Speedup and 100 Tflops Acceleration of Seismic Wave Propagation AWP-ODC on Heterogeneous Supercomputers, *Efecan Poyraz, Jun Zhou, Dong Ju Choi, Amit Chourasia, and Yifeng Cui* (Poster 035)

We have developed a highly scalable 3D finite difference GPU code based on AWP-ODC for earthquake simulations. This real world CUDA-MPI code allows efficient utilization of accelerators on multicore GPU systems. The performance is tuned through algorithm-level data locality for the GPU hierarchy, and novel overlapping design of data communication between GPUs. Benchmarks on M2090-based NCCS Titan demonstrated over 77-fold speedup and perfect weak scaling sustaining 100 TFlops in single precision for 49 billion mesh points using 952 GPUs. We also report the actual wave propagation simulations whose accuracy has been validated against the original AWP-ODC CPU production code. Further enhancement of this application is under development for hybrid multicore architectures towards production capabilities to meet petascale seismic computing needs.

Preservation of the seismic cycle in a continental low-angle, oblique-normal fault: West Salton detachment fault, USA, *Mitchell R. Prante, Susanne U. Janecke, and James P. Evans* (Poster 135)

The seismicity of low-angle normal faults (LANFs) has been a topic of persistent controversy. Previous studies have documented slip on normal faults at < 30° dip; however, the seismic potential of LANFs remains a subject of debate. Documentation of ancient seismicity along exhumed LANFs can test the hypothesis that LANFs generate large earthquakes. Pseudotachylite (Pt, rapidly quenched frictional melt) is the most convincing evidence for ancient seismicity in exhumed fault zones. We document evidence for multiple earthquakes along a LANF from 2.5-7.5 km depths. The West Salton detachment fault is a NNW-striking, shallowly-dipping LANF that accommodated transtension in the Salton Trough, CA, from L. Miocene to E. Pleistocene time. Fault rocks documented here and in previous work include Pt, fault breccia, cataclasite, and ultracataclasite. Thick (~ 1 m), laterally extensive, black, aphanitic, layered accumulations of Pt in the fault core and hanging wall and footwall, contain evidence for a melt origin. Pt is intermixed with cataclasites and proto-mylonite, with some cross-cutting quartz and calcite veins, and alteration. Brittle deformation includes cross-cutting faults and fractures as well as reworked Pt in fault-gouge and breccias. Calcite twin thickness and geometry constrain the ambient temperature conditions to $\geq 170^\circ\text{C}$. Assuming a typical geothermal gradient (25-30°C/km), calcite veins and older Pt formed at depths ≥ 5.6 km. Partial melt of quartz fragments in Pt matrix suggest a melt temperature $>1500^\circ\text{C}$, and a coseismic temperature increase of up to $\sim 1300^\circ\text{C}$. Crystal-plastic deformation of tonalite in the hanging wall includes: undulose extinction, subgrains, deformation lamellae, grain-boundary bulging in quartz, and limited undulose extinction in feldspar. The observed crystal-plastic deformation is consistent with temperatures between 300-500°C. Because the crystal-plastic deformation is pervasive in the fault core and hanging wall damage zone, we interpret this deformation to be associated with post-seismic recrystallization. Crystal-plastic deformation associated with Pt has been documented by other workers. We conclude that overprinted brittle and plastic deformation and multiple episodes of melt-injection are consistent with multiple large-magnitude earthquakes and local recrystallization associated with coseismic temperature perturbation in the WSDF at a low-angle.

Earthquake Nests as Natural Laboratories for the Study of Intermediate-Depth Earthquake Mechanics, *German A. Prieto* (Poster 179)

The physical mechanism of intermediate-depth earthquakes is still under debate. In contrast to conditions in the crust and shallow lithosphere, at temperatures and pressures corresponding to depths >50 km, rocks ought to yield by creep or flow rather than brittle failure. Some physical process has to enable brittle or brittle-like failure for intermediate-depth

earthquakes. The two leading candidates for that are dehydration embrittlement and thermal shear runaway. Given their great depth, intermediate-depth earthquake processes can't be observed directly. Instead we must rely on a combination of seismology and the study of laboratory analogs to understand them.

Earthquake nests are regions of highly concentrated seismicity that are isolated from nearby activity. In this paper we focus on three intermediate-depth earthquake nests - Vrancea, Hindu Kush and Bucaramanga, and what they reveal about the mechanics of intermediate-depth earthquakes. We review published studies of tectonic setting, focal

mechanisms, precise earthquake locations and earthquake source physics at these locations, with an emphasis on the Bucaramanga nest. All three nests are associated with subducting lithosphere and at least two of the nests have consistently larger stress drops compared to shallow seismicity. In contrast, the Bucaramanga nest has a larger b -value,

larger variability of focal mechanisms and shows no evidence of aftershock sequences unlike the other two. We also report for the first time finding a significant number of repeating earthquakes, some with reverse polarity.

Given the nature and characteristics of earthquake nests, they can be thought as natural laboratories. Future seismological studies of intermediate-depth earthquakes in nests will likely enlighten our understanding of their physical mechanisms.

SKS Splitting offshore California from ALBACORE, *Joseph Ramsay, Paul M. Davis, and Monica D. Kohler* (Poster 279)

The development and evolution of the Pacific-North America plate boundary offshore Southern California is of great geodynamical interest. For better understanding, the Asthenospheric and Lithospheric Broadband Architecture from the California Offshore Region Experiment (ALBACORE) was initiated. ALBACORE is a network of 24 broadband and 10 short-period ocean bottom seismometers (OBSs) deployed across the southwestern region of the Pacific-North American plate boundary. Other than at scattered island stations present seismic array data ends at the coastline due to the difficulty of measurements further to sea. The experiment is intended to study many aspects of the Pacific-North American plate boundary. In this study we calculate SKS splitting parameters in an effort to measure the anisotropy of the region. The first step involved determining the orientations of each seismometer due to twisting during deployment. P wave arrivals are used and waveforms of each OBS are compared to nearby island stations of the California Seismic Network. The horizontal waveforms from the OBS's are rotated until the rotated components achieved maximum correlation with North and East components at a nearby station. The rotation angle is further constrained by particle motion. Once orientations are established, we calculate SKS splitting parameters by minimizing energy in the transverse component.

Effects of Uncertain Primary Assumptions on Earthquake Source Imaging, *Hoby Razafindrakoto and Martin Mai* (Poster 158)

Robust kinematic source imaging is of great importance in earthquake seismology as diverse studies depend on accurate rupture models, for instance seismic hazard assessment, aftershock prediction and dynamic rupture modelling. However, when we design our method for earthquake source inversion, physical assumptions are required that are in general non-unique and an oversimplification of the reality. Particular choices in prior assumptions are mapped into the model space, but are rarely rigorously analyzed and quantified.

The main goal of this study is to investigate the contribution of variability in prior assumptions on the a posteriori model parameter uncertainty. For this purpose, we use a Bayesian technique that infers the ensemble of all possible source models that are consistent with data. We particularly explore the possibility of constraining the kinematic source inversion by taking into account the forward modelling uncertainty associated with the variability in Earth structure, which are in general neglected in previous studies. Additionally, we carry out a series of tests concerning the starting model and fault parameterization. We use synthetic test based on the

"Source Inversion Validation" exercise and describe the earthquake rupture in term of slip rate, rupture time and rise time defined on a regular grid on the fault surface. Our preliminary results show that the maximum posterior likelihood indicates a major slip patch located around the hypocenter, which is consistent with the true model. Additionally, the posterior probability density functions (PDFs) of the parameters at nodes of 3kmx4km and 3kmx2km grid in the shallow part of the fault and surrounding the hypocenter maintain the overall shape, independent of the chosen starting model, random or correlated. However, the use of correlated initial models is preferable, when we account for uncertainty in the Earth model. For the purpose of comparison, we perform two different analyzes: we first adopt a variation in velocity of $\pm 2\%$ for each layer. The second case consists of a more realistic model, which includes large variations in velocity for shallow layers as well as in the Moho. The second case allows us to seek evidence for a relation between the choice of velocity uncertainty and the posterior PDFs. Our analysis reveals that slip rate parameters are not sensitive to variability in Earth structure especially in the high slip-rate area of the fault that are maintained during jackknife test

Simulation of the 1994 Northridge Earthquake Including Nonlinear Soil Behavior, *Doriam Restrepo, Ricardo Taborda, and Jacobo Bielak* (Poster 015)

The importance of inelastic soil behavior on ground motion during strong earthquakes has been increasingly recognized in recent years. These effects are now customarily incorporated into the analysis of ground motion through one-dimensional nonlinear soil models subjected to vertically incident seismic waves. Despite the progress to date, three-dimensional (3D) effects of soil nonlinearity on the spatial and temporal distribution of ground shaking are still far from being well understood. We present initial results from a set of 3D simulations of the 1994 Mw 6.7 Northridge earthquake including nonlinear soil effects. Simulations are performed for frequencies up to 2 Hz and shear wave velocities (V_s) down to 200 m/s. We synthesize the earthquake source and material model in a volume domain of size equal to 85 km x 85 km x 42.5 km and solve the simulation using Hercules, a finite-element application for modeling ground motion in large basins. Inelastic soil behavior is represented using the Drucker-Prager model. Hercules implements a rate-independent approach for the solution of the displacement field that combines an implicit scheme for the integration of the soil evolution equations with an explicit formulation of the wave equation in solids. As a first approximation, plastic deformations are considered only in soft-soil deposits with V_s values between 200 and 500 m/s. Inelastic material parameters within these deposits were determined ad hoc, based on an initial simulation under elastic conditions, in order to force the occurrence of discernible plastic deformation at the upper soft-soil layers. Elastic properties of the material were based on SCEC's Community Velocity Model, CVM-S 4.1. Our results are qualitatively comparable to observations from past earthquakes. They indicate that nonlinear soil behavior affects significantly the spatial variability of the ground motion, causes permanent displacements, and reduces peak ground velocities and accelerations. They also indicate that nonlinearity is influenced by 3D effects that cannot be represented by alternative hybrid or pseudo-nonlinear approaches commonly used in seismic hazard analyses.

Information gains of a hybrid earthquake forecasting model, *David A. Rhoades* (Poster 054)

Optimal mixtures of three space-time-magnitude earthquake likelihood models are found for forecasting earthquakes with magnitudes of 5.0 and greater in the New Zealand and California catalogues, with forecasting time-horizons ranging from zero to 3000 days. The models are the Epidemic Type Aftershock (ETAS) short-term clustering model, the Every Earthquake a Precursor According to Scale (EPPAS) medium-term clustering model and the Proximity to Past Earthquakes (PPE) quasi-time-invariant smoothed seismicity model. The optimal mixture is called here the Janus model, after the Roman god of beginnings and doorways, often depicted as looking both ways. Beginning from each new earthquake that is added to the catalog, the model looks in two directions \square to the min

MEETING ABSTRACTS

or earthquakes (aftershocks) that are expected to follow it in the short term, which are targeted by the ETAS model, and to the major earthquake(s) that may follow it in the long term, which are targeted by the EEPAS model. The ETAS model is the most informative of the component models for short time-horizons of a few days, but even with a zero time-horizon the

Western Transverse Ranges Tsunami Project: Do Great Earthquakes Occur on a Linked Western Transverse Ranges Thrust System?, *Thomas K. Rockwell, Robert Peters, Eileen Hemphill-Haley, Mary McGann, Bruce Richmond, Bruce Jaffe, Rick Wilson, and Stephanie Ross* (Poster 136)

Large earthquakes and their associated tsunamis in Sumatra (2004) and Japan (2011) have brought into sharp focus the hazards associated with convergent margins. The Transverse Ranges is southern California's version of a convergent margin and recent work between Ventura and Carpinteria has demonstrated that the Ventura Avenue Anticline (VAA) and associated Pitas Point – Ventura thrust have produced large uplift events. The amount of inferred uplift, on the order of 6-9 m per event, likely resulted in the production of a sizable tsunami along the Santa Barbara – Ventura County coastline, although until recently no one has looked for tsunami deposits in this region. We have initiated an effort to collect cores from subsiding estuaries along the Santa Barbara coastline to search for evidence of past tsunami deposits. This year, four new Russian-peat cores were collected at the Carpinteria Salt Marsh Reserve that penetrated to about a meter depth, which likely captured the past several hundred years of sedimentation. Radiocarbon analysis is under way for organic components (plant lignans, seeds, other components) to confirm the expected age range. Preliminary analysis of foraminifera and diatoms from a possible post-1700 AD tsunami deposit (possibly associated with the 1812 earthquake) does not indicate the presence of deep-water species as may be expected for a tsunami origin, and therefore, does not support the presence of a shallow tsunami deposit at Carpinteria. Deeper cores using a hydraulic piston corer will be recovered in October (after the end of endangered species nesting season) to test for older tsunami deposits that may have originated from terrace uplift at Pitas Point.

Using Videogames in Geoscience Education, *Daniel Rohrlack, Alan Yang, and Debi Kilb* (Poster 259)

Can a videogame be a learning tool? Over the last five years we have been developing geoscience based educational games, experimenting with various forms of gaming techniques and player interaction. Our first game, "Deep-sea Extreme Environment Pilot (DEEP)", is an Xbox 360 game where players learn about deep-sea environments by playing the role of an Oceanographer controlling a Remotely Operated Vehicle (ROV). DEEP is a "traditional" videogame where players interact with a controller and a TV screen. In our seismology based "Quake Catcher Network (QCN)" game, instead of using a game controller, we incorporated the Microsoft Kinect motion sensor, which allows for controller free game play by obtaining input from the player using only the player's body motions (e.g., hands in the air, feet off the ground etc). In this game the player must quickly deploy seismic sensors in order to record aftershocks from a large earthquake. In both of these games we attempt to measure how effective videogames can be used to educate players.

After testing our games numerous times in museums, informal learning centers, and classrooms we learned which educational gaming techniques work and which do not work. Being placed in the role of the scientist and being able to interact with unique environments and gameplay goals gave players a different way to learn. We also found some people enjoy the traditional form of playing a videogame with a controller, whereas some of the more outgoing players were intrigued by the uniqueness of the Kinect motion sensor. Regardless of the input method, overall players were excited to use videogames to learn about science. More often than not, we noticed players having fun while learning. After creating our games on various formats and software suites, we ultimately hope to encourage educators to give educational gaming a chance to add variety to the learning process. Hopefully we can even motivate some to create their own games.

Mechanisms of Postseismic Deformation Following the 2010 El Mayor-Cucapah Earthquake, *John C. Rollins, Sylvain Barbot, and Jean-Philippe Avouac* (Poster 208)

In the Salton Trough, ongoing continental rifting has produced a regime in which the mechanically weak asthenosphere may extend up to within 40-45 km of the surface, compared to 60-80 km in much of southern California. As a result, viscous flow of the asthenosphere may more strongly affect surface deformation in the Salton Trough than elsewhere, and conversely, patterns of surface deformation in this region may provide insights into the nature of asthenospheric flow that are difficult to extract elsewhere. The 2010 El Mayor-Cucapah earthquake occurred within the Salton Trough and may have triggered shallow postseismic creep, deep creep, and viscous flow in the asthenosphere (and possibly the lower crust). Using the Fialko et al [2010] coseismic displacement model and the open-source deformation modeling software RELAX, we calculate the expected postseismic surface deformation resulting from coupled creep and viscous flow in a variety of hypothetical geometries, then compare these forward models to continuous GPS and INSAR data. Preliminary findings suggest that viscous flow in the shallow Salton Trough asthenosphere, and possibly within the lower crust, is required to explain postseismic uplift observed at several GPS stations in the Imperial Valley.

Testing seismic hazard models with Be-10 exposure ages for precariously balanced rocks, *Dylan H. Rood, Rasool Anooshehpour, Greg Balco, Glenn Biasi, James Brune, Richard Brune, Lisa Grant-Ludwig, Katherine Kendrick, Matthew Purvance, and Inyo Saleeby* (Poster 011)

Currently, the only empirical tool available to test maximum earthquake ground motions spanning timescales of 10 ky-1 My is the use of fragile geologic features, including precariously balanced rocks (PBRs). The ages of PBRs together with their areal distribution and mechanical stability ("fragility") constrain probabilistic seismic hazard analysis (PSHA) over long timescales; pertinent applications include the USGS National Seismic Hazard Maps (NSHM) and tests for ground motion models (e.g., Cybershake). Until recently, age constraints for PBRs were limited to varnish microlamination (VML) dating techniques and sparse cosmogenic nuclide data; however, VML methods yield minimum limiting ages for individual rock surfaces, and the interpretations of cosmogenic nuclide data were ambiguous because they did not account for the exhumation history of the PBRs or the complex shielding of cosmic rays. We have recently published a robust method for the exposure dating of PBRs combining Be-10 profiles, a numerical model, and a three-dimensional shape model for each PBR constructed using photogrammetry (Balco et al., 2011, Quaternary Geochronology). Here, we use our published method to calculate new exposure ages for PBRs at 6 sites in southern California near the San Andreas, San Jacinto, and Elsinore faults, including: Lovejoy Buttes (9 +/- 1 ka), Round Top (35 +/- 1 ka), Pacifico (19 +/- 1 ka, but with a poor fit to data), Beaumont South (17 +/- 2 ka), Perris (24 +/- 2 ka), and Benton Road (40 +/- 1 ka), in addition to the recently published age of 18.5 +/- 2.0 ka for a PBR at the Grass Valley site. We combine our ages and fragilities for each PBR, and use these data to test the USGS 2008 NSHM PGA with 2% in 50 year probability, USGS 2008 PSHA deaggregations, and basic hazard curves from USGS 2002 NSHM data.

Volumetric changes in source regions of earthquakes in the San Jacinto fault zone and the eastern California shear zone, *Zachary E. Ross, Yehuda Ben-Zion, and Lupei Zhu* (Poster 163)

Theoretical and observational studies indicate that earthquake ruptures can dynamically produce rock damage in the surrounding material leading to isotropic components of radiation. Typical source tensor inversions for tectonic earthquakes, however, are constrained by default to be deviatoric. Here we investigate the possible existence of isotropic radiation and volumetric changes of strain in earthquake source regions with two research directions.

(i) We use a methodology for source inversion that includes a parameter beta defined as the percentage of the isotropic component of radiation. The inversion is applied to a set of earthquakes with $3.5 < M < 5.4$ in the San Jacinto Fault Zone in southern California. In the analysis done so far

we find source tensors for tectonic earthquakes with beta ranging from 0% to >15%. We run a set of tests on the statistical robustness of the tensor parameters. The results are compared for different events to better understand the range of beta values, and assess the implications for the source process. To study how a neglected CLVD component may partition into double couple and isotropic components, we generate synthetics with a range of CLVD components and invert for source mechanism assuming zero CLVD component. The results suggest that the CLVD component is primarily mapped onto the double couple component, with a limited amount going to the isotropic component.

(ii) We examine the rotation angles between aftershock source mechanisms constrained to be double-couples and the parent event. The distributions of rotation angles are compared with the distribution of angles for background seismicity over large space-time scales. The aftershock sequences of the 1992 Landers mainshock and several earthquakes with $M > 5$ in the San Jacinto Fault Zone are investigated. The focal mechanisms of aftershocks near the edges of the Landers rupture are found, on average, to have larger misalignment with the mainshock than the mechanisms of the overall background seismicity. These differences are found to be statistically significant. The aftershock focal mechanisms become more aligned with the mainshock orientation as time increases and ultimately approach the average orientation of background events. Synthetic calculations show that the differences between early aftershock and background focal mechanisms can be the result of neglecting small isotropic components (as a constraint) in the derivation of the double couple source

Development of excess pore water pressure in liquefiable soils inferred from vertical array records, *Daniel Roten, Donat Fäh, and Fabian Bonilla* (Poster 013)

Strong motions recorded on liquefiable deposits during recent damaging earthquakes show that buildup of pore water pressure has a significant effect on ground motions. The phase transformation behavior of liquefiable soils may give rise to high-frequency dilation pulses which produce large accelerations. During the 2011 Tohoku earthquake, for example, such dilation pulses resulted in a peak ground acceleration (defined as the maximum of the 3D acceleration vector) of $\sim 2g$ at Onahama port (OP) in Iwaki (Fukushima prefecture).

Despite the growing number of borehole accelerometers operating today, only few vertical arrays are equipped with pore pressure transducers, and field observations of pore water pressure development in soils during strong motion remain scarce. We propose to derive excess pore water pressure time histories in liquefiable deposits indirectly by inverting strong motions recorded on vertical arrays.

The forward problem is represented by vertical SH wave propagation inside a horizontally layered medium with known geophysical and geotechnical properties but unknown dilatancy parameters. We use the nonlinear effective stress code NOAH to solve the forward problem and take the measured borehole signal as input at the bottom of the model. We sample the parameter space with the neighborhood algorithm and seek for a model that minimizes the misfit between simulated and observed free-surface acceleration time series.

Application of this approach to the OP records of the Tohoku earthquake results in synthetic acceleration time series which are consistent with the observations in shape and amplitude. The inversion suggests that pore water pressure eventually approached the effective mean stress in the upper part of the sand layer. Buildup of excess pore water pressure occurred mostly between 145 and 170 s, possibly triggered by a burst of high-frequency energy from a large slip patch below the Iwaki region.

With the increasing volume of strong motion data acquired on vertical arrays worldwide, this approach may contribute to a more comprehensive characterization of pore water pressure effects during strong ground motion.

The Grand Challenge: Documenting the Scientific Collaboration and other Experiential Learning Activities of the UseIT Class of 2012, *Nick Rousseau, Alysia Gonzales, Carlos Landa, Will Ilgen, Madeline Berger, Thomas Jordan, and Robert de Groot* (Poster 299)

The Southern California Earthquake Center (SCEC) is a community of over 600 scientists, students, and others at over 60 institutions worldwide, headquartered at the University of Southern California. SCEC's mission is to develop a comprehensive understanding of earthquakes in Southern California and elsewhere, and to communicate useful knowledge for reducing earthquake risk. As part of its mission SCEC hosts an 8-week summer internship program, Undergraduate Studies in Earthquake Information Technology (UseIT). UseIT interns work in multi-disciplinary, collaborative teams to tackle a scientific "Grand Challenge." The Grand Challenge varies each year but always entails performing computer science research that is needed by earthquake scientists or outreach professionals. The overall task of the UseIT Media Team was to document the process of addressing this year's Grand Challenge as well as documenting the experiences of the interns. The medium of film does something that no other medium can do. By immersing the viewer in a visual and aural experience, the viewer is able to feel as close as possible to actually experience the internship, without going through the entire 8-week program themselves. The Media Team began by gathering daily footage throughout the summer. This footage is called "A-Roll". Additionally, transition and contextualizing shots known as "B-Roll" are obtained. The next step is the writing of a script used to organize this footage. As interviews are gathered, the connections between each shot and segment are fine-tuned using professional editing software called Final Cut Pro. After gathering footage, scripting, and editing, the Media Team will have a film that both illustrates the summer 2012 program as well as present the products to the scientific community.

Laboratory Earthquakes: Measuring surface displacements with high-speed digital image correlation, *Vito Rubino, Ares J. Rosakis, and Nadia Lapusta* (Poster 069)

Mapping full-field displacements and strains on the Earth's surface during an earthquake is of paramount importance to enhance our understanding of earthquake mechanics. In this study, the feasibility of such measurements using image correlation methods is investigated in a laboratory earthquake setup. Earthquakes are mimicked in the laboratory by dynamic rupture propagating along an inclined frictional interface formed by two Homalite plates under compression, using the configuration developed by Rosakis and coworkers (e.g., Rosakis et al., 2007). In our study, the interface is partially glued, in order to confine the rupture before it reaches the ends of the specimen. The specimens are painted with a speckle pattern to provide the surface with characteristic features for image matching. Images of the specimens are taken before and after dynamic rupture with a 4 Megapixels resolution CCD camera. The digital images are analyzed with two software packages: VIC-2D (Correlated Solutions Inc.) and COSI-Corr (Leprince et. al, 2007).

Both VIC-2D and COSI-Corr are able to characterize the full-field static displacement of a dynamic crack. For example, in a case with secondary mode I cracks, the correlation analysis performed with either software clearly shows (i) the relative displacement (slip) along the frictional interface, (ii) the rupture arrest on the glued boundaries, and (iii) the presence of two wing cracks. The obtained displacement measurements are converted to strains, using de-noising techniques.

The digital image correlation method is then used in combination with high-speed photography. We will report our progress on the study of a spontaneously expanding sub-Rayleigh shear crack advancing along an interface containing a patch of favorable heterogeneity, such as a preexisting subcritical crack or a patch with higher prestress. According to the predictions of Liu and Lapusta (2008), intersonic transition and propagation can be achieved in the presence of a favorable heterogeneity for much lower prestress levels than those predicted by the Burridge-Andrews mechanism. Our current numerical work is directed towards elucidating this speed transition mechanism and designing full-field, dynamic experiments to validate our predictions.

The 2001 – Present Triggered Seismicity Sequence in the Raton Basin of Southern Colorado/Northern New Mexico, *Justin L. Rubinstein, William L. Ellsworth, and Arthur McGarr* (Poster 168)

MEETING ABSTRACTS

The occurrence of an earthquake of magnitude (M) 5.3 near Trinidad, CO, on 23 August 2011 renewed interest in the possibility that an earthquake sequence in this region that began in August 2001 is the result of industrial activities. Our investigation of this seismicity, in the Raton Basin of northern New Mexico and southern Colorado, led us to conclude that the majority, if not all of the earthquakes since August 2001 have been triggered by the deep injection of wastewater related to the production of natural gas from the coal-bed methane field here. The evidence that this earthquake sequence was triggered by wastewater injection is threefold. First, there was a marked increase in seismicity shortly after major fluid injection began in the Raton Basin. From 1970 through July of 2001, there were five earthquakes of magnitude 3 and larger located in the Raton Basin. In the subsequent 10 years from August of 2001 through the end of 2011, there were 95 earthquakes of magnitude 3 and larger. The statistical likelihood of this rate increase occurring naturally was determined to be 0.01%. Second, the vast majority of the seismicity is located close (within 5km) to active disposal wells in this region. Additionally, this seismicity is primarily shallow, ranging in depth between 2 and 8 km, with the shallowest seismicity occurring within 500 m depth of the injection intervals. Finally, these wells have injected exceptionally high volumes of wastewater. The 23 August 2011 M5.3 earthquake, located adjacent to two high-volume disposal wells, is the largest earthquake to date for which there is compelling evidence of triggering by fluid injection activities; indeed, these two nearly-co-located wells injected about 4.9 million cubic meters of wastewater during the period leading up to the M5.3 earthquake, more than 7 times as much as the disposal well at the Rocky Mountain Arsenal that caused damaging earthquakes in the Denver, CO, region in the 1960s. Much of the seismicity since 2001 falls on a 15km-long, NE-trending lineation of seismicity dipping steeply to the SE. The focal mechanisms of the largest earthquakes since mid-2001 are consistent with both the direction of the seismicity lineation and the regional tectonic regime of east-west extension centered on the Rio Grande rift.

Modeling Crack-like/Pulse-like Ruptures on Dip-Slip Faults using Rate-State Friction with a Normal-Stress-Dependent State, Kenny J. Ryan and David D. Oglesby (Poster 091)

It is well known that the asymmetric geometry of reverse and normal faults can lead to greater slip and a greater peak slip rate on reverse faults than on normal faults, given the same initial conditions for each (e.g., Nielsen, 1998; Oglesby et al., 1998; Oglesby et al., 2000A, Oglesby et al., 2000B). This result is associated with the effect of the free surface on the fault stress: as rupture approaches the free surface along a normal fault there is a decrease in normal stress ahead of the crack tip and an increase in normal stress behind the crack tip, with the opposite effect for reverse faults (Nielsen, 1998; Oglesby et al., 1998). To date, there has been no systematic investigation into how the laboratory-derived normal-stress dependence of the state variable (Linker and Dieterich, 1992) affects the asymmetric slip and slip rate patterns between reverse and normal faults. In principle, normal-stress dependence of the state variable should moderate the above normal-stress dependent frictional effects. In this study, we examine rupture along reverse and normal faults, each with a 45-degree dip. We use the 2D dynamic finite element method (Barall, 2009) with an ageing law implementation of rate- and state-dependent friction (Dieterich, 1978, 1979; Ruina 1983; Linker and Dieterich, 1992) to model our earthquakes. Specifically, we use the relation $d\psi/dt = -(\alpha/\sigma)(d\sigma/dt)$ (Linker and Dieterich, 1992), in which a change in normal stress leads to a change in state variable of the opposite sign. We investigate a range of values for alpha (which scales the impact of the normal stress change on state) from 0 to 0.8 (laboratory values range from 0.2 to 0.5). Additionally, we vary the value of loading stress among models to investigate possible different behaviors between crack-like and pulse-like ruptures (e.g., Zheng and Rice, 1998). We find that the asymmetry in peak slip rate and total slip between reverse and normal faults decreases with both increasing alpha and decreasing loading stress. The trend is less obvious for the slip, however, and may be influenced by the formation of daughter cracks in our normal fault models near the free surface. For more pulse-like normal fault models, rupture often does not reach the free surface within the time duration of the models. We examine our results in light of the associated energy budgets of both reverse and normal fault ruptures.

Salton Seismic Imaging Project Line 5—the San Andreas Fault and Northern Coachella Valley Structure, Riverside County, California,

Michael J. Rymer, Gary S. Fuis, Rufus D. Catchings, Mark R. Goldman, Jennifer M. Tarnowski, John A. Hole, Joann M. Stock, and Jonathan C. Matti (Poster 202)

The Salton Seismic Imaging Project (SSIP) is a large-scale, active- and passive-source seismic project designed to image the San Andreas Fault (SAF) and the adjacent basins (Imperial and Coachella Valleys) in southern California. Here, we focus on SSIP Line 5, one of four 2-D NE-SW-oriented seismic profiles that were acquired across the Coachella Valley. The 38-km-long SSIP-Line-5 seismic profile extends from the Santa Rosa Ranges to the Little San Bernardino Mountains and crosses both strands of the SAF, the Mission Creek (MCF) and Banning (BF) strands, near Palm Desert. Data for Line 5 were generated from nine buried explosive sources (most spaced about 2 to 8 km apart) and were recorded on approximately 281 Texan seismographs (average spacing 138 m). First-arrival refractions were used to develop a refraction tomographic velocity image of the upper crust along the seismic profile. The seismic data were also stacked and migrated to develop low-fold reflection images of the crust. From the surface to about 8 km depth, P-wave velocities range from about 2 km/s to more than 7.5 km/s, with the lowest velocities within a well-defined (~2-km-deep, 15-km-wide) basin (< 4 km/s), and the highest velocities below the transition from the Coachella Valley to the Santa Rosa Ranges on the southwest and within the Little San Bernardino Mountains on the northeast. The MCF and BF strands of the SAF bound an approximately 2.5-km-wide horst-type structure on the northeastern side of the Coachella Valley, beneath which the upper crust is characterized by a pronounced low-velocity zone that extends to the bottom of the velocity image. Rocks within the low-velocity zone have significantly lower velocities than those to the northeast and the southwest at the same depths. Conversely, the velocities of rocks on both sides of the Coachella Valley are greater than 7 km/s at depths exceeding about 4 km. The relatively narrow zone of shallow high-velocity rocks between the surface traces of the MCF and BF strands is associated with a zone of uplifted strata. Along SSIP Line 5, we infer that the MCF and BF strands are steeply dipping and merge at about 2 km depth. We base our interpretation on a prominent basement low-velocity zone (fault zone) that is centered southwest of the MCF and BF strands and extends to at least 8 km depth.

Imaging the upper crustal velocity structure in the northern Salton Sea: Results from the Salton Sea Imaging Project's (SSIP) marine refraction experiment, Valerie J. Sahakian, Annie Kell, Alistair Harding, Neal Driscoll, and Graham Kent (Poster 277)

Active-source marine refraction data collected in the Salton Sea in the spring of 2011 allow us to investigate earthquake hazards related to the southern San Andreas Fault (SAF), and to examine continental rifting processes within the Salton Trough. Performed in conjunction with the Salton Seismic Imaging Project (SSIP), this experiment deployed Ocean Bottom Seismometers (OBS) at 78 locations in the Salton Sea composing several linear tracks, as well as an array in the southern section of the sea. We invert by following the method of Van Avendonk, et. al (2004), trying to find the smoothest model that best fits our P-wave travel-time picks. We attempt to minimize the misfit between our predicted and observed travel-times, iterating until we achieve a suitable misfit and stable model.

Here we present results from the linear track Line 7, which runs perpendicular to the SAF in the northern section of the Salton Sea. The 2D model we obtain along this line shows velocity variations of 1.5 to 3 km/s in the upper 2 kilometers of the crust, to slightly over 4 km/s at 4 km depth. We attempt to constrain the upper crustal velocities to provide insight into the formation of this pull-apart basin, and investigate the geometry of the southern SAF.

Subjectivity of LiDAR-Based Offset Measurements: Results from a Public Online Survey, J. Barrett Salisbury, J. Ramon Arrowsmith, Thomas K. Rockwell, David E. Haddad, Olaf Zielke, and Christopher M. Madugo (Poster 148)

Rockwell, David E. Haddad, Olaf Zielke, and Christopher M. Madugo (Poster 148)

Geomorphic features (e.g., stream channels) that are offset in an earthquake can be measured to determine slip at that location. Analysis

of these and other offset features can provide useful information for generating fault slip distributions. Remote analyses of active fault zones using high-resolution LiDAR data have recently been pursued in several studies, but there is a lack of consistency between users both for data analysis and results reporting. Individual investigators typically make offset measurements in a particular study area with their own protocols for measurement, assessing uncertainty, and rating quality, yet there is no coherent understanding of the reliability and repeatability of the measurements from observer to observer. We invited the participation of colleagues, interested geoscience communities, and the general public to measure ten geomorphic offsets from active faults in western North America using remote measurement methods that span a range of complexity (e.g., paper image and scale, the Google Earth ruler tool, and a MATLAB GUI for calculating backslip required to properly restore tectonic deformation) to explore the subjectivity involved with measuring geomorphic offsets. We provided a semi-quantitative quality-rating rubric for a description of offset quality, but there was a general lack of quality rating/offset uncertainty reporting. Survey responses (including mapped fault traces and piercing lines) were anonymously submitted along with user experience information. We received 11 paper-, 28 Google Earth-, and 16 MATLAB-based survey responses, though not all individuals measured every feature provided. For all survey methods, the majority of responses are in close agreement. However, large discrepancies arise where users interpret landforms differently, specifically the pre-earthquake morphologies and total offset accumulation of geomorphic features. Experienced users make more consistent measurements, whereas beginners less-consistently choose the same interpretation for an offset feature. The Google Earth survey, for example, shows that the average percent difference between all expert measurements is significantly smaller (19%) than the percent difference between all beginner measurements (39%). One group of students was asked to perform the paper-based survey twice -- once before and once after an introductory lecture on the basic neotectonic principles. While the standard deviations for each feature were arbitrarily affected in this simple experiment, in 80% of the cases measurement uncertainties increased. In general, standardizing measurement and reporting methods will be a crucial first step towards enhancing consistency of LiDAR-based analyses of active faults and establishing community protocols for measurement and reporting.

The Role of Deep Creep in the Timing of Large Earthquakes, Charles G. Sammis and Stewart W. Smith (Poster 063)

The 1968 earthquake at Parkfield Ca was the sixth event in a fairly regular sequence of M6 events having a recurrence interval near 20 years. Consequently, the Parkfield segment of the San Andreas Fault was heavily instrumented to search for short-term physical precursors to the next M6 event expected in the early 1980s. When the anticipated event finally occurred in 2004, no physical precursors were observed. However, we have observed that the 2004 earthquake was preceded by a four-fold increase in the rate of off-fault seismicity in the distance range from 2 to 18 km from the fault axis having a sharp onset four years before the event. During the same time period there was no clear decrease in the recurrence interval of repeating events (all of which occur within 2 km of the fault axis). The spatial pattern of off-fault seismicity was unchanged during the 20 years leading up to the 2004 event and during the subsequent 8 years of aftershocks. The observed spatial pattern can be explained using an Okada dislocation model for deep creep (below 20 km) on the fault plane in which the slip rate decreases from North to South consistent with surface creep measurements and deepens south of the "Parkfield asperity" as indicated by recent tremor locations. The model predicts the off-fault events should have reverse mechanism consistent with observed topography. In this interpretation, the increase in off-fault seismicity is caused by an increase in deep creep on the fault, an interpretation that is consistent with Shelly's recent observation of an increase in tremor preceding the 2004 event. On a related topic, it has recently been observed that the seismic waves from large earthquakes can trigger tremor at the base of distant faults. If tremor is a proxy for deep creep, then triggered tremor offers a mechanism by which a large earthquake can advance the seismic cycles on distant faults. We present a coupled non-linear oscillator model that shows how this interaction can synchronize the seismic cycles of large earthquakes on a global scale.

Investigations into effects of different modeling codes and rheology on predicted coseismic and postseismic surface deformation, David T.

Sandwell, Sylvain D. Barbot, Charles A. Williams, Andrew Freed, Susan Ellis, Mong-Han Huang, and Bridget R. Smith-Konter (Poster 239)

A number of sophisticated modeling tools are presently available and under active development that allow geoscientists to take advantage of the ever-increasing accuracy and coverage being provided by geodetic observations. Many features have not been extensively tested, however, and it is frequently difficult to determine which modeling tool is best suited to a particular problem. We will present results contrasting several different modeling codes: the commercial Abaqus finite element code, the open-source PyLith finite element code, the available-by-collaboration SULEC finite element code, the open-source RELAX deformation code, and the Maxwell code of Smith and Sandwell (2006). We start with a simple benchmark of a strike-slip fault embedded in an elastic layer overlying a viscoelastic half-space. Particular points of difference arise for some of the codes in terms of whether the fault is represented by an infinitely thin fault, a thin layer of elements, or point dislocations. Only some of the codes allow heterogeneous elastic properties. We will concentrate on the strike-slip benchmark and variations of it, but also show some examples of further benchmarks such as the Savage and Prescott (1978) problem, and discuss implementation of a benchmark for a real-life examples from the El Mayor and Darfield earthquakes. We will summarise our results so far in terms of the abilities and suitabilities of each code to investigate a variety of tectonic problems.

Spatial Variability of Shallow Velocity Measurements in the Los Angeles Area, William H. Savran, Kim B. Olsen, and Bo H. Jacobsen (Poster 038)

As greater computational power allows earthquake scientists to push the frequency limits of deterministic ground motion estimates higher, understanding small-scale, near-surface heterogeneities becomes paramount. The variation of the soil amplification over short distances (from tens to hundreds of meters) is important for the design of smaller structures, including lifelines. These small-scale heterogeneities may significantly affect ground motion in geologic basins, and are not included in state-of-the-art Community Velocity Models (CVMs). The density of current (and expected future) direct and indirect measurements of these heterogeneities is insufficient to capture their variation in sedimentary basins. Toward characterizing the variability of shallow sediment amplification, we have collected readily available near-surface velocity data, including several datasets of direct and indirect Vs30 values (775 measurements) and downhole sonic logs from oil exploration surveys (687 measurements) in the Los Angeles area. We have prepared semi-variograms of the near-surface heterogeneities in an effort to quantify statistical parameters about the existing shear-wave velocities in Los Angeles Basin. Our preliminary analysis suggests that the data are conforming to a fractal distribution with fractal dimensions of 1.5-1.8 and related Hurst exponents of 0.2-0.5. We plan to generate statistical models of seismic velocities and densities in agreement with the results of the data analysis and integrate into the most recent SCEC CVMs. The effects of the near-surface heterogeneities on ground motion and scattering will be tested using simulations of selected historical earthquakes with a high density of strong motion recordings available. These simulations will be calculated for several values of Qs and Qp, up to at least 5 Hz, in order to examine the interdependency between intrinsic and scattering attenuation on the ground motion.

Earthquakes through the Big Bend: Comparison of earthquake ages from Frazier Mountain, Bidart Fan, and Pallett Creek, CA, Katherine M.

Scharer, Ray Weldon, and Ashley Streig (Poster 126)

We present a chronologic model for the timing of 10-11 earthquakes documented by trenching at the Frazier Mountain paleoseismic site. New ages confirm that sag-pond forming events initiated after ca. A.D. 500, and since then earthquakes have ruptured through the site on average every ~130 years. In detail, individual intervals between earthquakes can be shorter than 50 years or as long as 200 years, similar to variability documented at other southern San Andreas fault paleoseismic sites. We also present a comparison of the Frazier Mountain record with neighboring paleoseismic sites at Bidart Fan and

MEETING ABSTRACTS

Pallett Creek, 100 km to NW and SE, respectively. The timing of earthquakes at Frazier is more similar to Bidart than Pallett Creek. We explore how these records would predict different rupture extents and event patterns on the fault through time. We also evaluate the record completeness at each site (as determined by number of depositional events between earthquakes), and how this parameter might affect completeness of the record in periods where the events do not readily correlate based on their ages.

Dynamic rupture at low mean shear stress initiated with rate/state friction and sustained by thermal pressurization, Stuart V. Schmitt, Andrew M. Bradley, Eric M. Dunham, and Paul Segall (Poster 089)

Reconciling the frictional behavior of faults during nucleation and seismic slip remains a challenge in the study of fault mechanics. Multiple lines of evidence indicate that earthquakes frequently occur at low shear stress τ , and for effective normal stresses σ at seismogenic depths, the friction coefficient $f = \tau/\sigma$ must therefore be quite small (< 0.2) during seismic slip. Yet nearly all laboratory rock sliding experiments show that slip initiates at $f \sim 0.6$ to 0.9 . In order for sustained rupture to occur at low mean f , a likely scenario is that earthquakes nucleate where f is locally high and then propagate into regions of lower f . For a rupture to be self-sustaining, a strong weakening mechanism must operate during fast slip. One candidate mechanism is thermal pressurization, in which frictional heating pressurizes pore fluid in the fault zone and causes σ to drop, thereby weakening the fault. We have performed a suite of numerical simulations on 1D faults that shows that slip with thermal pressurization can produce some of the behavior observed in natural earthquakes. We consider two idealized nucleation conditions--one called "high stress" in which σ is uniform and τ locally grows, and another called "low strength" in which τ is uniform and σ locally decreases. In high-stress ruptures, thermal pressurization is substantial within the nucleation zone and is capable of producing a self-sustaining rupture that propagates far into low- τ regions. At sufficiently low τ , high-stress ruptures possess a pulse-like character, which has been inferred for many natural earthquakes. In low-strength ruptures, thermal pressurization is modest within the nucleation zone, but becomes significant as slip propagates outside of the low- σ region. With weak thermal pressurization inside the nucleation zone, slip there is less energetic and more prolonged than at the rupture tips so earthquakes are generally more crack-like in character. For ruptures that arrest, both high-stress and low-strength ruptures show a moment-length relationship of $M \sim L^2$, which in 1D also arises for cracks with constant stress drop. Moment-length relationships for populations of earthquakes are often interpreted in the framework of constant stress drop cracks, so the moment-length relationship in our simulated ruptures is consistent with observed source parameters for small earthquakes.

Mapping the Crust-Mantle Transition Beneath Parkfield and Tectonic Tremor, Han Yue, Susan Y. Schwartz, and Geoffrey Abers (Poster 176)

Tectonic tremor has been located beneath the creeping section of the San Andreas Fault near Parkfield. It was shown that many tremor families occurred over a 150 km length of the SAF (Shelly and Hardbeck, 2012). These events reveal a shallowing in depth from 25-30 km at the northwest and southeast ends to ~ 16 km, adjacent to the base of the seismogenic zone near Parkfield. The depth variation of these tremor events may have significant implications for understanding the mechanisms of tremor occurrence and the stress release near a transform plate boundary. The first question that needs to be addressed is whether the depth change of these tremor families correlates with variations in Moho depth or anisotropic properties of the lower crust along the San Andreas Fault. To study crustal structure, receiver functions from broadband stations of the PASO and PERMIT temporary arrays, as well as 8 permanent stations spanning over 100 km of the SAF were constructed. The Moho interface and crustal layers were clearly imaged using array migration techniques which show a sharp Moho step from 26 to 30 km across the San Andreas Fault and a velocity inversion at 12-14 km, the depth of the deepest earthquakes. This suggests that the base of the brittle deformation zone corresponds to a significant velocity decrease. Relocation of tremor event families (Thurber, 2012 SCEC report) indicates that most of the tremor events occur on the southwest side of the fault at depths between 15-26 km. Many of these

tremor events locate directly beneath the deepest earthquakes where the velocity inversion is the strongest. Single station receiver functions show that the azimuthal variation of transverse receiver functions is strongly influenced by the structural heterogeneity across the San Andreas Fault, which probably will not reveal the anisotropic property of the lower crust near the fault region as proposed by (Ozacar and Zandt, 2009).

Investigation of Seasonal Variations in the Response of the Soil-Foundation-Structure-Interaction Test Structure, Sandra H. Seale, Emily Stinson, Jamison H. Steidl, and Paul Hegarty (Poster 185)

The experimental soil-foundation-structure-interaction (SFSI) test structure installed at the NEES@UCSB Garner Valley field site is fully instrumented to record the response to ambient earthquakes. The SFSI experiment is unique in its ability to record in situ response of a structure in the field. A mobile shaker is installed on the underside of the roof slab of the SFSI. The shaker is run every night (60 sec sine sweep from 15 – 5Hz) and the response of the SFSI is recorded. Running this experiment daily has provided a valuable data set that documents the change in structural behavior with changes in the environment such as temperature and ground water level. Two years of nightly shaker test data were analyzed for behavior of the resonance of the structure. Fourier analysis shows a first mode (rocking) resonant frequency of ~ 5.6 Hz. That first resonance sometimes appears as two peaks in the amplitude spectrum. Comparing the resonance frequencies with the average daily temperature shows that the resonance frequencies are higher on warmer days. We expect that changing temperatures have the greatest impact on the steel members of the SFSI frame and that this, in turn, alters the resonance. It also appears that the "split" of the first resonance frequency is associated with higher temperatures. We also present a comparison of the rocking mode frequencies with water table depth.

Mapping offset features using high-resolution LiDAR data and field observations along the San Andreas fault in the San Bernardino/ Cajon Pass area, southern California, Ziad Sedki, Nate Onderdonk, and Sally McGill (Poster 127)

We have created a new tectonogeomorphic strip map along the San Andreas fault from Wrightwood 47 km south to Highland using B4 light detection and ranging (LiDAR) imagery and field observations. The primary purpose of this mapping was to look for small (1-5 m) offsets that would allow us to map out the extent and lateral slip distribution of the most recent ruptures along this section of the San Andreas fault. For the entire project area, field mapping coupled with high-resolution LiDAR imagery and aerial photos analysis was used to map the fault zone and to identify geomorphic offset features.

Our mapping shows that there are no offset features smaller than about 6 m. Calculated offsets range from 6 m to 48.6 m, with most above 10 m. However, we found abundant tectonic geomorphic offset features indicating recent fault slip along the fault zone including offset and deflected stream channels, shutter and pressure ridges, linear valleys and troughs, benches, aligned notches, saddles, sag ponds, and scarps. The general lack of offset (or deflected) streams less than 6 m suggests that smaller offsets from the last one or two ground-rupturing earthquakes were not preserved. The new mapping will be used to catalog and evaluate the distribution of offset features as well as to look for previously unexploited slip-rate sites.

Exploration of slip-rate discrepancies and distributed deformation via linkages between the Calico, Harper Lake and Blackwater Faults, Jacob Selander and Michael Oskin (Poster 269)

The combination of strike-slip and shortening across the central Mojave Desert illuminates how discrepancies between geologic and geodetic slip rates in this region may arise. Geologic studies show $\leq 6.2 \pm 1.9$ mm/yr of dextral slip distributed across six strike-slip faults. Geodetic block models and present Community Fault Model (CFM) configurations link faults across the central Mojave Desert and predict higher displacement rates than permitted by geologic data. However numerous faults in the Mojave Desert terminate into a region of widespread, un-quantified shortening around the latitude of Barstow. To address the impact of this shortening on the slip rate discrepancy, we constructed new balanced cross-sectional interpretations across the central Mojave Desert. These

sections show linkages between the Calico, Blackwater, and Harper Lake Faults, and sever connections between these and the Camp Rock Fault. Slip on the Calico fault is distributed on to a series of smaller north-dipping thrust ramps that link to the Harper Lake fault and strike-slip and reverse faulting in the Mud Hills. North-south shortening between these systems can account for the loss of displacement between the Calico and Blackwater faults. Simplified subsurface geometries from these cross-sections will be incorporated into an update of the Community Fault Model (CFM) and used as input for new elastic models of fault slip in this region.

Spatiotemporal evolution of the 2012 Mw 8.6 Sumatra earthquake constrained by teleseismic body and surface waves, *Guangfu Shao, Xiangyu Li, and Chen Ji* (Poster 192)

On 11 April 2012, a magnitude 8.6 earthquake occurred off coast of the Sumatra Island within the Indo-Australian plate. This unusual intra-plate earthquake is the largest strike slip event ever recorded by modern instruments. The distributions of its aftershocks and high-frequency radiations suggest that this earthquake may have ruptured a complex fault system with multiple fault segments orienting nearly perpendicular to each other [e.g., Meng et al., 2012; Yue et al, 2012]. However, the spatial and temporal evolution of the moment release of this earthquake is still not very clear. We have performed a multiple double couple (MDC) analysis using long-period (100 s – 333 s) seismic waves after calibrating the 3D path effects using a nearby foreshock. The preferred solutions consist of five or six point sources, with the first one locating coincidentally near the epicenter and contributing about 45% of the total seismic moment (9.7-10.1x10²¹ Nm). Before the cease of this subevent, bilateral rupture occurred along the NNE-SSW elongated fault zone about 80 km west of the epicenter and released 28% of the total seismic moment. The rest of seismic moment is associated with the two Mw 8 subevents along the SSE-NWW aftershock zone 150 km southwest of the epicenter, with the centroid of the last one right beneath the Ninetyeast Ridge and rupturing with a centroid time of 149 s. Interestingly, only the beginning subevent, where this giant earthquake initiated, and last subevent, where this rupture was arrested, have larger centroid depths of 28 km and 20 km, respectively. The rest of sub-events are generally shallow with a centroid depth of 12 km. Based on the nodal planes derived from this solution and the aftershock distribution, we further perform finite fault inversions to investigate preferred nodal planes by jointly modeling teleseismic broadband body waves and long-period surface waves. Our preliminary inversion results indicate that, for the first subevent, models based on the NNE striking nodal plane is more favorable by seismic waveform fits, especially for teleseismic P waves, which is inconsistent with the back-projection result of high-frequency P wave recorded by European array [e.g., Meng et al., 2012; Yue et al, 2012].

Detection of Strain Transient Anomalies in Southern California Using Retrospective and Near Real Time Analyses, *Gina Shcherbenko and William E. Holt* (Poster 236)

We present test results for a continuous, near real-time automated monitoring system of anomalous strain transients in Southern California. The modeling procedure involves interpolating velocities within a region to estimate the velocity gradient tensor field over time. These velocities are time-dependent estimates obtained from CGPS data. The smoothing of the strain rate solution is controlled through optimization of a functional in a formal least-squares inversion. Deviations from a reference strain field indicate the potential presence of a strain transient. Our previous models were successful in uncovering strain transient anomalies in synthetic CGPS time series from recent SCEC transient test exercises. We have updated our model to accommodate greater complexities in real data, such as GPS receiver failure or extreme outliers. Two types of analyses of modeled strain are presented: a retrospective and a daily solution. The retrospective analysis detects anomalous strain within a broad range of time intervals. The daily solution involves automated download and analysis of the most recent two weeks of accumulated strain. We will collaborate with CSEP and our model will be automated for daily analysis.

Dynamics of migrating earthquake swarms at Yellowstone and Mount Rainier: Evidence for fluid triggering?, *David R. Shelly, Seth C. Moran, David P. Hill, Frédérick Massin, Jamie Farrell, and Robert B. Smith* (Poster 094)

Volcanic and hydrothermal regions often exhibit high rates of seismicity and frequent seismic swarms. Two recent examples include a swarm September 20-23, 2009, beneath Mount Rainier and a January 15-February 6, 2010 swarm near the northwest rim of Yellowstone Caldera (Madison Plateau) in Yellowstone National Park. To help illuminate the underlying processes driving the activity, we attempt to identify low signal-to-noise earthquakes and to locate them precisely along with numerous cataloged events.

For each swarm, we use the waveforms of cataloged events to scan the continuous seismic data, with the goal of improving both event identification and relative locations. To do this, we measure both the height and precise timing of the correlation peaks between catalog events and the continuous waveform data. We then input the resulting differential times to a double-difference relative relocation algorithm. This results in successful location of a factor of ~4 more events than included in the catalog, or roughly 800 and 8000 events for the Rainier and Yellowstone sequences, respectively.

Despite differences in the depth range (2-3.5 km below mean station elevation at Rainier versus 6-11 km in Yellowstone), the swarms share many common characteristics. Both seismic swarms exhibit clear migration of event centroids, and in each case activity expands systematically outward in a largely planar pattern with time. Expansion of the seismicity front is episodic and seems to be led by smaller events, even when accounting for differences in source dimensions. Both the Rainier and Yellowstone swarms activate shallower, seismically disconnected structures later in the swarm evolution. A further similarity is that dominant structures, as defined by the earthquake locations, strike perpendicular to the direction of minimum regional compressive stress, and neither nodal plane of double-couple-constrained focal mechanisms generally matches the trend of event locations. This suggests the possibility of an echelon faulting and/or a component of fault opening, perhaps in a fracture mesh geometry similar to that envisioned by Hill [1977]. We hypothesize that both swarms were driven by sudden fluid pressure increases diffusing through the crust along pre-existing fractures, in combination with stress transfer from preceding events. If so, these swarms may represent natural analogs for seismicity induced by industrial injection.

Unified Western US Crustal Motion Map, *Zheng-Kang Shen and Min Wang* (Poster 221)

We collect and process GPS data observed in western US to produce a unified crustal motion map. Great efforts have been made by the USGS/SCEC geodesy group to produce a western US velocity map through combining velocity solutions produced by various groups. Such a solution has been successfully obtained, and used for assessing seismic hazard in the region. The solution nevertheless, could reduce but not eliminate errors arise from systematic biases among different solutions, which could amount up to a few millimeters per year for a large group of sites. Such a problem would not be resolved unless all the GPS data are reprocessed uniformly using the best and latest models and techniques, such as the most updated data processing softwares, satellite and receiver antenna phase center models, ocean tides and atmospheric delay models, and geodetic reference frame, etc.

We collected the campaign GPS data archived at the UNAVCO, SCEC, NCEDC, and USGS data centers, and obtained more than 30,000 RINEX data files observed during 1987-2011 period at more than 3700 campaign sites, plus data from more than 1300 continuous GPS sites. We use the GAMIT software version 10.40 to process the regional data to produce daily solutions, which are combined with SOPAC produced daily solutions of global and regional continuous networks. The combined daily solutions are subsequently aggregated using the QOCA software to solve for station initial positions, secular velocities, coseismic jumps, and postseismic displacements modeled as logarithmic decay functions. The final solution is referenced to the ITRF2008 reference frame, then transferred to the SNARF reference frame realized by constraining

MEETING ABSTRACTS

network translation, rotation, and dilatation of north America fiducial sites to their SNARF model predicted values.

In our current solution we have incorporated all the forementioned data collected 1993-2011, and are working toward to include all the pre-1993 data by the end of this year. Our current solution, after quality checking and filtering, has ~2600 velocity vectors, and ~1500 coseismic and ~1200 postseismic displacement vectors induced by eight strong earthquakes occurred during 1993-2011. This solution will be presented at the meeting, along with a number of transect velocity profiles across the western US. Detailed deformation patterns will also be assessed.

Ground Motions from Large-Scale Dynamic Rupture Simulations, *Zheqiang Shi and Steven M. Day (Poster 023)*

We investigate the characteristics of ground motions generated using an all-physics-based deterministic approach. The rupture events are simulated as dynamic ruptures along rough faults using large-scale three-dimensional models. The fault roughness assumed in our study follows self-similar fractal distribution with the roughness wavelength scales spanning three orders of magnitude from $\sim 10^2$ m to $\sim 10^5$ m. Frictional sliding on the fault is governed by a rate-and-state friction with strongly rate-weakening property and the inelastic yielding of the off-fault bulk material is subject to Drucker-Prager viscoplasticity. Our simulation results show that the fault roughness promotes the development of self-healing rupture pulses and causes loss of rupture coherence. The resulting rupture irregularity leads to ground motions of considerable complexity. Ground accelerations that show extensive high-frequency oscillations exhibit a rich variety of phases and near-flat power spectra between a few tenths of one Hz to slightly less than 10 Hz. The patterns of fault-parallel, fault-normal, vertical and geometric-mean PGAs all show considerable level of variability that appears to be quantitatively similar to that found in earthquake strong motion records. We also computed the orientation-independent RotD50 response spectra of the ground accelerations for representative periods from 0.1 to 3.0 seconds. Compared to the Ground Motion Prediction Equations for the Next Generation Attenuation project (Power et al., 2008), these RotD50 response spectra are highly consistent with those empirical estimates, within the epistemic uncertainty, giving credence to the usefulness of our approach. Our study will contribute to the better understanding of the theoretical aspects of ground motion and hopefully provide useful guidance for the future development of the seismic risk analysis in practice.

Bio-inspired Techniques for Novel Earthquake Research, *Liwen Shih (Poster 273)*

Integrating multiple disciplines to tackle vital research applications has become a recognized trend recently among earthquake researchers. We list here some emerging bio-inspired computing techniques which can play crucial keys for future vital earthquake research breakthrough. The demands for complex, high-throughput, data-intensive research in fine scale, at high frequency, on high-dimensional, big data, is pushing current computation and storage limits. Mimicking problem solving in nature may alleviate the everlasting chafe between fast computing advances and even faster application demands.

Hybrid Lossless/Lossy Image/Data Compression balances accuracy, storage, bandwidth and speed – Inspired by select-focus vision (central vs. peripheral), some seismic data may be lossily compressed for compact storage, reduced bandwidth and faster transmission, and still preserving high, lossless fidelity in critical regions of interest.

Artificial Neural Networks (ANN) approximate and predict – Data-oriented problem solving, such as statistics and ANN, is necessary when model is either not existing or the computation of would take too long. With proper training, good performing ANNs can be developed to intuitively connect the dots for regression, as well as extrapolate beyond existing data scope for prediction. Supervised or unsupervised ANNs are often chosen over statistics on high-dimensional, non-linear, or noisy data. However, ANN results are architecture-dependent, thus can be hard to assess the confidence level at times. ANN models were chosen for earthquake magnitude prediction using multiple seismicity indicators with no clear

correlations among them for two seismically different regions: Southern California and the San Francisco bay in [Panakkat07].

Cellular Automata (CA) cut complexity with local-effect propagation in distributed neighborhoods in discrete time steps – Spatial seismic motion matches well with the local neighbor cells interaction, especially for non-uniform movement due to varied geophysical composition. Coincidentally, distributed computer cores and GPUs are also emerging to synchronize with the needed support for CA computation paradigm.

Several bio-inspired techniques, e.g., ANN and CA, have been attempted in earthquake research with promising outcome. We are currently seeking earthquake data and research collaboration to explore further with hybrid data compression and other emerging computing techniques. rate on reverse faults than

Using the SCEC Broadband Platform for Strong Ground Motion Simulation and Validation, *Fabio Silva, Philip J. Maechling, Kim Olsen, Ralph Archuleta, Robert Graves, Christine Goulet, Paul Somerville, Thomas H. Jordan, and Broadband Platform Working Group (Poster 024)*

The Southern California Earthquake Center (SCEC) Broadband Platform is a collaborative software development project involving SCEC researchers, graduate students, and the SCEC Community Modeling Environment. The SCEC Broadband Platform is open-source scientific software that can generate broadband ground motions for earthquakes that may include deterministic low-frequency, and stochastic high-frequency simulations. SCEC scientists and software developers have integrated complex scientific modules for rupture generation, low-frequency deterministic seismogram synthesis, high-frequency stochastic seismogram synthesis, and non-linear site effects calculation into a software system that supports easy on-demand computation of broadband seismograms.

The SCEC Broadband Platform operates in two primary modes: validation simulations and scenario simulations. When running a validation simulation, the Broadband Platform runs the earthquake modeling software to calculate seismograms of a historical earthquake for which observed strong motion data is available. During the past year, we have modified the software to enable the addition of a larger number of historical events, and we are now adding validation simulation inputs and observational data for 23 historical events covering the Eastern and Western United States, Japan, Taiwan, Turkey, and Italy. When used in the validation mode, the Broadband Platform calculates a number of goodness of fit measurements that quantify how well the model-based broadband seismograms match the observed seismograms for a certain event. Based on these results, the Platform can be used to tune and validate different numerical modeling techniques. Users can also run a scenario simulation using the Broadband Platform. In this mode, users input a scenario event, and list of stations, and select a velocity model from the platform, which then calculates ground motions for the stations.

The SCEC software development group continues to add new capabilities to the Broadband Platform and to release new versions of the platform an open-source scientific software distribution that can be compiled and run on many Linux computer systems. New capabilities in our latest release include the ability to work with observed data in multiple formats; Husid plots to measure significant event duration; additional goodness of fit plots; and extra features and batching utilities that facilitate the execution of large-scale simulations on computing clusters.

A Recursive Division Stochastic Strike-Slip Seismic Source Algorithm Using Insights from Laboratory Earthquakes and Implications of a Big One in the Los Angeles Basin., *Hemant Siriki and Swaminathan Krishnan (Poster 018)*

There are a sparse number of credible source models available from past earthquakes and a stochastic source model generation algorithm thus becomes necessary for robust risk quantification using scenario earthquakes. We present an algorithm that combines the physics of fault ruptures as imaged in laboratory earthquakes with stress estimates on fault constrained by field observations to generate stochastic source models for high magnitude (6.0-8.0) strike-slip earthquakes. The algorithm is validated through a statistical comparison of peak ground

velocity at 636 sites in Southern California from synthetic ground motion histories simulated for 10 hypothetical rupture scenarios of a magnitude 7.9 earthquake along Southern San Andreas fault, using a stochastically generated “median” source model against that generated using a kinematic source model of similar magnitude earthquake from a finite-source inversion. This “median” model, selected from a set of 5 stochastically generated source models, produces ground shaking intensities in Southern California with a median that is closest to the median intensity of shaking from all 5 source models (and 10 rupture scenarios per model). A similar validation exercise is conducted for a magnitude 6.0 earthquake, the lower magnitude limit of the algorithm. The algorithm is then applied to generate 50 source models for a hypothetical magnitude 7.9 earthquake originating at Parkfield, with rupture propagating from north to south (towards Wrightwood), similar to the 1857 Fort Tejon earthquake. Peak ground velocities in the Los Angeles Basin are computed for each scenario earthquake and the sensitivity of ground shaking intensity to seismic source parameters (such as slip, rupture speed, and slip-velocity) is studied. Furthermore, 3-component ground motion waveforms computed at 636 sites in Southern California for the earlier mentioned ten hypothetical rupture scenarios (of magnitude 7.9 earthquake) are used to conduct non-linear dynamic response history analysis (using FRAME3D) of an 18-story building, designed according to the 1982 and 1987 Uniform Building Codes. Damage to the building under each scenario earthquake is quantified and mapped in terms of peak inter-story drift ratios (peak IDR).

Maximum peak ground velocity in Los Angeles Basin, Norman H. Sleep
(Poster 001)

Structural engineers would like to know that maximum past shaking and the maximum credible future shaking. I obtain such limits for large strike-slip earthquakes on the San Andreas Fault that produce reverberating long period (3-4 sec) Love waves in the Los Angeles and Palm Springs Basins. These basin waves pass through relatively stiff exhumed sedimentary rocks and less stiff accumulating sedimentary rocks. Exhumed sedimentary rocks and hard rocks are long-lasting ubiquitous fragile geological features. Seismic waves that exceed the frictional elastic limit produce damage that lowers the stiffness in the upper ca.100 meters. Basin Love waves are relatively simple to analyze. Their wavelength is long enough that they impose strain boundary conditions in the shallow subsurface. The dynamic stress is this strain times the shear modulus. Failure occurs when this stress exceeds the frictional strength. To the first order, frictional strength increases with lithostatic pressure and hence linearly with depth. Seismic regolith develops where the shear modulus increases linearly with depth so that the maximum dynamic strain brings the shallow subsurface to failure (modulus*strain = coefficient of friction * density * depth). S-wave velocity ($\sqrt{\text{modulus}/\text{density}}$) increases with the square root of depth. Typical exhumed sediments in this San Fernando Valley have not experienced strains greater than $1e-3$ corresponding to peak ground velocity (PGV) of 1.5 m/s. Exhumed sediments within the Mission Hills anticline have not experienced strains greater than $0.5e-3$ corresponding to PGV of 0.75 m/s. Conversely, nonlinear attenuation will sap seismic waves that cause strong shallow failure. Widespread accumulating sediments in the Los Angeles Basin will fail at PGV of ~ 3 m/s. The analysis of near-field velocity pulse from strike-slip events is similar. More precise PGV estimates can be obtained if information exists on the fluid pressure (here assumed to be zero) and the coefficient of internal friction (here assumed to be 1). Note this analysis assumes the long wavelength limit and thus does not provide details on the period of the waves. The dynamic Coulomb stress for vertically propagating S-waves is the dynamic acceleration in g's, again yielding simple scaling relationships. An analogous process produces damage from static deformation in the lids of blind faults. Overall the persistence of shallow stiff rocks and steep topography indicates that extreme ground motions greater than 3 m/s PGV or 1 g sustained acceleration are very rare or even nonexistent.

Earthquake source inversion with dense networks, Surendra Nadh Somala, Jean-Paul Ampuero, and Nadia Lapusta (Poster 172)

Inversions of earthquake source slip from the recorded ground motions typically impose a number of restrictions on the source parameterization, which are needed to stabilize the inverse problem with sparse data.

Such restrictions may include smoothing, causality considerations, predetermined shapes of the local source-time function, and constant rupture speed. The goal of our work is to understand whether the inversion results could be substantially improved by the availability of much denser sensor networks than currently available. The best regional networks have sensor spacing in the tens of kilometers range, much larger than the wavelengths relevant to key aspects of earthquake physics. Novel approaches to providing orders-of-magnitude denser sensing include low-cost sensors (Community Seismic Network) and space-based optical imaging (Geostationary Optical Seismometer). However, in both cases, the density of sensors comes at the expense of accuracy.

Inversions that involve large number of sensors are intractable with the current source inversion codes. Hence we are developing a new approach that can handle thousands of sensors. It employs iterative conjugate gradient optimization based on an adjoint method and involves iterative time-reversed 3D wave propagation simulations using the spectral element method (SPECFEM3D). To test the developed method, and to investigate the effect of sensor density and quality on the inversion results, we have been considering kinematic and dynamic synthetic sources of several types. In each case, we produce the data by a forward SPECFEM3D calculation, choose the desired density of stations, filter the data to 1 Hz, add noise of the desired level, and then apply our inversion approach.

The results indicate that dense networks produce sharper images of the considered sources than sparse networks, with better amplitude recovery and better resolution with depth. This is true even when noiseless sparse networks are compared with noisy dense networks, provided that the standard deviations of noise do not exceed $\sim 1\%$ of the maximum earthquake source amplitude. Substantial qualitative improvements arise when features of relatively narrow spatial extent are included in the source, in which case the dense networks can reproduce the features whereas the sparse networks cannot. We will report on our current efforts to incorporate the effect of errors in the bulk velocity model.

Importance of 1-point statistics in earthquake source modeling for ground motion simulation, Seok Goo Song and Luis A. Dalguer (Poster 002)

Both rupture and wave propagation affect strong ground motions on the surface. The complexity of finite earthquake source process may play a significant role in determining near-source ground motion characteristics, especially for large events. Spontaneous dynamic rupture modeling has been efficiently adopted for physics-based source and ground motion modeling for the last several decades, but input dynamic parameters and friction laws are still not well constrained in general. We demonstrate that at least two statistical measures, i.e., 1-point and 2-point statistics, are needed to quantify the heterogeneity of spatial data and that 1-point statistics such as mean, standard deviation, and shape of probability density function (PDF) of dynamic input parameters, is a separate quantity that we need to consider in addition to 2-point statistics in earthquake source modeling. We show that 1-point statistics of input dynamic parameters such as stress drop can significantly affect resulting kinematic source and near-source ground motions. The standard deviations of input stress drop affect both 1-point and 2-point statistics of kinematic source parameters derived from spontaneous rupture modeling significantly and even systematically. They also strongly control near-source ground motions, especially in the rupture directivity region. Quantifying the characteristics of both earthquake source and ground motions in the same format of 1-point and 2-point statistics may help us to construct a consistent framework for studying the effect of finite earthquake source process on near-source ground motions.

Post-1 Ma deformation history of the anticline forelimb above the Pitas Point-North Channel fault in Santa Barbara Channel, California.,

Christopher C. Sorlien, Courtney J. Marshall, Craig Nicholson, Richard J. Behl, James P. Kennett, Sarah H. Decesari, Marc J. Kamerling (Poster 123)

The north margin of rapidly-shortening, rapidly subsiding offshore and western onshore Ventura Basin is comprised of major N-dipping faults that step left. Offshore in Santa Barbara Channel, part of the shortening

MEETING ABSTRACTS

accommodated by the shallow Red Mountain fault is transferred farther offshore to the Pitas Point-North Channel faults (PP-NC). These faults project to merge down dip. We previously mapped the PP-NC to be made up of several left-stepping strands. The eastern 60 km of the offshore >100 km length of this fault system was investigated using dense grids of industry multichannel seismic reflection (MCS) data and local grids of high resolution MCS data. Transects of piston cores recovered from outcropping sediments along the Mid Channel trend in 2005 and 2008 were carefully analyzed using biostratigraphy, oxygen isotopic stratigraphy, and tephrochronology the 639 ka Lava Creek ash. The post-160 ka near-continuous section was earlier cored during ODP Site 893. A discontinuous section provides well-dated time windows back to 740 ka. A ~1 Ma horizon was identified and correlated from drill holes and cross sections by Yeats (1981, 1983).

The PP-NC is variably blind along strike, with its upper tips in places below the 1 Ma horizon and in other locations cutting up to higher levels. The blind slip is absorbed by a progressively-tilting S-dipping forelimb everywhere. Preliminary examination of cross sections through our 8 gridded, depth-converted horizons suggests that the rate of tilting has not significantly changed in the last 1 Ma, and that dips and structural relief, although variable, are not systematically more in the east than the west between Carpinteria and the UCSB campus. There is about 1.5 km of structural relief of the 1 Ma horizon across the forelimb. Given the gentle and moderate dips of the shallow faults, a couple of km of slip is needed to produce such relief. Simple trigonometry of a triangle representing the forelimb, results in only ~0.5 mm/yr. shortening being absorbed by forelimb tilting. Given the half cm/yr GPS shortening across eastern Santa Barbara Channel and the 1.5 km structural relief, additional shortening is expected in the backlimb, by tectonic wedging, pressure solution, sediment compaction, and across the Red Mountain fault system including onshore antithetic faults.

Evolution of the October 1999 Hector Mine Earthquake surface rupture: a decadal view, *Frank J. Sousa, Joann M. Stock, and Sinan O. Akciz* (Poster 238)

We report on the first ever decadal scale repetition of a high density 3D aerial laser scan covering practically all of a large earthquake surface rupture. The scan was acquired by the National Center for Airborne Laser Mapping (NCALM) on May 27, 2012 along a 50 km stretch of the surface rupture of the October 16, 1999 Mw 7.1 Hector Mine Earthquake. This new scan averages 1100 m total width, overlapping with and significantly increasing the breadth of a previous LiDAR scan acquired on April 19, 2000 by the USGS and Aerotech, LLC. Together, the two datasets comprise a 4D (12 year) snapshot of the post-event landscape evolution of a well-defined fault scarp and its immediate environs as well as a test case for characterization of the interplay between landscape evolution through human timescales and offset measurements made on geomorphic features visible in LiDAR derived DEMs. We investigate a 2 km long focus zone of the Lavic Lake fault where it cuts through Neogene volcanic rocks in the Bullion Mountains, a sparsely vegetated area which contains both the maximum horizontal offset measurements from field study and April 2000 LiDAR DEMs and the highest density of April 2000 LiDAR DEM offset measurements. After gridding both the 2000 and 2012 point cloud data for this zone into exactly congruent 0.5 m resolution DEMs we directly subtracted the two raster DEMs. This new raster elucidates specific and quantifiable areas of erosion and aggradation and shows that no measurable post-seismic slip has occurred within the focus zone during the interscan period. Within the focus zone, 28 offset measurements were made previously using the Ladicaoz matlab script by others at the USGS and Caltech. We revisit these 28 measurement locations and find that in roughly half of the locations the same geomorphic features used to measure offset in the April 2000 data are clearly identifiable in the 2012 data. Re-investigating the locations of the three largest offsets made in the April 2000 dataset (over 600cm), we find that each is complicated by the geomorphology of its specific locale. One is at a stream bifurcation point, one is on a stream bend that potentially existed pre-earthquake, and one is located on a slope with minimal along strike relief. High resolution pre-event aerial photography and field investigation of the specific locales is needed to confirm the validity of these large offset measurements.

Present-day loading rate of faults in southern California and northern Baja California, Mexico, and post-seismic deformation following the M7.2 April 4, 2010, El Mayor-Cucapah earthquake from GPS Geodesy, *Joshua C. Spinler and Richard A. Bennett* (Poster 218)

We use 142 GPS velocity estimates from the SCEC Crustal Motion Map 4 and 59 GPS velocity estimates from additional sites to model the crustal velocity field of southern California, USA, and northern Baja California, Mexico, prior to the 2010 April 4 Mw 7.2 El Mayor-Cucapah (EMC) earthquake. The EMC earthquake is the largest event to occur along the southern San Andreas fault system in nearly two decades. In the year following the EMC earthquake, the EarthScope Plate Boundary Observatory (PBO) constructed eight new continuous GPS sites in northern Baja California, Mexico. We used our velocity model, which represents the period before the EMC earthquake, to assess postseismic velocity changes at the new PBO sites. Time series from the new PBO sites, which were constructed 4-18 months following the earthquake do not exhibit obvious exponential or logarithmic decay, showing instead fairly secular trends through the period of our analysis (2010.8-2012.5). The weighted RMS misfit to secular rates, accounting for periodic site motions is typically around 1.7 mm/yr, indicating high positioning precision and fairly linear site motion. Results of our research include new fault slip rate estimates for the greater San Andreas fault system, including model faults representing the Cerro Prieto (39.0±0.1 mm/yr), Imperial (35.7±0.1 mm/yr), and southernmost San Andreas (24.7±0.1 mm/yr), generally consistent with previous geodetic studies within the region. Velocity changes at the new PBO sites associated with the EMC earthquake are in the range 1.7±0.3 to 9.2±2.6 mm/yr. The maximum rate difference is found in Mexicali Valley, close to the rupture. Rate changes decay systematically with distance from the EMC epicenter and velocity orientations exhibit a butterfly pattern as expected from a strike slip earthquake. Sites to the south and southwest of the Baja California shear zone are moving more rapidly to the northwest relative to their motions prior to the earthquake. Sites to the west of the Laguna Salada fault zone are moving more westerly. Sites to the east of the EMC rupture move more southerly than prior to the EMC earthquake. Continued monitoring of these velocity changes will allow us to differentiate between lower crustal and upper mantle relaxation processes.

Measuring Material Properties with a Permanently Deployed Cross-Hole Experiment, *Jamison H. Steidl, Timothy A. Lamere, Sandra H. Seale, Robin Gee, and Paul Hegarty* (Poster 191)

The NEES@UCSB Garner Valley facility was recently enhanced to include a unique cross-hole array experiment. The new permanent cross-hole array includes two geophones and a solenoid-activated dual-direction hammer source at 5m depth. A second set of geophones at 2m depth is deployed directly above the 5m geophones in the same casings. The system is set to trigger once per day automatically with both upward and downward hammer strikes, thus providing the capability to measure shear-wave velocity on a daily basis. The system is also programmed to automatically activate the hammer source at shorter time intervals immediately following a large earthquake. This cross-hole experiment is unique in that these velocity measurements will capture the decrease and recovery of shear wave velocity after a large event. As researchers wait for the Earth to provide an earthquake, the once daily hammer strikes are recorded and analyzed for potential temporal changes in velocity with seasons. The shear-wave velocity is determined by cross-correlation of the signals between the geophones at equal depth. Initial analysis performing cross correlations on the 5m sensors have given a shear-wave velocity of ~220m/s. Two years of daily hammer strike data are presented with comparison to ambient temperature and water table depth. There appears to be a relationship where higher water table (increased pore pressure) reduces the shear strength of the material and a reduction in the shear-wave speed is observed.

Fragile Geologic Features and Points in Hazardspace in New Zealand, *Mark W. Stirling and Dylan H. Rood* (Poster 005)

A major issue facing probabilistic seismic hazard analysis (PSHA) is the lack of established methods for testing or validation of PSH estimates for long return periods (i.e. >100 yrs). Testing or validation requires the use

of independent criteria (criteria that have not already been used in construction of the PSH model) to provide constraints on ground motions at a site, followed by a statistically rigorous comparison of these constraints to the PSH estimates. The use of ancient fragile geologic features such as precariously-balanced rocks (PBRs) to provide constraints on ground motions for return periods of 10-100,000 years has been the topic of considerable research over the last two decades. In our poster we present the initial stages of the first practical application of PBRs to the PSHA of a large hydro-electric dam. The seismic hazard of the Clyde Dam site in New Zealand has recently been reassessed for the first time since the mid-1980s. In this reassessment the Clyde dam was shown to be located on the hanging wall of the nearby Dunstan Fault, with consequent increases in estimated seismic hazard relative to the earlier estimates. Fortunately, the Clyde Dam is also located close to the well-studied Clyde-6 PBR site (see 2011 SCEC abstract). Detailed cosmogenic (Be-10) dating of the Clyde-6 PBR and assessment of the fragility indicates that the PBR has not experienced PGAs of more than about 0.1-0.2g for c. 40,000 years. The paleoseismology of the Dunstan Fault further implies that PBR has survived at least four $M_w > 7$ near-field Dunstan Fault earthquakes over the last c. 30kyrs. In our poster we examine this discrepancy by way of a "points in hazardspace" method. The method was developed during the Yucca Mountain Extreme Ground Motion project, and involves plotting the PBR on the Clyde Dam hazard curves with the fragility on the x-axis (0.1-0.2g) and the inverse of the age (1/40,000 yr) on the y-axis. The points in hazardspace graph shows the accelerations estimated from the Clyde PSH model to be at least a factor-of-two higher than the fragility (toppling acceleration) of the PBR for annual frequencies equivalent to 1/age of the PBR (1/40,000 yr). Follow-up studies of PBRs in the area will be used to further evaluate the PSHA of the Dam site.

Effects of Implementing Coulomb Stress Changes into Southern California Earthquake Forecasts, Anne E. Strader and David D. Jackson (Poster 152)

Previous studies, such as those by Deng & Sykes (1997) and Stein (1997), retrospectively show that a majority of earthquakes tend to occur in areas of positive Coulomb stress change (ΔCFF). We confirm these results for recent seismicity in southern California, but also observe widespread areas with positive ΔCFF where few earthquakes occur. In order to evaluate our hypothesis that ΔCFF influences future earthquake locations, it is necessary to examine how seismically quiescent areas affect its reliability through pseudoprospective testing.

Assuming uniform slip distribution and zero ΔCFF just before the 1812 Wrightwood earthquake, we calculate ΔCFF from seismic sources ($M_w \geq 5.8$) and tectonic loading at just after the 1999 Hector Mine and the 2010 El Mayor earthquakes. We use the average ΔCFF in $0.1 \times 0.1^\circ$ cells to calculate an arctangent index function, where earthquake rates increase monotonically with ΔCFF , using maximum likelihood to obtain the optimal function width and median. Our target earthquake catalog includes 7379 $M_w \geq 2.8$ events (Felzer, 2012) from after the Hector Mine earthquake to the present, which we divide into two time intervals: between the Hector Mine and El Mayor earthquakes, and after the El Mayor earthquake. We use uniform seismicity and smoothed seismicity (Hiemer, 2012) earthquake rates as null hypotheses to test against ΔCFF earthquake rates during both time intervals.

Our results indicate that, although it may potentially contribute to improved earthquake forecasts within a hybrid model, ΔCFF alone is insufficient against other factors, such as fault and previous seismicity locations. Likelihood ratio tests show that ΔCFF alone consistently outperforms uniform but not smoothed seismicity, and that a hybrid of ΔCFF and smoothed seismicity is subject to bias from earthquake clustering. Because earthquake rates calculated from smoothed seismicity decay over a shorter distance than earthquake rates calculated from ΔCFF , earthquake declustering methods play an important role in the forecasts' relative effectiveness. Additionally, introducing temporal dependence through combining ETAS (Zhuang, 2002) or rate- and state-friction (Dieterich, 1996 and Hainzl, 2010) with spatial earthquake density helps to account for aftershock effects and reduce variability in the forecasts' reliability.

Anisotropy of the Mexico Subduction Zone Based on Shear-Wave Splitting, Igor Stubailo and Paul M. Davis (Poster 186)

The Mexico subduction zone is an important region to investigate since it is characterized by both steep and flat subduction, a volcanic arc that appears to be oblique to the trench, and an excellent data coverage due to the 2005-2007 Middle America Subduction Experiment (MASE). Here, we study the anisotropy of the region using shear-wave splitting measurements. Our goal is to verify and complement the three-dimensional model of shear-wave velocity and anisotropy in the region constructed using Rayleigh wave phase velocity dispersion measurements (Stubailo, Beghein, and Davis, published at JGR, 2012). That model contains lateral variations in shear wave velocity consistent with the presence of flat and steep subduction as well as variations in azimuthal anisotropy that suggest a tear between the flat and steep portions of the slab. Shear-wave splitting is effective for studying upper mantle anisotropy beneath the receivers and has a better lateral resolution than the Rayleigh wave phase velocity dispersion measurements, although it suffers from a poor depth resolution. To better resolve the anisotropy at depth, we involve Fresnel zones and the shear-wave splitting based on the higher mode surface waves of different overtones. We will report on our shear-wave splitting results and their comparison and present an evidence of the deep origin of anisotropy under Mexico.

Data Democracy in Simultaneous Monte Carlo Optimizations of Geodetic and Seismic Data, Henriette Sudhaus and Sebastian Heimann (Poster 275)

Estimating the geometry of an earthquake source from seismological and/or geodetic data is a non-linear problem. Often, Monte Carlo methods are used to find the optimum earthquake model through a sophisticated sampling of a misfit function in the multidimensional model space. The topology of the misfit function and hence the best fitting model, however, very much depend on the weight we assign to the data. Moreover, there is a large variation between simple arbitrary data weight assignments and weights calculated from data error estimations or trial modeling results.

An accepted and regularly applied procedure to weight geodetic data, e. g. from GPS and InSAR data, is in accordance with their quality, as derived from a data error variance-covariance matrix. In this way, we consider correlations of densely spaced data with data weight factors that are independent of the model parametrization. In seismological source studies, the data weighting often appears to be done more simply. Qualitatively, the

azimuthal coverage is ensured, but relative weights for different stations are assigned only sometimes, e. g. based on apparent noise. For combining of geodetic and seismological data, it would be desirable to have an internally consistent rationale for assigning the weights within each data set. Thereafter, we need to find meaningful weighting between the different data sets.

We present our way of data weighting in a source optimization study of the 2010 Haiti earthquake. Here, we use a rich data set of teleseismic waveforms as well as measurements of the coseismic surface deformation derived from geodetic sources. The latter include GPS, several ALOS L-band interferograms and pixel offset measurements from TerraSAR-X radar amplitude images. With meaningful data weighting and an advanced joint optimization of the seismic and geodetic data, we aim for a robust estimation of the first-order kinematic parameters of the earthquake source.

Investigating the spatial and temporal distribution of earthquakes and tremor along the Cholame segment of the San Andreas fault, Danielle F. Sumy, Elizabeth S. Cochran, Rebecca M. Harrington, and Justin R. Brown (Poster 156)

The Parkfield Experiment to Record Microseismicity and Tremor (PERMIT) is a thirteen-station broadband array deployed between May 2010 and July 2011 near Cholame, California, to improve seismic network coverage south of the High Resolution Seismic Network (HRSN). The array is located along a portion of the San Andreas fault that transitions from locked to creeping northward along fault strike. The goal

MEETING ABSTRACTS

of the project is to explore the spatiotemporal relationships between low-frequency earthquakes (LFEs) and local earthquake activity reported in the Northern California Seismic Network (NCSN) catalog and identified in the temporary array data. We identify LFEs from a catalog of tremor episodes automatically detected using a neural network approach. Previous studies have shown that tremor activity increased along this section of the San Andreas fault before and after the 2004 Parkfield earthquake, suggesting that stress interactions exist between earthquakes in the shallow, seismogenic zone and processes in the deeper transition zone. Understanding the range of fault slip behaviors, including how tremor and earthquakes interact, will provide critical information for assessing seismic hazard.

Spatiotemporal Behaviors in Earthquake Multiplets at the Geysers Geothermal Field, CA, Taka'aki Taira (Poster 201)

The Geysers geothermal field is located in northern California and is characterized by a high rate of microseismicity. The Geysers seismicity is spatially and temporally correlated with the geothermal production and injection well activity. One of important signatures of the Geysers microseismicity involves earthquake multiplets or families of earthquakes with similar waveforms. Spatiotemporal variations in the state of stress or migration of geothermal fluids near the multiplet source area would be reflected by changes in multiplet occurrence in time and space. An investigation of temporal behaviors of multiplet characteristics is, in principle, capable of monitoring subsurface stress field and hydrothermal fluid migration. We construct a multiplet catalog by using broadband seismic data recorded by the STS2 installed at station GDXB. This station is located near the center of the Geysers geothermal area and has been operational since the middle of 2006. We focused on analyzing broadband data from station GDXB and analyzed over 65,000 Geysers local earthquakes (May 2006 through Dec. 2011) detected by the Northern California Seismic System earthquake catalog. A 8-24 Hz bandpass filter and a 5.12-s time window from the direct P-wave were used to identify multiplets. We measured cross-correlation values for 400 million seismogram pairs and used 0.95 for the waveform cross-correlation threshold for identifying multiplets. Our cross-correlation analysis identifies around 550 earthquake multiplets with magnitudes ranging from 0.06 to 1.77. The majority of the multiplets are earthquake doublets. The catalog of the Geysers multiplets appears to indicate an increased multiplet activity after 2010. We will examine spatial and temporal correlations between the multiplet seismicity and the production and injection well activity. With the double-difference earthquake catalog by Waldhauser and Schaff (2008, JGR), we find the majority of the event pairs (about 50 pairs) with shorter recurrence intervals (less than 1 hour) are located along the Big Sulphur Creek fault in a depth of 4 km. It appears that the occurrences of these events are not correlated with the water injections and larger earthquakes (M3+). To explore the underlying mechanisms, efforts are ongoing to evaluate the relative seismic moments for individual event pairs by using a method with the Singular Value Decomposition introduced by Rubinstein and Ellsworth (2010, BSSA).

Dynamic models of potential earthquakes within the San Gorgonio Pass, CA, Jennifer M. Tarnowski and David D. Oglesby (Poster 101)

We use numerical modeling to investigate the likelihood of a through-going earthquake along the San Andreas fault system in the San Gorgonio Pass (SGP). The SGP is a structurally complex area of Southern California often referred to as a "pinch-point" along the fault system, with several non-vertical and non-coplanar segments. It may or may not be a geometrical barrier that can slow or stop earthquake rupture propagation. The likelihood of through-going rupture in the SGP affects the maximum earthquake size in Southern California as well as the intensity and distribution of ground motion, with implications for seismic hazard. We use the finite element code FaultMod (Barall, 2009) to observe differences in rupture propagation and ground motion based on different input parameters in a simplified fault geometry of the SGP region. Models that include the San Bernardino, Garnet Hill, and Coachella Valley fault strands show that near-fault ground motion patterns are heterogeneous with pronounced asymmetry across the fault strands. Ground motion distribution farther from the strands varies with the hypocenter location. In models with faults close to failure, the

presence of well-defined Mach cones suggest that non-planar fault strands may not inhibit supershear rupture nor render Mach cones incoherent. The models presented here are the early stages of a series of test cases to develop more realistic models of rupture in the SGP that incorporate the complexity of fault geometry and stress distribution in the region.

Application of Cluster Analysis to Interpreting Regional GPS Velocity Fields in California, Wayne Thatcher, James Savage, and Robert Simpson (Poster 234)

Deformation fields from dense regional GPS networks can often be concisely described in terms of relatively coherent blocks bounded by active faults, although the choice of blocks, their number and size are subjective and usually guided by the distribution of known faults. Cluster analysis applied to GPS velocities provides a completely objective method for identifying groups of observations ranging in size from 10s to 100s of km in characteristic dimension based solely on the similarities of their velocity vectors. In the three regions we have studied (the Mojave Desert and the San Francisco Bay region in California, and the Aegean in the eastern Mediterranean), statistically significant clusters are almost invariably spatially coherent, fault bounded, and coincide with elastic, geologically identified structural blocks. Often, higher order clusters that are not statistically significant are also spatially coherent, suggesting the existence of additional blocks, or defining regions of other tectonic importance (e.g. zones of localized elastic strain accumulation near locked faults). These results can be used both to formulate tentative tectonic models with testable consequences and to suggest focused new measurements in under-sampled regions.

Cluster analysis applied to GPS velocities has several potential limitations, aside from the fact that any data set, even random data, can be clustered. First of all, the gap test for significance, when used to identify the number of clusters yielding the greatest significance level, typically selects a small number of clusters in a given region, usually 5 or fewer. Visual inspection of higher order clusters beyond this number may suggest additional smaller blocks, distributed strain, or geologic structures. Results may sometimes be refined by applying the method to smaller, more focused sub-regions. Finally, GPS data precision and spatial density limit the degree to which distinct clusters can be resolved. This highlights the importance of incorporating higher precision data (e.g. semi-continuous and continuous GPS sites) and, if possible, of other data types (for example, InSAR deformation maps) into the method.

Preliminary Results from the 2012 Dry Lake Valley Paleoseismic Site on the central Creeping Section of the San Andreas Fault, Nathan A. Toke, Tsurue Sato, Larry Kellum, Nicole Abueg, James Anderson, Jeff Selck, James B. Salisbury, and J.R. Arrowsmith (Poster 140)

A predominant hypothesis is that historical records of seismicity and fault creep are representative of the locations and mechanisms of San Andreas Fault (SAF) behavior over long time scales. We identified the Dry Lake Valley paleoseismic site (DLV site; 36.46791, -121.05564), located within the region of peak aseismic slip (~30 mm/yr) along the central SAF as a good location to test this hypothesis. The main 2012 trench (DLV-1) was cut across a fault bounded sag depression that developed within an alluvial fan complex emanating from the northeast. The sag is ~40 m wide and ~250 m long. It is steep-sided and asymmetric. The northeast fault scarp is 7 m high and the southwest scarp is 3 m. A modern channel enters the depression from the east. We excavated and logged a 45.5 m fault-perpendicular trench extending from the outflow of the modern channel to the top of the western scarp. We documented alluvial fan sediments underlying a series of clayey silt and sand packages that were deposited within the sag and overprinted by poorly-developed paleosols. DLV-1 exposed two regions of faulting. On the western side of the sag, the region of faulting is 7 m wide and parallel with the local trend of the SAF (315°). Whereas, on the eastern side of the sag the region of faulting is > 13 m wide and includes more than a dozen small faults. These faults are oriented ~40° clockwise from the SAF trend. They are characterized by modest opening and fill within the lower half of the 2.5 m exposure. Above these filled zones, narrow cracks extended to the surface. The region of faulting on the west side of the sag is concentrated within four zones. Curiously, the most prominent of these zones bounds a sub-

vertical mass of sand, cobbles, and boulders. The stratigraphy above the fault zone gravel is overprinted by soil alteration and an oblique to the SAF shear fabric that is common across the two regions of faulting in this trench. However, there is a remnant structure to the sediment that suggests the fault zone gravels are capped by bedding. We excavated a fault parallel trench (DLV-2) just west of the sag which revealed numerous channel deposits with varying clast size (pebbles to boulders) and structure (bedded to massive). It is likely that these paleochannels are the origin of the fault zone gravels. Two questions remain. Did a paleoearthquake induce these gravels to fall into the fault zone? Or, did fault creep rearrange the channel gravels into place?

A systematic estimation of fault creep rates along major faults in California from L-band radar interferometry, Xiaopeng Tong, David Sandwell, and Bridget Smith-Konter (Poster 205)

Accurate and continuous monitoring of fault creep is important for understanding fault behavior and evaluating seismic risk. Fault creep rate has been documented along major active faults in California using various techniques (e.g., alignment arrays, cultural offsets, GPS, InSAR, and creepmeters) since the 1970s. Using GPS and L-band InSAR, we have produced a new high-resolution interseismic velocity map that can be used to systematically evaluate the fault creep rates along all major faults of the San Andreas Fault System, including some that have not been well instrumented before. The L-band PALSAR onboard ALOS is less affected by temporal decorrelation, thus we can recover fault creep even in the vegetated areas in northern California. The creep rate measurements from space-born InSAR are low-cost and cover a wide range of faults, including the San Andreas fault, Maacama fault, Bartlett Springs fault, Concord fault, Rogers Creek fault, Calaveras fault, Hayward fault, Garlock fault, San Jacinto fault, and Superstition Hills fault. In this study we compared creep rates with ground-based instruments compiled in UCERF2 [Wisely et al., 2008] to evaluate the practicability and uncertainties of our method. Our results indicate a general agreement, although there are a few areas of statistically significant discrepancy, which may be attributed to temporal variation of fault creep.

Fault Nomenclature for the San Gorgonio Pass Region, Jerome A. Treiman, Jonathan C. Matti, William A. Bryant, and Katherine J. Kendrick (Poster 128)

The spatial distribution of late Cenozoic faults in the San Gorgonio Pass (SGP) region of southern California lends credence to the old adage "what's in a name?" The Pass, colloquially referred to as the "San Gorgonio Pass knot" in the San Andreas Fault (SAF), is traversed by an array of dextral and sinistral strike-slip faults, contractional thrust and reverse faults, and normal dip-slip faults that, collectively, represent ~10 Ma of tectonic history within the San Andreas Fault system (*sensu lato*). This long tectonic history has led to complex spatial and structural relations among the various faults. As might be expected, names historically applied to these faults are as diverse and complex as the faults themselves, with workers in some cases using different names for the same fault or using the same name in different ways. Vaughan (1922) first introduced the name "San Andreas Fault" in SGP. Subsequent fault names include the Banning Fault (Hill, 1928), the Mill Creek and Mission Creek faults (Allen, 1957), north and south branches of the San Andreas Fault (as used by Dibblee, 1964, 1968, 1975, 1982), and the San Gorgonio Pass Fault Zone as proposed by Smith (1979) and as extended by Matti and others (1985, 1992). The result is a maze of fault patterns and inconsistent nomenclatural usage.

With increasing SCEC focus on the seismotectonic framework of the SAF in SGP, including consideration of a Special Fault Study Area, the need for consistent fault nomenclature recognized and used by the entire earthquake community is evident. To this end, the California Geological Survey and U.S. Geological Survey are developing a nomenclatural scheme that represents the full range of fault types and their presumed fault-family associations. An example of the latter would be the strands of the dextral San Andreas Zone versus strands of the contractional San Gorgonio Pass Fault Zone versus older structures like the Banning Fault. The proposed fault nomenclature supports a coherent tectonic picture for the SAF zone in SGP that includes (1) how SAF strands are distributed, (2) how displacements on these strands have been sequenced, and (3)

how fault names intuitively allow the earthquake community to explore and evaluate late Holocene strain budgets, likely fault-rupture patterns, and earthquake hazards. Most importantly, the nomenclature attempts, as much as possible, to reflect historical usage while simultaneously accommodating recent mapping and current practice.

Potential of High-Performance Computing for Solid-Earth Science, Jeroen Tromp (Talk Tue 10:30a)

In recent years, modeling, simulation and computation have come to play a central role in modern solid-Earth science in general, and seismology in particular. With dramatic increases in the quality and quantity of geophysical data and the availability of sophisticated open-source numerical modeling tools, there is a need for a more organized, community-driven approach to computational solid-Earth science. As an example, the California Seismic Network, the EarthScope USArray Transportable Array, the permanent Backbone Array, and the Flexible Array are providing seismologists with a wealth of new data. Data analysis is keeping up with data acquisition only for the computationally simplest analysis methods, as even computationally modest analysis is often still labor intensive. Modeling of and imaging with this data requires powerful numerical modeling tools, automation of routine analysis tasks, and dedicated high-performance computing facilities.

Most simulations are currently performed on modest in-house facilities, or through grants at various national supercomputing centers. A dedicated simulation facility would accommodate the substantial computational demands of modern solid-Earth science, including, for example, kinematic and dynamic rupture simulations to assess seismic hazard, data assimilation simulations in geodynamics, seismology, and geomagnetism, and full waveform inversions in global and regional seismology. Such a facility would not obviate the need for local resources, instead the local facilities would be used for development, scenario testing, and education, acting as the on-ramp to the earth science HPC facility. The facility would benefit investigators at universities that have limited HPC resources by providing hardware, software engineering, training and a community specific environment to draw on. The goal of such a computational solid-Earth science center should be to provide our community a system structured specifically for our simulation/imaging needs, which include large fast storage capacity, large memory, and a large number of cores, configured in a system designed for long run-times, which also allows for user interaction between iterations in compute intensive inversions.

When Are Noise Correlation Amplitudes Useful?, Victor C. Tsai and Zhongwen Zhan (Poster 197)

The amplitudes of ambient-noise cross-correlation measurements depend on a number of factors, including noise source amplitude, site response, anelastic attenuation, and wavefield scattering by velocity heterogeneities. It has been suggested by various authors that certain noise processing techniques can suppress the dependence of these amplitudes on some of the factors so that the other factors can be more systematically analyzed. These processing techniques include spectral whitening, temporal normalization, temporal flattening, deconvolution, and C-cubed processing. Here, we find that while these techniques do help in many ways to reduce the systematic bias of factors like inhomogeneous noise source distributions, there remain some counterintuitive dependencies in many cases that resemble realistic Earth situations. We describe some of these dependencies. For example, we quantitatively describe the smoothness criteria for noise distributions that is necessary for amplitudes to decay with distance as predicted by equipartition theory; and we find that the results of C-cubed processing depends on the distribution of scatterers and the strength of scattering.

Array analysis of Love-wave data in the Southern California Seismic Network (SCSN) to Detect Azimuthal Anisotropy, Stephanie D. Tsang and Toshiro Tanimoto (Poster 167)

Love-wave data are particularly sensitive to the shear wave structure. Therefore, they should prove critical in evaluating the heterogeneity and anisotropy of the Earth's subsurface structure, particularly that of Southern California's. Using the Southern California Seismic Network (SCSN) as an array, the beamforming method (e.g., Johnson and

MEETING ABSTRACTS

Dudgeon, 1993) is applied to determine the Love-wave phase velocities and their backazimuth angles for 190 teleseismic events. The beamforming method should prove effective in detecting the azimuthal dependence in phase velocity measurements of the teleseismic events as they propagate through the network. This is essential in terms of yielding insight into the anisotropic subsurface structure.

One goal of this project will be to further constrain the anisotropic fast-axis orientation and its tectonic implications in detecting azimuthal anisotropy. Alvizuri and Tanimoto (2011) carried out array analysis while examining only the vertical components of this same data set spanning over ~10-year range (1998-2008). However, the depth resolution of the anisotropic structure in this case was limited: azimuthal anisotropy was detected for frequencies between 30 and 60 mHz, but below 10 mHz and above 60 mHz the resolution is reduced. Their results show a dominance in the azimuthal dependence for anisotropic phase velocities for the 2θ term and a negligible dependence on the 4θ term. Their results also show a fast-axis orientation in the SE-NW ($110/290^\circ$ relative to 0°) direction. This project aims to investigate the azimuthal dependence of the 2θ and 4θ terms in measuring phase velocities for Love-waves. The incorporation of the analysis of the Love-wave data using this approach will increase the depth resolution of, thereby providing insight for a more comprehensive and detailed understanding of the overall anisotropic structure.

Tracking the Moho and the lithosphere-asthenosphere boundary along the margin of the Salton Trough with variations in basaltic magmas,

Elinor S. Utevsky, Andrew P. Barth, and Drew S. Coleman (Poster 253)

The intersection of the East Pacific Rise with the subduction-related trench off Southern California approximately 29 Ma created a transform system, which evolved into the modern San Andreas fault. Demise of the subduction zone may have also formed a gap in the subducting oceanic slab, leaving space for upwelling asthenospheric mantle. A suite of Miocene to Recent volcanic systems are critically located between the southern portion of the San Andreas fault, the western extent of the Basin and Range, and the northern boundary of the East Pacific Rise, representing volcanism related to the transition from a subduction zone to a transform fault system. This study will influence future modeling of the San Andreas fault and related volcanism, as well as assist in understanding the characteristics and local variations in the mantle beneath this region. Past studies of adjacent volcanism suggest the presence of both a typical asthenospheric source mantle to the north and a depleted mantle to the south, with little to no evidence of an old lithospheric mantle carrying a subduction signature beneath the crust. Volcanic systems are grouped latitudinally, with silica-undersaturated alkali basalts to the north, older silica-oversaturated tholeiites dominating the central sites possibly related to the onset of Basin and Range extension, and silica-undersaturated olivine tholeiites to the south. Within the northern alkali basalt province, the $87\text{Sr}/86\text{Sr}$ ratios display a longitudinal gradient with the highest values the farthest east, supporting the involvement of an old lithospheric mantle. These analyses suggest the mantle is heterogeneous and atypical, and generated at least two distinct parent magmas. Past studies illustrate that both the crust and lithosphere are remarkably thin southwest of the San Andreas fault within the Salton Trough, but thicknesses appear less correlated northeast of the fault. Additional geochemical data for volcanic rocks immediately northeast of the fault will explore the possibility that the southern thinning is related to mid-ocean ridge volcanism and formation of oceanic lithosphere, whereas continental crust to the north is underlain by both thicker and possibly older lithospheric mantle and an upwelling asthenospheric mantle.

Observation of far-field Mach waves generated by the 2001 Kokoxili supershear earthquake,

Martin Vallée and Eric M. Dunham (Poster 073)

Regional surface wave observations offer a powerful tool for determining source properties of large earthquakes, especially rupture velocity. Supershear ruptures, being faster than surface wave phase velocities, create far-field surface wave Mach cones along which waves from all sections of the fault arrive simultaneously and, over a sufficiently narrow frequency band, in phase. These waves are essentially the Mach waves that have been

the focus of ground motion studies in the near-source region. We present the first observation of far-field Mach waves from the major Kokoxili earthquake (Tibet, 2001/11/14, Mw 7.9) and confirm that ground motion amplitudes are indeed enhanced on the Mach cone. Theory predicts that on the Mach cone, bandpassed surface wave seismograms from a large supershear rupture will be identical to those from much smaller events with similar focal mechanisms, with an amplitude ratio equal to the ratio of the seismic moments of the two events. Cross-correlation of 15 \times 25 s Love waves from the Kokoxili event with those from a much smaller (Mw 5) foreshock indicates a high degree of similarity (correlation coefficient

Earthquake Preparedness Education Program, *Michelle J. Vanegas, Monica Barajas, Nick Scruggs, Aaron Hoogstraten, and Robert M. de Groot (Poster 251)*

This project consisted of creating an educational, interactive presentation that explores the science of earthquakes, and proper earthquake preparedness and safety practices. The presentation is designed to be performed in a free-choice learning institution (i.e. museums, science centers, etc.), and is designed with an all-ages audience in mind. A script, background information packet, and supply list were also created as curriculum for the program. The main goals of this program are: raising public awareness of seismic hazards throughout California, as well as piquing public interest – especially in children – in the fields of earth science and geology. The target audience age-range of program is children ages 6-12, and because of this, one of the major challenges was figuring out how to communicate complex ideas of geology and natural disasters in a way that would be easy for a young audience to understand. The first half of the presentation explores basic concepts of geology, such as the composition of the earth, plate tectonics, and strike-slip fault systems. The second portion of the presentation focuses on the proper assembly of a disaster supply kit, and staying safe during an earthquake with the “drop, cover, and hold on” method. Ultimately, the objective of the project is to export this presentation for use in other institutions throughout California to continue to spread earthquake preparedness education to the public.

3-D Rocking Response of Precariously Balanced Rocks, *Swetha*

Veeraraghavan and Swaminathan Krishnan (Poster 017)

There are several precariously balanced rocks (PBRs) in western US. Analyzing the toppling behavior of these rocks can provide limits on the largest ground motions (of the type that the rocks are sensitive to) that could have occurred at the rock sites in the time that they have been precarious. We are creating detailed 3-D models of some of the PBRs that have been imaged using Terrestrial Laser Scanning (TLS) techniques in order to analyze the toppling behavior accurately. To establish the proof of concept, we are modeling the Echo Cliff PBR which is located in the Western Santa Monica Mountains. We first obtain equally spaced nodes throughout the rock using Matlab. Then, under the assumption that the rock and the pedestal behave like rigid bodies, we use rigid body dynamics to solve for the response of the rock to different ground motions. The state of the rigid body at any instant in time can be fully described by the position vector of the center of mass (CM), velocity of CM, a rotation matrix (which is a transformation mapping between the local body fixed configuration and the global configuration) and the angular momentum of the rigid body about CM. At each time step, these state variables are updated using force and moment balance equations. Forces and moments arise out of the inertia of motion as well as the normal contact and tangential friction between the rock and pedestal. The impact from the collision is forced to be perfectly inelastic (i.e., no bouncing) by applying an impulse at each contact point to reduce the relative normal velocity between the rock and the pedestal to zero at that point. Two linear complementarity problems are solved, one for the impulse force to be applied, and the other for the contact normal and frictional forces simultaneously. Using this algorithm, we have performed some preliminary analysis on the Echo Cliff PBR. We are analyzing the 3-D response of the rock to idealized saw tooth ground velocity pulses with varying peak ground velocity (PGV), time period (T) and number of cycles (n). This will provide an estimate of the combinations of PGV, T and n that will topple the rock. The toppling analysis are being performed on several

precariouly balanced rocks in southern California to help characterize seismic hazard in the region.

Steady slip pulses on faults with rate- and state-dependent friction and strong velocity-weakening friction due to flash heating, *Robert C. Viesca and Dmitry I. Garagash* (Poster 097)

We present solutions for steadily propagating slip pulses whose underlying frictional evolution is dependent on both the rate of slip and the evolution of a state parameter (of a slip-law type), with strong velocity-dependent weakening of friction at high slip rates (via flash heating of asperity contacts). Such a dynamic weakening mechanism has been suggested as a mean through which the majority of strength is lost during an earthquake rupture and by which earthquakes may occur despite low levels of fault-resolved shear stress (e.g., Noda et al., JGR 2009).

The behavior immediately behind the tip, where the state-evolution effect is dominant, is universal for solutions in which the characteristic slip velocity is much greater than V_w . In this region, strength weakens exponentially with slip and is representable by a tip solution with an associated flash-weakening fracture energy (Brantut & Rice, GRL 2011; Garagash & Viesca, AGU 2011). Further behind the tip, the direct effect (relating velocity changes to instantaneous changes in friction) again becomes important. Considering the trailing edge, as state evolution of the slip-law type does not provide frictional restrengthening at zero slip velocity, the slip pulse heals asymptotically with distance behind the rupture tip. A robust, effective pulse length can be established in this case by setting a threshold value of the slip velocity.

We find a relation between background stress levels and steady rupture velocity (lower background stress implies propagation velocities approaching the limiting seismic speed). These solutions (which contain no information on nucleation) are found for wide range of background stress levels (e.g., as also in Garagash, JGR 2012), suggesting that pulse-like ruptures may be observable over the range of background stress, including large, near the nominal strength values which are usually associated with the crack-like mode. This is encouraged by the observation in full elastodynamic simulations with strong rate-weakening friction that the background stress levels marking the phase boundaries between arresting and growing pulses, and between growing pulses and crack-like ruptures, respectively, depend on manner of nucleation and may span a large range of the background stress (Gabriel et al., rev. JGR 2012; Noda et al., 2009).

Estimation of path effects on the ground motion standard deviation based on the empirical data and the simulated waveforms from the CyberShake platform, *Manuela Villani and Norman Abrahamson* (Poster 012)

In seismic hazard analysis (SHA), an ergodic assumption is typically made when the variability in the ground-motion at a single site-source combination is assumed to be the same as the total standard error of a classical ground motion prediction equation (GMPE). The latter is the misfit between observations and the corresponding predicted ground motions at multiple stations. Thus, the standard deviation of empirical GMPEs includes both the variability due to different sites and that of different ray paths. When physics-based numerical simulations of ground motion, such as CyberShake, are used as input for a PSHA, the ergodic assumption is removed. In this case, the predicted variability in the ground motion at a given site directly includes the 3D path and rupture characteristics specific and unique to the studied site for a specified rupture. The modeling error of the GMPEs can be partitioned into five components: two true aleatory components of variability for the source and path effects due to the simplified parameterization of the source and wave propagation used in PSHA (inter- and intra-event terms), and three repeatable effects due to the average source effect, path effects, and site effects that apply to a given site/source combination.

In this work, we explore the spatial correlation of residuals to estimate path effects and the path-specific standard deviation. To this end, we used two sets of residuals of the response spectral values: one empirical set of single-station intra-events residuals from a preliminary version of the Abrahamson and Silva updated NGA model and one set derived from simulated waveforms of the CyberShake platform. These residuals are

used to develop spatial maps of the path effects and the results reduction in the standard deviation for a single ray path. We compare the empirical and CyberShake results for selected sites in Los Angeles basin at an oscillator period of 3 s.

Rupture to Rafters on a Global Scale, *David J. Wald* (Talk Sun 18:00)

The U.S. Geological Survey's Prompt Assessment of Global Earthquakes for Response (PAGER) system provides rapid and automated alerting of estimated economic and human impacts following earthquakes around the globe. Although PAGER's primary purpose is to quantitatively any earthquake's severity for situational awareness and response decision-making, the underlying tools developed are utilized for many other scientific and mitigation efforts. PAGER is an end-to-end system of scientific and engineering results combined for the purpose of loss estimation, analogous to SCEC's notion of "rupture to rafters" computations. There are four components of the PAGER system. First, earthquakes trigger rapid source characterization; second, these source parameters inform our estimates of shaking-distribution (e.g., ShakeMap). Third, losses are then modeled by computed populations exposed per shaking intensity level, and country-specific and shaking-dependent loss functions are used to provide estimates of economic impact and potential casualties. Finally, these uncertain loss estimates are communicated in an appropriate form for actionable decision-making among a variety of users. Rapidly and automatically assessing the wide range of seismological, demographic, building inventory, and vulnerability information necessary to make such loss estimates entails a requisite balance of empirical & physics-based modeling strategies. Several aspects of our problem cannot yet be adequately solved with purely empirical, nor solely mechanistic, approaches. The "physics-based" model components of the PAGER system are essential for informing empirical models where they are data-limited, and for providing a framework for better understanding the causative pathways that dominate earthquake losses around the globe. In the course of explaining the end-to-end strategies and science/engineering employed by the PAGER system, we also describe what pragmatic choices were made in balancing the uncertainties in and benefits provided by our empirical, semi-empirical, expert-opinion, and physical models. We then relate these trade-offs to similar challenges faced by SCEC scientists. Recognizing and reconciling the complimentary benefits of data-driven versus theoretical problem-solving is at the core of the PAGER system, as it is for a wide variety of other challenges within the earth sciences.

UNAVCO-PBO Southwest Region Network Operations, *Christian Walls, Doerte Mann, Andre Basset, Jacob Sklar, Chelsea Jarvis, Travis Pitcher, Shawn Lawrence, and Karl Feaux* (Poster 224)

The UNAVCO Southwest region of the Plate Boundary Observatory manages 470 continuously operating GPS stations located principally along the transform system of the San Andreas Fault, Eastern California Shear Zone and the northern Baja peninsula. In the past year, network uptime averaged 98% with greater than 99% data acquisition. Communications range from CDMA modem (314), radio (100), Vsat (30), DSL/T1/other (25) to manual download (1). Thirty-four stations have WXT520 metpacks. Sixty-four stations stream 1 Hz data over the VRS3Net typically with <0.5 second latency. Over 650 maintenance activities were performed during 341 onsite visits out of approximately 346 engineer field days. Within the past year there have been 7 incidences of minor (attempted theft) to moderate vandalism (solar panel stolen) with one total loss of receiver and communications gear. Security was enhanced at these sites through fencing and more secure station configurations.

UNAVCO is working with NOAA to stream real-time GPS and met data from PBO stations with WXT520 meteorological sensors and high rate data communications. These streams support watershed and flood analyses for regional early-warning systems related to NOAA's work with California Department of Water Resources. Network-wide NOAA receives a total of 54 streams including stations in Cascadia.

In 2008 PBO became the steward of 209 existing network stations ("Nucleus stations") of which 140 are in the SW region that included SCIGN, BARD, BARGEN stations. Due to the mix of incompatible equipment used between PBO and existing network stations a project

MEETING ABSTRACTS

was undertaken to standardize existing network GPS stations to PBO specifications by upgrading antenna cabling, power systems and enclosures. In 2012 the Nucleus upgrade project was completed.

Using Averaging-Based Factorization to Compare Seismic Hazard Models Derived from 3D Earthquake Simulations with NGA Ground Motion Prediction Equations, Feng Wang and Thomas H. Jordan (Poster 009)

Seismic hazard models based on empirical ground motion prediction equations (GMPEs) employ a model-based factorization to account for source, propagation, and path effects. An alternative is to simulate these effects directly using earthquake source models combined with three-dimensional (3D) models of Earth structure. We have developed an averaging-based factorization (ABF) scheme that facilitates the geographically explicit comparison of these two types of seismic hazard models. For any fault source k with epicentral position x , slip spatial and temporal distribution f , and moment magnitude m , we calculate the excitation functions $G(s, k, x, m, f)$ for sites s in a geographical region R , such as 5% damped spectral acceleration at a particular period. Through a sequence of weighted-averaging and normalization operations following a certain hierarchy over f , m , x , k , and s , we uniquely factorize $G(s, k, x, m, f)$ into six components: A , $B(s)$, $C(s, k)$, $D(s, k, x)$, $E(s, k, x, m)$, and $F(s, k, x, m, f)$. Factors for a target model can be divided by those of a reference model to obtain six corresponding factor ratios, or residual factors: a , $b(s)$, $c(s, k)$, $d(s, k, x)$, $e(s, k, x, m)$, and $f(s, k, x, m, f)$. We show that these residual factors characterize differences in basin effects primarily through $b(s)$, distance scaling primarily through $c(s, k)$, and source directivity primarily through $d(s, k, x)$. We illustrate the ABF scheme by comparing CyberShake Hazard Model (CSHM) for the Los Angeles region (Graves et. al. 2010) with the Next Generation Attenuation (NGA) GMPEs modified according to the directivity relations of Spudich and Chiou (2008). Relative to CSHM, all NGA models underestimate the directivity and basin effects. In particular, the NGA models do not account for the coupling between source directivity and basin excitation that substantially enhance the low-frequency seismic hazards in the sedimentary basins of the Los Angeles region. Assuming CyberShake simulations are representative of earthquake excitation in this region, we show the degree to which regionally modified versions of the NGA models can reduce epistemic uncertainties.

Triggering of Tremor along the San Jacinto Fault near Anza, California, Tien-Huei Wang, Elizabeth S. Cochran, Duncan Agnew, and David D. Oglesby (Poster 195)

Remote triggering of tremor has been widely documented in various tectonic regions; however, the dominant factor required to trigger tremor remains unclear. We examine the conditions necessary to trigger tremor along the San Jacinto Fault (SJF) near Anza, California where previous studies suggest triggered tremor occurs, but observations are sparse. The two main factors influencing tremor occurrence are thought to be the stress imposed on the fault plane and the period of the applied stress. We use continuous broadband seismograms from 11 stations located near Anza, California. We analyze 44 $M_w \geq 7.4$ teleseismic events between 2001 and 2011; these events occur at a wide range of backazimuths and hypocentral distances. The maximum shear stress estimated from velocity seismograms are verified by surface strain measurements at station PFO. We find that stress estimated from seismograms is consistent with that from surface strain measurements.

We find the only episode of triggered tremor, which occurs during the 3 November 2002 M_w 7.8 Denali earthquake. The tremor episode starts at the Love wave arrival, when surface-wave particle motions are primarily in the transverse direction. The Denali earthquake induces the highest stress among the 44 teleseismic events. The dominant period of the Denali surface wave is 22.8 seconds, at the lower end of the range observed for all events (20-100 seconds). This value is similar to periods shown to trigger tremor in other locations. We also examined one smaller magnitude event, the 2009 M_w 6.5 Gulf of California earthquake, because it induced extremely high strains at Anza. The surface waves from the 2009 M_w 6.5 Gulf of California earthquake had higher observed strain than the Denali earthquake, but a shorter dominant period of 11 seconds. This event did not trigger any obvious tremor at Anza. This result suggests that not only the amplitude of the induced strain, but also

the period of the incoming surface wave control triggering of tremor near Anza. In addition, we find that the transient shear stress required to trigger tremor along the San Jacinto Fault at Anza may be higher (34-70kPa) than reported for other regions (7-60kPa in subduction zones; 10-30 kPa along crustal strike-slip faults). Future work will include using dynamic modeling to investigate possible amplitude- and period-dependent tremor triggering mechanisms.

Multiple sources inversion techniques on GPU/CPU hybrid platform, Yongfei Wang and Sidao Ni (Poster 161)

Source parameter of earthquakes is a fundamental issue of seismology. Accurate and timely determination of the earthquake parameters (such as moment, depth, strike, dip and rake of fault planes) is significant for both the earthquake dynamic study and ground motion simulation. And the rupture process study, especially for the moderate and large earthquakes, is essential as the more detailed kinematic study has become the routine work of seismologists. However, among these events, some events behave very specially and intrigue seismologists. These earthquakes usually consist of two similar size sub-events which occurred with very little time interval, such as m_b 4.5 Dec.9, 2003 in Virginia. The studying of these special events including the source parameter determination of each sub-events will be helpful to the understanding of earthquake dynamics. However, seismic signals of two distinctive sources are mixed up bringing in the difficulty of inversion. As to common events, the method(Cut and Paste) has been proven effective for resolving source parameters, which jointly use body wave and surface wave with independent time shift and filters. CAP could determinate fault orientation and focal depth using a grid search algorithm without exact velocity model. Based on this method, we developed an algorithm(MUL_CAP) to simultaneously acquire parameters of two distinctive events. However, the simultaneous inversion of both sub-events make the computation very expensive, so we develop a hybrid GPU and CPU version of CAP(HYBRID_CAP) to improve the computation efficiency. Thanks to advantages on multiple dimension storage and processing in GPU, we obtain excellent performance of the revised code on GPU-CPU combined architecture and the speedup factors can be as high as 40x-90x compared to classical cap on traditional CPU architecture. As the benchmark, we take the synthetics as observation and inverse the source parameters of two given sub-events and the inversion results are very consistent with the true parameters. For the events occurring in Virginia, USA on 9 Dec, 2003, we re-inverse source parameters and detailed analysis of regional waveform indicates that Virginia earthquake included two sub-events which are M_w 4.05 and M_w 4.25 at the same depth of 10km with focal mechanism of strike65/dip32/rake135, which are consistent with previous study. Moreover, compared to traditional two-source model method, MUL_CAP is more automatic with no need for extra manipulation of administrators.

An old question revisited: the mechanics of shallow creep events on strike slip faults, Meng Wei, Yajing Liu, and Jeff McGuire (Poster 085)

As shown in geodetic data following the 1966 Parkfield, 1979 Imperial and 1987 Superstition Hills earthquake, rapid decaying afterslip consists of continuous and episodic creep events. Although many studies focus on the mechanics of individual creep events, no numerical simulation has been done to reproduce the afterslip that mainly consists of creep events. We use a physics-based model in the frame of rate-and-state friction to simulate slip in an earthquake cycle on the Superstition Hills Fault, reproducing surface deformation that is consistent with all available geological and geophysical observations. We started our simulation based on a 2-layer model proposed by Bilham and Behr [1992]. In their model, the region above the seismogenic zone is divided into 2 layers: stable sliding occurs from the surface to a transition depth, below which episodic creep events were initiated. We found that the 2-layer model couldn't reproduce both the afterslip and creep events in the right amount. The problem is that a strong velocity-strengthening layer that creates enough afterslip prevents creep events from propagating to the surface, and vice versa. Therefore, we propose a 3-layer model above the seismogenic zone. In our model, creep events arise from a shallow velocity-weakening layer between two velocity-strengthening layers. The top velocity-strengthening layer reproduces the continuous creep between creep events, whereas the other velocity-strengthening

layer creates rapid afterslip. Our results imply the complexity of fault zone and improve our understanding of the mechanics of episodic creep on strike-slip faults such as the San Andreas near Parkfield, Imperial, and Superstition Hills Fault.

Source and Basin Structure Studies using the 8 August 2012 Yorba Linda Earthquake Sequence, Shengji Wei, Robert W. Graves, Dunzhu Li, and Don Helmberger (Poster 027)

The 8 August 2012 Mw 4.0 and 4.1 Yorba Linda earthquake doublet were strike-slip events occurring within 10 hours of one another along a SW-NE trend of recent seismicity near the intersection of the Elsinore, Chino and Whittier faults. Recent earthquakes along this trend include a M4 strike-slip event on 6 June 2012 and the Mw 5.4 oblique-slip Chino Hills event on 29 July 2012. All of these events have been well recorded by the dense network of broadband and strong motion stations throughout the Los Angeles basin region. Modeling the mid- to higher-frequency (0.2 – 5 Hz) waves of these events can provide a better understanding of source processes and wave propagation effects within the complex 3D basin structure, which can help to improve the estimate of the seismic hazard. With the high quality and dense coverage of the data, detailed investigation of source properties for these events becomes possible, such as delineation of rupture directivity and robust stress drop estimates. Recent analyses of other LA basin events using empirical path corrections from smaller events whose mechanisms were determined with Amplitude Amplification Factors (AAFs) from the larger events have placed tight constraints on the source rupture process. Similar techniques will be applied to the Yorba Linda earthquake sequence. A preliminary assessment of the Yorba Linda doublet indicates that despite their close hypocentral proximity, and similar mechanism and magnitude, their radiated waveforms show significant differences at some close-in stations, particularly for the direct S wave. This indicates differences in source processes, and/or wave propagation effects that require further investigation.

Aftershock Decay with Distance from a Fault, Deborah A. Weiser, Lucile M. Jones, and Egill Hauksson (Poster 175)

We test the hypothesis presented in Dieterich's (1994) rate and state friction model, that p -value is a function of distance from the mainshock. Dieterich's model predicts that the duration of the aftershock sequence (the time to return to background level) is the same at all distances from the fault. However, the change in earthquake rate is proportional to the stress drop, and thus decreases with distance away from the fault. Together, these imply that the apparent decay of aftershock rate should be faster near the fault, where a high stress drop produces a large increase in seismicity, than far from the fault where the change is smaller.

The rate and state friction hypothesis can be evaluated with the new data available with accurate relocations of aftershocks. We compile aftershock data from four major earthquakes: Landers, Hector Mine, Northridge, and Sierra El Mayor that have been relocated with waveform cross correlation and double difference locations. The distance of each aftershock from the principal slip surface in the SCEC Community Fault Model is determined and used to group the events. The change in earthquake rate from the pre-mainshock level is plotted for aftershocks within concentric annuli around the fault surface. Preliminary results show that the decay of aftershocks for the Landers earthquake occurs at the same rate for events very near and those at larger (>50 km) distances from the fault. These results will be compared with the sequences following the Northridge, Hector Mine, and Sierra El Mayor events, to see if our preliminary results are generally applicable.

Very Short-Term (Sub-24h) and Event-Based Earthquake Forecasting Experiments in California, Maximilian J. Werner, Agnes Helmstetter, David D. Jackson, and Yan Y. Kagan (Poster 046)

Most theories of short-term earthquake triggering invoke rapid changes of the crustal stress field during periods of active seismicity. The observed seismicity patterns thus present a unique window into triggering mechanisms, and forecasting experiments within the Collaboratory for the Study of Earthquake Predictability (CSEP) can be designed to better evaluate such occurrence hypotheses by reducing (and eliminating) the current one-day forecast updating periods. Similarly,

providing the public with up-to-date hazard information may require operational forecasts that are updated at sub-daily frequencies. Here, we present progress along two paths toward these goals: we present retrospective, very short-term ETAS forecasts for California at forecast update periods of 12h, 6h, 2h and 1h; and we present a prototype event-based predictability experiment that does not require any discrete forecast horizons or spatial cells but instead evaluates a model by calculating its likelihood function at the exact times, locations and magnitudes of observed earthquakes. These experiments have higher resolution and more power: for example, we find that 24h ETAS forecasts for $m > 4$ earthquakes during 1992 achieve a likelihood gain of about 63 over a time-independent long-term forecast, while the gains of 12h, 6h, 2h and 1h forecasts reach 331, 448, 633 and 781, respectively (preliminary results for 1992 to 2012 show smaller gains near 100, but a preserved trend of increasing gains with higher update frequency).

The prototype event-based experiment is designed for the popular class of point-process models and conforms to the design principles of CSEP testing centers. By requiring models to be expressed by a conditional intensity function, which software can sample at any point in the testing volume, no discretized forecasts are required, and yet likelihood-based inference and model diagnostics provided by point-process theory are accessible. To allow a wide range of conditional intensity functions (e.g., non-analytical functions), the testing software faces the challenge of multi-dimensional numerical integration of the conditional intensity over the test volume to calculate the likelihood. Here, we assess the accuracy and feasibility of numerical integration techniques by comparing numerical results to analytical solutions available for simple conditional intensities.

A user-friendly online tool for inferring surface ages from ^{10}Be depth profiles, A. Joshua West and John Yu (Poster 280)

Accurate dating of geomorphic surfaces that have been offset by faults provides vital information about rates of fault slip over time scales of 10^3 - 10^5 years. Constraints on surface ages can be inferred from concentrations of terrestrial cosmogenic nuclides, and particularly concentrations of ^{10}Be produced in-situ in quartz. TCN concentrations of alluvial deposits are determined not only by surface age, but also by a variable inherited nuclide signal carried by parent sediment. Depth profiles can help to quantify this inheritance, and have been widely applied in studying fault slip rates. However, their accurate interpretation requires careful attention to the range of parameters that determine the systematic variation in concentration with depth in sedimentary deposits, including rates of surface erosion or burial, which vary from one surface to another.

In this work, a new online tool ("BeDeCalc") is presented for interpreting depth trends of ^{10}Be concentration. The goal is to enhance the capacity for researchers to assess the multi-dimensional space of surface age-inheritance-erosion rate associated with depth profiles. BeDeCalc generates 3D plots for visualizing the parameter space, reports best-fit values, and allows for Monte Carlo analysis to determine uncertainty ranges. It also allows for considering variation in density with depth, and over time. It is intended as a user-friendly, widely accessible complement to existing tools for depth profile interpretation, such as the Dalhousie Depth Profile Simulator.

Application of this tool to a range of natural and synthetic datasets suggests that, in the absence of independent information about either inheritance or erosion rate, depth profile data can generally only place a lower limit on surface age. This is true even for profiles extending to many meters depth where muonic production dominates, because unknown inheritance complicates inferences about age. These results emphasize that depth profile chronology should carefully consider the full erosion-inheritance-age parameter space, using all available constraints, and that careful attention should be paid to potential surface erosion when collecting samples for dating.

Using Static Coulomb Models with Rate- and State-Friction Models to Estimate Seismicity Rates for the Canterbury, New Zealand, Earthquake

MEETING ABSTRACTS

Sequence, Charles A. Williams, Sandy Steacy, Matthew Gerstenberger, and David Rhoades (Poster 058)

The Canterbury earthquake sequence began with the Mw 7.1 Darfield earthquake in September, 2010, and continues to the present. This event was followed by events in February, 2011 (Mw 6.2) and June, 2011 (Mw 6.0), causing severe damage to the city of Christchurch, where the level of seismic hazard was previously thought to be moderate. Most recently, a sequence of three events with magnitudes ranging from Mw 5.4 to Mw 5.9 occurred east of Christchurch in Pegasus Bay. Prior to the Darfield event, this region had little to no historical seismicity. Since the initial event, however, the region is extremely active. We are using a variety of approaches to constrain the predicted seismicity rates for this region, and we hope to develop a methodology to apply to similar events in the future.

The approach described here uses stress changes computed by static Coulomb models and uses them in a rate- and state-friction formulation to predict aftershock rates. An alternative approach (not described here) involves using the Coulomb model to redistribute predicted seismicity rates for the STEP model. Our goal is to develop methods that can be used very quickly following a large event in a previously quiescent area, as well as developing more long-term models. To do this, we first restrict our information to what is available within 10 days following an event, including focal mechanism, aftershock locations, fault plane geometry, and any previous background information. This information goes into our Coulomb models and then into the rate- and state-friction models to provide a predicted seismicity rate. For each subsequent large event, we again use information within 10 days of the event, along with any updated information for previous events, and thus update the seismicity rate predictions. We plan to compare these models with observed seismicity rates to determine how effective they are. We also plan to do the same thing for longer-term predictions, but in this case we will use the best available information. Our hope is that these models will prove to be useful prediction tools for future earthquakes.

Deterministic High-Frequency Ground Motions from Simulations of Dynamic Rupture along Rough Faults, Kyle B. Withers, Kim B. Olsen, Zheqiang Shi, Rumi Takedatsu, and Steve Day (Poster 019)

The accuracy of the earthquake source description is a major limitation in high-frequency (>1 Hz) deterministic ground motion prediction, which is critical for performance-based design by building engineers. Here we compute the ground motions generated by dynamic rupture propagation along a rough (non-planar) fault with the goal of studying the effects of fault roughness and heterogeneity of velocity structure on the resultant ground motion. As a first step, the simulation of rupture process along the rough fault is carried out in a homogeneous half-space model using SORD (Shi and Day, 2012), in which the assumed fault roughness follows a self-similar fractal distribution with wavelength scales spanning three orders of magnitude from $\sim 10^2$ m to $\sim 10^5$ m. The rupture irregularity caused by fault roughness leads to ground motions of considerable complexity and generates high-frequency accelerations with near-flat power spectra for up to slightly less than 10 Hz. Next, by using a fourth-order staggered-grid finite difference method (AWP-ODC) with a uniform grid spacing of 20 m, we take the slip-rate time history from the dynamic rupture simulation as our seismic source for the computation of wave propagation in several different crustal models: a high-velocity half space, characteristic 1D rock and basin models and a 3D subset of the CVM-S. We quantify how realistic our ground motion results are by computing PGAs and performing comparisons of PSAs obtained from our simulations with the empirical curves given by recent Next Generation Attenuation (NGA) relations. The purpose of this study is to examine whether the resemblance of the characteristics of ground motion to earthquake strong motion records can be further extended by using more realistic velocity models. The high-frequency ground motions from the rough fault simulations are compared to those obtained by a hybrid deterministic-stochastic technique using scattering operators as the high-frequency component (Mai et al, 2010).

New Earthquake Classification Scheme for Mainshocks and Aftershocks in the NGA – West2 Ground Motion Prediction Equations (GMPEs), Kathryn E. Wooddell and Norman A. Abrahamson (Poster 020)

Over the past 20 years, it has been observed that median ground motions from aftershocks are systematically lower than median ground motions from mainshocks by about 20 - 40% at short spectral periods (Boore and Atkinson, 1989; Boore and Atkinson, 1992; Abrahamson and Silva, 2008); however, classifying an earthquake as a mainshock or aftershock is not a straightforward problem. At best, aftershock is a loosely defined term because there is no clear distinction between aftershocks, triggered events, clusters, etc., all of which are presumably responding to different physical processes following the mainshock. We have developed a new earthquake classification method that captures the differences in the ground motion but is unambiguous to avoid confusion between the seismology and engineering communities.

In accordance with our new methodology, the earthquakes are separated into Class 1 and Class 2 based on their location and time of occurrence with respect to the rupture plane of the largest event in the earthquake cluster. Class 1 earthquakes include the classically defined mainshock, foreshocks, triggered events, and aftershocks that occur off of the Class 1 rupture plane or are outside of the time window for aftershocks. Currently, our methodology uses the time window as defined by Gardner and Knopoff (1974). Distance between the Class 1 earthquake and the potential Class 2 earthquakes is measured using a distance metric we call the centroid Joyner-Boore distance CRJB, which is defined as the shortest distance between the centroid of the Joyner-Boore rupture surface of the potential Class 2 earthquakes and the closest point on the edge of the Joyner-Boore rupture surface of the Class 1 event.

With this classification, we find lower median ground motions for Class 2 events than for Class 1 events with the same magnitude and distance. This new classification scheme allows for a consistent interface between the source characterization (e.g. UCERF) and the ground motion models (NGA-West2).

Quantifying the seismic risk with Gutenberg-Richter relation, Yi-Hsuan Wu, Chien-Chih Chen, Donald L. Turcotte, and John B. Rundle (Poster 060)

The island of Taiwan is a part of the complex boundary between the Eurasian plate and the Philippine Sea plate. The interaction of the plates results in large, shallow earthquakes in west Taiwan such as the Chi-Chi earthquake (Mw=7.6) and extensive seismicity in east and northeast Taiwan and the offshore. Most of the main cities that are high populated are in west Taiwan and the nuclear power plants are built along the coast adjacent to two subduction zones. In this study, we quantify the seismic hazard on the island of Taiwan using the frequency-magnitude statistics of earthquakes since 1900. The seismic data from CWBSN is in good agreement with Gutenberg-Richter relation taking $b \approx 1$ when $M < 7$. For large earthquakes, that is, $M \geq 7$ the seismic data fit Gutenberg-Richter relation with $b \approx 1.5$. This transition is important because it greatly lower the risk of catastrophic earthquakes. Without the change in scaling a $M > 8$ earthquake would be expected about every 25 years. With the change in scaling a $M > 8$ earthquake would be expected about every 200 years. However, the level of seismicity on Taiwan, with area about 35,883 km², is still about 12 times greater than in Southern California, with area about 146,365 km².

Numerical and theoretical analyses of in-plane dynamic rupture on a frictional interface and off-fault yielding patterns at different scales, Shiqing Xu and Yehuda Ben-Zion (Poster 074)

We perform numerical simulations of in-plane ruptures with spontaneous Mohr-Coulomb yielding in the bulk and analyze properties of the ruptures and yielding zones at different scales. Using a conventional polar coordinate system, we show that the overall shapes and patterns of the simulated yielding zones can be well explained by combining the slip-induced Coulomb stress change and the background stress. The preferred sense of shear may be different for off-fault fractures at different scales. While there is no apparent mechanism to prefer either synthetic or antithetic shearing at a scale much smaller than the yielding zone size, this is not the case at larger scales. For low angle reverse faults, large-scale off-fault synthetic fractures are dominant but there are two conjugate sets of fractures with a typical size comparable to the thickness of the yielding zone. For smooth rupture propagation on large strike-slip faults, most of the off-fault fractures that grow across the

entire yielding zone are of the synthetic type. The less preferred antithetic set may become more pronounced for rupture propagation encountering fault heterogeneities. In particular, a strong fault barrier promotes antithetic fractures with a comparable size to those of the synthetic type around the barrier, where very high permanent strain is also observed. A consideration of the non-local properties of the stress field, both in space at a fixed time and in time with changing configuration of the rupture front, can explain the above differences.

Our numerical results and theoretical analysis provide an alternative way to understand Riedel shear structures and the potentially preferred synthetic shear set R suggested in previous studies. The dynamic processes in our study may be distinguished from quasi-static patterns by the timing, location, and inclination angle of characteristic fracture elements. In agreement with other studies, we propose that backward-inclined antithetic shear fractures, may be used as a geological signal that reflects abrupt changes of rupture behavior in a strike-slip fault system. This seems to be true at least for cases when rupture experiences a sudden deceleration, with the intensity of the fracture signal generally proportional to the abruptness of rupture deceleration. Fault locations associated with strong mechanical or geometrical barriers may be recognized by very large permanent off-fault strain.

Continuous Record of Permeability inside the Wenchuan Earthquake Fault Zone, *Lian Xue, Emily E. Brodsky, Haibing Li, Huan Wang, and Junling Pei* (Poster 270)

Faults are complex hydrogeological structures which include a highly permeable damage zone with fracture-dominated permeability. Since fractures are generated by earthquakes, we would expect that in the aftermath of a large earthquake, the permeability would be transiently high in a fault zone. Over time, the permeability may recover due to a combination of chemical and mechanical processes. However, the in situ fault zone hydrological properties are difficult to measure and have never been directly constrained on a fault zone immediately after a large earthquake. In this work, we use water level response to solid Earth tides to constrain the hydraulic properties inside the Wenchuan Earthquake Fault Zone. The transmissivity and storage determine the phase and amplitude response of the water level to the tidal loading. By measuring phase and amplitude response, we can constrain the average hydraulic properties of the damage zone at 800-1200 m below the surface (~200-600 m from the principal slip zone). We use Markov chain Monte Carlo methods to evaluate the phase and amplitude responses and the corresponding errors for the largest semidiurnal Earth tide M2 in the time domain. The average phase lag is $\sim 30^\circ$, and the average amplitude response is 6×10^7 strain/m. Assuming an isotropic, homogenous and laterally extensive aquifer, the average storage coefficient S is 2×10^{-4} and the average transmissivity T is 6×10^{-7} m² using the measured phase and the amplitude response. Calculation for the hydraulic diffusivity D with $D=T/S$, yields the reported value of D is 3×10^3 m²/s, which is two orders of magnitude larger than pump test values on the Chelungpu Fault which is the site of the Mw 7.6 Chi-Chi earthquake. If the value is representative of the fault zone, then this means the hydrology processes should have an effect on the earthquake rupture process. This measurement is done through continuous monitoring and we could track the evolution for hydraulic properties after Wenchuan earthquake. We observed the permeability decreases 35% per year. For the purpose of comparison, we convert the permeability measurements to into equivalent seismic velocity. The possible range of seismic wave velocity increase is 0.03%~0.8% per year. Our results are comparable to the results of the previous hydraulic and seismic studies after earthquakes. This temporal decrease of permeability may reflect the healing process after Wenchuan Earthquake.

Seismotectonic Crustal Stress Field and Style of Faulting Along the Pacific North America Plate Boundary in Southern California, *Wenzheng Yang and Egill Hauksson* (Poster 153)

Using recent high quality earthquake focal mechanisms catalog (1981-2010) we invert for the state of stress in the southern California crust. To interpret the stress field we determine the maximum horizontal compressive stress (SHmax) orientations and the style of faulting across southern California at four different scales of resolution, with grid spacing

of 5 and 10 km, and with 15 or 30 events per grid. The stress field is best resolved where seismicity rates are high but sufficient data are available to constrain the stress field across most of the region. The trend of SHmax exhibits significant regional and local spatial heterogeneities. The regional trend of SHmax varies from north along the San Andreas system to NNE to the east in the Eastern California Shear Zone as well as to the west, within the Continental Borderland and the western Transverse Ranges. The transition zones from one state of stress to the other are very sharp and occur over a distance of a few kilometers, following a trend from Yucca Valley to Imperial Valley to the east, and the western edge of the Peninsular Ranges to the west. The local scale heterogeneities in the SHmax trend include NNW trends along the San Andreas Fault near Cajon Pass, Tejon Pass, and the Cucapa Range, as well as NNE trends near the northern San Jacinto Fault and the Wheeler Ridge region. The style of faulting exhibits similar complexity, ranging from predominantly normal faulting in the high Sierra Nevada, to strike-slip faulting along the San Andreas system, to three consecutive bands of thrust faulting in the Wheeler Ridge area and the western Transfer Ranges. The local variations in the style of faulting include normal faulting at the north end of the San Jacinto Fault and scattered regions of thrust faulting. We compare the pattern of SHmax trend in the crust with the GPS measured maximum shortening strain rate tensor and upper mantle anisotropy. The regional variations in the SHmax trends are very similar to the pattern of the maximum shortening axes of surface strain rate tensor field although the strain field tends to be smoother and appears to capture some of the upper mantle deformation field. The mean trend of SHmax depart about approximately 14° to the east from the trend of the maximum shortening directions of anisotropy in the upper mantle.

Biases in the Coseismic Slip Models of Shallow Subduction Zone Earthquakes Induced by Using Elastic Green's Functions, *Qian Yao and Shuo Ma* (Poster 162)

Elastic dislocation theory has been widely used to infer earthquake rupture processes in the shallow subduction zone. However, the assumption that materials deform elastically during the rupture process is questionable. In the classic critical taper theory of accretionary wedges (Davis et al., 1983; Dahlen, 1990) wedge materials are on the verge of Coulomb failures everywhere, including the basal fault. Due to the proximity to failure an updip-propagating rupture on a shallow-dipping plate interface can significantly increase the pore pressure, lowering the wedge strength and leading to widespread Coulomb failures in the wedge, which is greatly enhanced by the shallow dip of the fault (Ma, 2012). The widespread failures in the wedge give rise to slow rupture velocity and large seafloor uplift. They have also been demonstrated to lead to the deficiency of high-frequency seismic radiation and low overall radiated energy (Hirakawa and Ma, 2012), which has been documented for shallow subduction zone earthquakes (especially tsunami earthquakes) for four decades.

The displacement field calculated by incorporating this poroplastic mechanism is distinctly different from the one predicted by an elastic model – the slip near the trench is small and the largest seafloor uplift is landward from the trench. If this mechanism operates during the rupture process how biased can the inverse models by using elastic Green's functions be? Could the large inferred slip near the trench for the 2011 Tohoku earthquake be an artifact or manifestations of extensive moment release in the wedge? In this work, we will use elastic Green's functions to invert the numerically simulated seafloor displacement field by incorporating this poroplastic mechanism and discuss these issues.

Ground Shaking and Seismic Source Spectra for Large Earthquakes Around the Megathrust Fault Offshore of Northeastern Honshu, Japan, *Lingling Ye, Thorne Lay, and Hiroo Kanamori* (Poster 077)

Large earthquake ruptures on or near the plate boundary megathrust fault offshore of northeastern Honshu, Japan, produce variable levels of regional high frequency ground shaking. Analyses of 0.1-10 Hz strong ground motion recordings from K-net and KiK-net stations and 0.3-3.0 Hz short-period recordings from Hi-net stations establish that the shaking variations result from a combination of differences in seismic source spectra and path attenuation. Eleven earthquakes with Mw= 6.0 to 7.6 are analyzed, including interplate events at different positions on

MEETING ABSTRACTS

the megathrust within the rupture zone of the 11 March 2011 Tohoku (Mw 9.0) event, and nearby intraplate events within the underthrusting Pacific slab. The relative ground shaking for frequencies of 5-10 Hz is strongest for the 7 April 2011 (Mw 7.2) intra-slab event near the coast, followed by intraplate events beneath the outer trench-slope. Decreasing levels of high frequency shaking are produced by interplate megathrust events moving from the down-dip edge of the seismogenic zone to the up-dip region near the trench. Differential attenuation measurements from averaged spectral ratios of strong-motion recordings indicate that average path attenuation is lower for events deeper on the megathrust or within the slab below the coast. Empirical Green's function analysis isolates the source spectra for the passband 0.3-3.0Hz, indicating higher corner frequencies for intraplate events and deep megathrust events than for shallow megathrust events. Similar differences in average source spectra are found for teleseismic P waves. Depth-varying source radiation and path attenuation thus account for the high frequency shaking for the 2011 Tohoku mainshock originating from the down-dip portion of the megathrust.

1/f and the Earthquake Problem: Scaling constraints to facilitate operational earthquake forecasting, Mark R. Yoder, John B. Rundle, and Donald L. Turcotte (Poster 057)

The difficulty of forecasting earthquakes can fundamentally be attributed to the self-similar, or "1/f", nature of seismic sequences. Specifically with respect to earthquakes, the rate of occurrence of earthquakes is inversely proportional to their magnitude m , or more accurately to their scalar moment M . With respect to this "1/f problem," it can be argued that catalog selection (or equivalently, determining catalog constraints) constitutes the most significant challenge to seismicity based earthquake forecasting. Here, we address and introduce a potential solution to this most daunting problem. Specifically, we introduce a framework to constrain, or partition, an earthquake catalog (a study region) in order to resolve local seismicity. In particular, we combine Gutenberg-Richter (GR), rupture length, and Omori scaling with various empirical measurements to relate the size (spatial and temporal extents) of a study area, or bins within a study area, to the local earthquake magnitude potential – the magnitude of earthquake the region is expected to experience. From this, we introduce a new type of time dependent hazard map for which the tuning parameter space is nearly fully constrained. In a similar fashion, by combining various scaling relations and also by incorporating finite extents (rupture length, area, and duration) as constraints, we develop a method to estimate the Omori (temporal) and spatial aftershock decay parameters as a function of the parent earthquake's magnitude m . From this formulation, we develop an ETAS type model that overcomes many point-source limitations of contemporary ETAS. Both of these models demonstrate promise with respect to earthquake forecasting applications. Moreover, the methods employed suggest a general framework whereby earthquake and other complex-system, 1/f type, problems can be constrained from scaling relations and finite extents.

Comparison of earthquake forecasting tests in Kanto district and all over Japan, Sayoko Yokoi, Hiroshi Tsuruoka, Kazuyoshi Nanjo, and Naoshi Hirata (Poster 045)

The Earthquake Research Institute, the University of Tokyo joined the CSEP and started the Japanese testing center called as CSEP-Japan since November 2009. Now more than 100 earthquake forecast models were submitted on the prospective experiment. These results provide new knowledge concerning statistical forecasting models. We started a study for constructing a 3-dimensional earthquake forecasting model for Kanto district in Japan based on the CSEP experiments under the Special Project for Reducing Vulnerability for Urban Mega Earthquake Disasters. Because seismicity of the area ranges from shallower part to a depth of 80 km due to subducting Philippine Sea plate and Pacific plate, we need to study effect of depth distribution. We will develop models for forecasting based on the results of 2-D modeling. We defined the 3D - forecasting area in the Kanto region with test classes of 1 day, 3 months, 1 year and 3 years, and magnitudes from 4.0 to 9.0 as in CSEP-Japan. In the first step of the study, we will install RI10K model (Nanjo, 2011) and the HISTETAS models (Ogata, 2011) to know if those models have good performance as in the 3 months 2-D CSEP-Japan experiments in the

Kanto region before the 2011 Tohoku event (Yokoi et al., in preparation). We use the CSEP-Japan experiments as a starting model of non-divided column in a depth. In the presentation, we will discuss the performance of the models comparing results of the Kanto district with those obtained in all over Japan by the CSEP-Japan.

Analysis of Terrain Proxy Using Measured Vs30 Data, Alan Yong (Poster 007)

Data on measurement-based estimates of Vs30, the time-averaged shear-wave velocity to a depth of 30 meters, is often sparse or not readily available. Until site-specific measured results become available, the engineering community has instead relied on map-based proxy approaches to estimating Vs30. One promising approach, employing geometric parameters (slope gradient, local convexity and surface texture) that directly or indirectly encapsulate proxies (slope and geology, respectively) employed by other methods, is the terrain-based method of Yong et al. (2012) (herein referred to as Y12). Y12, however, developed their model using 853 data points that included both measured and inferred Vs30 values, that is, a mixture of measurements from recorded waveforms and extrapolations from other map-based proxy methods, respectively. In this study, the Y12 approach is reapplied to the California region by combining 503 measured Vs30 values acquired through separate projects funded by the 2009 American Recovery and Reinvestment Act (ARRA) and National Earthquake Hazards Reduction Program (NEHRP). Included are 202 measured values from the earlier Y12 study. Using results from the ARRA-funded project, Vs30 values acquired at "rock" sites appear to reduce the predictive capabilities of the Y12 classes describing well-indurated terrains (mountains and plateaus). A scarcity of data from "rock" sites and training on inferred data are factors that possibly influence the performance of the Y12 model. Observed Vs30 values in other terrain classes (alluvial fans and basins) remain consistent with Y12 estimates. The correlation coefficient (r) for $\log(Vs30)$ as described by slope gradient (0.43) matches results from an earlier study by Yong and Iwahashi (2012). Analyses of local convexity ($r = 0.17$) and surface texture ($r = 0.37$), however, yield reduced correlations by 32 and 14%, respectively. Regressing Vs30 values on groups of explanatory variables also result in lower correlations. Of the three variables and their correlations to Vs30, slope gradient is consistently the strongest and most reliable parameter. Alluvial and basin features used to estimate Vs30 values at softer shallow sediment sites seem to remain stable. Mountain and plateau features, however, do not appear to be as well correlated to measured Vs30 values. By recalibrating the Y12 model with only measured data, an improvement to the overall predictive capabilities of the terrain-based Vs30 model is expected.

Products and Services Available from the Southern California Earthquake Data Center (SCEDC) and the Southern California Seismic Network (SCSN), Ellen Yu, Aparna Bhaskaran, Shang-Lin Chen, Faria Chowdhury, Doug Given, Kate Hutton, Egill Hauksson, and Rob Clayton (Poster 193)

Currently the SCEDC archives continuous and triggered data from nearly 7700 data channels from 505 SCSN recorded stations, processing and archiving an average of 12,000 earthquakes each year. The SCEDC provides public access to these earthquake parametric and waveform data through its website www.data.scec.org and through client applications such as STP and DHI. This poster will describe the most significant developments at the SCEDC in the past year.

New data holdings:

- Real time GPS displacement waveforms are now archived at SCEDC. The 1 sps displacement waveforms are produced by the California Real Time Network (CRTN - <http://sopac.ucsd.edu/projects/realtime/>). They are archived at regular intervals and converted into miniseed format by SCEDC. Users can retrieve these waveforms through a special client called AISTstp in miniseed or sac formats. This project was funded by the NASA Advanced Information System Technologies program.
- Strong motion waveforms from the California Geological Survey are now archived at SCEDC. These waveforms are made available from CGS in V0 format following events in the SCSN region where the peak ground

acceleration amplitude at the station exceeds 0.1% g. They are archived as miniseed along with other SCSN waveforms for a given event.

- Triggered data from the Quake Catcher Network (QCN) and Community Seismic Network (CSN): The SCEDC in cooperation with QCN and CSN is exploring ways to archive and distribute data from high density low cost networks. As a starting point the SCEDC will store a dataset from QCN and CSN and distribute it through a separate STP client.

New distribution methods:

- The SCEDC continues to develop web services. In addition to web services that describe station metadata, StationXML, and event parametric data, QuakeML, the SCEDC has developed a waveform web service. This work was done in cooperation with the Northern California Earthquake Data Center and IRIS.

- Starting September 1, 2012, SCEDC will version its catalog on a daily basis.

- The SCEDC is developing a search interface for its focal mechanism catalog.

SCEC Workshop on San Gorgonio Pass: Structure, Stress, Slip, and the Likelihood of Through-Going Rupture, Doug Yule, Michele L. Cooke, and David Oglesby (Talk Tue 15:30b)

This workshop explored the San Gorgonio Pass "knot" region as a candidate for a SCEC Special Fault Study Area and outlined a plan to fill existing knowledge gaps. Specific topics included the geometry of active subsurface faulting, the potential for earthquakes on the complex fault system in this region, and the likelihood of a 'super-earthquake' that would propagate along the San Andreas system through the pass, leading to a very large-magnitude and damaging event. The workshop brought together geoscientists from a wide spectrum of interests including tectonic geomorphology, structural geology, mechanical modeling, rupture modeling, gravity and magnetic modeling, seismology, geochronology, geodesy, and fault and rock mechanics. The first day was a blend of short science talks on case studies with discussions of specific topics. On the second day, we took a field trip to view key sites in San Gorgonio Pass. Our discussions focused on three major questions for the San Gorgonio Pass.

1. How do we reconcile near-surface observations with subsurface evidence for active fault configuration? The pattern of active faulting revealed by seismicity seems to be quite different below about 10-12 km from that expressed in the upper crust or at the surface. Potential field data suggest fault configurations representative of older fault strands with larger cumulative displacements than those interpreted as currently active from other data sets.

2. What is the earthquake potential of faults in the San Gorgonio Pass? Slip rates, slip per event and uplift rates provide critical data for assessment of earthquake potential. While the UCERF3 seeks to provide critical seismic hazard information, it fails to capture active deformation within the SGP because of erroneous fault geometry. Forward mechanical models show that small changes in fault geometry can produce large differences in slip rates and uplift patterns.

3. Can large earthquakes rupture through the San Gorgonio Pass? The patterns of precarious rocks and temporal correlation of slip events between trenches provide some constraints on the rupture extent of paleo-earthquakes through the Pass. In addition to these constraints, dynamic earthquake rupture models can determine the likelihood of the SGP allowing a 'super-event' to propagate through this region of extreme fault complexity. Recent advances in numerical methodology indicate that we are ready to incorporate enough realism into such models.

Comparing the Size and Frequency of Ruptures of the San Andreas fault system at the Burro Flats, Millard Canyon, and Cabazon Paleoseismic Sites, Doug Yule, Paul McBurnett, Shahid Ramzan, and Kerry Sieh (Poster 131)

Recent findings from the Millard Canyon and Cabazon paleoseismic sites reveal that the most recent rupture of the San Andreas fault system (here the San Gorgonio Pass fault zone) occurred there ~650 yrs ago with no evidence for rupture during the more recent quakes that affected the San Bernardino and Coachella Valley regions in 1812 and ~1680 A.D.,

respectively. It is noteworthy that the late Medieval rupture in San Gorgonio Pass was large (>6 m of slip) and correlates in time with paleo ruptures on the Mojave/San Bernardino, and Coachella Valley segments. The data therefore support two types of San Andreas ruptures for the region: 1) ~M7 events whose ruptures die out as they approach the Pass from the SE or NW; and 2) relatively infrequent but M7.8 events that rupture through the structural complexity of the Pass and involve both the Coachella Valley and San Bernardino/Mojave segments of the fault (as depicted by the 2008 ShakeOut Scenario earthquake). Implicit in this model is the concept that paleoseismic sites located on strike-slip segments where they approach San Gorgonio Pass ought to experience both types of earthquakes. The Burro Flats site is one such site whose trench logs can be studied to see if one can distinguish ruptures that die out as they approach San Gorgonio Pass (small slip events) from those that propagate through the Pass (large slip events). Interestingly subtle fold growth, and minor fissuring and faulting characterize the three most recent events at Burro Flats (BF1 - 1812, BF2 - 1670-1730, and BF3 - 1480-1520 A.D.). It may be possible that deformation during events BF1 and 2 is not due to rupture along faults in San Gorgonio Pass but rather to liquefaction (the site is a yr-round marsh) during the 1812 Wrightwood and ~1680 Coachella Valley events. In contrast to the BF1-3 events, greater folding, abundant fissures, and faults that exhibit strata thickness mismatches across them characterize rupture events BF4 and BF5 at 1300-1360 and 1060-1160 A.D, respectively. The most recent event at Cabazon (1320-1470 A.D.) and at Millard Canyon (poorly constrained to >800 A.D.) may therefore record a through-the-Pass San Andreas rupture that generated large slip at the Burro Flats as well as the Millard and Cabazon sites. Deepening trenches at the Cabazon site is slated for Fall 2012 to test whether another large through-the-Pass rupture occurred ~900 yrs ago when large displacement affected the Burro Flats site (BF5).

Different types of seismicity clusters in southern California: A case study of non-universal behavior, Ilya Zaliapin and Yehuda Ben-Zion (Poster 053)

We document systematic changes in properties of seismic clustering in southern California on spatial scales of tens of kilometers that are correlated with the effective viscosity of the crust (related to heat flow, fluids and deep sedimentary basins). The findings challenge the universality of seismicity parameters and offer an approach for developing improved region-specific parameterizations. Specifically, we work with the waveform-relocated 1981-2011 southern California catalog of Hauksson et al. [2012]. The seismic clusters are identified using the approach of Zaliapin et al. [2008]. The cluster detection method is tested using the ETAS model and reshuffled catalog analyses. It is shown to be effective in detecting the cluster structure of ETAS catalogs and stable with respect to earthquake location errors, completeness magnitude and various algorithm parameters. The seismicity of southern California is decomposed into a sequence of spatio-temporal clusters. Each cluster is considered as a rooted time-oriented tree with vertices representing earthquakes and edges representing nearest-neighbor links. A simple topological characterization of a cluster – average leaf depth – is shown to (i) depict the essential variability of the cluster structure, and (ii) be significantly correlated with a dozen of statistics traditionally considered in aftershocks studies (number of events, duration, area, time decay rate, etc.). The existence of two principal modes of cluster formation, based on the average leaf depth scaling with cluster size, is demonstrated for the observed seismicity. Importantly, the ETAS model does not have the reported bimodality. The two main detected modes of seismic clusters are referred to as burst-like clusters and swarm-like clusters. The burst-like clusters occur predominantly in regions characterized by relatively low heat flow and mild-to-no geothermal activity. The swarm-like sequences occur predominantly in regions characterized by relatively high heat flow and geothermal activity. The developed approach can also be used to study spatio-temporal development of singles (parents with no offspring), repeaters of small magnitudes, and deviations of the background seismicity from a stationary inhomogeneous Poisson process. Our findings are consistent with the existing knowledge on earthquake clustering associated with large events, while providing more detailed, uniform and robust approach to detection and analysis of seismic sequences.

MEETING ABSTRACTS

Engineering Validation of Ground Motion Simulation: Part 2. Skewed Bridges, *Farzin Zareian, Carmine Galasso, and Peyman Kaviani* (Poster 031)

This is a companion poster to the one dealing with the engineering validation of ground motion simulations using tall buildings models. This study focuses on the engineering validation of hybrid broadband ground motion simulations in terms of seismic response of reinforced concrete bridges with skew-angled seat-type abutments (or simply 'skewed bridges'). Synthetic records, simulated at fine grid spacing, represent an attractive option for loss estimation purposes, e.g., if transportation networks are of interest. Moderate and strong earthquake events may cause system interruption over a long period of time, resulting in unacceptable socioeconomic losses and societal disruption. In order to assure that the damage estimates of a bridge (or a portfolio of bridges) computed using simulated and real recordings exhibit similar statistics, the equality, in statistical sense, between seismic responses to these two kinds of accelerograms needs to be tested. To this aim, three short bridges located in California are selected as seed bridges here, from which different models are developed by varying key bridge structural parameters such as column-bent height, symmetry of span arrangement, and abutment skew angle. Through extensive nonlinear dynamic analysis conducted using simulations and actual recordings for two historical earthquakes; i.e., 1989 Mw 6.8 Loma Prieta earthquake and 1994 Mw 6.7 Northridge earthquake, it is demonstrated that median deck rotations and column drift ratios produced by simulations agree reasonably well with those produced by recorded ground motions. However, the intra-event dispersion in the structural response due to the simulations is generally lower than that for recorded ground motions, consistently with the findings of previous studies on the same topic. Hypothesis tests on selected samples are carried out to quantitatively assess the results' statistical significance for both demand parameters. Finally, the sensitivity of the two demand parameters to some ground motion intensity measures is investigated for both simulations and recorded waveforms. It is important to note that results of this study are valid with respect to the assumptions made in the validation process.

Betting against the house and peer-to-peer gambling: a Monte Carlo view of earthquake forecasting, *Jeremy D. Zechar and Jiancang Zhuang* (Poster 043)

Using an analogy between prediction and gambling, we consider earthquake forecasts as wagers of professional reputation. We have previously discussed a "gambling score" based on comparing earthquake predictions with a reference model, and this is akin to betting against the house: the reference model is the oddsmaker and a gambler can win a large amount in a single bet. One might criticize this as an unstable score because it is sensitive to the occurrence of low-probability events, and constructing an appropriate reference model is itself a difficult problem. There is another gambling paradigm in which bettors compete directly against each other and share the winnings among themselves--this is sometimes called peer-to-peer betting. This too has an analogue in earthquake forecasting and model development, where it is increasingly common to compare and rank multiple forecasts which have a common format. In this presentation, we consider the case of gridded rate forecasts, in which one wants to forecast the distribution of seismicity (in space, time, magnitude, etc.) rather than individual events. We treat each grid node as a separate wager in which each forecast can abstain or bet 1 credit of reputation distributed over the number of expected earthquakes. After the observation period, each forecast that bet on this node is rewarded with an amount that is proportional to its correct wager. We applied this method to compare forecasts from the RELM (Regional Earthquake Likelihood Models) five-year experiment in California. In this presentation, we demonstrate how a peer-to-peer gambling score can be calculated in a roundtable setting to simultaneously compare multiple earthquake forecasts, and we also present a head-to-head mode which we compare to using a likelihood ratio metric. We also discuss how the gambling score can be used when developing new seismicity models.

A Fault-based Crustal Deformation Model for UCERF3 and Its Implication to Seismic Hazard Analysis, *Yuehua Zeng and Zhengkang Shen* (Poster 051)

We invert GPS data to determine slip rates on major California faults using a fault-based crustal deformation model with geological slip rate constraints. The model assumes buried elastic dislocations across the region using fault geometries defined by the Uniform California Earthquake Rupture Forecast version 3 (UCERF3) project with fault segments slipping beneath their locking depths. GPS observations across California and neighboring states were obtained from the UNAVCO western US GPS velocity model and edited by the SCEC UCERF3 geodetic deformation working group. The geologic slip rates and fault style constraints were compiled by the SCEC UCERF3 geologic deformation working group. Continuity constraints are imposed on slips among adjacent fault segments to regulate slip variability and to simulate block-like motion. Our least-squares inversion shows that slip rates along the northern San Andreas fault system agree well with the geologic estimates provided by UCERF3, and slip rates for the Calaveras-Hayward-Maacama fault branch and the Greenville-Great Valley fault branch are slightly higher than that of the UCERF3 geologic model. The total slip rates across transects of the three fault branches in Northern California amount to 39 mm/yr. Slip rates determined for the Garlock fault closely match geologic rates. Slip rates for the Coachella Valley and Brawley segment of the San Andreas are nearly twice that of the San Jacinto fault branch. For the off-coast faults along the San Gregorio, Hosgri, Catalina, and San Clemente faults, slip rates are near their geologic lower bounds. Comparing with the regional geologic slip rate estimates, the GPS based model shows a significant decrease of 6-14 mm/yr in slip rates along the San Andreas fault system from the central California creeping section through the Mojave to the San Bernardino Mountain segments, whereas the model indicates significant increase of 1-3 mm/yr in slip-rates for faults along the east California shear zone and northern Walker Lane. This implies a significant increase in seismic hazard in the eastern California and northern Walker Lane region, but decreased seismic hazard in the southern San Andreas area, relative to the current model used in the USGS 2008 seismic hazard map evaluation. Overall the geodetic model suggests an increase in total regional moment rate of 24% compared with the UCERF2 model and the 150-yr California earthquake catalog.

Study on the Earthquake Potential Risk in Western United States by LURR Method Based on Seismic Catalogue, Fault Geometry and Focal Mechanisms, *Yongxian Zhang, M. Burak Yikilmaz, and John B. Rundle* (Poster 044)

The Load-Unload Response Ratio (LURR) method is a medium-term earthquake prediction approach that has shown considerable promise. The physical essence of an earthquake is precisely the failure or instability of the focal region. When a seismogenic system is in a stable state, its response to loading is nearly the same as its response to unloading, whereas when the system is in an unstable state, the response to loading and unloading becomes quite different.

According to the LURR idea, when a seismogenic system is in a stable or linear state, response ratio Y equals to about 1, whereas when the system lies beyond the linear state, Y is greater than 1. In earthquake prediction practice with LURR, loading and unloading periods are determined by calculating perturbations in the Coulomb Failure Stress (CFS) induced by earth tides, and the response rate could be chosen as the Benioff strain which could be calculated from earthquake magnitude M .

The experimental and numerical simulations have confirmed the validation of LURR. In retrospective studies, high Y values have been observed months to years prior to most events and some successful intermediate-term earthquake predictions have been made.

Based on the theory of LURR and its recent development, we chose the western United States (31~44°N, -128~-112°E) as our study area. For this area, we compiled an earthquake catalogue from ANSS, the fault geometry is from USGS, and the focal mechanisms are from Harvard University. We divided the area in 20 sub-regions, and in each sub-region the fault geometry and the focal mechanisms are generally consistent

with each other, so that the loading or unloading attributes of earthquakes occurred in each region could be determined by the same result of Coulomb Failure Stress (CFS) change induced by earth tide.

The results show that obvious LURR anomaly regions near most of the epicenters of the strong earthquakes in California occur months to years before the earthquakes. According to the characteristics of LURR anomalies in western US, two regions were detected with high risk of big earthquakes. One is between the north of Bay Area and the Mendocino triple junction ($38\sim 40^{\circ}\text{N}$, $-124\sim -122^{\circ}\text{E}$) and the other is between Lake Tahoe and Mono Lake ($37.5\sim 39.5^{\circ}\text{N}$, $-120\sim -118^{\circ}\text{E}$) along the border of California and Nevada.

Modeling slow slip events, non-volcanic tremor and large earthquakes in the Guerrero subduction zone (Mexico) with space-variable frictional weakening and creep, *Dimitri Zigone, Yehuda Ben-Zion, and Michel Campillo* (Poster 081)

We explore with numerical simulations the range of conditions leading to key observed features of NVT in relation to SSE and earthquakes along the Guerrero segment of the Mexican subduction zone. The Guerrero segment is known to produce some of the largest slow slip events (SSE) recorded so far with equivalent magnitude up to 7.5 Mw. These SSE, with apparent durations of about 4 years, are accompanied by strong activity of Non Volcanic Tremor (NVT) in central Guerrero. Recently, NVT triggered by the 8.8 Mw Maule earthquake were also been reported in that region. The geometry of the Guerrero subduction zone remains sub-horizontal between 150 km to 250 km from the coast, making it easy to model with a simple flat frictional interface.

We use a model with a planar interface governed by space-varying static/kinetic friction and dislocation creep in elastic solid. The model is tailored through the employed dimensions, distribution of rheological properties and boundary conditions to the Guerrero segment, with particular attention to conditions of the past 15 years for which observations are available. A section of the fault with zero weakening during frictional slip fails in a mode corresponding to a “critical depinning transition” that produces many observed features of NVT. When a high creep patch representing a section sustaining SSE is added, strong interactions between NVT and SSE are observed as in the natural fault system. We also examine triggering of NVT by larger remote earthquakes, implemented by adding periodic triggering oscillations to the regular tectonic loading. In addition to modeling observations of NVT and SSE made in Guerrero during the past 15 years, the simulations allow us to distinguish aspects of the observed behavior that are robust over long time intervals from aspects that change during intervals longer than the observational period.

Meeting Participants

AAGAARD Brad, USGS
ABERS Geoffrey, Columbia 176
ABRAHAMSON Norman, PG&E 004, 012, 020
ABUEG Nicole, 140
AGNEW Duncan, IGPP/SIO/UC San Diego 174, 195, 233
AGRAM Piyush, Caltech 041, 229
AIKEN Chastity, Georgia Tech 194
AKCIZ Sinan, UC Irvine 238, 252
ALLAM Amir, USC 160
AMERI Gabriele, INGV 006
AMOS Colin, Western Washington 105
AMPUERO Jean-Paul, Caltech 159, 165, 172, 278, Talk Tue 08:00
ANDERSON Greg, NSF
ANDERSON James, CalSAE 140
ANDERSON James, Utah Valley
ANDERSON John, UNR
ANDERSON Robert, CSSC/CEA
ANDERSON Tiffany, CSU San Bernardino 222
ANDINO Eduardo, ELAC 297, 298
ANDREWS Dudley, USGS (Retired)
ANGSTER Stephen, USGS 008
ANOOSHEHPOOR Abdolrasool, US NRC 011
ARCHULETA Ralph, UC Santa Barbara 014, 024, 084, 093, 103
ARGUS Donald, NASA JPL 226
ARMSTRONG Gregory, Georgia Tech 194
ARROWSMITH J Ramon, ASU 140, 148, 214
ASPIOTES Aris, USGS 213
ASSATOURIANS Karen, Western Ontario
ASSIMAKI Dominic, Georgia Tech 010
ATHENS Noah, USGS 117, 120
ATKINSON Gail, Western Ontario 003
AVOUAC Jean-Philippe, Caltech 078, 112, 206, 208
AYOUB Francois, 078, 080, 206
BAKER Jack, Stanford 029
BAKER Scott, UNAVCO
BALCO Gregory, LLNL 011
BALTAY Annemarie, Stanford 021
BAMBAKIDIS Gust, Wright State 267
BANESH Divya, UC Davis 143
BANNISTER Stephen, GNS Science 169
BARAJAS Monica, USC 251
BARBOT Sylvain, Caltech 112, 208, 229, 230, 239
BARBOUR Andrew, SIO/UC San Diego 071
BARNEICH John, GeoPentech
BARNHART William, Cornell 204
BARRERA Wendy, UCLA 138, 142, 147
BARRETT Sarah, Stanford 198
BARRY Robert, 146
BARTH Andrew, Indiana 253
BARTLOW Noel, Stanford 169
BASSET Andre, UNAVCO 224
BAUER Robert, Missouri 121
BAYLESS Jeff, URS
BEAUDOIN Bruce, IRIS
BEAVAN John, GNS Science 169
BECKER Julia, GNS Science 258
BECKER Thorsten, USC 064, 113, 114, 150
BEELER Nick, USGS 092
BEHL Richard, CSU Long Beach 123
BEHR Whitney, UT Austin 263
BEMIS Sean, U Kentucky 145
BEN-ZION Yehuda, USC 003, 053, 066, 074, 081, 160, 163, 171, 183, 187
BENNETT Jonathan, Missouri/UC Santa Barbara 121
BENNETT Richard, Arizona 215, 218, 232
BENNINGTON Ninfa, UW Madison 177
BENTHIEN Mark, SCEC/USC
BERG Joseph, CSU San Bernardino 133, 232
BERGEN Kristian, USGS 138
BERGER Madeline, USC 299
BERNARDIN Tony, UC Davis 130
BERNARDO Kevin, UC Santa Cruz 256
BEROZA Gregory, Stanford 016, 021, 036, 182, 198
BEUTIN Thomas, GFZ Potsdam
BHASKARAN Aparna, Caltech 193
BIASI Glenn, UNR 011, 034, 139, 144
BIELAK Jacobo, CMU 015
BILHAM Roger, Colorado
BIRD Peter, UCLA
BLANPIED Michael, USGS
BLEWITT Geoffrey, UNR 235
BLISNIUK Kimberly, UC Davis 129
BOCANEGRA Joseph, Citrus Valley HS
BOCANEGRA Melissa, Citrus Valley HS
BOCANEGRA Richard, Citrus Valley HS
BOCK Yehuda, SIO/UC San Diego 042, 225, 237
BOESE Maren, Caltech 040
BOHON Wendy, ASU
BONILLA Fabian, UC Santa Barbara 013
BOOKER Cecilia, NAVFAC ESC
BORMANN Jayne, UNR 235
BOWMAN David, CSU Fullerton
BRADLEY Brendon, Canterbury 265, 266
BRADLEY Andrew, Stanford 089
BRINKMAN Braden, UIUC 183
BROCHER Thomas, USGS
BRODSKY Emily, UC Santa Cruz 178, 190, 256, 270
BROWN Justin, Caltech/USGS 156, 165, 177
BROWN Kevin, SIO/UC San Diego 075, 088
BRUNE James, UNR 011, 025, 026, 102, 144
BRUNE Richard, UC Irvine 011, 025
BRYANT William, CGS 128
BUCKLEY William, 232
BUITER Susanne, 111
BÜRGMANN Roland, UC Berkeley 105, 129
BURKHART Eryn, UC Santa Barbara
BURKS Lynne, Stanford 029
BYDLON Samuel, Stanford 087
CALLAGHAN Scott, SCEC/USC 037, 040
CAMPBELL Brian, Missouri 121
CAMPBELL Kenneth, EQECAT
CAMPILLO Michel, Joseph Fourier 081
CARLSON Jean, UC Santa Barbara 067, 106
CASTIGLIONE Thomas, Riverside USD 215, 219
CATCHINGS Rufus, USGS 120, 155, 202, 203
CELEBI Mehmet, USGS 028
CENTENO Kevin, USC 295
CHAN Kevin, USC 262
CHAO Kevin, Georgia Tech 194
CHEHAL Simarjit, CSU Northridge
CHEIFFETZ Terry, UC Irvine 252
CHEN Chien-chih, Natl Central Univ Taiwan 060
CHEN Jiangzhi, Oregon 070
CHEN Po, Wyoming 036
CHEN Shang-Lin, Caltech 193
CHEN Xiaofei, Univ of Sci & Tech of China
CHEN Xiaowei, IGPP/SIO/UC San Diego 164
CHEN Yu, 228
CHESTER Judith, Texas A&M
CHIANG Yao-Yi, USC 297
CHIOU Ray, NAVFAC ESC
CHOI Dong Ju, SDSC/UC San Diego 035
CHOURASIA Amit, SDSC/UC San Diego 035
CHOWDHURY Faria, Caltech 193
CHUANG Yun-Ruei, Indiana 220
CHUNG Karina, Wellesley 260
CIVILINI Francesco, UC Santa Barbara 231
CLAYTON Robert, Caltech 193, 274
COCHRAN Elizabeth, USGS 154, 156, 195, 262
COCKETT Rowan, British Columbia 209
COLEMAN Drew, UNC Chapel Hill 253
COMPTON Tracy, UC Davis 130
CONRAD John, UC Riverside
COOK Matthew, UC Santa Barbara 255
COOKE Michele, UMass Amherst 033, 119, 149
COPELAND Breeanna, 133
CORMIER Marie-Helene, Missouri 121
CORRAL-BONNER Helen, Sherman Indian HS 215, 219
COVARRUBIAS Ashley, 232
COWGILL Eric, UC Davis 100, 130
CRANE Thomas, CSU San Bernardino
CREAGER Kenneth, Washington 188
CREMPIEN Jorge, UC Santa Barbara 103
CROUSE C.B., URS Talk Mon 16:00

MEETING PARTICIPANTS

CROWELL Brendan, *UC San Diego* 042, 225
CRUZ Jennifer, 041
CRUZ Jose, *USGS* 298
CUI Yifeng, *SDSC/UC San Diego* 035
CURREN Ivy, *UCLA* 276
DAHMEN Karin, *UIUC* 183
DALGUER Luis, *ETH Zürich* 002
DANZIGER Galen, 055
DAVIS Paul, *UCLA* 186, 200, 279
DAY Steven, *SDSU* 019, 023
DE CRISTOFARO Jason, *USGS*
DE GROOT Robert, *SCEC/USC* 215, 219, 251, 257, 260, 262, 295, 296, 297, 298, 299
DE PASCALE Gregory, 065
DEBOCK David, *Colorado* 032
DECESARI Sarah, 123
DENOLLE Marine, *Stanford* 016, 036
DEPOLO Craig, *UNR* 034
DETERMAN Daniel, *USGS* 213
DEWOLF Scott, *IGPP/SIO/UC San Diego* 233
DIETERICH James, *UC Riverside* 062, 079
DIFO Ohilda, *UMass Amherst* 149
DMITRIEVA Ksenia, *Stanford* 210
DOLAN James, *USC* 078, 080, 138, 147, 206, Talk Tue 15:30
DOMINGUEZ Luis, *UNAM* 200
DONNELLAN Andrea, *NASA JPL* 207, 217, 268
DONOVAN Jessica, *USC* 026
DORSEY Rebecca, *Oregon* 109, 272
DOUILLY Roby, *Purdue*
DRAKE Jacob, 215
DRAKE Joshua, 215
DRAKE Vicki, 226
DREILING Jennifer, *USGS*
DRESEN Georg, *GFZ Potsdam* 064, 150
DRISCOLL Neal, *SIO/UC San Diego* 120, 155, 196, 277
DUAN Benchun, *Texas A&M* 068, 082, 134
DUCKETT Harlee, *John W North HS*
DUNBAR Sean, *CA DWR* 146
DUNHAM Eric, *Stanford* 073, 086, 087, 089, 095, 189
DUPUTEL Zacharie, *Caltech*
EBERHART-PHILLIPS Donna, *UC Davis*
ELBANNA Ahmed, *UC Santa Barbara* 067, 084, 106
ELLIOTT Austin, *UC Davis* 100, 134
ELLIOTT Don, *SIO/UC San Diego* 233
ELLIS Susan, *GNS Science* 111, 239
ELLSWORTH William, *USGS* 168
ELY Geoffrey, *Argonne National Lab*
ERICKSON Brittany, *Stanford* 189
EVANS Eileen, *Harvard* 212
EVANS James, *Utah State* 135
FÄH Donat, 013
FANG Peng, *SIO/UC San Diego* 225
FARRELL Jamie, *Utah* 094
FATTARUSO Laura, *Umass Amherst* 033
FEAUX Karl, *UNAVCO* 224
FIALCO Yuri, *SIO/UC San Diego* 075, 088, 237, 240
FIELD Edward, *USGS* 048
FIELDING Eric, *NASA JPL* 041
FLETCHER John, *CICESE* 240
FLOYD Michael, *MIT* 216, 240
FOUTZ Anna, *John W North HS* 215, 219
FREED Andrew, *Purdue* 239
FREEMAN Stephen, *GeoPentech*
FREYMUELLER Jeffrey, *Alaska*
FUIS Gary, *USGS* 117, 120, 155, 202, 203
FUKUDA Jun'ichi, *U Tokyo* 083
FUNNING Gareth, *UC Riverside* 209, 240
GALASSO Carmine, 030, 031
GALLOVIC Frantisek, *Charles U Prague* 006
GARAGASH Dmitry, *Dalhousie* 090, 097
GARLAND Erica, *CSU Fullerton* 254
GARRISON Jack, 032
GEE Robin, *UC Santa Barbara* 191
GELLER Robert, 052
GERBI Laura, *USC* 297, 298
GERSHENZON Naum, *Wright State* 267
GERSTENBERGER Matthew, *GNS Science* 058, 061
GHOFRANI Hadi, *Western Ontario*
GHOSH Abhijit, *UC Santa Cruz* 188
GHOSH Attreyee, *USC* 113, 228
GILCHRIST Jacquelyn, *UC Riverside* 079
GILL David, *SCEC/USC*
GIVEN Doug, *USGS* 193
GLASSCOE Margaret, *NASA JPL* 207
GOEBEL Thomas, *USC* 064, 150
GOLD Peter, *UT Austin* 100
GOLD Ryan, *USGS* 130
GOLDMAN Mark, *USGS* 120, 155, 202, 203
GOLTZ James, *CalEMA*
GOMEZ Luis, *Etiwanda HS*
GONZALES Alysia, *USC* 299
GONZÁLEZ-GARCÍA Jose Javier, *CICESE* 240
GONZALEZ-HUIZAR Hector, *UTEP* 194
GONZALEZ-ORTEGA Alejandro, *CICESE* 240
GOODING Margaret, *LSA Assoc*
GORBUNOV Val, *UC Santa Barbara* 261
GORDON Erik, 124
GORMLEY Deborah, *SCEC/USC*
GOULET Christine, *PEER/UC Berkeley* 024
GOW Irene, *USC* 257
GRANT-LUDWIG Lisa, *UC Irvine* 011, 025, 144, 252
GRAVELY Darren, *Canterbury* 065
GRAVES Robert, *USGS* 024, 027, 037, 040
GRAY Harrison, *Cincinnati*
GREENWOOD Rebecca, *Cal Poly Pomona* 297
HAASE Jennifer, *SIO/UC San Diego*
HADDAD David, *ASU* 148
HADDON Elizabeth, *CGS* 105
HAGOS Lijam, *CGS*
HALL Kelley, *UNR* 250
HAMANN Bernd, *UC Davis* 143
HAMMOND William, *NBMG* 235
HAMON Jennifer, *Caltech*
HANKS Thomas, *USGS* 021
HARDEBECK Jeanne, *USGS* 107
HARDING Alistair, *UC San Diego* 120, 155, 196, 277
HARRINGTON Rebecca, *UCLA* 156
HARRIS Ruth, *USGS* 104
HARTZELL Stephen, *USGS* 008
HATFIELD Billy, *SIO/UC San Diego* 233
HAUKSSON Egill, *Caltech* 040, 122, 153, 164, 175, 181, 193, Talk Tue 08:00
HEARN Elizabeth, 116
HEATON Thomas, *Caltech* 040, 271
HEERMANCE Richard, *CSU Northridge* 125
HEFLIN Michael, *NASA JPL* 226
HEGARTY Paul, *UC Santa Barbara* 185, 191, 255
HEIEN Eric, *UC Davis* 055
HEIMANN Sebastian, *Hamburg* 275
HELLIGE Bridget, *USC* 295, 298
HELMBERGER Donald, *Caltech* 027, 159
HELMSTETTER Agnes, *Grenoble* 046
HEMPHILL-HALEY Eileen, *Humboldt State* 136
HENRY Pamela, *Fault Line LLC*
HERBERT Justin, *UMass Amherst* 119, 149
HERNANDEZ Janis, *CGS*
HERNANDEZ Stephen, *UC Santa Cruz* 190
HERRING Thomas, *MIT* 216
HILL David, *USGS* 094
HINOJOSA-CORONA Alejandro, *CICESE* 100
HIRAKAWA Evan, *UC San Diego* 173
HIRATA Naoshi, *U Tokyo* 045
HIRTH Greg, *Brown* 092, 263
HODGES Michael, *USC* 296
HODGKINSON Kathleen, *UNAVCO*
HOIRUP Don, *CA DWR* 146
HOLE John, *Virginia Tech* 120, 155, 202, 203
HOLLIDAY James, *UC Davis* 059
HOLLINGSWORTH James, *USC* 078, 080, 206
HOLLIS Daniel, *NodalSeismic LLC* 200
HOLMES James, *SIO/UC San Diego*
HOLT William, *SUNY Stony Brook* 228, 236
HONG Bo, *Georgia Tech* 180
HOOGSTRATEN Aaron, *USC* 251, 295
HOUGH Susan, *USGS* 151, 165
HSU Ya-Ju, *Caltech* 112
HUA Hook, 041
HUANG Mong-Han, *UC Berkeley* 239
HUDNUT Kenneth, *USGS* 141, 213
HUMPHREYS Eugene, *Oregon* 113
HUSA Steve, *Fontana HS* 215, 219
HUTTON Kate, *Caltech* 193
HUYNH Tran, *SCEC/USC*
IGARASHI Toshihiro, 083
IIBA Masanori, 028
ILGEN William, *USC* 299
IMPERATORI Walter, *KAUST* 166

MEETING PARTICIPANTS

INBAL Asaf, *Caltech* 159
JACKSON David, *UCLA* 046, 052, 152
JACOBSEN Bo, *U of Aarhus Denmark* 038
JAFFE Bruce, *USGS* 136
JANECKE Susanne, *Utah State* 135
JARA Marianne, *USC* 297
JARVIS Chelsea, *UNAVCO* 224
Ji Chen, *UC Santa Barbara* 170, 192
JIANG Junle, *Caltech* 098
JOHNSON Kaj, *Indiana* 115, 220, 227
JOHNSON Kameron, *USC* 295
JOHNSON Leonard, *NSF*
JOHNSON Marilyn, *PCC*
JOHNSTON David, *GNS Science* 258
JONES Lucile, *USGS* 175, Talk Mon 11:00
JORDAN Frank, *CSU Los Angeles* 141
JORDAN Thomas, *USC* 009, 024, 026, 036, 037, 047, 062, 171, 257, 262, 281, 295, 296, 297, 298, 299
JOSHI Varun, *Canterbury* 265
JUVE Gideon, *ISI/USC* 037
KAGAN Yan, *UCLA* 046, 052
KAMAI Ronnie, *PEER/UC Berkeley* 004
KAMERLING Marc, *UC Santa Barbara* 123
KANAMORI Hiroo, *Caltech* 077
KANEKO Yoshihiro, *WHOI* 096
KASHIMA Toshidate, 028
KATO Aitaro, *U Tokyo* 083
KAVIANI Peyman, *UC Irvine* 031
KEDAR Sharon, *NASA JPL* 225
KELL Annie, *UNR* 120, 155, 196, 277
KELLOGG Louise, *UC Davis* 055
KELLUM Lawrence, *Utah Valley* 140
KENDRICK Katherine, *USGS* 011, 025, 128, 132
KENNETT James, *UC Santa Barbara* 123
KENT Graham, *UNR* 120, 155, 196, 277
KENT Tyler, *UNR*
KENYON Scott, *CSU Long Beach* 137
KHODAVIRDI Katere, *UCLA*
KILB Debi, *UC San Diego* 184, 259
KING Nancy, *USGS* 213
KIRKPATRICK James, *UC Santa Cruz* 072
KLINE Mark, *Banning HS*
KLOTSKO Shannon, *SIO/UC San Diego*
KNUDSEN Keith, *USGS*
KOCH Franklin, *Caltech*
KOHLENBERGER Chris, *USC* 296
KOHLER Monica, *Caltech* 118, 199, 279
KOYAMA Shin, 028
KOZDON Jeremy, *Stanford* 086, 087, 095, Talk Tue 10:30
KREEMER Corné, *UNR* 235
KREYLOS Oliver, *UC Davis* 100, 143
KRISHNAN Aravindhan, 214
KRISHNAN Swaminathan, *Caltech* 017, 018, 022
KROLL Kayla, *UC Riverside* 154
KURZON Ittai, *IGPP/SIO/UC San Diego* 003
LAJOIE Lia, *UC Santa Cruz* 178
LAMERE Timothy, *UMass Amherst* 191
LANDA Carlos, *USC* 299
LANGENHEIM Victoria, *USGS* 117, 120, 272
LANGER James, *UC Santa Barbara* 067
LAPUSTA Nadia, *Caltech* 069, 098, 157, 172
LAVALLEE Daniel, *UC Santa Barbara* 014
LAWRENCE Shawn, *UNAVCO* 224
LAWSON Michael, *UCLA* 138, 142, 147
LAY Thorne, *UC Santa Cruz* 077
LEBLANC Michael, *UIUC* 183
LEE En-Jui, *Wyoming* 036
LEEPER Robert, *USGS*
LEGG Mark, *Legg Geophysical* 118
LEITH William, *USGS*
LEMME Nathan, *NAVFAC ESC*
LEPRINCE Sebastien, *Caltech* 078, 080, 206
LI Dunzhu, *Caltech* 027, 274
LI Haibing, 270
LI Xiangyu, *UC Santa Barbara* 170, 192
LI Yong-Gang, *USC* 065
LIEL Abbie, *Colorado* 032
LIEOU Charles, *UC Santa Barbara* 067
LIN Fan-Chi, *Caltech* 199, 274
LIN Ting, *Stanford*
LIN Yen-Yu, *Caltech* 157
LINDSEY Eric, *SIO/UC San Diego* 237
LIPOVSKY Brad, *UC Riverside* 240
LIPPOLDT Rachel, *USC*
LIU Ming, *NAVFAC ESC*
LIU Pengcheng, *USBR*
LIU Qiming, *UC Santa Barbara* 093
LIU Xin, *USC* 171
LIU Yajing, *Harvard* 085
LIU Zaifeng, *Texas A&M* 068, 134
LIU Zhen, *NASA JPL/Caltech* 225, 226, 230
LIU-ZENG Jing, 134
LIUKIS Maria, *SCEC/USC* 047
LLENOS Andrea, *USGS* 056
LOHMAN Rowena, *Cornell* 204
LONG Kate, *CalEMA*
LOUIE John, *UNR* 034, 250
LOZOS Julian, *UC Riverside* 102
LUCO Nicolas, *USGS*
LUEDTKE William, *USC* 262
LUNDGREN Paul, *NASA JPL* 041, 226, 230
LUO Yingdi, *Caltech* 278
LUPTOWITZ Rainer, *CSU San Bernardino* 133, 232
LUTTRELL Karen, *USGS* 039
LYNCH David, *USGS* 141
LYNETTE Jennifer, *FEMA*
MA Kuo-Fong, *Natl Central Univ Taiwan* 157
MA Shuo, *SDSU* 162, 173
MACCARTHY Dawn, *USGS*
MADDEN Elizabeth, *Stanford* 182
MADDEN MADUGO Christopher, *Earth Consultants Intl* 148
MAECHLING Philip, *SCEC/USC* 024, 036, 037, 040, 047
MAI P. Martin, *KAUST* 158
MALONEY Jillian, *SIO/UC San Diego*
MANN Doerte, *UNAVCO* 224
MAO Youli, *Texas A&M*
MARLIYANI Gayatri, *ASU*
MARQUIS John, *SCEC/USC*
MARSHALL Courtney, *CSU Long Beach* 123
MARSHALL Scott, *Appalachian State* 108, 119
MASSIN Frédérick, *Utah* 094
MATTI Jonathan, *USGS* 128, 132, 202, 203
MATTOX Nolan, *USC* 296
MAURER Jeremy, *Indiana* 227
MAVROMMATIS Andreas, *Stanford* 211
MAZZONI Silvia, *Degenkolb Engineers*
MCAULIFFE Lee, *USC* 147
MCBRIDE Sarah, 258
MCBURNETT Paul, *CSU Northridge* 125, 131
MCCARTHY Christine, *Columbia*
MCCLURE John, 258
MCGANN Mary, *USGS* 136
MCGARR Arthur, *USGS* 168
MCGILL Sally, *CSU San Bernardino* 124, 127, 133, 147, 215, 219, 232
MCGUIRE Jeff, *WHOI* 085
MCHATTIE Sam A., *Canterbury* 266
MCNABB James, *Oregon* 109, 272
MCRANEY John, *SCEC/USC*
MEADE Brendan, *Harvard* 212
MEHTA Gaurang, *ISI/USC* 037
MELGAR Diego, *UC San Diego* 042
MELTZNER Aron, *Earth Observatory of Singapore*
MENCIN David, *UNAVCO*
MENG Lingsen, *Caltech* 076
MENG Xiaofeng, *Georgia Tech* 180
MENGES Christopher, *USGS*
MERRIAM Martha, *Caltrans*
MICHAEL Andrew, *USGS* 056
MILLER M. Meghan, *UNAVCO*
MILLINER Chris, *USC* 078, 080
MILNER Kevin, *SCEC/USC* 048, 062, 296
MITCHELL Erica, *UC San Diego* 075
MIYAZAKI Shin'ichi, *Stanford* 211
MONTELLI Raffaella, *NSF*
MOONEY Walter, *USGS*
MOORE Angelyn, *NASA JPL* 041, 211, 225, 226
MORAN Seth, *USGS* 094
MORELAN Alexander, *UNR* 139
MORENO Bladimir, 194
MORESI Louis, *Monash* 114
MORRIS Anna, 108
MORRIS Justin, 261
MOSCHETTI Morgan, *USGS* 008
MOURHATCH Ramses, *Caltech* 022
MURARI Madhav, 138
MURRAY George, *SCE/SONGS*

MEETING PARTICIPANTS

MURRAY Jessica, USGS
NADEAU Robert, UC Berkeley 110
NANJO Kazuyoshi, U Tokyo 045
NAVA Alex, CICESE 240
NI Sidao, URS 161
NICHOLSON Craig, UC Santa Barbara 122, 123
NIGBOR Robert, UCLA
NISSEN Edwin, ASU 214
NOLL Erika, UC Riverside 223
NOMURA Shunichi, ISM 110
NORDSTRÖM Jan, Uppsala 086
NORIEGA Gabriela, LA EMD
O'REILLY Ossian, Stanford 086
OCHOA Guadalupe, UCLA 142
OGATA Yoshiko, ISM 110
OGLESBY David, UC Riverside 079, 091, 099, 101, 102, 195
OKAWA Izuru, 028
OKUBO Steven, UCLA 147
OKUMURA Koji, Hiroshima
OLSEN Anna, USGS 271
OLSEN Kim, SDSU 019, 024, 037, 038, 102
OLSON Brian, CGS
ONDERDONK Nate, CSU Long Beach 124, 127, 133, 137
ORCHISTON Caroline, Otago 258
ORTEGA Gustavo, Caltrans
OSKIN Michael, UC Davis 100, 134, 143, 269
OWEN Lewis, Cincinnati 138
OWEN Susan, NASA JPL 041, 211, 226
OZAKIN Yaman, USC 187
PACOR Francesca, INGV 006
PAGE Morgan, USGS 048
PANCHA Aasha, Optim 034
PANKOW Kristine, Utah 184
PARKER Jay, NASA JPL 207, 268
PARSONS Thomas, USGS Talk Wed 08:00
PATON Douglas, 258
PAULSON Elizabeth, USC
PAYNE Ryan, Texas A&M
PAZOS Celia, Cal Poly Pomona
PEARCE Justin T., Fugro Consultants 146
PEI Junling, 270
PENG Zhigang, Georgia Tech 160, 180, 194
PEREZ Nicholas, 261
PERSONIUS Stephen, USGS 008
PETERS Robert, 136
PETERSEN Mark, USGS
PETERSON Dana, UW Madison 177
PITARKA Arben, LLNL
PITCHER Travis, UNAVCO 224
PLATT John, Harvard 090
PLATT John, USC 114
PLESCH Andreas, Harvard 122, 281
POLET Jascha, Cal Poly Pomona
POLLARD David, Stanford 182
PONCE-ZEPEDA Moises, UC Santa Barbara 268
PORTER Keith, Colorado
POTTER Hannah, Cal Poly Pomona
POWELL Robert, USGS
POWERS Peter, USGS 050
POYRAZ Efekan, SDSC/UC San Diego 035
PRANTE Mitchell, Utah State 135
PRIETO German, Universidad de los Andes 179
PRUDENCIO Ernesto, UT Austin
PULLAMMANAPPALLIL Satish, Optim 034
PURASINGHE Rupa, CSU Los Angeles
PURVANCE Matthew, UNR 011
RAMIREZ-GUZMAN Leonardo, CMU 008
RAMSAY Joseph, UCLA 279
RAMZAN Shahid, CSU Northridge 125, 131
RAZAFINDRAKOTO Hoby, KAUST 158
REDINGER Tara, SBCM
REED Samuel, PCC 298
REICHLIN Robin, NSF
REMPEL Alan, Oregon 070
RESTREPO Doriam, CMU 015
REUVENI Yuval, NASA JPL
REZAEIAN Sanaz, USGS
RHOADES David, GNS Science 054, 058
RHODES Edward, UCLA 138, 142, 147
RICE James, Harvard
RICHARDS-DINGER Keith, UC Riverside 062, 079, 154
RICHMOND Bruce, USGS 136
ROCKWELL Thomas, SDSU 066, 124, 129, 133, 136, 148
RODER Belinda, UCLA 142, 147
RODRIGUEZ-PINTO Ivan, NASA JPL 226
ROGERS-MARTINEZ Marshall, Columbia 296
ROHRLICK Daniel, UC San Diego 259
ROLLINS John, Caltech 208
ROMANO Mark, USC
ROOD Dylan, SUERC 005, 011
ROSAKIS Ares, Caltech 069
ROSE Elizabeth, USGS 120
ROSEN Paul, NASA JPL 041
ROSS Stephanie, USGS 136
ROSS Zachary, USC 163
ROTEN Daniel, ETH Zürich 013
ROUSSEAU Nick, SCEC/USC 262, 295, 296, 297, 298, 299
ROUSSET Baptiste, Caltech 112
RUBINO Vito, Caltech 069
RUBINSTEIN Justin, USGS 168
RUHL Christine, UNR
RUNDLE John, UC Davis 044, 055, 057, 059, 060
RYAN Kenny, UC Riverside 091
RYMER Mike, USGS 120, 129, 155, 202, 203
RYNGE Mats, ISI/USC 037
SACHS Michael, UC Davis 055
SAHAKIAN Valerie, SIO/UC San Diego 196, 277
SAHL Eric, Fontana HS 215, 219
SALEEBY Inyo, UC Santa Barbara 011
SALISBURY James, ASU 140, 148
SAMMIS Charles, USC 063
SANDWELL David, UC San Diego 039, 205, 239, 240
SARIPALLI Srikanth, ASU 214
SATO Tsurue, ASU 140, 252
SAVAGE James, USGS 234
SAVRAN William, UC San Diego 038
SCHARER Katherine, USGS 126, 129, 130, 145
SCHEIRER Daniel, USGS 117, 120
SCHMANDT Brandon, Caltech 274
SCHMEDES Jan, UC Santa Barbara 014
SCHMITT Stuart, Stanford 089
SCHORLEMMER Danijel, USC 047, 064
SCHWARTZ David, USGS
SCHWARTZ Susan, UC Santa Cruz 176
SCOTT Eric, SBCM
SCRUGGS Nick, CA Science Center 251
SEALE Sandra, NEES@UCSB 185, 191, 255, 261
SEDKI Ziad, CSU Long Beach 127
SEGALL Paul, Stanford 089, 169, 210, 211, 227
SELANDER Jacob, UC Davis 269
SELCK Jeff, Utah Valley 140
SELIGSON Hope, MMI Engineering
SELLNOW Timothy, U Kentucky Talk Mon 11:00
SHAO Guangfu, UC Santa Barbara 170, 192
SHARP Warren, BGC 129
SHAW John, Harvard 122, 138, 281
SHCHERBENKO Gina, SUNY Stony Brook 236
SHEARER Peter, UC San Diego 096, 164
SHELLY David, USGS 094, 177
SHEN ZhengKang, UCLA 051, 221
SHI Jian, 010
SHI Zheqiang, SDSU 019, 023, 066
SHIH Liwen, U of Houston Clear Lake 273
SHINTAKU Natsumi, CSU Northridge 118
SIEH Kerry, Caltech 131
SILVA Fabio, USC 024
SIMILA Gerry, CSU Northridge
SIMONS Mark, Caltech 041
SIMPSON Robert, USGS 234
SIRIKI Hemanth, Caltech 018
SKLAR Jacob, UNAVCO 224
SLEEP Norman, Stanford 001
SMITH Dave, USC 295
SMITH Michelle, USC 133
SMITH Robert, Utah 094
SMITH Stewart, Washington 063
SMITH-KONTER Bridget, UTEP 039, 205, 239
SOMALA Surendra Nadh, Caltech 172
SOMERVILLE Paul, URS 024
SONG Seok Goo, ETH Zürich 002
SONG Xin, USC
SORLIEN Christopher, UC Santa Barbara 121, 123
SOUSA Frank, Caltech 238
SPINLER Joshua, Arizona 215, 218, 232
SPRINGER Kathleen, SBCM 260
STANG Dallon, UCLA

MEETING PARTICIPANTS

STARK Keith, *Strata Info Tech Inc* 213
STEACY Sandy, *Ulster* 058
STEIDL Jamison, *UC Santa Barbara* 185, 191, 231, 255, 261
STEPANCIKOVA Petra, *Czech Acad Sciences*
STEPHENSON William, *USGS* 008
STINSON Emily, *UC Santa Barbara* 185
STIRLING Mark, *GNS Science* 005
STOCK Joann, *Caltech* 120, 155, 202, 203, 238
STRADER Anne, *UCLA* 152
STREIG Ashley, *Oregon* 126
STUBAILO Igor, *UCLA* 186
SU Feng, *USBR*
SUDHAUS Henriette, *GFZ Potsdam* 275
SUMY Danielle, *USGS* 154, 156, 262
SWIFT Mark, *SBCM*
SYMITHE Steeve, *Purdue*
TABORDA Ricardo, *CMU* 015
TAIRA Taka'aki, *UC Berkeley* 201
TAKEDATSU Rumi, *SDSU* 019
TANIMOTO Toshiro, *UC Santa Barbara* 167
TARNOWSKI Jennifer, *UC Riverside* 101, 120, 202, 203
TAYLOR Michael, *Kansas* 100
TAYLOR Patrick, *NASA GSFC* 145
TERAN Orlando, *CICESE*
THATCHER Wayne, *USGS* 234
THIO Hong Kie, *URS*
THURBER Clifford, *UW Madison* 177
TOKE Nathan, *Utah Valley* 140
TONG Xiaopeng, *IGPP/SIO/UC San Diego* 205
TOWNSEND Meredith, *Stanford*
TREIMAN Jerome, *CGS* 128
TROMP Jeroen, *Princeton* Talk Tue 10:30
TSAI Victor, *Caltech* 197
TSANG Stephanie, *UC Santa Barbara* 167
TSURUOKA Hiroshi, *U Tokyo* 045
TULLIS Terry, *Brown*
TURCOTTE Donald, *UC Davis* 057, 060
UHL Jonathan, *UIUC* 183
UTEVSKY Elinor, *Occidental* 253
VAHI Karan, *ISI/USC* 037
VALLÉE Martin, *Nice* 073
VAN DER ELST Nicholas, *UC Santa Cruz* 190, 256
VANDERWALL Christian, *USC* 296
VANEGAS Michelle, *PCC* 251
VARGAS Bernadette, *Etiwanda HS* 215, 219
VEERARAGHAVAN Swetha, *Caltech* 017
VELASCO Aaron, *LANL* 184
VERNON Frank, *UC San Diego* 003
VIDALE John, *Washington* 188
VIESCA Robert, *Tufts* 090, 097
VILLANI Manuela, *UC Davis* 012
VINCI Margaret, *Caltech*
WALD David, *USGS* Talk Sun 18:00
WALKER Laurel, *U Kentucky* 145
WALLACE Laura, *UTIG* 169
WALLACE Seth, *Bloomington HS* 219
WALLS Christian, *UNAVCO* 224
WANG Feng, *USC* 009
WANG Huan, 270
WANG Min, *UCLA* 221
WANG Tien-Huei, *UC Riverside* 195
WANG Xin, 143
WANG Yongfei, *USTC* 161
WARD Steven, *UC Santa Cruz*
WEAVER Craig, *Washington* 258
WEBB Frank, *NASA JPL* 041
WECH Aaron, 169
WECHSLER Neta, *IPGP* 124, 133
WEERARATNE Dayanthie, *CSU Northridge* 118, 199
WEI Meng, *WHOI* 085
WEI Shengji, *Caltech* 027
WEISER Deborah, *UCLA* 175
WELDON Ray, *Oregon* 126, 146
WERNER Maximilian, *Princeton* 046, 047
WESNOUSKY Steven, *UNR* 139
WEST A. Joshua, *USC* 280
WESTERTEIGER Rolf, *Kaiserslautern* 130
WHITCOMB James, *NSF*
WHITTAKER Andrew, *MCEER/U Buffalo*
WICKER Cary, *CSU Long Beach*
WILLIAMS Charles, *GNS Science* 058, 111, 239
WILLIAMS Patrick, *SDSU* 129
WILLIAMSON Shanna, *USC* 298
WILLS Chris, *CGS*
WILSON Rick, *CGS* 136
WILSON Tom, *Commonwealth Insurance* 258
WITHERS Kyle, *SDSU* 019
WOLF Evan, *UCLA* 147
WOOD Michele, *UCLA* 254
WOODDELL Kathryn, *PG&E* 004, 020
WU Francis, *SUNY Binghamton*
WU Yi-Hsuan, *UC Davis* 060
WYATT Frank, *UC San Diego* 174, 233
XU Shiqing, *USC* 066, 074
XUE Lian, *UC Santa Cruz* 270
YANG Alan, *UC San Diego* 259
YANG Wenzheng, *Caltech* 153
YANO Tomoko, *UC Santa Barbara*
YAO Qian, *SDSU/UC San Diego* 162
YE Lingling, *UC Santa Cruz* 077
YIKILMAZ Mehmet, *UC Davis* 044
YODER Mark, *UC Davis* 057
YOKOI Sayoko, *U Tokyo* 045
YONG Alan, *USGS* 007, 010
YOUNG Karen, *USC*
YU Ellen, *Caltech* 193
YU John, *USC* 047, 280
YU Xiao, *Georgia Tech* 180
YUE Han, *UC Santa Cruz* 176
YULE Doug, *CSU Northridge* 125, 131, Talk Tue 15:30
YUN Sang-Ho, *NASA JPL* 041
ZALIAPIN Ilya, *UNR* 053
ZAREIAN Farzin, *UC Irvine* 030, 031
ZECHAR Jeremy, *ETH Zürich* 043, 047, 150
ZENG Yuehua, *USGS* 051
ZHAN Zhongwen, *Caltech* 197
ZHANG Ding, *USC*
ZHANG Haijiang, *UW Madison* 177
ZHANG Yongxian, *China EQ Networks Center* 044
ZHONG Peng, 030
ZHOU Jun, *SDSC/UC San Diego* 035
ZHU Jianbo, *Caltech*
ZHU Lupei, *Saint Louis* 163
ZHUANG Jiancang, *ISM* 043
ZIELKE Olaf, *KAUST* 148
ZIGONE Dimitri, *USC* 081
ZUMBERGE Mark, *SIO/UC San Diego* 233
ZUZA Andrew, *UCLA*

The Southern California Earthquake Center (SCEC) is an institutionally based organization that recognizes both **core institutions**, which make a major, sustained commitment to SCEC objectives, and a larger number of **participating institutions**, which are self-nominated through the involvement of individual scientists or groups in SCEC activities and confirmed by the Board of Directors. Membership continues to evolve because SCEC is an open consortium, available to any individual or institution seeking to collaborate on earthquake science in Southern California.

Core Institutions and Representatives

| | | | | |
|---------------------------------|--------------------------------|--|---------------------------------------|------------------------------------|
| USC, Lead Tom Jordan | Harvard Jim Rice | UC Los Angeles Peter Bird | UC Santa Cruz Emily Brodsky | USGS Pasadena Rob Graves |
| Caltech Nadia Lapusta | MIT Tom Herring | UC Riverside David Oglesby | UNR Glenn Biasi | |
| CGS Chris Wills | SDSU Steve Day | UC San Diego Yuri Fialko | USGS Golden Jill McCarthy | |
| Columbia Bruce Shaw | Stanford Paul Segall | UC Santa Barbara Ralph Archuleta | USGS Menlo Park Ruth Harris | |

Core institutions are designated academic and government research organizations with major research programs in earthquake science. Each core institution is expected to contribute a significant level of effort (both in personnel and activities) to SCEC programs, as well as a yearly minimum of \$35K of institutional resources (spent in-house on SCEC activities) as matching funds to Center activities. Each core institution appoints an **Institutional Director** to the Board of Directors.

SCEC membership is open to participating institutions upon application. Eligible institutions may include any organization (including profit, non-profit, domestic, or foreign) involved in a Center-related research, education, or outreach activity. An invitation was sent this summer to all SCEC3 domestic participating institutions and institutions new to SCEC that were funded in 2012 to apply for participating institution status in SCEC4, as called for in the SCEC by-laws. As of August 2012, the following institutions have applied for participating institution status for SCEC4 (2012-2017).

Domestic Participating Institutions and Representatives

| | | | | |
|--|--|--|--|--|
| Appalachian State Scott Marshall | Colorado Sch. Mines Edwin Nissen | Smith John Loveless | U Illinois Karin Dahmen | U Wisconsin Madison Clifford Thurber |
| Arizona State J Ramon Arrowsmith | Cornell Rowena Lohman | SUNY at Stony Brook William Holt | U Kentucky Sean Bemis | URS Corporation Paul Somerville |
| Brown Terry Tullis | Georgia Tech Zhigang Peng | Texas A&M Judith Chester | U Massachusetts Michele Cooke | Utah State Susanne Janecke |
| CalPoly Pomona Jascha Polet | Indiana Kaj Johnson | U Alaska Fairbanks Carl Tape | U Michigan Ann Arbor Eric Hetland | Utah Valley Nathan Toke |
| CSU Fullerton David Bowman | JPL Andrea Donnellan | UC Berkeley Roland Bürgmann | U New Hampshire Margaret Boettcher | WHOI Jeff McGuire |
| CSU Long Beach Nate Onderdonk | Oregon State Andrew Meigs | UC Davis Michael Oskin | U Oregon Ray Weldon | |
| CSU San Bernardino Sally McGill | Penn State Eric Kirby | UC Irvine Lisa Grant Ludwig | U Texas El Paso Bridget Smith-Konter | |
| Carnegie Mellon Jacobio Bielak | Purdue Andrew Freed | U Cincinnati Lewis Owen | U Texas Austin Whitney Behr | |

Participating institutions do not necessarily receive direct support from the Center. Each participating institution (through an appropriate official) appoints a qualified **Institutional Representative** to facilitate communication with the Center. The interests of the participating institutions are represented on the Board of Directors by two Directors At-Large.

International Participating Institutions

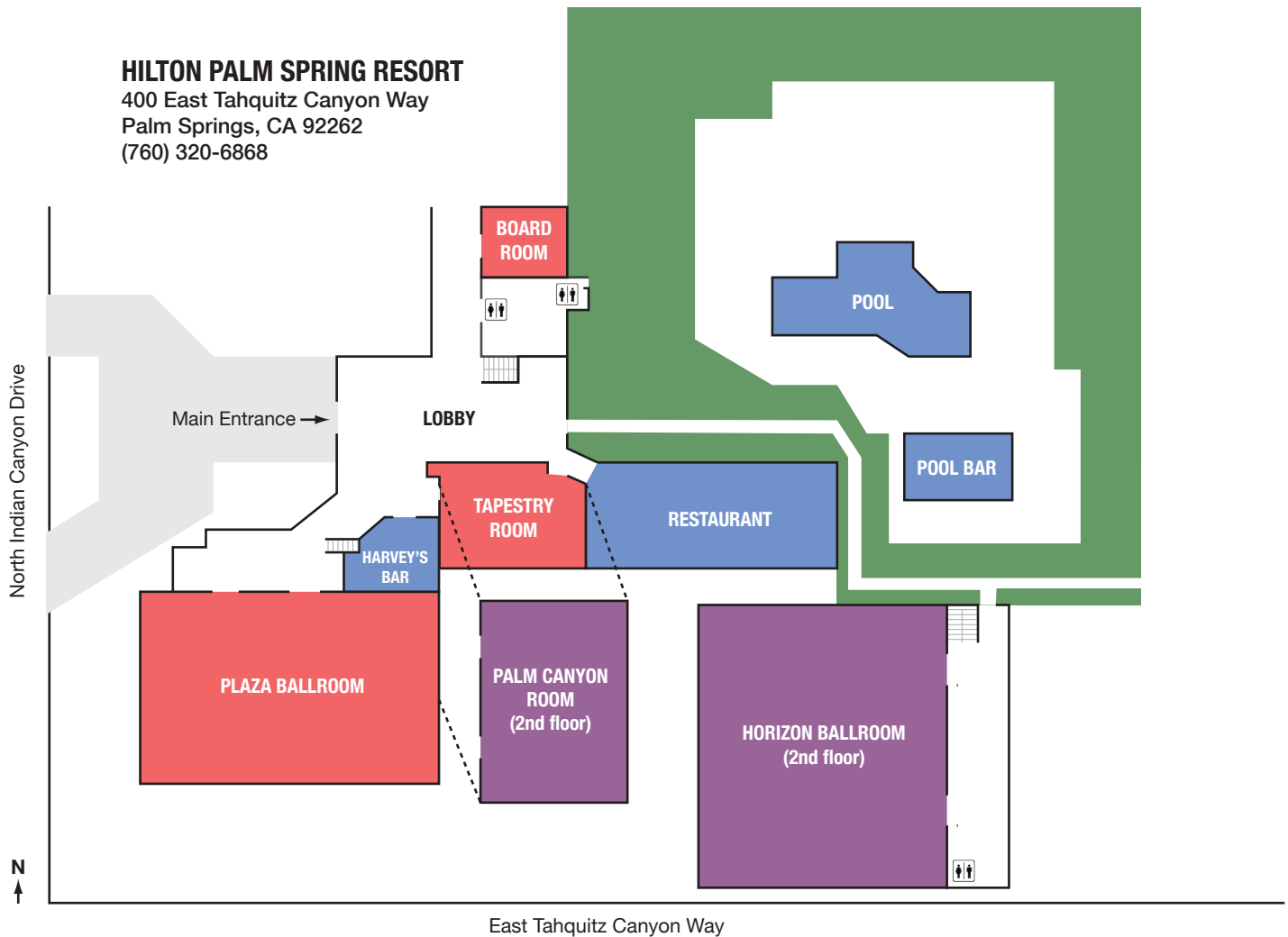
| | | | |
|---------------------------------|---------------------------------|-----------------------------------|-----------------------------------|
| Academia Sinica (Taiwan) | ERI Tokyo (Japan) | Nat'I Central U (Taiwan) | U Western Ontario (Canada) |
| CICESE (Mexico) | ETH Zürich (Switzerland) | Nat'I Chung Cheng (Taiwan) | |
| DPRI Kyoto (Japan) | IGNS (New Zealand) | Nat'I Taiwan U (Taiwan) | |

How to apply to be a SCEC Participating Institution

E-mail application to John McRaney [mcraney@usc.edu]. The application should come from an appropriate official (e.g. department chair or division head) and include a list of interested faculty and a short statement on earthquake science research at your institution. Applications will be approved by a majority vote of the SCEC Board of Directors.

HILTON PALM SPRING RESORT

400 East Tahquitz Canyon Way
Palm Springs, CA 92262
(760) 320-6868



SATURDAY, September 8

- 10:00-21:00 SoSAFE Fieldshop (depart from Lobby)
- 14:00-17:00 Registration and Check-In (Lobby)

SUNDAY, September 9

- 07:00-18:30 Registration and Check-In (Lobby)
- 07:00-08:00 Breakfast (Poolside)
- 08:00-20:00 Poster Set-Up (Plaza)
- 08:00-12:00 Source Inversion Validation (Palm Canyon)
- Modeling Advances in SCEC Geodesy (Horizon)
- Community Modeling Environment Group Meeting (Tapestry)
- 09:00-16:00 NEES@UCSB Workshop and Site Visit (Spa Resort Hotel**)
- 12:00-13:00 Lunch (Restaurant and Poolside)
- 13:00-17:00 SoSAFE Fieldshop (Palm Canyon)
- Ground Motion Simulation Validation Progress (Horizon)
- 17:00-18:00 Annual Meeting Ice-Breaker (Lobby, Harvey's, Plaza)
- 18:00-19:00 Distinguished Speaker Presentation (Horizon)
- 19:00-20:30 Welcome Dinner (Poolside)
- 19:00-20:30 SCEC Advisory Council Dinner Meeting (Tapestry)
- 20:30-22:00 Poster Session (Plaza)

MONDAY, September 10

- 07:00-08:00 Registration and Check-In (Lobby)
- 07:00-08:00 Breakfast (Poolside)
- 08:00-10:30 General Session (Horizon)
- 11:00-13:00 General Session (Horizon)
- 13:00-14:30 Lunch (Restaurant, Tapestry, Poolside)

MONDAY, September 10 (continued)

- 13:00-14:30 Lunch (Restaurant, Tapestry, Poolside)
- 14:30-16:00 Poster Session (Plaza)
- 16:00-18:00 General Session (Horizon)
- 19:00-21:00 SCEC Honors Banquet (Poolside)
- 21:00-22:30 Poster Session (Plaza)

TUESDAY, September 11

- 07:00-08:00 Breakfast (Poolside)
- 08:00-10:00 General Session (Horizon)
- 10:30-12:30 General Session (Horizon)
- 12:30-14:00 Lunch (Restaurant, Tapestry, Poolside)
- 12:30-14:00 SCEC AC Executive Session (Boardroom)
- 14:00-15:30 Poster Session (Plaza)
- 15:30-17:30 General Session (Horizon)
- 19:00-21:00 Dinner (Poolside)
- 20:00-22:00 SCEC AC Executive Session (Boardroom)
- 21:00-22:30 Poster Session (Plaza)

WEDNESDAY, September 12

- 07:00-08:00 Poster Removal (Plaza)
- 07:00-08:00 Breakfast (Poolside)
- 08:00-10:00 General Session (Horizon)
- 10:30-12:00 General Session (Horizon)
- 12:00 Adjourn 2012 SCEC Annual Meeting
- 12:00-14:00 SCEC PC Lunch Meeting (Palm Canyon)
- SCEC Board Lunch Meeting (Tapestry)

** Meet at Cahulla Room, Spa Resort Hotel across North Indian Canyon Drive from Hilton Palm Springs Resort